R-10-02

Modelling of present and future hydrology and solute transport at Forsmark

SR-Site Biosphere

Emma Bosson, Svensk Kärnbränslehantering AB

Mona Sassner, Ulrika Sabel, Lars-Göran Gustafsson
DHI Sverige AB

October 2010

Svensk Kärnbränslehantering AB
Swedish Nuclear Fuel
and Waste Management Co

Box 250, SE-101 24 Stockholm
Phone +46 8 459 84 00

ISSN 1402-3091
SKB R-10-02
ID 1260478
Updated 2013-01

Modelling of present and future hydrology and solute transport at Forsmark

SR-Site Biosphere

Emma Bosson, Svensk Kärnbränslehantering AB

Mona Sassner, Ulrika Sabel, Lars-Göran Gustafsson
DHI Sverige AB

October 2010

Update notice

The original report, dated October 2010, was found to contain editorial errors which have been corrected in this updated version.

Abstract

Radioactive waste from nuclear power plants in Sweden is managed by the Swedish Nuclear Fuel and Waste Management Co, SKB. SKB has performed site investigations at two different locations in Sweden, referred to as the Forsmark and Laxemar-Simpevarp areas, with the objective of siting a final repository for high-level radioactive waste. In 2009 a decision was made to focus on the Forsmark site. This decision was based on a large amount of empirical evidence suggesting Forsmark to be more suitable for a geological repository /SKB 2010b/.

This report presents model results of numerical flow and transport modelling of surface water and near-surface groundwater at the Forsmark site for present and future conditions. Both temperate and periglacial climates have been simulated. Also different locations of the shoreline have been applied to the model, as well as different models of vegetation and Quaternary deposits. The modelling was performed using the modelling tool MIKE SHE and was based on the SDM-Site Forsmark MIKE SHE model (presented by Bosson et al. in SKB report R-08-09). The present work is a part of the biosphere modelling performed for the SR-Site safety assessment.

The Forsmark area has a flat, small-scale topography. The study area is almost entirely below 20 m.a.s.l. (metres above sea level). There is a strong correlation between the topography of the ground surface and the ground water level in the Quaternary deposits (QD); thus, the surface water divides and the groundwater divides for the QD can be assumed to coincide. No major water courses flow through the catchment. Small brooks, which often dry out in the summer, connect the different sub-catchments with each other. The main lakes in the area, Lake Bolundsfjärden, Lake Fiskarfjärden, Lake Gällsbo-träsket and Lake Eckarfjärden, all have sizes of less than one km^2. The lakes are in general shallow.

Approximately 70% of the catchment areas are covered by forest. Agricultural land is only present in the south-eastern part. Till is the dominating type of QD. The QD are often shallow; the mean depth is approximately 5 m and the maximum depth observed on land is 16 m. Most of the lakes are underlain by fine-grained sediments. Bedrock outcrops are frequent but constitute only 5% of the area. Granitic rock is dominating bedrock of the area.

The main changes between the SDM-Site MIKE SHE model and the present SR-Site MIKE SHE model are the size of the model area and the grid resolution, which both are larger in the SR-Site version, and the updated description of the geometry and hydraulic properties of the bedrock. Also, the uppermost part of the QD-profile has been taken into consideration when describing the hydraulic properties in the unsaturated zone compartment of the MIKE SHE model. In previous model versions the distribution of the QD has been the same in both the saturated and unsaturated zone description. In the present version the information from the QD-mapping regarding the upper 0.5 m has been included in the description of the unsaturated zone. The hydrology under different future conditions with regard to shoreline positions and climate conditions has been simulated. Three different shorelines were studied, corresponding to 2000 AD, 5000 AD and 10,000 AD, and three different climates, temperate (i.e. the present climate), wet (i.e. temperate with increased precipitation), and periglacial (cold climate with permafrost).

No full-scale sensitivity analysis of the different model parameters was carried out, but a quality check and calibration of the model was made by comparing model results to measured data. Based on the calibrated model describing present conditions at the Forsmark site the different cases were defined for simulating future shorelines and climates.

A simulation case describing present conditions, i.e. the present climate and the 2000 AD shoreline, was compared to measured data from the site. To obtain an acceptable response when modelling a pumping test performed at the site, the vertical hydraulic conductivity was reduced by a factor of two in the upper 200 m of the bedrock and the specific storage was reduced to a constant value of $5 \cdot 10^{-9}$ m^{-1}. These were the only changes of the given input data that were made. It was concluded that increasing the horizontal grid resolution did not have a large negative effect on the ability of the model to reproduce measured groundwater levels, surface water discharges and surface water levels. The model results for the SR-Site MIKE SHE model for present conditions in Forsmark did not differ much from the results obtained with the SDM-Site MIKE SHE model. Thus, the model describing present conditions was used as the basis for the cases describing future conditions at the site.

Calculated water balances for different areas, time periods and climate conditions indicate that the variations in the overall water balance are small as long as the climate is the same. Under the present (temperate) climate conditions the distribution of the water precipitated during a year is approximately 30% runoff and 70% evapotranspiration. Independently of the shoreline position the variations in the distribution of the precipitated water are within 10%. Under wet climate conditions, the runoff constitutes 20% of the precipitated water and 80% leaves the model volume as evapotranspiration.

However, for the simulated wet climate there is an absolute increase in the total annual runoff from c.180 mm to c. 380 mm, i.e. the runoff increases with more than 100%. The transpiration increases from approximately 145 mm with a temperate climate to approximately 470 mm under wet conditions. When applying a periglacial climate and permafrost condition to the model, the distribution of the precipitated water is approximately 50% runoff and 50% evapotranspiration. The transpiration constitutes only 10% of the total evapotranspiration. This is due to the poor vegetation cover under periglacial conditions.

The modelling results show that the local topography has a strong impact on the pattern of recharge and discharge areas in the QD. The weather conditions have a stronger impact on the recharge and discharge areas in the QD than in the bedrock. In the bedrock, the discharge areas are concentrated to lakes and depressions connected to the streams. The pattern is the same for all applied shorelines under temperate climate conditions. In general the discharge areas, both in QD and bedrock, are stronger in the models with the shorelines of 5000 AD and 10,000 AD. This is due to a more distinct topography in the future land areas. Under periglacial conditions the through taliks function as either recharge or discharge taliks and have a consistent flow direction up or down with exception to the vertical flow pattern and exchange between the active layer and the upper permafrost layer which fluctuates seasonally.

Two local models were created within the regional model area, denoted local model A and B. The numerical grid resolution was changed from 80 m in the regional model to 20 m in the local models. The local models were based on conditions for the year 10,000 AD. However, the local model A was made in two versions with different descriptions of the QD layers (corresponding to modelled present and future QD). For local model A, transport simulations were conducted with both the particle tracking (PT) module and the advection-dispersion (AD) module in MIKE SHE. For the local model B only AD simulations were made.

A particle release at 150 m.b.s.l. showed that after 1,000 years of simulation time, more than 50% of the introduced particles were still left in the model volume. If the particles were introduced at 40 m.b.s.l. more than 80% left the model within 1,000 years of simulation. Particles were concentrated to the lake shorelines rather than the centres of the lakes. One reason for this is that since the lake sediments are less conductive than other QD (i.e. below the sediments and also those around the lake) the particles were forced to move towards the shorelines rather than through the sediments. Another explanation is that the evapotranspiration along the shoreline and in surrounding areas creates an upward hydraulic gradient from deeper parts of the model volume.

Particles released at 40 m.b.s.l. were transported more or less vertically upwards to the surface and the exit locations were concentrated to the streams and lake areas. When the particles were released at c. 150 m.b.s.l. no particles are found in areas underlain by layers with a high horizontal conductivity in the bedrock. Once the particles entered a layer with a high horizontal conductivity, they were transported horizontally in the bedrock towards the northern part of the model domain.

Profiles of calculated solute concentrations across the lake objects showed that once the solute reached the surface it started spreading horizontally across the lake area. When applying plant uptake to the model, the solute concentration was strongly reduced in the central parts of the lakes. Plant uptake from the saturated zone is higher than the uptake from the unsaturated zone. The reason is that most of the solute appears in lake areas and in connection to the water courses, i.e. in areas that are saturated or close to saturated. Decreasing the hydraulic conductivity in the lake sediments by a factor 100 did not change the transport pattern, but it caused a delay of the transport through the sediments. Increasing the dispersion coefficients of the QD layers causes a faster spreading of the solute in the uppermost layers, although the differences are not very large.

Sammanfattning

Radioaktivt avfall från kärnkraftsanläggningar i Sverige tas om hand av Svensk Kärnbränslehantering AB (SKB). SKB har utfört platsundersökningar på två platser, vilka benämns som Forsmark och Laxemar/Simpevarp, med syfte att lokalisera en plats för ett slutförvar för använt kärnbränsle. 2009 togs ett beslut att fokusera på Forsmark. Beslutet baserades på en stor mängd empiriska fakta som pekade på att Forsmark var den mest lämpliga platsen för ett geologiskt slutförvar /SKB 2010b/.

Denna rapport presenterar modellresultat från numeriska flödes- och transportsimuleringar av ytvatten och ytnära grundvatten i Forsmark, både för dagens och för framtida förhållanden. Både tempererade och periglaciala klimat har simulerats. Även olika lägen för havslinjen har applicerats på modellen, likaväl som olika modeller för vegetation och kvartära avlagringar. Modelleringen har utförts med modellverktyget MIKE SHE och baserades på MIKE SHE modellen för Forsmark SDM-Site (presenteras av Bosson et al. i SKB-rapporten R-08-09). Arbetet som presenteras i denna rapport är en del av den biosfärsmodellering som görs inom projektet för säkerhetsanalysen av Forsmark, SR-Site.

Forsmarksområdet karakteriseras av en småskalig topografi. I princip hela modellområdet ligger under 20 meter över havet. Det finns en stark korrelation mellan markytans topografi och grundvattennivån i jordlagren (QD); och således kan man anta att ytvattendelare och grundvattendelare i princip sammanfaller. Det finns inga större vattendrag som rinner igenom området. Små bäckar, som ofta torkar ut under sommarens torrperioder, förbinder de olika delavrinningsområdena med varandra. De största sjöarna i området, Bolundsfjärden, Fiskarfjärden, Gällsboträsket och Eckarfjärden, är alla mindre än en km^2. Sjöarna är i huvudsak grunda.

Ungefär 70% av avrinningsområdena täcks av skog. Jordbruksmark finns enbart i den sydvästra delen av modellområdet. Morän är den dominerande jordarten och jordlagrena är oftast tunna; medeldjupet är cirka 5 meter och det maximala observerade djupet på land är 16 meter. Sjöarna underlagras av finkorniga sediment. Berg-i-dagen är vanligt, men tar enbart upp ca 5% av markytan. Granit är den dominerande bergarten.

De största förändringarna mellan MIKE SHE-modellen för SDM-site och den nuvarande MIKE SHE- modellen för SR-site är storleken på modellområdet och gridupplösningen, som båda är större för SR-site versionen. Beskrivningen av de geometriska och hydrauliska egenskaperna av berget har också uppdaterats. Den översta delen av jordprofilen har tagits i beaktande vid beskrivningen av de hydrauliska egenskaperna av den omättade zonen i MIKE SHE. I de föregående modellversionerna har fördelningen av jordarterna varit densamma i både beskrivningen av den mättade och den omättade zonen. I den nuvarande versionen har information från jordartskartan för den översta halvmetern inkluderats i beskrivningen av den omättade zonen. Hydrologin under olika framtida förhållanden med avseende på kustlinjens läge och klimatförhållanden har simulerats. Tre olika lägen för kustlinjen har studerats, motsvarande 2000 AD, 5000 AD och 10 000 AD, och tre olika klimat, tempererat (d v s nuvarande klimat), vått (d v s tempererat med ökad nederbörd) och periglacialt (kallt klimat med permafrost).

Ingen fullskalig känslighetsanalys av de olika modellparametrarna utfördes, men en kvalitetskontroll och kalibrering av modellen gjordes genom att jämföra modellresultat med mätdata. Baserat på den kalibrerade modellen för nuvarande förhållanden vid Forsmark definierades de olika fallen för att simulera framtida kustlinjer och klimat.

Ett simuleringsfall som beskriver dagens förhållanden, d v s med nuvarande klimat och med kustlinjens läge enligt 2000 AD, jämfördes med mätdata från platsen. Vid kalibrering mot ett pumptest som utförts på platsen reducerades den vertikala hydrauliska konduktiviteten med en faktor 2 i de översta 200 m av berget och magasinstalet reducerades till det konstanta värdet $5 \cdot 10^{-9}$ m^{-1}. Dessa var de enda ändringarna av givna indata som gjordes. Det konstaterades att ökningen av den horisontella gridstorleken inte hade någon större negativ effekt på modellens möjligheter att reproducera uppmätta grundvattennivåer, ytvattenflöden eller ytvattennivåer. Modellresultaten för MIKE SHE SR-site modellen skiljde inte mycket från resultaten som erhölls med MIKE SHE SDM-site modellen. Således kunde den modell som beskriver dagens förhållanden användas som utgångspunkt för fallen som beskriver framtida förhållanden på platsen.

Beräknade vattenbalanser för olika områden, tidsperioder och klimatförhållanden indikerar att variationerna i de övergripande vattenbalanserna är små så länge som de klimatiska förhållandena är desamma. Under nuvarande (tempererade) klimatförhållanden är fördelningen av nederbörden under ett år ca 30% avrinning och 70% evapotranspiration.. Oberoende av kustlinjens läge är variationen i fördelningen av nederbörden inom 10%. Under det våta klimatförhållandet utgör avrinningen 20% av nederbörden and 80% lämnar modellvolymen som evapotranspiration.

För det våta klimatet sker däremot en absolut ökning i den totala årliga avrinningen från ca 180 mm till ca 380 mm, d v s avrinningen ökar med mer än 100%. Transpirationen ökar från ungefär 145 mm vid ett tempererat klimat till ungefär 470 mm under våta förhållanden. När man applicerar ett periglacialt klimat och permafrostförhållanden till modellen blir fördelningen av nederbörden ca 50% avrinning och 50% evapotranspiration. Under periglaciala förhållanden utgör transpirationen bara 10% av den totala evapotranspirationen. Detta beror framförallt på en lägre potential för vattenupptag hos det tunna vegetationstäcket som applicerats i modellen.

Modellresultaten visar att den lokala topografin har en stor betydelse på mönstret för in- och utströmningsområden i jordlagren. Väderförhållandena har en större betydelse för in- och utströmningsmönstren i jorden än i berget. I berget är utströmningsområdena koncentrerade till sjöar och sänkor i anslutning till vattendrag. Mönstret är detsamma för alla applicerade kustlinjer under tempererade förhållanden. I allmänhet är utströmningsområdena, både i berget och i jorden, starkare i modellerna med kustlinjerna för 5000 AD och 10 000 AD. Detta beror på en mera distinkt topografi i de framtida landområdena. Under periglaciala förhållanden fungerar talikarna antingen som inströmnings- eller som utströmningstalikar och har en konsekvent flödesriktning upp eller ner med undantag av det vertikala flödesmönstret och utbytet mellan det aktiva lagret och det övre permafrostlagret som fluktuerar säsongsmässigt.

Två lokala modeller skapades inom det regionala modellområdet, vilka benämns som modell A och B. Den numeriska gridupplösningen ändrades från 80 m i den regionala modellen till 20 m i de lokala modellerna. De lokala modellerna baserades på förhållanden för år 10 000 AD. Den lokala modellen A gjordes dock i två versioner med olika beskrivningar av jordlagren (motsvarande modellerade nuvarande och framtida jordlager). För den lokala modellen A gjordes transportsimuleringar både med MIKE SHEs partikelspårningsmodul (PT) och advektions-dispersionsmodul (AD). För den lokala modellen B gjordes enbart transportsimuleringar med AD-modulen.

Ett partikelsläpp på 150 meter under havsytan (m u h) visade att efter 1000 års simulering så är mer än 50% av de introducerade partiklarna fortfarande kvar i modellvolymen. Om partiklarna i stället introduceras på 40 m u h har mer än 80% av partiklarna lämnat modellen inom 1000 års simulering. Partiklarna koncentrerades till sjökanterna snarare än till mitten av sjöarna. En anledning till detta är att eftersom sjösedimenten är mindre konduktiva än andra jordlager (d v s under sedimenten och också runt sjöarna) tvingades partiklarna att röra sig runt sjöarna snarare än genom sedimenten. En annan förklaring är att evapotranspirationen längs med sjökanten och i angränsade områden skapar en uppåtgående hydraulisk gradient från lägre delar av modellen.

Partiklar som släpps på 40 m u h transporterades mer eller mindre vertikalt uppåt mot ytan och utgångspunkterna koncentrerades till vattendrag och sjöområden. När partiklarna släpptes på 150 m u h återfanns inga partiklar i områden som ligger under lager med hög horisontell konduktivitet i berget. När partiklarna väl kommit in i ett lager med hög horisontell konduktivitet transporteras de horisontellt i berget mot den norra delen av modellområdet.

Profiler av beräknade föroreningskoncentrationer tvärs över sjöobjekten visade att när väl föroreningen når ytan så börjar den sprida sig horisontellt över sjöområdet. När växtupptag introduceras till modellen reduceras föroreningskoncentrationen markant i de centrala delarna av sjön. Växtupptag från den mättade zonen är högre än upptaget från den omättade zonen. Anledningen är att huvuddelen av massan kommer upp i sjöområden och i anslutning till vattendrag, d v s till områden som är mättade eller nästan mättade. En minskning av den hydrauliska konduktiviteten i sjösedimenten med en faktor 100 ändrade inte transportmönstret men orsakade en försening i transporten genom sedimenten. En ökning av dispersionskoefficienterna i jordlagren ger en snabbare spridning i de översta lagren; skillnaden är dock inte särskilt stor.

Contents

1 Introduction

1.1 Background

Radioactive waste from nuclear power plants in Sweden is managed by the Swedish Nuclear Fuel and Waste Management Co, SKB. Within SKB's program for the management of spent nuclear fuel, an interim storage facility and a transportation system are in operation today (2010). SKB has performed site investigations at two different locations in Sweden, referred to as the Forsmark and Laxemar areas, with the objective of siting a final repository for high-level radioactive waste. In 2009 a decision was made to focus on the Forsmark site. This decision was based on a large amount of empirical evidence suggesting Forsmark to be more suitable for a geological repository /SKB 2010b/.

Data from the site investigations have been used in a variety of modelling activities; the results are presented within the frameworks of Site Descriptive Models (SDM), Safety Assessment (SA), and Environmental Impact Assessment (EIA). The SDM provides a description of the present conditions at the site, which is used as a basis for developing models intended to describe the future conditions in the model volume considered within the SA.

This report presents model results of numerical flow and transport modelling of surface water and near-surface groundwater at the Forsmark site for present and future conditions. Both temperate and periglacial climates have been simulated. Also different locations of the shoreline have been applied to the model, as well as different models of the vegetation and the Quaternary deposits (QD, for short). The modelling was performed using the modelling tool MIKE SHE and is based on the SDM-Site MIKE SHE model. The present work is a part of the biosphere modelling performed for the SR-Site safety assessment. The present report and the hierarchy of background reports in the overall SR-Site reporting are illustrated in Figure 1-1 and further described below.

1.2 SR-Site Biosphere

The safety assessment SR-Site is focused on three major fields of investigation: the performance of the repository, the geosphere and the biosphere. The surface system or biosphere part of SR-Site, which is summarised in /SKB 2010a/, mainly describes the information and modelling needed to calculate effects on humans and the environment in case of a radionuclide release from the planned repository.

The calculated effects are then used to show compliance with regulations related to the future repository performance for time spans up to one million years /SSM 2008/. Because of the uncertainties associated with the prediction of the future development of the considered systems in this time frame, a number of future cases are analysed to describe a range of possible site developments. The following text briefly describes the SR-Site biosphere modelling and how the knowledge resulting from the work presented in this report was utilised there.

The SR-Site biosphere modelling is divided into a number of subtasks, see Figure 1-1. The overall work flow can be summarised as follows:

- Describe the site and the site development under different future conditions.
- Describe properties and processes of importance for modelling radionuclide behaviour in present and future ecosystems.
- Identify and describe areas in the landscape that potentially can be affected by releases of radionuclides from the planned repository (biosphere objects).
- Calculate radiological exposure to humans at constant unit release in future ecosystems in order to estimate Landscape Dose conversion Factors (LDFs), and also to calculate the radiological exposure of the environment.
- Describe and motivate the simplifications and assumptions made in the biosphere radionuclide model and in the underlying models.

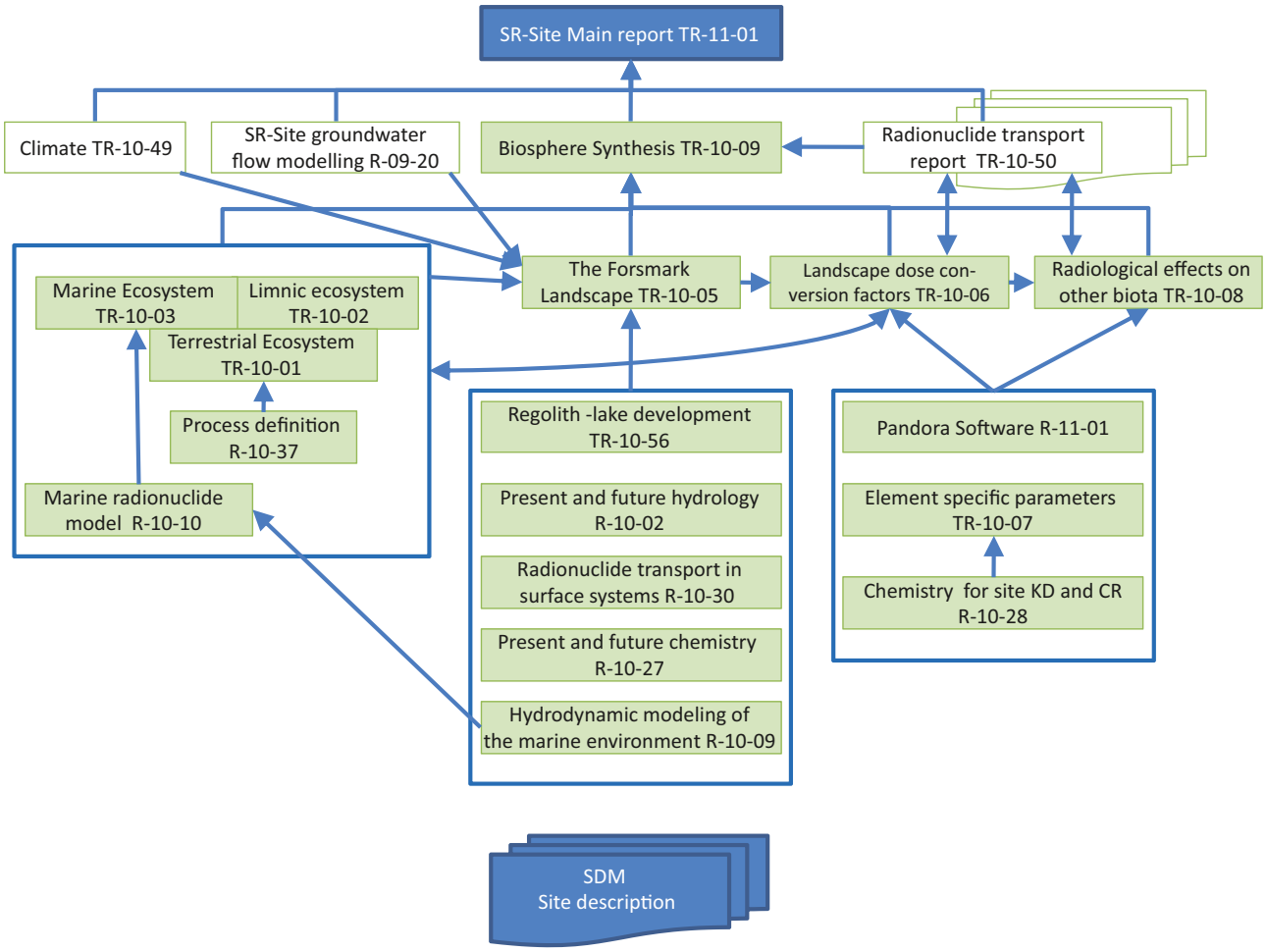

Figure 1-1. *The hierarchy of reports produced in the SR-Site biosphere modelling.*

1.3 Objective and scope

The general objectives of the SR-Site modelling and the specific objectives of the SR-Site Biosphere modelling are presented in /SKB 2010a/. The present report is a background report describing the numerical modelling of surface hydrology and near-surface hydrogeology in Forsmark for future conditions and different climates.

Within the site descriptive hydrological modelling presented in /Bosson et al. 2008/, only the present conditions at the site were described and analysed. The present work aims to describe future hydrological conditions at the site taking shoreline displacement, sedimentation processes and development of the climate into consideration. The water fluxes within and between different ecosystems are of great importance when describing the different ecosystems at landscape level. The water fluxes are the driving force in the radionuclide model and results from the descriptive and numerical hydrological modelling are used as input to the radionuclide model /Avila et al. 2010/.

The results from the numerical modelling presented in this report are also an important input to the overall understanding of the future hydrology in Forsmark. The different model cases defined in this report and the results from the model cases are used as supporting information when analysing which processes in the landscape development that are of importance for the hydrology at the site. Supporting transport calculations have been carried out to be able to analyse the water flow paths in a more detailed way. The transport calculations aim to better understand the flow paths of a potential release from the repository in the near-surface system.

The objectives of the modelling reported in this document are to:

1 With the SDM MIKE SHE model as a starting point update the MIKE SHE model and simulate future land areas and apply different climate cases to the model.

2 Evaluate the performance of the updated MIKE SHE water flow model by controlling the ability to reproduce measured groundwater levels, surface water discharges and surface water levels from the site.

3 Present the methodology of the modelling of future conditions, especially describe the methodology of the permafrost simulations.

4 Present the results of the flow modelling of present and future conditions at the Forsmark site.

5 Describe the results from the flow modelling delivered to the radionuclide model.

6 Analyse which processes that are of importance for the description and understanding of the future hydrological conditions in Forsmark.

7 Analyse solute transport under different climate conditions from potential sources at large depth in the bedrock to and within near-surface and surface systems.

1.4 Setting

The Forsmark area is located approximately 120 km north of Stockholm, in northern Uppland within the municipality of Östhammar. Figure 1-2 shows the regional model area and the so-called candidate area considered by the site investigation and within the site descriptive modelling. Also some lakes and other objects of importance for the hydrological modelling are shown in the figure.

The candidate area is situated in the immediate vicinity of the Forsmark nuclear power plant and the underground repository for low- and medium-active nuclear waste, SFR. It is located along the shoreline of Öregrundsgrepen (a part of the Baltic), and extends from the nuclear power plant and the access road to the SFR facility in the northwest to the Kallrigafjärden bay in the southeast. The candidate area is approximately 6 km long and 2 km wide.

A description of the present meteorological, hydrological and hydrogeological conditions in the Forsmark area is presented in /Johansson 2008/. /Lindborg 2008/ gives a description of the whole surface and near-surface system, including the most recent models of, e.g. the topography and the regolith. Possible future conditions and the succession of the landscape are described in /Lindborg 2010/. The site characteristics and parameters considered in the present work are summarised and described in Chapter 2.

In this report, the reference system for altitude levels is RHB70. Depending on type of data presented, levels will be given in metres above sea level (m.a.s.l.) or metres below sea level (m.b.s.l.) according to RHB70.

The regolith in Forsmark consists mainly of Quaternary deposits. In this report all the regolith, including lake and sea bottom sediments, is named Quaternary deposits and in the following text abbreviated as QD.

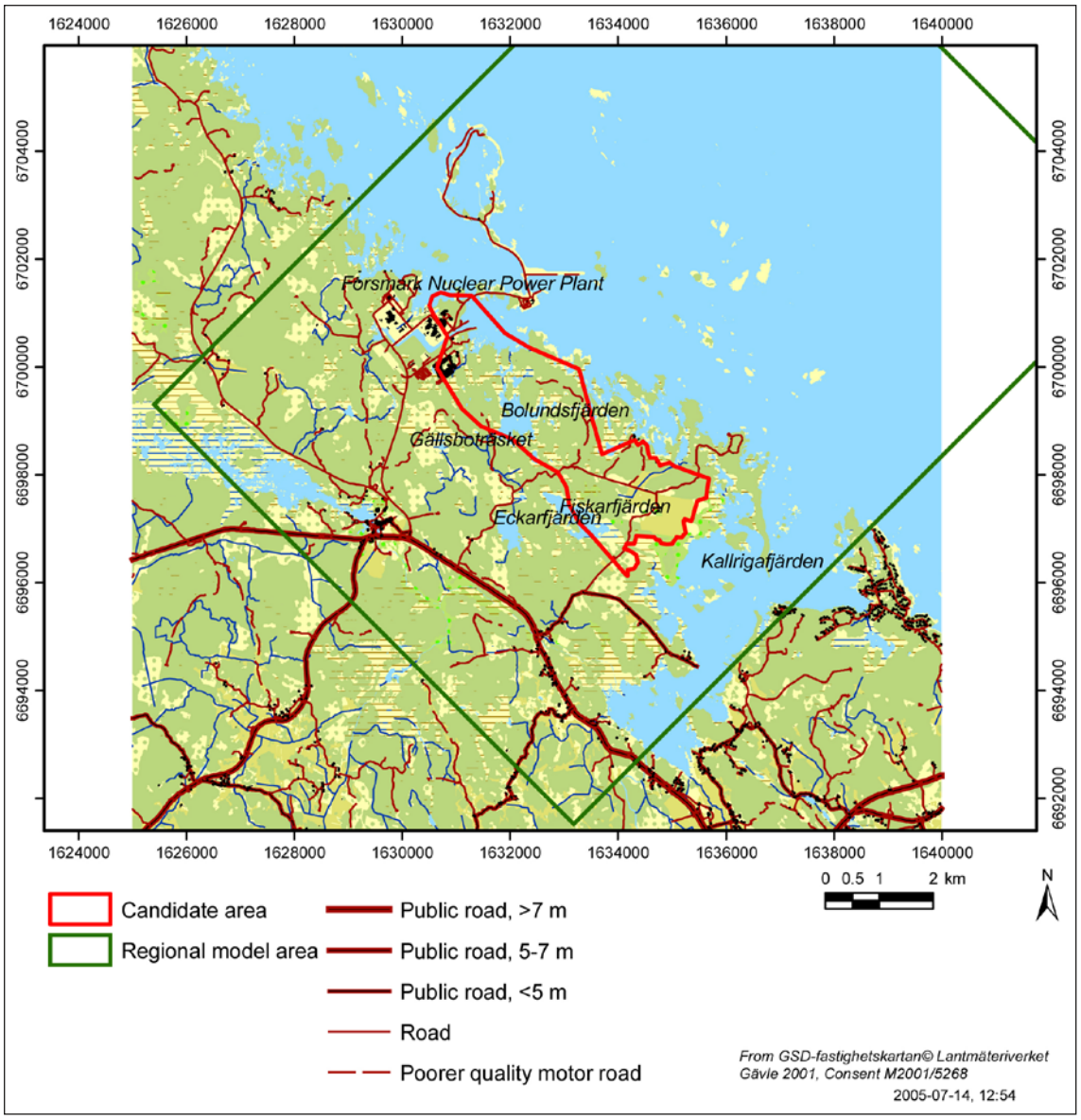

Figure 1-2. *Map of the land part of the regional model area and some objects of particular interest for the hydrological modelling.*

1.5 Related modelling activities

Several modelling activities have provided the various external input data and models required for the SR-Site hydrological and near surface hydrogeological numerical modelling. The MIKE SHE SDM-Site model is the starting point for all model cases in this report. Data for the modelling of future condition and different climate cases are presented in Chapter 2 whereas all data used for the MIKE SHE SDM modelling are described or referred to in /Bosson et al. 2008/ and /Johansson 2008/. We discuss here briefly the interactions with other modelling activities that consider flow modelling of the integrated bedrock-Quaternary deposits system.

The work described in this report is focused on the surface systems, i.e. the Quaternary deposits and the upper part of the bedrock. The numerical model was developed using the MIKE SHE tool. The ground surface, as obtained from the topographic model of the site, is the upper model boundary and the bottom boundary was set at 600 m.b.s.l. The modelling activities that provided inputs to the various parts of this work can be summarised as follows:

- The SDM-Site conceptual modelling of the hydrology and near-surface hydrogeology at the Forsmark site /Johansson 2008/ provided a basic hydrogeological parameterisation and a hydrological-hydrogeological description that were used in the numerical SDM-Site MIKE SHE modelling /Bosson et al. 2008/.
- The SR-Site hydrogeological modelling performed with the ConnectFlow modelling tool /Joyce et al. 2010/ delivered the hydrogeological properties of the rock and the starting positions of the particles traced in some of the MIKE SHE transport calculations.
- The Forsmark version 2.3 geological models of the QD /Hedenström and Sohlenius 2008/ provided the geological-geometrical framework for the stratigraphical description for present conditions used in the MIKE SHE model.
- The stratigraphical description of the QD for future conditions is described in /Lindborg 2010/ and /Brydsten and Strömgren 2010/.
- Inputs to the descriptions of vegetation and land use under periglacial conditions was provided from /Löfgren 2010/.
- Meteorological data for wet and periglacial conditions were provided from /Kjellström et al. 2009/.

1.6 This report

This report provides an integrated presentation of the modelling activities corresponding to objectives 1–7 in Section 1.3. Chapter 2 describes the input data (objective 1). Chapter 3 describes the modelling tool and the methodology of the numerical modelling of different time periods and climate conditions (objective 3). Chapter 4 describes the numerical flow models (objective 3). In Chapter 5, the initial calibration and the results from the regional modelling describing present and future conditions in terms of different shorelines and QD models are presented (objectives 2, 4 and 6). The results for different climate cases are described in Chapter 6 (objectives 4, 6 and 7). Results of solute transport modelling using the local models are presented in Chapter 7 (objectives 6 and 7). In Chapter 8, the delivery of the MIKE SHE modelling results to the radionuclide transport calculations is summarised (objective 5) and finally the conclusions and a discussion of the work are presented in Chapter 9 (objective 6).

2 Site description and input data

2.1 Site overview

The Forsmark area has a flat, small-scale topography. The study area is almost entirely below 20 m.a.s.l. (see Figure 2-1). In Figure 2-1 the surface water divides are marked. As a part of the site investigations, 25 “lake centred” catchments and sub catchments were delineated. Catchment areas and lakes are described in /Brunberg et al. 2004/. There is a strong correlation between the topography of the ground surface and the ground water level in the QD. Thus, the surface water divides and the groundwater divides in the QD can be assumed to coincide.

There is a strong east-western gradient in the precipitation in north-eastern Uppland. At the SMHI station located approximately 15 km west of the Forsmark area the long term mean annual precipitation is 690 mm, whereas at Örskär, an SMHI station located c. 15 km north-east of Forsmark, it is only 490 mm. The annual corrected precipitation in the Forsmark area during the site investigation period, May 2003 to May 2007, was 563 mm. There is also a gradient in the temperature with a slightly milder climate on the coast than at the inland stations. The dominating wind direction in the area is from southwest.

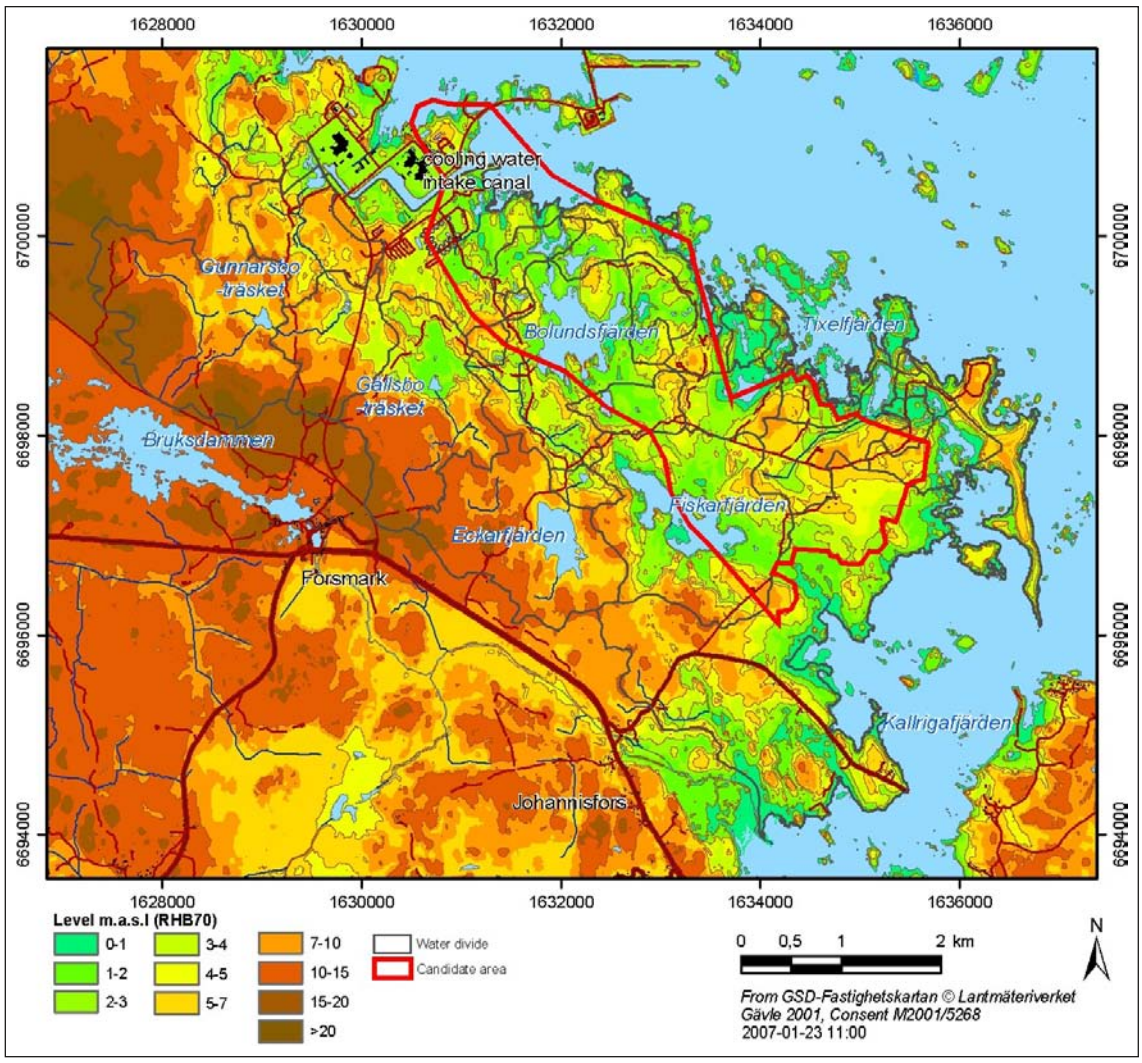

Figure 2-1. *Topographical map of the Forsmark area. Surface water divides are indicated in the figure.*

No major water courses flow through the catchments shown in Figure 2-1. Small brooks, which often dry out in the summer, connect the different sub-catchments to each other. The brooks downstream Lake Gunnarsboträsket, Lake Eckarfjärden and Lake Gällsboträsket carry water most of the year but can be dry during dry years. The long term annual runoff in the area has been estimated to 150–160 mm; this will be further discussed in the section describing the water balance of the area. The highest recorded specific discharge in the area during the site investigation period, 64.5 L/s/km^2 (10 min mean value), was observed at the PFM002669 station (Figure 2-21). Due to the relatively short time series, firm conclusions regarding the long term specific discharge in the area cannot be drawn. However, the mean specific discharge of the largest catchment (PFM005764) was 4.88L/s/km^2 (154 mm/y), which value is based on a measured time series of 35.5 months.

The main lakes in the area, Lake Bolundsfjärden, Lake Fiskarfjärden, Lake Gällsboträsket and Lake Eckarfjärden, all have sizes of less than one km^2. The lakes are in general shallow. For all the lakes in the study area, the mean depth ranges from 0.1 m to 1 m. Due to the limited depth, the vertical mixing is likely to be complete. The vertical mixing is mainly driven by wind and shear. The inlets and outlets of the lakes are often located at opposite ends of the lake. The lakes are assumed to be well mixed also in the horizontal plane. The horizontal mixing is driven by flow and wind shear. In the shallow reed covered areas of the lake, often close to the shore, there is a risk of more stagnant water. However, the degree of mixing must be related to the flow, which in this area is small. Velocities induced by flow will therefore be small compared to velocities induced by wind shear. This supports the notion of well mixed lakes.

During periods of high sea water levels, salt water intrusion from the sea to the lakes may occur. Both under the storm “Gudrun” in January 2005 and during “Per” in January 2007 salt water intrusion occurred in Lake Norra Bassängen and Lake Bolundfjärden. This was observed as an increased electrical conductivity in the lake water. The surface water levels in the lakes in the area seem to be dependent on the lake threshold and the amount of surface- and groundwater discharging into the lakes. However, the surface water levels in Lake Bolundsfjärden and Lake Norra Bassängen are more dependent on the sea water level /Johansson and Öhman 2008/.

Approximately 70% of the catchments areas are covered by forest. Agricultural land is only present in the south-eastern part, north-east of Lake Fiskarfjärden (Figure 2-1). Wetlands are frequent in the area and cover more than 25% of some sub-catchments. From a hydrological point of view it is important to distinguish between bogs, fens and marshes /Kellner 2003/. The only source of water to a bog is the precipitation falling within the area of the bog, whereas a fen partly is supplied also with surface water and/or groundwater flowing into the area. Marshes are wetlands with little or no peat. Bogs are only found in the most elevated areas of the site investigation area and fens and marches are frequent in the low-lying areas.

Till is the dominating type of Quaternary deposit (QD) in Forsmark. The QD are often shallow; the mean depth is approximately 5 m and the maximum depth observed on land is 16 m (in a QD borehole south-east of Lake Fiskarfjärden). Measurements performed at the site indicate anisotropy of the hydraulic conductivity of the till with a decreasing conductivity with depth. Also, the vertical hydraulic conductivity is in general lower than the horizontal. Most of the lakes are underlain by fine-grained sediments. The typical sediment stratigraphy from down and up consists of glacial and/or post glacial clay, sand and gravel, clay-gyttja, and gyttja. A detailed description of the QD in the Forsmark area is given in /Hedenström and Sohlenius 2008/. Bedrock outcrops are frequent but constitute only 5% of the area. Granitic rock is dominating bedrock of the area.

2.2 Hydrogeological conditions

In Figure 2-2 the overall conceptual model of the present near-surface hydrogeology is illustrated. Direct groundwater recharge from precipitation is the dominating source of recharge. During summer, some of the lakes in the area may act as recharge areas. Water uptake from plants lowers the groundwater level in the vicinity of the lakes and some of the lakes change from discharge to recharge conditions. Due to the high infiltration capacity of the upper QD, overland flow rarely occurs, except from in saturated areas where the groundwater level reaches the ground surface. The runoff in the brooks is dominated by water of groundwater origin. During intensive rain events or snow melt, overland flow may contribute significantly to the runoff.

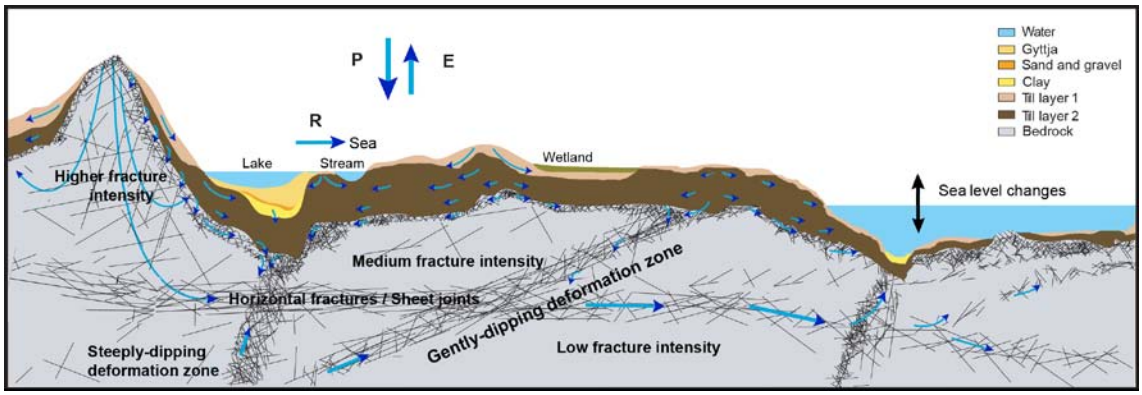

Figure 2-2. *Conceptual model of the surface hydrology and near-surface hydrogeology at Forsmark.*

The small-scale topography implies that many small catchments are formed with local, shallow groundwater flow systems in the QD. Combined with the decreasing hydraulic conductivity with depth and the anisotropy of the tills dominating in the area (implying higher horizontal than vertical hydraulic conductivities), it is obvious that a dominating part of the groundwater will move along very shallow flow paths. Groundwater levels in QD are very shallow with mean levels within a depth of less than a metre in most of the area. The groundwater level in the QD is highly correlated with the topography of the ground surface. This local flow system in the QD overlays larger-scale flow system in the bedrock.

The upper part of the bedrock is characterised by a high frequency of horizontal fractures (sheet joints). Results from the site investigations indicate that these sheet joints interconnect hydraulically across large distances /Follin 2008, Johansson 2008/. The bedrock between the sheet joints is less conductive. Below the upper c. 200 m of the bedrock there are no horizontal fractures/sheet joints of this type and the overall fracture frequency is very low, and is mainly related to steeply dipping deformation zones. The groundwater recharge from the QD to the upper bedrock is easily transmitted in the upper bedrock even at low gradients due to the high-transmissive sheet joints and other structures there. The groundwater level in the upper bedrock is very flat and not correlated to the surface topography as the groundwater levels in the QD. The groundwater level in the upper bedrock is approximately at 0.5 m within the candidate area.

2.3 Climate data

The MIKE SHE model uses data on temperature, precipitation and potential evapotranspiration. Three different types of climate are used in the model simulations in this report. For most of the simulations, a meteorological year representing a normal climatic year was selected, i.e. an actual year with meteorological conditions as close to mean values as possible. Besides the cases with the selected normal year with a temperate climate, simulations with a wet (temperate) climate and a periglacial climate were performed.

For the simulations with the present climate, locally measured data are available for the period between 2003 and 2007. The meteorological input data are taken from two meteorological stations within the SKB site investigations area, the Högmasten and Storskäret stations.

Based on precipitation data from the local meteorological stations, average monthly sums were calculated. The monthly sums were then compared to monthly mean values for the reference period 1961–1990 for the meteorological station Örskär /Larsson-McCann et al. 2002/ and /Johansson 2008/. In the same way, the mean yearly precipitation for the reference period was compared to the accumulated yearly precipitation for each year in the measured data. The year that gave the best fit to mean values was then selected to represent a normal year with regard to precipitation.

The selected year was from October 2003 to September 2004. Table 2-1 shows the monthly mean values for the selected year as well as the monthly average values for the reference period. Figure 2-3 shows the precipitation time series for the selected year and Figure 2-4 shows the potential evapotranspiration for the selected year. For all simulations with a normal climate, the selected year was cycled for the entire calculation period.

For the MIKE SHE simulation with a wet climate, climatic data are based on data for a wet period of 50 years presented in /Kjellström et al. 2009/. The mean annual precipitation for the 50-year period is approximately 1,280 mm. The objective was to find a 3-year period within the 50-year period that included both a very wet year and a year similar to the mean year among the 50 wet years. To find the most representative period, a moving three-year sum was calculated and the maximum three-year sum was found. Since the period with the maximum three-year sum also contains a year with a mean close to the 50-years average, this period was selected.

Table 2-1. Average monthly precipitation (mm) for station Örskär for the reference period 1961–1990 and monthly sums for the selected year, October 2003 – September 2004.

Month	Average monthly sums 1961–1990 (mm)	Monthly precipitation for selected year (mm)
October	53	74
November	61	60
December	50	73
January	44	43
February	33	16
March	29	26
April	35	31
May	27	44
June	39	46
July	71	84
August	66	55
September	61	29
Yearly sum	569	583

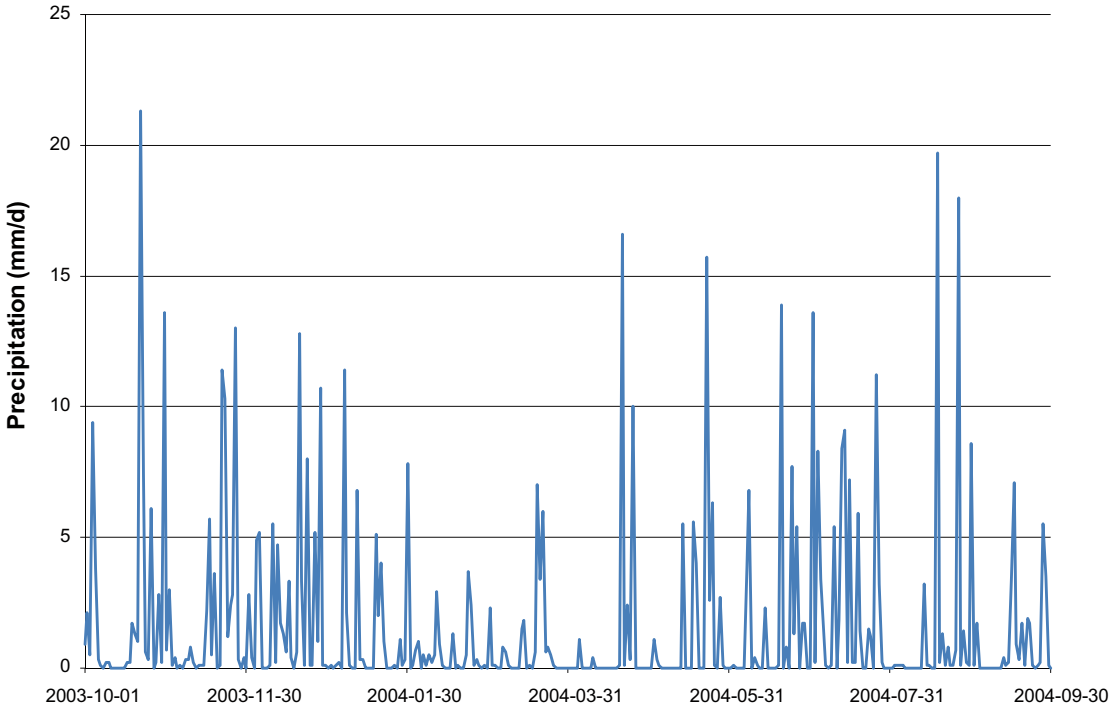

Figure 2-3. *Precipitation during the selected year, October 2003 to September 2004.*

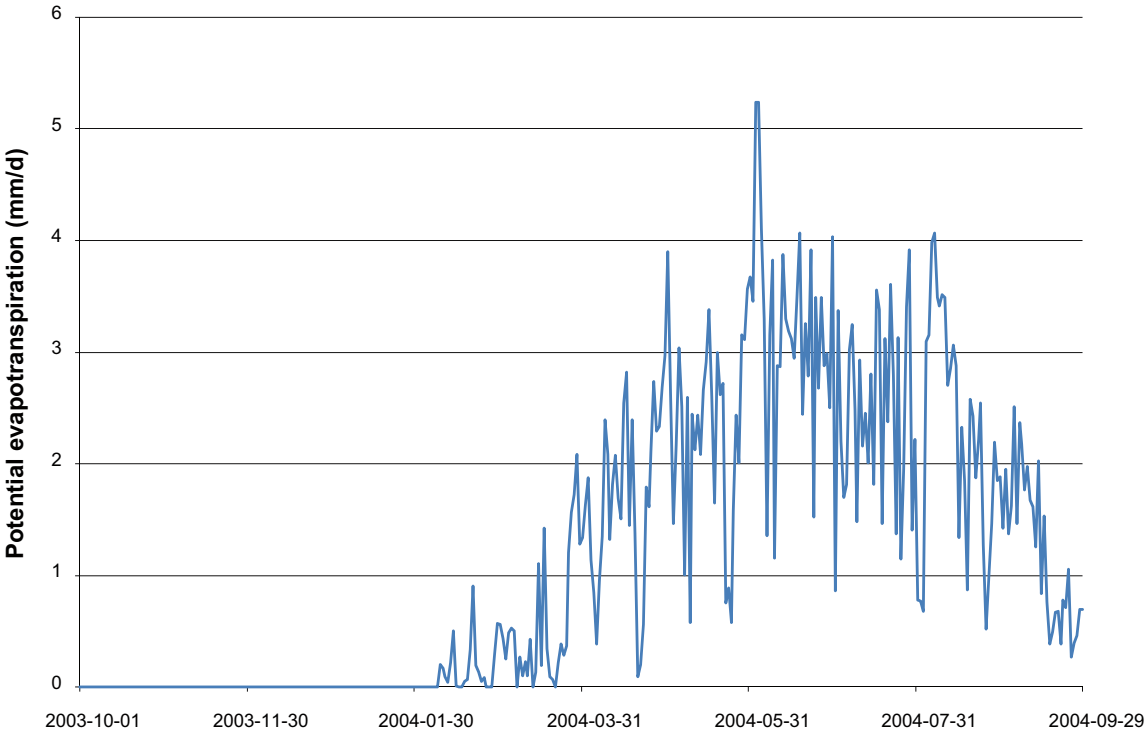

Figure 2-4. *Potential evapotranspiration for the selected year, October 2003 to September 2004. The original values were reduced by 15% in accordance with results from /Bosson et al. 2008/.*

Figure 2-5 shows the precipitation time series for the selected period (blue line). The total accumulated precipitation for the period is approximately 4,390 mm, which gives a mean annual precipitation of 1,463 mm. The second year has an annual precipitation of 1,218 mm. Figure 2-6 shows the potential evapotranspiration for the three-year period.

In the same way as for the wet year, climatic data were obtained from /Kjellström et al. 2009/ for the simulation with a periglacial climate. The data is based on results from 50 years of simulation of a cold climate.

The average yearly precipitation was calculated for the entire 50-year period. Furthermore, the average monthly precipitation during the 50 years was calculated. For each year in the period, the monthly mean values were compared to the 50-year average values and in the same way the yearly mean values were compared to the 50-years average value. Based on this comparison, the year with values most similar to the average values was selected. The selected year was then cycled for the entire length of the permafrost simulations.

Figure 2-7 shows the precipitation for the selected permafrost year. The yearly precipitation is 411 mm. Figure 2-8 shows the corresponding potential evapotranspiration (PET) during the permafrost year, and Figure 2-9 shows the temperature during the selected year. The annual PET was calculated to 216 mm. The model used for calculations of the PET overestimates the PET, especially during periods of cold temperatures. To avoid numerical instabilities due to a too high PET, which would result in a too high actual evapotranspiration, the PET was reduced by a factor of 4. The reduced PET is shown in Figure 2-8.

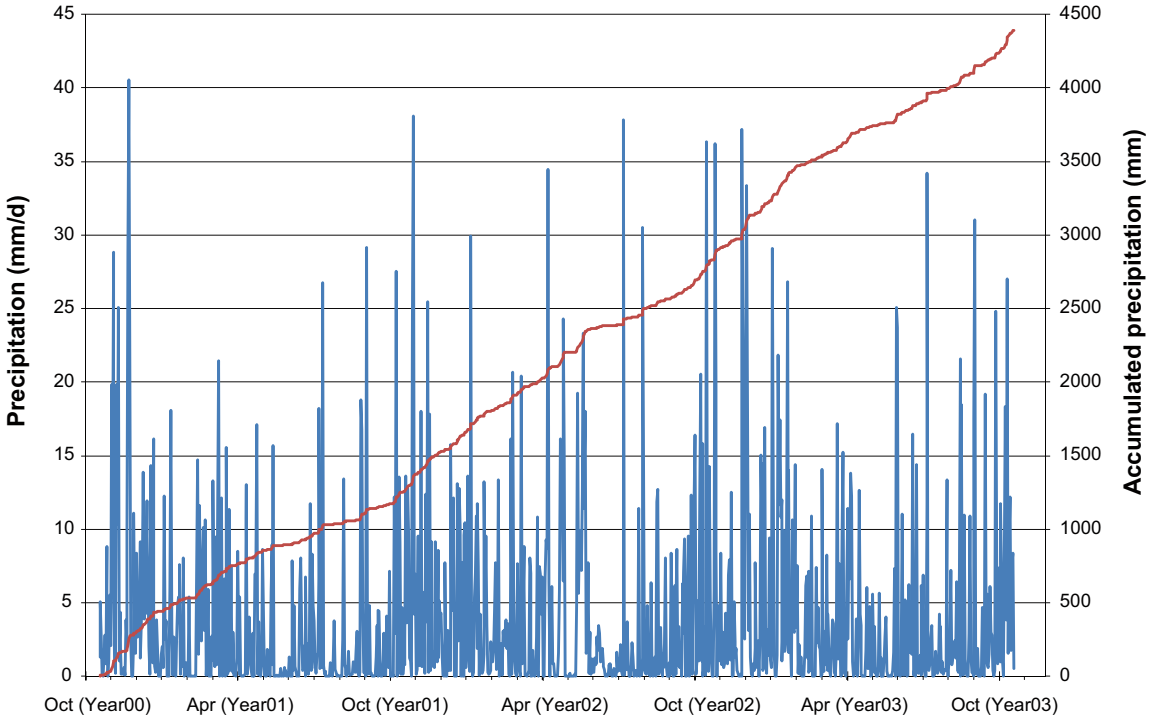

Figure 2-5. *Precipitation (blue line) and accumulated precipitation (red line) for the selected three years used in the wet climate calculations.*

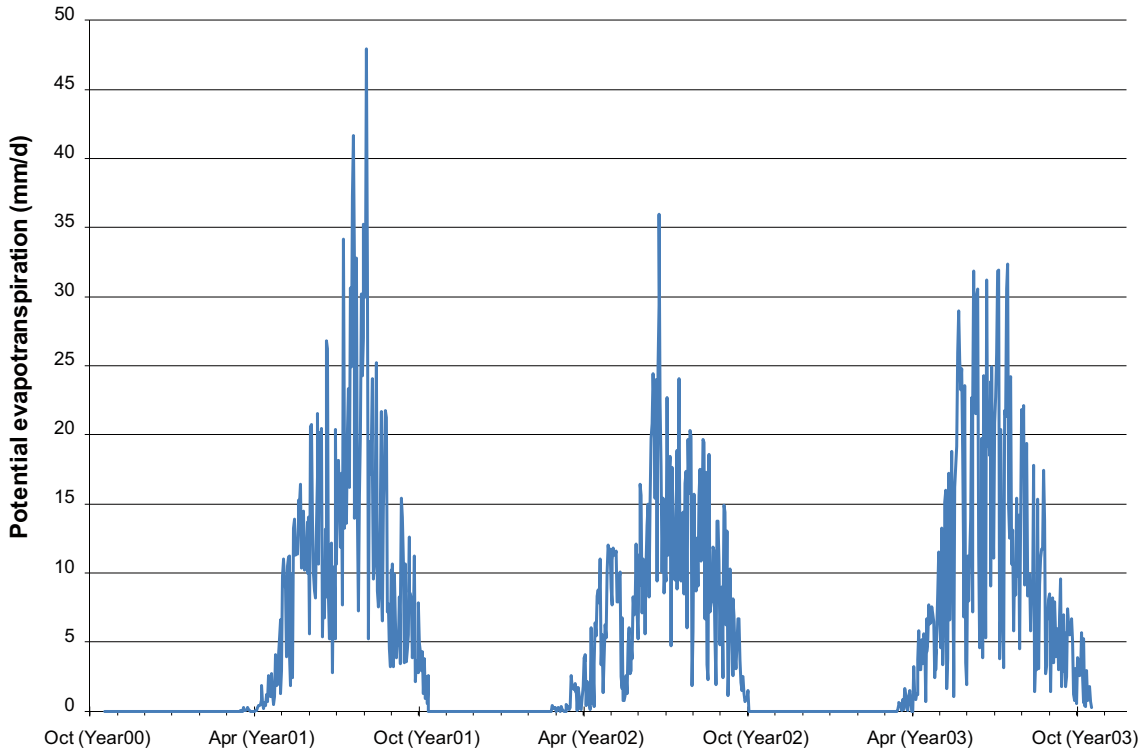

Figure 2-6. *Potential evapotranspiration for the three years considered in the wet climate calculations.*

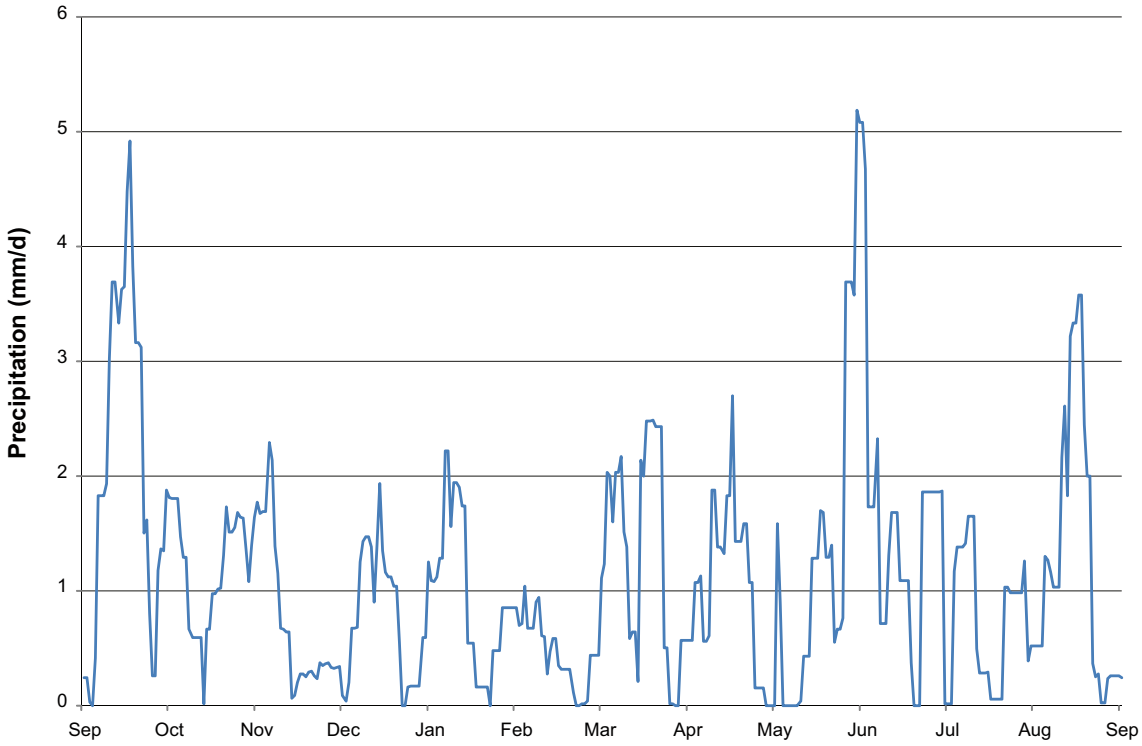

Figure 2-7. *Precipitation for the selected year for the permafrost climate simulations.*

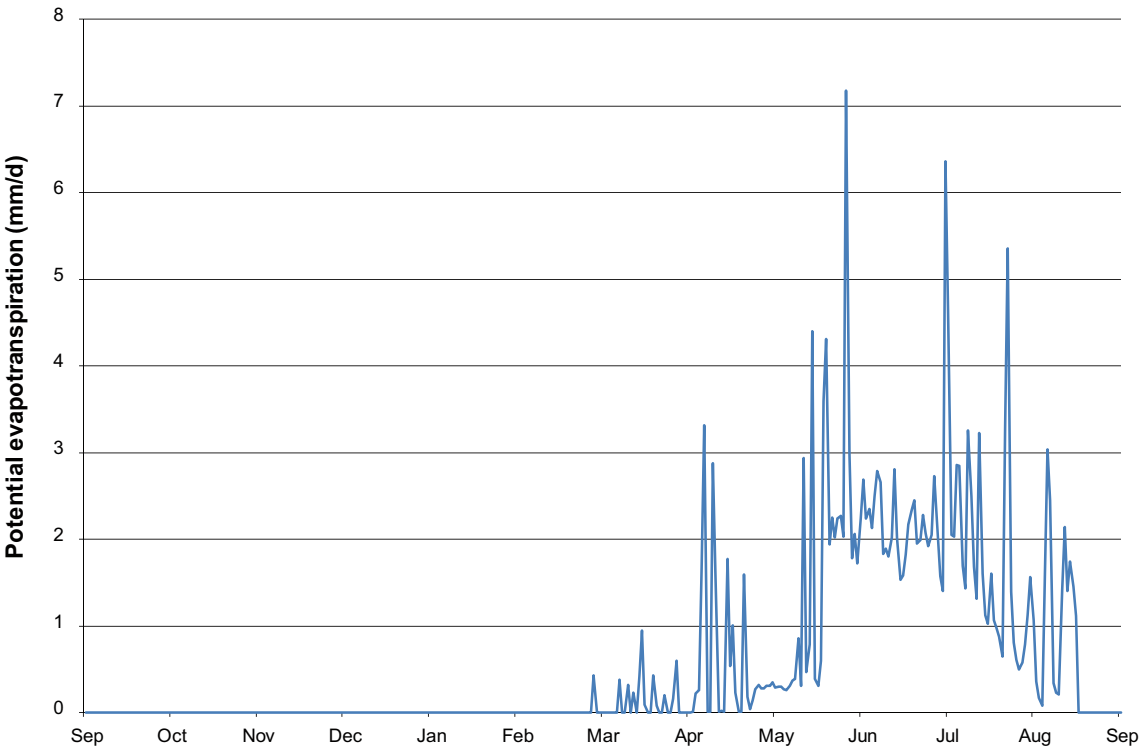

Figure 2-8. *Potential evapotranspiration for the selected year for the permafrost climate simulations.*

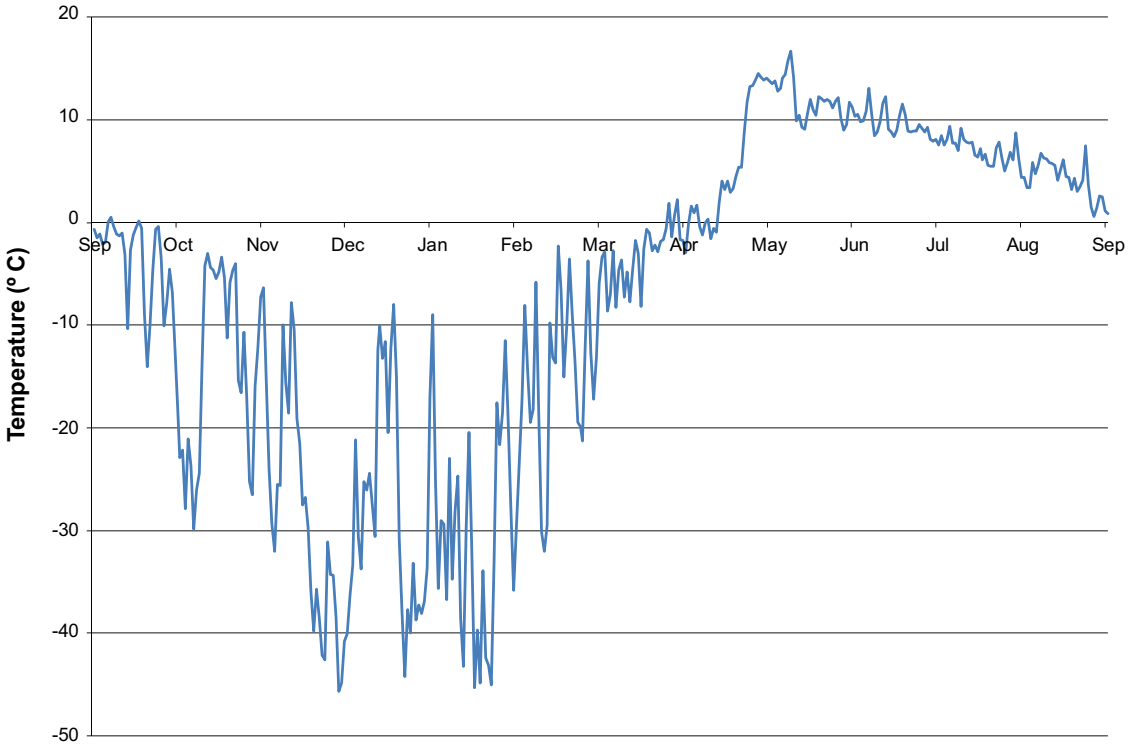

Figure 2-9. *Temperature for the selected year for the permafrost climate simulations.*

2.4 Quaternary deposits

The shoreline displacement is crucial when simulating future hydrological conditions. Today the land rises with approximately 6 mm per year in the Forsmark area /Hedenström and Risberg 2003/. The shore-line displacement as described in /Brydsten and Strömgren 2010/ has been applied to the hydrological models. Three different shoreline positions have been studied, i.e. those that according to the model represent 2000 AD, 5000 AD and 10,000 AD. The corresponding shorelines are placed at –0.17 m.a.s.l., –14.96 m.a.s.l. and –31.42 m.a.s.l. (Figure 2-10). For a detailed description of the development of the QD model the reader is referred to /Brydsten and Strömgren 2010/.

Within the hydrological modelling no time period when the shoreline is above the present shoreline has been studied; all the studied time periods have sea levels below the present one. The shoreline displacement causes a development of the landscape in the area. In particular, it influences the development of lakes and wetlands, the vegetation cover and the QD in the area. Three different QD models have been applied to the MIKE SHE model, describing the QD layers at 2000 AD, 5000 AD and 10,000 AD.

2.4.1 Model for present conditions

Geological model

The geological model of the Quaternary deposits is developed using the modelling tool MIKE Geomodel /DHI Software 2007/. The conceptual model is presented in Figure 2-11. The model consists of nine units referred to as layers. The model is geometrical and presents the total regolith depth and the bedrock topography. The conceptual model for the construction of the different layers is based on knowledge from the site as well as on general geological knowledge on similar formations. The layers are denoted Z1–Z6 and L1–L3. All layers may have zero thickness in parts of the model area. The lower level of each layer is specified and the layers are used as direct input to the MIKE SHE model. Each layer in the geological model of the Quaternary deposits represents a geological layer in MIKE SHE.

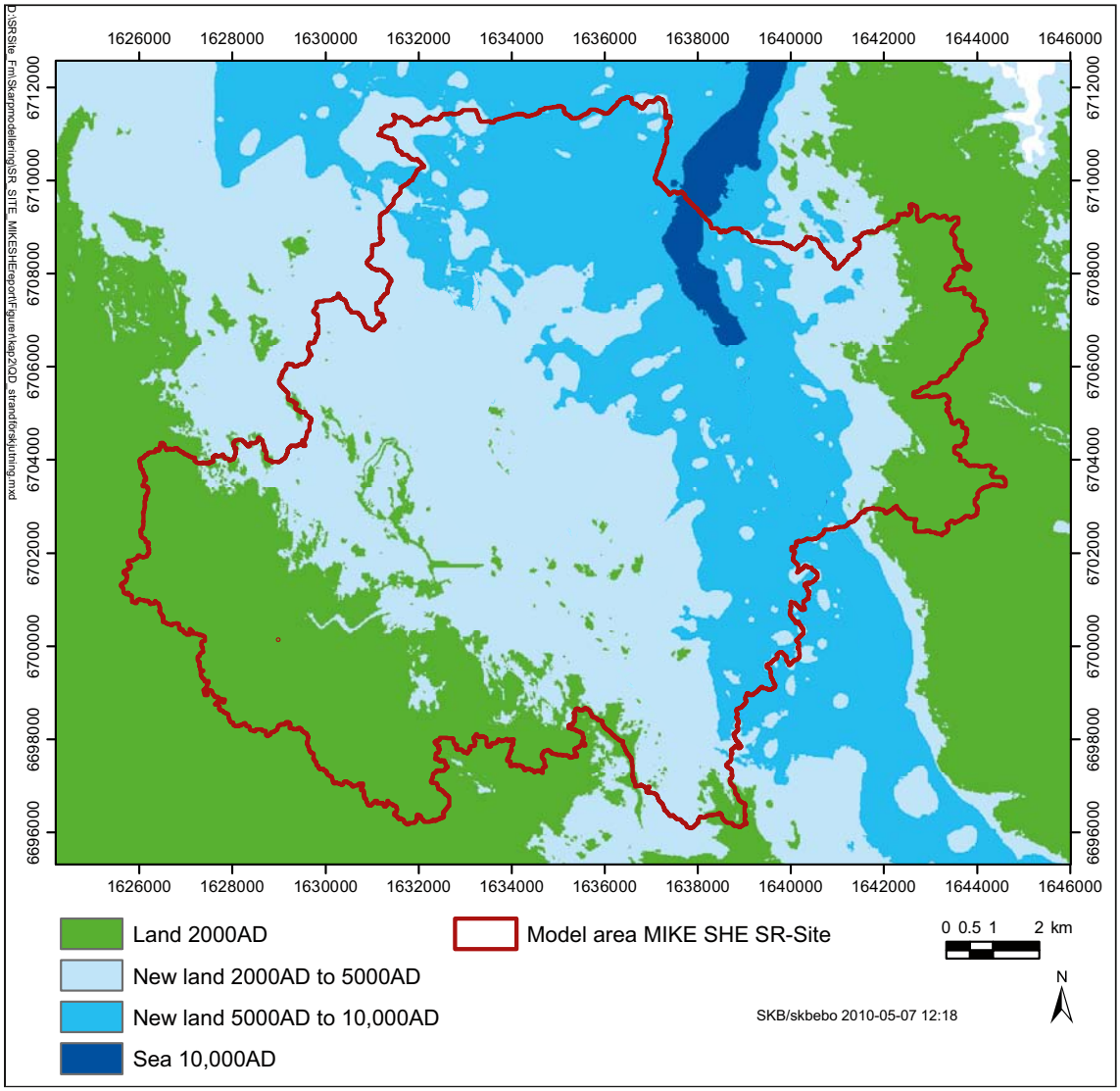

Figur 2-10. *The shoreline positions at 2000 AD, 5000 AD and 10,000 AD in the Forsmark area.*

The model presents the geometry of the lower level of each layer in terms of elevation above sea level (RHB70). The model has a spatial resolution of 20×20 m^2. The lower level of Z5 is interpolated from the dataset of information on the total depth of the Quaternary deposits, as well as the bedrock outcrops. Thus, the lower level of Z5 represents the bedrock surface regardless of whether it is covered by deposits or not. The bottom layer, Z6, is characterised by fractured bedrock. This layer is included in the model because a high-conductive layer has been recorded in the contact zone between bedrock and QD, see e.g. /Werner and Johansson 2003/, which implies that it may be of interest to vary the properties of this layer in the flow modelling. The geometrical-geological model of the QD is described in detail in /Hedenström et al. 2008/. Each layer consists of one or several types of Quaternary deposits; the layers are described in Table 2-2. The layers L1–L3 describe the extension of the lake sediments.

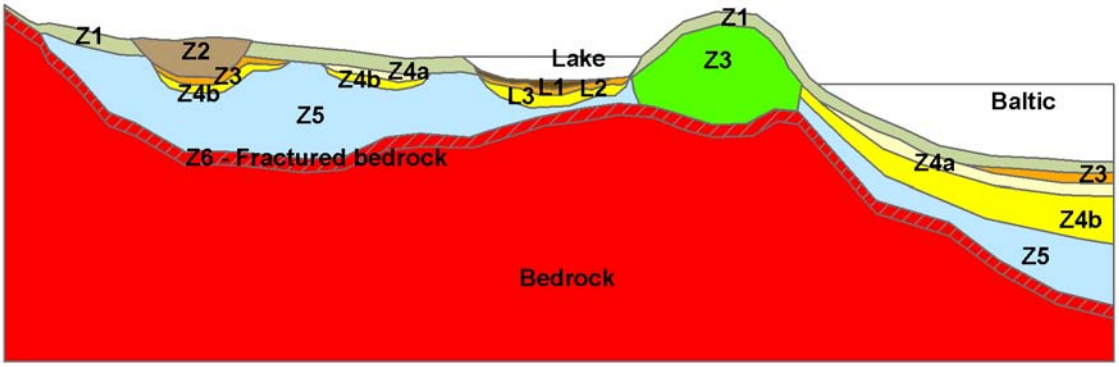

Figure 2-11. *Conceptual model of the QD geometry.*

Table 2-2. Deposits, simplified codes and occurrence for the nine layers.

Description of layer	Simplified code	Description/Occurrence
Gyttja (algal gyttja, calcareous gyttja, clay gyttja-gyttja clay)	L1	When peat is present as surface layer in the vicinity of a lake area, this is included in the L1 layer.
Postglacial sand and/or gravel	L2	
Clay (glacial and postglacial)	L3	
Surface layer	Z1	The layer is affected by soil forming processes and is present within the entire modelled area, except where the surface is covered by peat or where the model has a lens (under lakes). The layer is 0.1 m on bedrock outcrops and 0.6 m in other areas. If the total modelled regolith depth is less than 0.6 m, Z1 will be the only layer. The layer can be connected to the map of Quaternary deposits and assigned properties in accordance to the properties of the deposits.
Peat	Z2	This layer is only present where peat is presented on the QD map.
Postglacial sand/gravel, glaciofluvial sediment and artificial fill	Z3	The layer is only present where the surface layer consists of postglacial sand/gravel, glaciofluvial sediment or artificial fill.
Postglacial clay	Z4a	
Glacial clay	Z4b	
Till	Z5	This layer is present in a major part of the model area. The lower limit of Z5 represents the bedrock surface, i.e. Z5 represents a Digital Elevation Model for the bedrock surface.
Fractured bedrock	Z6	This layer has a constant depth of 0.5 m and represents the upper part of the bedrock, calculated from the interpolated Z5. The layer represents a highly hydraulically conductive zone that has been observed in many of the hydraulic tests in Forsmark.

Hydrogeological data for the saturated zone

Hydraulic properties were assigned to each layer in the geological model according to the parameterisation of the final model of the SDM-Site MIKE SHE model /Bosson et al. 2008/. The values are based on site data and knowledge from the calibration process of the SDM-Site MIKE SHE model. Table 2-3 presents the setup of hydraulic properties in the MIKE SHE model. The spatial distribution of the QD in Z1 is presented in Figure 2-12. The map has its origin in the QD map of the Forsmark area presented in /Hedenström and Sohlenius 2008/.

The different QD categories in the original map have been lumped together according to their hydraulic properties. All clay areas have been assigned the same hydraulic properties, “clay” in Table 2-3 below. The QD-types sand and glaciofluvial deposits have also been lumped together and assigned the same properties, cf. “Sand” in Table 2-3. In addition, the areas with artificial fill are lumped into the “Till” category and the post glacial silt has been assigned the same properties as the clayey till in Table 2-3.

Table 2-3. Hydraulic parameters assigned to each layer in the QD model.

Layer	K_h (m/s)	K_v (m/s)	S_y (–)	S_s (m^{-1})
L1, Gyttja	$3 \cdot 10^{-7}$	$3 \cdot 10^{-7}$	0.03	0.006
L1, Peat	$1 \cdot 10^{-6}$	1·10–6	0.2	0.006
L2, Sand/gravel	$1.5 \cdot 10^{-4}$	1.5·10–4	0.2	0.004
L3, Clay	$1.5 \cdot 10^{-8}$	1.5·10–8	0.05	0.006
Z1:				
Till	$1.5 \cdot 10^{-4*}$	$1.5 \cdot 10^{-5}$	0.15	0.001
Gyttja	$3 \cdot 10^{-7*}$	$3 \cdot 10^{-7}$	0.03	0.006
Clay	$5 \cdot 10^{-6*}$	$5 \cdot 10^{-7}$	0.05	0.006
Sand	$7.5 \cdot 10^{-4*}$	$7.5 \cdot 10^{-5}$	0.2	0.004
Peat	$5 \cdot 10^{-6*}$	$5 \cdot 10^{-7}$	0.2	0.02
Bedrock	$1 \cdot 10^{-7*}$	$1 \cdot 10^{-7}$	0.15	0.001
Z2, Peat	$3 \cdot 10^{-7}$	$3 \cdot 10^{-7}$	0.05	0.005
Z3, Glaciofluvial deposit	$1.5 \cdot 10^{-4}$	$1.5 \cdot 10^{-4}$	0.2	0.35
Z4, Clay	$1.5 \cdot 10^{-8}$	$1.5 \cdot 10^{-8}$	0.03	0.006
Z5:				
Fine till	$5 \cdot 10^{-7*}$	$5 \cdot 10^{-8}$	0.03	0.001
Coarse till	$7.5 \cdot 10^{-6*}$	$7.5 \cdot 10^{-7}$	0.05	0.001
Z6	$1.5 \cdot 10^{-6}$	1.5·10–6	0.15	0.001

* K_h is multiplied by 2 in the catchment area of Lake Eckarfjärden.

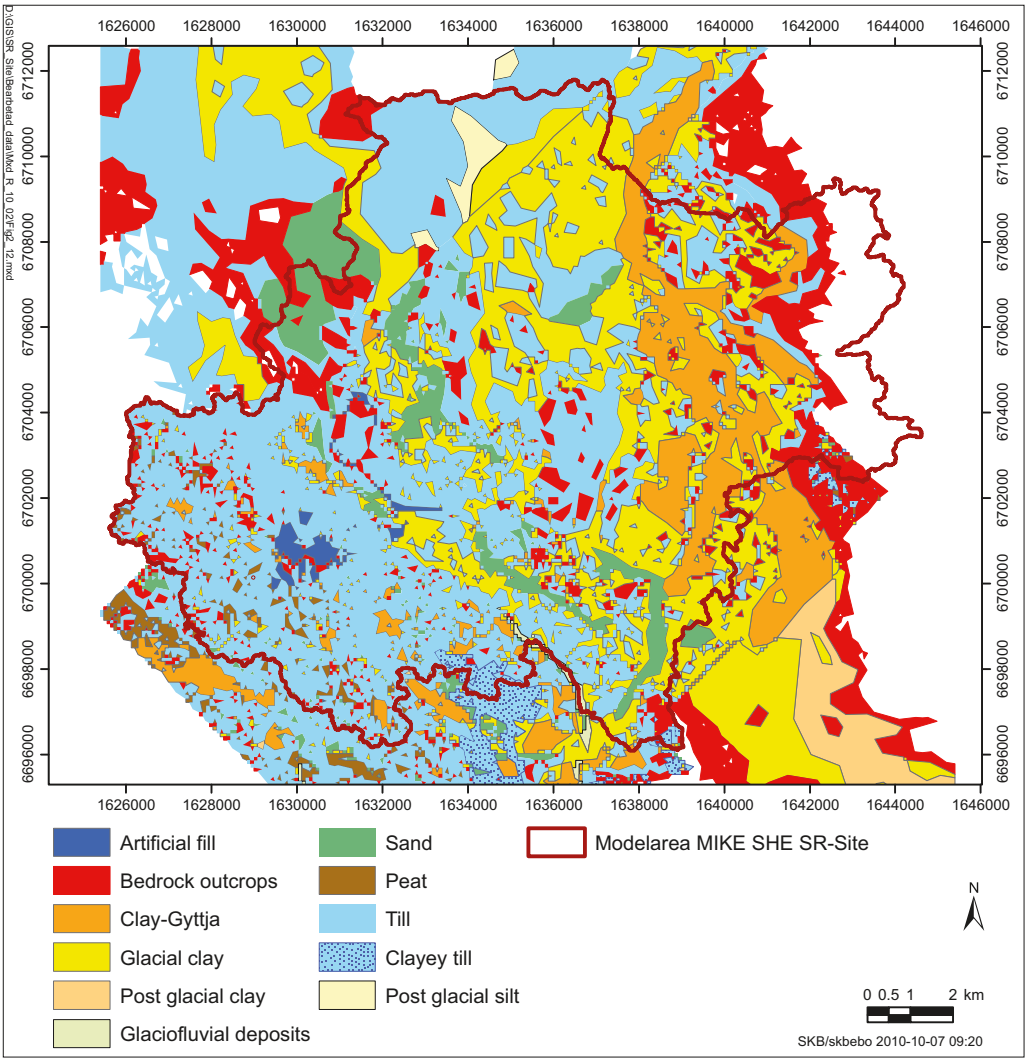

Figure 2-12. Spatial distribution of the QD in layer Z1, the uppermost geological layer of the saturated zone.

Hydrogeological data on the unsaturated zone

The description of the spatial distribution of the QD in the unsaturated zone is more detailed than the description of the QD in the saturated zone. The mapping depth of the QD is 0.5 m. In the QD map /Hedenström and Sohlenius 2008/, there is also information on the surface layer above a depth of 0.5 m. This information has been used as input data for the UZ-calculations in the MIKE SHE model. The QD map used in the unsaturated zone calculations is shown in Figure 2-13. The detailed UZ-description with a spatial distribution of the QD according to Figure 2-13 is used in the upper 30 cm of the unsaturated zone model. For larger depths the information from the spatial distribution of the QD in Figure 2-12 is used. The detailed description of the spatial distribution of the QD in UZ was not implemented in the SDM-Site MIKE SHE model of Forsmark.

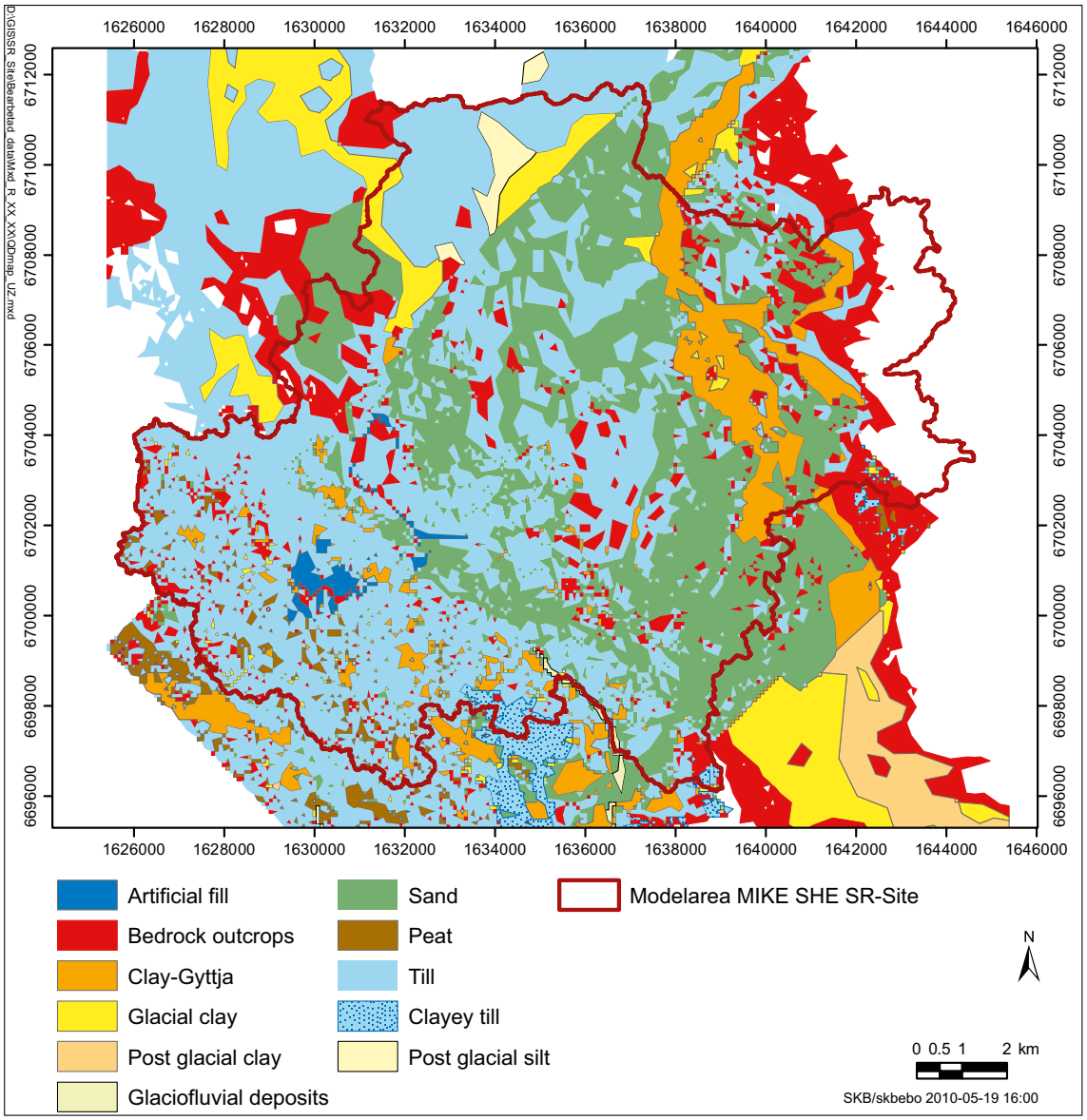

Figure 2-13. *Spatial QD distribution used in the unsaturated zone description.*

2.4.2 Models of future conditions

The QD models describing the geometry of the QD layers at 5000 AD and 10,000 AD have their origin in the QD model describing the present geometry of the QD. The models of the future QD are described in detail in /Brydsten and Strömgren 2010/. The bedrock surface, the till layer Z5 and the lower level of Z4b are the same in all the QD-models. The layers Z1–Z4a are replaced by new layers representing each time period. Also the ground surface topography and the lacustrine and marine sediment layers are adjusted to reflect the modelled landscape development.

Due to time constraints, the final model of the Quaternary development at the site has not been used in the present numerical modelling. In particular, the lake module describing the sedimentation processes within the lakes is not implemented in the hydrological modelling. Thus, the lake development has been handled manually in MIKE SHE in a simplified way: the lakes are either lakes or fully developed wetlands or mires. The lakes that have turned into wetlands at each modelled time step (5000 AD and 10,000 AD) have in the MIKE SHE model been filled with peat up to the level of the lake threshold. The lakes that have turned into mires at 5000 AD and 10,000 AD are marked in Figure 2-14 and Figure 2-15. The two QD models used were delivered on April 23, 2009 (svn_SrSite-Bio_Forsmark/Indata/GIS/Landscape/Delivered_MIKE_SHE_rev_3702, also part of the dataset stored as SKBdoc 1263189).

The spatial distribution of the QD changes when the land is rising. The QD maps representing the spatial distributions of the QD at 5000 AD and 10,000 AD (Layer Z1) was divided into the following groups: postglacial clay, glacial clay, thin postglacial clay, till, other deposits, and bedrock. The QD map for 5000 AD is shown in Figure 2-14 and the QD-map for 10,000 AD in Figure 2-15. As seen, the difference between the two time periods is very small. The same hydraulic properties for each QD-type as in the 2000 AD model have been assigned to the 5000 AD and 10,000 AD models.

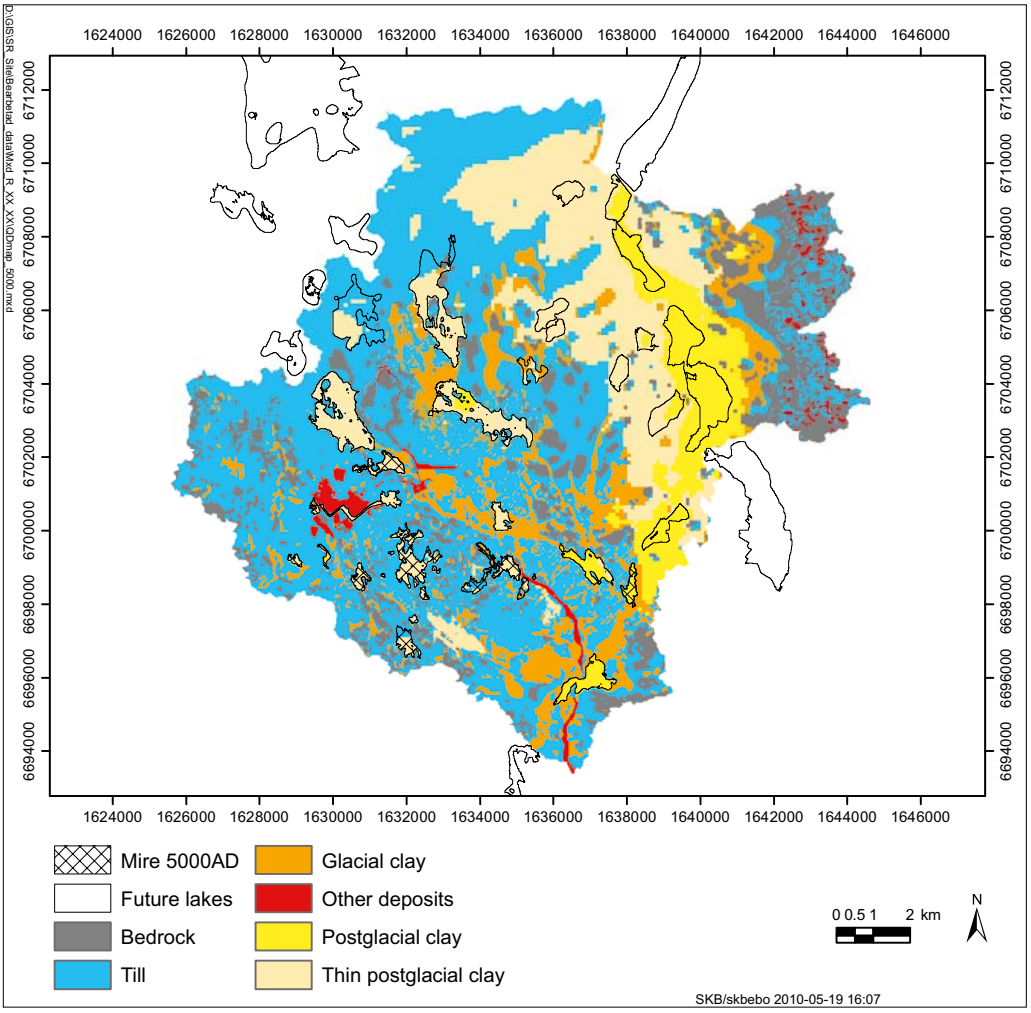

Figure 2-14. QD map representing the spatial distribution in the year 5000 AD.

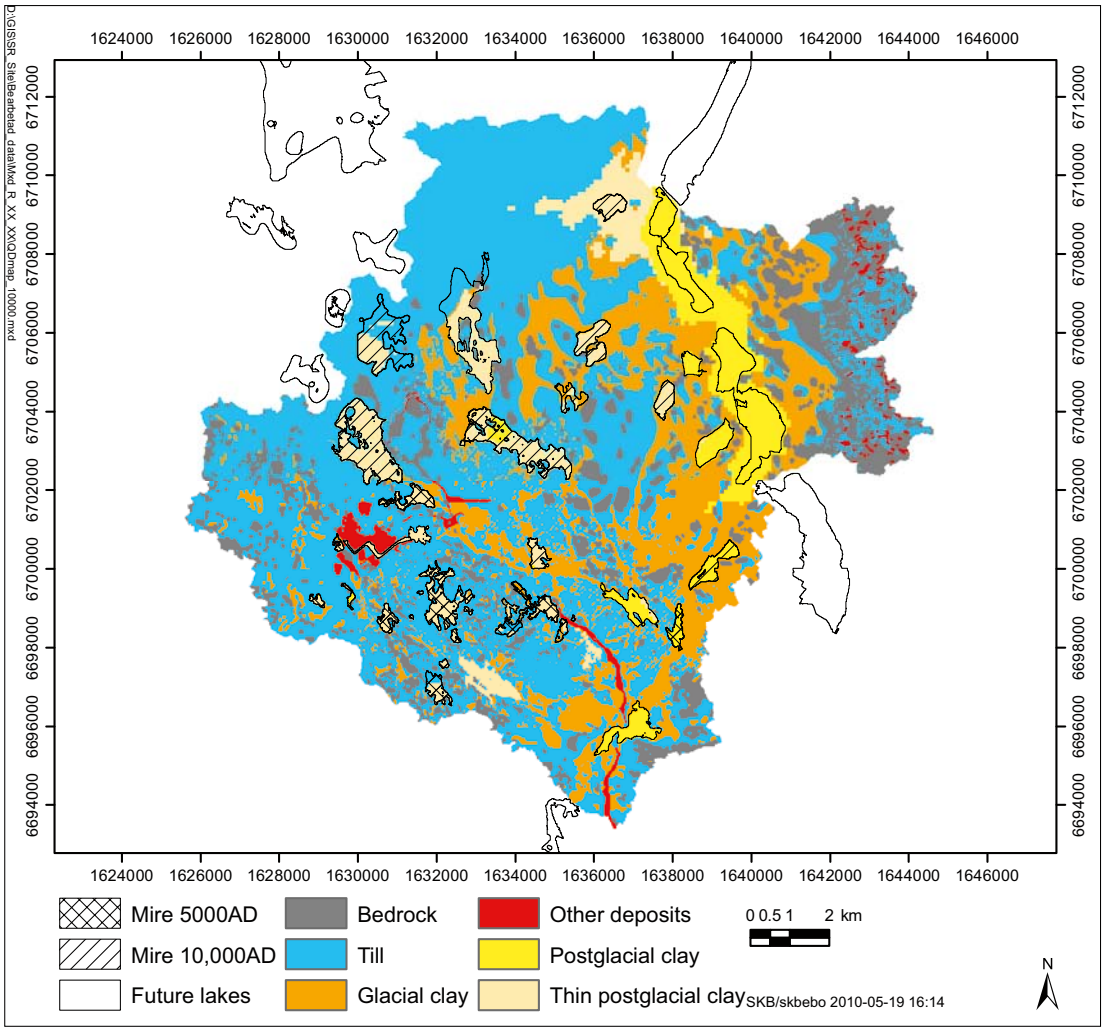

Figure 2-15. *QD-map representing the spatial distribution 10,000 AD .*

2.5 Bedrock hydrogeology

Input to the geological description of the bedrock is obtained from the ConnectFlow groundwater flow model /Joyce et al. 2010/. The horizontal and vertical resolutions of the data on the hydraulic conductivity, specific storage and porosity of the bedrock are 80 m (i.e. the grid cells are 80×80×80 m^3). Data representing the properties are introduced to the MIKE SHE model as geological layers every 80 m. The ID-number of the ConnectFlow delivery is:

SRS_HCD2h100A2b_HRD5r1_phi6F_HSD5d_IC3Mat_MD2_MOW_mikeshe

The upper c. 200 m of the bedrock are highly fractured and water conductive. Horizontal sheet joints are present in the upper bedrock and are interconnected hydraulically. According to hydraulic tests performed in percussion-drilled boreholes, the horizontal hydraulic conductivity of the fractures/ sheet joints in the upper rock is very high, and the groundwater flow in the areas is dominated by the horizontal component. Figures 2-16 and 2-17 show the horizontal and vertical hydraulic conductivities at 40 m.b.s.l., respectively.

There is a distinct difference in the conductivity fields between the horizontal and vertical conductivities, which is that the sheet joints dominate the pattern of the horizontal conductivity in Figure 2-16. In general the hydraulic conductivities of the non-fractured bedrock are in the range 10^{-10} to 10^{-8} m/s, whereas the hydraulic conductivities of the fractured parts vary from 10^{-6} to 10^{-4} m/s.

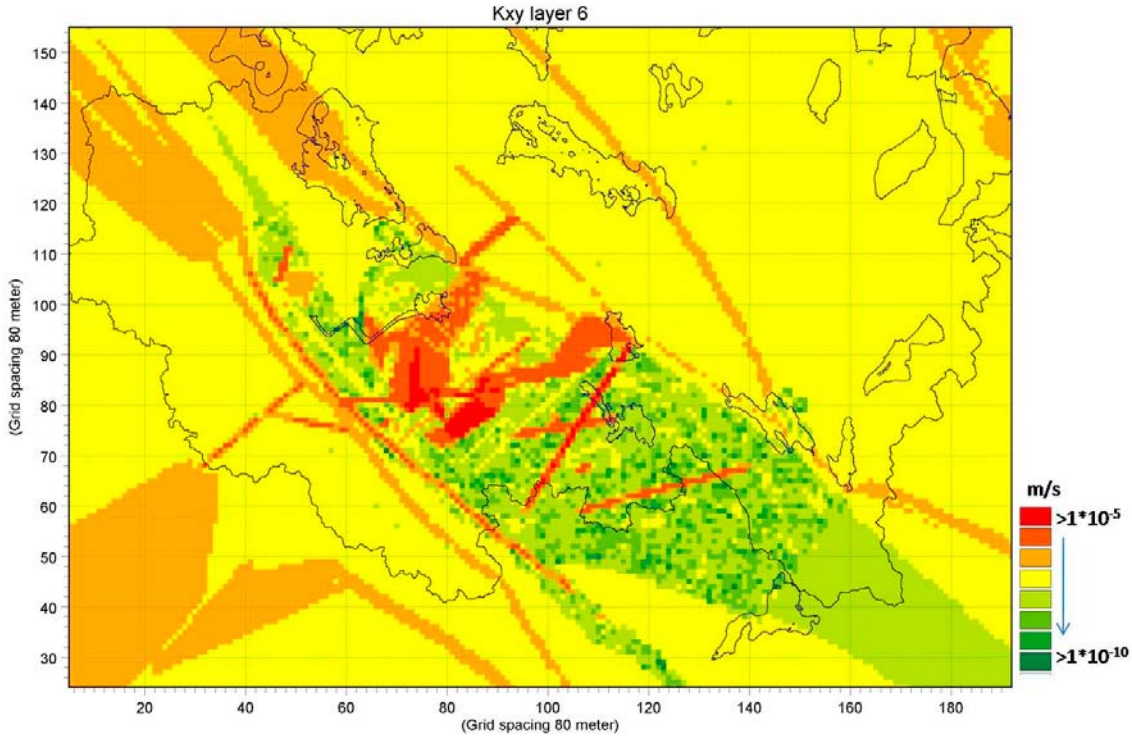

Figure 2-16. *Horizontal hydraulic conductivity at approximately 40 m.b.s.l.*

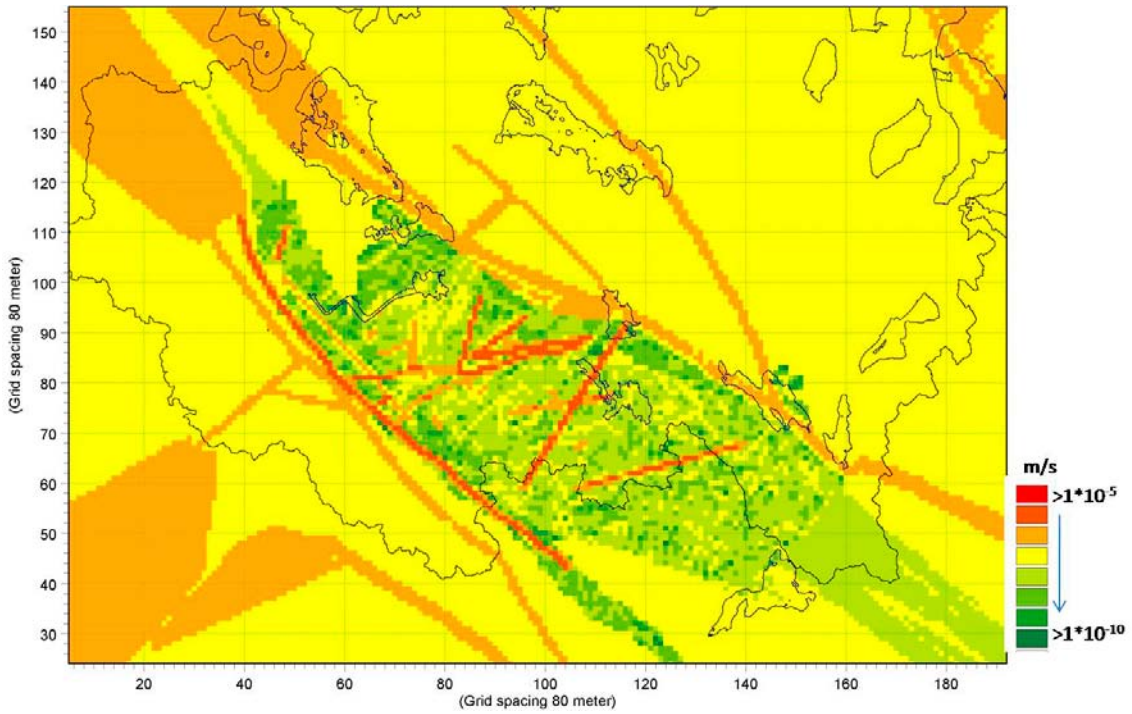

Figure 2-17. *Vertical hydraulic conductivity at approximately 40 m.b.s.l.*

2.6 Stream and lake data

Data on lake threshold levels and bathymetries from the Forsmark area have been used as input to the geometric and hydraulic description of the surface water system (the lakes and the water courses) in the surface water component of MIKE SHE (MIKE 11, see Section 3.1.1). A description of the surface water models is given in Chapter 4. The corresponding model reported in /Bosson et al. 2008/ was used as a basis for the SR-Site models developed for the different QD models and simulated time periods described in Section 4.1.2. Figure 2-18 shows the water courses described in the surface water model and points where bottom elevations and cross sections of the water courses have been measured.

2.6.1 Model for present conditions

Cross sections and bottom elevations have been measured every ten meters along the water courses. The X- and Y-coordinates of the stretches of the water courses, data on the cross sections and data on the lake thresholds, see /Brydsten and Strömgren 2004/, are used in the surface water model. Figure 2-19 shows an example of a cross section in the water course downstream Lake Eckarfjärden. The lake thresholds used as input data to the surface water model are also marked in Figure 2-18. Table 2-4 shows data on the lake thresholds marked in Figure 2-18.

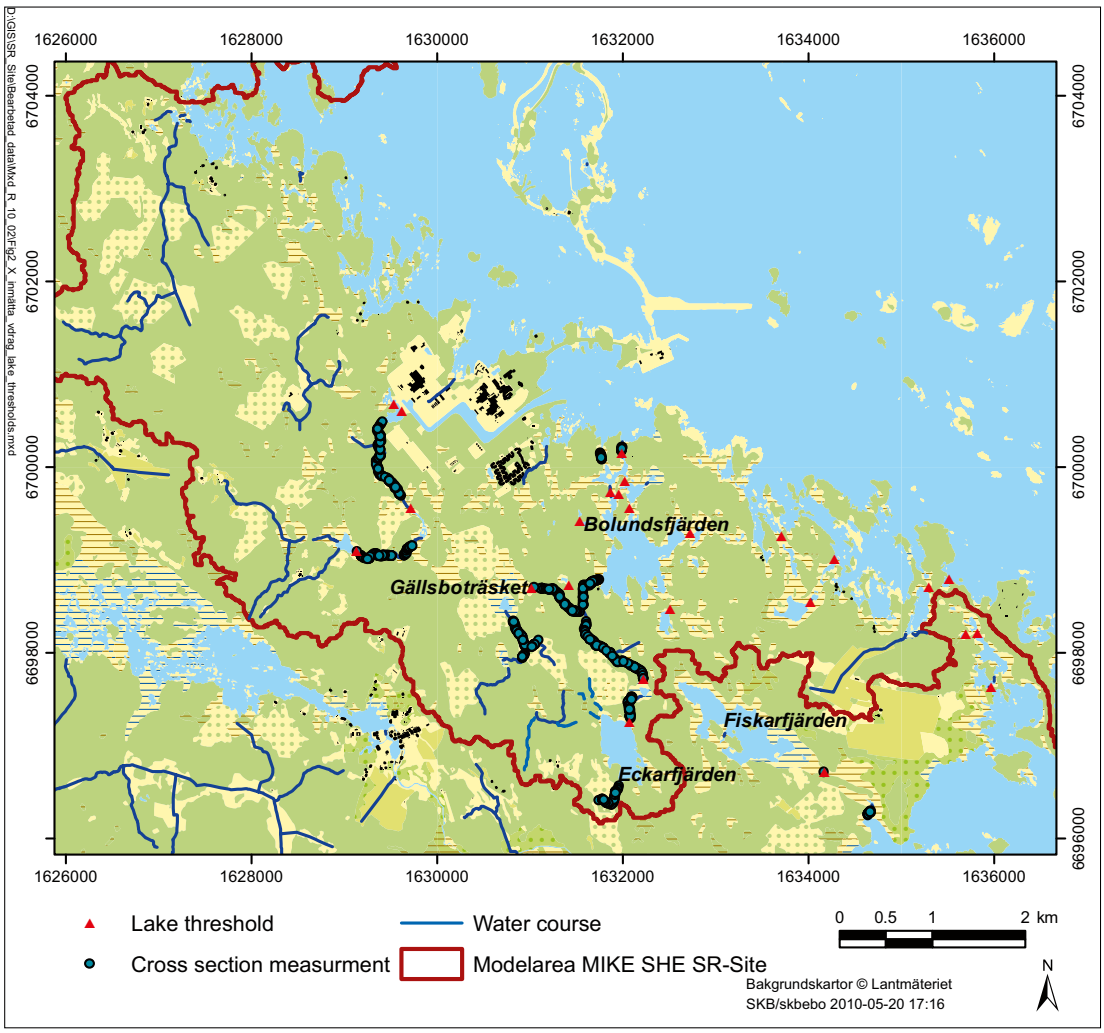

Figure 2-18. Field controlled water courses, measured cross sections in water courses and measured lake thresholds used in the surface water modelling. The red line indicates the boundary of the regional MIKE SHE model area.

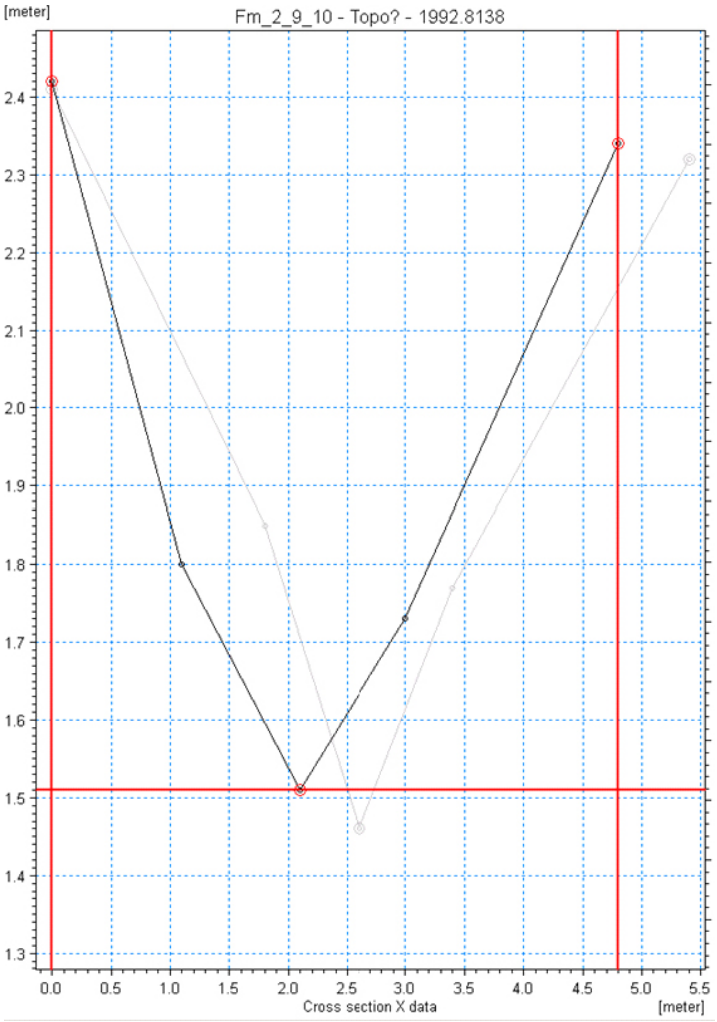

Figure 2-19. *Example of a cross section (black line) along the water course downstream Lake Eckarfjärden. The grey line indicates the cross section 10 m downstream the one marked by the black line.*

Table 2-4. Data on lake thresholds in the area.

ID code	Name	Threshold level (m.a.s.l.)
AFM000010	Eckarfjärden	5.15
AFM000048	Labbotträsket	2.65
AFM000049	Lillfjärden	–0.35
AFM000050	Bolundsfjärden	0.28
AFM000051	Fiskarfjärden	0.28
AFM000052	Bredviken	–0.26
AFM000073	Gunnarsbo – Lillfjärden (south)	1.92
AFM000074	Norra Bassängen	0.19
AFM000081	Märrbadet	–0.29
AFM000084	Simpviken	–0.32
AFM000086	Tallsundet	–0.23
AFM000087	Graven	0.44
AFM000089	Vambörsfjärden	1.02
AFM000090	Stocksjön	2.70
AFM000091	Puttan	0.48
AFM000093	Kungsträsket	2.31
AFM000094	Gällsboträsket	1.47
AFM000095	Gunnarsboträsket	5.68
AFM000096	Gunnarsbo – Lillfjärden (north)	1.07

The parameter describing the bed resistance in the water courses, i.e. the Manning number, has not been changed since the previous version of the model reported in /Bosson et al. 2008/. Thus, the Manning number is 10 $m^{1/3}s^{-1}$ in the whole model area, except from the branch downstream Lake Eckarfjärden where a value of 3 $m^{1/3}s^{-1}$ is used. The leakage coefficient, which affects the conductance used in the calculation of the water exchange between the stream network and the saturated groundwater zone in the model, is also the same as in the previous model; the value is set to 10^{-5} s^{-1}. This means that the leakage coefficient is not limiting the contact between the groundwater and the surface water.

2.6.2 Models for future conditions

The locations of the streams at 5000 AD and 10,000 AD were modelled in the ArcGIS hydrology extension and presented in /Brydsten and Strömgren 2010/. The locations of the streams are shown in Figure 2-20. The digital elevation model (DEM) including lacustrine and marine sediments for each time period 5000 AD and 10,000 AD is also an important input when building the MIKE 11 surface water models. The bank levels of the streams are defined by the DEM. Since the streams in Forsmark are very small and the widths of the streams are smaller than the resolution of the DEM, the DEM defines the bank level. The major parts of the streams are assumed to have a width of 2 m and a depth of 1 m.

Downstream of the point where the present streams Forsmarksån and Olandsån are connecting to each other all streams have a width of 8 m and a depth of 1 m. Also, all lakes that have turned into mires are assumed to have a small stream running through the wetland. The geometries of these streams are the same as described above.

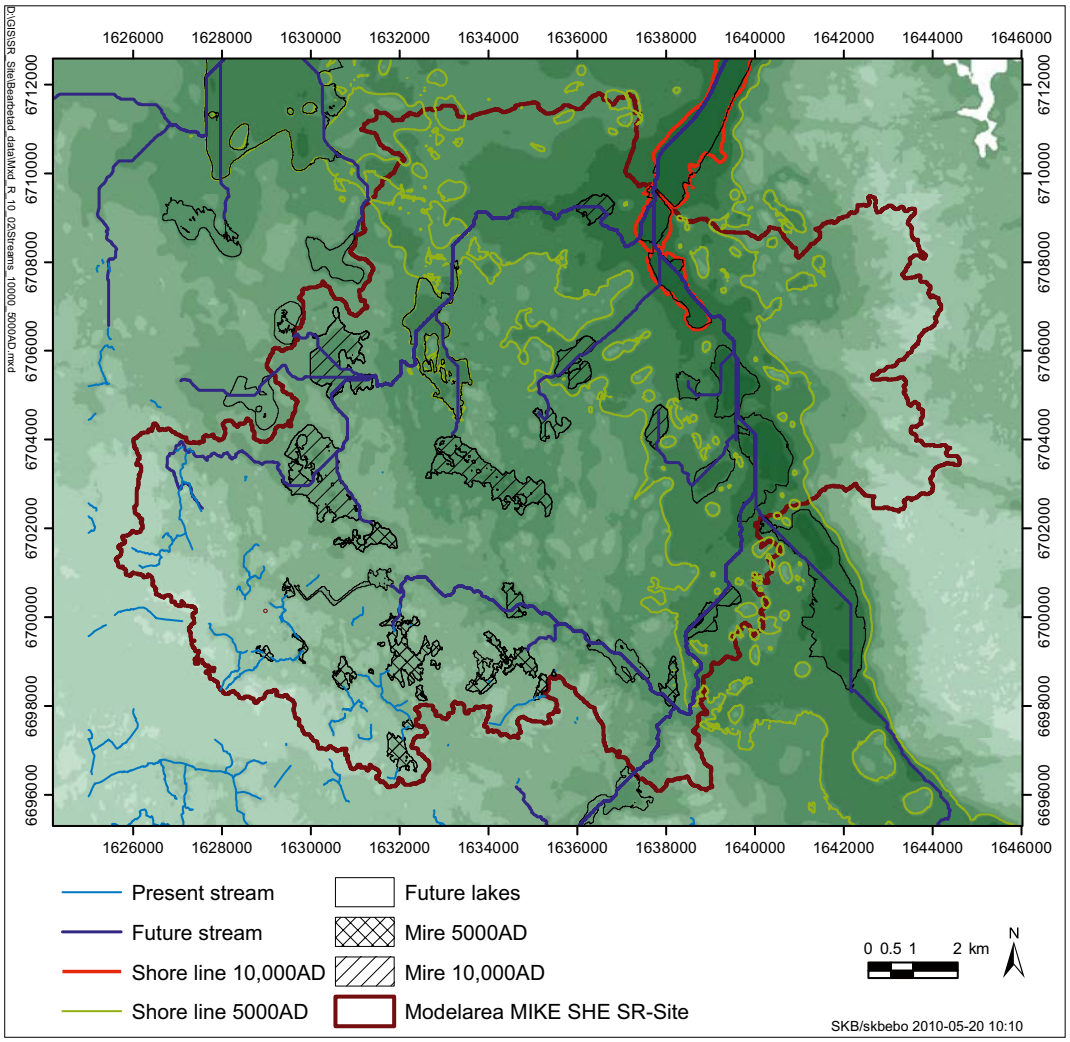

Figure 2-20. *Locations of streams at 5000 AD and 10,000 AD.*

2.7 Vegetation and overland flow parameters

In the hydrological modelling, vegetation parameters are used to specify vegetation input data for the evapotranspiration calculations. The vegetation parameters are time varying vegetation characteristics for each type of vegetation specified in the model domain. Calculations with the overland flow module are required when water courses are modelled using the MIKE 11 surface water model in MIKE SHE (see Section 3.1.1 for a description of the MIKE SHE program compartments). This is because the overland flow module provides lateral runoff to the water courses in MIKE 11.

For present conditions and in all the future models with temperate climate conditions, the same parameters for overland flow and vegetation are used as in the SDM-Site modelling. Therefore, the reader is referred to /Bosson et al. 2008/ for a detailed description of the vegetation and overland flow parameters for present conditions at the Forsmark site. However, the distribution of the vegetation changes when the shoreline displacement and the development of the QD are implemented in the models. This is further described in Section 2.7.1 below. Both the overland flow parameters and the distribution of the vegetation are changed when simulating periglacial conditions. This is further described in Sections 2.7.2 and 4.2. A general description of the different vegetation parameters in the evapotranspiration calculations in MIKE SHE is also found in /Bosson et al. 2008/.

2.7.1 Temperate conditions

The future distributions of Quaternary deposits described in Section 2.4.2, described in more detail in /Brydsten and Strömgren 2010/, provide the basis for the modelling of future vegetation in the Forsmark area. The spatial distribution of the present vegetation has been compared to the present QD-map. The dominating vegetation on each QD-category has been identified and the vegetation representing each QD-category is listed in Table 2-5. It is assumed that the vegetation type dominating a QD-category at present will also be the dominating vegetation on that specific QD-category in the future. The future QD-categories and the corresponding vegetation types are listed in Table 2-6.

The exception to this is found in the assignment of arable land to the categories of postglacial clay and glacial clay. These QD categories are associated to former lake or deep marine bottoms. It is assumed that these are used as arable land in the future if they are deep, which means that there is an overestimation of the future arable land compared to how the present land use is manifested in the distribution of vegetation type on these two QD categories (Table 2-5). A detailed description of the vegetation prevailing under different climate conditions is found in /Löfgren 2010/. The future vegetation types were assigned values of the leaf area index (LAI) and the root zone depth in accordance with the description in /Bosson et al. 2008/.

Table 2-5. The present distribution of vegetation types on different QD. Figures are in percent and are derived from the QD map /Hedenström and Sohlenius 2008/ and the vegetation map /Löfgren 2010/.

QD map Forsmark	Needle-leaved forest	Dry pine forest	Mixed-deciduous forest	Poor regrowth	Forest wetland	Open wetland	Arable land	Other open land
Peat	29	0	11	1	19	34	2	5
Gyttja	23	2	3	0	8	65	0	1
Clay gyttja	10	0	5	0	8	58	13	4
Post-glacial sand	38	0	17	1	8	22	3	12
Post-glacial gravel	68	2	8	4	0	6	5	8
Glacial clay	38	0	11	0	3	12	21	14
Fluvial sediment	72	1	12	0	3	8	0	3
Till	75	2	11	3	1	4	1	4
Clayey till	42	0	10	0	1	5	29	13
Bedrock	63	21	8	3	1	1	1	4

Table 2-6. The future QD and the corresponding vegetation types on the map of the future vegetation.

Future QD	Resulting vegetation type
Post glacial clay	Arable land
Glacial clay	Arable land
Thin postglacial clay	Wetland
Till	Needle-leaved forest
Bedrock	Scots pine-dominated forest

2.7.2 Periglacial conditions

Under periglacial conditions the same QD-model was used as for the future model representing the distribution of the QD at 10,000AD for temperate conditions, and the resulting vegetation types assigned to these are presented in Table 2-7. No agricultural land was assumed to be present under these conditions. The LAI values are presented in Table 2-8 and the root zone depth values in Table 2-9.

Table 2-7. The vegetation found on different Quaternary deposits under periglacial conditions.

Future QD	Resulting vegetation type	Dominating functional groups
Post glacial clay	Wetland	Dominated by sedges and bryophytes
Thin postglacial clay	Wetland	Dominated by sedges and bryophytes
Till	Heathland	Dominated by dwarf shrubs, grasses, bryophytes and lichens
Bedrock	Barrens	No vegetation other than epilitic lichens and some cushion forming forbs

Table 2-8. Parameterisation of leaf area index (LAI) for the different vegetation types in a future landscape under periglacial conditions.

Resulting vegetation type	LAI		Reference
	Maximum	Minimum	
Wetland	0.75	0	/Spadavecchia et al. 2008/
Heathland	0.75	0	/Spadavecchia et al. 2008/
Barrens	0	0	/Spadavecchia et al. 2008/

Table 2-9. Parameterisation of root depth for the different vegetation types in a future landscape under periglacial conditions.

Resulting vegetation type	Root zone depth	Reference
Wetland	30 cm	/Canadell et al. 1996/
Heathland	30 cm	/Canadell et al. 1996/
Barrens	No other vegetation than epilitic lichens and some cushion forming forbs = 0 cm	

2.8 Calibration data

When comparing the performance of the model with the SDM-Site MIKE SHE model, time series of surface water discharges and levels, groundwater levels in the QD and groundwater head elevations in the bedrock were used as calibration data. The monitoring stations providing calibration data to the present modelling are presented in Figure 2-21. A pumping test in HFM14 performed in the summer of 2006 was an important input to the calibration of the bedrock model.

Figure 2-21. *Locations of the surface water discharge stations and groundwater monitoring wells used in the calibration of the present model.*

2.9 Transport calculations input data

All the transport calculations performed are based on the calculated flow fields from the MIKE SHE water movement calculations. No additional input data except from the porosity are required. The porosity of the bedrock is described in /Joyce et al. 2010/ and is included in the delivery denoted as:

SRS_HCD2h100A2b_HRD5r1_phi6F_HSD5d_IC3Mat_MD2_MOW_mikeshe

The porosity of the QD is assumed to be the same as the specific yield. The specific yield of each QD layer is listed in Table 2-3 in Section 2.4.1.

One of the aims with the transport calculations performed within this work has been to analyse the water flow paths towards and within specific areas in the landscape. In the hydrogeological modelling /Joyce et al. 2010/ particle tracking has been performed and the water flow paths from the repository towards the ground surface have been calculated. The so-called exit or discharge points, i.e. the areas where the water flow paths from the repository reach the ground surface, have been identified. In the SR-Site landscape modelling, which is described in detail in /Lindborg 2010/, a number of landscape objects have been identified by using the discharge points from the hydrogeological modelling. These objects are referred to as "biosphere objects" in the safety assessment (in this report, they are sometimes called just "objects").

The biosphere objects considered in the present modelling are shown in Figure 2-22. The process of defining the biosphere object is described in detail in /Lindborg 2010/. The biosphere objects, which contain both lake and wetland areas, are the geometrical boundaries for the areas of interest when setting up and evaluating the transport models. In the MIKE SHE transport modelling in the present work, focus has been on biosphere objects 116, 118, 120 and 121_01, since these objects receive many discharge points according to the ConnectFlow modelling described below

In addition to the coordinates of the discharge points at the ground surface, coordinates along the flow paths from canister positions in the repository to the ground surface have also been extracted from the ConnectFlow model results. The coordinates of the flow paths at a selected level (c. 40 m.b.s.l.) have been used as source locations in some of the MIKE SHE transport calculations presented below (e.g. as starting positions of particles in particle tracking simulations).

2.10 Summary of model updates

This section summarises the model updates between the SDM-Site MIKE SHE model and the SR-Site MIKE SHE model describing the Forsmark site at present, Table 2-10. The main changes are the new bedrock model and the enlargement of the model area. Also, the description of the spatial distribution of the uppermost soil layer has been refined compared to the SDM-Site version of the MIKE SHE model.

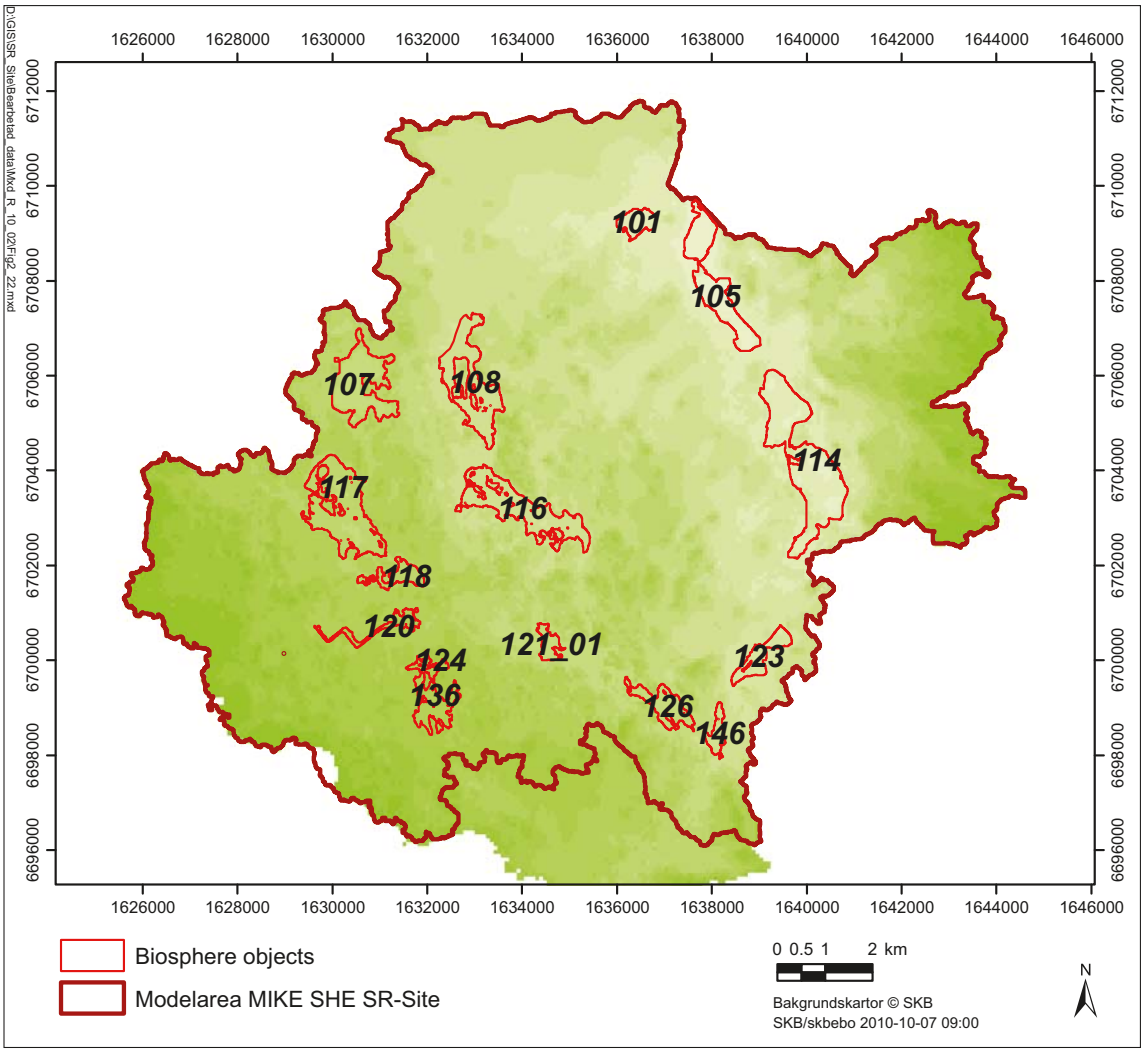

Figure 2-22. Biosphere objects, the MIKE SHE model area is also shown in the figure.

Table 2-10. Summary of model updates from the SDM-Site MIKE SHE model to the regional SR-Site MIKE SHE model.

	SDM-Site	SR-Site
Model area	37 km^2	180 km^2
Horisontal resolution	40 m × 40 m	80 m × 80 m
Vertical extent	600 m.b.s .l	600 m.b.s.l.
Shoreline	2000 AD	2000 AD, 5000 AD, 10,000 AD
Climate	Site data	Site data, modelled data (wet and periglacial conditions)
QD-map, unsaturated zone	Same as saturated zone, Z1	Detailed description of soil layers, upper 0.3 m.
Bedrock model	SDM23_HCD2h100A2b_ HRD5r1_phi4F_HSD5d_ IC3Mat_MD2_MOW18	SRS_HCD2h100A2b_HRD5r1_phi6F_HSD5d_IC3Mat_ MD2_MOW_mikeshe

3 Modelling tool and methodology

3.1 The MIKE SHE modelling tool

The modelling tool used in the present analysis is MIKE SHE. MIKE SHE is a dynamic, physically based modelling tool that describes the main processes in the land phase of the hydrological cycle. The code used in this project is software release version 2009 /DHI Software 2009/.

3.1.1 Water movement

In the model, the precipitation can either be intercepted by leaves or fall to the ground. The water on the ground surface can infiltrate, evaporate or form overland flow. Once the water has infiltrated the soil, it enters the unsaturated zone. In the unsaturated zone, it can either be extracted by roots and leave the system as transpiration, or it can percolate down to the saturated zone. The water can also be extracted by roots in the saturated zone if the vegetation is classified as hydrophilic. MIKE SHE is fully integrated with a channel-flow code, MIKE 11. The exchange of water between the two modelling tools takes place during the whole simulation, i.e. the two programs run simultaneously. The modelled processes are summarised in Figure 3-1.

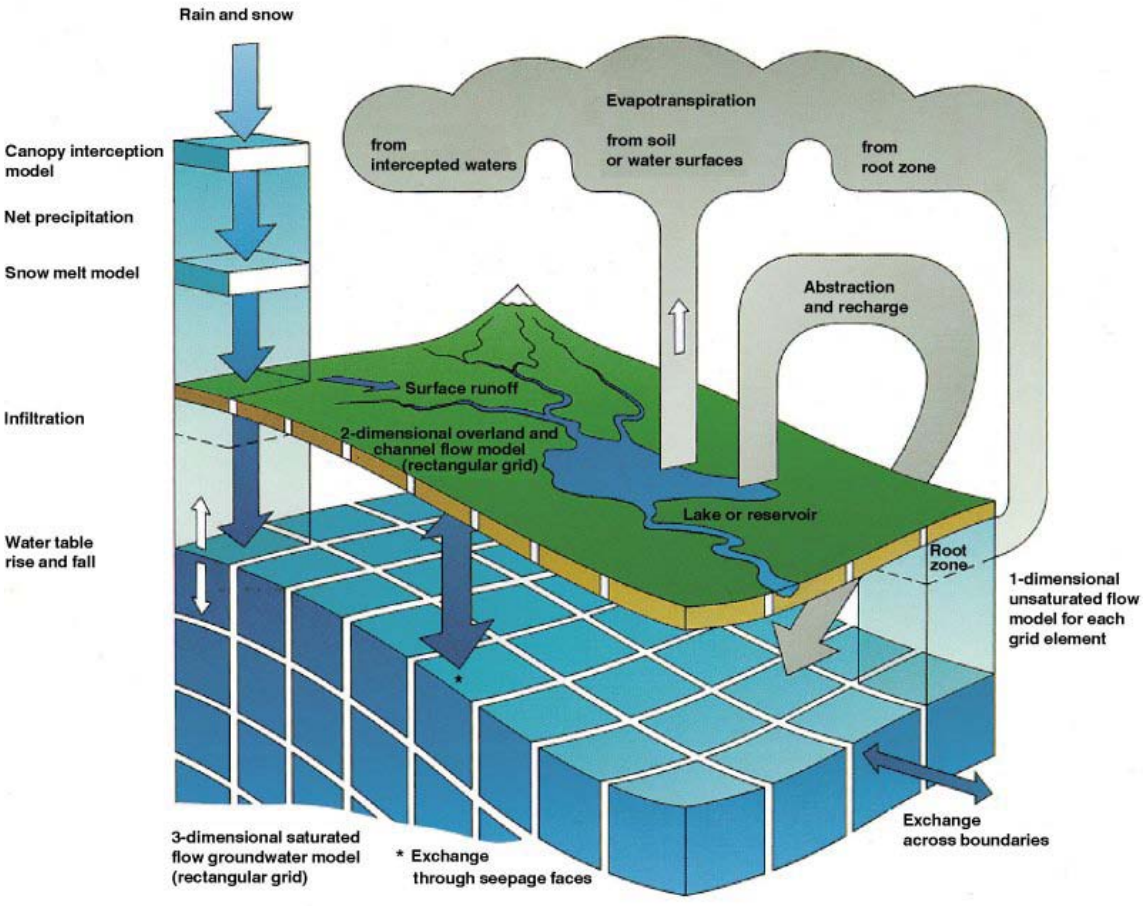

Figure 3-1. *Overview of the model structure and the processes included in MIKE SHE /DHI Software 2009/.*

MIKE SHE consists of the following model components:

- Precipitation (rain or snow).
- Evapotranspiration, including canopy interception, which is calculated according to the principles of /Kristensen and Jensen 1975/.
- Overland flow, which is calculated with a 2D finite difference diffusive wave approximation of the Saint-Venant equations, using the same 2D mesh as the groundwater component. Overland flow interacts with water courses, the unsaturated zone, and the saturated (groundwater) zone. The overland flow is abbreviated OL in the following text.
- Channel flow, which is described through the river modelling component MIKE 11, which is a modelling system for river hydraulics. MIKE 11 is a dynamic, 1D modelling tool for the design, management and operation of river and channel systems. MIKE 11 supports any level of complexity and offers simulation tools that cover the entire range from simple Muskingum routing to high-order dynamic wave formulations of the Saint-Venant equations.
- Unsaturated water flow, which in MIKE SHE is described as a vertical soil profile model that interacts with both the overland flow (through ponding) and the groundwater model (the groundwater table provides the bottom boundary condition for the unsaturated zone). MIKE SHE offers three different modelling approaches, including a simple two-layer root-zone mass balance approach, a gravity flow model, and a full Richards equation model. The unsaturated zone is abbreviated UZ in the following text.
- Saturated (groundwater) flow, which allows for 3D flow in a heterogeneous aquifer, with conditions shifting between unconfined and confined. The spatial and temporal variations of the dependent variable (the hydraulic head) are described mathematically by the 3D Darcy equation and solved numerically by an iterative implicit finite difference technique. The saturated zone is abbreviated SZ in the following text.

For a detailed description of the processes included in MIKE SHE and MIKE 11, see /Werner et al. 2005/, /DHI Software 2009/ and /Graham and Butts 2005/.

The communication between the river network in MIKE 11 and the overland component in MIKE SHE can be defined in two different ways:

- using so-called flood codes, where water levels from MIKE 11 simply are transferred to MIKE SHE, or
- using a two-way communication based on a so-called overbank spilling option.

In this version of the Forsmark model, the two-way overbank spilling option is applied. This option allows river water to spill onto the MIKE SHE model as overland flow. The overbank spilling option treats the river bank as a weir. When the overland water level or the river water level is above the left or right bank elevation, water will spill across the bank based on the weir formula:

$$Q = \Delta x \cdot C \cdot (H_{us} - H_w)^k \cdot \left[1 - \left(\frac{H_{ds} - H_w}{H_{us} - H_w} \right)^k \right]^{0.385}$$

where Q (m^3/s) is the flow across the weir, Δx (m) is the cell width, C ($m^{½}/s$) is the weir coefficient, H_{us} (m) and H_{ds} (m) refer to the height of water on the upstream and downstream side of the weir, respectively, H_w (m) is the height of the weir, and k is a head exponent.

If water levels are such that water is flowing to the river, overland flow to the river is added to MIKE 11 as lateral inflow. If the water level in the river is higher than the level of ponded water, river water will spill onto the MIKE SHE cell and become part of the overland flow. If the upstream water depth over the weir approaches zero, the flow over the weir becomes undefined. Therefore, the calculated flow is reduced to zero linearly when the upstream level drops below a threshold.

The communication between the river network and the groundwater aquifer is calculated in the same way as in the previous versions of the code. The exchange flow between a saturated zone grid cell and a river link is calculated as a conductance multiplied by the head difference between the river and the grid cell. The conductance between the grid cell and the river link depends on the conductivity of both the river bed and the aquifer material /DHI Software 2009/.

3.1.2 Solute transport

Solute transport simulations with the MIKE SHE model may be performed by either the particle tracking module or the advection-dispersion module. In both cases, the three-dimensional flow field calculated by the MIKE SHE water movement module is the basis for the transport simulations.

Particle tracking modelling in the MIKE SHE model system is per definition a purely advective transport modelling, without other dispersion effects than those arising due to velocity variations. This means that the solute particles move with the Darcy flow vectors only. The particles themselves can have any locations in the water movement grid net, i.e. their positions are interpolated within the grid cells.

In particle tracking simulations, hypothetical inert particles or "water parcels" are traced as they are transported by the groundwater flow field in the model volume. The resulting flow paths provide important information as such; they connect the selected starting points with groundwater discharge points or other exit points on the model boundaries. Furthermore, travel or residence times along the flow paths can be calculated. The three-dimensional flow field calculated by MIKE SHE is the basis for the advective transport of the particles. In addition to the input required for the flow modelling, the particle tracking simulations require input data on the number of particles introduced and the starting point of each particle.

The particles are traced in the saturated zone only. When a particle moves from the saturated zone to another compartment of the model that particle is not traced any further. It is registered to which sink/compartment the particle moves; the time step, travel distance and position of the particle is also registered. Thus, it is possible to get information on where the particle leaves the saturated zone and where it goes. A more detailed description of the methodology of the particle tracking calculation is given in /Bosson and Berglund 2006/ and /DHI Software 2009/.

With the MIKE SHE advection-dispersion (AD) module, it is possible to calculate solute transport in all of the different parts of the hydrological cycle. The solute transport module for the saturated zone in MIKE SHE allows the user to calculate transport in 3D, 2D, or even 1D. However, the transport formulation is controlled by the water movement discretisation. If the vertical discretisation is uniform (except for the top and bottom layers), the transport scheme is described in a fully three-dimensional numerical formulation. If the numerical layers have different thicknesses a multi-layered 2D approach is used, where each layer exchanges flows with other layers as sources and sinks.

Temporal and spatial variations of the solute concentration in the soil matrix are described mathematically by the advection-dispersion equation and solved numerically by an explicit, third-order accurate solution scheme. The forcing function for advective transport is the cell-by-cell groundwater flow, as well as groundwater head, boundary, drain and exchange flows, which are all read from the MIKE SHE water movement results files.

Advection-dispersion modelling includes, except advective transport, also dispersion, which allows the substance to move in other directions than the modelled velocity field. The strength of the solute transport through dispersion is controlled by given dispersivities in different directions. The physical interpretation behind the dispersion is diffusion and small-scale heterogeneities that are not part of the model description but affect the solute spreading. Thus, it follows that the more accurately the spatial variability in the hydrogeological regime is described (i.e. the variations in the advective velocity), and if the grid resolution is sufficiently fine, the smaller the dispersivities that need to be applied in the model.

A drawback with the advection-dispersion description is that the model may create so-called numerical dispersion, i.e. model-related "dispersion" caused by the numerical approximations in the model. Numerical dispersion may appear even though the given dispersivities are zero. This phenomenon arises when the grid cells are too large in relation to the advective velocities.

Several reaction processes can be considered in the MIKE SHE solute transport calculations, including sorption and desorption, degradation, and plant uptake. Sorption includes a number of geochemical and chemical reactions. If these processes occur sufficiently fast compared with the water flow velocity they can be described by an equilibrium sorption isotherm. Different equilibrium sorption isotherms have been identified from experimental results. The MIKE SHE AD module includes three of the most commonly applied isotherms, namely the linear, the Freundlich and the Langmuir equilibrium sorption isotherms.

MIKE SHE AD is also able to simulate solute transport in fractured media through a so-called dual porosity description, with mobile and immobile phases representing water in fractures and matrix, respectively. Further details on available process models in MIKE SHE are found in /DHI Software 2009/.

3.2 Overview of models

Three different models were defined, one regional model covering the main part of the Forsmark regional model area situated on land, and two local models within the regional model area. The local models are referred to as (local) models A and B, see Figure 3-2. The regional model covers an area of 180 km^2 and the local models 15.6 km^2 (model A) and 17.3 km^2 (model B). The calibrated SDM-Site MIKE SHE model /Bosson et al. 2008/ was used as a starting point when setting up the SR-Site MIKE SHE model. The calibrated properties of the QD from the SDM modelling have been used directly and no further sensitivity analyses of the hydraulic properties have been performed within the SR-Site modelling.

However, an initial calibration of the new model was carried out in order to analyse the performance of the updated version of the model. Simulations of the pumping test in HFM14 resulted in a reduction of the vertical hydraulic conductivity of the upper 200 m of the bedrock with a factor of 2. This is further described in Section 5.2. Different time periods and climate cases have been simulated with the regional model. A selected year describing a normal (temperate) climate, defined from present long-term meteorological data, a periglacial climate with permafrost conditions, case with wet (temperate) conditions have been simulated with the regional MIKE SHE model. The simulations performed with the local models have only been performed using the model describing the shoreline, QD composition and vegetation cover at 10,000 AD.

In Table 3-1 the different simulation cases are listed, both for the local and the regional MIKE SHE models. The grid resolution of the regional model is 80 m by 80 m and the grid resolution of the local models is 20 m by 20 m. Also the vertical resolution of the local models is finer; there are three calculation layers in the QD compared with two in the regional model. The total number of calculation layers in the local models is increased from 14 layers (in the regional model) to 24 layers. The main purpose of the local models was to use perform transport calculations.

When simulating future conditions in MIKE SHE, the shoreline position, the QD model and the vegetation cover change between the different simulated time periods. The sea has been lowered to the level at that specific period of time. The short-term (daily) variations in the sea level are assumed to be the same as those measured today for all time periods considered. Thus, the time series of the sea level has been corrected to the level of the shoreline at each time period, but the variation during the year is kept the same as in the measured time series of the present sea level in Forsmark.

Each model case is named after the time period (which directly corresponds to a modelled shoreline position, and the applied QD model. Thus, the simulation case 2000AD_2000QD means the MIKE SHE model with the shoreline of 2000 AD and the QD model describing the Quaternary geology at 2000 AD.

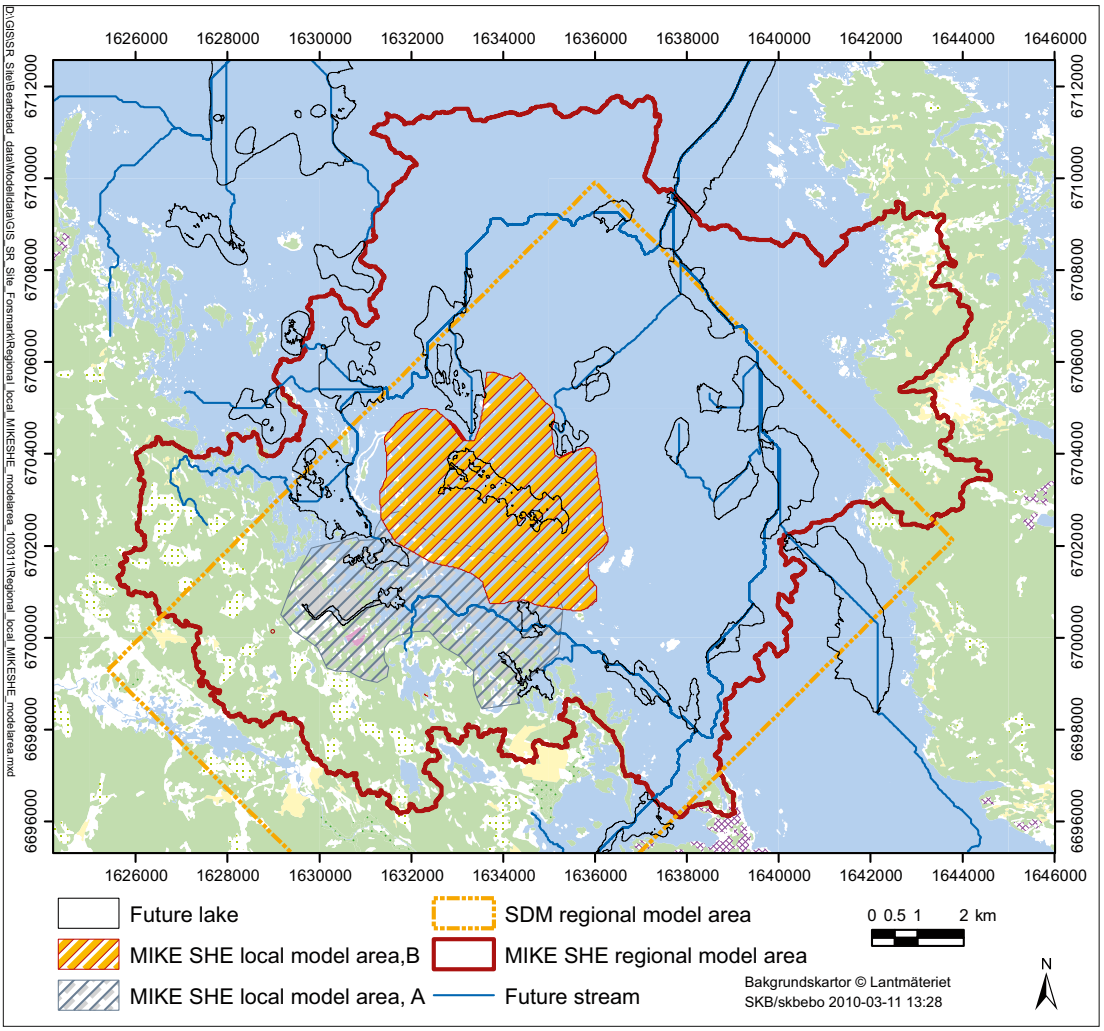

Figure 3-2. *The regional and local MIKE SHE model areas. In the figure the SDM regional model area and the future lakes and streams are also marked.*

Table 3-1. Simulation cases in the MIKE SHE SR-Site modelling. The table also gives information about the QD-model and climate applied in each simulation case.

Regional model, flow modelling		**QD model**			**Transport modelling**	
Shoreline	**Climate**	**2000**	**5000**	**10,000**	**AD****	**PT****
2000 AD	Measured site data*	x				
10,000 AD	Temperate, normal year	x		x		x
5000 AD	Temperate, normal year	x	x			x
2000 AD	Temperate, normal year	x				x
10,000 AD	Periglacial			x		x
10,000 AD	Wet year			x		
Local models, flow modelling						
10,000 AD	Temperate, selected year			x	x	x

*The same climate data series and simulation period as in the SDM-Site modelling. This simulation was performed to analyse the results in order to compare measured and simulated groundwater levels and surface water discharges and levels.

**AD = advection-dispersion, PT = particle tracking.

3.3 Shoreline displacement

The shoreline displacement, as described in /Brydsten and Strömgren 2010/, has been applied to the hydrological models. Three different shorelines have been studied; 2000 AD, 5000 AD and 10,000 AD. The corresponding shorelines are placed at –0.17 m.a.s.l. –14.96 m.a.s.l. and –31.42 m.a.s.l. The time varying sea level measured at the site is applied to all different models, i.e. the short-term variations in the sea level are assumed to be the same over time. The time series of the sea level have been lowered to the level of the sea at each simulated time period 5000 AD and 10,000 AD.

3.4 Modelling of wet conditions

When simulating the wet case the 10000AD_10000QD model was used. No changes in the methodology or the numerical grid were made; only the meteorological input data was changed. The meteorological data for the wet period are described in Section 2.3.

3.5 Modelling of periglacial conditions

Two periglacial cases have been studied for the 10000AD_10000QD model. The cases exemplify two of several possible futures when the Forsmark site is covered by permafrost. These cases are relevant examples of future hydrological processes during permafrost conditions using site specific data. The examples are based on chosen reconstructed conditions from the Weichsel glaciation. The definitions of permafrost and taliks given below are used throughout the text and the different types of formations are illustrated in Figure 3-3.

Permafrost: A condition where a layer of soil or rock below the ground surface remains frozen for at least two consecutive years /French 2007/. In other words, the definition of permafrost is permanently frozen ground. The term ***continuous permafrost*** refers to permafrost when it exists over the landscape as a continuous layer /Summerfield 1991 pp 293–294/.

Active layer: Deposits with permafrost have an upper active layer. This active layer is frozen or unfrozen depending on the weather conditions at each time of the year and a repeated cyclic thaw and freeze.

Taliks: Taliks are unfrozen pockets of water located on top of, underneath or within masses of permafrost. In areas of continuous permafrost, taliks are often found under lakes because of the ability of water body to store and vertically transfer heat energy.

Open talik: An open talik is an area of unfrozen ground that is open to the ground surface but otherwise enclosed in permafrost.

Through talik: Through taliks are unfrozen ground exposed to the ground surface and to a larger mass of unfrozen ground beneath it.

Closed talik: Unfrozen ground enclosed in permafrost is known as a closed talik.

3.5.1 Permafrost simulation cases

Two simulation cases covering the seasonal time variations during a year have been specified. The permafrost depth is different in the two cases and extends down to 100 m or 240 m below the ground surface, as illustrated in Figure 3-4. The definitions of the depth of the permafrost in the two simulation cases are given in the following section. The permafrost is continuous and covers the entire model area, with exception of several through taliks. Superimposing the permafrost is an active layer with a thickness of 1 m. There is no ice sheet present within the model area in periglacial model cases.

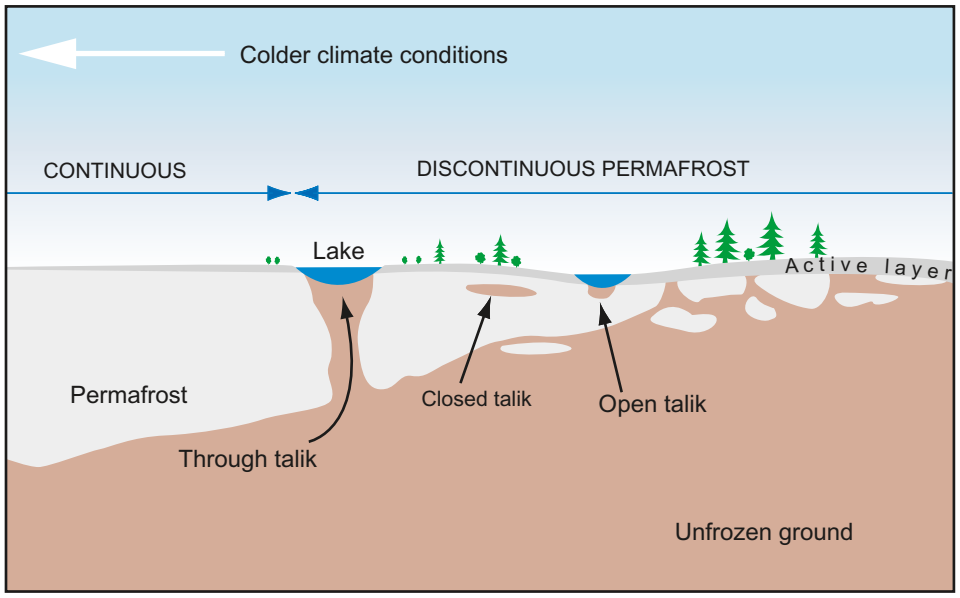

Figure 3-3. *A schematic profile through a permafrost area with an upper active layer and presence of different types of taliks (open, through and closed taliks).*

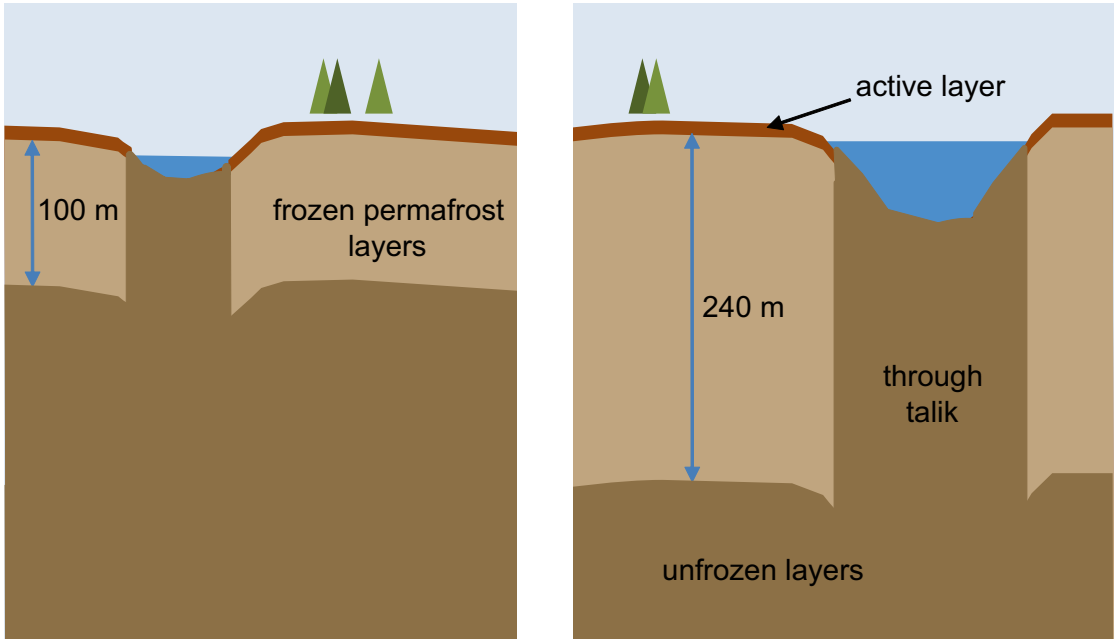

Figure 3-4. *Schematic profiles describing the modelled cases with a permafrost thickness of 100 m or 240 m, and an active layer with a thickness of 1 m.*

Permafrost thickness

The permafrost thickness of 240 m was identified in a previous study /SKB 2006/. The results and conclusions of that study have been applied also here. According to /SKB 2006/ the permafrost thickness for an average surface temperature of –4°C is approximately 240 m, which correlates to the temperature conditions found in the applied periglacial climate data /Kjellström et al. 2009/. Thus, one of the studied model cases in this work has a permafrost thickness of 240 m. The case with a permafrost thickness of a 100 m was added to simulate a potential future situation with more taliks occurring, since the definition of taliks is dependent on the thickness of the surrounding permafrost.

The thickness of the permafrost may vary, in the area of Markha river, Russia, the estimated depths of permafrost range up to at least 1,500 m. Rates of permafrost aggradation can be of the order of only a few centimetres a year, so the development of thick permafrost formations have progressed under a very long period of time /Summerfield 1991 pp 293–294/. The selected permafrost depths are just two examples resulting in different numbers of taliks within the model area. In this work, the presence and effects of taliks are of interest; therefore, no case with a permafrost depth greater than 240 m has been studied. This is because a larger permafrost depth would result in even fewer through taliks in the model area, due to the relation between permafrost depth and presence of taliks.

Through taliks

The planned repository is in both permafrost depth cases positioned below the permafrost at a depth of approximately 500 m below the ground surface where the bedrock is unfrozen. Both open and closed taliks are completely or partly enclosed in the continuous permafrost and will thereby be delimited from the planned repository. Only through taliks are therefore included in the periglacial simulation cases. These formations allow communication between the ground surface with the active layer, and the unfrozen bedrock below the permafrost where the repository will be placed; therefore, only through taliks are of interest in the present modelling.

Active layer

The active layer can be up to 3 m in depth /Summerfield 1991 pp 293–294/. In the climate data used in this work /Kjellström et al. 2009/ the ground temperature at a depth of 1.89 m never reaches above zero and the ground is always frozen independently of the season. The ground temperature at a depth of 0.72 m, illustrated in Figure 3-5, varies seasonally above and below the freezing point, and the ground is frozen/unfrozen only seasonally. This indicates that the "permafrost table" is present at a depth between 0.7 m and 1.9 m.

However, a very thin active layer is difficult to handle in the numerical model, since it requires very short simulation time steps. For the permafrost simulations the active layer has therefore been generalised to a thickness of 1 m covering the entire model area. It should also be emphasised that the general focus is not on the thickness of the active layer, but on the processes in the active layer and the through taliks. This means that a somewhat generalised and simplified system description is justified.

3.5.2 Identification of through taliks

The presence of taliks will differ depending on the thickness of the permafrost. To find out whether a through talik can be maintained beneath a lake or pond in a permafrost landscape, a generalised definition taken from /SKB 2006/ has been applied. This definition means that the presence or absence of a talik under a lake can be assessed if the lake radius and depth and the thickness of the surrounding permafrost are known. The criterion to maintain an open talik is otherwise independent of the site and also of the ground temperature. The definition is valid for a surface temperature of –4°C.

To maintain a through talik beneath a circular lake, one of the two following conditions should be fulfilled /SKB 2006/:

i) the radius of a shallow lake with an average depth of 0.5 m has to exceed the thickness of the surrounding permafrost.
ii) the radius of a deep lake with an average depth of 4 m should be 0.6 times greater than the thickness of the surrounding permafrost. I.e. the radius of the lake has to be 1.6 times the depth of the permafrost if a talik should be maintained.

The definition limits the taliks to only exist beneath a lake. The development of overland water at the surface in the 10000AD_10000QD model has therefore been studied and cells with an annual mean depth of overland water greater than 1 cm was defined as a lake cell. The exact criteria for the through taliks in each simulation case with 240 m respectively 100 m permafrost depth are listed in Appendix 1.

The above definition has resulted in 7 through taliks for the case with 240 m deep permafrost and 45 through taliks in the case with 100 m deep permafrost. The locations of the taliks are presented in Figure 3-5.

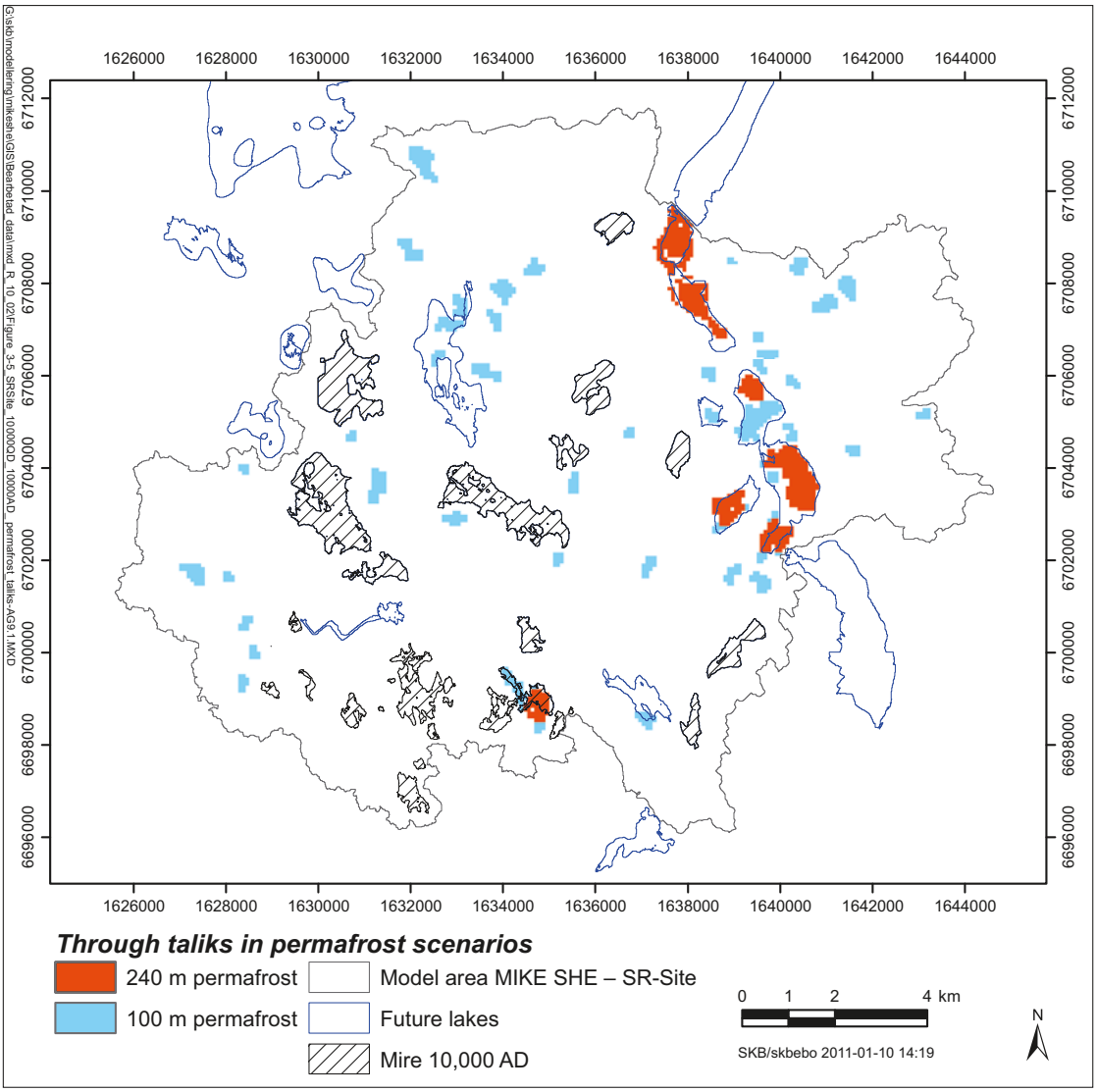

Figure 3-5. *Defined through taliks in the periglacial model cases with permafrost thicknesses of 100 m or 240 m. The areas defined as taliks in the case with a permafrost thickness of 240 m are taliks also in the case with 100 m of permafrost.*

3.5.3 Describing permafrost processes in MIKE SHE

To simulate the processes associated with permafrost conditions, several model parameters, important for the description of the permafrost conditions, have been identified in MIKE SHE. The modelling methodology is to change these parameters to reflect freeze and thaw processes in the active layer, the frozen state in the permafrost and the unfrozen conditions found in the through taliks and the unfrozen layers below the permafrost deposits. A full description of the processes in MIKE SHE that are important when simulating the processes occurring in a periglacial climate with permafrost conditions are described in Appendix 1. In Appendix 1 each natural process, how this process is described in the MIKE SHE model, and the parameters describing each process are listed. A short summary of the most important processes and parameters to change in the model is given below.

The main and most important parameters that have to be changed in the MIKE SHE model when describing a hydrological system with permafrost are the hydraulic properties of the QD and bedrock connected to the permafrost layers. The hydraulic conductivity has to be reduced to imitate the frozen ground. Also the overland flow parameters have to be changed to prevent surface runoff during periods of temperature below zero degrees. The unsaturated zone is a part of the active layer

where melting and freezing processes are going on throughout the year and the layer can be totally or partly frozen or unfrozen. The unsaturated zone parameters are changed to mimic the dynamics of the freezing and thawing processes, i.e. to allow water to infiltrate when the active layer is not frozen and to prevent water from infiltrating when it is frozen.

The permafrost modelling was based on a selected year with time varying climate data (see Section 2.3) and vegetation data (see Section 2.7.2), which both reflect permafrost conditions. Since the permafrost simulations are based on the initial conditions in the 10000AD_10000QD model the selected year is cycled until steady permafrost conditions are met. The applied climate year is repeated and each year is initiated by initial conditions from the end of the previous simulation through so-called hot starts /DHI Software 2009/.

A current limitation in MIKE SHE prevents the use of time varying spatial grid data. This makes a gradual time varying change of permafrost specific parameters impossible and the methodology has therefore been a step-by-step solution. Each year has been divided into periods identified as either a freeze, frozen, thaw or active period where the parameters are changed step by step from period to period. Each period is initiated with initial conditions from the end of the previous simulation period through a hot start.

3.5.4 Definition of simulation periods

The available climate data includes modelled temperatures in the ground (0.01 m down to 1.89 m below ground). These temperatures indicate when the ground starts to freeze/melt and when the ground is frozen/unfrozen. These temperature curves for the selected year have been used to determine when and for how long the freeze and thaw periods occur as well as the frozen and active period. In Figure 3-6 a running weekly average of temperatures at depths of 0.01 m and 0.72 m are found during the selected year.

When the temperature in the soil at a depth of 0.01 m drops below 0°C the soil begins to freeze at the surface. When the temperature in the soil at a depth 0.72 m also drops below 0°C the soil in the entire active layer is considered frozen. When the temperature rises above 0°C at the depth of 1 cm the thawing begins, but the entire active layer is not active until the bottom temperature also rises above 0°C. The freeze period starts in the beginning of October and lasts until the active layer is completely frozen at the end of October. The active layer stays completely frozen until thawing commences in April and continues until the start of the summer period in June. The active period is from the beginning of June until September. The freeze period is shorter than the thaw period.

The freeze and thaw seasons are divided into 15-day periods. The modelled year starts at the 1st of October and the method is to repeat a yearly cycle using hot starts from the end of the previous simulation period until stable conditions are established. Each yearly cycle includes seven simulation periods (see Table 3-2), and the identified MIKE SHE parameters are changed step by step from period to period (see Appendix 1). This modelling sequence simulates the thermal processes in water and soil during a year to reflect the seasonal variations (see Table 3-3) under periglacial conditions.

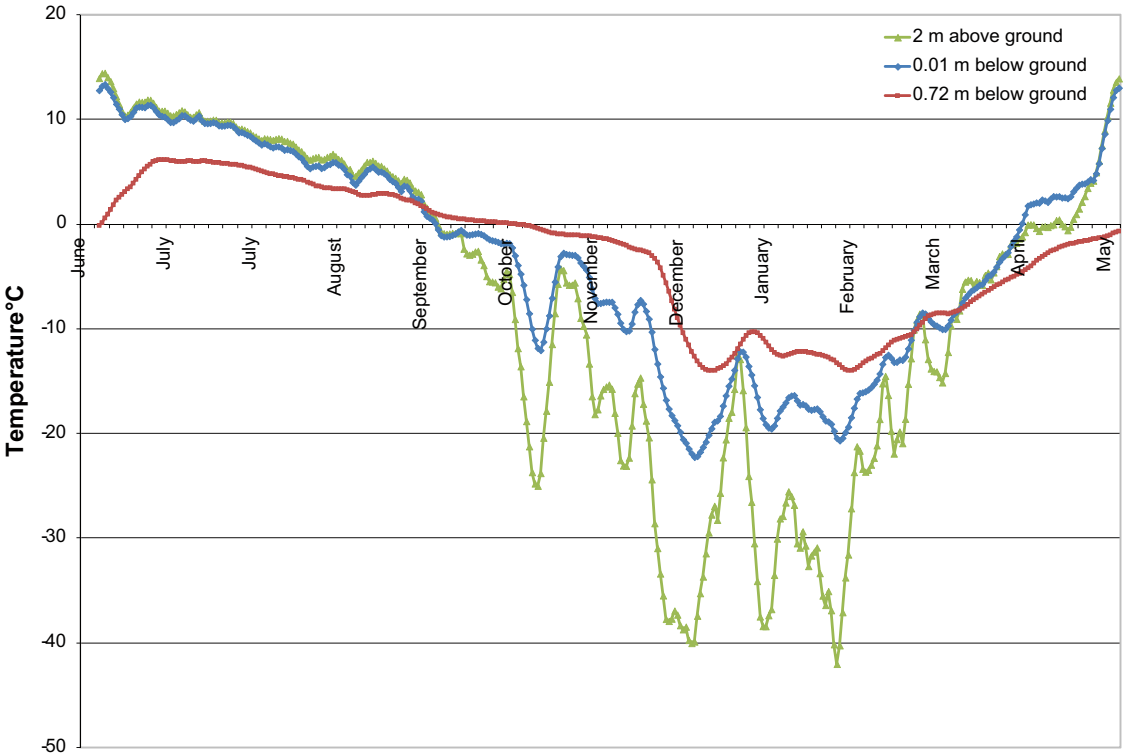

Figure 3-6. *Surface and ground temperatures used to define the modelling sequence.*

Table 3-2. The different periods of the year described as freezing, thawing, frozen and active periods.

	One-year cycle						
Simulation period	**freeze 1**	**freeze 2**	**frozen**	**thaw 1**	**thaw 2**	**thaw 3**	**active**
Length of period (days)	15	15	175	15	15	15	115
Date	1/10 – 16/10	16/10 – 31/10	31/10 – 23/4	23/4 – 8/5	8/5 – 23/5	23/5 – 7/6	7/6 – 1/10
Ground temperature (0.01 m below surface)	T<0	T<0	T<0	T>0	T>0	T>0	T>0
Ground temperature (0.72 m below surface)	T>0	T>0	T<0	T<0	T<0	T<0	T>0

Table 3-3. Cyclic modelling scheme; the asterisk indicates original model input data from the 10000AD_10000QD model.

Compartment	Data type	Parameter	freeze 1	freeze 2	frozen	thaw 1	thaw 2	thaw 3	active
Climate	Time varying	Precipitation (P) Temperature (T) Potential Evapotranspiration (PET)	P T PET	P T PET	P T PET	P T PET	P T PET	P T PET	P T PET
Vegetation	Time varying	Leaf area index (LAI) root depth (RD)	LAI RD	LAI RD	LAI RD	LAI RD	LAI RD	LAI RD	LAI RD
Snow	Constant	Energy melting coefficient	0.013	0.013	0.013	0.013	0.013	0.013	0.013
		Snow sublimation factor	0.1	0.1	0.1	0.1	0.1	0.1	0.1
Overland	Spatial grid	Overland-groundwater leakage coefficient	1E–7	1E–20	1E–20	1E–7	0.1	0.1	0.1
		Overland-groundwater leakage coefficient in taliks	0.1	0.1	0.1	0.1	0.1	0.1	0.1
		Manning M	5E–6	5E–19	5E–19	5E–6	5*	5*	5*
		Manning M in taliks	5*	5*	5*	5*	5*	5*	5*
Unsaturated zone	Spatial grid	Saturated hydraulic conductivivty (Ks)	Ks*/30	Ks*/300	1E–10	Ks*/1,000	Ks*/100	Ks*/10	Ks*
		Saturated hydraulic conductivivty (Ks) in taliks	Ks*	Ks*	Ks*	Ks*	Ks*	Ks*	Ks*
Saturated zone	Spatial grid	Horizontal and vertical conductivity (K) in active layer	K*/30	K*/300	1E–20	K*/1,000	K*/100	K*/10	K*
		Horizontal and vertical conductivity (K) in permafrost	1E–20	1E–20	1E–20	1E–20	1E–20	1E–20	1E–20
		Horizontal and vertical conductivity (K) in taliks	K*	K*	K*	K*	K*	K*	K*
		Horizontal and vertical conductivity (K) in unfrozen layers below permafrost	K*	K*	K*	K*	K*	K*	K*
		Drain time constant (TC)	TC*/30	TC*/300	1E–20	TC*/1,000	TC*/100	TC*/10	TC*
		Drain time constant (TC) in taliks	0	0	0	0	0	0	0

3.6 Transport modelling

Transport simulations were performed both in the regional and the local models. In the regional model only particle tracking simulations were made, while in the local models both particle tracking simulations and simulations with the advection-dispersion module were performed.

3.6.1 Regional model

Table 3-4 shows a summary of the particle tracking (PT) simulations performed with the regional model. As discussed above, the regional model was run for three different times (i.e. three different shoreline positions) and with three different QD models, resulting in the following models: 2000AD_2000QD, 5000AD_2000QD, 5000AD_5000QD, 10000AD_2000QD and 10000AD_10000QD. Particle tracking simulations were made using the 2000AD_2000QD, 5000AD_5000QD and 10000AD_10000QD models, i.e. for the three different times studied and each time with the corresponding QD model /Brydsten and Strömgren 2010/. In all of these three PT simulations the particles were introduced at a depth 150 m.b.s.l. and with one particle per cell in the whole model area. The simulations were run for a 1000-year period by cycling the flow results for the second year of the water flow simulations 1,000 times.

Table 3-4. Transport simulations performed with the regional MIKE SHE model.

Model	Climate	Source location	Flow results circulation	Introduction of particles	Length of simulation (years)
2000AD_2000QD	Temperate	150 m.b.s.l.	1 year	1 part/cell	1,000
5000AD_QD10000	Temperate	150 m.b.s.l.	1year	1 part/cell	1,000
10000AD_10000QD	Temperate	150 m.b.s.l.	1 year	1 part/cell	1,000
Permafrost, 240 m	Periglacial	Active layer	Frozen period	1 part/cell	5,000
Permafrost, 240 m	Periglacial	Active layer	Active period	1 part/cell	5,000
Permafrost, 240 m	Periglacial	240 m.b.s.l.	Frozen period	1 part/cell	5,000
Permafrost, 240 m	Periglacial	240 m.b.s.l.	Active period	1 part/cell	5,000
Permafrost, 100 m	Periglacial	Active layer	Frozen period	1 part/cell	5,000
Permafrost, 100 m	Periglacial	Active layer	Active period	1 part/cell	5,000
Permafrost, 100 m	Periglacial	100 m.b.s.l.	Frozen period	1 part/cell	5,000
Permafrost, 100 m	Periglacial	100 m.b.s.l.	Active period	1 part/cell	5,000
Permafrost, 100 m	Periglacial	Repository*	Active period	5 part/cell within repository	16,000
Permafrost, 240 m	Periglacial	Repository*	Active period	5 part/cell within repository	16,000
10000AD_10000QD	Temperate	Repository*	1 year	5 part/cell within repository	16,000
Wet	Wet	Repository*	1 year	5 part/cell within repository	16,000

*The results of the PT-simulations with particle release within the repository are presented in Chapter 8.

For the permafrost model, i.e. the regional model run for a periglacial climate, six PT simulations were performed, see Table 3-4. All PT simulations for the permafrost model were run for 5000 years. In the first two PT simulations, the particles were introduced in the uppermost calculation layer, i.e. the active layer. One particle per cell was introduced at a depth of 90% of the thickness of the uppermost layer. The first simulation was made for the frozen period by cycling the flow results for the frozen period with a total length of 175 days. The second simulation was run for the active period, i.e. the non-frozen period which is 115 days.

The next two PT simulations for the permafrost flow simulation were made by introducing the particles below the permafrost layer, at a depth of c. 240 m.b.s.l. or c. 100 m.b.s.l. (depending of the permafrost depth). In the same way as for the first two simulations, one simulation was made for the frozen period and one for the active period.

The last two permafrost PT simulations were made by introducing the particles at the depth and position of the repository. Five particles were introduced in each cell situated within the repository area. In the same way as for the other permafrost PT simulations, one simulation was made for the frozen period and one for the active period.

3.6.2 Local models

For the local models named A and B, transport simulations were made both with particle tracking and the advection-dispersion model. Table 3-5 shows a summary of the transport simulations performed using the local SR-Site model covering objects 118, 120, and 121 (local model A) and Table 3-6 the transport simulations made with the local SR-Site model covering object 116 (local model B).

Table 3-5. Transport simulations using the local MIKE SHE SR-Site model A.

Transport simulation type	QD model (AD)	Source	Source depth (m.b.s.l)	Source type	Plant uptake factor (-)	Dispersion	Mult factor for K-values in lake sediments	Length of simulation (years)
PT	10,000	Layer	150	initial	–	–	–	1,000
PT	10,000	CF	40	initial	–	–	–	1,000
PT	10,000	CF	40	continuous	–	–	–	100
AD	10,000	CF	40	continuous	0	low	1	100
AD	10,000	CF	40	continuous	1	low	1	100
AD	10,000	Layer	30	initial	0	low	1	100
AD	10,000	Layer	30	initial	0	high QD, low bedrock	1	100
AD	10,000	Layer	30	initial	0	low	100	100
AD	2000	CF	40	continuous	0	low	1	100
AD	2000	Layer	30	initial	0	low	1	100
AD	10,000	selected deposition holes	40	continuous	0	low	1	100

Table 3-6. Transport simulations using the local MIKE SHE SR-Site model B.

Transport simulation type	QD model (AD)	Source	Source depth (m.b.s.l)	Source type	Plant uptake factor (-)	Dispersion	Mult factor for K-values in lake sediments	Length of simulation (years)
AD	10,000	Layer	40	initial	0	low	1	100
AD	10,000	Layer	40	initial	0	high QD, low bedrock	1	100
AD	10,000	selected deposition holes	40	continuous	0	low	1	100

In the tables, the transport simulation type refers to either particle tracking (PT) or advection-dispersion (AD) simulations. There are two different approaches for how the concentration or particles are introduced in the model. Either there is a continuous source, which is introduced at a depth of 40 m.b.s.l., or there is an initial concentration, which is introduced uniformly in the cells at a depth of approximately 30–40 m.b.s.l.

When the source is an initial concentration, the concentration is set to 1 g/m^3 all over a calculation layer. Since the upper and lower levels of the layer follow the topography, the depth varies. Consequently, when the source is an initial concentration it is introduced at higher levels in some areas whereas at lower levels in other areas. When the source is a continuous source it is not introduced in a layer but in a grid cell located at a given depth of 40 m.b.s.l. Since the concentration source is introduced at a specific depth it means that the source may be introduced into different calculation layers along the horizontal plan, but always in cells located at 40 m.b.s.l. The height of the cell is 5 m and the source is introduced in the entire grid cell height.

In Table 3-5, the source type referred to as CF means that the source is introduced at locations obtained from the ConnectFlow modelling. Based on the discharge points according to ConnectFlow transport simulations /Joyce et al. 2010/, the corresponding positions of the particles when they passed the depth 40 m.b.s.l. were extracted, i.e. the coordinates of the flow paths at 40 m depth were extracted and used as starting points for concentration sources or particles in the MIKE SHE transport simulations. In the MIKE SHE model, it is not possible to give exact starting positions of the particles within a cell, but only the cell in which they are introduced. Since one MIKE SHE cell might be passed by several CF flow paths the initial particle concentration was calculated based on the number of CF flow paths passing each MIKE SHE cell. Each flow path passing a MIKE SHE cell was given a concentration of 1g/m^3. Figure 3-7 shows the positions and concentrations of the continuous source. The highest concentration strengths are located within the lakes in the north and western parts of the model area. The maximum concentration is 176 g/m^3, i.e this cell has been passed by 176 CF flow paths.

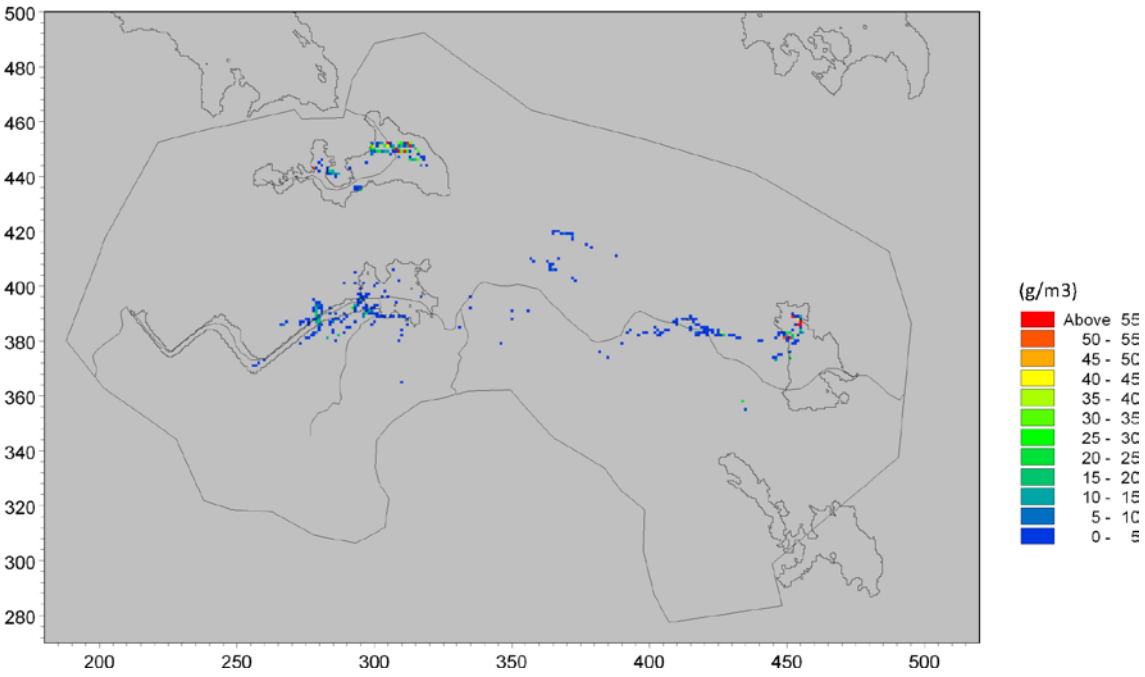

Figure 3-7. *Locations of point sources used for the simulations with a continuous source at a depth of 40 m.b.s.l.*

Furthermore, when the source type is referred to as "selected deposition holes", the source is introduced along the flow paths from ten selected depositions holes in the repository towards the surface. The flow paths from the repository are calculated in the ConnectFlow model /Joyce et al. 2010/. The ten selected deposition holes represent canister positions in the repository with relatively high groundwater flow rates and relatively short travel time to the surface (typically less than 1,000 years). Thus, the canister positions and the hydrological transportation in the repository and the geosphere should be seen as an example only.

The coordinates of the flow paths from the ten selected deposition holes at approximately 40 m.b.s.l. are extracted from the ConnectFlow model and the sources in the MIKE SHE transport calculations are placed at these coordinates. This exchange of information between the two hydro(geo)logical models makes it possible to analyse the transport in the near-surface system in more detail. This means that the effects of the more detailed representation of the surface processes included in the MIKE SHE model on e.g. discharge locations can be investigated.

Figure 3-8 shows the locations of the flow paths at 40 m.b.s.l. within the local model area for the model including objects 118, 120 and 121. In total, seven flow paths from the ten selected deposition holes are contained within the model area. Figure 3-9 shows the coordinates of the flow paths from the selected deposition holes within object 116. In total, three flow paths are located within object 116. However, since two of the flow paths are located within the same grid cell the initial source strength in that cell was set to 2 g/m^3 instead of 1 g/m^3.

For the local model A including objects 118, 120 and 121, three different PT simulations were made, all for the 10000AD_10000QD model, see Table 3-5. The first two PT simulations were run for 1,000 years. The third PT simulation was run only for 100 years, since the purpose was to compare the results to an AD simulation. All AD simulations were run for 100 years. In Section 7.2.1, the particle tracking simulations are further discussed and in Section 7.2.2 the results of the simulations with the advection-dispersion module are described.

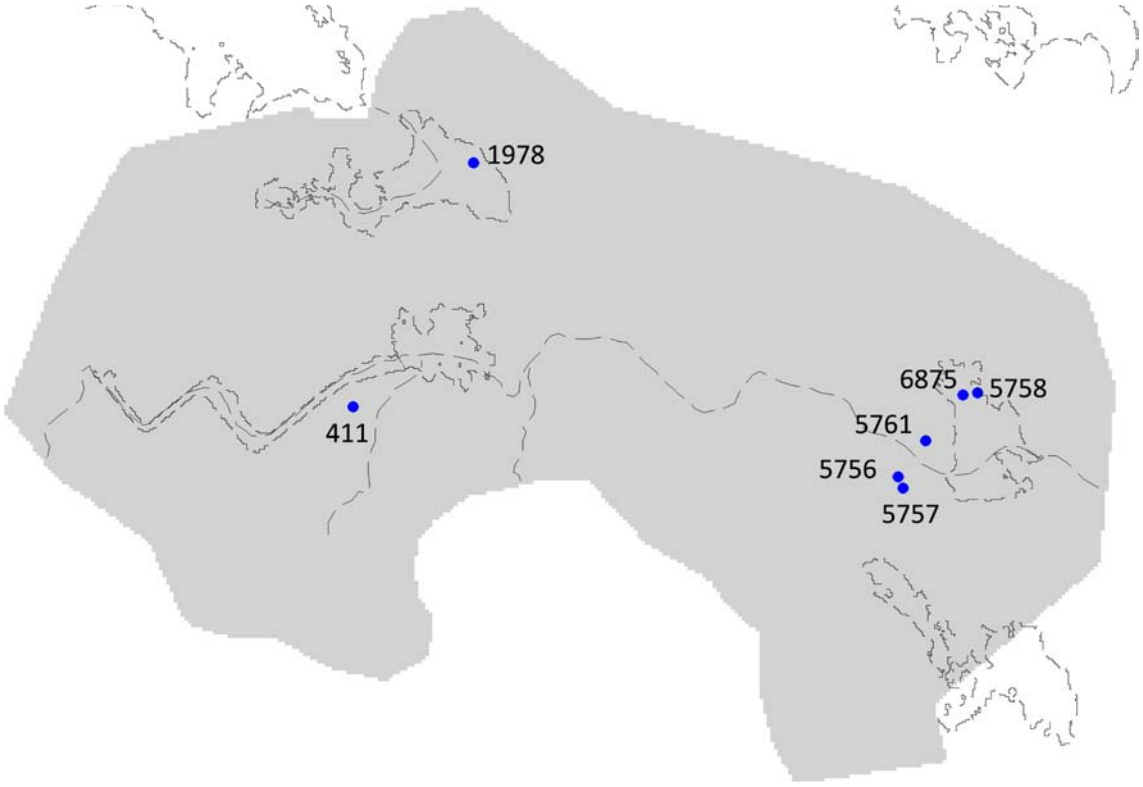

Figure 3-8. *Locations and ID numbers of the flow paths from the selected deposition holes at c. 40 m.b.s.l. within the model area for the local model containing objects 118, 120 and 121.*

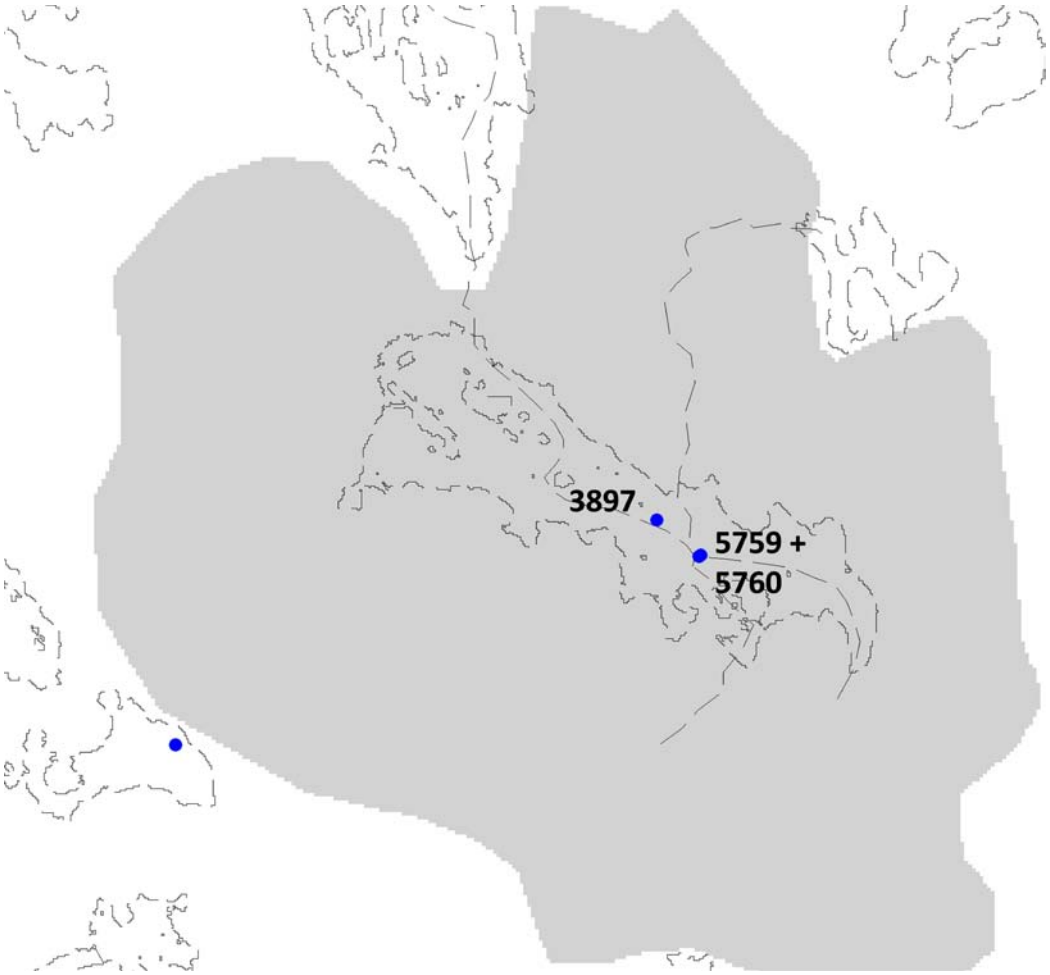

Figure 3-9. *Locations and ID numbers of the flow paths from the selected deposition holes at c. 40 m.b.s.l. within the model area for the local model containing object 116. Flow paths from canisters 5759 and 5760 are located within the same model grid cell.*

4 Description of numerical flow models

4.1 Regional flow models for normal and wet temperate conditions

4.1.1 Model domain and grid

The regional model (Figure 3-2) covers an area of 180 km^2. Most of the on-shore part of the SDM Forsmark regional model area is included in the MIKE SHE regional model area considered in the present work. However, the upstream (inland) boundary follows the water divide towards the stream Forsmarksån catchment rather than the boundary of the SDM Forsmark regional model area.

When defining the horizontal extent of the regional MIKE SHE model area, the candidate area, the surface water divides and the regional deformation zones were taken into consideration. The surface water divide towards the stream Forsmarksån catchment is a natural boundary for the south western part of the model area. In addition, the field-controlled catchment area boundaries identified in the surface-hydrological modelling were used to determine the position of the on-shore part of the north-western boundary. Compared to the SDM-Site MIKE SHE model area /Bosson et al. 2008/, the model area in the SR-Site MIKE SHE modelling has been extended further from the present shoreline. The main reason for this is that the model should include the future land areas in the cases to be simulated in the SR-Site project. Thus, the model area was extended to include the shoreline at 10,000 AD.

The horizontal resolution of the calculation grid in the regional model is 80 m by 80 m in the whole model area. This resolution is used for all flow components in MIKE SHE, i.e. the overland flow, the unsaturated zone (including evapotranspiration), and the saturated zone. The unsaturated zone, which is a 1D vertical model description, is however treated in a semi-distributed manner, see below. Hydrogeological input data for the bedrock and the Quaternary deposits and geometrical data for the bedrock and QD layers are also given on a 80 m × 80 m grid.

The vertical resolution varies with depth, both for the unsaturated and the saturated zone, according to the description below. The vertical distributions given by the parameterised geological model are interpolated to the vertical grid in the following manner: In each horizontal model grid cell, the geologic model is scanned in the vertical direction and the properties from the geological model are assigned to the cell. The properties are based on the average of the values found in the cell weighted by the thickness of each of geological layer /DHI Software 2009/. For example, if there are three different geological layers in a model grid cell, each with a different value for the specific yield, then the specific yield for the model grid cell is calculated as:

$$S_y = \frac{S_{y1} \cdot z_1 + S_{y2} \cdot z_2 + S_{y3} \cdot z_3}{z_1 + z_2 + z_3}$$, where z_i is the thickness of geological layer *i*.

The vertical hydraulic conductivity is not calculated as described above. Vertical flow depends mostly on the lowest hydraulic conductivity in the geological layers presented. A harmonic weighted mean value is therefore used instead. The vertical hydraulic conductivity for the three geological layers described above will be calculated as follows:

$$K_v = \frac{z_1 + z_2 + z_3}{\frac{z_1}{K_{v1}} + \frac{z_2}{K_{v2}} + \frac{z_3}{K_{v3}}}$$

In the Quaternary deposits, several geological layers may be included in the same calculation layer (with parameter values averaged as described above). The calculation layers in the bedrock follow the geological layers given by the ConnectFlow modelling team, see Section 2.5, which means that no averaging of parameter values was needed.

4.1.2 The surface stream network

For the regional model area, five different MIKE 11 model set ups were created, one for each shoreline time step and each QD model, i.e. 2000AD_2000QD, 5000AD_2000QD, 5000AD_5000QD, 10000AD_2000QD, and 10000AD_10000QD. The MIKE 11 model has to be adjusted to the model topography used in each model case otherwise the river banks might be higher than the topography and surface water cannot flow into the MIKE 11 river branches.

The first setup was made for the 2000 AD case, for which surface stream cross sections and boundaries were based on levels from the 2000 QD model. The MIKE 11 model reported in /Bosson et al. 2008/ was the basis for the model, but since the grid size was changed from 40 m to 80 m the surface stream cross section levels were adjusted to the new topography. The model contains MIKE 11 surface stream branches with a total length of approximately 25 km and with 122 surface stream cross sections. Figure 4-1 shows the surface stream networks for shoreline location (2000 AD, 5000 AD and 10,000 AD).

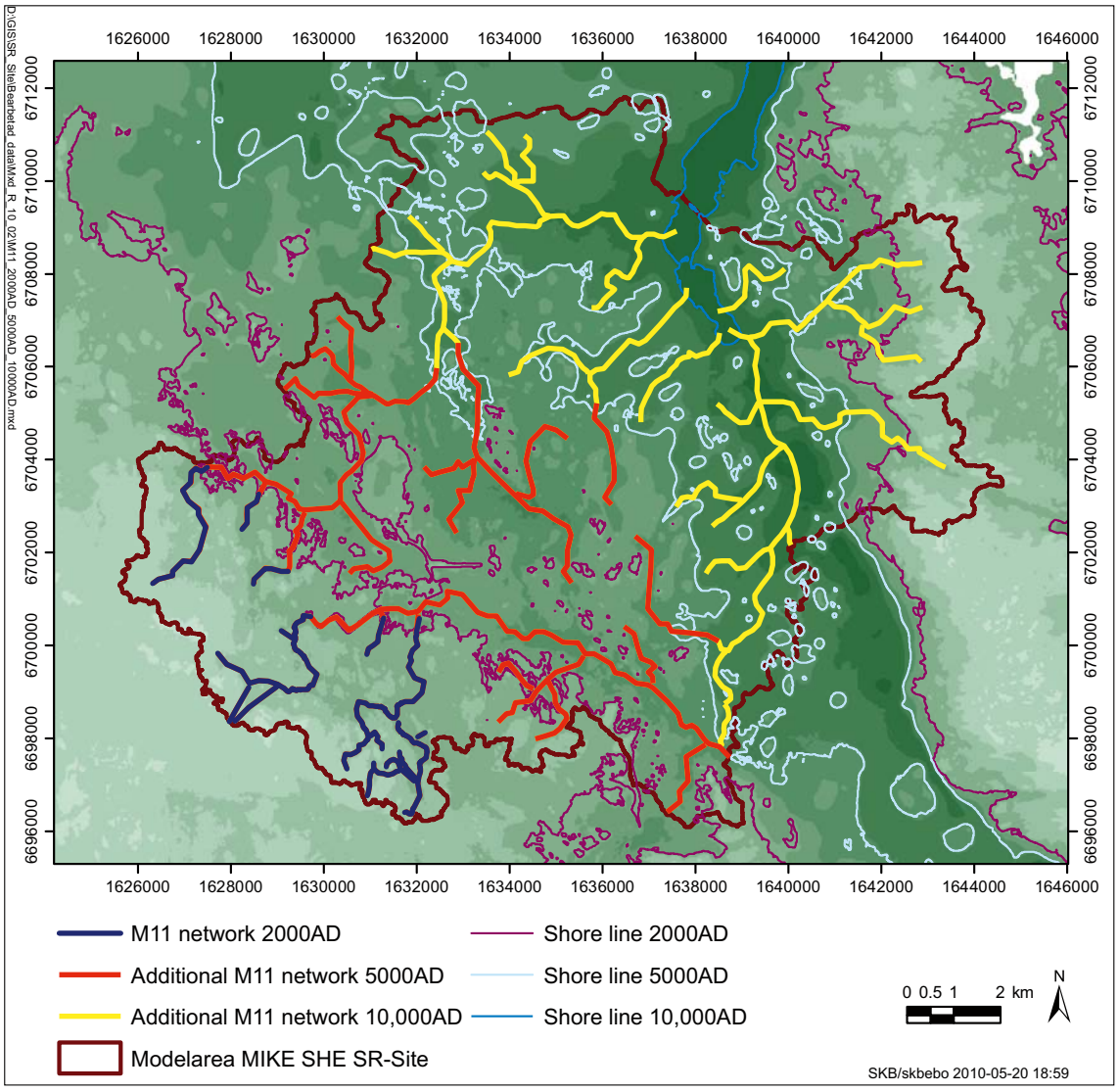

Figure 4-1. *Surface stream networks for the 2000 AD, 5000 AD and 10,000 AD shorelines.*

For the 5000 AD model, the surface stream network for 2000 AD was extended to include new land areas. Since two different QD models were used in the 5000 AD simulation case, the network levels were adjusted for each QD model. However, the positions of branches and cross sections were the same for both QD models. Figure 4-1 shows the stream network for the 5000 AD cases. The length of the MIKE 11 surface stream branches is approximately 80 km and 268 cross sections are included in the model.

In the same way as for the 5000 AD models, the surface stream networks were further extended for the 10,000 AD models (Figure 4-1). All cross section data were updated for the two different QD models. In total, the MIKE 11 model for 10,000 AD includes 430 cross sections and the total MIKE 11 surface stream branch length is approximately 145 km.

For branches contributing to an inflow of surface water crossing the model boundary to the MIKE SHE model, surface discharges were calculated in the MIKE NAM module, which is a hydrological rainfall/runoff module. The NAM module was calibrated by use of field observations from monitoring station PFM005764, situated just upstream of Lake Bolundsfjärden, see Figure 2-21. The calibrated NAM parameters were considered to be applicable for the entire model area and used for calculations of all boundary discharges.

4.1.3 The unsaturated zone

In order to speed up the simulation, only a limited number of grid cells are simulated in the unsaturated zone modelling. The selection of which cells to consider in the simulation is made through a classification system where those unsaturated zone columns that have the same conditions (i.e. the same QD profile, land use, meteorology and groundwater depth) are grouped together. From each group only one column, randomly selected, is simulated.

In the Forsmark model, an exception from this is made in areas with ponding water on the surface, i.e. lakes and wetland areas (excluding the sea). In these areas, the unsaturated zone simulation is executed in all grid cells. This has been found important in order to ensure a proper simulation of the evapotranspiration /Aneljung and Gustafsson 2007/. The vertical discretisation is the same for all QD profiles, see Table 4-1, starting with a resolution of a few centimetres in the top soil and increasing to a few decimetres at the depth where the groundwater table is typically reached in Forsmark.

Table 4-1. The vertical discretisation of the unsaturated zone.

Depth interval	Cell height (m)	Number of cells
0–1 m	0.1	10
1–5 m	0.5	8
5–10 m	1	5
10–20 m	2	5

4.1.4 The saturated zone

The ground surface, as given by the topographic model, is the upper model boundary. The bottom boundaries in both the regional model and the local models are at 600 m.b.s.l. MIKE SHE distinguishes between geological layers and calculation layers. The geological layers (see Section 2.4) are the basis for the model parameterisation, which means that the hydrogeological parameters are assigned to the different geological layers. The calculation layers are the units considered in the numerical flow model. In cases where several geological layers are included in one calculation layer, the properties of the latter are obtained by averaging of the properties of the former, see Section 4.1.1. The regional model consists of 16 calculation layers, two in the QD and 14 in the bedrock.

In general, the calculation layers follow the geological layers. However, one exception is the calculation layers in the Quaternary deposits. The lake sediments and other Quaternary deposits are included in the two uppermost calculation layers of the regional model. The uppermost calculation layer has a minimum thickness of 2.5 m and the other calculation layers have a minimum thickness of 1 m. The lake sediments are included in the uppermost calculation layer. If the depth of the lake sediments is larger than 2.5 m, the lower level of calculation layer 1 follows the lower level of the lake sediments. The coupling between geological layers and calculation layers in the QD is illustrated in Figure 4-2.

In the sea, the lower boundary of the uppermost calculation layer follows the sea bottom. Modelling large volumes of overland water is very time-consuming in MIKE SHE and may cause numerical instabilities. Therefore, the sea is described as a geological layer filled with gravel of high hydraulic conductivity. The "sea-gravel" is present from the sea bottom up to the level of the lowest measured sea level during the simulation period.

The "sea-gravel" is included in the uppermost calculation layer; therefore, the model topography is flat in the sea. The reason why the minimum sea level is chosen as the upper limit for the "sea gravel" is that the littoral zone in the model should be able to vary with time. When the measured sea level rises above the minimum sea level, overland water is built up in the littoral zone and the water level (the sea level) can rise and move towards land during periods of high water levels.

The model topography (i.e. the upper boundary of the uppermost calculation layer) is defined as follows:

If DEM (Digital elevation model) > minimum sea level → Topography = DEM
If DEM < minimum sea level → Topography = minimum sea level

The part of calculation layer 1 containing the sea has an internal boundary condition with a prescribed time-varying head given by the measured sea level. Since the internal boundary is set from the sea bottom up to the minimum sea level, the littoral zone may vary during the simulation. The lower layer of calculation layer one is calculated in six steps:

1. If lake sediment is present → Lower level = Lower level of L3.
2. If ***Topography*** > minimum sea level → Lower level = Topography – 2.5 m.
3. If ***Topography*** < minimum sea level → Lower level = Sea bottom (DEM).
4. Calculate the thickness, T, of calculation layer one based on step 1 and 2.
5. Correct for the littoral zone: If T < 2.5 m → set T to 2.5 m.
6. Lower level of calculation layer 1 = ***Topography*** – T

The lower layer of calculation layer 2 follows the lower level of Z6, with the condition that the minimum thickness of the layer has to be 1 m. In areas where the thickness is smaller than 1 m, calculation layer 2 enters the uppermost geological bedrock layer (with a maximum of one meter).

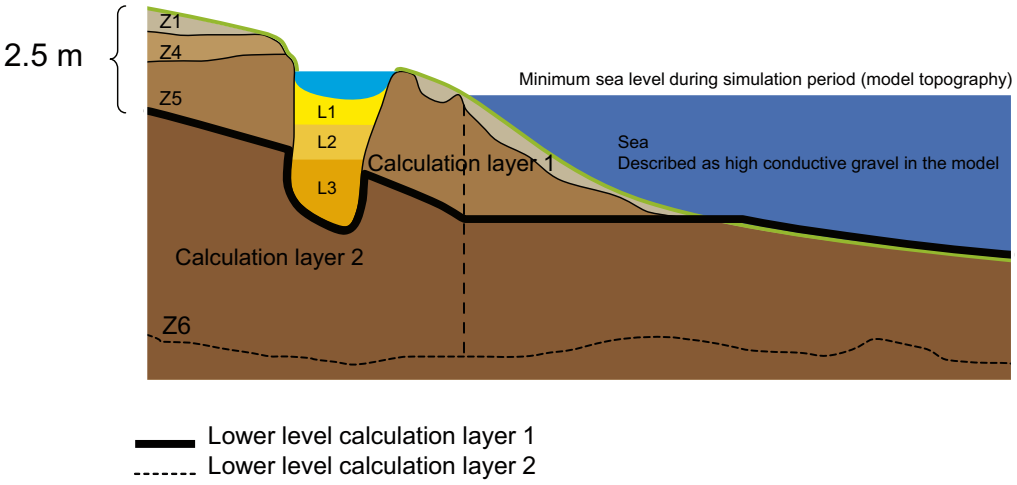

Figure 4-2. *Illustration of the calculation layers in the QD.*

4.1.5 Initial and boundary conditions and time stepping

The groundwater divides are assumed to coincide with the surface water divides; the latter are reported in /Brunberg et al. 2004/. Thus, a no-flow boundary condition is used for the on-shore part of the model boundary. The sea forms the uppermost calculation layer in the off-shore parts of the model. As described above, the sea is represented by a geological layer consisting of highly permeable material. The hydraulic conductivity of this material is set to 0.001 m/s. The sea part of the uppermost calculation layer has a time-varying head boundary condition. The measured time-varying sea level is used as input data.

The top boundary condition is expressed in terms of the precipitation and potential evapotranspiration (PET). The precipitation and PET are assumed to be uniformly distributed over the model area, and are given as time series. The actual evapotranspiration is calculated during the simulation. The bottom boundary condition is a no-flow boundary condition. The effect of different bottom boundary conditions was analysed in the SDM-Site MIKE SHE modelling /Bosson et al. 2008/.

The simulations for present conditions were run for the selected hydrological year October 1st 2003 to October 1st 2004, see Section 2.3. The selected year was cycled twice and all the results have been evaluated for the second year. The initial conditions were defined using modelling results from the second run of the cycled period.

In MIKE SHE a maximum time step is defined for each compartment of the model. During the simulation the time step may be reduced. The maximum time step for all compartments are listed in Table 4-2.

4.2 Regional flow model for periglacial conditions

4.2.1 Model domain and grid

The permafrost cases have been studied with the 10000AD_10000QD model. The horizontal extent and resolution of the grid are kept unchanged in the permafrost cases. To describe the permafrost deposits and formations included in the cases, the 10000AD_10000QD model setup has been adjusted to include an active layer, permafrost layers and through taliks. This modification has resulted in a slightly altered vertical resolution, see Figure 4-3 and 4-4 and Table 4-3.

In the 10000AD_10000QD model the lower levels of some of the geological layers differ from the calculation layers. To be able to change the hydraulic properties delimited to the periglacial formations as described in Section 3.5, the geological layers were processed to have the same vertical extent as the calculation layers. The hydraulic properties have also been modified accordingly. In this process the boundary between the two QD layers were slightly altered to create a top layer with a thickness of 1 m. This top QD layer, calculation layer 1, is the active layer and consists of the upper part of layer QD1 and replaces the previous QD1. Consequently the thickness of the layer QD2 will be greater than in the 10000AD_10000QD model for temperate conditions, i.e. all QD are still included in the two upper calculation layers.

The permafrost formations consist of several calculation layers. The upper boundary of the permafrost is defined by the lower level of the active layer in both permafrost cases. For the case with a permafrost thickness of 100 m the lower boundary is defined by the lower level of calculation layer 7 (B5_CF9 in Table 4-3). A total of 6 calculation layers are frozen permafrost.

Table 4-2. Maximum time steps for the different compartments of the MIKE SHE-MIKE 11 model.

Compartment	Maximum timestep
Overland	1 h
Unsaturated zone	1 h
Saturated zone	3 h
MIKE 11 (water courses)	5 s

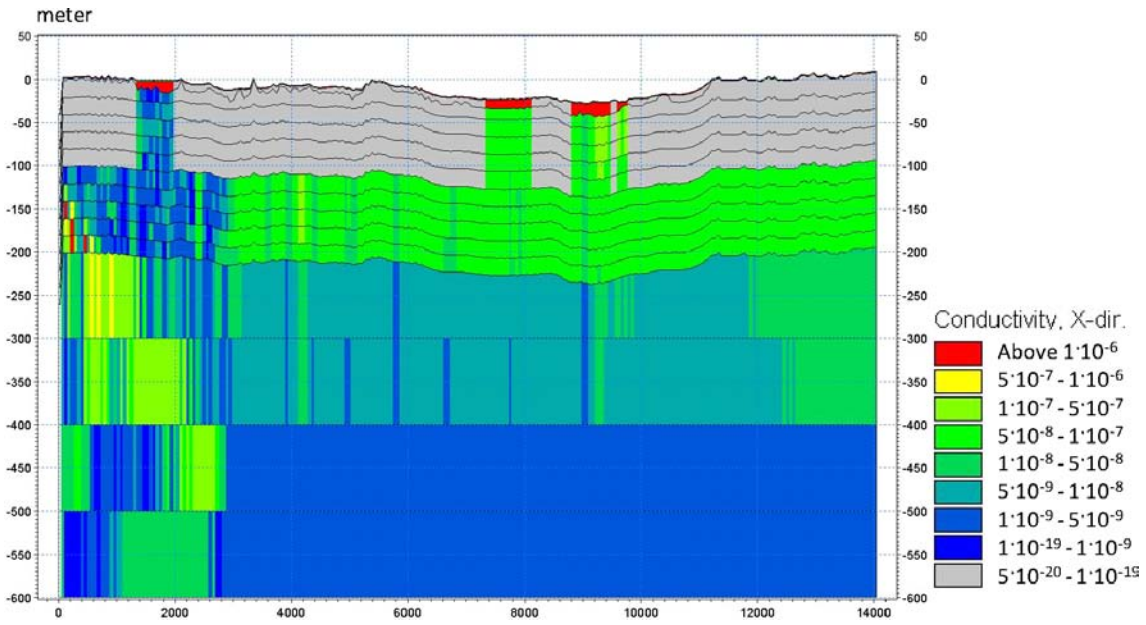

Figure 4-3. *Profile with horizontal conductivity and calculation layers used in the simulation case with 100 m permafrost.*

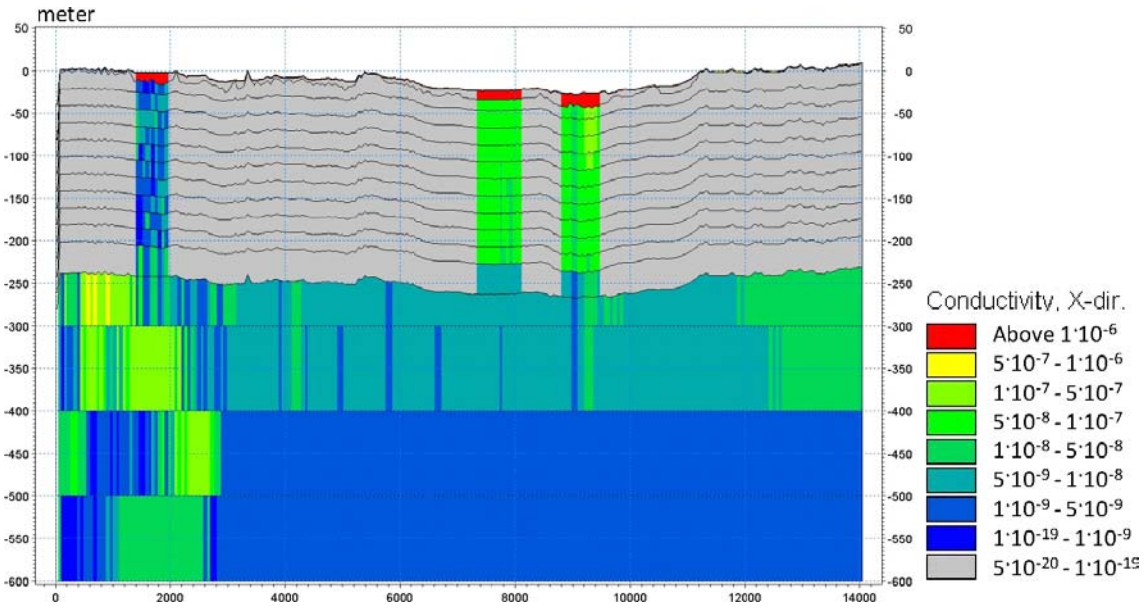

Figure 4-4. *Profile with horizontal conductivity and calculation layers used in the simulation case with 240 m permafrost.*

Table 4-3. Layers in the regional models for temperate climate and permafrost conditions (240 m and 100 m permafrost cases).

Layers in regional model 10000AD_10000QD			Layers in case with 100 m thick permafrost			Layers in case with 240 m thick permafrost		
Name	**Mean thick-ness**	**Mean lower level**	**Name**	**Mean thick-ness**	**Mean lower level**	**Name**	**Mean thick-ness**	**Mean lower level**
QD1	2.5	–10.3	Active	1.0	–8.8	Active	1.0	–8.8
QD2	4.1	–14.4	Permafrost	5.6	–14.4	Permafrost	5.6	–14.4
B1_CF5	17.4	–31.8	Permafrost	17.4	–31.8	Permafrost	17.4	–31.8
B2_CF6	20.0	–51.8	Permafrost	20.0	–51.8	Permafrost	20.0	–51.8
B3_CF7	20.0	–71.8	Permafrost	20.0	–71.8	Permafrost	20.0	–71.8
B4_CF8	20.0	–91.8	Permafrost	20.0	–91.8	Permafrost	20.0	–91.8
B5_CF9	20.0	–111.8	Permafrost	20.0	–111.8	Permafrost	20.0	–111.8
B6_CF10	20.0	–131.8	Unfrozen	20.0	–131.8	Permafrost	20.0	–131.8
B7_CF11	20.0	–151.8	Unfrozen	20.0	–151.8	Permafrost	20.0	–151.8
B8_CF12	20.0	–171.8	Unfrozen	20.0	–171.8	Permafrost	20.0	–171.8
B9_CF13	20.0	–191.8	Unfrozen	20.0	–191.8	Permafrost	20.0	–191.8
B10_CF14	20.0	–211.8	Unfrozen	20.0	–211.8	Permafrost	20.0	–211.8
B11_CF15	88.2	–300	Unfrozen	88.2	–300	Permafrost	36.0	–247.8
						Unfrozen	52.2	–300
B12_CF16	100.0	–400	Unfrozen	100.0	–400	Unfrozen	100.0	–400
B13_CF17	100.0	–500	Unfrozen	100.0	–500	Unfrozen	100.0	–500
B14_CF18	100.0	–600	Unfrozen	100.0	–600	Unfrozen	100.0	–600

For the case with a permafrost thickness of 240 m an additional boundary was placed at a depth of 240 m below the ground surface to define the lower level of the permafrost. Calculation layer 13 (B11_CF15 in Table 4-3) was subsequently divided into an upper permafrost part and a lower unfrozen part. A total of 12 calculation layers are frozen permafrost. The through taliks are active and never frozen and can be described as columns of unfrozen ground and water from the ground surface down to the unfrozen layers beneath the permafrost. The through taliks are described in the active and permafrost layers as always unfrozen windows. Three through taliks are in Figure 4-3 and 4-4 seen as vertical corridors through the grey permafrost formation and layers.

4.2.2 Vegetation

The vegetation map and vegetation types in the 10000AD_10000QD model are replaced by vegetation input reflecting permafrost conditions (see Section 2.7.2). The applied vegetation parameters vary over time as seen in Table 4-4. The different periods (Freeze 1, Freeze 2, etc) are defined in Section 3.5.

4.2.3 The surface stream network

The MIKE 11 setup used in the permafrost cases is identical to the setup applied in the regional model 10000AD_10000QD.

Table 4-4. Seasonal variations in leaf area index (LAI) and root depth reflecting permafrost conditions.

Date	Period	End day	Wetland and heath land		Barrens	
			LAI	Root depth	LAI	Root depth
Start 1/10	Freeze 1		1	0	0	0
End 16/10	Freeze 1	15	0	0	0	0
Start 16/10	Freeze 2	16	0	0	0	0
End 31/10	Freeze 2	30	0	0	0	0
Start 31/10	Frozen	31	0	0	0	0
End 23/4	Frozen	205	0	0	0	0
Start 23/4	Thaw 1	206	0	0	0	0
End 8/5	Thaw 1	220	0	0	0	0
Start 8/5	Thaw 2	221	0.75	1	0	0
End 23/5	Thaw 2	235	0.75	1	0	0
Start 23/5	Thaw 3	236	0.75	1	0	0
End 7/6	Thaw 3	250	0.75	1	0	0
Start 7/6	Active	251	0.75	1	0	0
End 1/10	Active	366	0.75	1	0	0

4.2.4 Overland flow

In the 10000AD_10000QD model, full contact between the saturated zone and overland is applied in the entire model catchment. In the permafrost cases reduced contact is introduced to decrease the infiltration capacity when the ground is frozen. This is done through the overland-groundwater leakage coefficient during the freeze, frozen and initial thaw periods, see Table 4-5. During the other periods and always in the taliks, full contact is attained through a high leakage coefficient, which means that the infiltration capacity is the same as under temperate climate conditions.

With the same principles as for the leakage coefficient, the constant value of the Manning number (M) used in the temperate 10000AD_10000QD model is modified during the freeze, frozen and initial thaw periods, see Table 4-6. This is done to avoid water to flow on the surface when the temperature is below zero and, consequently, the water is frozen. The water in the overland compartment of the model cannot freeze; thus, the flow resistances during the freeze periods and the first thaw period are set very high so that the water cannot be routed downhill.

Table 4-5. Variations in overland leakage coefficient (i.e. infiltration capacity) reflecting permafrost conditions. The overland leakage coefficient influences the infiltration capacity of the soil.

	Freeze 1	Freeze 2	Frozen	Thaw 1	Thaw 2	Thaw 3	Active
Overland-groundwater leakage coefficient outside taliks	$1 \cdot 10^{-7}$	$1 \cdot 10^{-20}$	$1 \cdot 10^{-20}$	$1 \cdot 10^{-7}$	0.1	0.1	0.1
Overland-groundwater leakage coefficient in taliks	0.1	0.1	0.1	0.1	0.1	0.1	0.1

Table 4-6. Variation in overland flow Manning numbers reflecting permafrost conditions.

	Freeze 1	Freeze 2	Frozen	Thaw 1	Thaw 2	Thaw 3	Active
Manning number outside taliks	$5 \cdot 10^{-6}$	$1 \cdot 10^{-19}$	$1 \cdot 10^{-19}$	$5 \cdot 10^{-6}$	5	5	5
Manning number in taliks	5	5	5	5	5	5	5

4.2.5 The unsaturated zone

The specific yield of the top layer in the saturated zone is always calculated from the hydraulic properties of the QD in the unsaturated zone. This calculation is performed at the start of a simulation and the hydraulic parameters applied depend on where the initial water table is positioned in each soil profile column and the QD type present at that level, see Section 2.4 and Table 4-7. Since the cyclic modelling scheme is based on continuous hot starts, a new specific yield will be calculated at the start of each simulation depending on where the groundwater level is situated. When the specific yield is not kept constant through all of the simulations a numerical error will be introduced and reflected in the simulation results. To avoid this inconsistency a simplified QD profile column in the unsaturated zone has been applied where only one QD type can be present. Note that the unsaturated zone numerically only is present in the top calculation layer which has a thickness of one metre. Therefore, only the QD type in the uppermost metre of the profile is of interest.

To simulate the freeze, ground frost and thaw processes in the unsaturated zone the saturated hydraulic conductivity (Ks) of each QD type has been altered step by step by dividing the Ks with specified factors (Table 4-8), which also are applied to the conductivities in the saturated zone to when the soil is freezing or thawing. The minimum Ks is limited to $1 \cdot 10^{-10}$ m/s. Lower values can introduce instabilities during model calculations and are therefore not recommended. The unsaturated zone in the through taliks is described as active/unfrozen throughout all simulated periods.

Table 4-7. UZ columns in the regional model and in the permafrost cases.

	QD profile definition in the 10000AD_10000QD model		QD profile definition in the permafrost cases	
QD profile columns	**QD types in QD profile**	**Depth**	**QD types in simplified UZ column**	**Depth**
Bedrock	Soil on bedrock	0.1	Bedrock	20
	Bedrock	20		
Till	Coarse till 0–0.5m	0.5	Coarse till 0–0.5m	20
	Coarse till 0.5–2m	2		
	Fine till	20		
Glacial clay	Clay	1	Clay	20
	Coarse till 0.5–2m	2		
	Fine till	20		
Artificial fill	Coarse till 0–0.5m	0.5	Coarse till 0–0.5m	20
	Coarse till 0.5–2m	2		
	Fine till	20		
Postglacial clay	Clay	1	Clay	20
	Fine till	20		
Thin glacial clay with thin layer of peat	Peat	2	Peat	20
	Clay	4		
	Fine till	20		

Table 4-8. Step by step changes in the saturated hydraulic conductivity (Ks) in the different QD types present in the unsaturated zone to reflect permafrost conditions.

Period / QD type	Active Ks	Freeze 1 Ks/30	Freeze 2 Ks/300	Frozen Ks_{min}	Thaw 1 Ks/1,000	Thaw 2 Ks/100	Thaw 3 Ks/10
Bedrock	$1.00 \cdot 10^{-10}$	$1.00 \cdot 10^{-10}$	$1.00 \cdot 10^{-10}$	$1.00 \cdot 10^{-10}$	$1.00 \cdot 10^{-10}$	$1.00 \cdot 10^{-10}$	$1.00 \cdot 10^{-10}$
Till	$3.00 \cdot 10^{-5}$	$1.00 \cdot 10^{-6}$	$1.00 \cdot 10^{-7}$	$1.00 \cdot 10^{-10}$	$3.00 \cdot 10^{-8}$	$3.00 \cdot 10^{-7}$	$3.00 \cdot 10^{-6}$
Clay	$1.00 \cdot 10^{-8}$	$3.33 \cdot 10^{-10}$	$1.00 \cdot 10^{-10}$	$1.00 \cdot 10^{-10}$	$1.00 \cdot 10^{-10}$	$1.00 \cdot 10^{-10}$	$1.00 \cdot 10^{-9}$
Peat	$1.00 \cdot 10^{-6}$	$3.33 \cdot 10^{-8}$	$3.33 \cdot 10^{-9}$	$1.00 \cdot 10^{-10}$	$1.00 \cdot 10^{-9}$	$1.00 \cdot 10^{-8}$	$1.00 \cdot 10^{-7}$

Table 4-9. Vertical discretisation in the unsaturated zone profiles.

Vertical discretisation in the QD profiles in the 10000AD_10000QD model		Vertical discretisation in the QD profiles in the permafrost cases	
Cell height (m)	**Number of cells**	**Cell height (m)**	**Number of cells**
0.1	10	0.05	8
		0.1	6
0.5	8	0.5	8
1	5	1	5
2	5	2	5

The vertical discretisation in the 10000AD_10000QD model has been refined with smaller intervals in the upper soil to give a better resolution in the unsaturated zone in order to capture the processes in the active layer. The discretisations of the models for temperate and permafrost conditions are shown in Table 4-9. The calculation cells in the unsaturated zone are defined according to the same methodology as for temperate climate, see Section 4.1.3. This means that the unsaturated zone calculations are only carried out in a number of representative cells. An exception is made to lake and wetland areas where the calculations are carried out in all cells.

4.2.6 The saturated zone

Calculation layer 1 is the active layer for which the horizontal and vertical conductivities are altered step by step during the different simulation periods (Table 4-10). The layers defined as permafrost have a constant and very low hydraulic conductivity ($1 \cdot 10^{-20}$ m/s). This means that in the case with a permafrost thickness of 100 m layers 2–7 have this very low and constant conductivity, whereas layers 2–13 have this low conductivity in the case with 240 m of permafrost. One exception is the windows produced by the through taliks where the conductivity is kept unchanged. The calculation layers beneath the permafrost layers (layer 8–16 with a permafrost thickness of a 100 m, layer 14–17 with a permafrost thickness of 240 m) are always unfrozen and have conductivities according to the 10000AD_10000QD model.

Since the drainage time constant is related to the hydraulic conductivity in the upper calculation layer, the drainage time constant used in the 10000AD_10000QD temperate model is modified according to the new K-values in Table 4-10. No drainage is applied in cells defined as through taliks. The drainage time constants for all periods are listed in Table 4-11.

Table 4-10. Variations in horizontal and vertical conductivity in the different saturated layers to reflect permafrost conditions.

	Freeze 1	Freeze 2	Frozen	Thaw 1	Thaw 2	Thaw 3	Active
Horizontal and vertical conductivity (K) in active layer	K/30	K/300	$1 \cdot 10^{-20}$	K/1,000	K/100	K/10	K
Horizontal and vertical conductivity (K) in permafrost layers	$1 \cdot 10^{-20}$	$1 \cdot 10^{-20}$	$1 \cdot 10^{-20}$	$1 \cdot 10^{-20}$	$1 \cdot 10^{-20}$	$1 \cdot 10^{-20}$	$1 \cdot 10^{-20}$
Horizontal and vertical conductivity (K) in taliks	K	K	K	K	K	K	K
Horizontal and vertical conductivity (K) in unfrozen layers beneath the permafrost	K	K	K	K	K	K	K

Table 4-11. Variations in the drainage time constant reflecting permafrost conditions.

	Freeze 1	Freeze 2	Frozen	Thaw 1	Thaw 2	Thaw 3	Active
Drainage time constant (TC)	TC/30	TC/300	1E–20	TC/1,000	TC/100	TC/10	TC
Drainage time constant (TC) in taliks	0	0	0	0	0	0	0

4.2.7 Initial and boundary conditions and time stepping

No changes in the outer boundary conditions have been made compared to the 10000AD_10000QD model for temperate conditions. The initial conditions at the start of each simulation period are extracted by using a hot start from the previous model simulation. Table 4-12 shows the time steps and model control parameters used in the permafrost modelling.

Table 4-12. Time steps and model control parameters for regional models with permafrost, OL = overland flow, SZ = saturated zone, UZ = unsaturated zone, and ET = evapotranspiration.

Parameter	Value
Initial time step	1.0 h
Maximum allowed OL, UZ, ET time step	1.0 h
Maximum allowed SZ time step	3.0 h
MIKE 11 time step	5 s
Maximum Courant number OL	0.75
Maximum profile water balance error, UZ/SZ coupling	0.001 m
Maximum allowed UZ iterations	50
Iteration stop criteria	0.005 m
Time step reduction control: Maximum water balance error in one node (fraction)	0.05
Maximum allowed SZ iterations	80
Maximum head change per SZ iteration	0.05 m
Maximum SZ residual error	0.005 m/d
Saturated thickness threshold	0.05 m

4.3 Local flow models for temperate conditions

4.3.1 Model domains and grids

Two different local models, denoted local model A and B, were created within the regional model area in order to make more detailed studies of areas that received many discharge points in the ConnectFlow modelling. In both local models, the numerical grid size was reduced from 80×80 m to 20×20 m. Furthermore, the number of calculation layers was increased from 14 layers to 24 layers in the local models. Tables 4-13 and 4-14 show the mean thicknesses and mean lower levels of the calculation layers in both the regional and the local models.

In both of the local models, the lower QD layer was divided into two separate layers. In addition, the two uppermost bedrock layers were divided into four layers each, with an approximate thickness of 5 m. Also the third bedrock layer was divided, but only into two layers with thicknesses of 10 m each. The differences in mean thickness and mean lower level between the local and regional models given in Table 4-13 and 4-14 depend on the differences in the grid size. The mean elevation of the topography in the 80×80 m DEM and the 20×20 DEM is not the same and consequently the lower level of each calculation layer is not exactly the same in the regional and local models. For example, the lower level of QD1 in the regional model is –4.9 m whereas the lower level of QD1 in the local models is –4.6 m.

The locations of the two local models, A and B, within the regional model area are illustrated in Figure 3-2. The local model A is the model that includes biosphere objects 118, 120 and 121. This model has an area of approximately 15.6 km^2 and c. 39,000 grid cells. Local model B is the model that includes biosphere object 116. This model has an area of approximately 17.3 km^2 and c. 43,000 grid cells. The two local models are overlapping each other. The reason for this is that the boundaries of the local models are set some distance from the surface water divides surrounding each one of the local models. This is done to avoid boundary effects in the area of interest for the transport calculations.

Table 4-13. Calculation layers in the regional model and in local model A (containing biosphere objects 118, 120 and 121).

Layers in regional model; local model area			Layers in local model; Objects 118, 120, and 121		
Name	**Mean thickness**	**Mean lower level**	**Name**	**Mean thickness**	**Mean lower level**
QD1	2.6	-4.9	QD1	2.4	-4.6
QD2	2.7	-7.6	QD2_1	0.9	-5.5
			QD2_2	2.0	-7.5
B1_CF5	18.1	-25.7	B1_CF5_1	4.2	-11.7
			B1_CF5_2	4.6	-16.3
			B1_CF5_3	4.6	-20.9
			B1_CF5_4	4.6	-25.5
B2_CF6	20.0	-45.7	B2_CF6_1	5.0	-30.5
			B2_CF6_2	5.0	-35.5
			B2_CF6_3	5.0	-40.5
			B2_CF6_4	5.0	-45.5
B3_CF7	20.0	-65.7	B3_CF7_1	10.0	-55.5
			B3_CF7_2	10.0	-65.5
B4_CF8	20.0	-85.7	B4_CF8	20.0	-85.5
B5_CF9	20.0	-105.7	B5_CF9	20.0	-105.5
B6_CF10	20.0	-125.7	B6_CF10	20.0	-125.5
B7_CF11	20.0	-145.7	B7_CF11	20.0	-145.5
B8_CF12	20.0	-165.7	B8_CF12	20.0	-165.5
B9_CF13	20.0	-185.7	B9_CF13	20.0	-185.5
B10_CF14	20.0	-205.7	B10_CF14	20.0	-205.5
B11_CF15	94.3	-300.0	B11_CF15	94.5	-300.0
B12_CF16	100.0	-400.0	B12_CF16	100.0	-400.0
B13_CF17	100.0	-500.0	B13_CF17	100.0	-500.0
B14_CF18	100.0	-600.0	B14_CF18	100.0	-600.0

Table 4-14. Calculation layers in the regional model and in local model B (containing biosphere object 116).

Layers in regional model; local model area			Layers in local model; Object 116		
Name	**Mean thickness**	**Mean lower level**	**Name**	**Mean thickness**	**Mean lower level**
QD1	2.6	-11.6	QD1	2.4	-11.3
QD2	3.1	-14.7	QD2_1	1.9	-13.2
			QD2_2	1.6	-14.8
B1_CF5	17.9	-32.6	B1_CF5_1	4.2	-19.0
			B1_CF5_2	4.5	-23.5
			B1_CF5_3	4.5	-28.0
			B1_CF5_4	4.5	-32.5
B2_CF6	20.0	-52.6	B2_CF6_1	5.0	-37.5
			B2_CF6_2	5.0	-42.5
			B2_CF6_3	5.0	-47.5
			B2_CF6_4	5.0	-52.5
B3_CF7	20.0	-72.6	B3_CF7_1	10.0	-62.5
			B3_CF7_2	10.0	-72.5
B4_CF8	20.0	-92.6	B4_CF8	20.0	-92.5
B5_CF9	20.0	-112.6	B5_CF9	20.0	-112.5
B6_CF10	20.0	-132.6	B6_CF10	20.0	-132.5
B7_CF11	20.0	-152.6	B7_CF11	20.0	-152.5
B8_CF12	20.0	-172.6	B8_CF12	20.0	-172.5
B9_CF13	20.0	-192.6	B9_CF13	20.0	-192.5
B10_CF14	20.0	-212.6	B10_CF14	20.0	-212.5
B11_CF15	87.4	-300.0	B11_CF15	87.5	-300.0
B12_CF16	100.0	-400.0	B12_CF16	100.0	-400.0
B13_CF17	100.0	-500.0	B13_CF17	100.0	-500.0
B14_CF18	100.0	-600.0	B14_CF18	100.0	-600.0

The local models were only used for water flow simulations with the selected normal year and for the 10,000 AD shoreline case. However, for local model A (objects 118, 120 and 121) both the 2000 QD model and the 10,000 QD model were used, i.e. two cases of the model A domain were modelled. The motivation for using both QD models in the calculations is that the influence of the development of the QD on the transport pattern in the surface and near-surface systems needs to be investigated. The most correct description of the QD-layers in a possible future in Forsmark is the QD-model where the sedimentation processes are taken into consideration, i.e. the 10,000 QD model.

The two different QD models are applied to the 10,000 AD model in order to analyse the sensitivity to the geometry and stratigraphy of the QD. Figures 4-5 and 4-6 show the topography of the two different cases. Although the general pattern for the topography is the same, there are a few important differences. For example, the inlet canal is not as deep in the 10,000 QD model as in the 2000 QD model. Furthermore, the area north of the inlet canal differs between the two QD models; in the 10,000 AD model this area is significantly lower than in the 2000 QD model. Figure 4-7 shows the local topography for the local model for object 116. It should be noted that the scale of the topography is given in RHB 70 meaning that both local models are above the shoreline 10,000 AD.

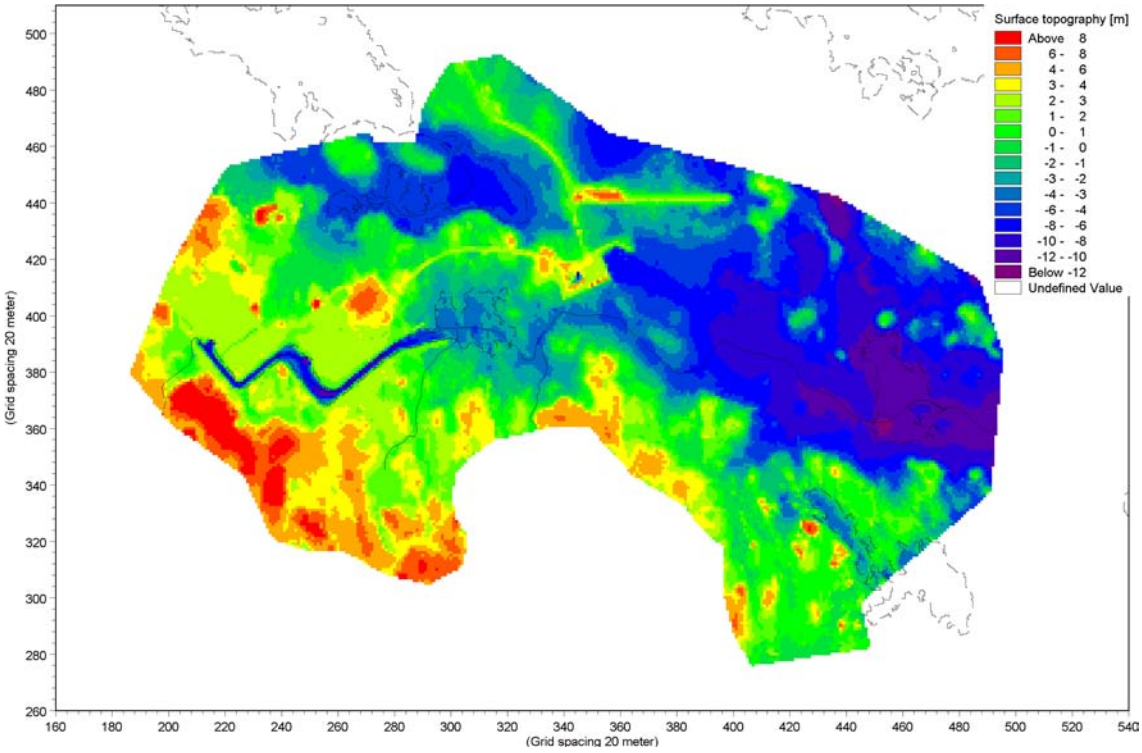

Figure 4-5. *Surface topography of local model A (biosphere objects 118, 120 and 121), based on the 2000 QD model.*

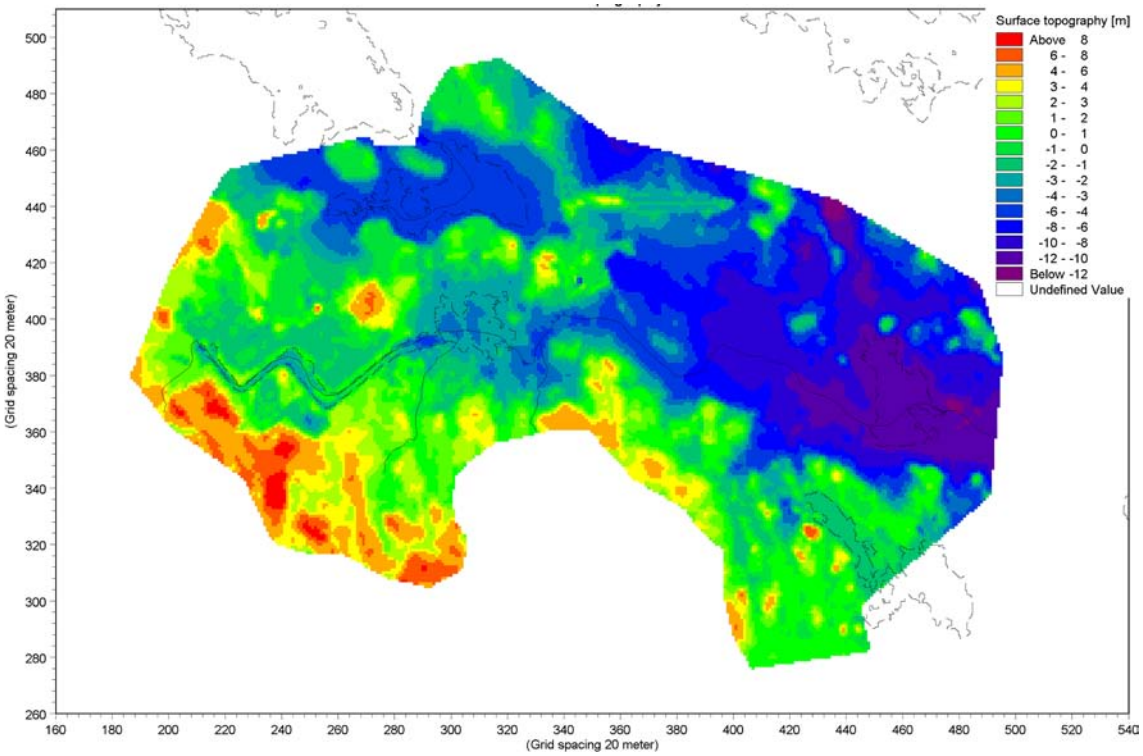

Figure 4-6. *Surface topography of local model A (objects 118, 120 and 121), based on the 10,000 QD model.*

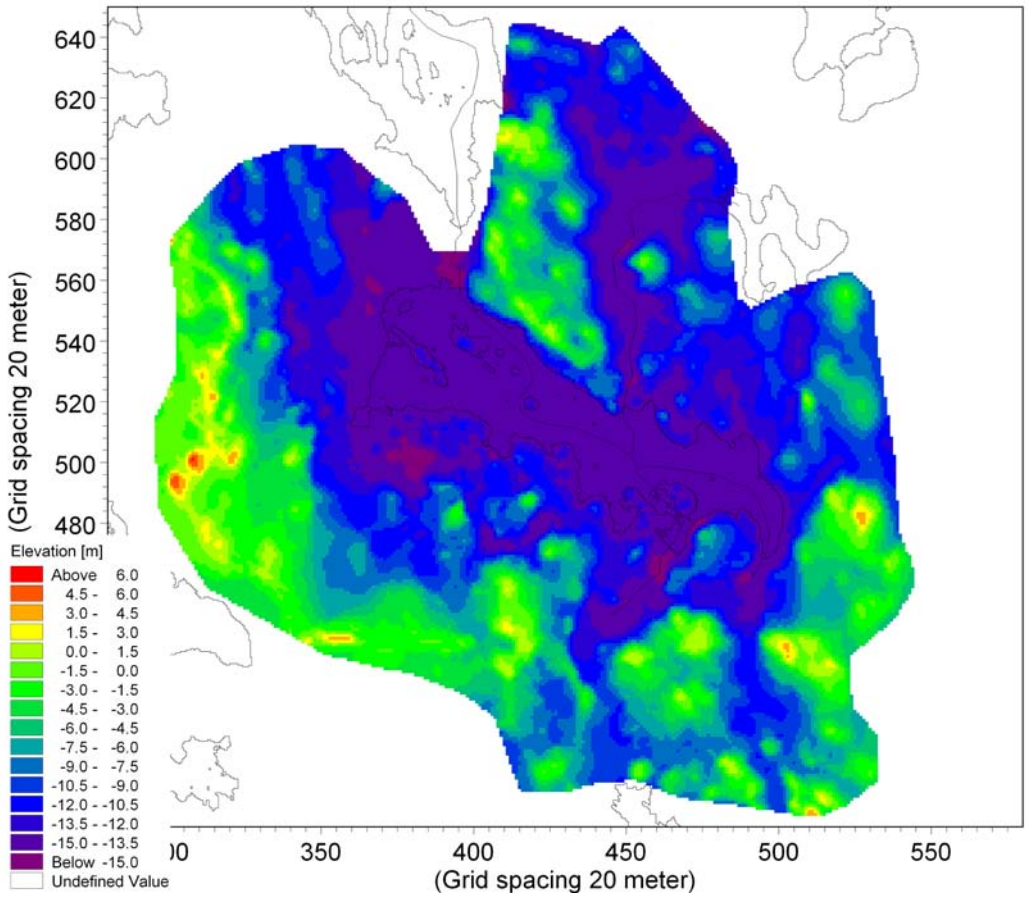

Figure 4-7. *Surface topography of local model B (object 116).*

4.3.2 The surface stream network

In local model A, the surface stream network model was updated with regard to the finer discretisation of the topography, but based on the stream branches in the regional model. Figure 4-8 shows the surface stream network. More surface stream cross sections were added to the model. At the upstream model boundaries, calculated surface water discharges from the regional model were set as boundary conditions. At the downstream boundary of the main stream, a time-varying water level, obtained from the regional model, was applied. In total, the local MIKE 11 model contains 78 cross sections and the total length of the branches is 11.2 km.

Figure 4-8 also shows the surface stream network in the model including object 116 (model B). In the regional model, the area situated downstream of the area of local model B consists of several lakes before the sea is reached. In order to get a downstream boundary that does not affect the upstream area, the MIKE 11 surface stream branch was extended further downstream of the local model boundary. Since the entire area for object 116, has a flat topography there is no need for many cross sections along the main MIKE 11 branch. In total, the local MIKE 11 model in Figure 4-8 contains 25 cross sections and the total length of the branches is 10.8 km.

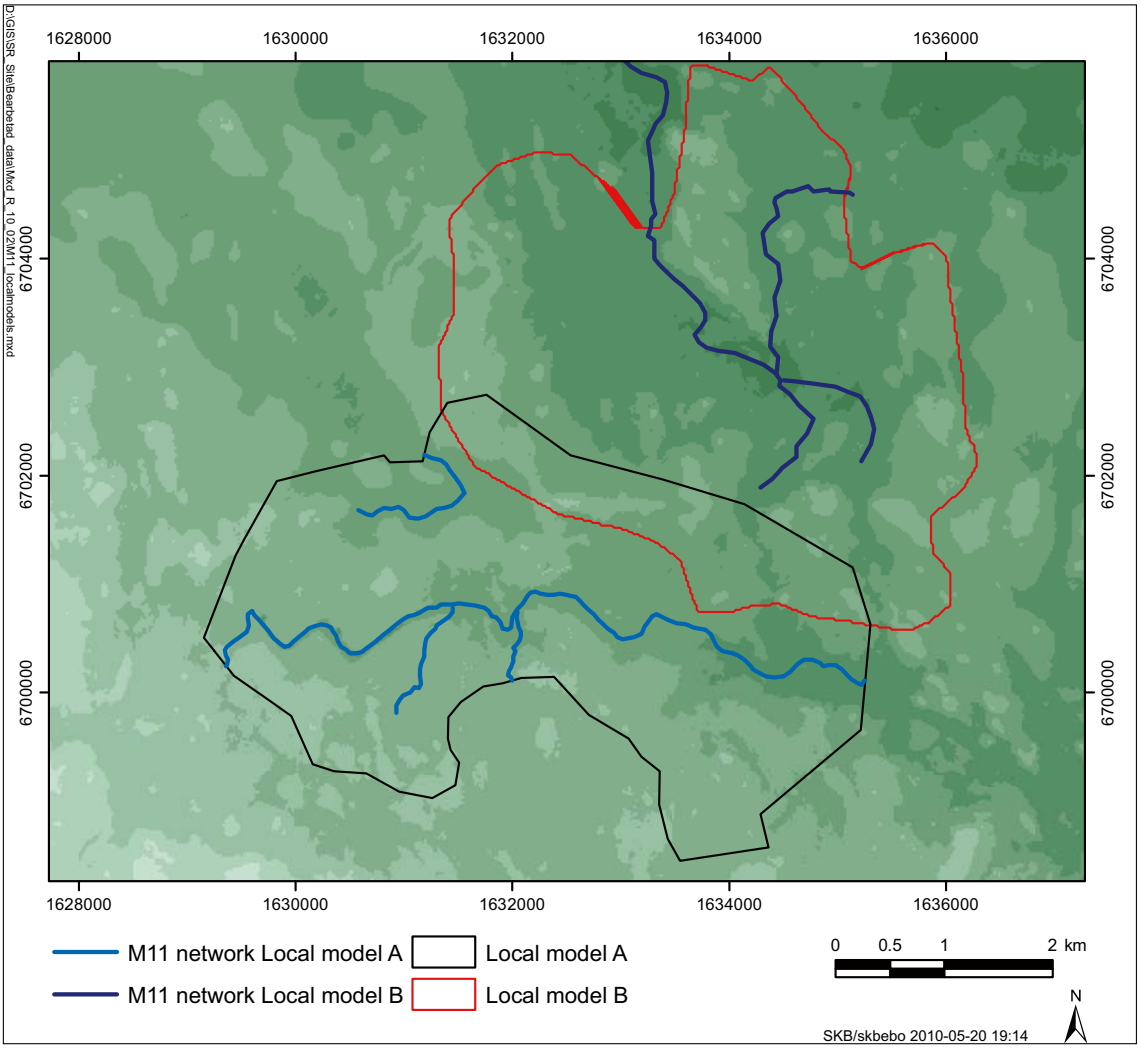

Figure 4-8. *Surface stream network in the areas of local models A and B.*

4.3.3 The unsaturated zone

The description of the unsaturated zone in the local models was made in the same way as in the regional model, although based on input data with a grid size of 20 m instead of 80 m. The codes and vertical discretisations are the same for the local models as for the regional model.

4.3.4 The saturated zone

For the bedrock, all parameters are the same for the local models as for the regional model. Since the main objective with the local models is to study the transport pattern close to the surface it was decided that the horizontal discretisation of the geological description of the bedrock was sufficient based on the regional model, i.e. the hydraulic properties of the bedrock are described on a 80×80 m grid. The properties of the QD layers on the other hand, were implemented based on a 20 m grid size. The numerical grid used in the calculations is 20×20 m in the whole model, which means that the geological model of the bedrock described on 80 m×80 m grid is interpolated to the 20×20 calculation grid.

All QD codes for the local model were set up in the same way as for the regional model. Since the purpose of the local model is to study the transport in connection to the lake areas, the uppermost calculation layer was given a thickness of 2.5 m in all areas except under the lakes. Under the lakes the thickness of the uppermost layer is equal to the thickness of the lake sediments. For the local model A, and with the 2000 QD model, the thickness of the lake sediments was calculated as the total sum for all QD layers L1 to Z4b. For the same local model, but using on the 10,000 QD model, the thickness was calculated as the difference between the topography and the lower level of the marine sediments.

Figures 4-9 and 4-10 show the resulting thicknesses of the two QD models for the local model including objects 118, 120, and 121 (model A). For the present-day (2000 AD) QD model, thick sediments are mainly found in object 121_01, but also in the south-eastern part of object 118. In general, the thickness of the sediments is smaller in the QD model for 10,000 AD. The thickest sediments are found in the inlet canal. For object 118, the sediments have approximately the same thickness in the 10,000 AD model as in the 2000 AD model, although the sediments are located in the middle of the lake for the 10,000 AD model. For object 121_01 the sediment thickness is less than 2.5 m in the entire object for the 10,000 AD model.

Figure 4-11 shows the thickness of the uppermost calculation layer in local model B. A large part of the lake area has only a thin sediment layer. In the central part of object 116, however, the sediment thickness is several meters.

4.3.5 Initial and boundary conditions and time stepping

In order to get accurate boundary conditions for the local models, the outer boundary conditions were extracted from the regional flow model. For each calculation layer, files with time-varying head elevations in the saturated zone were extracted and added as boundary conditions in the local models.

Initial conditions in terms of initial head elevations and initial depths of overland water were also extracted from the regional models. Table 4-15 shows the time steps and model control parameters used in both of the local models.

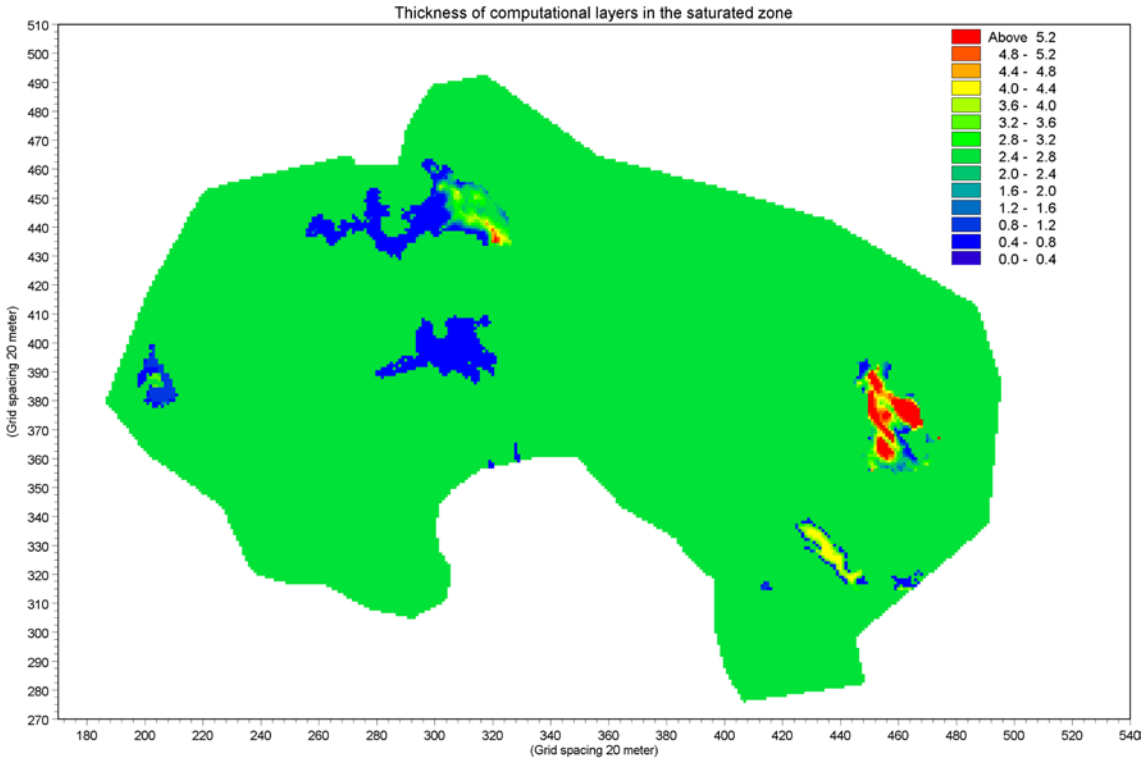

Figure 4-9. *Thickness of the uppermost calculation layer in the 10000AD_2000QD version of local model A (objects 118, 120 and 121).*

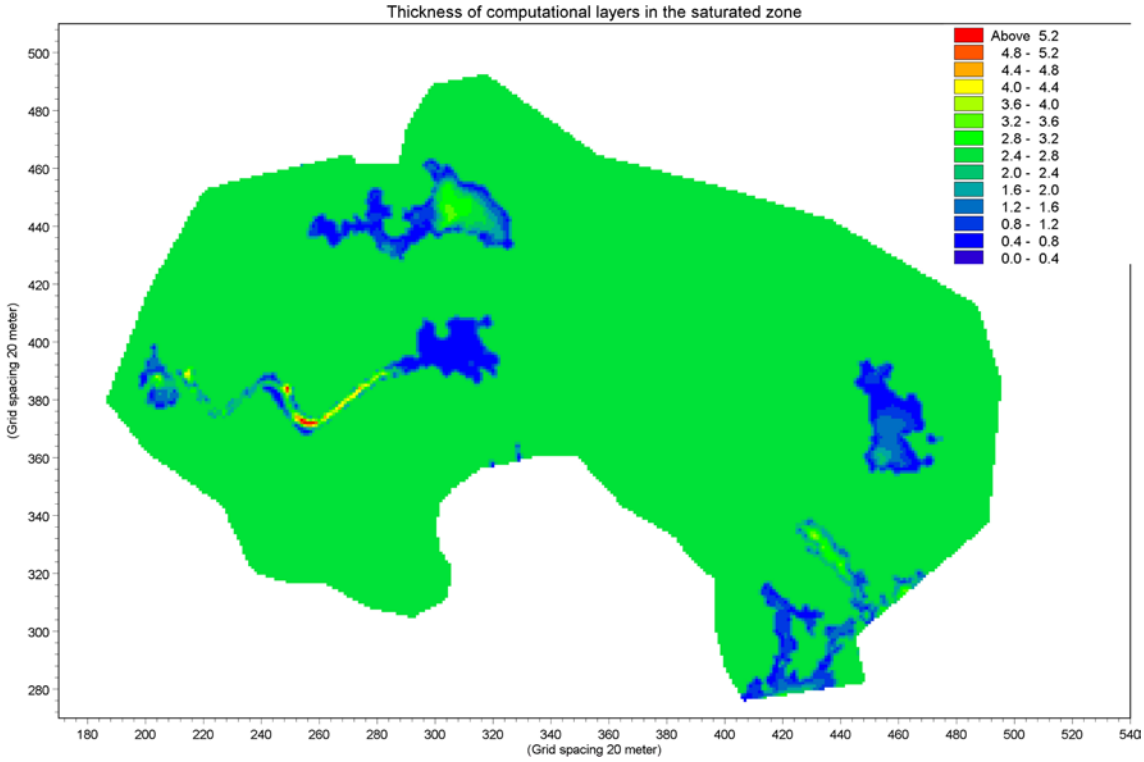

Figure 4-10. *Thickness of the uppermost calculation layer in the 10000AD_10000QD version of local model A (objects 118, 120 and 121).*

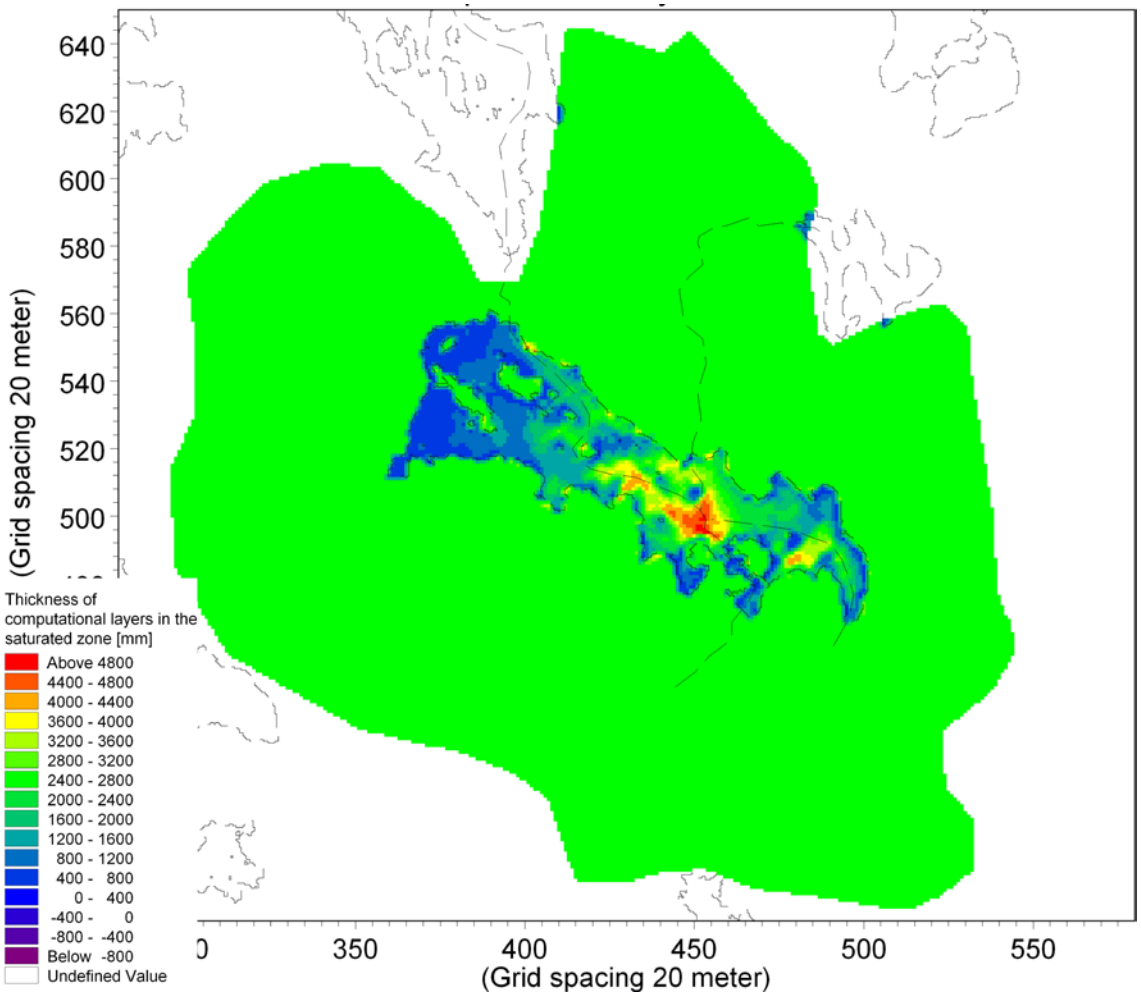

Figure 4-11. *Thickness of the uppermost calculation layer in local model B (object 116).*

Table 4-15. Time steps and model control parameters used in the local models; OL = overland flow, SZ = saturated zone, UZ = unsaturated zone, and ET = evapotranspiration.

Parameter	Value
Initial time step	0.5 h
Maximum allowed OL, UZ, ET time step	0.5 h
Maximum allowed SZ time step	1.5 h
MIKE 11 time step	5 s
Maximum Courant number OL	0.75
Maximum profile water balance error, UZ/SZ coupling	0.001 m
Maximum allowed UZ iterations	50
Iteration stop criteria	0.002 m
Time step reduction control: Maximum water balance error in one node (fraction)	0.03
Maximum allowed SZ iterations	80
Maximum head change per SZ iteration	0.01 m
Maximum SZ residual error	0.0001 m/d
Saturated thickness threshold	0.05 m

5 Results from regional model for normal temperate conditions

In this chapter, flow and transport modelling results for the regional model are presented for present and future conditions with a climate corresponding to the present climate. The flow modelling results are presented in Section 5.1 and Section 5.2. In Section 5.3, transport simulation results from particle tracking are presented.

5.1 Flow modelling cases

Shorelines positions and QD models corresponding to three different points of time, i.e. 2000 AD, 5000 AD and 10,000 AD, have been used when describing the hydrology at the Forsmark site today and in the future. Table 5-1 lists all the simulation cases from which results will be presented in the following sections.

The 2000AD_2000QD model (a model with shoreline and QD at 2000 AD) was run with meteorological data both from the selected year, defined in Section 2.3, and with meteorological input data from the whole site investigation period. The later was done to evaluate the differences between the SR-Site model and the SDM-Site Forsmark MIKE SHE model.

Table 5-1. The different simulation cases from which results will be presented in Section 5-2 and 5-3. The meteorological data period "selected year" is described in Chapter 2, section 2.3.

Simulation case	Time period (shoreline)	QD-model	Meteorological input data period
2000AD_2000QD_sitedata	2000 AD	2000 AD	15th May 2003 to 31th March 2007
2000AD_2000QD	2000 AD	2000 AD	Selected year
5000AD_2000QD	5000 AD	2000 AD	Selected year
5000AD_5000QD	5000 AD	5000 AD	Selected year
10000AD_2000QD	10,000 AD	2000 AD	Selected year
10000AD_10000QD	10,000 AD	10,000 AD	Selected year

5.2 Comparison with the SDM-Site model

To evaluate the effect on the MIKE SHE model when updating the SDM model, especially the increase of the horizontal grid spacing from 40 m to 80 m, the 2000AD_2000QD model was run with the same input data as the SDM-Site MIKE SHE model /Bosson et al. 2008/. The results were compared to measured surface water and groundwater levels and surface water discharges. The aim with running the SR-Site MIKE SHE model with the same meteorological input data as in the SDM-Site MIKE SHE model was to test and compare the model performance. It was investigated if the same agreement between measured and calculated water levels and discharges in the surface water and groundwater was achieved with the new model version.

The drainage of the SFR repository was included in the model with an updated description of the tunnel system and repository, see /Gustafsson et al. 2009/ for a detailed description of the implementation of the SFR repository in the MIKE SHE model. It should be noted that the drainage of the SFR repository is only active in the case *2000AD_2000QD_sitedata.*

5.2.1 Pumping test responses

In the calibration process for the SDM site model, a pumping test performed in HFM14 was used to investigate the response in the saturated zone, see /Bosson et al. 2008, Section 6.2.2/. Since the results from the pumping test led to several model improvements of the SDM-Site model, the same pumping test was simulated in the SR-Site 2000AD_2000QD model. The results based on the original bedrock in the SR-Site model indicated that the bedrock hydraulic conductivity was too high; the calculated response in the monitoring wells was too small compared to measured drawdown. As a consequence, a new sensitivity analysis of the hydraulic properties of the bedrock was made for the SR-Site MIKE SHE model presented in this report. The results from the sensitivity analysis performed within the SDM work were used as supporting information when defining the new sensitivity cases to be run for the SR-Site MIKE SHE model.

In the SDM-Site MIKE SHE modelling it was concluded that the vertical conductivity in the upper bedrock had to be reduced to obtain the right magnitude of the drawdown in the observation wells. Also the specific storage had to be reduced to get the right response in the observation wells. Besides the original values for the vertical hydraulic conductivity, one case with values reduced by a factor of 2 and one case with values reduced by a factor of 5 were defined for the SR-Site MIKE SHE model. The changes in the conductivity values were only applied to the upper 200 m of the bedrock. All three cases were run with both the original values of the specific storage and with a constant value of $5 \cdot 10^{-9}$ m^{-1}.

It was found that the best results were obtained with the vertical bedrock hydraulic conductivity reduced by a factor of 2 and with the low constant saturated zone specific storage. For all monitoring wells situated on the same side of Lake Bolundsfjärden as the pumping well HFM14 (see Figure 2-21 in Section 2.8), the results were similar to those obtained with the SDM-Site model /Bosson et al. 2008/. Figure 5-1 shows a comparison of results from the SDM-Site model and the SR-Site model for monitoring well HFM2. The difference between the two models is small, although the modelled drawdown is somewhat smaller for the SR-Site model.

Figure 5-2 shows the same comparison for monitoring well HFM16, which is situated on the other side of Lake Bolundsfjärden. The drawdowns calculated with the two models differ significantly and the measured drawdown in HFM16 is not captured by the SR-Site model. The reason is that the sheet joints layers that are underlying Lake Bolundsfjärden are not as distinct in the SR-Site model as in the SDM-Site MIKE SHE model. The hydraulic conductivity within the sheet joints was increased in the SDM-Site model, whereas no such correction was made in the SR-Site MIKE SHE model.

For the sensitivity case with the vertical conductivity divided by a factor 5, the drawdown in the monitoring wells located close to HFM14 was increased and the drawdown was over-estimated compared to measured values. However, the wells located on the opposite side of Lake Bolundsfjärden this conductivity change did not affect the drawdown significantly and the drawdown was only slightly increased. Therefore, the reduction by a factor of 2 was considered to be the best case.

Table 5-2 shows a comparison between measured and modelled drawdowns based on the pumping test in HFM14 for both the SDM-Site model and the SR-Site model. For the evaluated monitoring wells, the mean values are very similar for the two models. However, for the SR-Site model the results show that the drawdown is underestimated for the monitoring wells located on the opposite side of Lake Bolundsfjärden, such as HFM4 and HFM16.

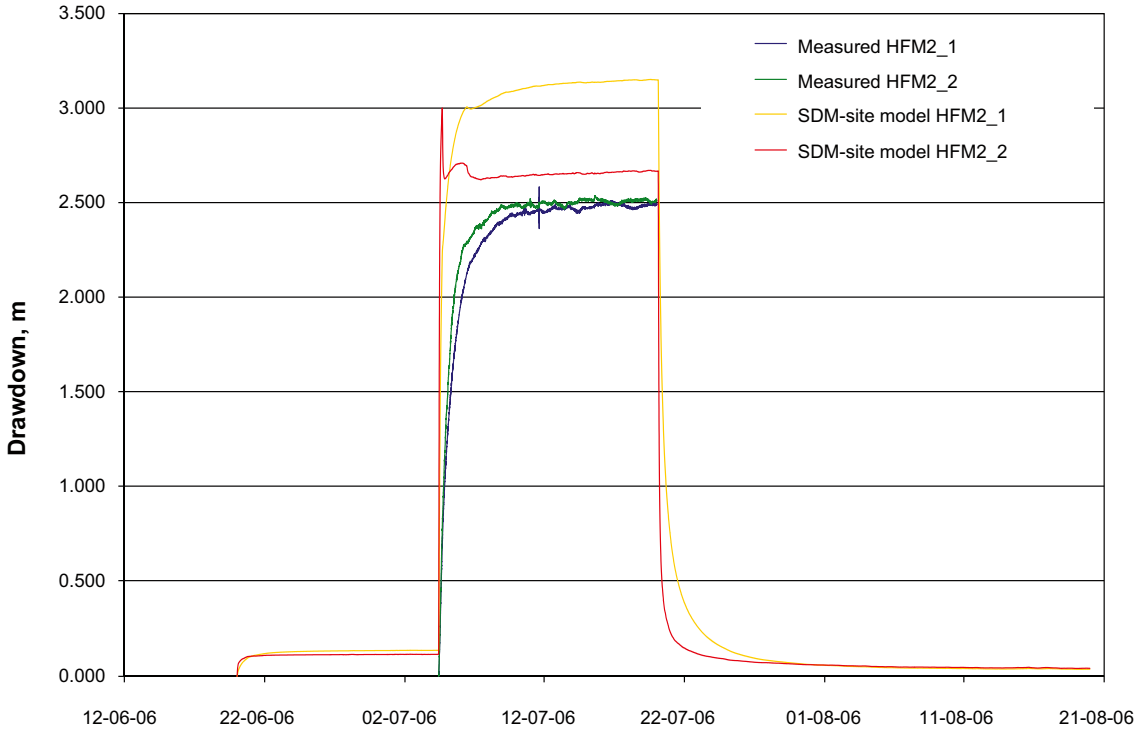

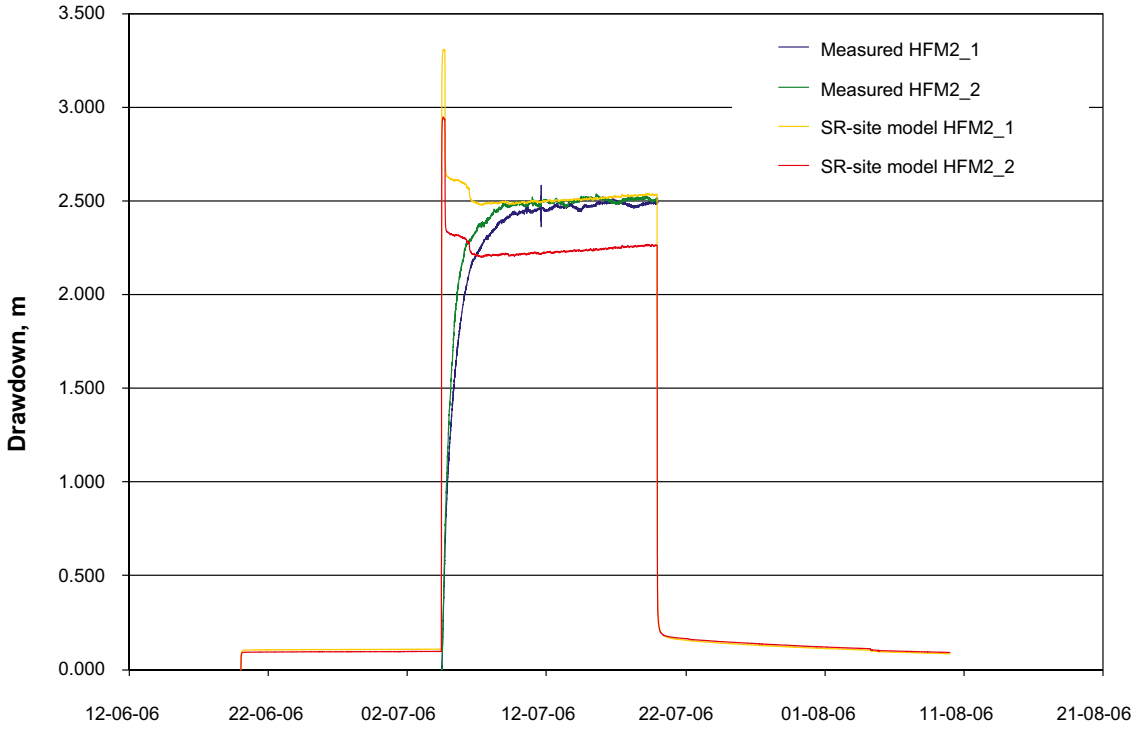

Figure 5.1. *Comparison between measured and modelled drawdowns in monitoring well HFM2 for the SDM-Site model and the SR-Site model, based on a pumping test in HFM14.*

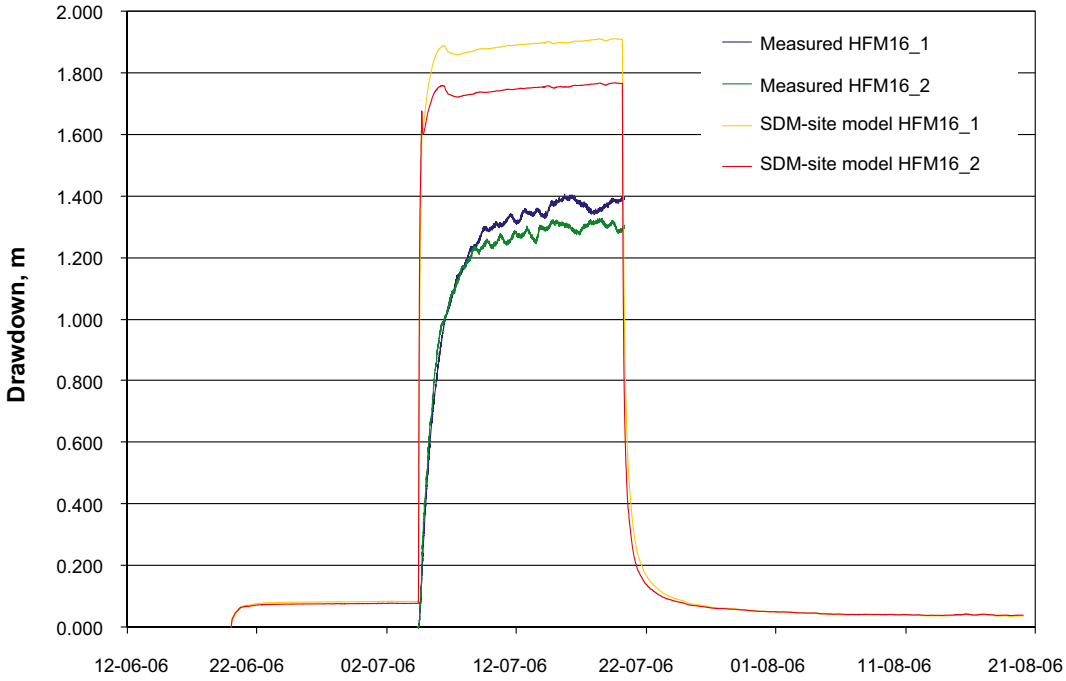

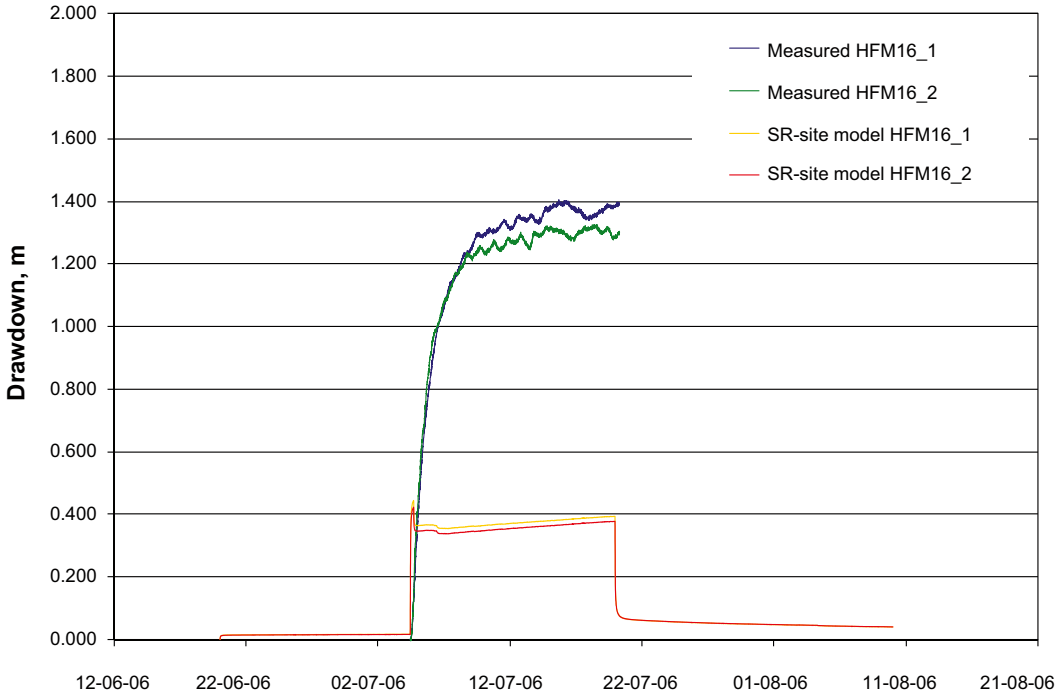

Figure 5-2. *Comparison between measured and modelled drawdowns in monitoring well HFM16 for the SDM-Site model and the SR-Site model, based on a pumping test in HFM14.*

Table 5-2. Comparison of maximum drawdowns in HFM-wells in the SDM-Site and SR-Site models calculated for the pumping test in HFM14.

HFM ID code	Measured	SDM-site model	SR-site model; Kv/2+const SS
HFM1_1	2.3	*2.8*	3.4
HFM1-2	2.3	*3*	3
HFM2_1	2.6	*2.9*	2.5
HFM2_2	2.5	*2.35*	2.3
HFM2_3	2.5	*2.35*	1.9
HFM3_1	2.4	*2.45*	0.85
HFM3_2	2.5	*2.45*	0.85
HFM4_1	0.2	*0.1*	0.16
HFM4_2	0.25	*0.08*	0.03
HFM4_3	0.1	*0.08*	0.02
HFM10_1	0.2	*0.6*	0.6
HFM10_2	0.2	*0.4*	0.7
HFM16_1	1.4	*1.7*	0.4
HFM16_2	1.3	*1.6*	0.4
HFM20_2	1	*1.4*	0.8
HFM20_3	1.3	*1.45*	0.7
HFM32_1	0.15	*1.85*	2.2
HFM32_2	0.17	*2.15*	2
HFM32-3	2	*0.86*	1.1
HFM13-2	5.8	*1.2*	3.6
HFM19_2	6.1	*3.15*	7.4
HFM9	0.25	*0.8*	0.3
mean	**1.71**	**1.62**	**1.60**

5.2.2 Surface water discharges

Figures 5-3 to 5-10 show a comparison between measurements, results from the SDM-Site model, and results from the SR-Site model for the surface water discharges in terms of discharge time series and accumulated water volumes. For Lake Gunnarsboträsket (Figures 5-7 and 5-8) and Lake Bolundsfjärden (Figures 5-9 and 5-10) the differences between the SDM-Site model and the SR-Site model are small. The peaks in the discharge are higher for the SR-Site model, but the differences in accumulated discharge are small.

For Lake Eckarfjärden (Figures 5-3 and 5-4) and Lake Stocksjön (Figures 5-6 and 5-7) the differences between the SDM-Site model and the SR-Site model are larger than for Lake Gunnarsboträsket and Lake Bolundsfjärden. The discharge peaks are higher for the SR-Site model than for the SDM-Site model, resulting in a larger volume of accumulated discharge. However, the general discharge pattern is still well reflected at all stations. Furthermore, for both Lake Eckarfjärden and Lake Stocksjön the accumulated discharge volume was underestimated for the SDM-Site model, whereas the results from the SR-Site model are overestimated compared to the measurements. Since the results for all four stations have errors within the same order of magnitude as the results from the SDM-Site model, the results were considered to be satisfactory and no further calibration was made.

There are two main reasons for the increased runoff: the change of the horizontal model resolution, which affects the drainage system in the model, and the updated bedrock properties. The drainage constant, TC, is dependent on the horizontal grid resolution and has to be calibrated. Small changes in the TC affect the amount of discharged water. The updated bedrock model causes higher groundwater levels in the bedrock than the groundwater levels obtained with the MIKE SHE SDM model. By increasing the hydraulic conductivity within the sheet joints, as was done in the SDM-Site model, the groundwater levels would decrease in the bedrock and the discharge of groundwater at the ground surface be reduced. Since the hydraulic conductivities within the sheet joints were not changed, the calculated groundwater levels are higher than the measured values and a higher groundwater discharge to the water courses occurs.

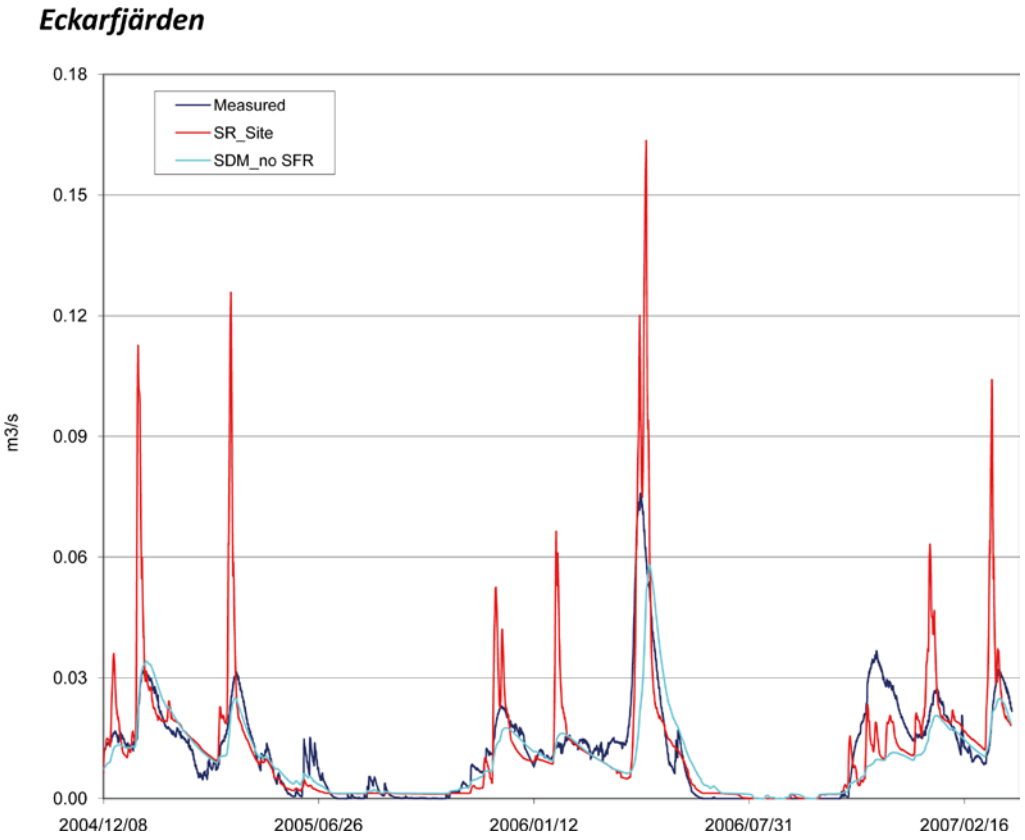

Figure 5-3. *Comparison between measured and modelled surface water discharges at the Lake Eckarfjärden station (PFM002668). The blue line is measured discharge, the turquoise line is modelled discharge with the SDM-Site model and the red line is modelled with the SR-Site model.*

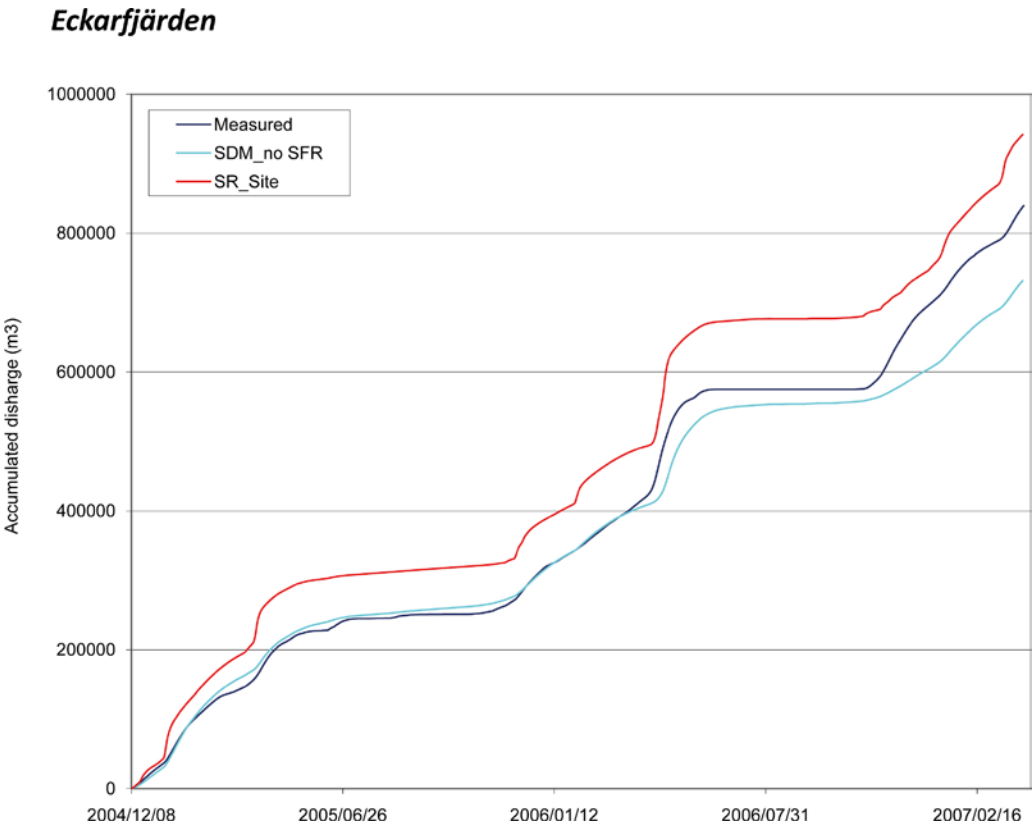

Figure 5-4. *Comparison between measured and modelled accumulated discharges at the Lake Eckarfjärden station (PFM002668). The blue line is measured discharge, the turquoise line is modelled discharge with the SDM-Site model and the red line is modelled with the SR-Site model.*

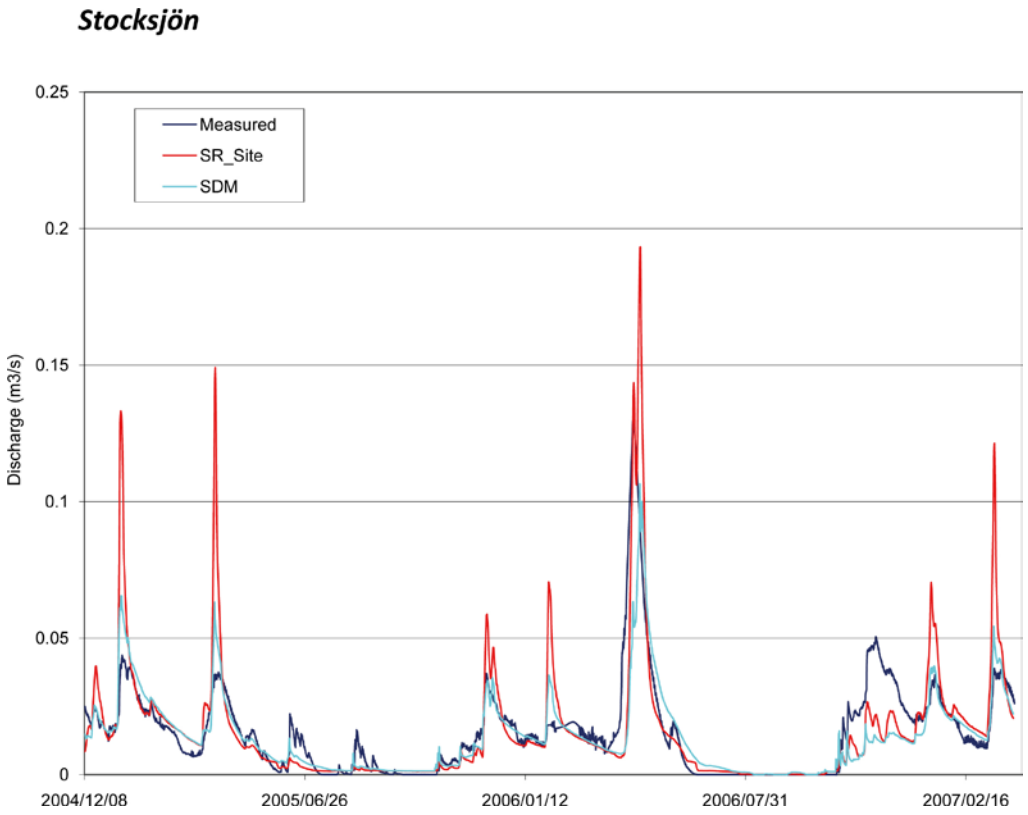

Figure 5-5. *Comparison between measured and modelled surface water discharges at the Lake Stocksjön station (PFM002667). The blue line is measured discharge, the turquoise line is modelled discharge with the SDM-Site model and the red line is modelled with the SR-Site model.*

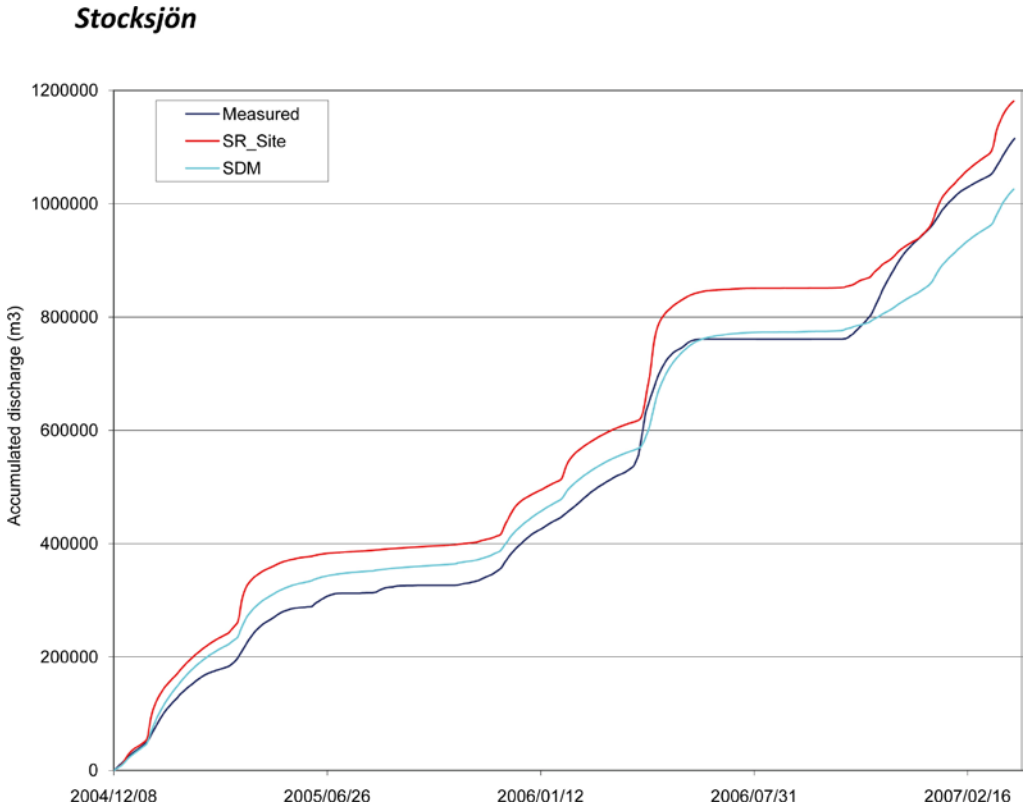

Figure 5-6. *Comparison between measured and modelled accumulated discharges at the Lake Stocksjön station (PFM002667). The blue line is measured discharge, the turquoise line is modelled discharge with the SDM-Site model and the red line is modelled with the SR-Site model.*

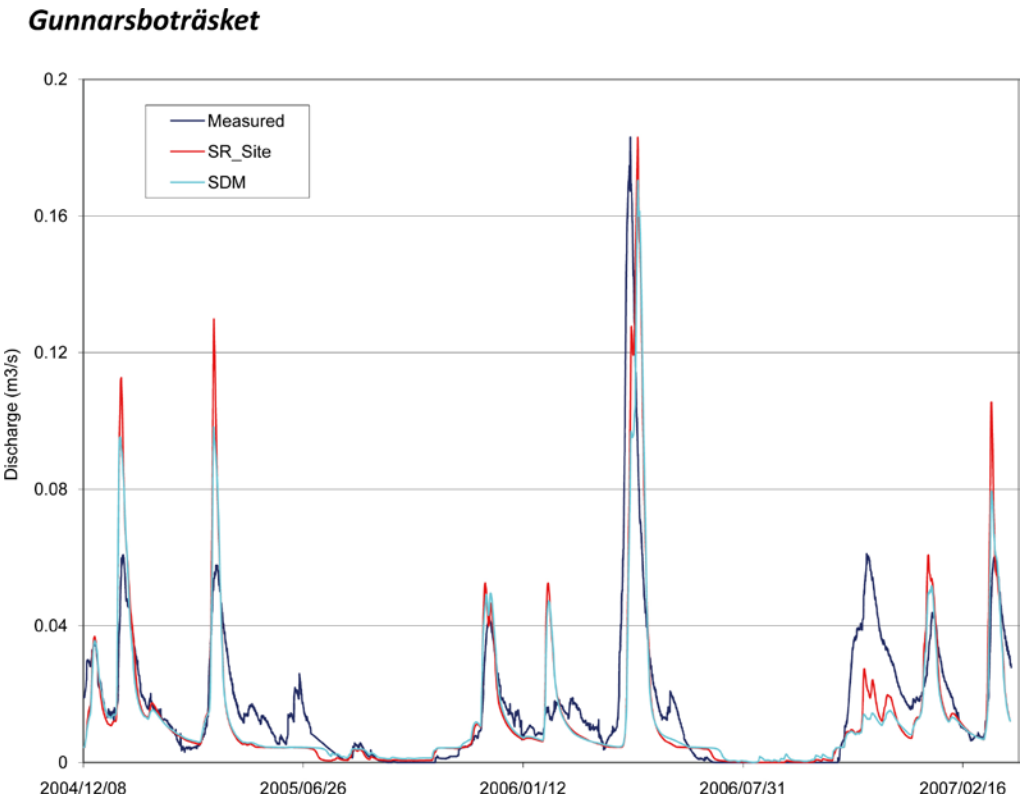

Figure 5-7. *Comparison between measured and modelled surface water discharges at the Lake Gunnarsboträsket station (PFM002669). The blue line is measured discharge, the turquoise line is modelled discharge with the SDM-Site model and the red line is modelled with the SR-Site model.*

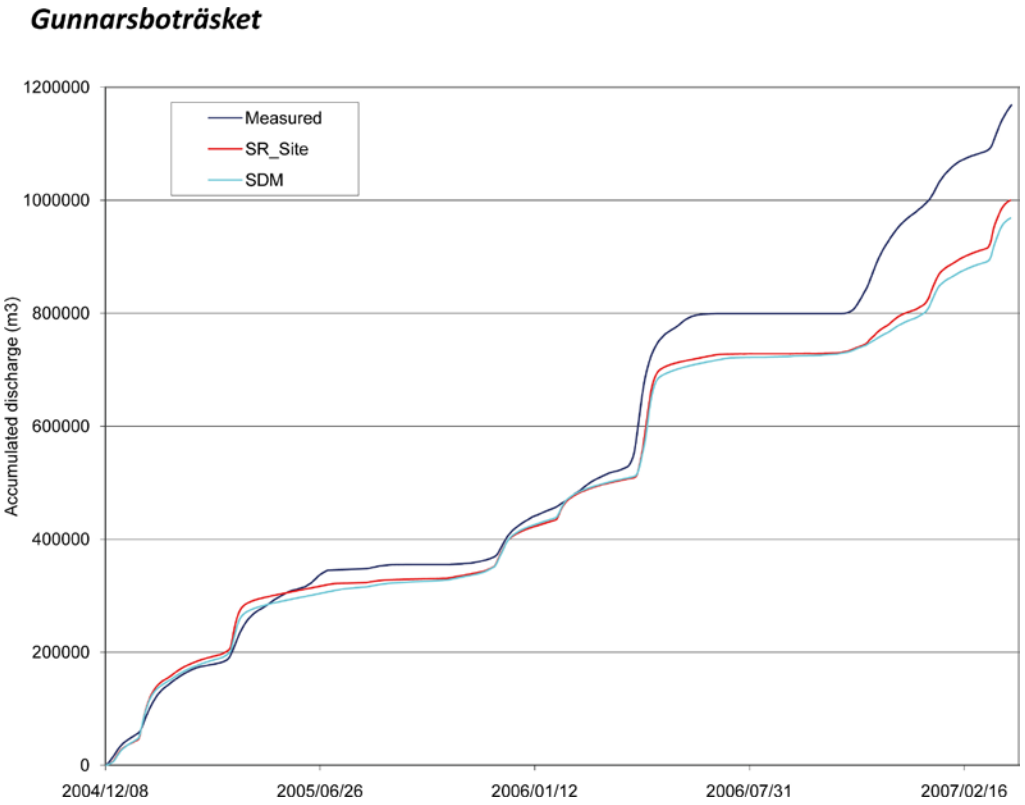

Figure 5-8. *Comparison between measured and modelled accumulated discharges at the Lake Gunnarsboträsket station (PFM002669). The blue line is measured discharge, the turquoise line is modelled discharge with the SDM-Site model and the red line is modelled with the SR-Site model.*

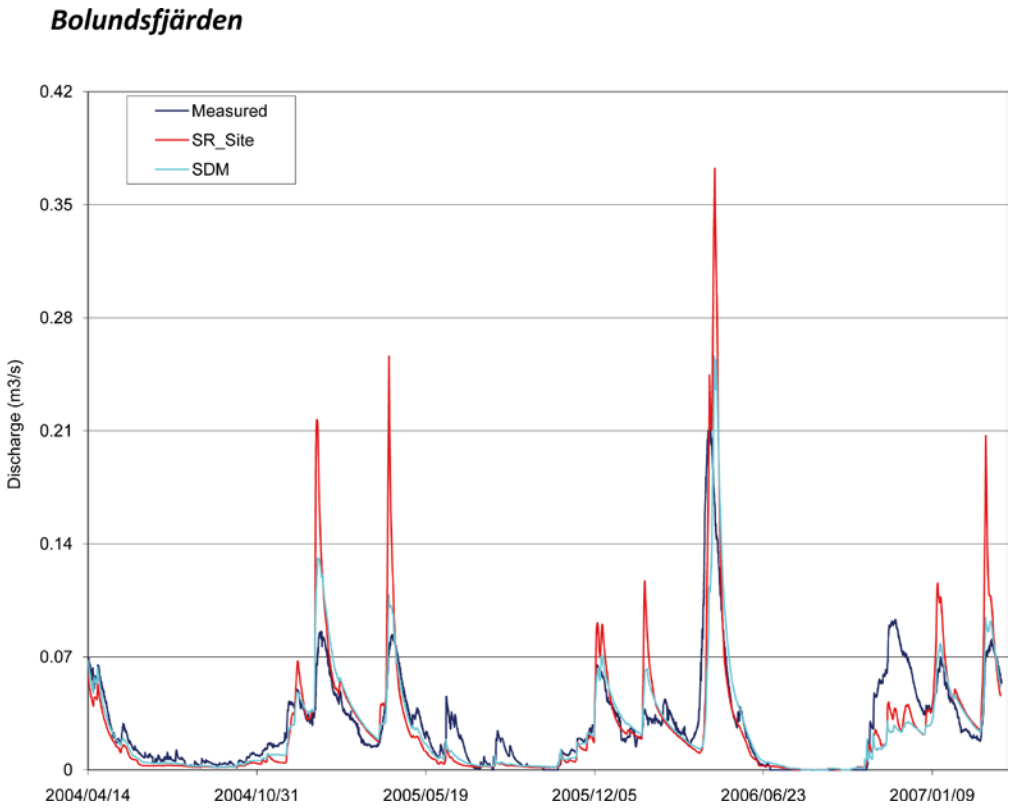

Figure 5-9. *Comparison between measured and modelled surface water discharges at the Lake Bolundsfjärden station (PFM005764). The blue line is measured discharge, the turquoise line is modelled discharge with the SDM-Site model and the red line is modelled with the SR-Site model.*

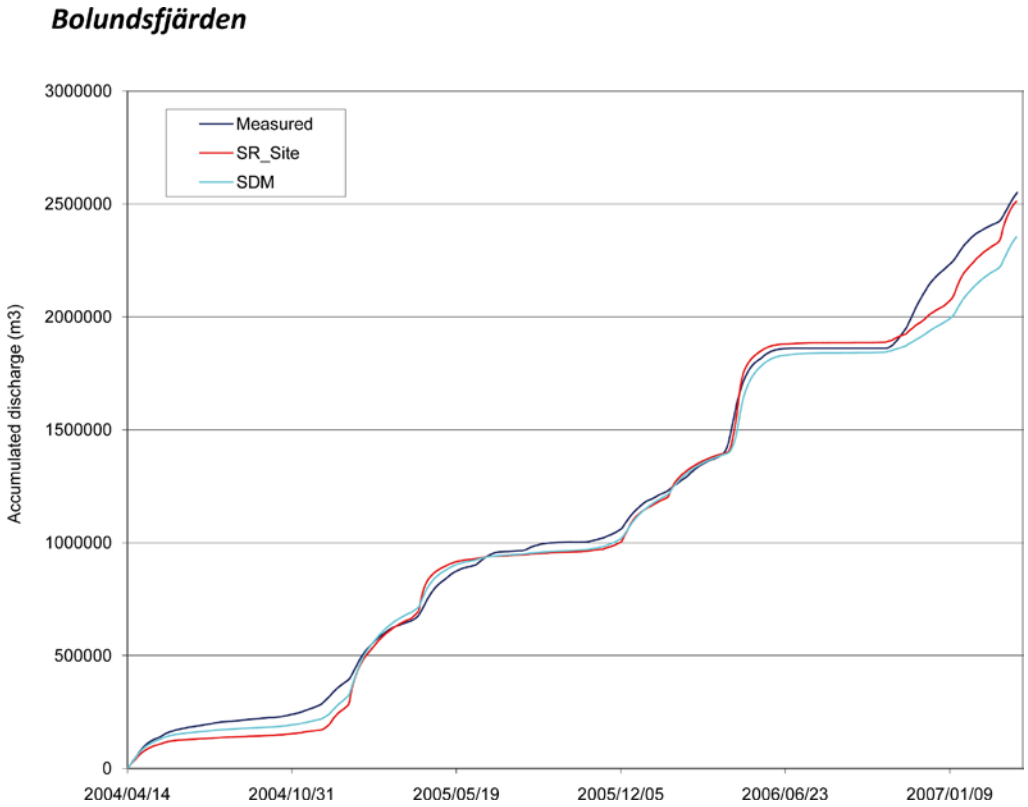

Figure 5-10. *Comparison between measured and modelled accumulated discharges at the Lake Bolundsfjärden station (PFM005764). The blue line is measured discharge, the turquoise line is modelled discharge with the SDM-Site model and the red line is modelled with the SR-Site model.*

5.2.3 Groundwater and surface water levels

The results for the groundwater monitoring wells in the QD layers and in the bedrock are shown in Tables 5-3 and 5-4 in terms of mean absolute errors (MAE) and mean errors (ME), the MAE and ME are defined below. The results are listed both for the SDM-Site model and the SR-Site model.

Mean error, ME

$$ME = \frac{1}{n}\sum_{t}(q_{obs_t} - q_{sim_t})$$

Mean absolute error, MAE

$$MAE = \frac{1}{n}\sum_{t}\left|(q_{obs_t} - q_{sim_t})\right|$$

The SR-Site mean MAE and ME for both the SFM- and the HFM-wells are almost the same as in the SDM modelling. The mean MAE for the SFM-wells is 0.30 m compared to 0.26 cm in the SDM-Site model, and the mean ME is reduced from 0.02 m to 0.00 m in the SR-Site model. There is a good agreement between the measured and the calculated values for the SFM-wells. The low mean error indicates that the mean groundwater table in the model area is very well described by the model. Also the mean absolute error is rather low, indicating that also the temporal variations are resolved by the model.

Extending the model area and decreasing the horizontal resolution have not decreased the model performance in terms of reproducing the measured groundwater levels in the QD. For the HFM-wells, the mean difference between the MAE in the SR-Site and the SDM-Site models is only 0.02 m. However, in the SDM model, the drainage of the SFR repository was not included. This caused high groundwater levels in the wells having hydraulic contact with SFR. For example, HFM34 is influenced of the drawdown caused by the SFR drainage. The MAE for HFM34 in the SDM model was 1.09 m and in the SR-Site model the MAE was reduced to 0.25 m.

The measured head elevations during the summer of 2006 drop to levels well below the lowest levels for the other summer periods. The calculated groundwater levels are quite well captured by the model. Both in SFM0003 and SFM0011 the decrease of the groundwater level during the summer 2006 are better captured by the SR-Site model than by the SDM-Site model (Figures 5-11 and 5-12). The contact between the lakes and the underlying till is also well described by the model. Figures 5-13 to 5-15 show the calculated surface water level and the head elevation in the till under each lake. In the model, all lakes have gyttja, sand and clay sediments between the lake bottom and the till.

The horizontal extent of the clay is much smaller in Lake Bolundsfjärden than in the other lakes. However, a low conductive layer of gyttja reduces the contact with the underlying till. Results from pumping tests during the site investigation indicate that there is only a very limited contact through the lake sediments, and the hydraulic conductivity of the clay is therefore set to 10^{-8} m/s and the hydraulic conductivity of the gyttja to 10^{-7} m/s. It was not needed to correct the conductivity values for the lake sediments during the calibration process; the initial low values have been kept.

Table 5-3. Comparison of mean absolute errors (MAE) and mean errors (ME) for groundwater monitoring wells in QD for the SDM-Site model and the SR-Site model.

ID code SFM-well	SDM-Site		SR-Site		
Calculated head	MAE	ME	MAE	ME	Diff. MAE
SFM0001	0.21	0.16	0.41	0.40	–0.20
SFM0002	0.37	0.37	0.40	–0.07	–0.03
SFM0003	0.19	–0.09	0.54	–0.54	–0.35
SFM0004	0.21	–0.01	0.43	0.43	–0.21
SFM0005	0.21	–0.15	0.36	0.15	–0.15
SFM0009	0.36	0.35	0.63	0.63	–0.26
SFM0010	0.31	0.29	0.33	–0.03	–0.02
SFM0011	0.10	–0.09	0.20	0.19	–0.10
SFM0012	0.08	0.01	0.10	–0.07	–0.02
SFM0013	0.27	0.00	0.46	–0.06	–0.18
SFM0014	0.34	–0.34	0.00	0.10	0.34
SFM0015	0.09	–0.08	0.05	–0.03	0.04
SFM0016	0.14	–0.14	0.17	–0.16	–0.04
SFM0017	0.63	–0.63	0.36	0.25	0.27
SFM0018	0.17	–0.04	0.38	0.31	–0.21
SFM0019	0.32	–0.29	0.38	0.37	–0.06
SFM0020	0.26	–0.26	0.26	–0.07	0.00
SFM0021	0.48	0.48	0.39	–0.28	0.09
SFM0023	0.07	–0.05	0.06	–0.02	0.01
SFM0028	0.15	–0.04	0.32	–0.32	–0.17
SFM0030	0.63	0.61	0.45	–0.37	0.18
SFM0033	0.35	0.32	0.29	0.27	0.06
SFM0034	0.29	-0.10	0.62	-0.33	-0.33
SFM0036	0.24	-0.15	0.35	0.33	-0.10
SFM0039	0.05	-0.03	0.05	-0.03	0.00
SFM0049	0.20	0.01	0.52	-0.39	-0.31
SFM0057	0.63	-0.59	0.87	-0.87	-0.24
SMF0058	0.43	-0.28	0.77	-0.69	-0.34
SFM0062	0.11	0.05	0.15	0.11	-0.04
SFM0065	0.21	-0.08	-0.45	0.46	0.66
SFM0066	0.12	0.03	-0.35	0.36	0.47
MEAN SFM	**0.26**	**-0.02**	**0.31**	**0.00**	**-0.04**

Table 5-4. Comparison of mean absolute errors (MAE) and mean errors (ME) for groundwater monitoring wells in the bedrock for the SDM-Site model and the SR-Site model.

ID code HFM-well	SDM-Site		SR-Site	
Calculated head	MAE	ME	MAE	ME
HFM01_1	0.82	–0.82	0.74	–0.74
HFM01_2	0.90	–0.90	0.97	–0.97
HFM02_1	0.82	–0.82	0.94	–0.94
HFM02_2	0.79	–0.79	0.96	–0.96
HFM02_3	0.81	–0.81	0.97	–0.97
HFM03_1	0.75	–0.75	0.92	–0.92
HFM03_2	0.74	–0.74	0.91	–0.91
HFM04_1	0.08	0.01	0.44	–0.44
HFM04_2	0.15	–0.12	0.46	–0.46
HFM04_3	0.17	0.17	0.24	–0.24
HFM10_1	0.39	–0.39	0.85	–0.85
HFM10_2	0.27	–0.22	0.53	–0.52
HFM11_1	0.29	–0.28	0.23	–0.15
HFM11_2	0.25	–0.22	0.51	–0.49
HFM15_1	0.68	–0.68	0.85	–0.85
HFM15_2	0.62	–0.62	0.70	–0.70
HFM16_1	0.41	–0.41	0.39	–0.38
HFM16_2	0.47	–0.47	0.39	–0.38
HFM16_3	0.56	–0.56	0.42	–0.41
HFM20_2	0.48	–0.48	0.17	–0.10
HFM20_3	0.44	–0.44	0.37	–0.37
HFM20_4	0.79	–0.79	0.66	–0.66
HFM32_1	1.39	–1.39	1.40	–1.40
HFM32_2	1.43	–1.43	1.36	–1.36
HFM32_3	1.32	–1.32	1.07	–1.07
HFM32_4	1.37	–1.37	1.08	–1.08
HFM34_3	1.09	–1.09	0.25	–0.23
Mean HFM	**0.68**	**–0.66**	**0.70**	**–0.69**

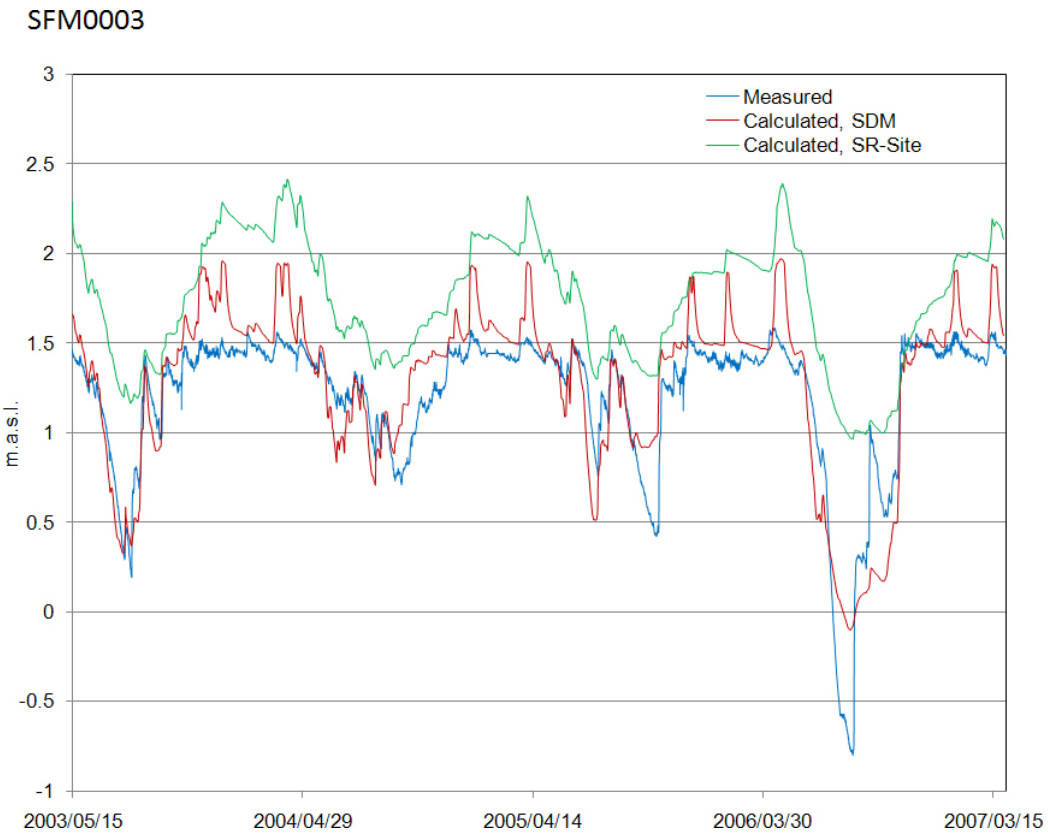

Figure 5-11. *Measured and calculated groundwater depths in SFM0003. Calculated groundwater levels are from both the SDM-Site and the SR-Site MIKE SHE models.*

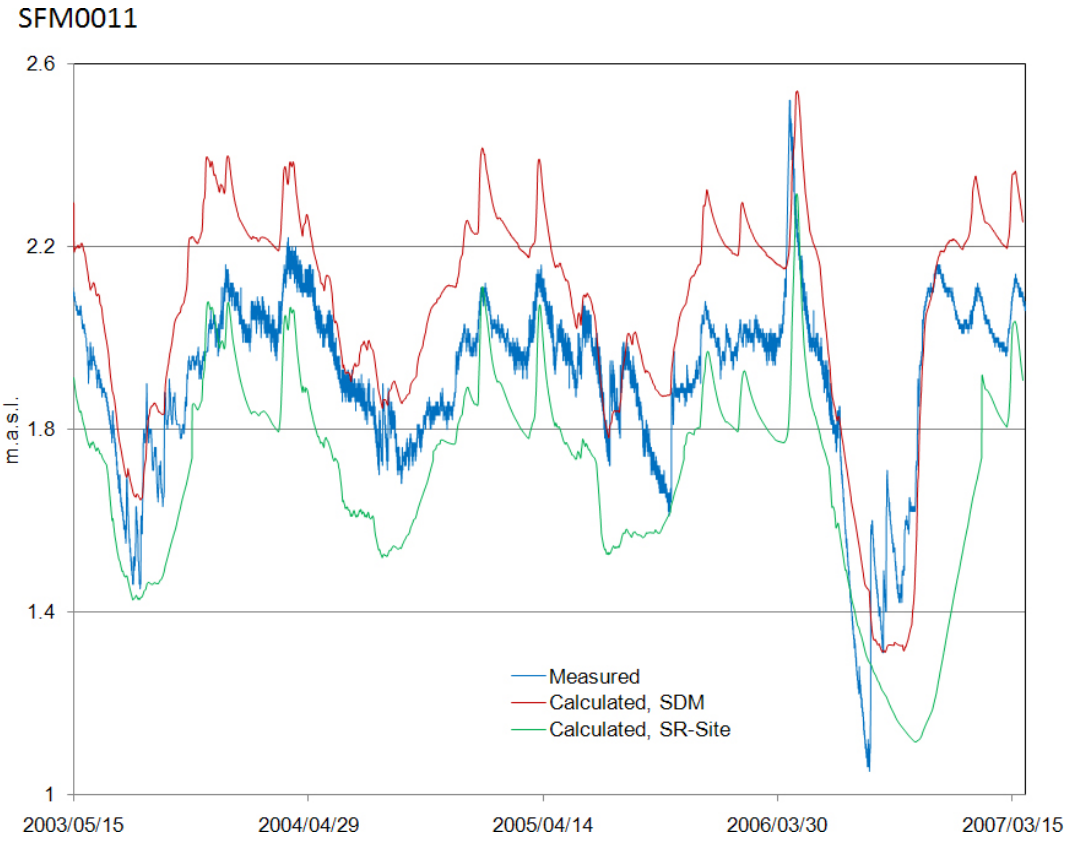

Figure 5-12. *Measured and calculated groundwater depths in SFM0011. Calculated groundwater levels are from both the SDM-Site and the SR-Site MIKE SHE models.*

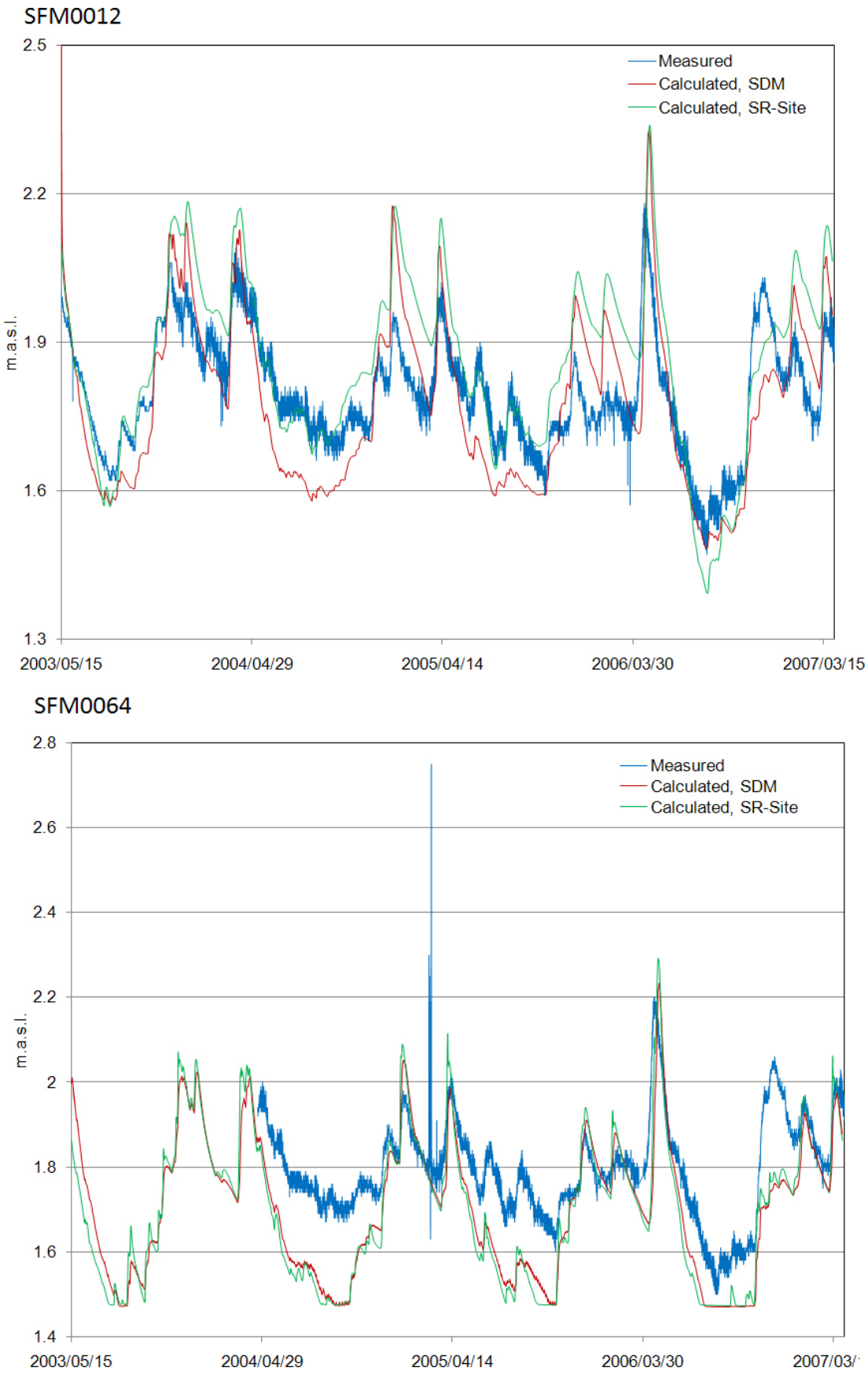

Figure 5-13. *Comparison between measured and calculated surface water levels and head elevations in the till under Lake Gällsboträsket. The lower figure shows a comparison between the measured (SFM0064) and calculated surface water levels in the lake, and the upper figure shows a comparison between the measured (SFM0012) and calculated groundwater heads in the till below the lake.*

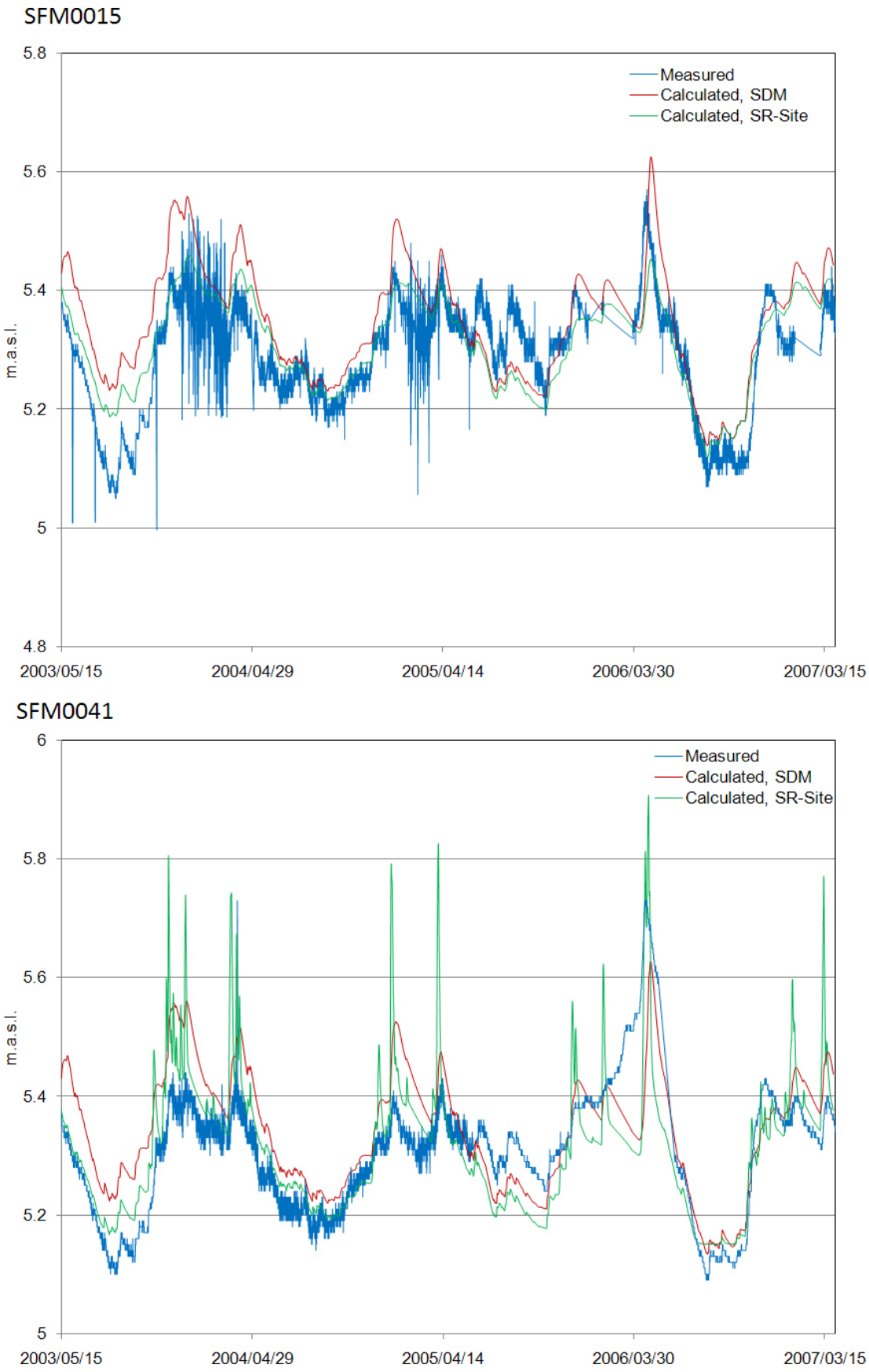

Figure 5-14. *Comparison between measured and calculated surface water levels and head elevations in the till under Lake Eckarfjärden. The lower figure shows a comparison between the measured (SFM0041) and calculated surface water levels in the lake, and the upper figure shows a comparison between the measured (SFM0015) and calculated groundwater heads in the till below the lake.*

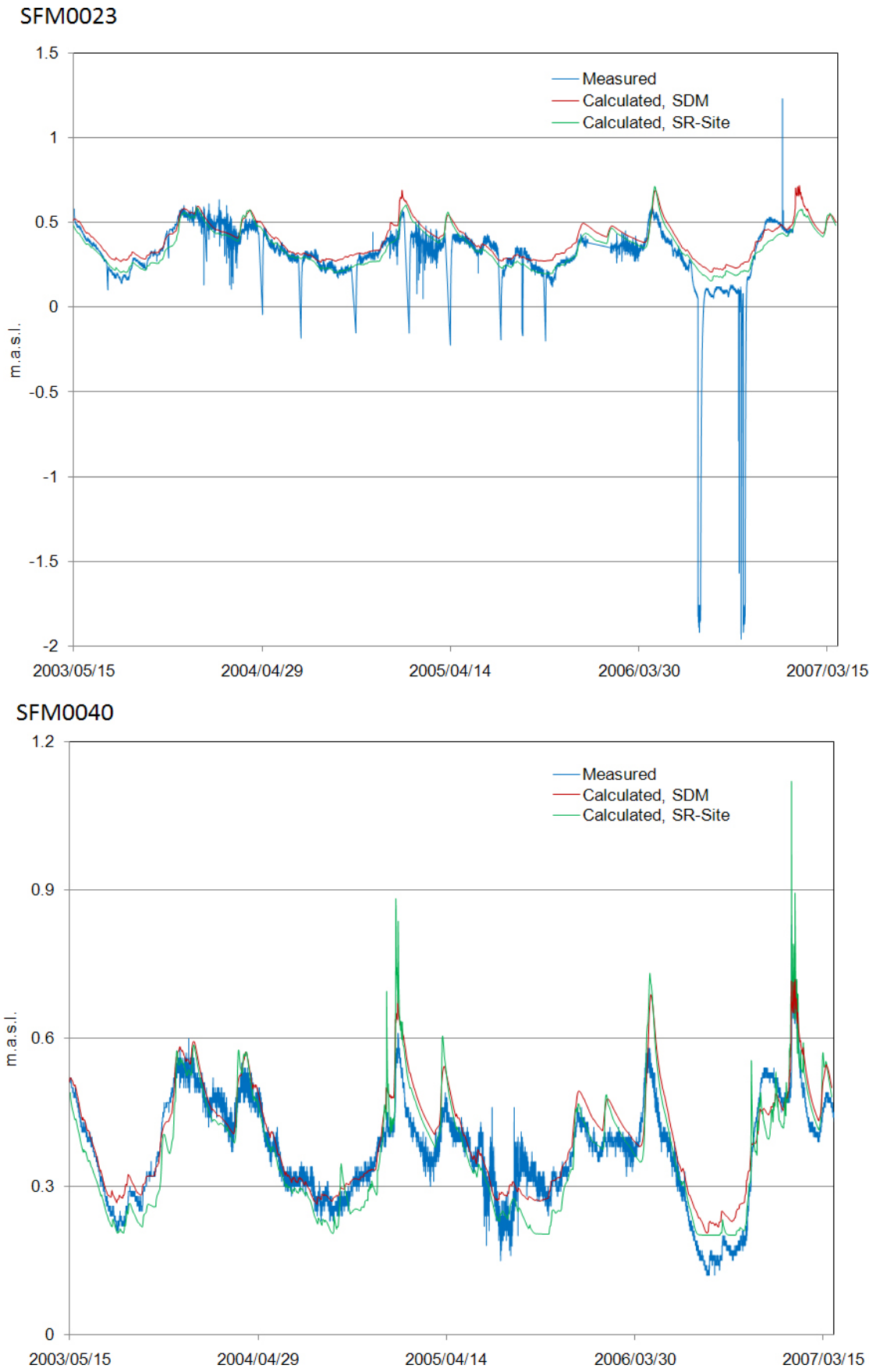

Figure 5-15. *Comparison between measured and calculated surface water levels and head elevations in the till under Lake Bolundsfjärden. The lower figure shows a comparison between the measured (SFM0040) and calculated surface water levels in the lake, and the upper figure shows a comparison between the measured (SFM0023) and calculated groundwater heads in the till below the lake.*

5.3 Flow modelling results

In the following sections the water balance, the depth to the groundwater table, the distribution and depth of surface waters and the spatial distribution of recharge and discharge areas are presented. Simulations have been performed with the same climate input data but different QD-models, land uses and shorelines have been applied to the models in order to describe the landscape development of the site.

The aim with the different simulation cases is to analyse which processes in the landscape development that are important when describing the future hydrology of the site. Additionally to each future model case describing the shoreline and QD for that specific time period, a sensitivity case was run with the present QD model. This was done to evaluate the effect of the development of the QD where sedimentation and erosion processes had been taken into consideration.

5.3.1 Water balance

The water balances of the different simulation cases listed in Table 5-1 have been evaluated for different areas, depending on which time period that is simulated. For all cases, the area constituting land at the studied point of time (2000 AD, 5000 AD or 10,0000 AD) was studied. Also the water balance of the area constituting land at 2000 AD was studied in all cases to see how the land area of today is affected by the shoreline displacement and the development of the vegetation and QD-layers (Figure 5-16).

The water balances of the catchment areas of Lake Bolundsfjärden and object 116 at 2000 AD and 10,000 AD were evaluated separately to analyse how the water balance of a delineated catchment area is affected by the shoreline displacement and the development of QD and vegetation. All the water balances are evaluated for the second cycle of the selected year (data from the period October 1, 2003 to September 30, 2004). All the numbers are annual mean values and given in mm (i.e. mm/year).

Studying the water balances for the five models for the area constituting land at 2000 AD there are small changes in evaporation and runoff, less than 10%. The mean annual runoff is approximately 180 mm in all cases and the total evapotranspiration is 400 mm. The annual precipitation is 583 mm for all cases since the same meteorological input data are used in all the models. The maximum total evapotranspiration is achieved in the model 5000AD_2000QD and is calculated to 410 mm. The minimum total evapotranspiration, 399 mm, is calculated with the 10000AD_2000QD model.

The runoff varies between 194 mm in the 10000AD_10000QD model and 175 mm for the model describing present conditions, 20000AD_2000QD. The water balances for the area constituting land at 2000 AD are presented in Figure 5-17. In Figure 5-18 the main changes in the water balance when taking shoreline displacement and the development of the QD into consideration are summarised. All water balances for each time period for the area constituting land at 2000 AD are presented in Appendix 2.

The largest changes in the flow between different model compartments occur when changing the QD-model. The infiltration is almost the same for all time periods when using the 2000 QD model. When applying the 5000 or 10,000 QD model the infiltration decreases with approximately 30 mm. Still the change in the infiltration is less than 10% for all cases. The decreased infiltration leads to an increased amount of water flowing from the overland compartment to the surface stream system and the water flow from the saturated zone to the surface streams decreases.

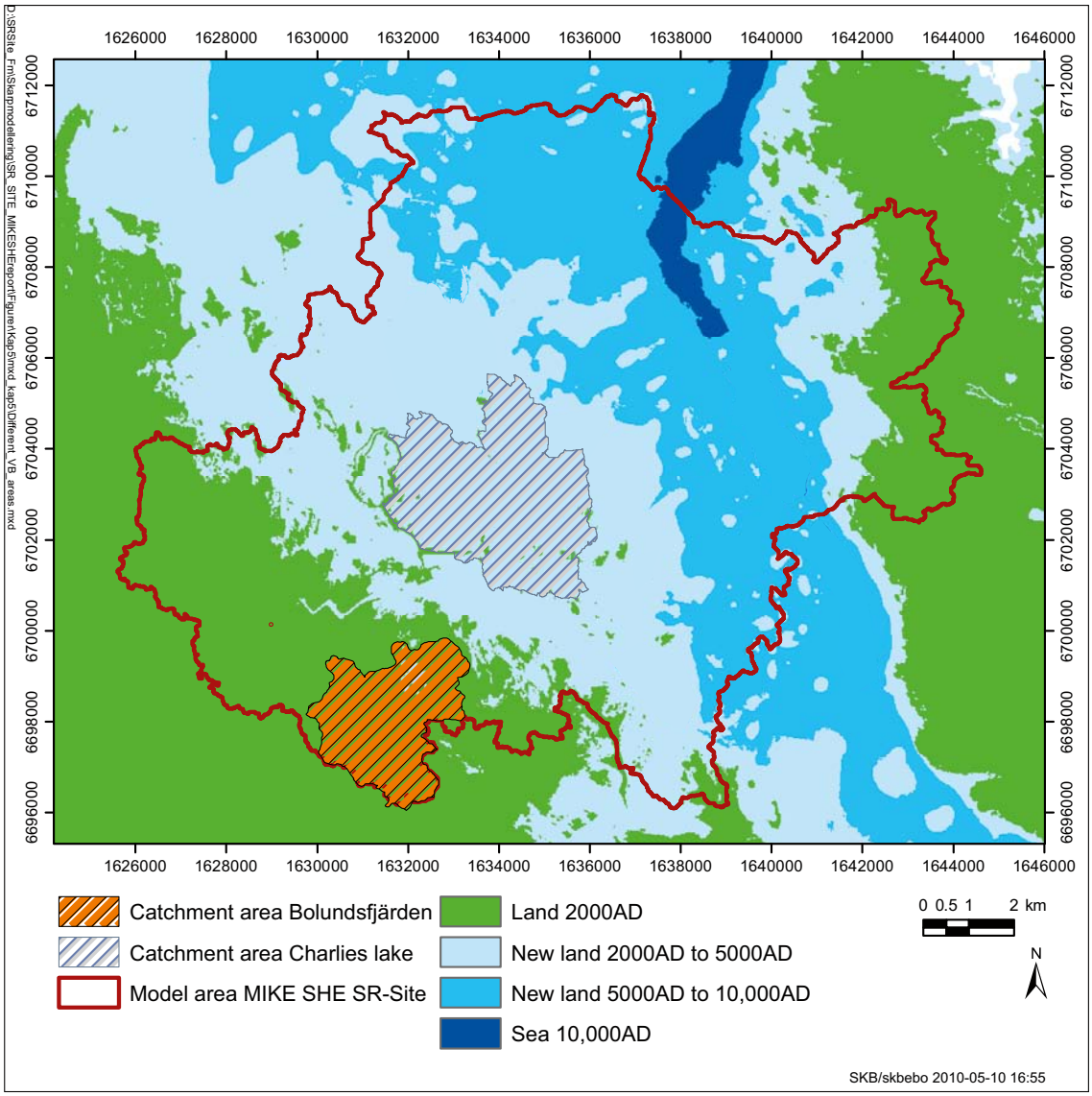

Figure 5-16. *The different areas studied when calculating water balances for the different simulation cases. A water balance for the green area, the area constituting land at 2000 AD, has been calculated for all simulation cases. For the 5000 AD models water balances were also extracted for the green and light blue area, i.e. the area constituting land at 5000 AD. For the 10,000 AD models, a water balance was extracted for the green, light blue and blue area, i.e. the area constituting land at 10,000 AD.*

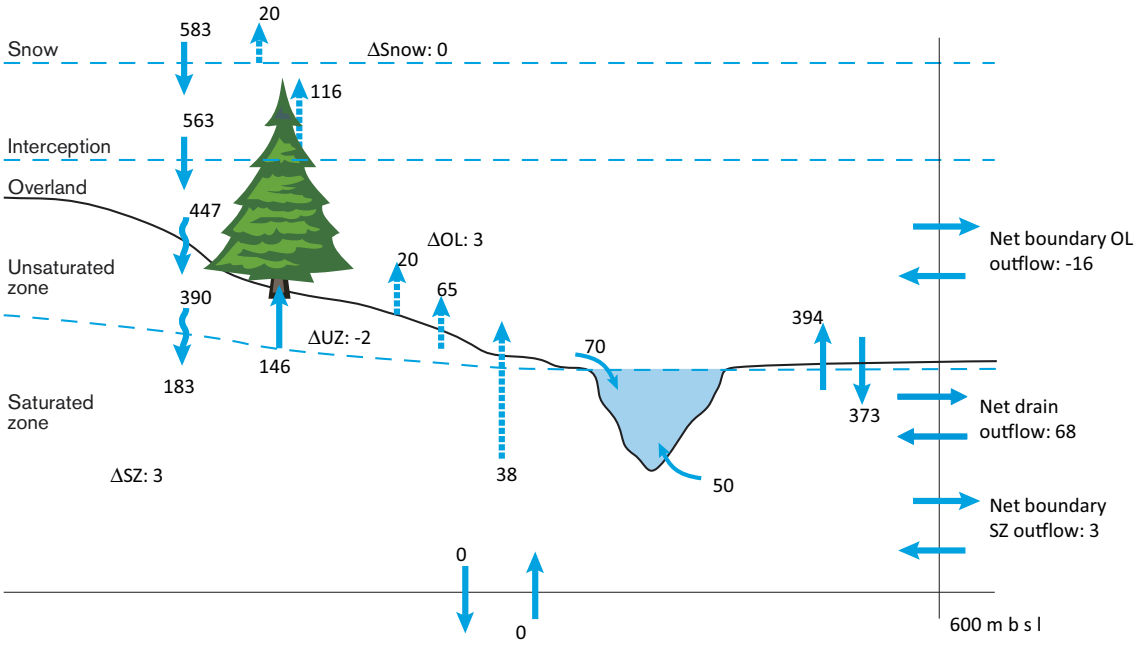

Figure 5-17. *Water balance from the 2000AD_2000QD model for the area constituting land at 2000 AD.*

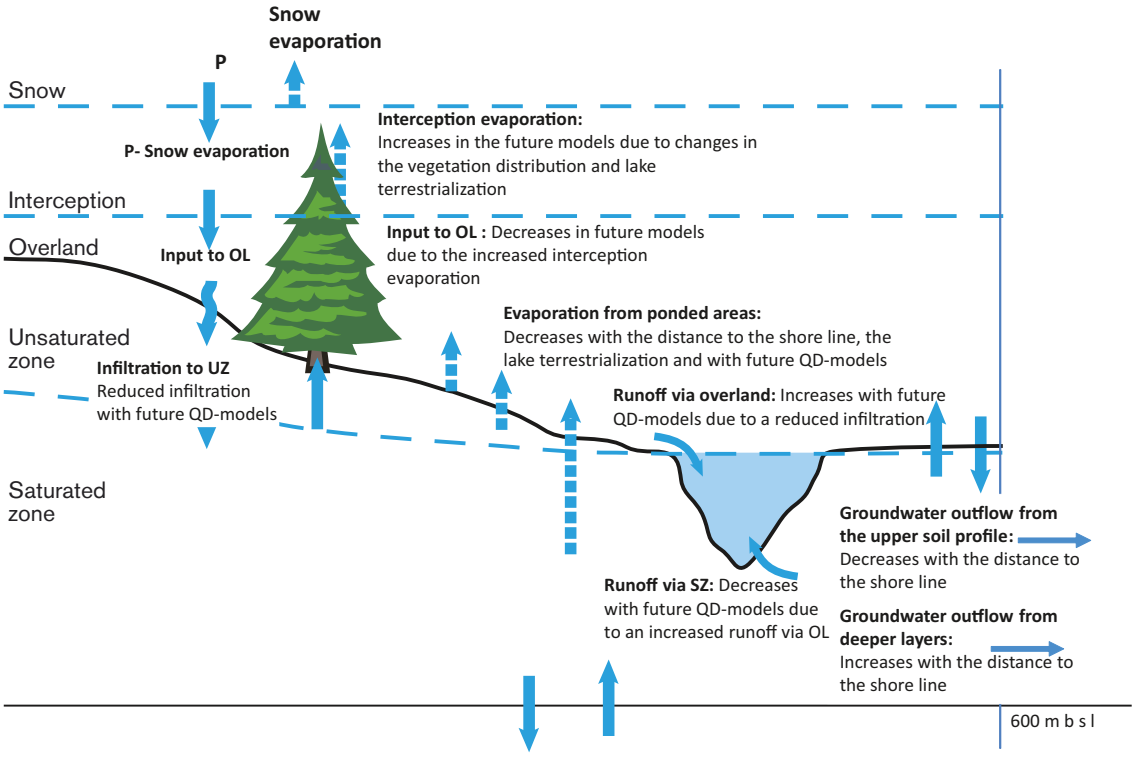

Figure 5-18. *Summary of the main changes in the water balance of the area constituting land at 2000 AD when taking the development of the landscape into consideration, i.e. the changes in the water balances from the different models from 2000 AD, 5000 AD and 10,000 AD.*

For the three models having the same QD-model, i.e. the 2000AD_2000QD, 5000AD_2000QD and 10000AD_2000QD models, the drain outflow decreases from 68 mm at 2000 AD to 29 mm at 10,000 AD. When only studying the water balance for the part of the model volume constituting land at each time step the drain boundary outflow is the groundwater discharging from the upper 0.5 m to the sea and the part of the model volume underlying the sea. The SZ outflow is the groundwater discharge from the remaining part of the saturated zone of the model. In the same time the SZ outflow increases from 3 mm at 2000 AD to 10 mm at 10,000AD. This is because the sea area is moved from the present shoreline, out to the shoreline of 5000 AD and 10,000 AD. The reason for the decreased drain outflow is also the shoreline displacement. The drainage function implemented in the model, is only active when the groundwater table rises above 0.5 m.b.g.s (meter below ground surface). The sea in the 2000AD_2000QD model causes relatively large areas along the coastline with groundwater levels close to or above ground surface and consequently larger amount of water discharged via the drainage system. In the 5000 AD and 10,000 AD models the shoreline is far away from the studied area of the water balance. Thus, the amount of water leaving the model area via the drainage system decreases.

Also when studying the area constituting land at each time period the changes in the total calculated runoff and evapotranspiration are small. Different vegetation covers, lake percentages and properties of the unsaturated zone in the areas result in a varying interception, transpiration and evaporation from overland waters, but the variation of the total calculated evapotranspiration is less than 10% for all the cases. All the water balances for the areas constituting land at each time period are shown in Appendix 2; only the water balance for the 10000AD_10000QD model is presented below (Figure 5-19).

The simulations with a wet and a periglacial climate are based on the 10000AD_10000QD model. Water balances are extracted for the area constituting land at 10,000 AD and the results from the simulations describing different climates will be compared. The total runoff for the area constituting land at 10,000 AD is 185 mm compared to 194 mm for the area constituting land at 2000 AD calculated with the same model (10000AD_10000QD). The main reason for the larger runoff when studying the area constituting land at 2000 AD is the runoff components associated with the model boundaries. Direct runoff via overland and the saturated zone is higher when only studying the area constituting land at 2000 AD. This is due to the continuous flow towards lower areas in the model area and a flow towards the sea.

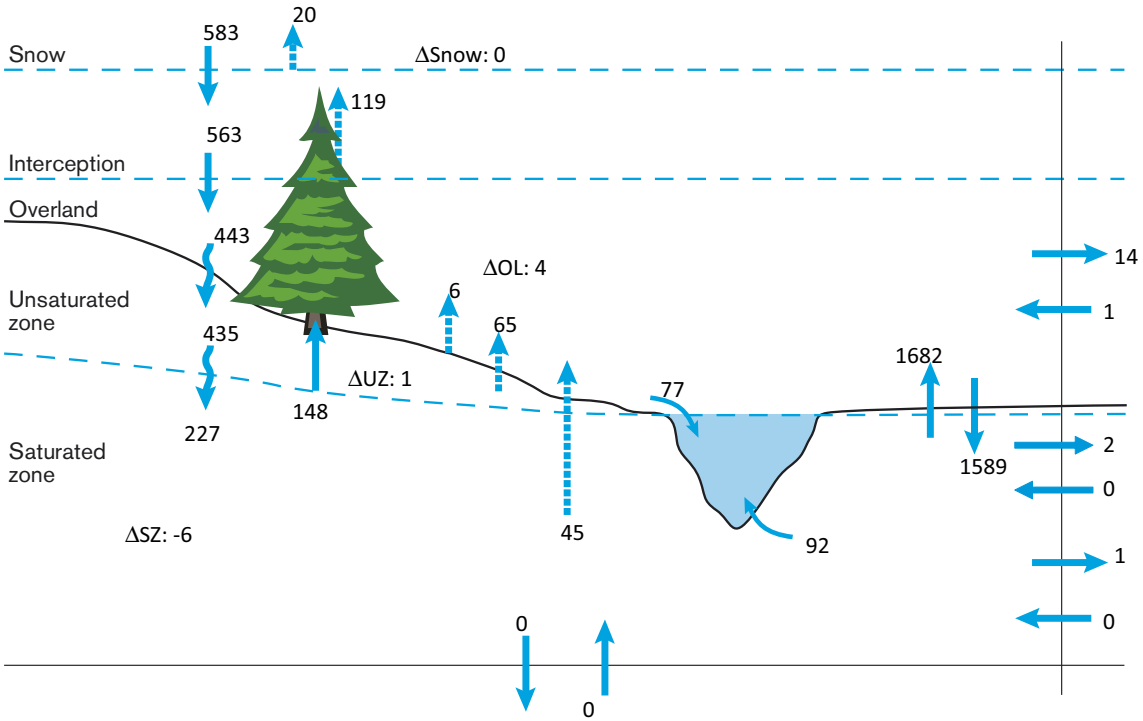

Figure 5-19. *Water balance from the 10000AD_10000QD-model for the area constituting land at 10,000 AD.*

The other difference in the water balance between the two studied areas is the amount of water infiltrating to the unsaturated zone. For the area constituting land at 2000 AD, the infiltration is 364 mm whereas the infiltration is 435 mm when taking the whole area constituting land at 10,000 AD into consideration. The higher infiltration depends on a higher net inflow of water from the saturated zone to the overland water via the exchange of water between the overland water and saturated zone compartments. The increased exchange of water between OL, water on the ground surface, and SZ depends on the drainage function, which is dependent on the hydraulic properties of the uppermost QD layer.

The catchment area of Lake Bolundsfjärden and the catchment area of object 116 have been analysed separately. Water balances have been extracted for the two areas from the 2000AD_2000QD model and from the 10000AD_10000QD model. Since object 116 is below sea level at 2000 AD, a water balance for this area has been extracted from the 10,000 AD model only. The three different water balances are shown in Figures 5-20 to 5-22.

Comparing the water balances of the Lake Bolundsfjärden area at 2000 AD and 10,000 AD, it can be noticed that there is a higher evapotranspiration at 2000 AD than at 10,000 AD, 411 mm versus 398 mm. The runoff increases from 169 mm at 2000 AD to 198 mm at 10,000 AD, an increase with 17%. The amount of water flowing into the surface stream system in the catchment area of Lake Bolundsfjärden is almost the same in the 2000 AD and 10,000 AD models, 182 mm at 2000 AD and 194 mm at 10,000 AD. However, the amount of water flowing from OL to the surface stream is much higher at 2000 AD. The opposite can be noticed for the water flow from SZ to the surface stream, which is much lower at 2000 AD compared to 10,000 AD. At 10,000 AD the shoreline is far away from the studied area and the groundwater table is situated deeper down in the ground, allowing more water to infiltrate and the recharge from UZ to SZ increases. More water is available for runoff from the saturated zone to the surface stream system. The increased flow from SZ to the river system cannot be noticed when studying the whole area constituting land at present. In general the development of the QD-model from 2000 AD to 10,000 AD generates a lower infiltration and a larger amount of water flow on the surface to the streams. However, in the catchment area of Lake Bolundsfjärden the effect of the shore line displacement is more important than the development of the QD-model since at present the shore line is situated close to the lake which results in a very shallow groundwater table.

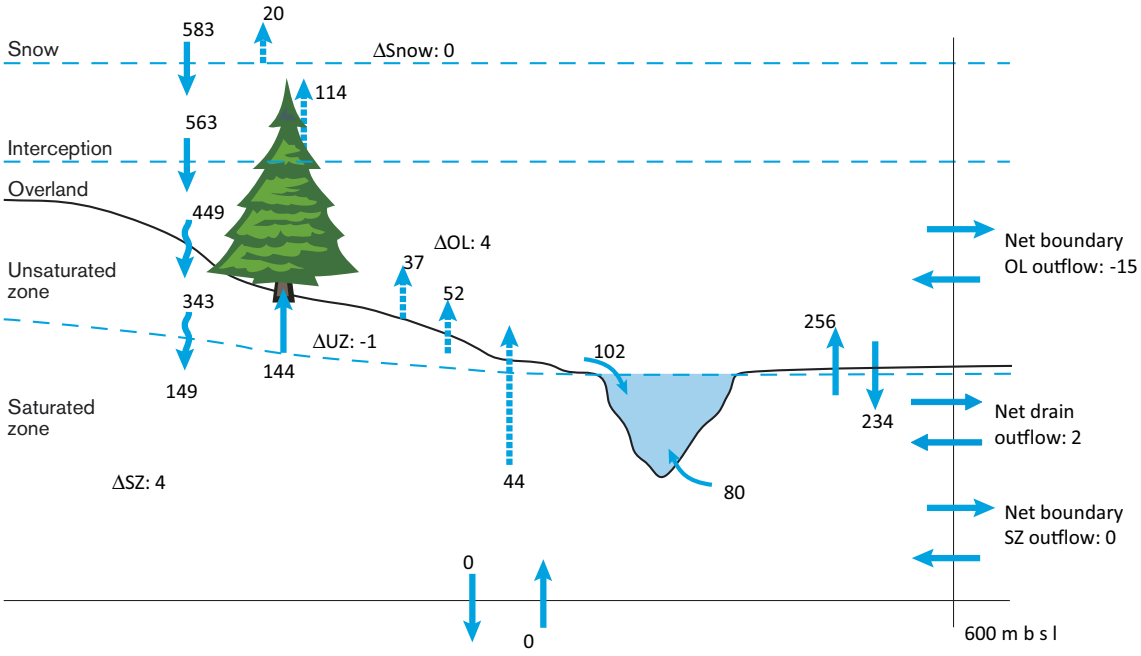

Figure 5-20. *Water balance from the 2000AD_2000QD model for the catchment area of Lake Bolundsfjärden.*

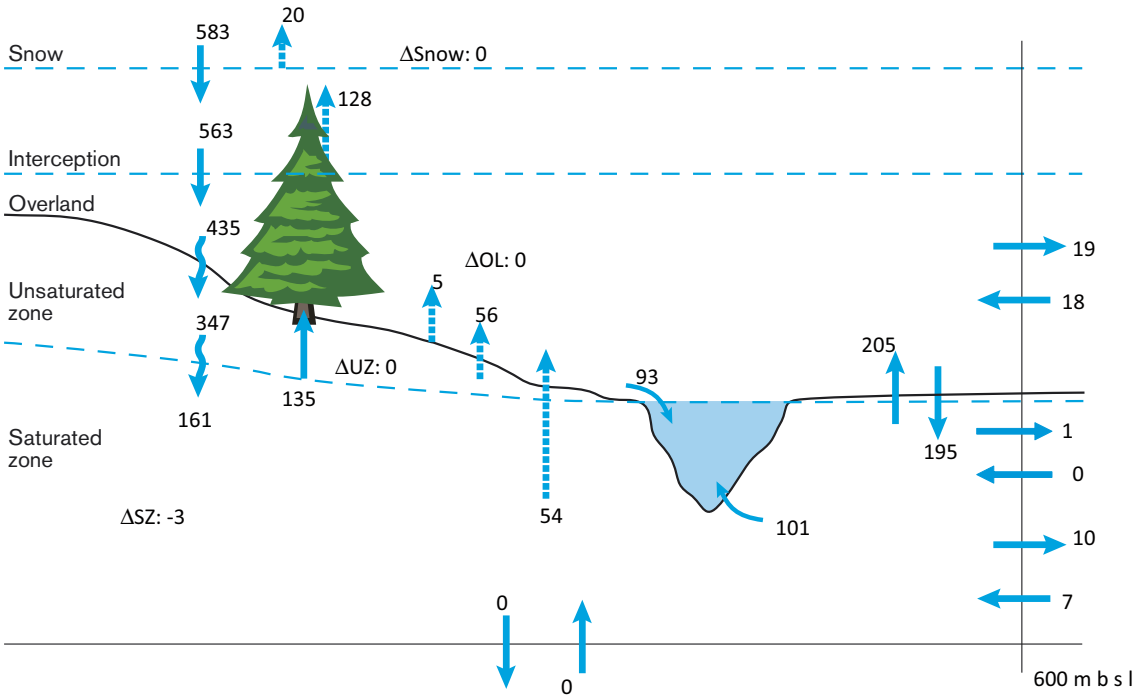

Figure 5-21. *Water balance from the 10000AD_10000QD model for the catchment area of Lake Bolundsfjärden.*

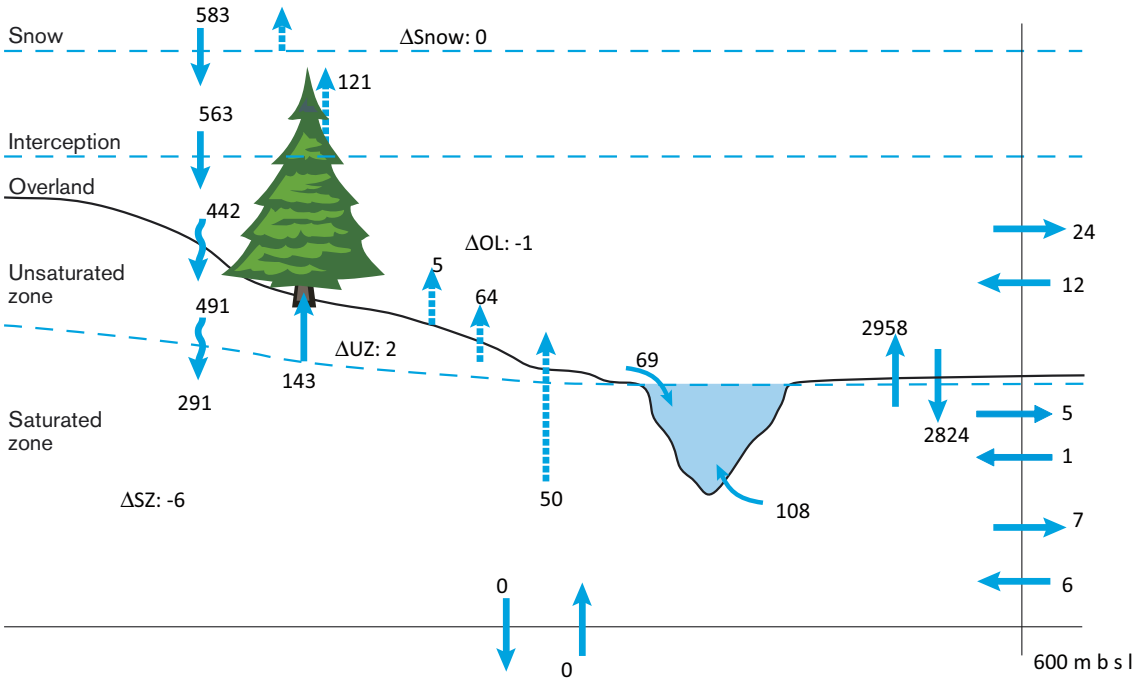

Figure 5-22. *Water balance from the 10000AD_10000QD model for the catchment area of object 116.*

There is an inflow of overland water, 15 mm, to the catchment at 2000 AD, whereas at 10,000 AD the net inflow of water is only 1 mm. This is also due to the more distant shoreline in the 10,000 AD model. At 2000 AD the fluctuation of the sea causes an inflow of overland water to the catchment area of Lake Bolundsfjärden during some periods of the year. Still the net runoff from the area via the surface water streams is directed out of the catchment area.

It can be noticed that the evaporation from overland water, i.e. surface waters and wetlands, is lower in the 10,000 AD model in the catchment area of Lake Bolundsfjärden compared to the 2000 AD model for the same area. At 2000 AD the evaporation from surface water is 37 mm. This value decreases to 5 mm in the 10000AD_10000QD model. This is due to that Lake Bolundsfjärden has turned into a mire at 10,000 AD, which means that less water is available for evaporation from the overland compartment.

Studying the water balances for the catchment area of Lake Bolundsfjärden and the catchment area of object 116 from the model 10000AD_10000QD the overall water balance is almost the same for the two drainage areas. The total evapotranspiration in the catchment area of Lake Bolundsfjärden is 398 mm, whereas it is 403 mm for the catchment area of object 116. The runoff in the catchment area of Lake Bolundsfjärden is 198 mm, as compared to 195 mm in the area of object 116.

The transpiration is 135 mm and 143 mm in the Lake Bolundsfjärden area and the area of object 116, respectively. The small differences that can be observed are due to differences in vegetation and QD (i.e. different hydraulic properties of the unsaturated zone). The lake percentages in the two catchment areas are almost the same, 8% in the catchment area of Lake Bolundsfjärden is covered by open water and compared to 11% in the catchment area of object 116. The area of open water affects the actual evapotranspiration in the area since the actual evapotranspiration equals the potential evapotranspiration in areas with overland water.

The results for the total runoff in the different model cases have been compared to the measured long-term runoff from a discharge station in Vattholma, see Table 5-5. The surface water discharge in Vattholma has been recorded since 1917, and is considered to be a representative long-term mean of the discharge in the region /Larsson-McCann et al. 2002/. The statistics of the calculated runoff is in the same range as the measured long-term mean.

However, the calculated values are lower than the measured. The minimum discharge at the Vattholma station is above zero since the stream in Vattholma never dries out during summer. Almost all streams in the Forsmark area dry out during dry summer periods. The mean specific discharge for the largest catchment area (that of station PFM005764) from local measurements within the site investigation program is 4.88 l/s km^2, value is based on 35.5 months of measurements.

Table 5-5. Total calculated runoff in the different simulation cases, and measured data from the SMHI station at Vattholma; all values in l/s/km^2.

Model or station	min	max	mean	stdev
2000AD_2000QD	0.00	32.85	5.49	7.55
5000AD_5000QD	0.00	37.34	5.81	10.90
10000AD_10000QD	0.00	34.42	5.81	7.18
Vattholma	1.14	26.90	7.36	5.09

5.3.2 Depth of overland water

The calculated depth of overland water is an indication of where future lakes and wetlands will be built up. The overland water depth calculated in the 2000QD_2000AD model is also gives a possibility to check whether the calculated depth of overland water coincides with present field-controlled lakes and wetlands in the area. Figures 5-23 and 5-24 show the depth of overland water from the 2000AD_2000QD model for wet and dry conditions, i.e. during periods of heavy rain and long draught, respectively. A large part of the 2000 AD model area is covered by the sea. It can be seen that in the model overland water is accumulating inside the field-controlled shorelines of the lakes. Under wet conditions, the water depth within the lakes is somewhat larger and the number of saturated cells, i.e. cells with overland water, also increases.

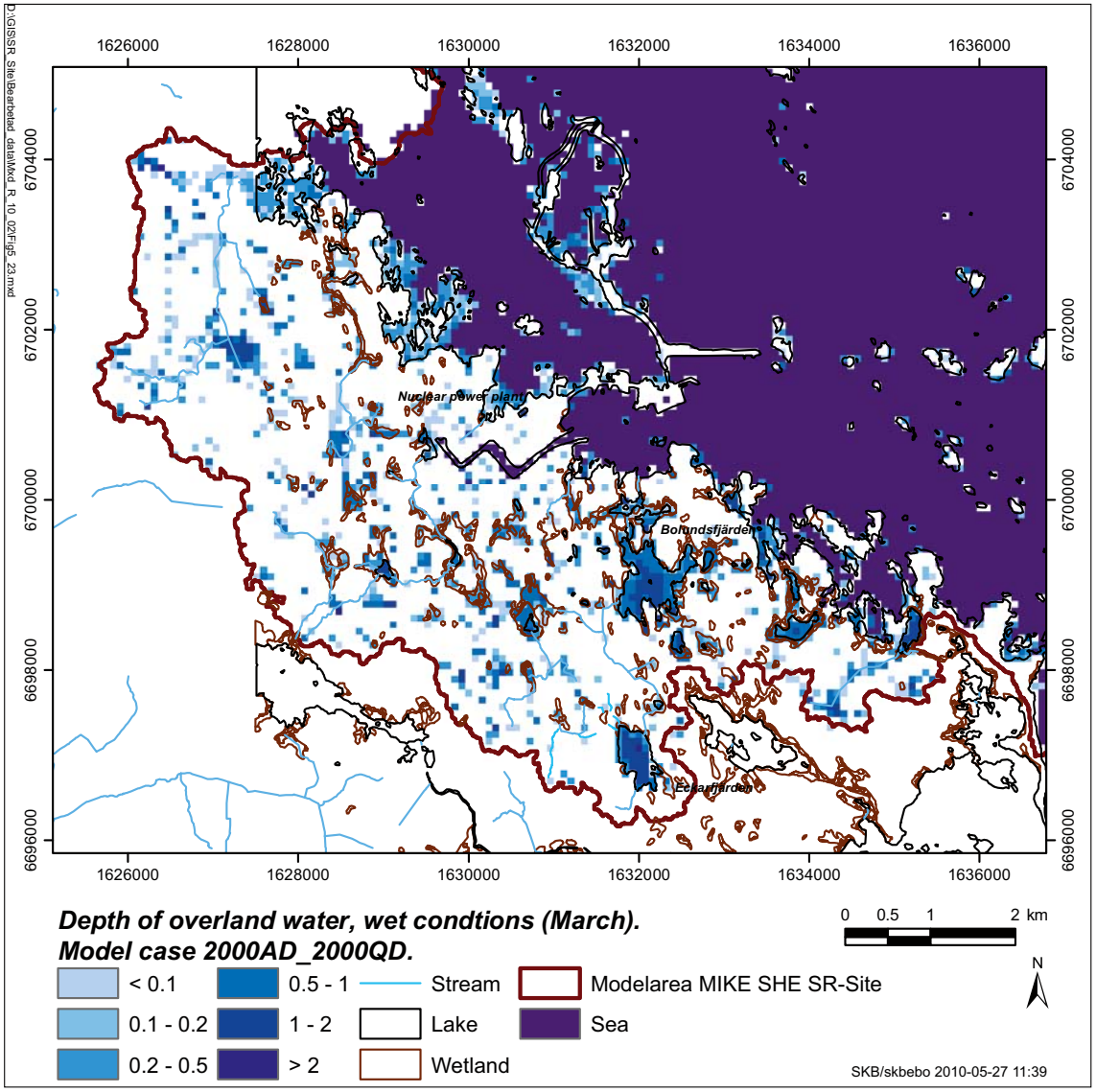

Figure 5-23. Depth of overland water, i.e. lakes and wetlands, from the 2000AD_2000QD model, results for a period of wet conditions. Field-controlled wetlands and lakes are marked in the figure. The western part of the model area is outside the area of the vegetation map; no wetlands are marked in this area.

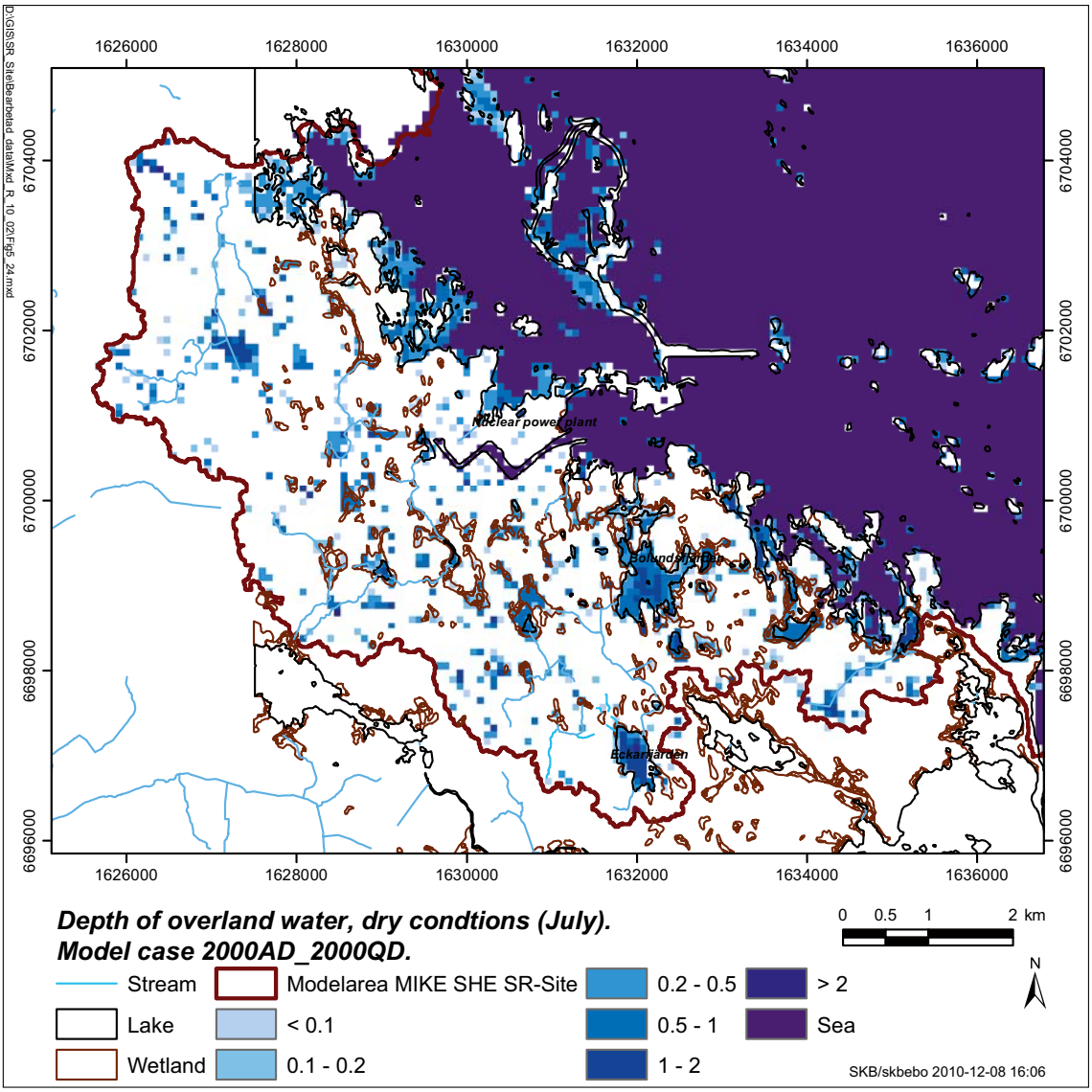

Figure 5-24. *Depth of overland water, i.e. lakes and wetlands, from the 2000AD_2000QD model, results for a period of dry conditions. Field-controlled wetlands and lakes are marked in the figure. The western part of the model area is outside the area of the vegetation map; no wetlands are marked in this area.*

Studying the depth of overland water for the 5000 AD and 10,000 AD models it can be seen that the calculated depth coincides with the GIS-modelled future lakes in the area. When using the 2000 QD model the succession of the lakes is not included in the model, i.e. no lakes have turned into mires. Thus, in the 5000AD_2000QD and 10000AD_2000QD models lakes are built up within the areas of the GIS-modelled lakes. The differences between dry and wet conditions are the same as in the 2000AD_2000QD case; the depths of overland water are somewhat less under dry conditions and the saturated areas are less extensive. Thus, example figures from the 5000AD_2000QD and 10000AD_2000QD models are shown for the period of wet conditions only (Figures 5-25 and 5-26).

In the 5000 QD and 10,000 QD models, some lakes have turned into mires. When applying these models to the MIKE SHE model, the surface water within the GIS-modelled lakes disappears or becomes very shallow. However, the terrestrialised lakes are still topographical low points in the area, and under wet conditions water is accumulating on the ground surface and shallow lakes/wetlands are built up. This phenomenon is clear in the 10000AD_10000QD models. The lakes that switch from almost dry areas to shallow lakes or wetlands under wet conditions in the 10000AD_10000QD model are marked with red circles in Figures 5-27 and 5-28.

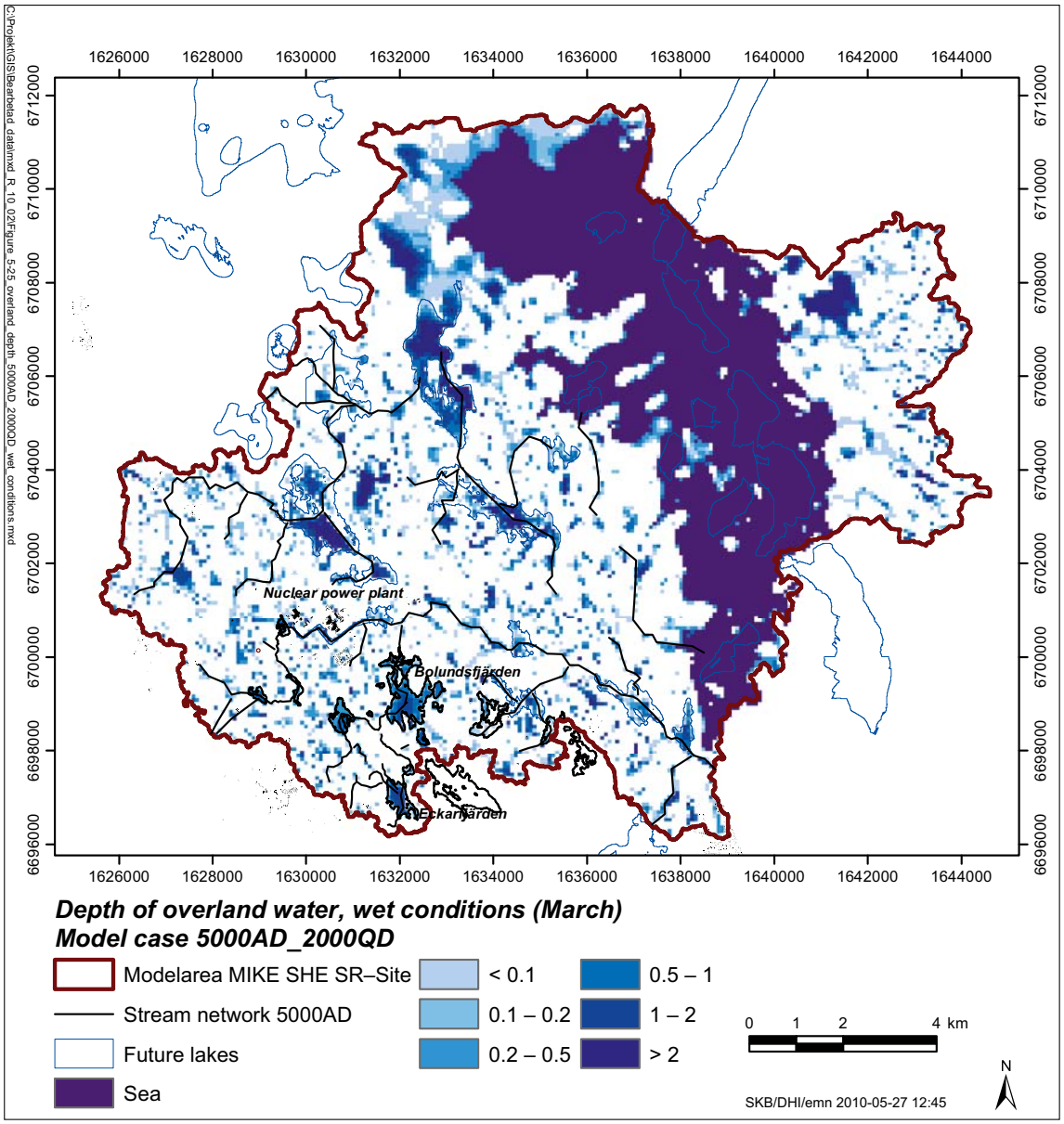

Figure 5-25. *Calculated depth of overland water in the 5000AD_2000QD model, results for a period of wet conditions.*

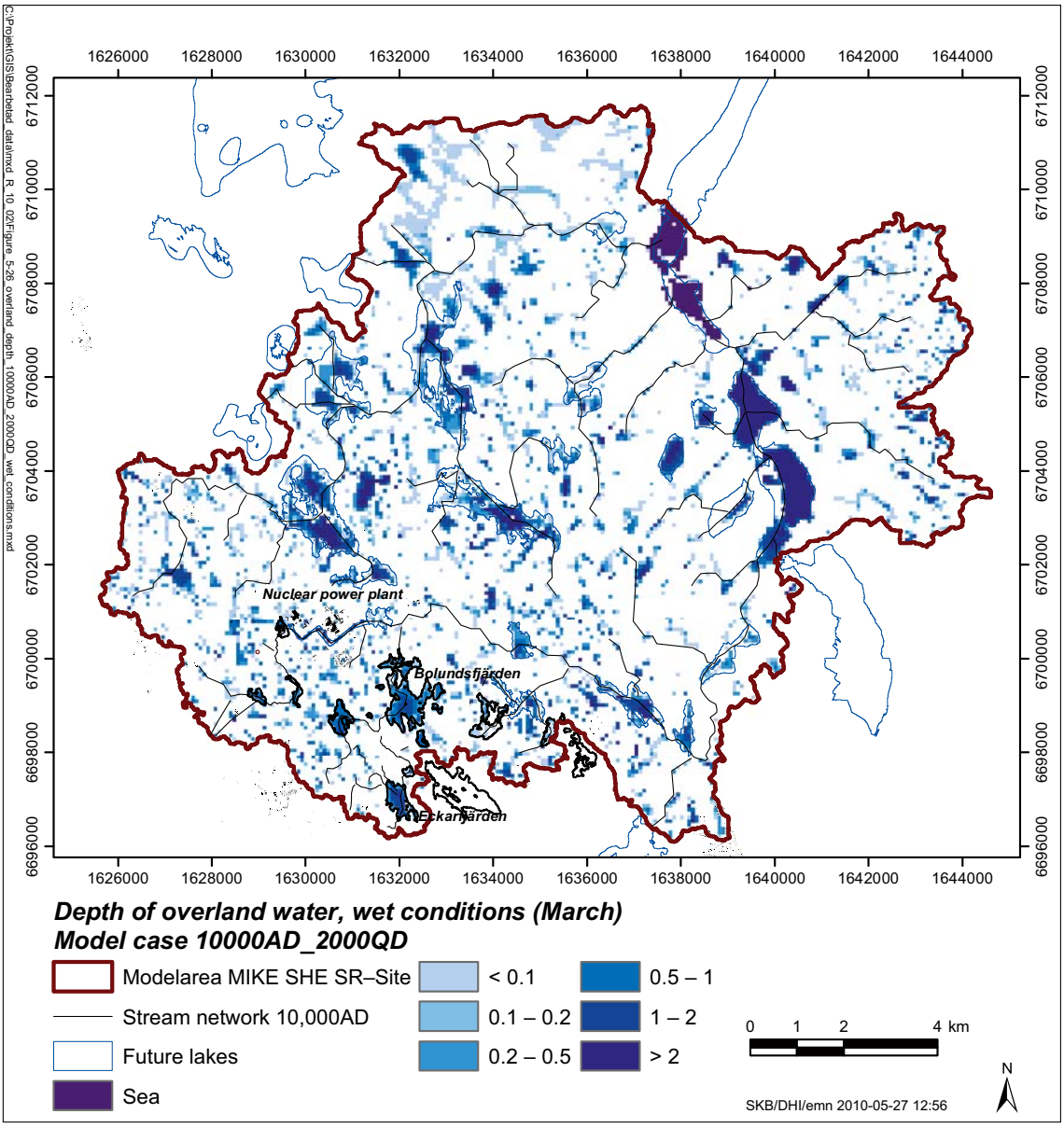

Figure 5-26. *Calculated depth of overland water in the 10000AD_2000QD model results for a period of wet conditions.*

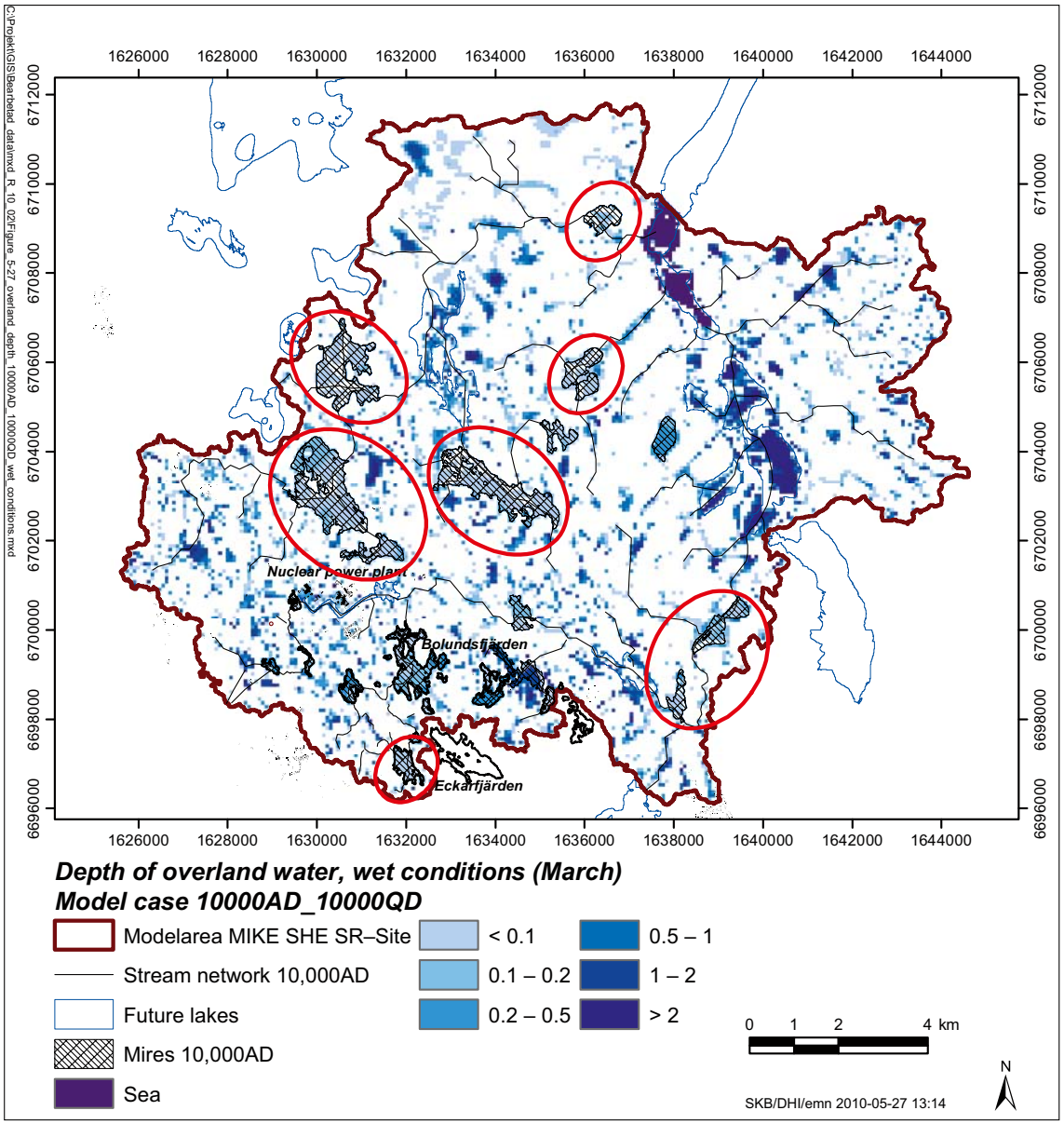

Figure 5-27. *Calculated depth of overland water in the 10000AD_10000QD model, results for a period of wet conditions. The areas that switch from almost dry areas under dry conditions to shallow lakes or wetlands under wet conditions are marked with red circles.*

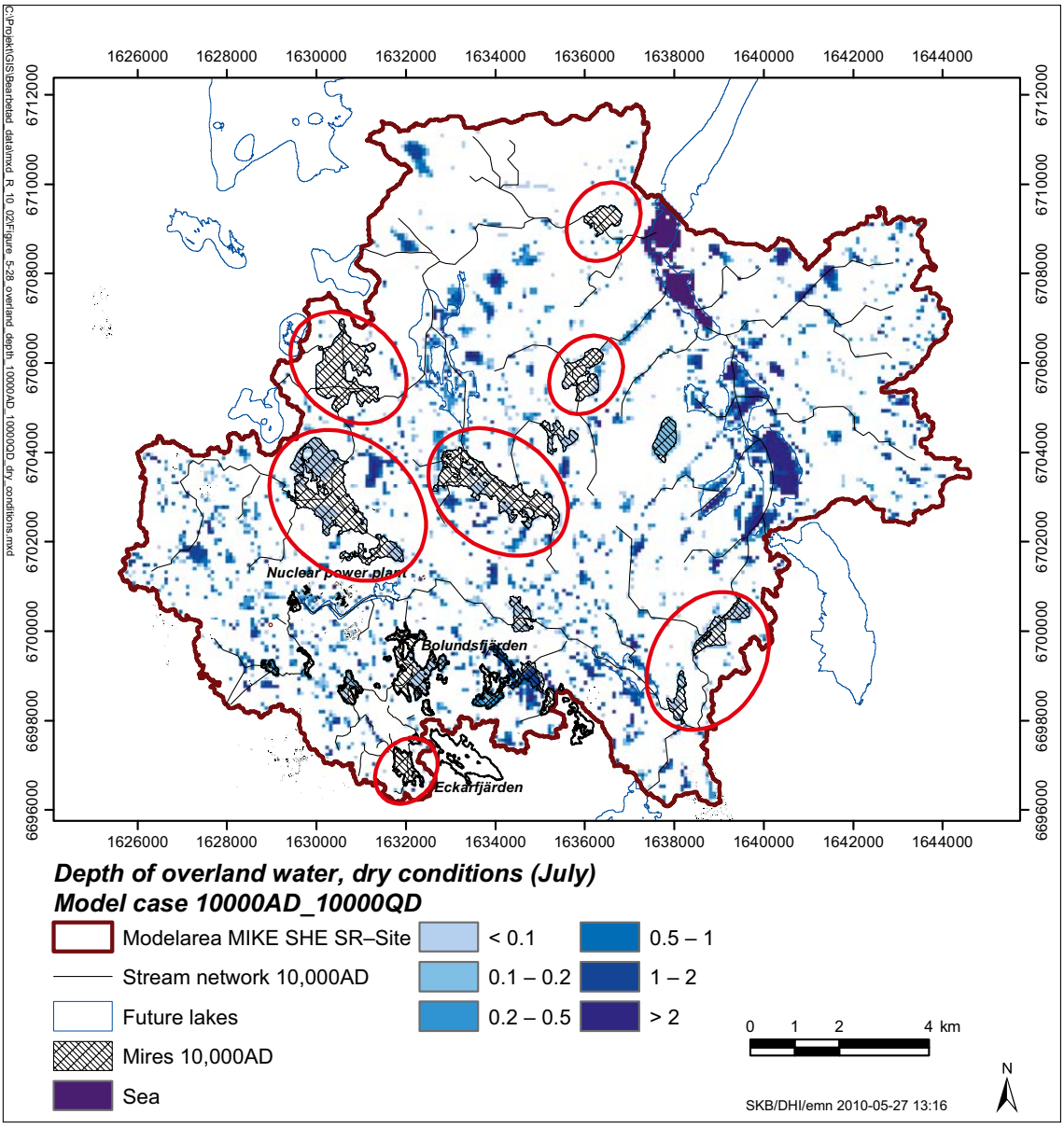

Figure 5-28. *Calculated depth of overland water in the 10000AD_10000QD model, results for a period of dry conditions. The areas that switch from almost dry areas under dry conditions to shallow lakes or wetlands under wet conditions are marked with red circles.*

5.3.3 Groundwater table

The groundwater table in the Forsmark area is very shallow under present conditions. In the major part of the model area the depth to groundwater table is less than 1 m. Figure 5-29 illustrates the cumulative frequency distribution of the groundwater depth within the area constituting land at 2000 AD for the different simulation cases. There is a slight increase of the depth to the groundwater table for all cases compared to the 2000AD_2000QD model which has a mean depth to the ground water table of 0.88 m. The mean depth to the groundwater table for the other cases varies between 0.98 m and 1.19 m, This is due to the more distant shoreline.

When applying the 2000 QD model the groundwater table depth distribution is almost the same. In most of the area, the depth is less than 1.5 m. Approximately 85% of the areas have depths less than 1.5 mm in all the cases (2000AD_2000QD, 5000AD_2000QD and 10000AD_2000QD). In the 5000AD_5000QD and 10000AD_10000QD cases, the frequencies of larger depths are higher. Approximately 20% of the depths are below 2 m compared to 5–10% for the cases where the year 2000 QD model is applied.

A deviation in the 2000AD_2000QD curve can be noticed in the depth interval between 0.5 m and the ground surface. This is due to the drainage function in the MIKE SHE model. The drainage function is activated when the groundwater table rises above 0.5 m depth. This water is moved from the actual cell to the surface stream system or to a topographical low point within the catchment area, resulting in a relative low frequency of depths between 0.5 m and 0 m. Since the shoreline of 2000 AD defines the boundary of the area shown in Figure 5-29, the sea is close to this area with a shallow groundwater table as a result. This means that a lot of cells are handled within the drainage system, the drainage system of the model is described in detail in /Bosson et al. 2008/. A minor deviation due to the same reason can be noticed for the other cases. Since the sea is more distant in the other cases, with a deeper groundwater table as a result, this phenomenon is not as obvious as for the 2000AD_2000QD simulation.

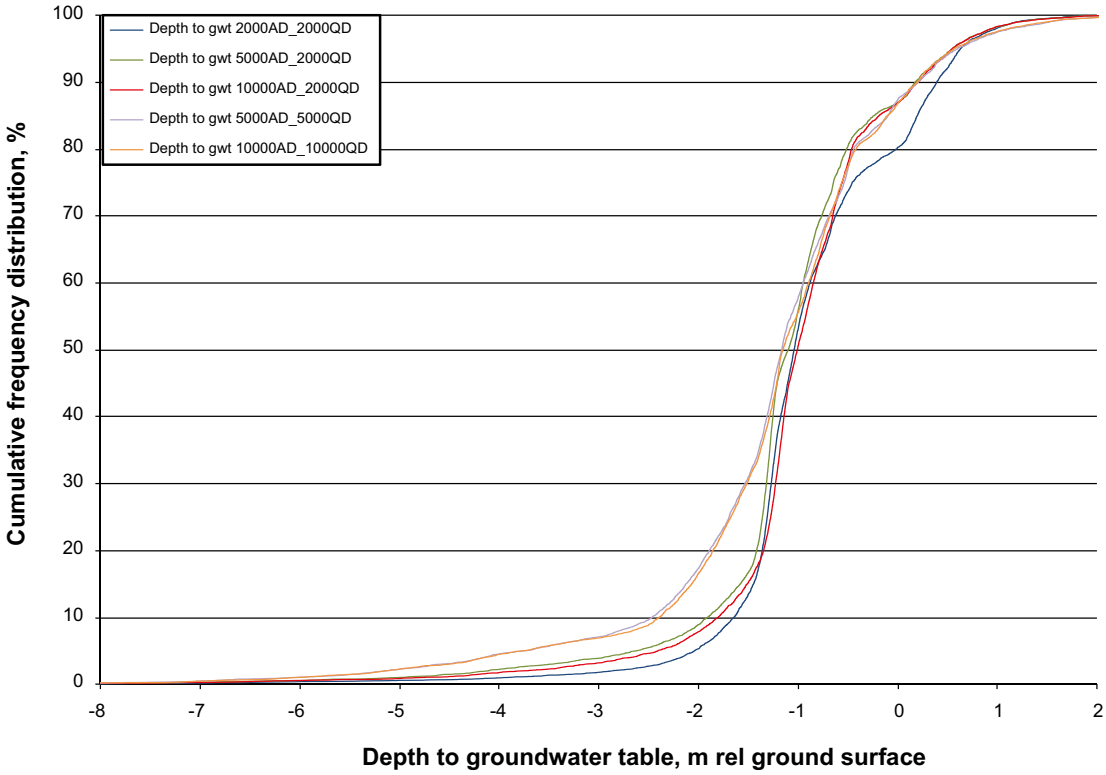

Figure 5-29. *The cumulative frequency of the depth to the groundwater table for all simulation cases. The depths are evaluated for the same area in all cases, i.e. the area constituting land at 2000 AD.*

5.3.4 Recharge and discharge areas

The model results indicate that, as expected, lakes and stream valleys are discharge areas and the high altitude areas are recharge areas. The distribution of recharge and discharge areas changes somewhat with the shoreline displacement, but the overall pattern is the same for all time periods and QD-models. The average situation during the simulation period from October 2003 to October 2004 is presented in Figures 5-30 to 5-34. These figures show the head difference between layers 1 and 2, i.e. the local recharge and discharge areas in the Quaternary deposits. Figures 5-35 to 5-39 show the head difference between layers 4 and 5 (c. 40 m below ground), i.e. the recharge and discharge in the upper bedrock (quantified as head differences).

The sea, stream valleys and lakes in the model area are discharge areas both in the Quaternary deposits and in the upper bedrock. However, the pattern of recharge and discharge areas is more diffuse in the QD, where the local topography creates a varying, small-scale pattern of recharge and discharge areas.

The majority of the terrestrialised lakes in the 5000AD_5000QD and 10000AD_10000QD models still act as discharge areas, even if the lake itself has dried out. However, the strengths of the discharge areas (measured as head differences) are in general less when the lake is terrestrialised. These areas are still topographical low points in the area, which means discharge areas are built up. One exception is found in object 116, which acts as a discharge area in the 10000AD_2000QD model but when applying the 10,000 QD model most of the previous lake area switches into a recharge area. This lake is a very shallow lake and the topography around it is not very distinct. However, 50 m down in the bedrock the whole area is a discharge area; it is only the QD layers that show varying recharge/discharge conditions.

Changing QD model from the 2000 QD model to the 5000 QD or 10,000 QD model does not have a strong influence on the pattern of recharge and discharge areas. It does have an impact on the strengths of the recharge or discharge areas, but areas with an upward or downward gradient in the 2000 QD model still have a gradient in the same direction when applying the 5000 QD or 10,000 QD model. There are some exceptions, but in general the overall pattern seems to be governed by the topography and not the stratigraphy, thickness or type of QD.

In the bedrock the discharge areas (i.e. areas of groundwater flow directed upwards) are concentrated to the areas close to and under the lakes. Also, the depressions around the streams are reflected as discharge areas in the bedrock. In particular, the valley of the stream dewatering the catchment area of Lake Bolundsfjärden and the catchment area of Lake Gunnarsboträsket is a very strong discharge area in the 5000 AD and 10,000 AD models. In general the discharge areas, both in QD and bedrock, are stronger in the models with the shoreline of 5000 AD and 10,000 AD. This is due to a more distinct topography in the future land areas. The Forsmark area of today has small-scale topography. The highest point within the model area at 2000 AD is at approximately 20 m.a.s.l.

In all model cases Lake Bolundsfjärden deviates from the other lakes. The average situation during the year in the QD-layers of the 2000AD_2000QD model is that the lake acts as a discharge area. However, during summer periods the lake may act as recharge area due to the transpiration of the plants in the catchment area /Johansson 2008, Bosson et al. 2008/. In the upper bedrock some parts of the area under the lake have a downward gradient (Figure 5-35). The sheet joints in the upper rock, see Section 2.5, short circuit the vertical flow and water is transported towards the sea. The recharge area under the lake increases in size when the shoreline moves further away from the lake. In the 10,000 AD models almost the whole lake acts as a recharge area, both in the QD and in the bedrock.

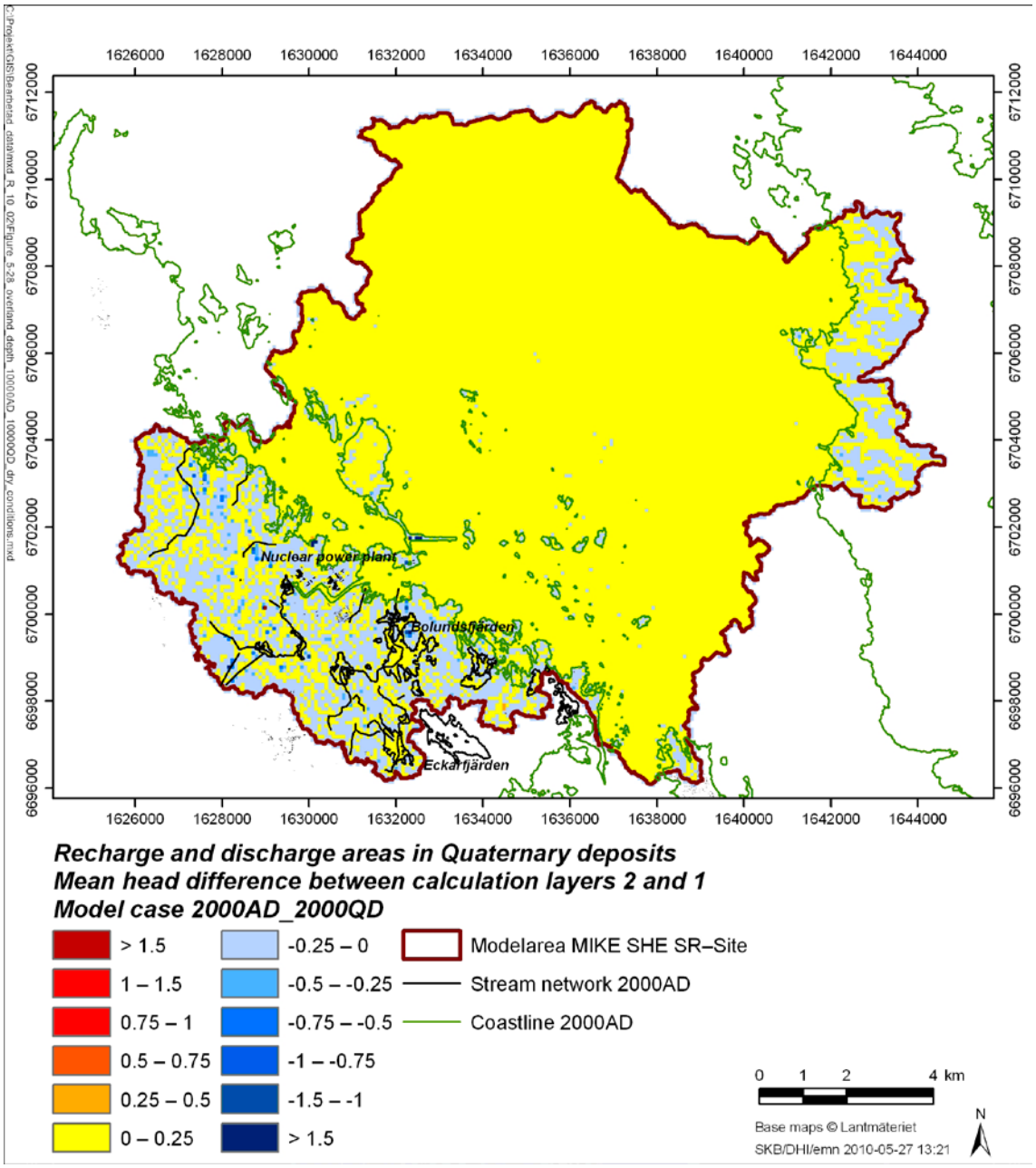

Figure 5-30. *The recharge and discharge areas in the Quaternary deposits of the 2000AD_2000QD model, calculated as the head difference between the two QD layers of the model.*

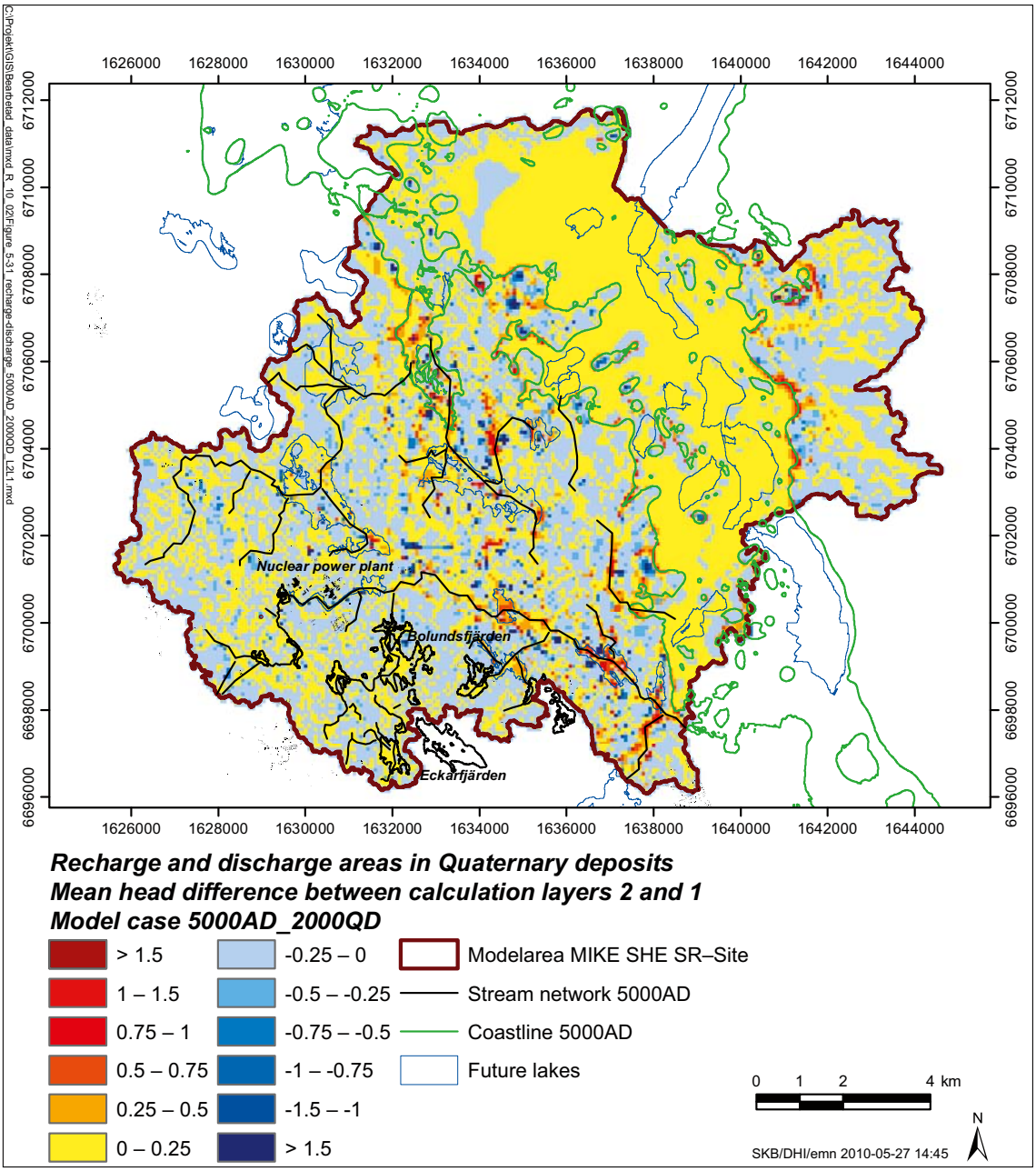

Figure 5-31. *The recharge and discharge areas in the Quaternary deposits of the 5000AD_2000QD model, calculated as the head difference between the two QD layers of the model.*

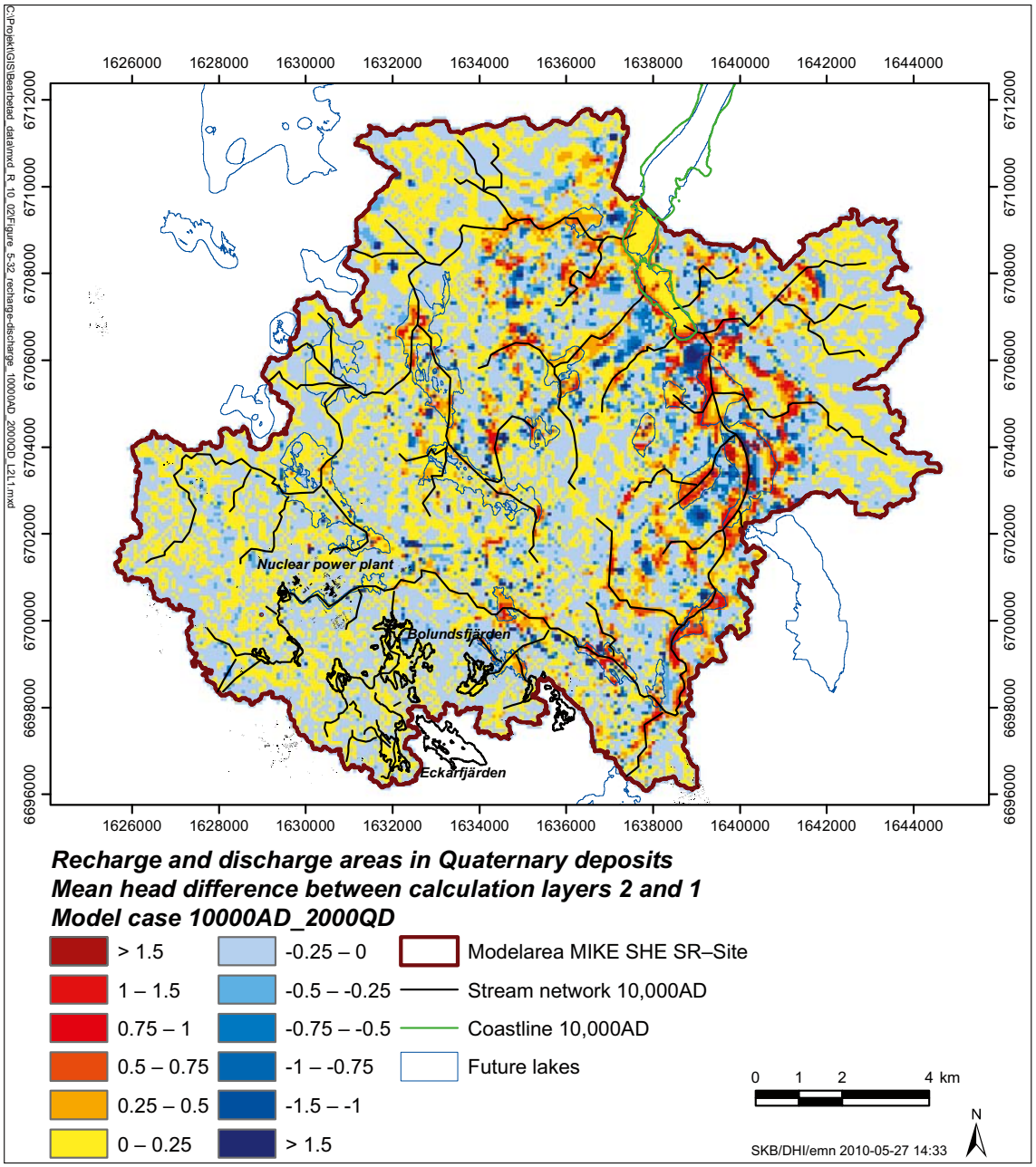

Figure 5-32. *The recharge and discharge areas in the Quaternary deposits of the 10000AD_2000QD model, calculated as the head difference between the two QD layers of the model.*

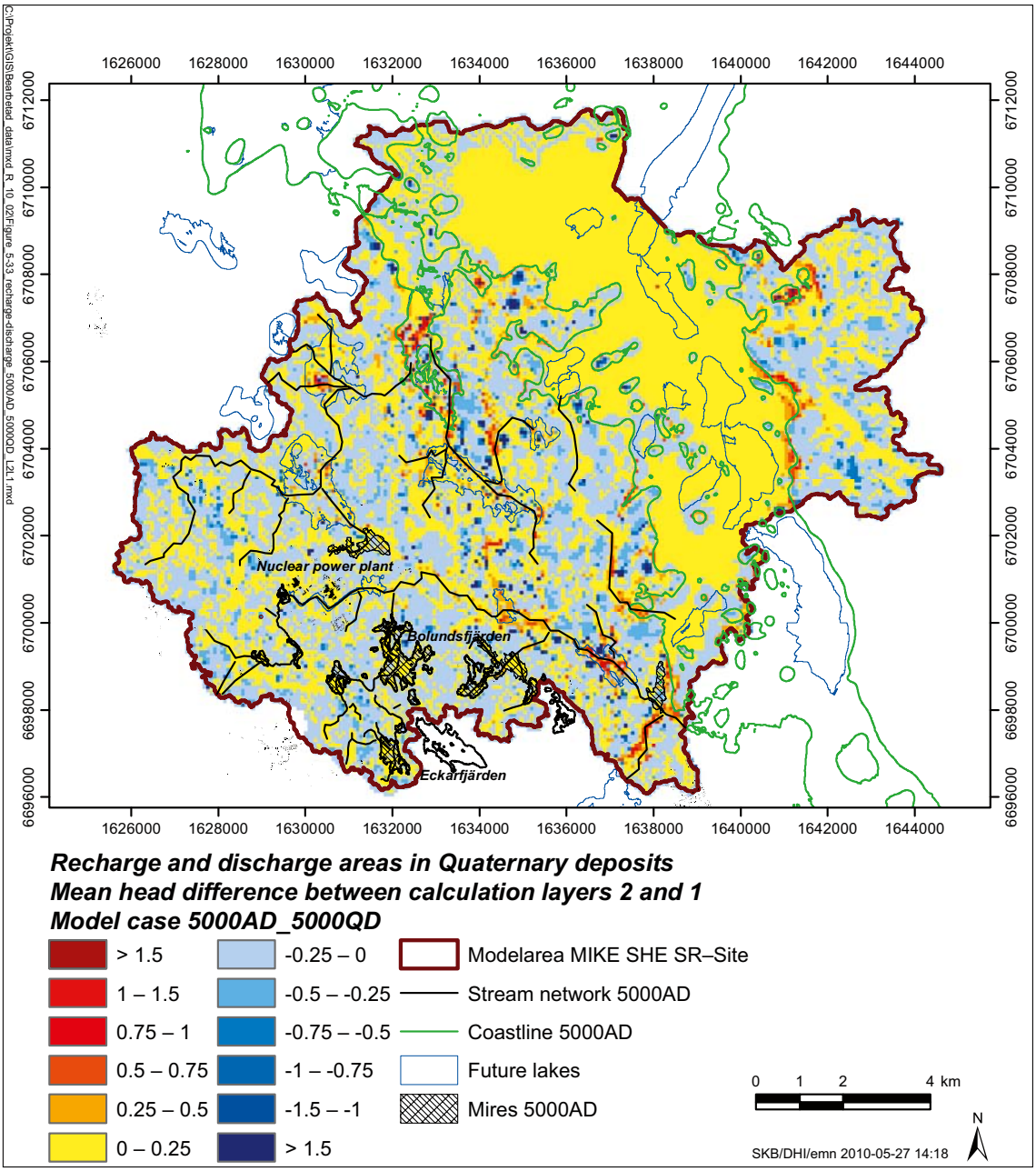

Figure 5-33. *The recharge and discharge areas in the Quaternary deposits of the 5000AD_5000QD model, calculated as the head difference between the two QD layers of the model.*

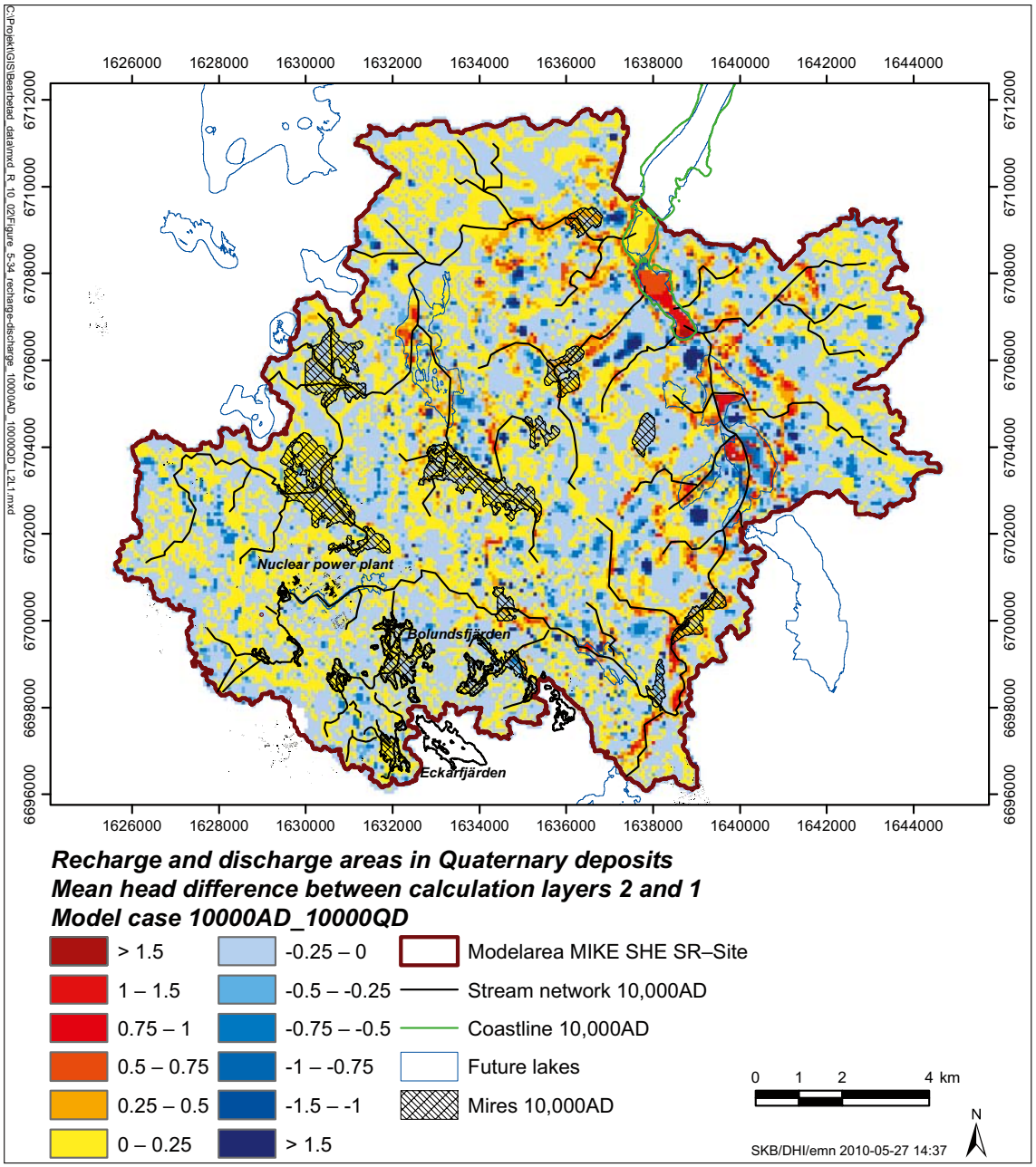

Figure 5-34. *The recharge and discharge areas in the Quaternary deposits of the 10000AD_10000QD model, calculated as the head difference between the two QD layers of the model.*

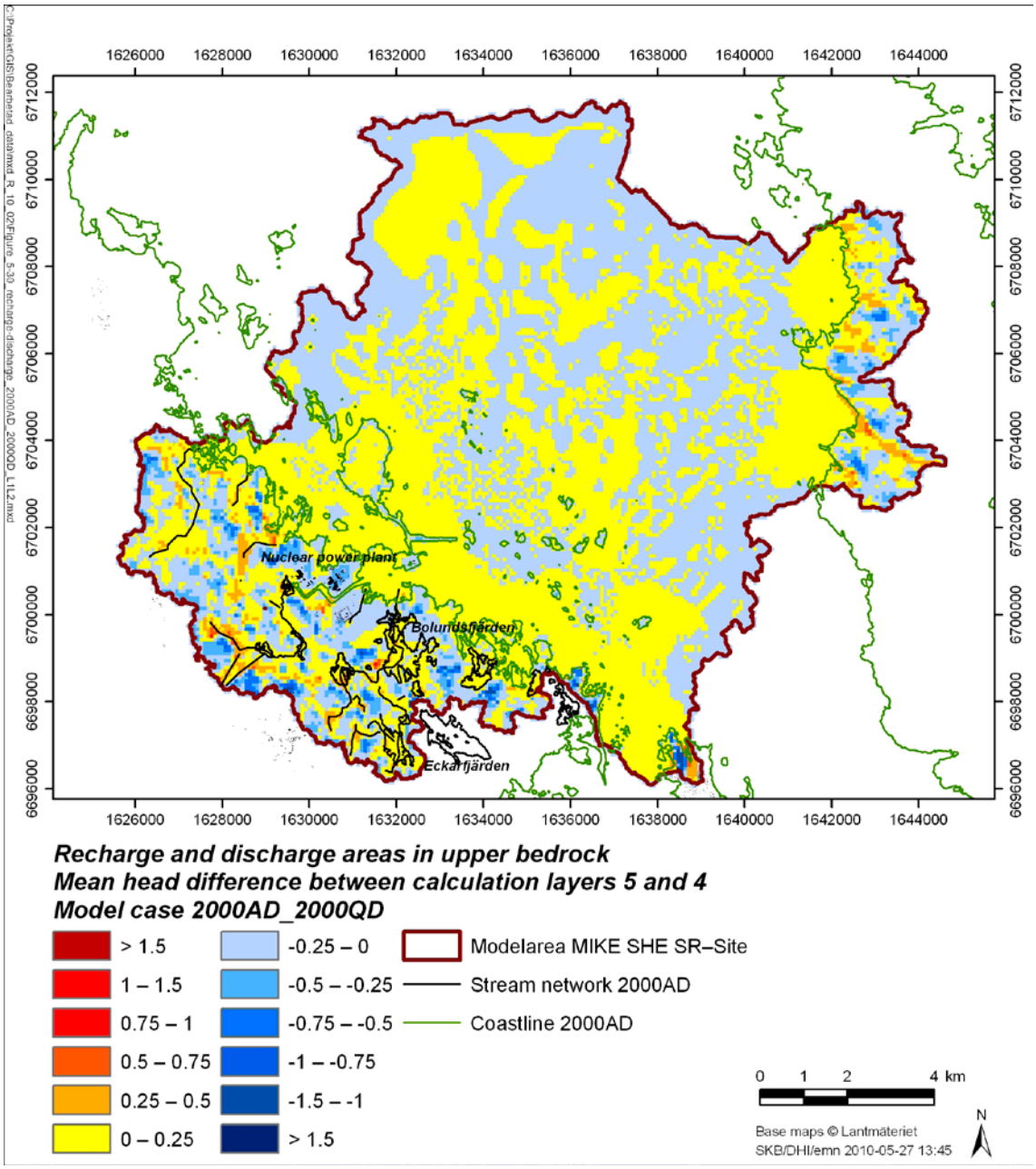

Figure 5-35. *The recharge and discharge areas in the upper bedrock of the 2000AD_2000QD model at a depth of approximately 50 m, calculated as the head difference between two adjacent bedrock layers at that depth.*

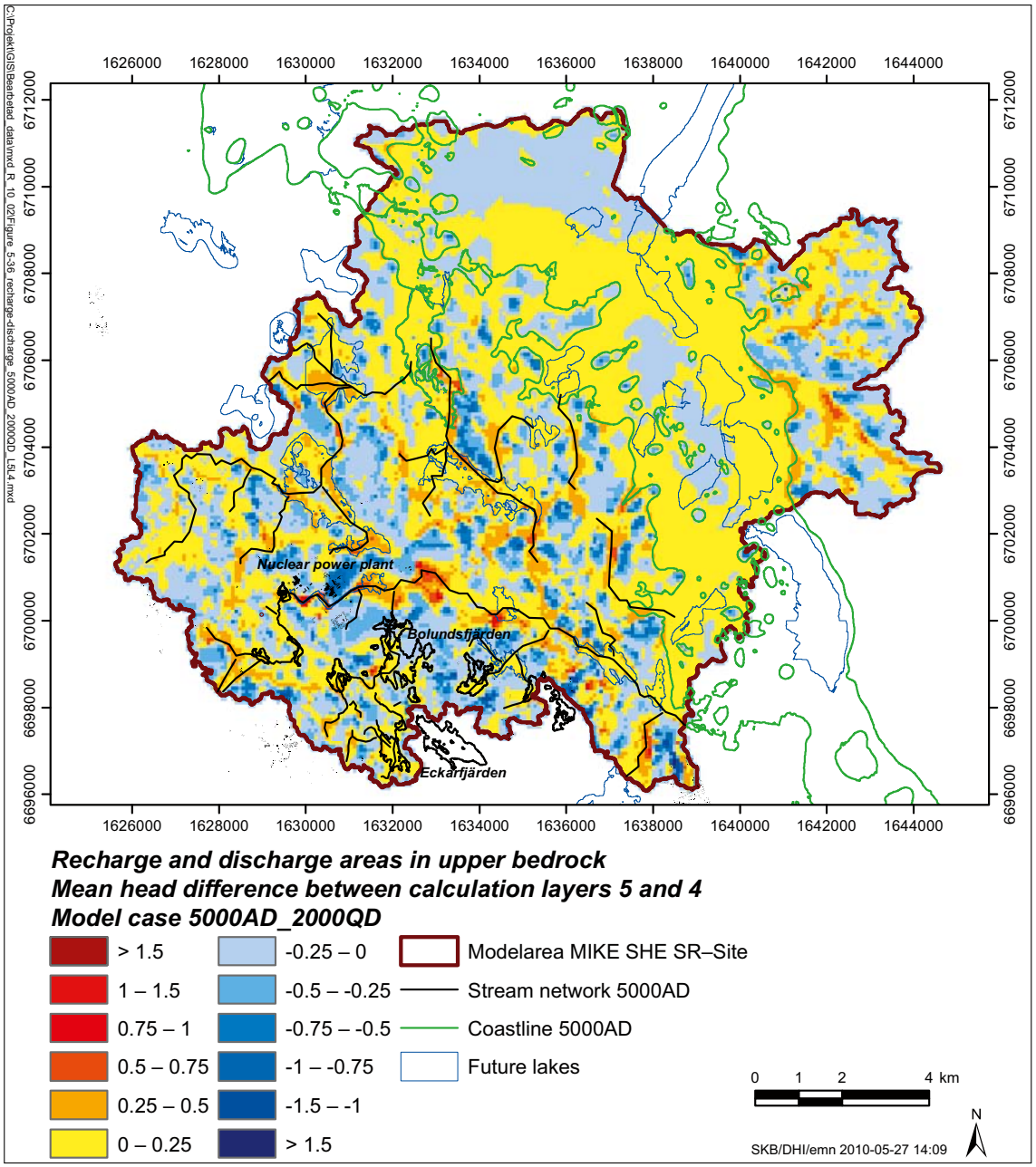

Figure 5-36. *The recharge and discharge areas in the upper bedrock of the 5000AD_2000QD model at a depth of approximately 50 m, calculated as the head difference between two adjacent bedrock layers at that depth.*

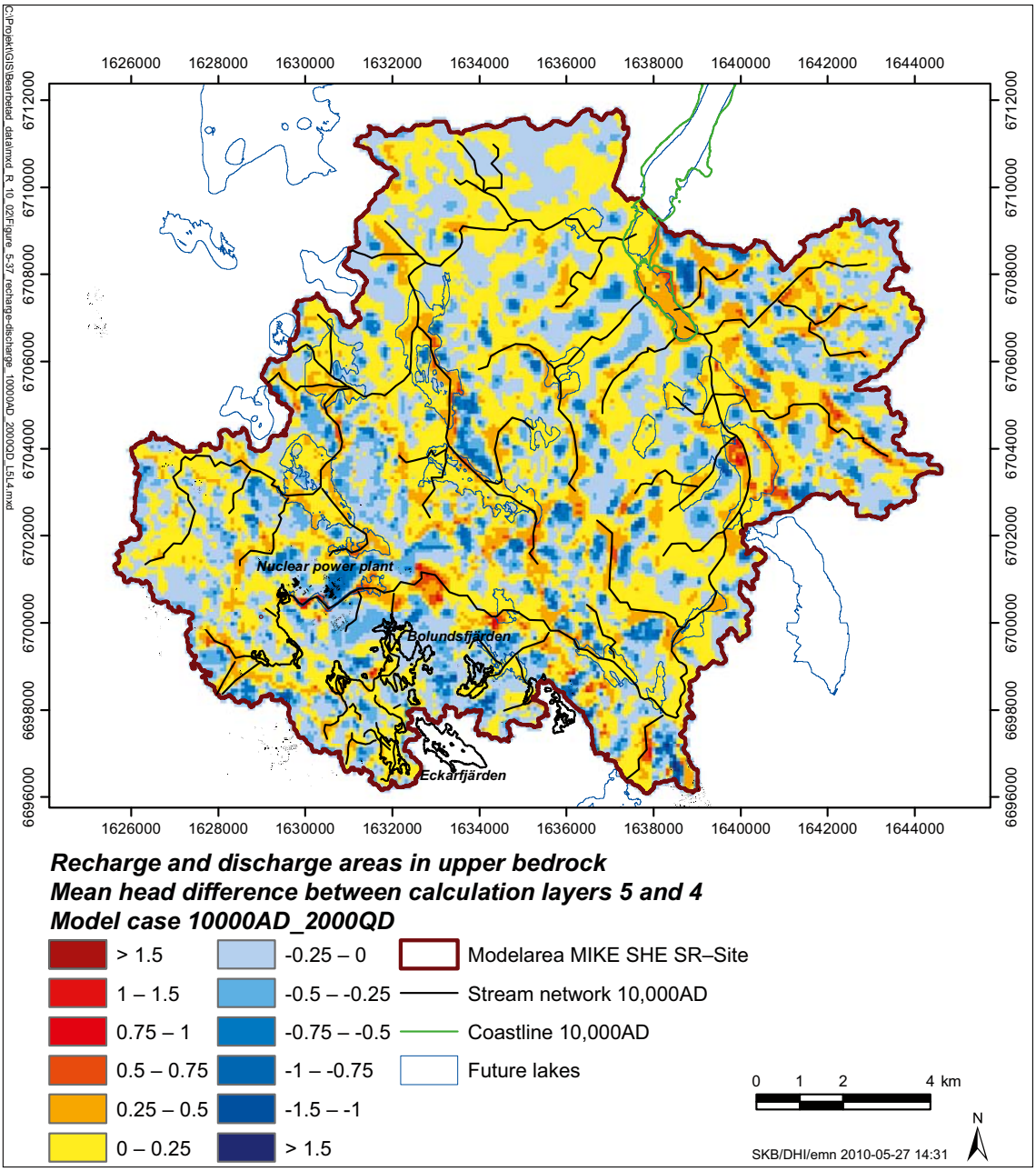

Figure 5-37. *The recharge and discharge areas in the upper bedrock of the 10000AD_2000QD model at a depth of approximately 50 m, calculated as the head difference between two adjacent bedrock layers at that depth.*

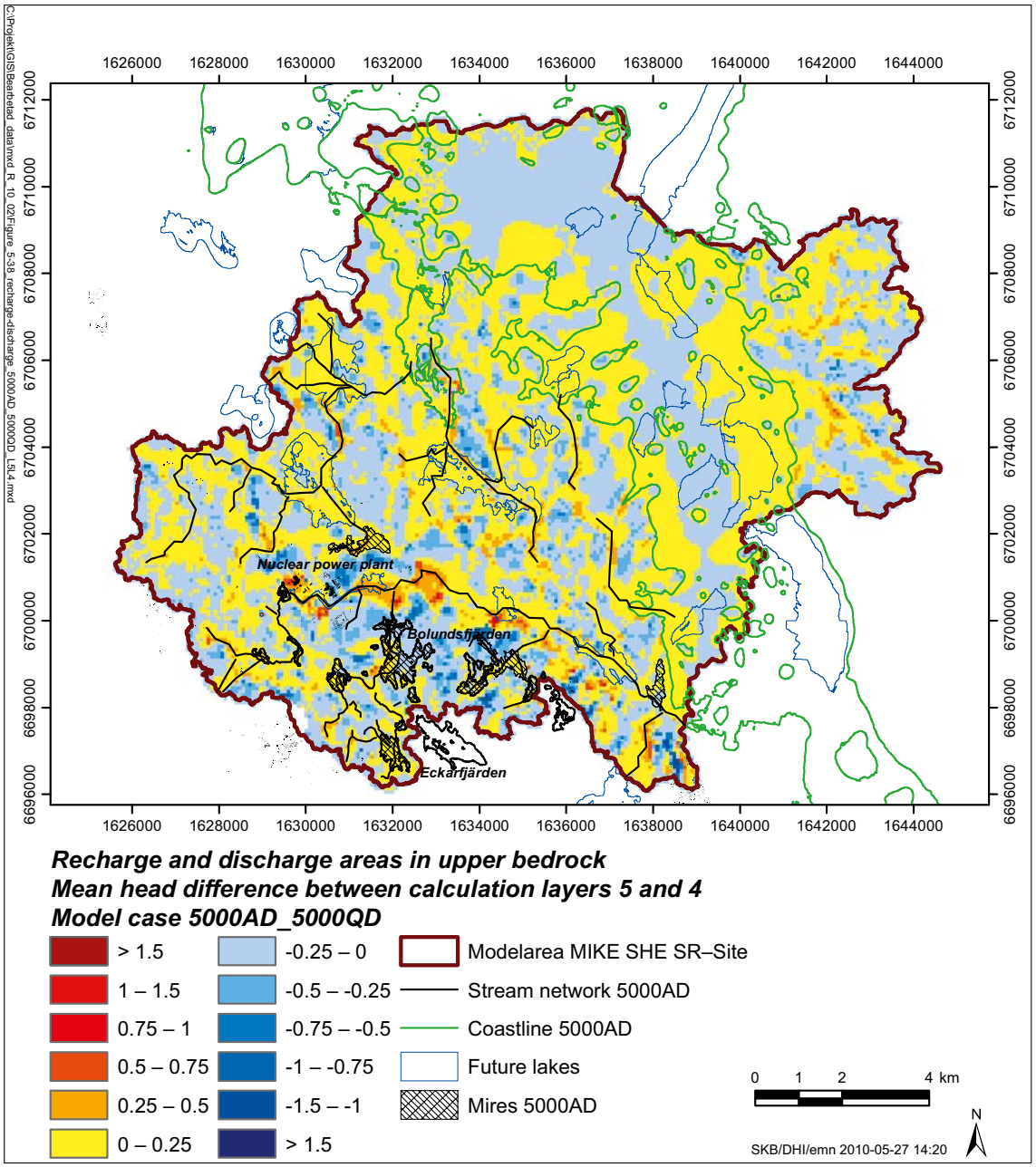

Figure 5-38. *The recharge and discharge areas in the upper bedrock of the 5000AD_5000QD model at a depth of approximately 50 m, calculated as the head difference between two adjacent bedrock layers at that depth.*

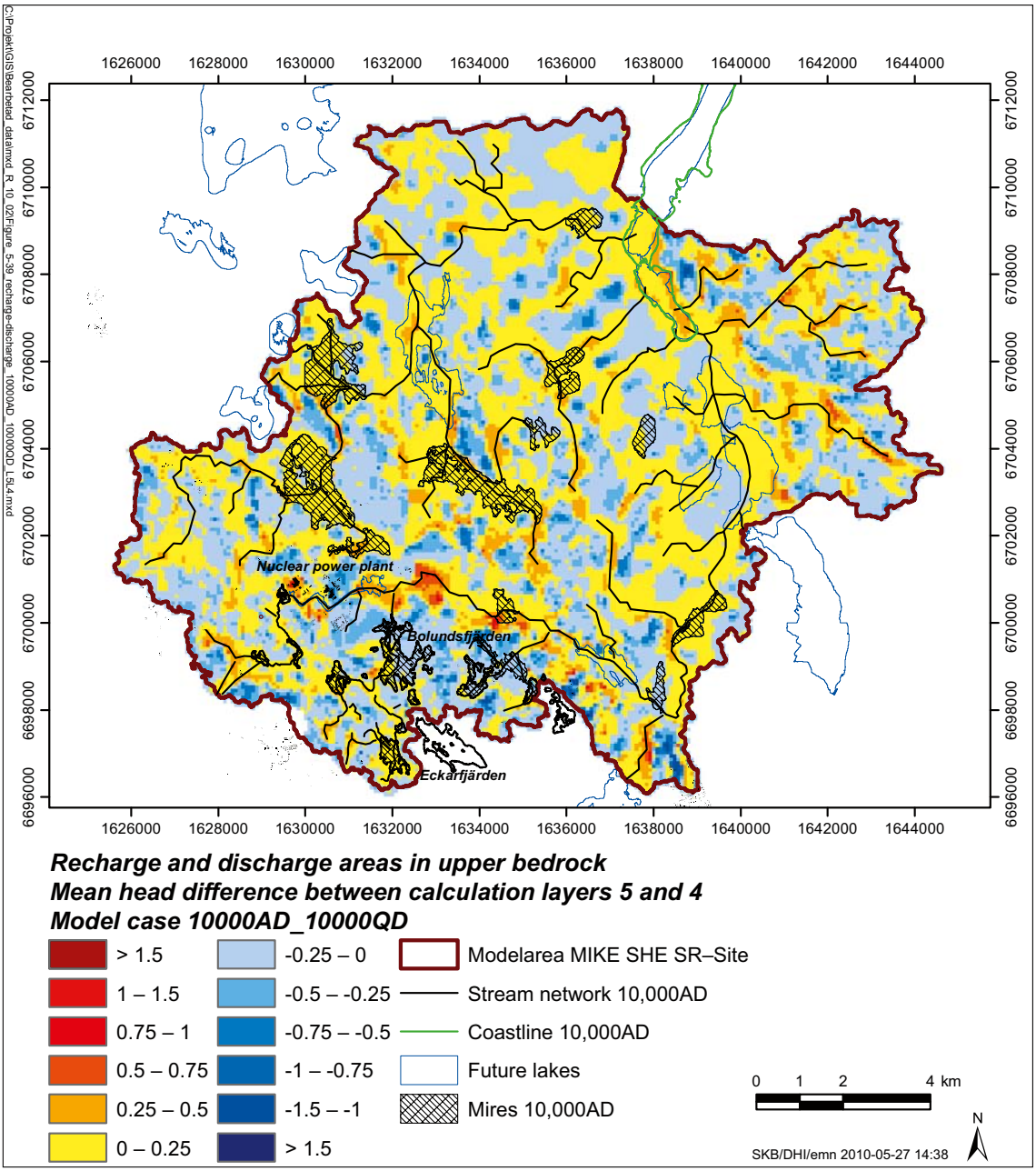

Figure 5-39. *The recharge and discharge areas in the upper bedrock of the 10000AD_10000QD model at a depth of approximately 50 m, calculated as the head difference between two adjacent bedrock layers at that depth.*

The particle tracking results from the regional models are presented in Section 5.4. In this section particle tracking results have been used as supporting information to study the recharge and discharge pattern under Lake Bolundsfjärden during different time periods. Figures 5-40 and 5-41 illustrate particle tracking results and head profiles, respectively, from the 2000AD_2000QD and 10000AD_10000QD models. One particle was released in each cell at 150 m.b.s.l. Only the flow paths of the particles released under Lake Bolundsfjärden are illustrated in Figure 5-40. It is seen in the 2000AD_2000QD model results that the majority of the particles move up towards the south-eastern shoreline of the lake. Some particles cross the sheet joints and move towards the sea and some are moving downwards. The simulation was run for 1,000 years. Many of the particles have not reached the surface at the end of the simulation.

Studying the 2000AD_2000QD head profile in Figure 5-41, showing the upper 50 m of the model, it is seen that the main flow direction is towards the lake. Also, looking at the horizontal views, the main part of the lake has an upward gradient (yellow to brown colours) in both QD and bedrock. The number of cells having a downward gradient (blue colours) in the bedrock is somewhat larger than in the QD. In the 10000AD_10000QD model only a few particles move towards the former lake. The rest of the particles flow in the sheet joints towards the sea and end up in the future lakes further north. Studying the head profile of the upper 50 m of the former lake area it is seen that the major part of the area has a downward gradient.

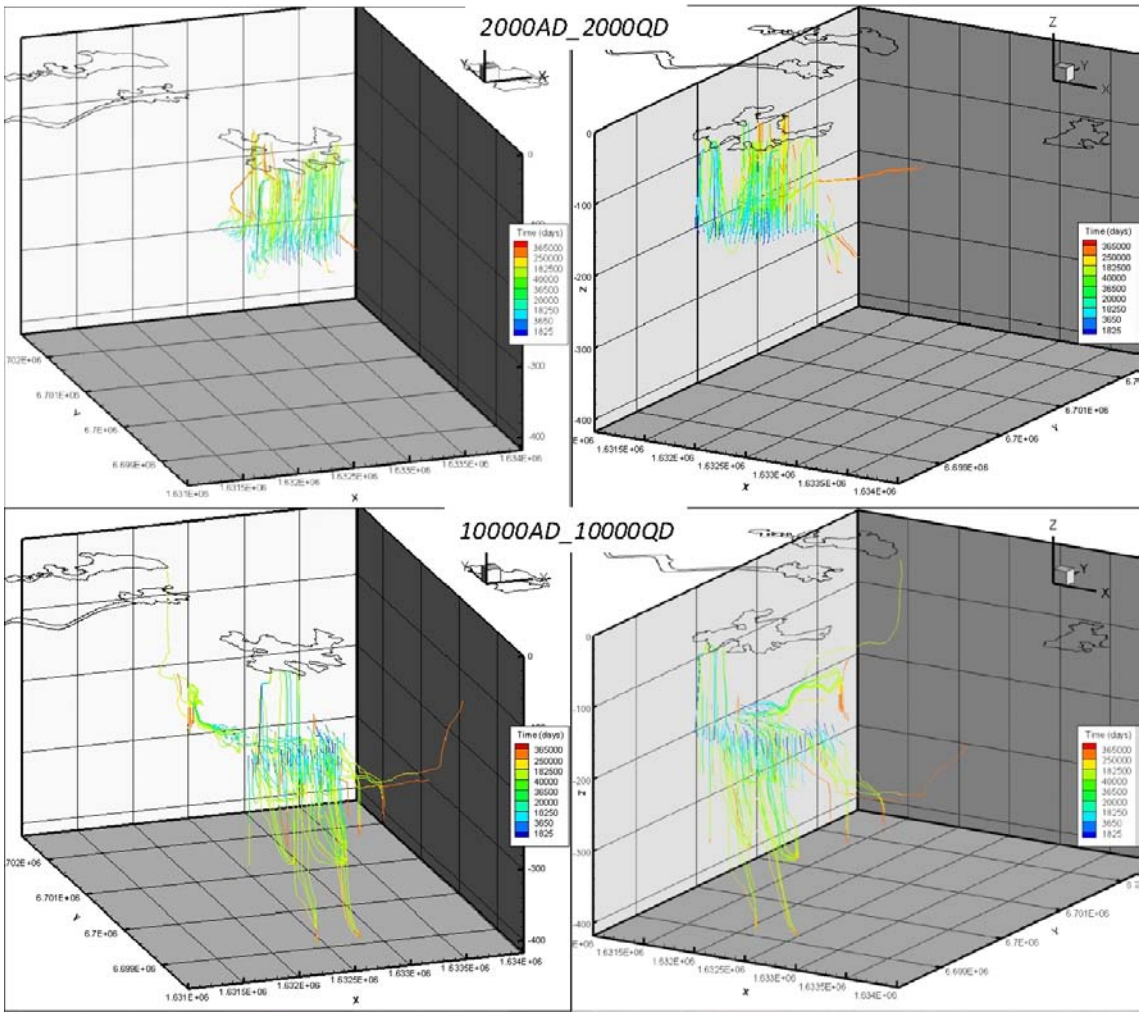

Figure 5-40. *Particle flow paths, one particle released in each cell at 150 m.b.s.l. Only particles released under Lake Bolundsfjärden are illustrated in the 3D-figures. The upper two figures are from the 2000AD_2000QD model and the two lower figures from the 10000AD_10000QD model. Two different views are shown for each time period. Lake Bolundsfjärden, the inlet canal and some future lakes are shown as an orientation.*

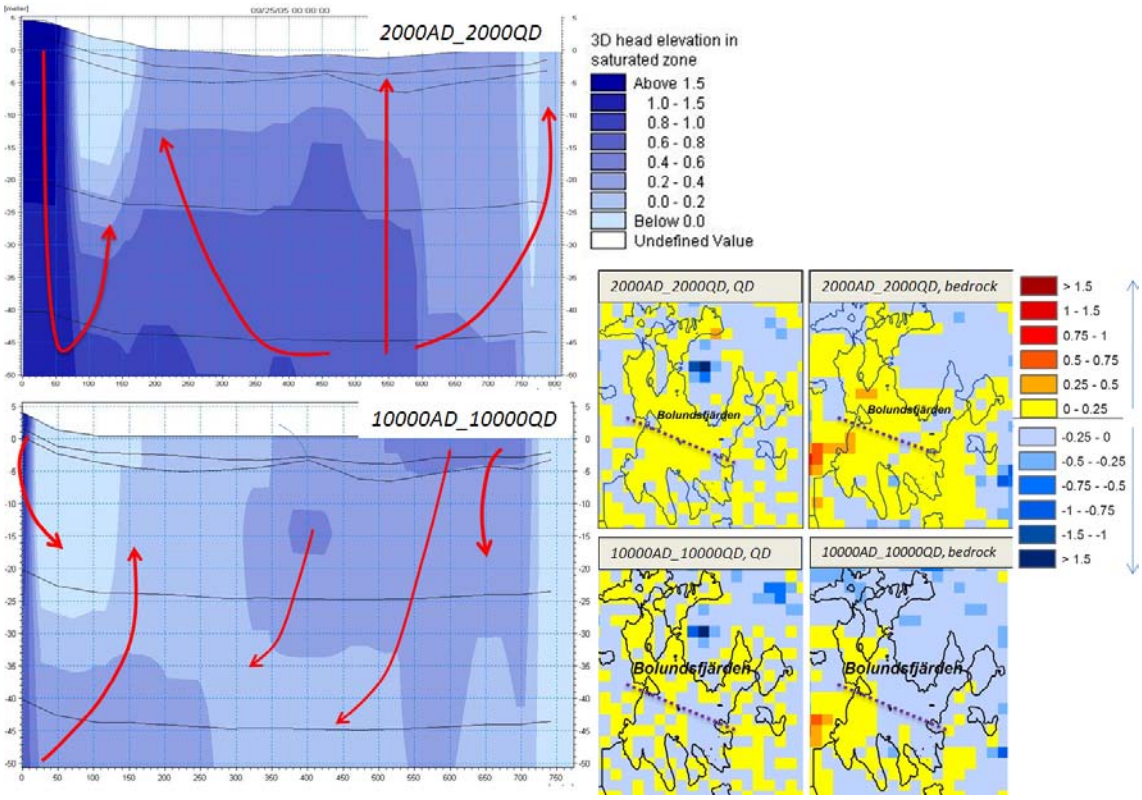

Figure 5-41. *Head profiles in the upper 50 m of the models. The uppermost figure shows results from the 2000AD_2000QD model and the one at the bottom from the 10000AD_10000QD model. Also, the head differences in QD and the upper bedrock are shown as horizontal views. The location of the profile is shown as a dotted line.*

Particle flow paths for particles released under object 116 are shown in Figure 5-42. As described above, the lake mainly act as a discharge area independently of the shoreline. The gradient in the bedrock is always directed upwards, but in the 10000AD_10000QD model the gradient in the QD-layers has a downward direction. At 2000 AD the lake is still below sea level. Some areas under the future lake are discharge areas and the flow paths of the particles are directed towards topographical low points within the future shoreline of the lake. The majority of the particles are still below the lake after 1,000 years of simulation. The low gradients below the sea result in long transport times and short flow paths.

At 10,000 AD the lake is above sea level, but also filled with peat. At this stage the whole lake has turned into a discharge area; all the particles released below the lake are rapidly transported towards ground surface. However, the velocity is reduced when the particles reach the QD layers and many of the particles are stuck in the bottom sediments due to the downward gradient in the QD. In Figure 5-43 a head profile across the lake from the 10000AD_10000QD model is shown. The right figure shows the head profile for the whole model depth and the left figure for the upper 25 m of the model. In the bedrock there is a clear upward gradient from the bedrock towards the QD layers, but in the upper part of the model the gradient is directed downwards. This is also seen in the horizontal views showing the head differences, i.e. the recharge and discharge areas in the QD and in the bedrock, shown at the bottom of Figure 5-43.

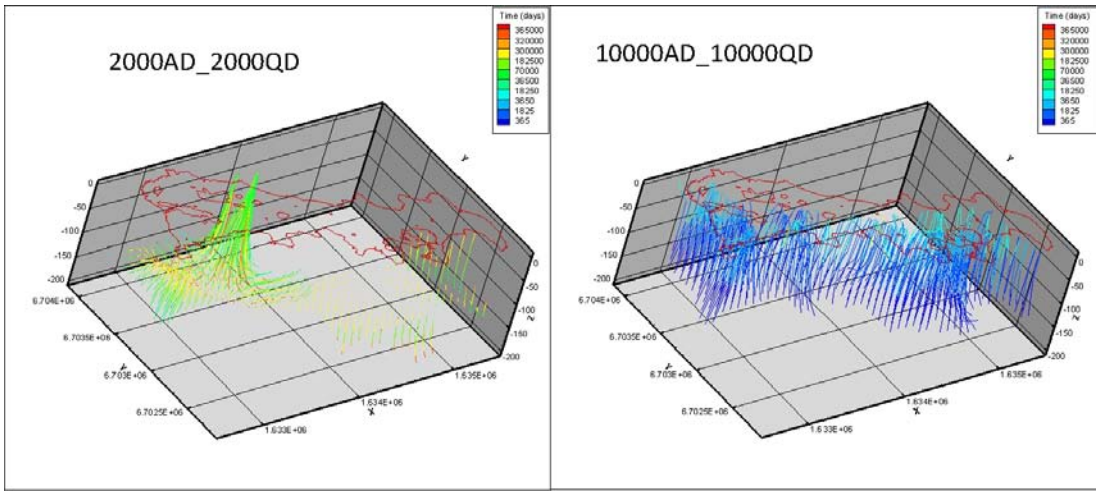

Figure 5-42. *Particle tracking results illustrating the flow path of the particles released below object 116. At 2000 AD only some parts of the future lake act as discharge areas, whereas at 10,000 AD all the particles released under the lake are rapidly transported up towards the lake.*

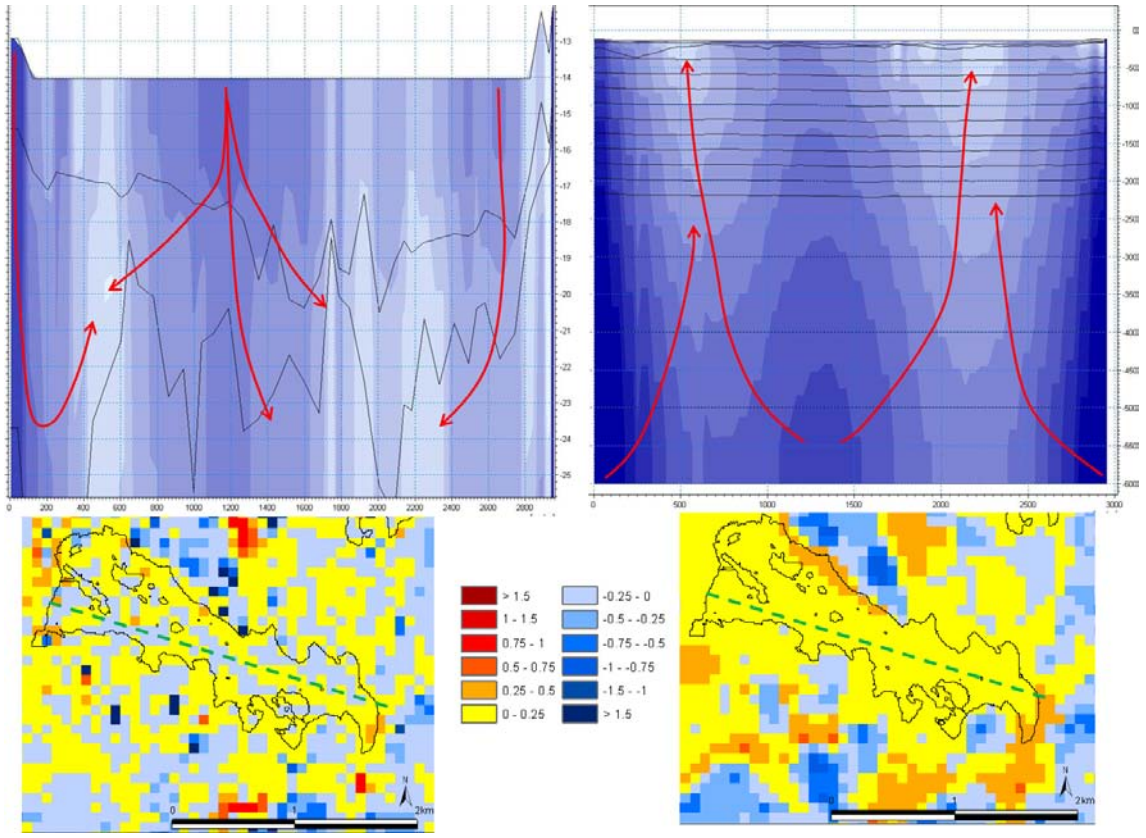

Figure 5-43. *Head profiles across object 116, showing results from the 10000AD_10000QD model. The right figure illustrates the head profile for the whole model extent down to 600 m.b.s.l. and the left figure shows the head profile for the upper 25 m of the model. At the bottom left the head difference between the two QD-layers is shown as a horizontal view and to the right the head difference at approximately 50 m depth. Blue colours indicate a downward gradient and yellow-red colours indicate an upward gradient.*

5.4 Transport modelling results

Based on the water flow field from the regional water movement simulations three particle tracking (PT) simulations were performed. The PT simulations were carried out using the 2000AD_2000QD model, the 5000AD_5000QD model, and the 10000AD_10000QD model. In each case, one particle per cell was introduced at approximately 150 m.b.s.l.

The aim with the PT simulations is to better understand and analyse the water flow paths in the upper bedrock and the QD and how the water flow paths are influenced by the landscape development. To identify the discharge areas associated with flow from the deep bedrock to the ground surface and to investigate whether locations of discharge areas are changing in time are important parts of the assessment of a potential release of radionuclides from the repository.

All PT simulations were run for 1,000 years. Table 5-6 lists the different sinks to which the particles went in the different simulations. Also the number of particles left in the model after 1,000 years of simulation is listed for each case; all results are given in percent. Due to the shoreline displacement, the sea part of the model area decreases with time. At 10,000 AD only 1% of the model area is covered by sea, compared to 70% at 2000 AD. The low gradients below the sea lead to very small flow velocities and many particles released below the sea are still left in the model after 1,000 years. At 2000 AD 67% of the particles are still left in the model volume compared to 11% at 10,000AD.

The locations and elevations of the particles left in the model at the end of the simulations with the 2000AD_2000QD model and the 10000AD_10000QD model are shown in Figures 5-44 and 5-45. The grey colour in almost the whole area under the sea in the 2000AD_2000QD model (Figure 5-44) indicates that the most of the particles are still left at the level where they were released.

The exit points at the ground surface are concentrated to lakes, wetlands and the surface water network (Figure 5-46). At 2000 AD, most of the exit points are concentrated to the part of the model area constituting land. The particles discharging at sea are concentrated to near-shore bays and some smaller islands within the model area. At 10,000 AD the exit points reflect the surface stream network. Also some future lakes and wetlands in topographical low points have a high concentration of discharged particles, Figure 5-47.

In both simulations the dominating sink is the combined overland water/unsaturated zone sink. It is not possible in MIKE SHE to separate the particles going to the overland compartment and the unsaturated zone. However, since the majority of the exit points are within the area of future lakes and wetlands it is assumed that the overland compartment, i.e. surface water, is the dominating sink.

Figure 5-48 shows the birth locations of all the particles that have been registered within the shoreline of Lake Bolundsfjärden. At 2000 AD a larger area contributes to the discharge of particles to the lake. The extent of the area contributing to a groundwater discharge in Lake Bolundsfjärden changes with the shoreline displacement and the applied QD model.

Table 5-6. Different sinks for the released particles in the three different PT simulations.

	2000AD_2000QD	5000AD_5000QD	10000AD_10000QD
Particles introduced, %	100	100	100
Particles left in the model, %	67	21	11
Particles gone to stream, %	3	15	27
Particles gone to boundary, %	7	16	4
Particles gone to OL or Unsaturated zone, %	23	48	58

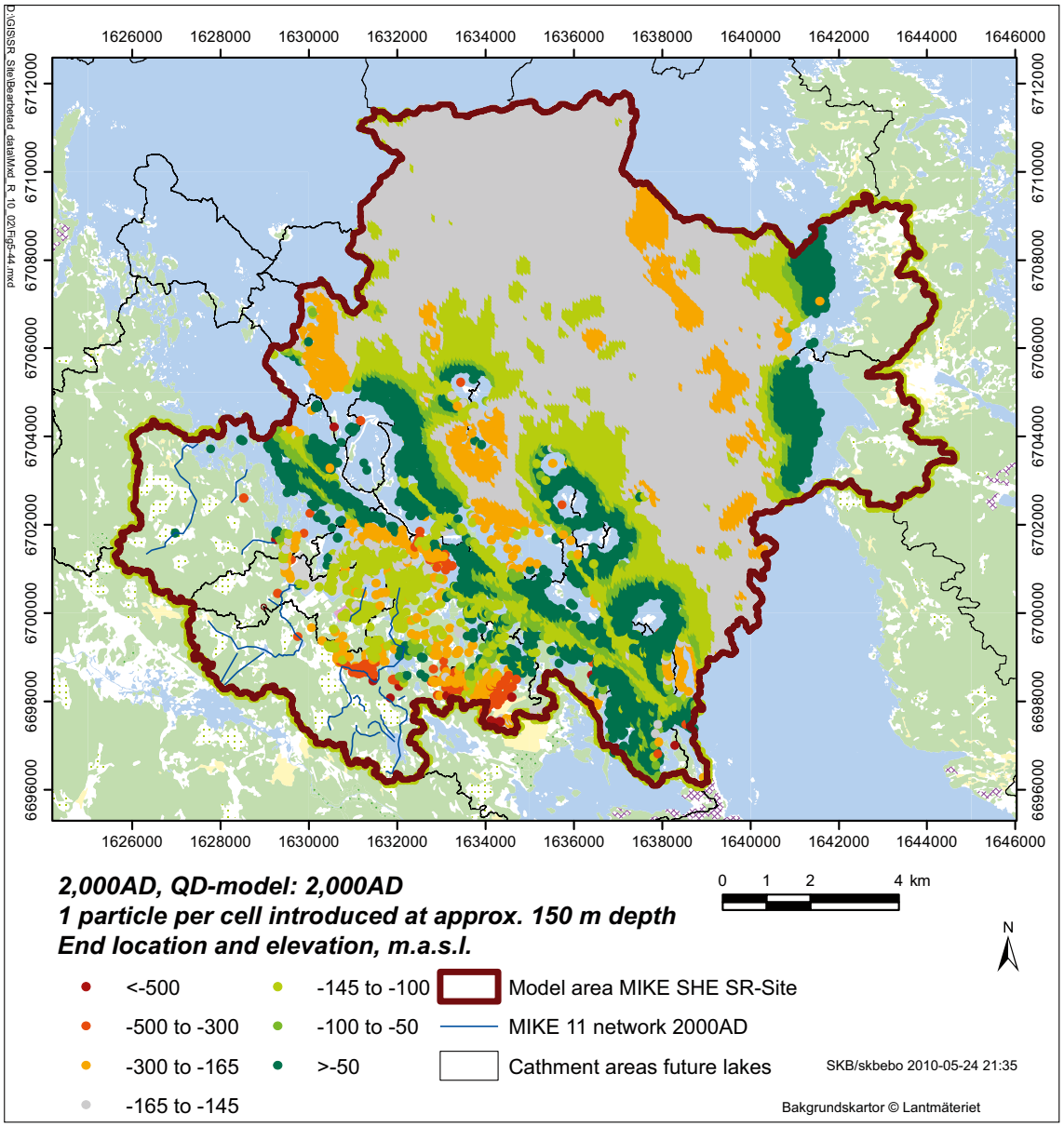

Figure 5-44. *Locations and elevations of the particles left in the model volume after 1,000 years of simulation, results from the 2000AD_2000QD model. Red and yellow colours mean that the particles are below the level where they were released, the particles situated above the level of release are marked with dark green colour. Grey particles are particles that are still left in the layer where they were released.*

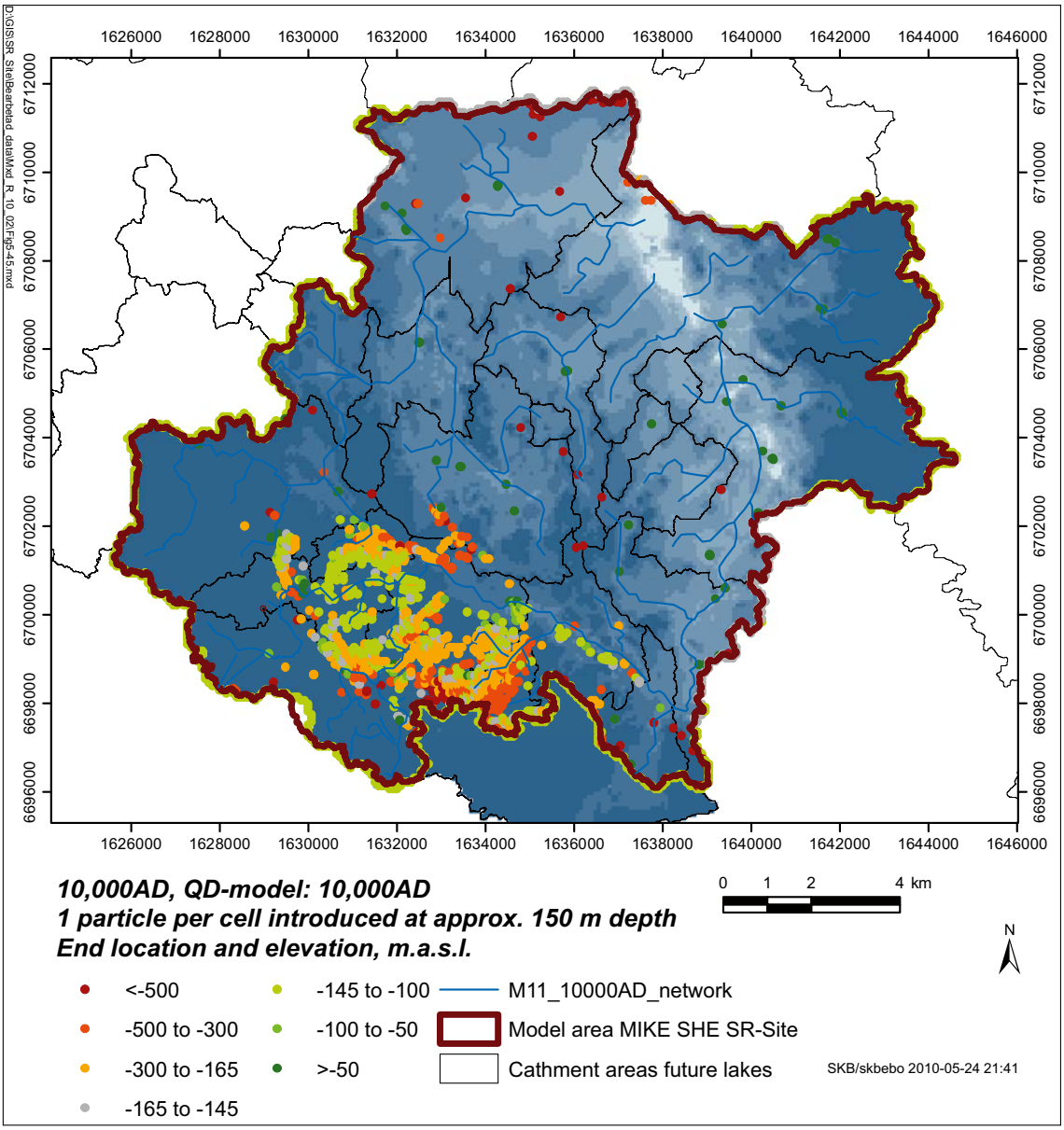

Figure 5-45. *Locations and elevations of the particles left in the model volume after 1,000 years of simulation, results from the 10000AD_10000QD model. Red and yellow colours mean that the particles are below the level where they were released, the particles situated above the level of release are marked with dark green colour. Grey particles are particles that are still left in the layer where they were released. As a background the model topography is illustrated in a blue scale, dark blue areas are heights and light blue areas are depressions.*

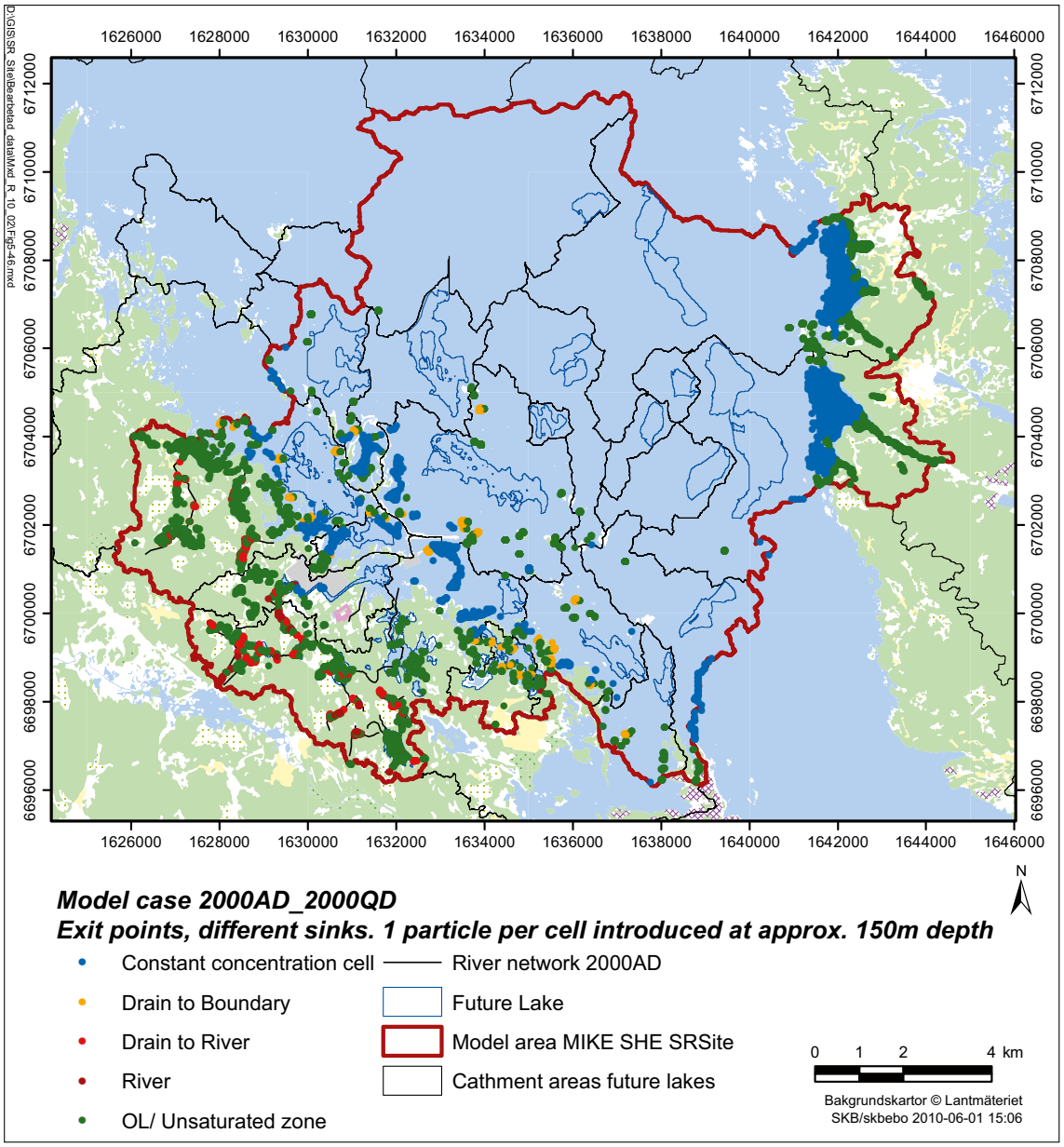

Figure 5-46. *Exit points at ground surface from the 2000AD_2000QD model; one particle per cell was introduced at approximately 150 m.b.s.l. The exit points are concentrated to the surface stream network and wetlands and lakes.*

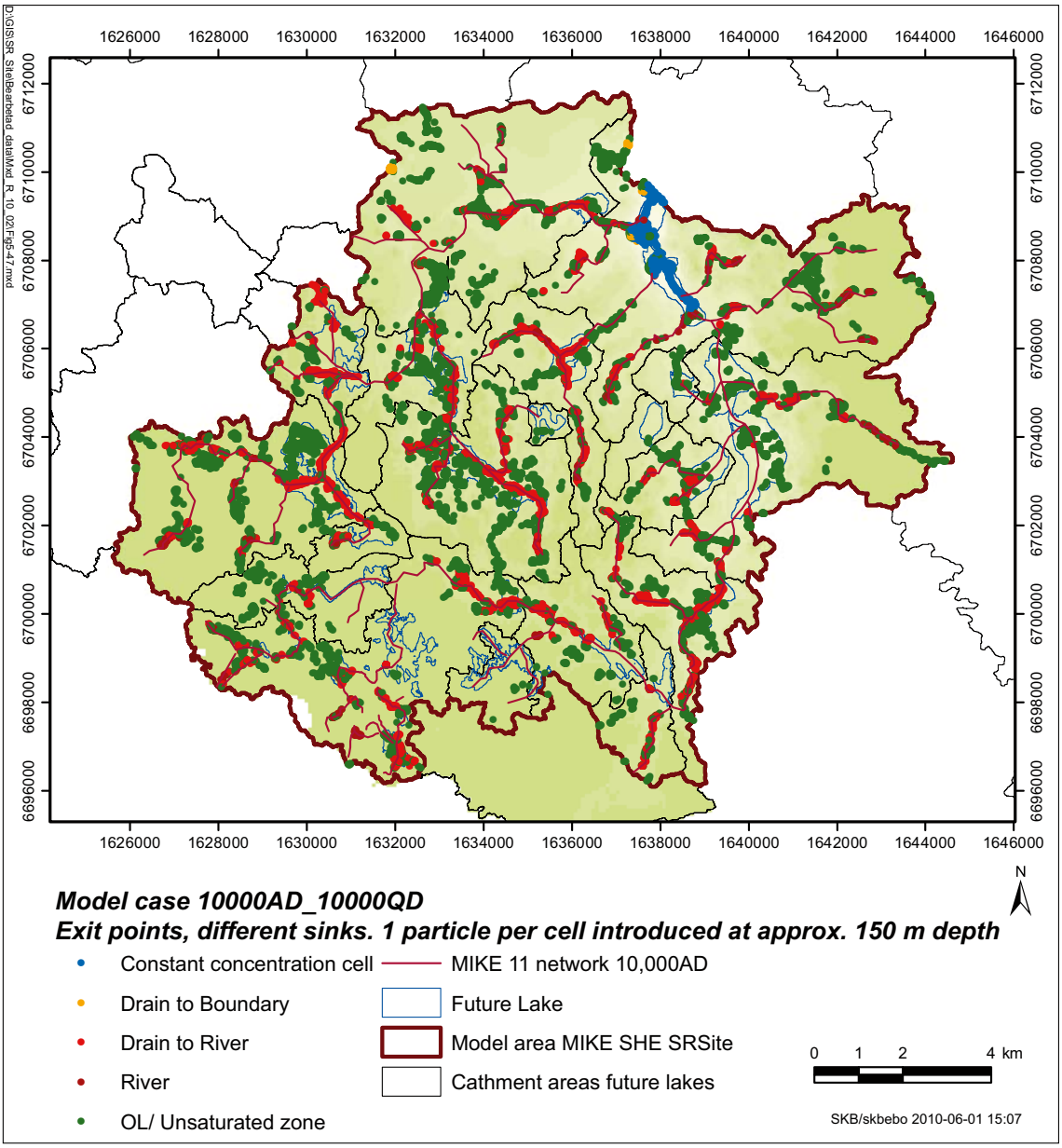

Figure 5-47. *Exit points at ground surface from the 10000AD_10000QD model; one particle per cell was introduced at approximately 150 m.b.s.l. The exit points are concentrated to the surface stream network and wetlands and lakes.*

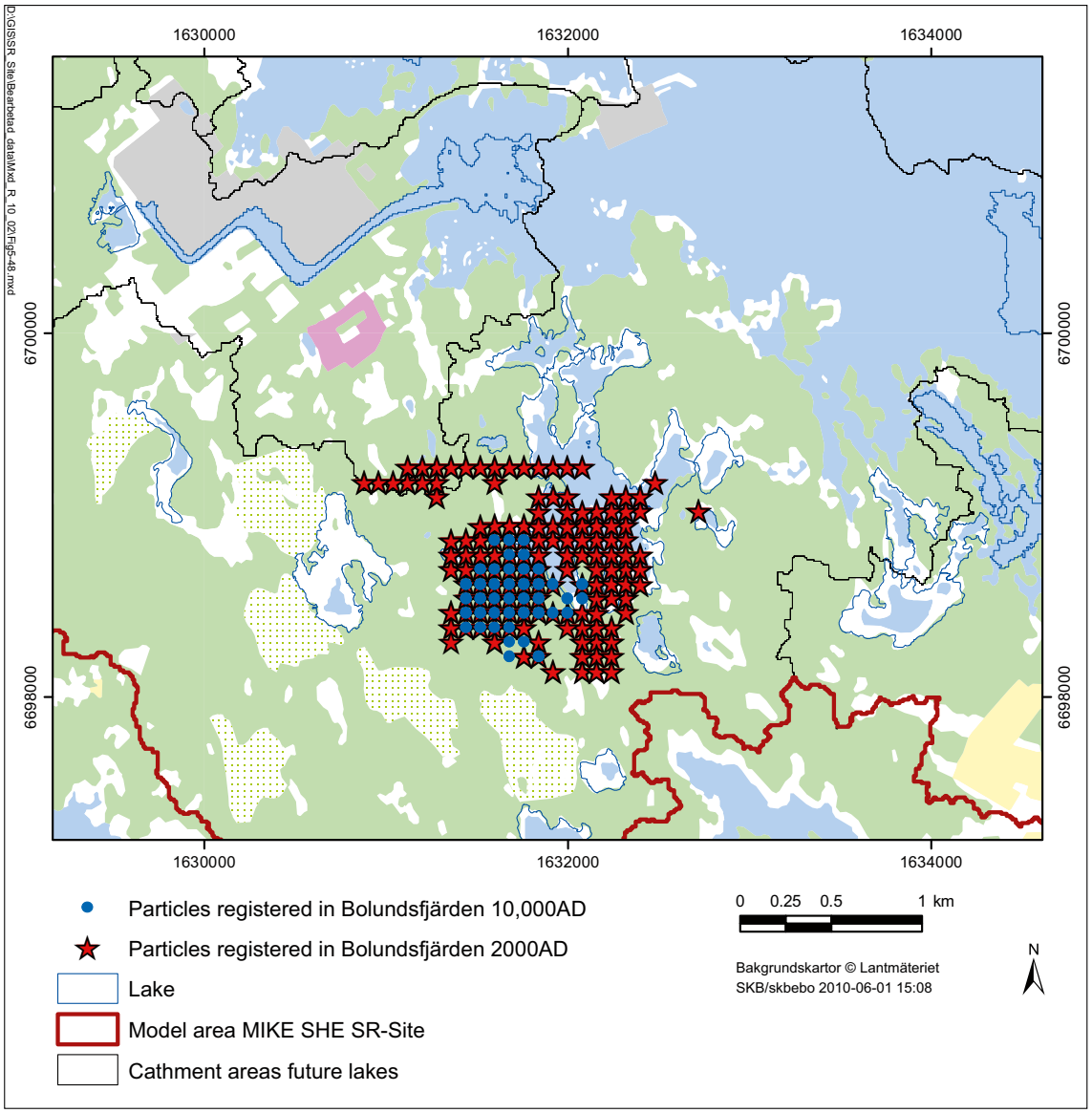

Figure 5-48. *Birth locations of particles registered within the shoreline of Lake Bolundsfjärden at 2000 AD and 10,000 AD.*

5.5 Summary of results from the regional model for temperate climate

The main conclusions from the regional modelling of flow and transport under normal temperate climate conditions are summarised below.

- The pumping test in HFM14 (performed in July 2006) and time series of surface water levels and discharges, groundwater levels in the QD and hydraulic heads in the upper bedrock were used in the initial calibration of the model. The simulation case describing present conditions, i.e. present climate and shoreline, was compared to measured data from the site. To obtain an acceptable response in the modelling of the pumping test the vertical hydraulic conductivity was reduced by a factor of 2 in the upper 200 m of the bedrock. In addition, the specific storage was reduced, from an approximate mean value of $2 \cdot 10^{-6}$ m^{-1} to a constant value of $5 \cdot 10^{-9}$ m^{-1}. These were the only changes of the given input data (as described in Chapter 3) that were made in the modelling.
- The measured water balance for the Forsmark site, which is based on local measurements of discharges and meteorological parameters, is in agreement with the calculated water balance from the SR-Site MIKE SHE model for present conditions.
- It was concluded that the reduction of the horizontal grid resolution made in the SR-Site MIKE SHE model, i.e. the grid cell size was increased compared to that in the previous SDM-Site model, did not have large negative effects on the ability of the model to reproduce measured groundwater levels, surface water discharges and surface water levels. The model results from the SR-Site MIKE SHE modelling of the present conditions in Forsmark were found not to differ significantly from the results obtained with the SDM-Site MIKE SHE model. This, together with the agreement between measurements and modelling results, led to the conclusion that the SR-Site model describing present conditions was an adequate basis for the development of models describing the future conditions at the site.
- Calculated water balances for different areas and time periods indicate that the variations in the overall water balance are small. Studying the water balances for the area constituting land today for the cases with different shorelines and a normal temperate climate, the modelled runoff is approximately 180 mm and the total calculated evapotranspiration approximately 400 mm. For the area constituting land at present, the largest difference in the water balance is found in the water exchange over the boundaries. The direct runoff via overland flow and the amount of water leaving the saturated zone to areas located downstream increase with the distance to the shoreline. As the gradient towards the sea increases with the distance to the sea, the surface and groundwater flows across the present shoreline increase.
- Also when studying modelling results for the areas constituting land at each time period modelled, the changes in the total calculated runoff and evapotranspiration are found to be small. Different vegetation covers, lake percentages and properties of the unsaturated zone in the studied areas result in a varying interception, transpiration and evaporation from overland waters, but the variations in the total calculated evapotranspiration are less than 10% for all the cases.
- For the present (temperate) climate conditions, the distribution of the precipitated water is approximately 30% runoff and 70% evapotranspiration. When comparing results from water balances for different shoreline positions the variation in the distribution of the precipitated water is within 10%.
- The future GIS-modelled lakes /Brydsten and Strömgren 2010/ coincide with the lake areas that appear in the MIKE SHE model. There are some small local sinks in the area, where surface water builds up; these areas are too small to be defined as lakes in the GIS-modelling /Brydsten and Strömgren 2010/. Thus, there are more lakes in the MIKE SHE model, both at 5000 AD and 10,000 AD, than in /Brydsten and Strömgren 2010/. Due to the transient conditions, some areas are ponded during wet periods of the year, whereas they dry out under drier periods.
- Since the flooded areas along the streams are limited, the applied MIKE 11 stream network models for the 5000 AD and 10,000 AD cases are concluded to have capacity enough to transport away the surface water.

- When applying the QD models for future conditions to the MIKE SHE model, taking lake succession into consideration, some lakes are terrestrialised at 5000 AD and 10,000 AD. The terrestrialisation of the lakes affects the ponded areas in the MIKE SHE model and the depth of the overland water decreases. The lakes that turn into mires are still low points in the area, and wetlands build up under wet weather conditions. However, according to the model some wetlands dry out during summers, whereas small lakes build up in the previous lake areas during periods of high precipitation.
- There is a lowering of the modelled water table within the area constituting land at 2000 AD when the distance to the sea shoreline increases. The present land area becomes more and more elevated relative to the sea, and the depth to the groundwater table increases. Still the main part of the model area has a groundwater table located less than 1.5 m below ground.
- Local topography has a strong impact on the pattern of recharge and discharge areas in the QD. The weather conditions have a stronger impact on the recharge and discharge areas in the QD than in the bedrock. In the bedrock, the discharge areas are concentrated to lakes and depressions connected to the streams. The pattern is the same for all applied shorelines under temperate climate conditions. In general, the discharge areas, both in QD and bedrock, are stronger (i.e. the hydraulic gradients are larger) in the models with the shorelines of 5000 AD and 10,000 AD. This is due to the more distinct topography in the future land areas than in the present ones, with larger gradients between land and sea.
- In parts of Lake Bolundsfjärden, there are discharge conditions in parts of the QD and recharge conditions in the bedrock (i.e. downward groundwater flow). The groundwater flow towards the sea in the horizontal fractures/sheet joints generates a downward gradient in the bedrock under the lake. The flow in the sheet joints under Lake Bolundsfjärden increases when the land is rising and the shoreline becomes more distant. At 10,000 AD the discharge areas from the bedrock to the QD in Lake Bolundsfjärden disappears and the water is mainly transported towards the sea in the sheet joints. This is due to the terrestrialisation of the lake and the shoreline displacement.
- The majority of the terrestrialised lakes in the 5000AD_5000QD and 10000AD_10000QD models still act as discharge areas even if the lake itself has dried out. However, the upward hydraulic gradients are in general smaller when the lakes have turned into mire. The areas are still topographical low points in the area, which means that discharge conditions prevail. Changing QD model from the one describing the present QD to those for future conditions (i.e. QD at 5000 AD or 10,000 AD) does not have a strong influence on the pattern of recharge and discharge areas. It has an impact on the strengths of the recharge or discharge areas, but an area with an upward or downward gradient in the model for the present QD has the same flow direction when applying the QD models for 5000 AD or 10,000 AD, which is confirmed by supporting particle tracking calculations. There are some exceptions, but in general the overall pattern seems to be governed by the topography and not the stratigraphy, thickness or type of QD.

6 Modelling results for other climate cases

In this chapter the results from simulations with a periglacial or a wet climate are presented. The different climates are applied to the 10000AD_10000QD model to see how the future hydrology, when landscape development has been taken into consideration, is influenced by climate changes.

6.1 Flow under wet conditions

6.1.1 Water balance

Three wet years in a row have been simulated to see how the area is affected by a longer time period with high precipitation; the precipitation increases during the three-year period (see Section 2.3 for details). The input data for a wet period have been applied to the 10000AD_10000QD model. The water balances for the second and the third year are evaluated and presented here. The water balances for the wet climate during simulation years 2 and 3 are shown in Figures 6-1 and 6-2, respectively. The figures illustrate the yearly water balances for the area constituting land at 2000 AD. The precipitation is 1,522 mm the second year and 1,568 mm the third year, which is almost 3 times the precipitation applied to the cases simulating present (normal) weather conditions. Due to a high potential evapotranspiration and also a high actual evapotranspiration, which is calculated to 1,181 mm year 2 and 1,223 mm year 3, the runoff is only 256 mm during year 2 and 360 mm year 3.

During the second year there is a larger storage change than the third year, indicating that water is accumulating in the system. A storage change between the years is natural since the climate data for the three years are transient. The system is not in balance and there will be a storage change in the water balance if the input data for the years differ. The largest storage change is found in the unsaturated zone; the storage increases with 61 mm during the second year. The total storage change for the same period is 80 mm. Since the amounts of water in both SZ and UZ increase during the second year, the groundwater table is rising. This leads to a decreased infiltration the third year, 943 mm year 3 compared to 974 mm year 2, whereas the runoff from the overland compartment to the surface stream system increases during the third year.

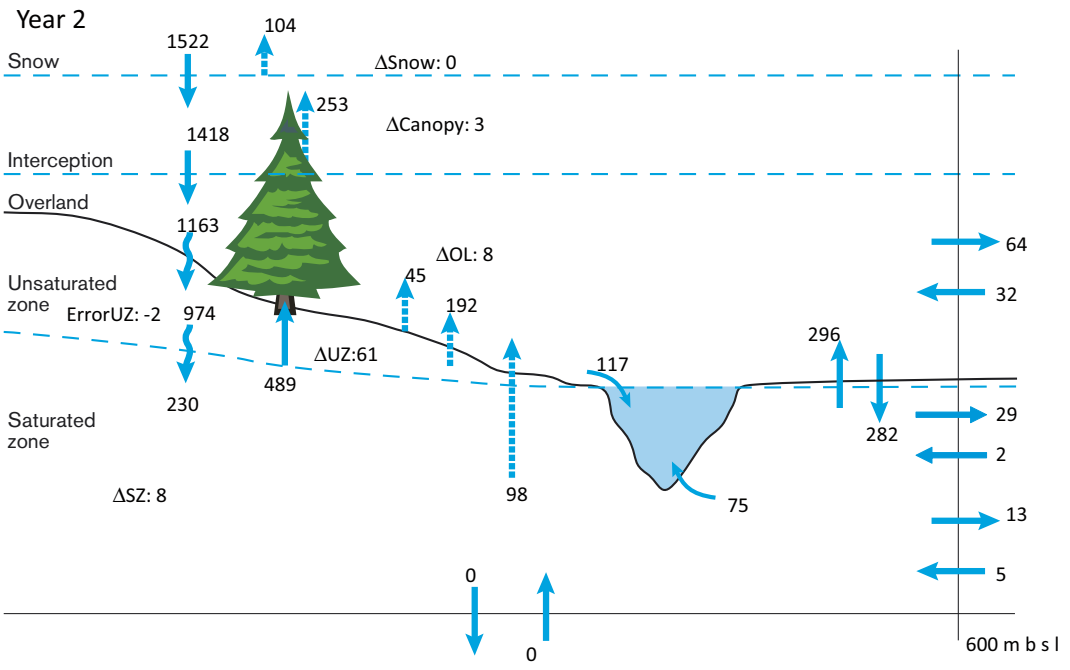

Figure 6-1. *Water balance from the simulation with a wet climate; the water balance is calculated for the area constituting land at 2000 AD. Results are illustrated for the second year of the three-year wet period simulation.*

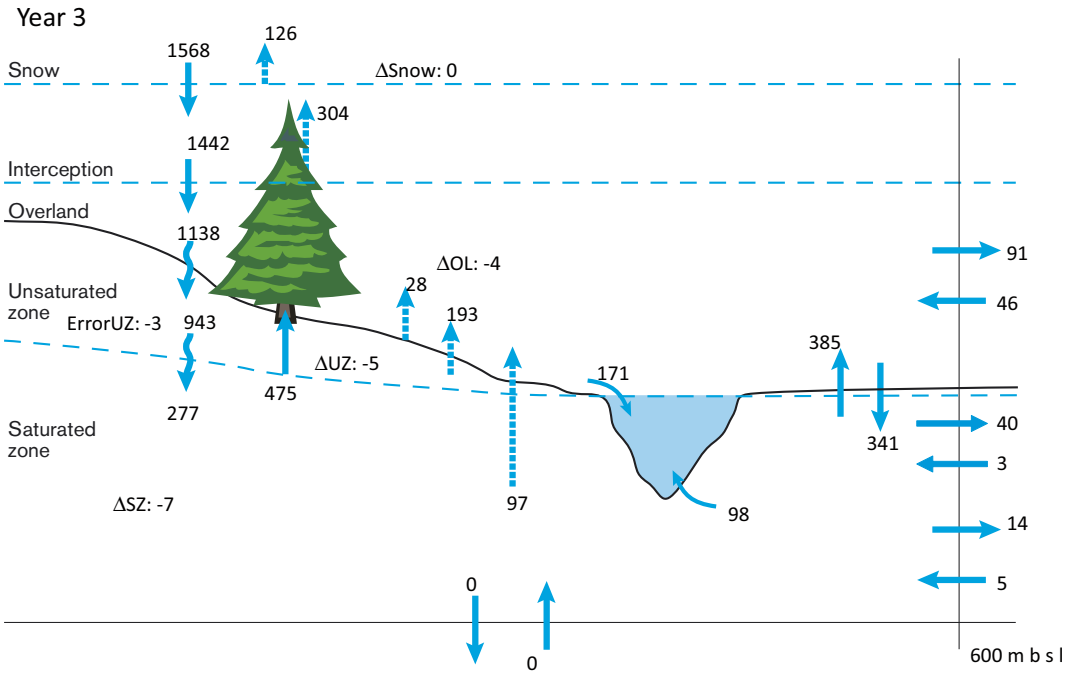

Figure 6-2. *Water balance from the simulation with a wet climate; the water balance is calculated for the area constituting land at 2000 AD. Results are illustrated for the third year of the three-year wet period simulation.*

The distribution of the precipitated water during both the second and the third year is approximately 20% runoff, whereas 80% of the water leaves the model volume as evapotranspiration. During the second year the runoff is some percent lower than during the third year, which is due to the increased storage. In this case the storage change is 5%. The results from the wet period simulation could be compared to the 70% evapotranspiration and 30% runoff obtained in the simulation with the selected year representing a normal temperate climate. Thus, the change of the relative internal distribution of water is not very large; all changes are within 10%.

The runoff from overland water to the surface stream system is significantly higher under wet conditions compared to normal weather conditions. This is due to additional saturated areas close to the stream system in the model area. There is a strong increase in the transpiration from plants both in saturated and unsaturated areas. The total transpiration from plants under wet conditions is approximately 580 mm (587 mm year 2 and 573 mm year 3) compared to 182 mm for a normal climate.

The water demand of the plants is sustained during the modelled period of wet conditions, which means that there is never a lack of water for the plants. However, the transpiration constitutes approximately 50% of the total actual evapotranspiration during both the second year and the third year of the simulation. Under normal temperate climate conditions the transpiration is 36% of the total calculated evapotranspiration; thus, the relative difference in the transpiration fraction between normal and wet climate conditions is small.

During the third year the evaporation from interception increases from 253 mm to 304 mm. The amount of water intercepted by the leaves is dependent on when the precipitation falls. If a large part of the precipitation falls during summer, when the leaf area index (LAI) is high, a larger amount of water will leave the model volume as interception evaporation. During the third year more rain is added to the model during periods of high LAI, giving a higher evaporation via interception. Due to the increased interception during year 3, the water input to the overland compartment decreases.

To be able to compare the water balances between normal temperate, wet temperate and periglacial climates, the water balances for the part of the model area that constitutes land at 10,000 AD are presented below (Figure 6-3). The total calculated evapotranspiration is 1,190 mm, as compared to 1,223 mm when only studying the part of the model area constituting land at 2000 AD. There is a slight increase in the total evapotranspiration compared to when only studying the area 2000 AD land area. The transpiration is 36% of the total calculated evapotranspiration, just as the results for the temperate climate.

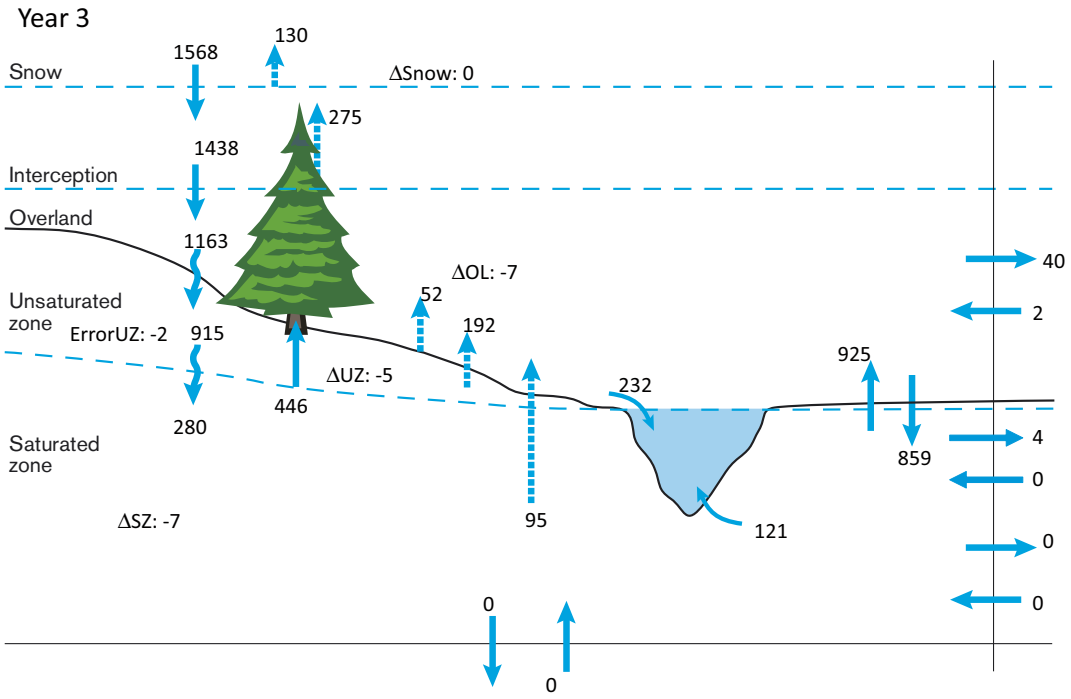

Figure 6-3. *Water balance from the simulation with a wet climate; the water balance is calculated for the area constituting land at 10,000 AD. Results are illustrated for the third year of the three-year wet period simulation.*

Based on the results illustrated in Figure 6-3, the total runoff is calculated to 395 mm, i.e. 25% of the precipitation. Thus, the results are very similar to the water balance presented in Figure 6-2, where only the area constituting land at 2000 AD is considered. The largest differences are in the boundary flows in the overland (OL) and saturated zone (SZ) compartments. More water flows across the studied area in Figure 6-2, due to a flow both in SZ and OL towards more low-lying areas downstream within the model area.

6.1.2 Recharge and discharge areas

The distribution of recharge and discharge areas under wet conditions is similar to the pattern under present conditions. No illustrations of the spatial distributions of recharge and discharge areas will be presented in this section, since the patterns of recharge and discharge areas in the bedrock and in the QD are similar to those presented in Figures 5-30 to 5-39 for a normal temperate climate.

In the bedrock, the total number of cells having a particular direction of the flow gradient (either upward or downward) is almost the same for wet conditions as for normal temperate conditions (Table 6-1). The difference is only one percent between the results for normal and wet climate conditions. However, the difference is larger in the QD where the total area with an upward gradient decreases during the wet period; 36% of the area has an upward gradient for wet climate compared to 44% when applying a normal temperate climate to the model.

Table 6-1. Fractions (%) of the MIKE SHE model area with upward or downward gradients under different weather conditions.

	Wet climate		Normal climate	
	Upward gradient (%)	Downward gradient (%)	Upward gradient (%)	Downward gradient (%)
QD	36	64	44	56
Bedrock	52	48	53	47

6.1.3 Groundwater table and overland water depths

The mean depth to the groundwater table is almost the same during the second and the third year of the wet period. Looking at the results for the depth to the groundwater table for the area constituting land at 2000 AD, the groundwater depth is in general larger than for the area constituting land at 10,000 AD. This is as expected, since the area constituting land at 2000 AD contains almost no lakes and is also situated further away from the sea. However, the results from both wet years show a deeper groundwater table than the results from the selected year with a normal climate. The same results are seen independently of the area studied, i.e. irrespective of whether the 2000 AD or 10,000 AD land area is considered.

This perhaps somewhat unexpected result is due to the high evapotranspiration. The very high transpiration, together with the other evapotranspiration components, result in a lower groundwater table. The increased precipitation does not cause a rise of the groundwater levels in the area because of the high applied potential evapotranspiration (PET). However, the uncertainties in the calculation of the PET are relatively large and could have a large impact on the results. The accumulated frequency of the depths to the groundwater table within the land areas at 2000 AD and 10,000 AD for the different simulation cases are shown in Figure 6-4.

Due to the high evapotranspiration, the ponded areas decrease when applying the wet climate to the model. The total area having a depth of overland water larger than 0.05 m decreases with approximately 20% compared to the simulation cases with a normal temperate climate. Still the lake areas and wetlands in the area are ponded; the GIS-modelled lakes coincide with the MIKE SHE modelled lakes for a wet climate.

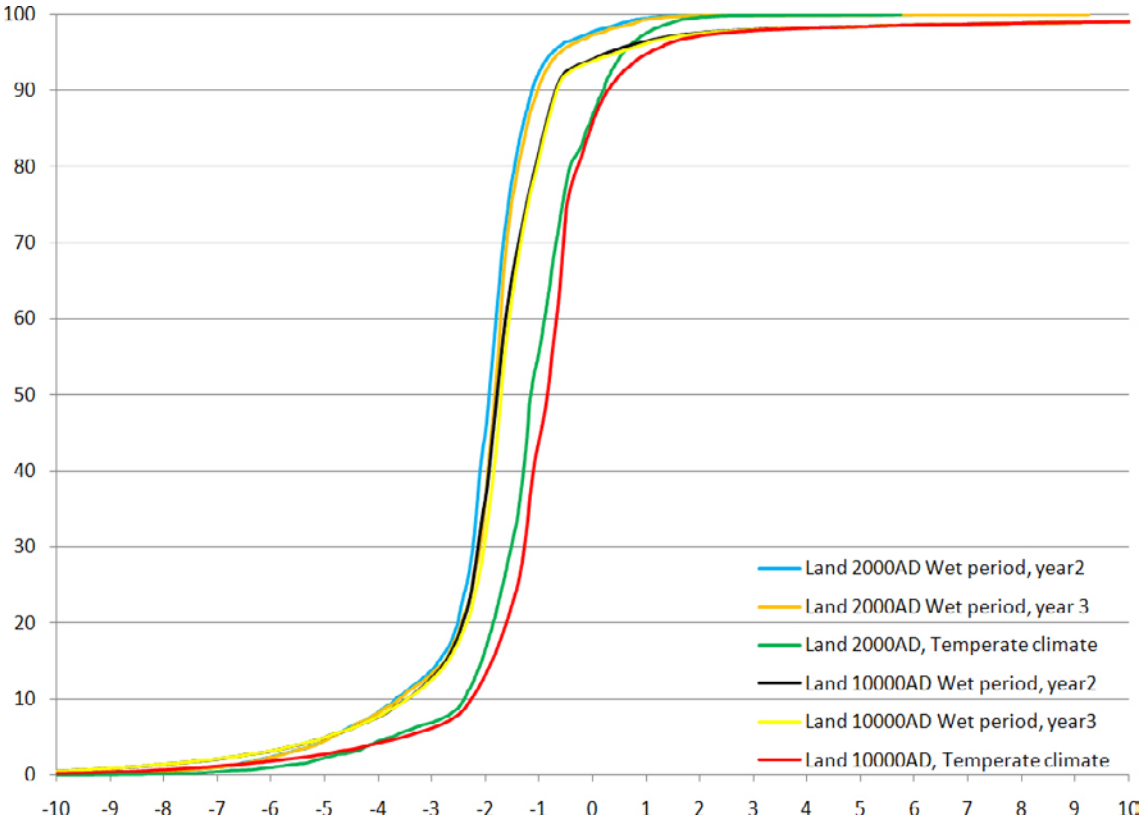

Figure 6-4. *Cumulative frequencies of the depth to the groundwater table in the model area for three different simulation years: the second wet year, the third wet year and the selected year with a normal climate. Results are shown for the areas constituting land at 2000 AD and 10,000 AD.*

6.2 Flow under periglacial conditions

Two cases including permafrost under periglacial conditions have been simulated: one case with a 240 m deep permafrost layer and one case with 100 m of permafrost. The selection of the permafrost depths is described in Section 3.5. The number of through taliks varies with the permafrost depth, see Section 3.5.2. The case with 240 m permafrost results in 7 taliks and the case with 100 m deep permafrost results in 45 taliks. The locations and numbers of the taliks are illustrated in Figure 6-5. The results from the flow modelling with a permafrost depth of 240 m are presented in Section 6.2.1, the flow modelling results from the 100 m case are presented in Section 6.2.2, and finally the particle tracking results in Section 6.3.

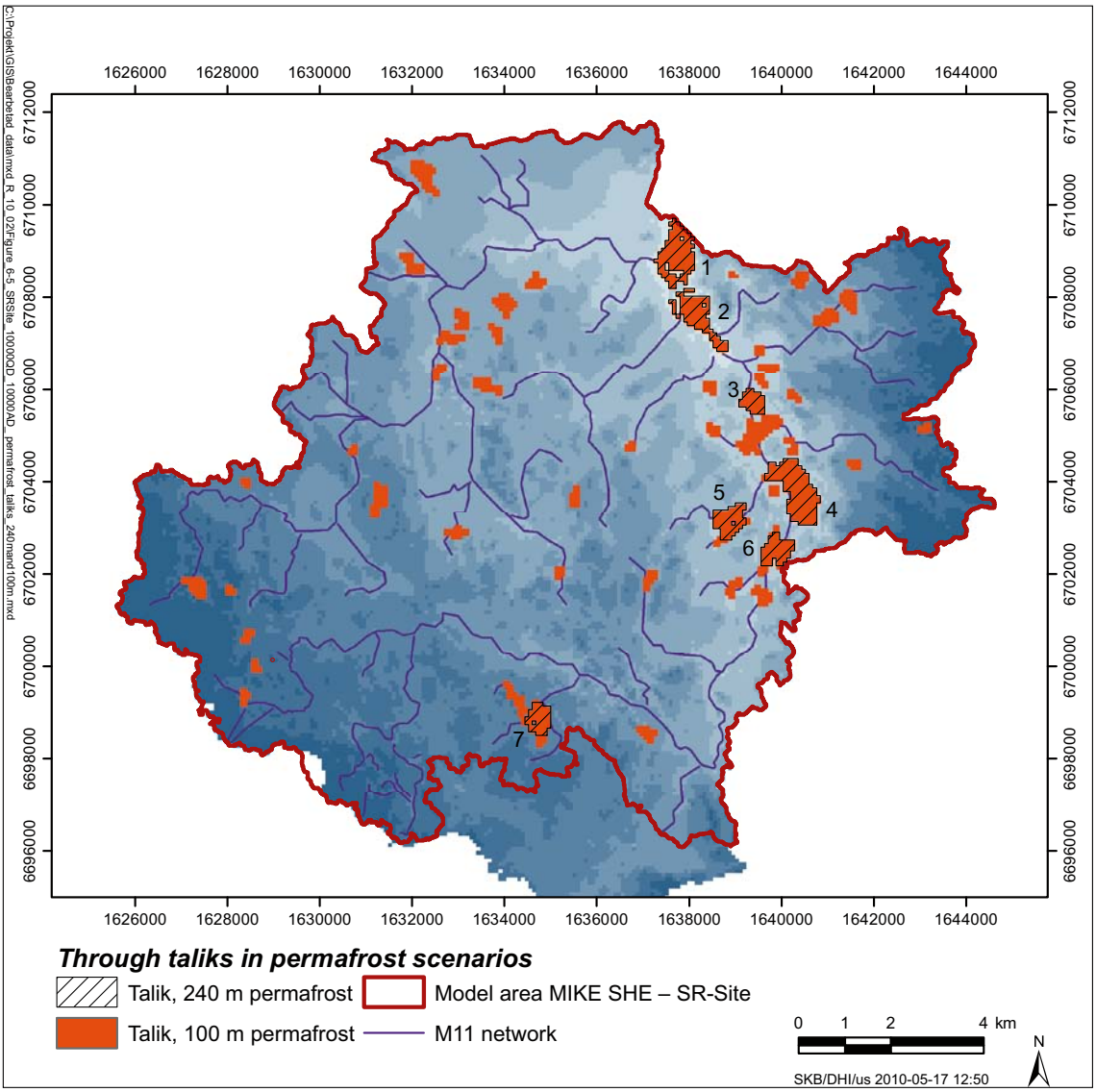

Figure 6-5. *Studied through taliks in the cases with permafrost thicknesses of 100 m and 240 m. Taliks 1 and 2 are a part of the sea.*

6.2.1 Model with 240 m permafrost

Water balance

The water balances for the permafrost case with a permafrost thickness of 240 m are shown in Figures 6-6, 6-7 and A3-1 to A3-7. Figures 6-6 and 6-7 illustrate the water balance over a one-year cycle. In Appendix 3 (Figures A3-1 to A3-7), the yearly water balance has been divided into partial balances for each simulation period, i.e. the freeze 1, freeze 2, frozen, thaw 1, thaw 2, thaw 3 and active periods. The figures illustrate the water balance for the area constituting land at 10,000 AD. The different periods of thawing and freezing and active and frozen conditions during the year are defined in Section 3.5.4, where it can be seen how the year is divided into the 7 periods mentioned above.

The annual precipitation is 412 mm, which is slightly lower than the precipitation applied in the simulation cases with the present (normal) climate. The calculated actual evapotranspiration is 193 mm and the total runoff sums up to 217 mm. The distribution of the precipitated water is approximately 50% runoff and 50% evapotranspirated water. This should be compared to 70% evapotranspiration and 30% runoff for the temperate climate. This indicates that a significant change in the internal distribution of water takes place when applying a periglacial climate together with permafrost to the model.

Less water is in circulation in the saturated zone under permafrost conditions compared to the temperate climate. There is a reduced infiltration into the unsaturated zone under permafrost conditions, 180 mm compared to 491 mm. Also the percolation to the saturated zone is reduced, 89 mm compared to 291 mm for normal temperate conditions.

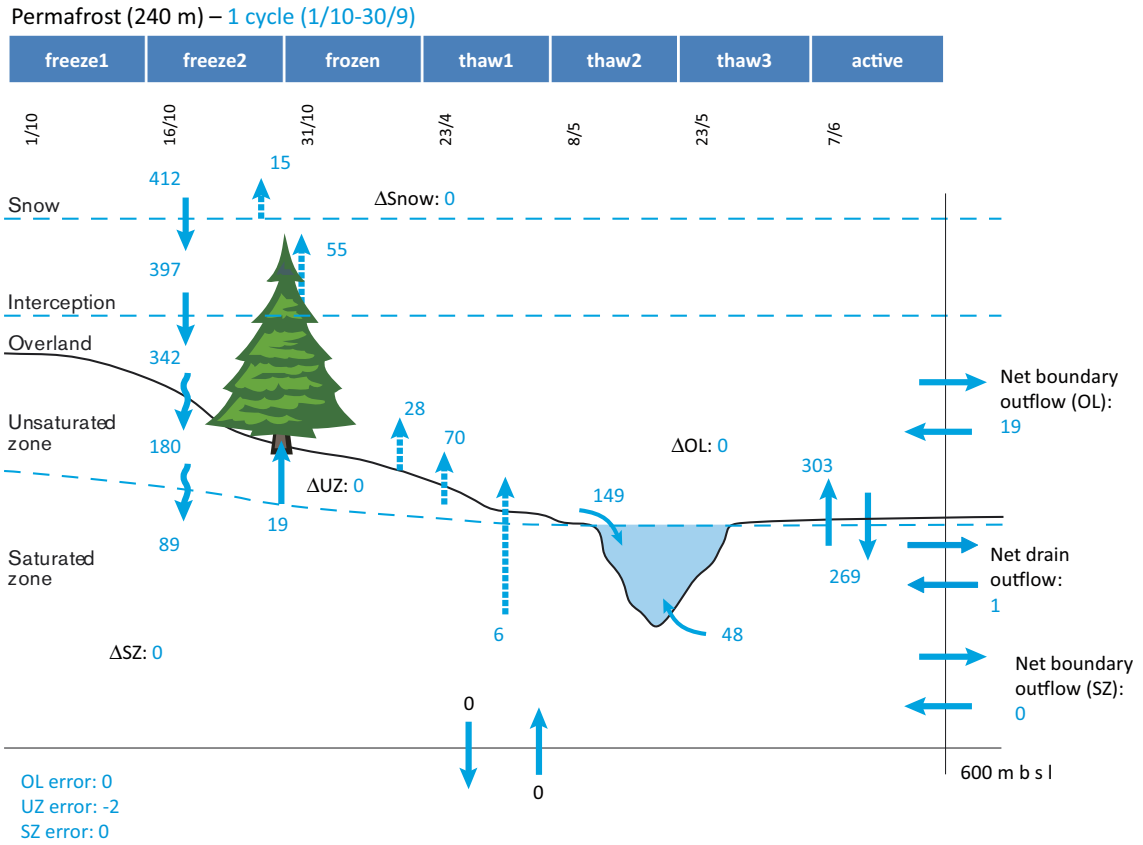

Figure 6-6. *Calculated water balance (units in mm) of the 10000AD_10000QD model under permafrost conditions (one-year period) with a permafrost thickness of 240 m for the 10,000 AD land area.*

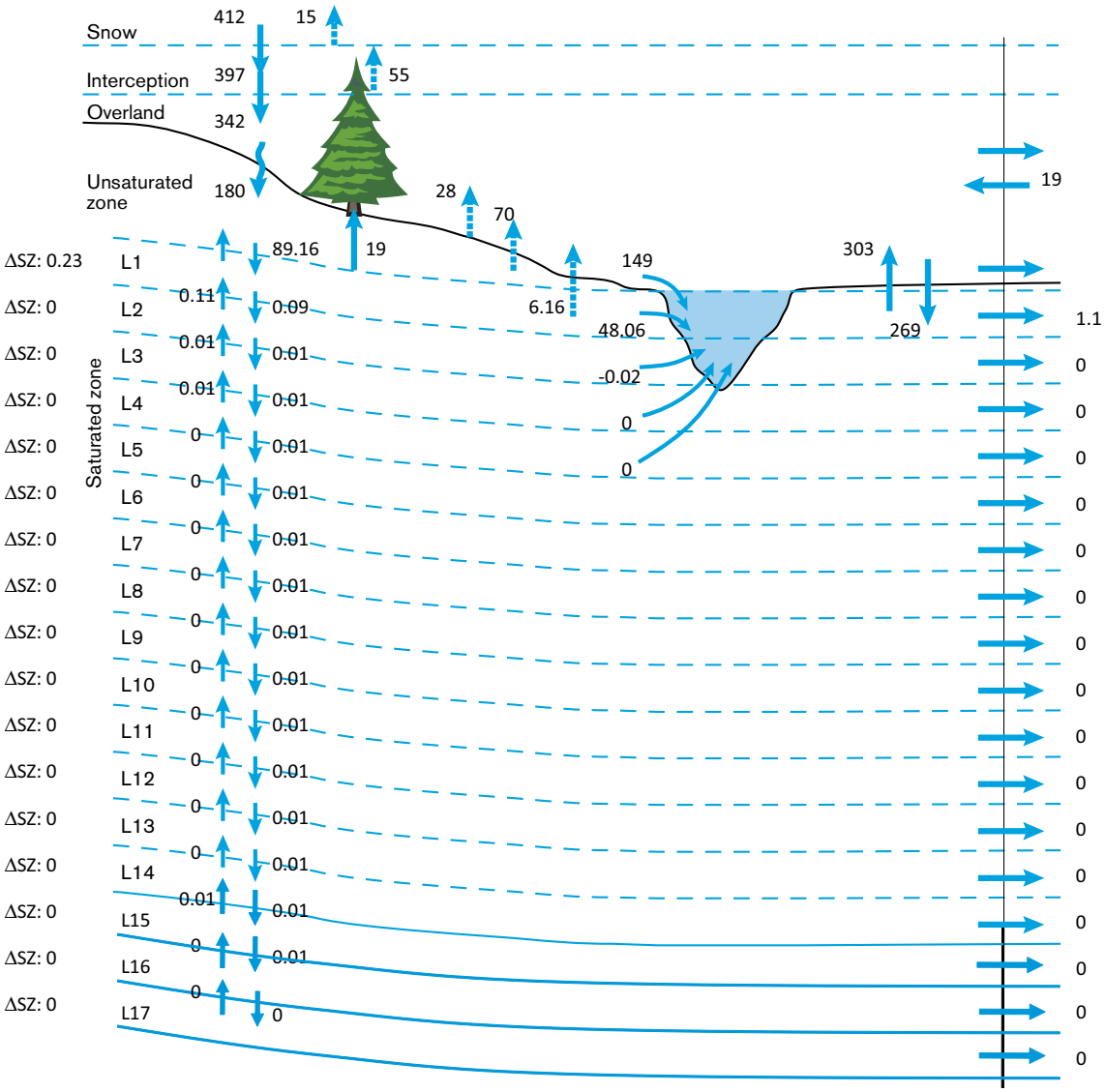

Figure 6-7. *Detailed calculated water balance (units in mm) illustrating the exchanges of water between layers in the saturated zone during the simulated year with a permafrost thickness of 240 m for the area constituting land at 10,000 AD. Permafrost is present in layers 2 to 13.*

The evapotranspiration is approximately halved during the permafrost period. A change is also observed in the internal distribution of the evapotranspirated water. Due to the applied tundra vegetation the transpiration from plants such as mosses and lichens is reduced from approximately 36% to 10% of the total evapotranspirated water. The calculated evaporation in the saturated zone is reduced from approximately 12% to 3% of the total evapotranspiration. The distribution has shifted towards a larger evapotranspiration from the soil (from 16% to 36%) and overland water (from 2% to 15%).

In Figure 6-7 a detailed water balance of the saturated zone for the 10,000 AD land area is illustrated (the sea-taliks 1 and 2 are not included). The recharge from the unsaturated zone to the saturated zone is 89 mm, as compared to 291 mm under normal temperate climate conditions. Almost all of that water (approximately 99%) is removed from the saturated zone through the exchange with overland water (38%), through the MIKE 11 streams (54%) and through evaporation (7%). Only very little water is left to percolate further down into the saturated zone resulting in very little water movement through the taliks. If the taliks were included in the calculation of the water balance illustrated in Figure 6-7 the water flows in the layers below the active layer would have been higher. This is further discussed in the section “Recharge and discharge areas” below.

Studying the active layer (layer 1) and the top permafrost layer (layer 2) in detail, only 0.11 mm is moving from layer 2 to layer 1 and 0.09 mm from layer 1 to layer 2. It is noticed that there is a leakage of water (0.02 mm) from the streams to layer 2. This is causing an upward movement of water from layer 2 to layer 1, which is deviant from the general downward movement. However, the vertical flows are very small and almost neglectible compared to the vertical flows under temperate climate conditions where the flow from layer 1 to layer 2 is 29.8 mm and 29.7 mm in the opposite direction.

In Figure 6-8 the flows between layers 1 and 2 and between layers 13 and 14 during the simulated year are illustrated. The flow in the upper part of the saturated zone is larger than that in the lower part. However, the flow is still very small. The mean flow in the deeper part has a continuous flow direction downwards, but is only a few percent of the flow in the upper layers. The direction in the upper part fluctuates. During the colder periods (freeze 1, freeze 2, frozen, thaw 1 and partly thaw 2) the vertical flow direction is upwards. The flow direction changes during thaw 3 due to the large snow melt. At the end of the active period the flow direction again turns downwards due to the leakage of water from the surface streams into layer 2.

The flow of water between the model compartments is transient during the year and varies between the different simulation periods. The water balance varies during the seasons and the different simulation periods. This is illustrated in the accumulated time series found in Figures 6-9 to 6-12. In these figures, the accumulated water balance for each model compartment is illustrated as time series. The exchanges of water between the compartments are illustrated as time series showing the input and output of water during the year. The input of water to each compartment is illustrated as a negative value and the output is always positive. For example, the graph illustrating the precipitation input to the evapotranspiration compartment in Figure 6-9 has negative values and the throughfall from the evapotranspiration compartment to the overland compartment has positive values. The different periods of thawing and freezing are marked in the figures.

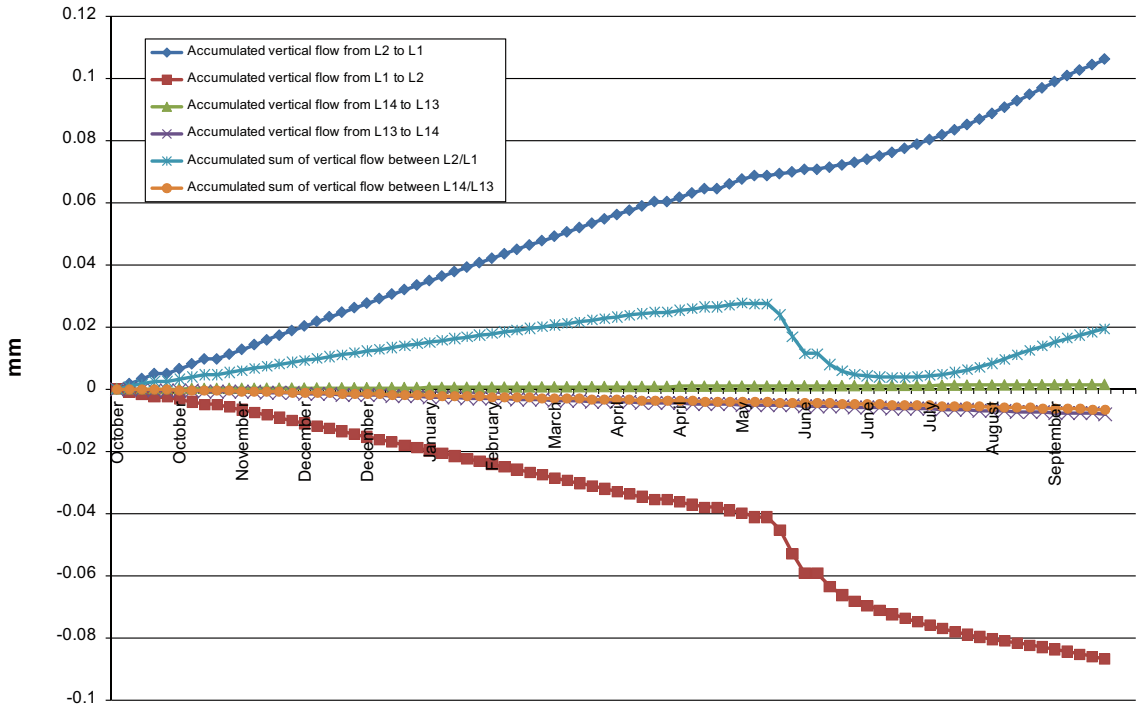

Figure 6-8. *Calculated accumulated vertical flow during the simulated year between layers L2 and L1 and between layers L14 and L13 for the area constituting land at 10,000 AD. An upward flow direction is positive and a downward flow direction is negative. The lighter blue and orange curves are the net fluxes to and from layers L2 and L14.*

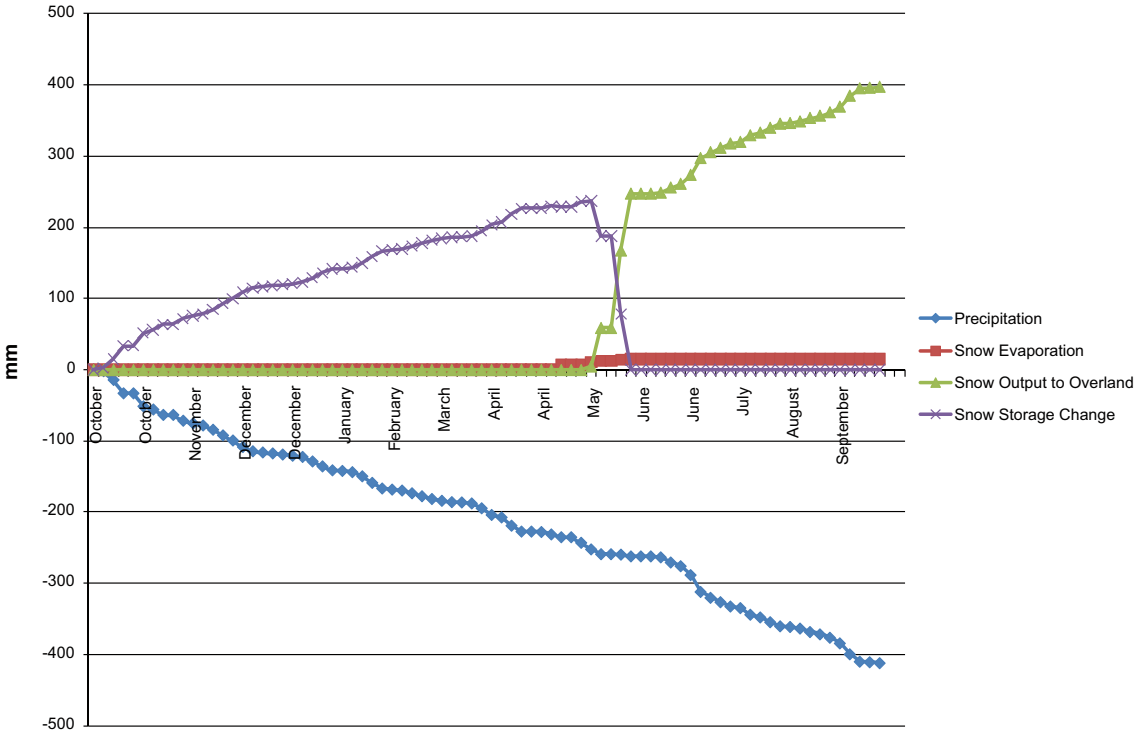

Figure 6-9. *Calculated accumulated precipitation, snow evaporation, snow throughfall and change in snow storage during the simulated year with a permafrost thickness of 240 m for the area constituting land at 10,000 AD.*

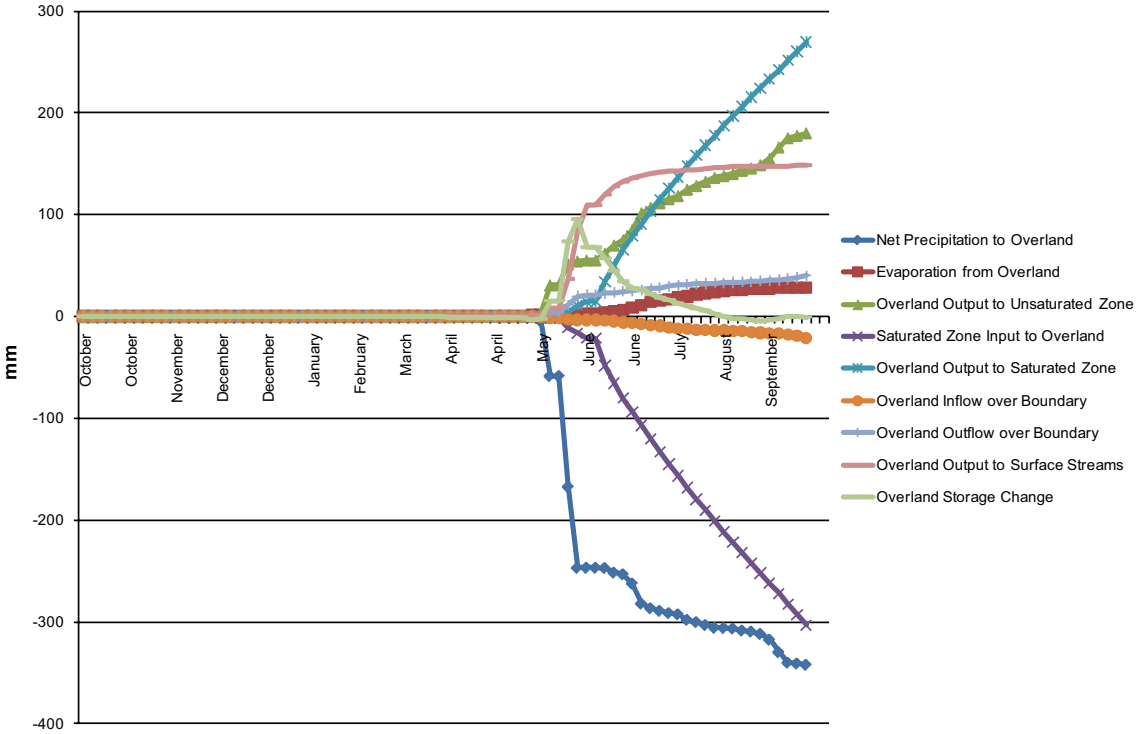

Figure 6-10. *Calculated accumulated net precipitation to OL, evaporation from OL, infiltration to UZ from OL, exchange between OL and SZ, boundary inflow and outflow, OL water to surface stream and change in OL storage during the simulated year with a permafrost thickness of 240 m for the area constituting land at 10,000 AD.*

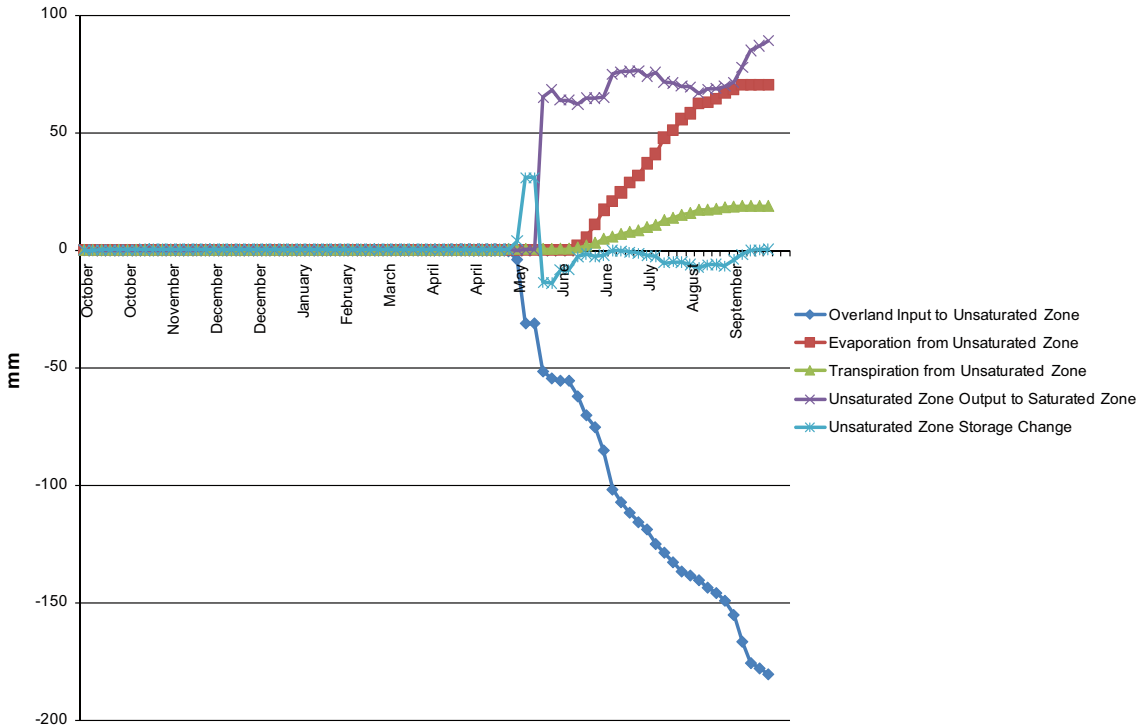

Figure 6-11. *Calculated accumulated infiltration to UZ, evaporation from soil, plant transpiration, recharge to SZ from UZ and change in UZ storage during the simulated year with a permafrost thickness of 240 m for the area constituting land at 10,000 AD.*

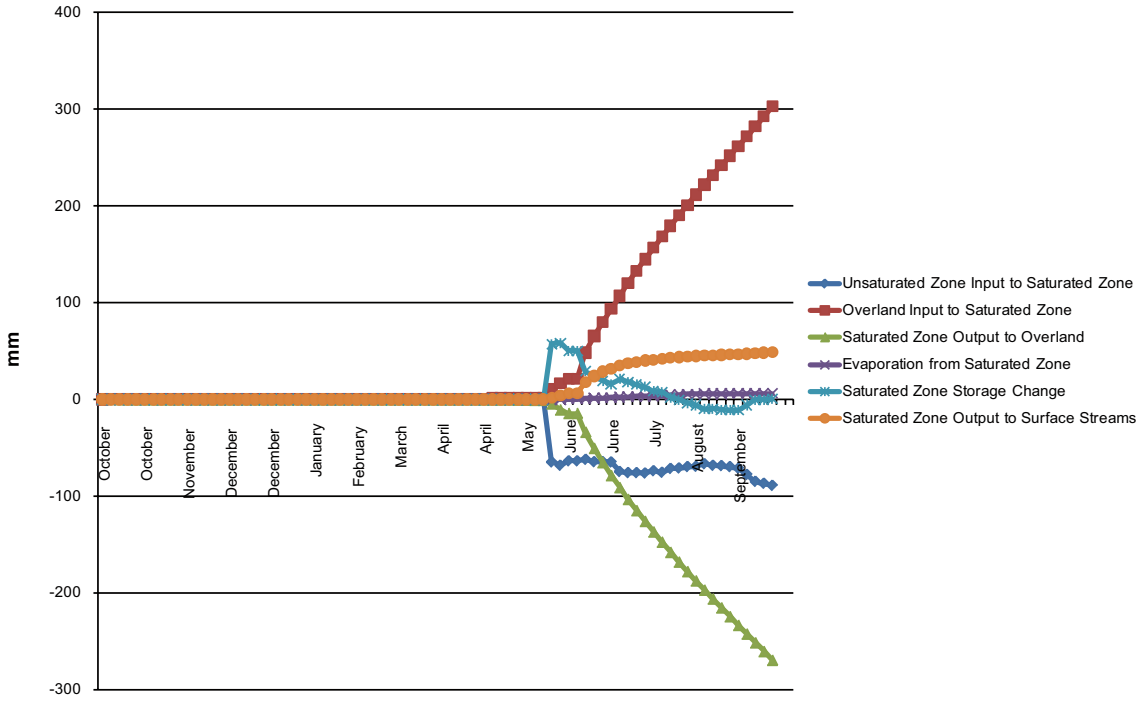

Figure 6-12. *Calculated accumulated recharge to SZ, exchange between OL and SZ, evaporation from SZ, SZ drainage to streams and change in SZ storage during the simulated year with a permafrost thickness of 240 m for the area constituting land at 10,000 AD.*

During the colder periods (freeze 1, freeze 2, frozen and thaw 1) the storage of water in the evapotranspiration compartment increases when the precipitation is accumulating as snow (Figure 6-9). Almost no evapotranspiration or runoff occurs. During thaw 2, the temperature increases and the ground begins to thaw. The snow storage slowly starts to melt and the snow evaporation increases. Melted snow and precipitation fall through the evapotranspiration compartment and the output from this compartment in Figure 6-9 is input to the overland compartment illustrated in Figure 6-10. The input from the evapotranspiration compartment to the overland compartment contributes to a small runoff and an infiltration to unsaturated zone, and also an increased storage in the unsaturated zone (Figure 6-11).

The evapotranspiration is also activated as the temperature more continuously rises above zero and the snow cover gradually disappears. During thaw 3, the snow melt reaches its peak contributing to a large runoff and an increased storage in the overland compartment (Figure 6-10). Water is transferred from overland to the surface stream network. Thaw 3 is the wetter period and water percolates to the saturated zone resulting in a storage increase as well as a rise of the groundwater table (Figure 6-12).

The active summer period is relatively dryer. The evapotranspiration is high and there is still a relatively large runoff at the expense of a reduction in overland and saturated storage. Consequently, the groundwater table falls. The total water balance for each period during the year is presented in Appendix 3. In this appendix, the illustrations show the same results as in Figure 6-6, but with each period illustrated by a separate figure.

Depth of overland water

With the permafrost as an almost impermeable formation below the active layer, the infiltration of overland water to the UZ, the exchange to the SZ and to the MIKE 11 stream is limited to the active layer and the through taliks during the unfrozen periods. This has resulted in the presence of a vaster coverage of overland water on the ground surface under permafrost conditions than for a temperate climate. Approximately 73% of the surface is covered with overland water at the end of thaw 3, which illustrates the conditions during a wet period. At the end of the active period the coverage is reduced to 58% and further to 45% at the end of the frozen period.

In comparison with the situation during a normal temperate climate, there are several similarities. The larger modelled lakes coincide with the GIS-modelled future lakes. In Figures 6-13 to 6-15 the depth of overland water is illustrated at the end of thaw 3, the active period and the frozen period. The main snow melt occurs during thaw 3, when the depth of overland water is building up. The overland water depth has decreased at the end of the relatively dryer active period.

Groundwater table depth

In this study the permafrost table is assumed to be saturated and defines the lower boundary of the active layer. Thus, the depth of the groundwater table is limited to the bottom of the active layer which is one metre below the ground surface. Fluctuations in the groundwater table position occur mostly in till dominated areas. At the end of thaw 3 the groundwater table in these areas is high and water is frequently occurring on the ground surface due to intense snow melt. During the active period the water table is lowered and in some parts the water table drops to the bottom of the active layer.

Figure 6-16 illustrates the cumulative frequency distribution of the groundwater depth within the area constituting land at 10,000AD at the end of the simulation periods thaw 3, active and frozen. The depth to the groundwater table is very similar at the end of the active and the frozen periods with a mean depth of 0.46 m and 0.44 m, respectively. The groundwater table at the end of thaw 3 is higher with a mean depth 0.12 m. The groundwater table is very shallow under permafrost conditions in comparison to the calculated groundwater table for a normal temperate climate.

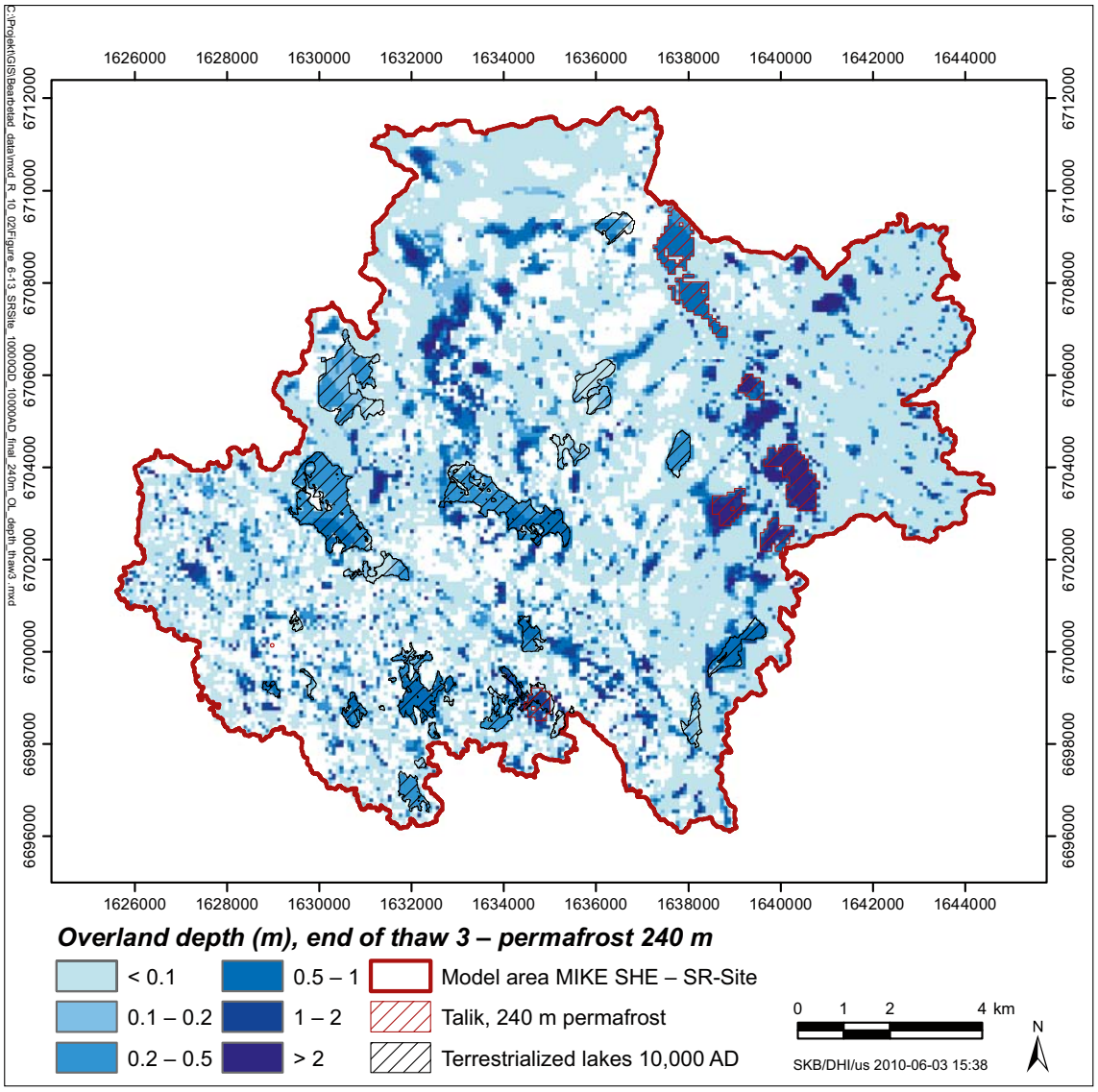

Figure 6-13. *Calculated depth of overland water from the 10000AD_10000QD model under permafrost conditions with a permafrost thickness of 240 m. Results are extracted at the end of the thaw periods (thaw 3), when the areas is characterised by wet and semi-frozen conditions.*

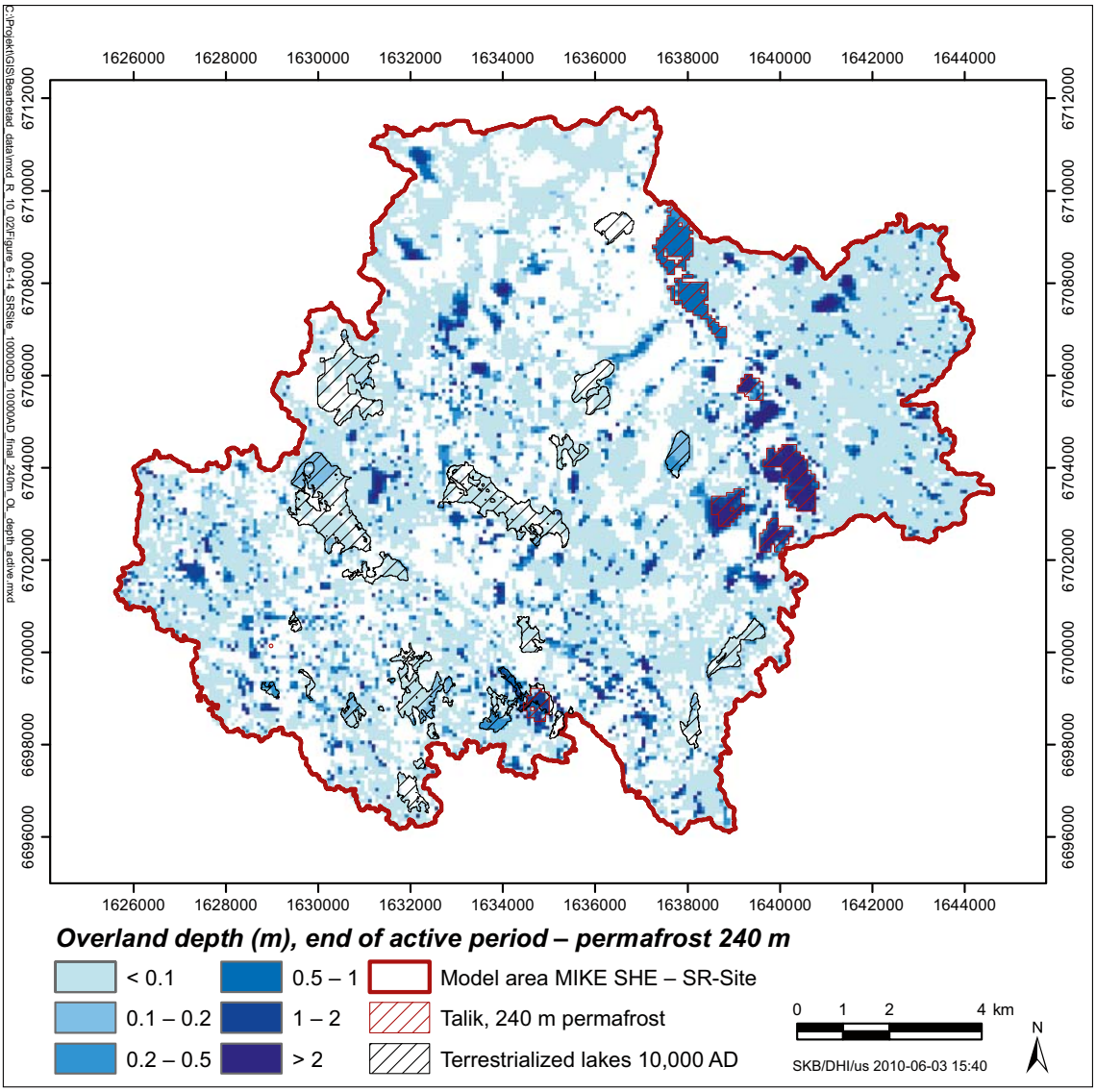

Figure 6-14. *Calculated depth of overland water from the 10000AD_10000QD model under permafrost conditions with a permafrost thickness of 240 m. Results are extracted at the end of the active period, when the area is characterised by dry and unfrozen conditions.*

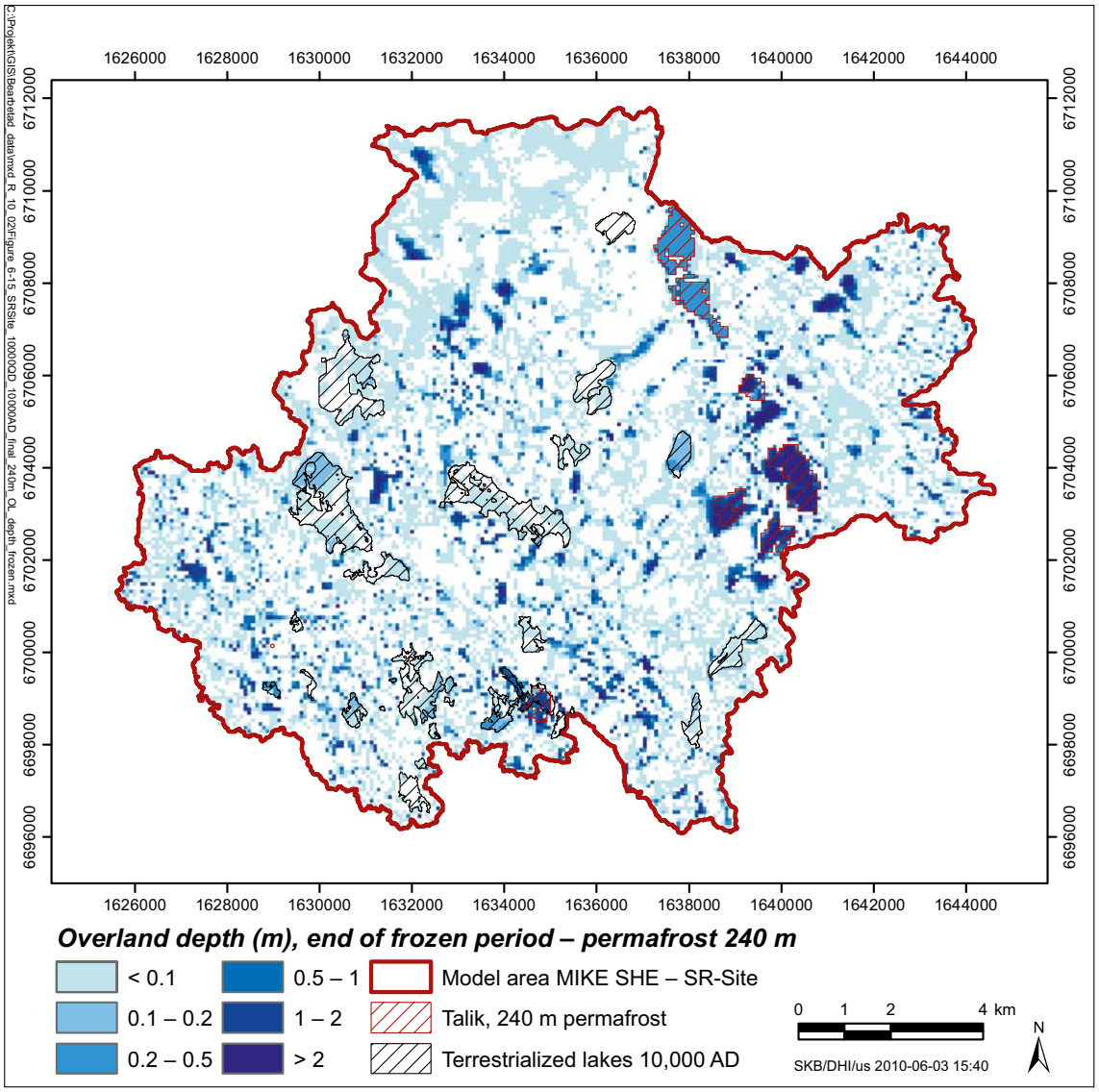

Figure 6-15. *Calculated depth of overland water from the 10000AD_10000QD model under permafrost conditions with a permafrost thickness of 240 m. Results are extracted at the end of the frozen period, i.e. after a long period of frozen conditions.*

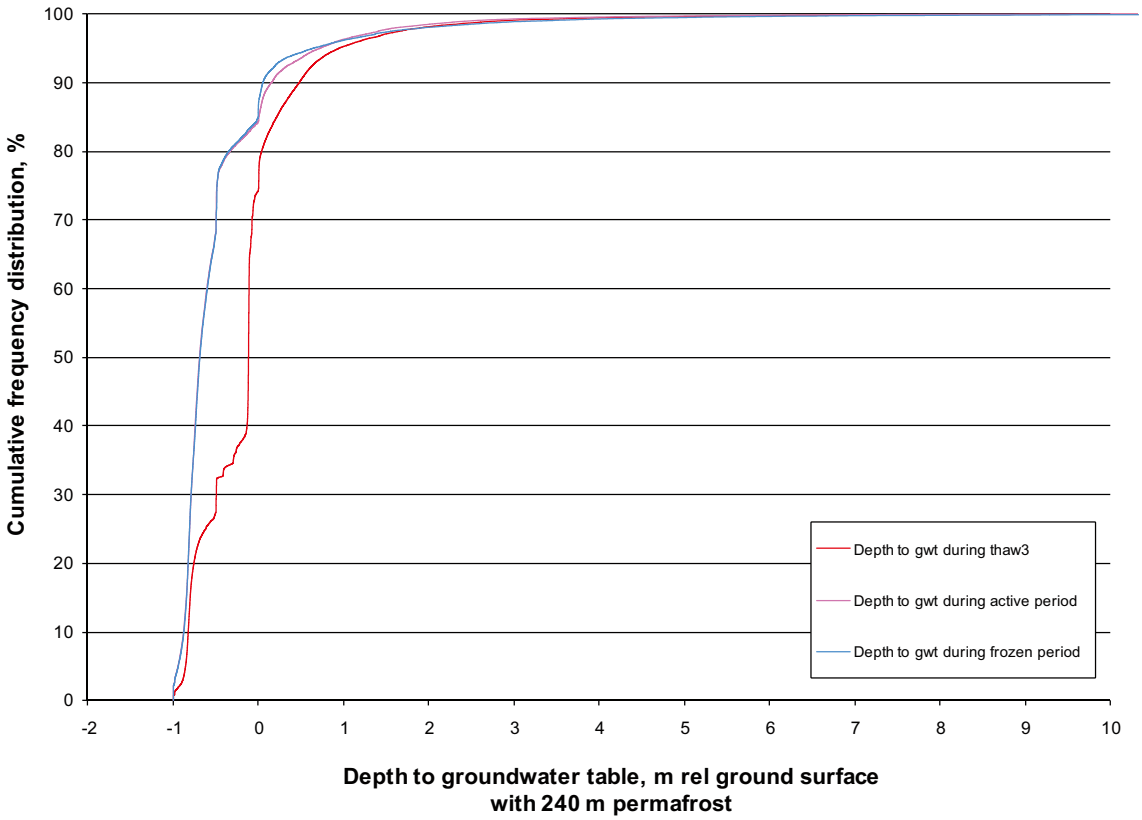

Figure 6-16. *Calculated cumulative frequency distributions of the depth to the groundwater table within the area constituting land at 10,000 AD at the end of the thaw 3, active and frozen periods under permafrost conditions with a permafrost thickness of 240 m.*

Recharge and discharge areas

The majority of the Quaternary deposits act as a recharge area as seen in Table 6-2 and Figures 6-17 to 6-19 where the head difference between the active layer and the top permafrost layer is compared. However, it should be emphasised that the actual flow rates in areas of permafrost are close to zero even though recharge/discharge patterns can be identified based on head gradients, as illustrated in Figures 6-17 to 6-19. The vertical flow is focused to the through taliks as seen in Figures 6-22 to 6-28.

The discharge areas are limited to the through taliks. The seasonal variations make several of the taliks switch from recharge to discharge areas and vice versa. During thaw 3 (Figure 6-17), the recharge to the taliks is dominating due to the intense snow melt contributing to a seasonal head increase in layer 1. The discharge from the taliks grows stronger during the active period (Figure 6-18), when the water contributing to the flow in the taliks is reduced and the head difference between layers 1 and 2 gradually changes, and is dominating during the frozen period as seen when comparing Figures 6-17 to 6-19.

The recharge and discharge areas in the upper bedrock are not influenced by the seasonal variations observed in the Quaternary deposits (Figure 6-20). The active recharge and discharge areas are limited to the taliks, since no recharge or discharge is occurring within the permafrost formation. In talik 7, a dominant recharge area is seen. The pattern is the same in all bedrock layers containing the permafrost. The recharge and discharge conditions (i.e. the flow gradients) in each layer are presented in Appendix 3. When reaching depths in the deeper bedrock just below the permafrost, the recharge/discharge pattern changes, see Figure 6-21. Talik 7 is still a dominant recharge area, but in areas outside the through taliks a pattern has emerged with both recharge and discharge areas determined by the bedrock hydrogeology under the permafrost.

Table 6-2. Distributions (in %) of recharge and discharge areas within the area constituting land at 10,000 AD under permafrost conditions with a permafrost thickness of 240 m. The distributions are calculated based on the mean head differences illustrated in Figures 6-17 to 6-21 (L1, L2 etc denote calculation layers in the MIKE SHE model).

Simulation period	Areas (%) of recharge/discharge L2–L1	Areas (%) of recharge/discharge L5–L4	Areas (%) of recharge/discharge L15–L14
Thaw 3	99/1	1/1	51/45*
Active period	98/2	1/1	52/45*
Frozen period	96/4	1/1	51/45*

*When calculating the mean head difference for each time period some areas are neither discharge nor recharge areas. Consequently the sum of the recharge and discharge areas given in the table are not always equal to 100%.

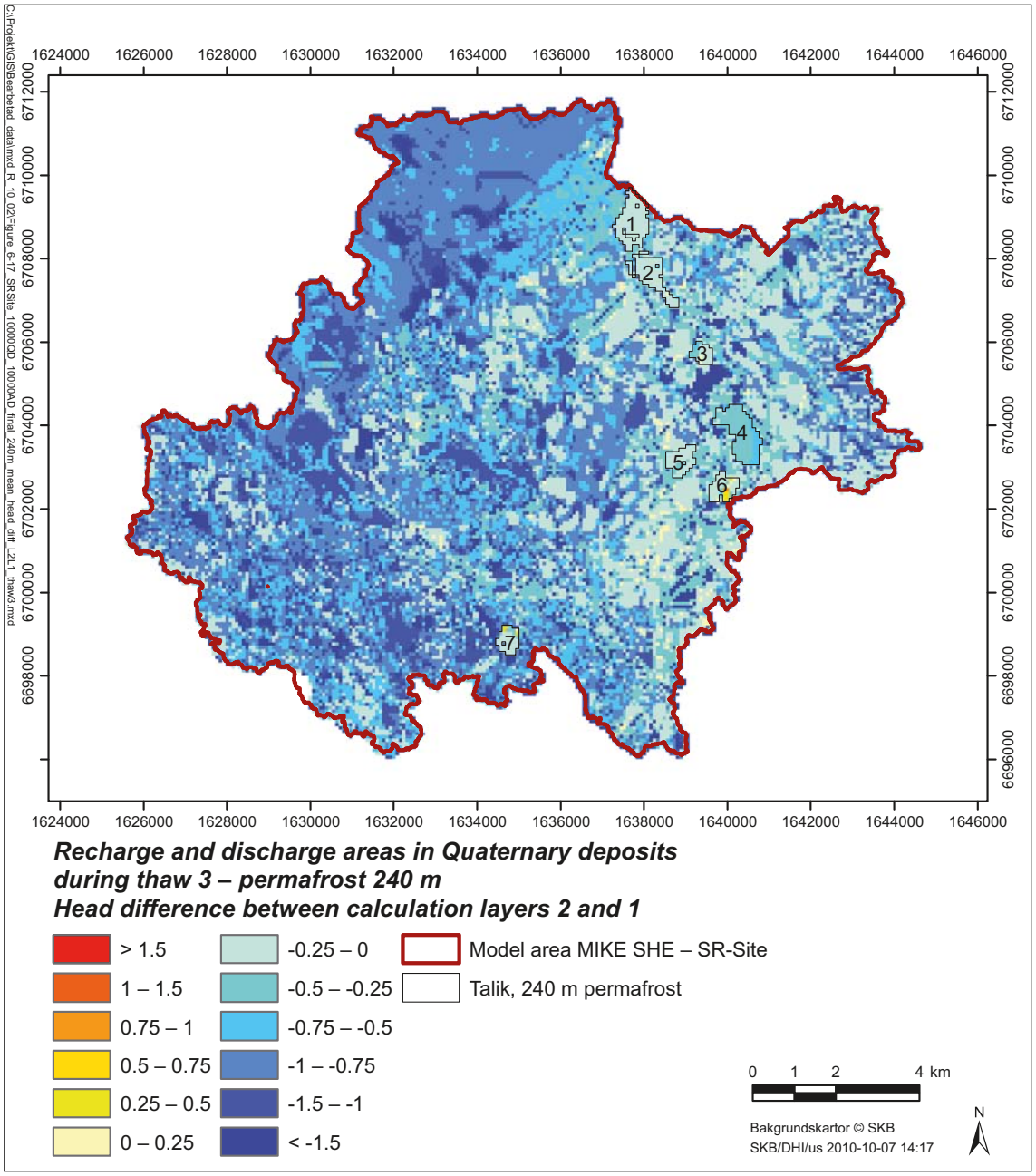

Figure 6-17. *The recharge (blue scale) and discharge (yellow to red scale) areas in the Quaternary deposits from the 10000AD_10000QD model under permafrost conditions with a permafrost thickness of 240 m, calculated as the mean head difference between the two QD layers of the model during the last thaw period (thaw 3).*

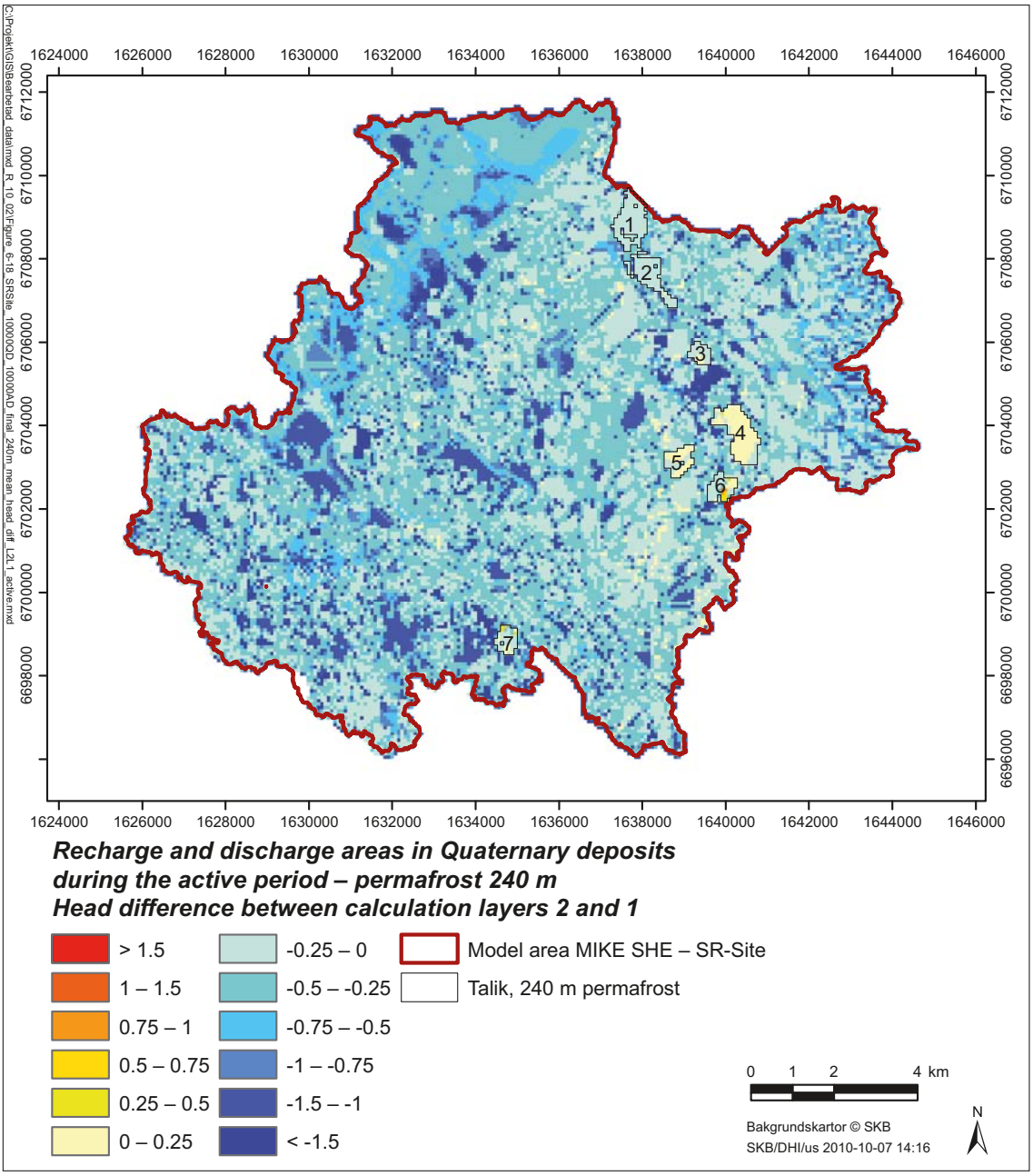

Figure 6-18. *The recharge (blue scale) and discharge (yellow to red scale) areas in the Quaternary deposits from the 10000AD_10000QD model under permafrost conditions with a permafrost thickness of 240 m, calculated as the mean head difference between the two QD layers of the model during the active period.*

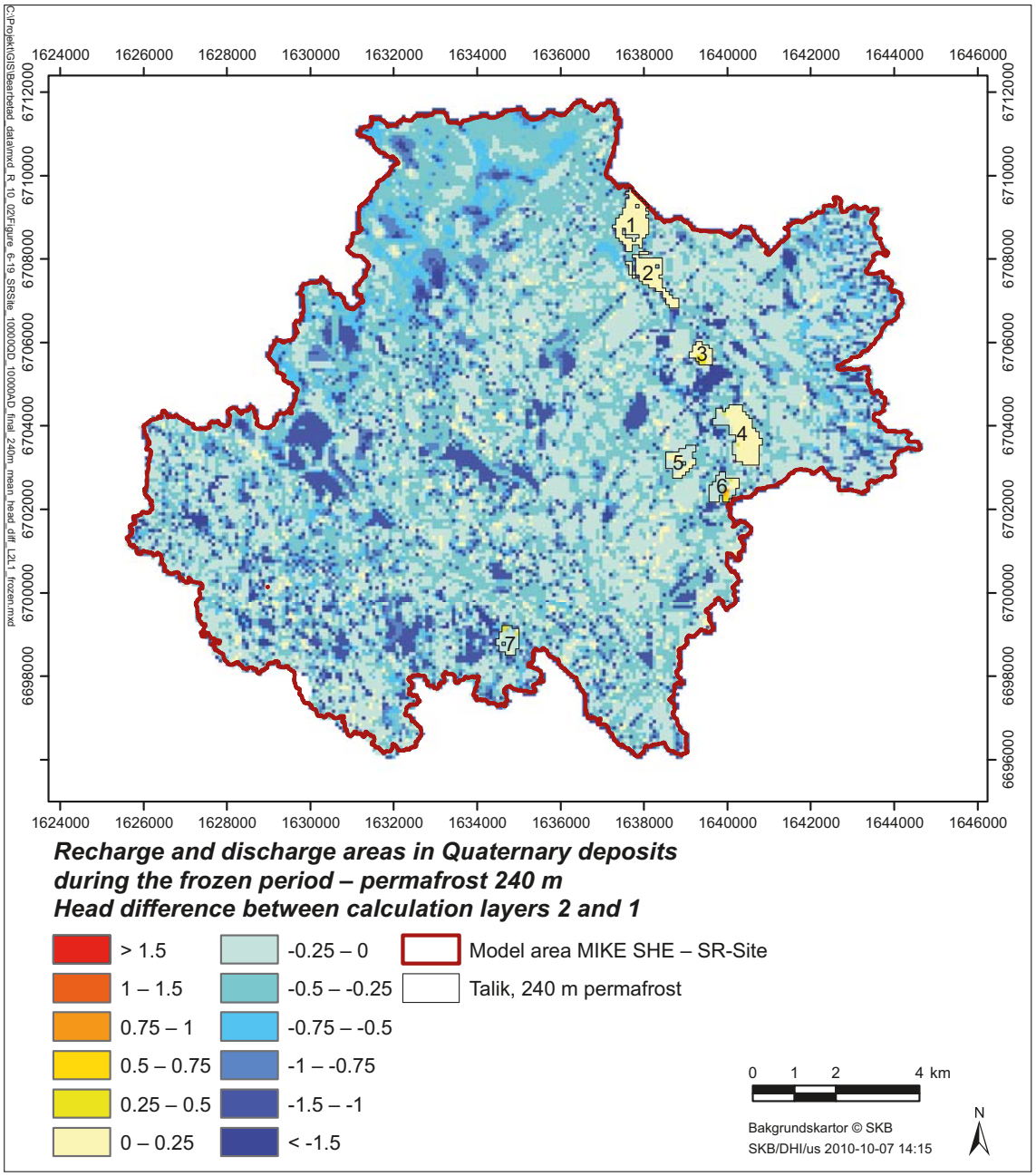

Figure 6-19. *The recharge (blue scale) and discharge (yellow to red scale) areas in the Quaternary deposits from the 10000AD_10000QD model under permafrost conditions with a permafrost thickness of 240 m, calculated as the mean head difference between the two QD layers of the model during the frozen period.*

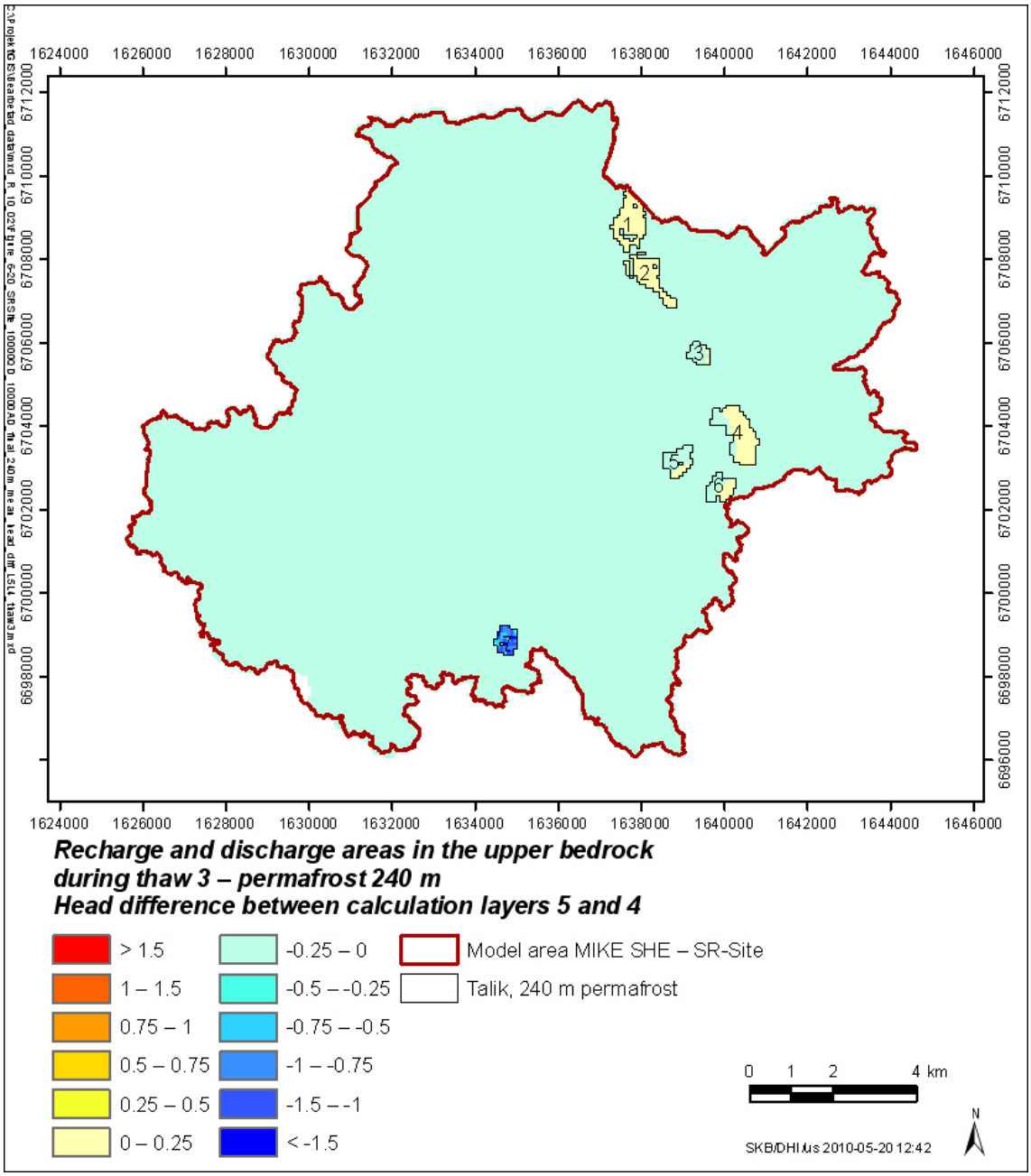

Figure 6-20. *The recharge (blue scale) and discharge (yellow to red scale) areas within the permafrost formation in the upper bedrock from the 10000AD_10000QD model under permafrost conditions with a permafrost thickness of 240 m, calculated as the mean head difference between calculation layers 5 and 4 during the last thaw period (thaw 3).*

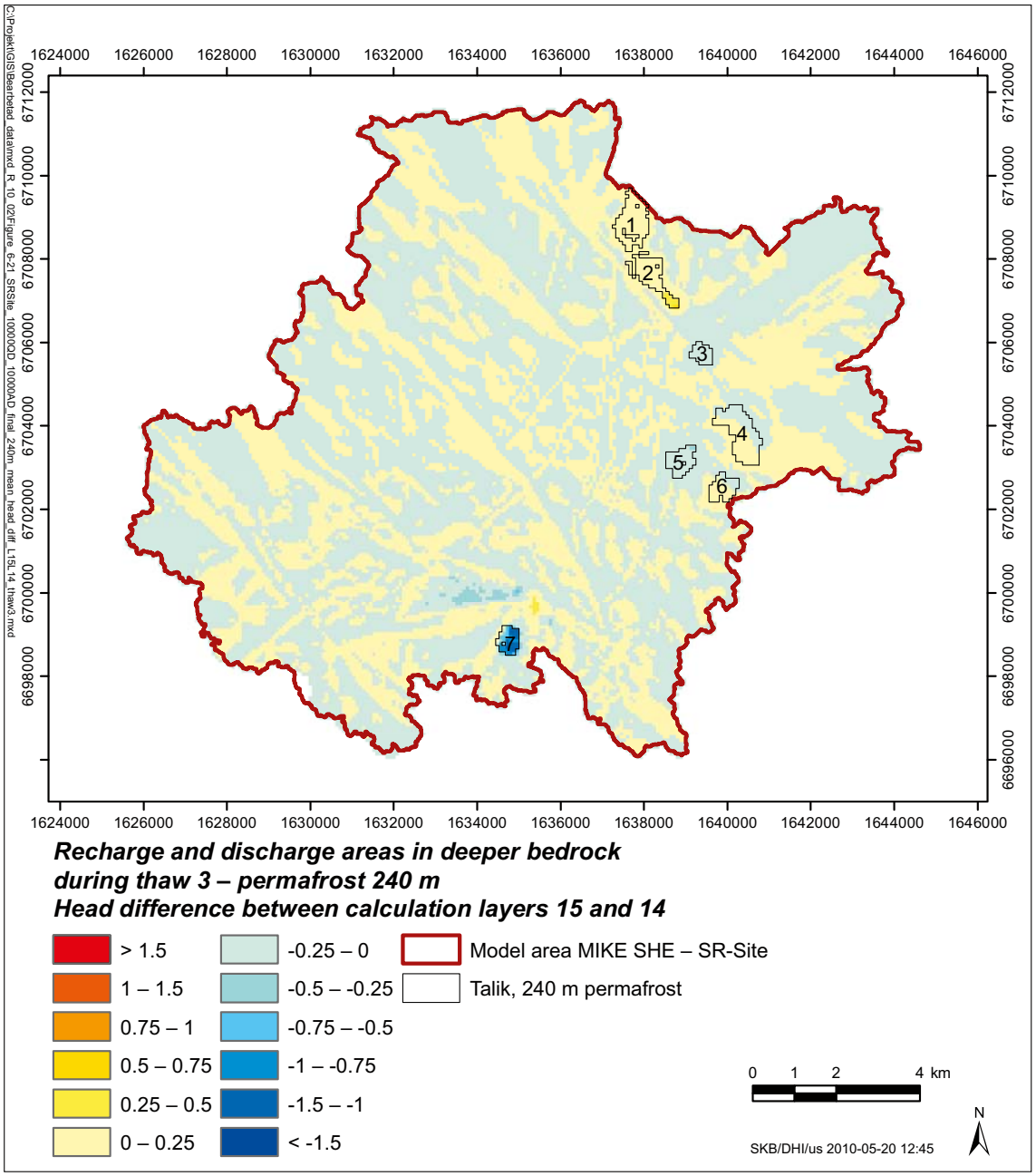

Figure 6-21. *The recharge (blue scale) and discharge(yellow to red scale) areas below the permafrost formation in the deeper bedrock from the 10000AD_10000QD model under permafrost conditions with a permafrost thickness of 240 m, calculated as the mean head difference between calculation layers 15 and 14 during the last thaw period (thaw 3).*

Vertical groundwater flow

Despite the recharge and discharge patterns illustrated in Figures 6-17 to 6-21, the only noticeable vertical flow that takes place is in the through taliks. This is because of the extremely low hydraulic conductivity of the permafrost.

The vertical flow between the active layer and the upper permafrost layer and the flow between the two upper permafrost layers in each talik and for each period are illustrated in Appendix 3. Figures 6-23 to 6-29 illustrate the mean flow direction over time in each through talik during the different periods describing seasonal variations in permafrost conditions during the year. The colour of the uppermost section in each profile indicates whether the active layer is frozen, thawed or in some intermediate semi-frozen state, as seen in Figure 6-22. The location of each talik is shown in Figure 6-5.

Each talik has a dominant flow direction (up or down) but seasonal variations are seen in the upper part of the talik, where the flow temporarily can switch direction in the top layers. The change of flow direction is controlled by the hydrological and meteorological variations in layer 1, i.e. the active layer. During summer and parts of the freezing and thawing periods water exchange may occur between the talik areas and the surrounding active layer. Also, in some areas the MIKE 11 model is deeper than the lower level of the active layer. Water exchange between parts of calculation layer 2 and MIKE11 might take part during periods when the active layer is thawed, however this only occurs in areas where MIKE 11 is connected to a talik.

The general water movement in the model is from talik 7 towards the sea, i.e. towards taliks 1 and 2, which are discharge taliks. However, the surface water level of the sea is transient during the simulation and the sea water level has an influence on the flow direction of the upper parts of taliks 1 and 2; this phenomenon is further discussed in Section 6.3.1.

Talik 3 is a recharge talik with a general flow direction downwards, except for the upper part where the flow direction is upwards during all periods except thaw 3 and the active period. Talik 4 is a discharge talik with an upward water movement except during the strongest period of snow melt during thaw 3.

Talik 5 is also a recharge talik with a general downward movement, but with seasonal variations in flow direction in the upper part. Talik 6 is also a discharge talik with the same flow pattern as talik 4. Talik 7 is located upstream and is the apparent recharge talik with a strong downward flow without influence of seasonal variations in the upper part of the talik.

The vertical flow between the active layer and the upper permafrost layer during the active period is shown in Figure 6-30. The direction of the water flow differs within each talik, and a particular talik can have both upward and a downward gradients in different parts of the talik. This is further discussed in Section 6.3.1, which describes the results of the particle tracking simulations for periglacial conditions.

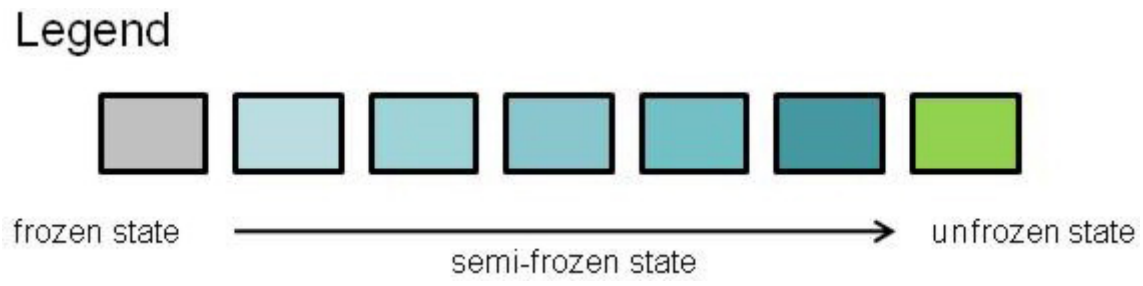

Figure 6-22. *Legend defining the state of the active layer, as illustrated in Figures 6-23 to 6-29 for the different periods of the permafrost simulation.*

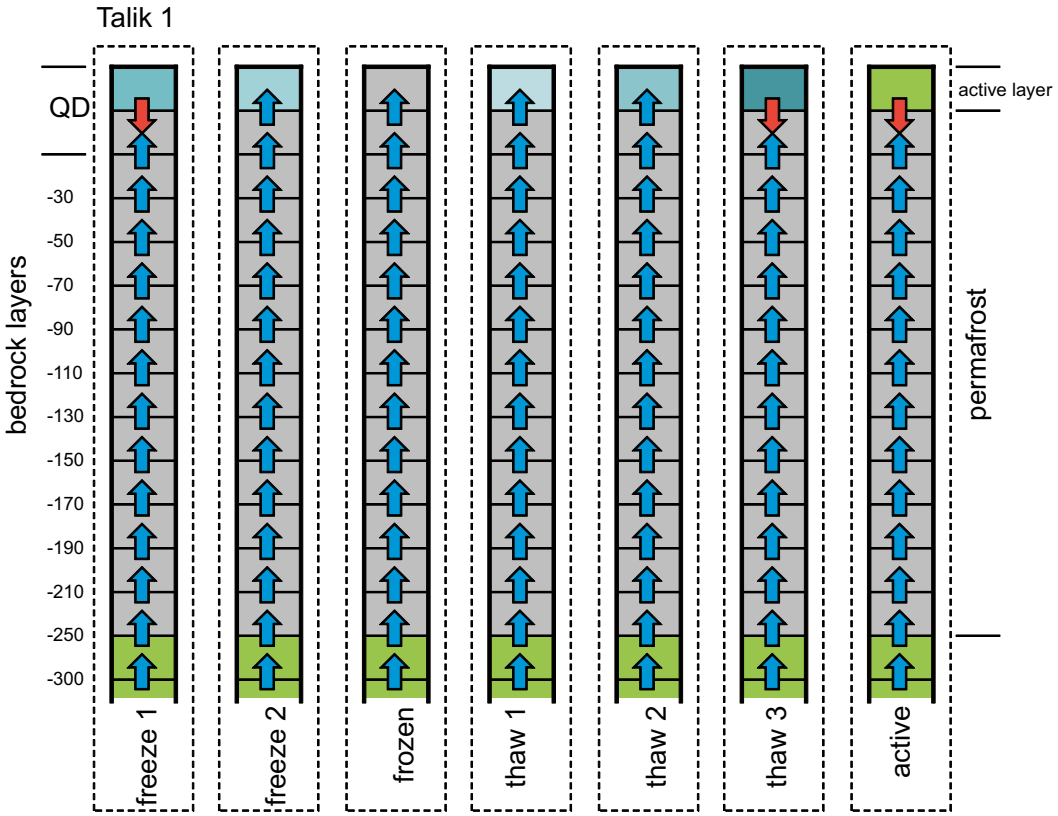

Figure 6-23. *Calculated mean vertical flow direction in talik 1 during the simulated periods with the 10000AD_10000QD model under permafrost conditions with a permafrost thickness of 240 m.*

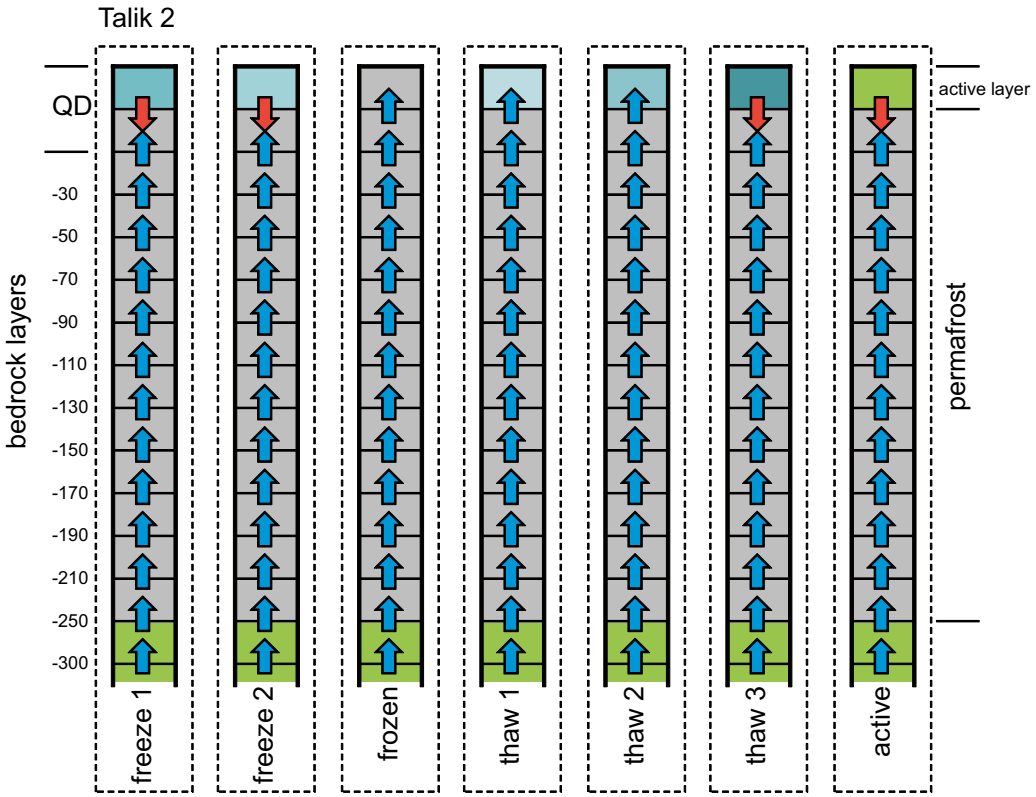

Figure 6-24. *Calculated mean vertical flow direction in talik 2 during the simulated periods with the 10000AD_10000QD model under permafrost conditions with a permafrost thickness of 240 m.*

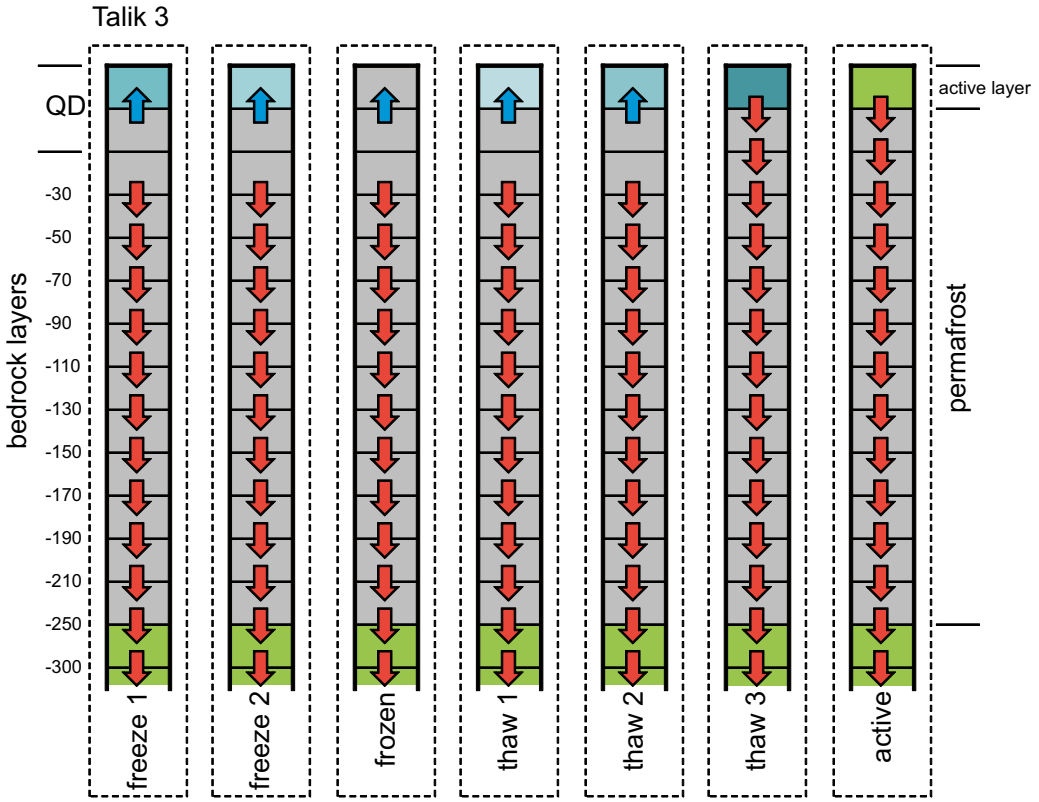

Figure 6-25. *Calculated mean vertical flow direction in talik 3 during the simulated periods with the 10000AD_10000QD model under permafrost conditions with a permafrost thickness of 240 m.*

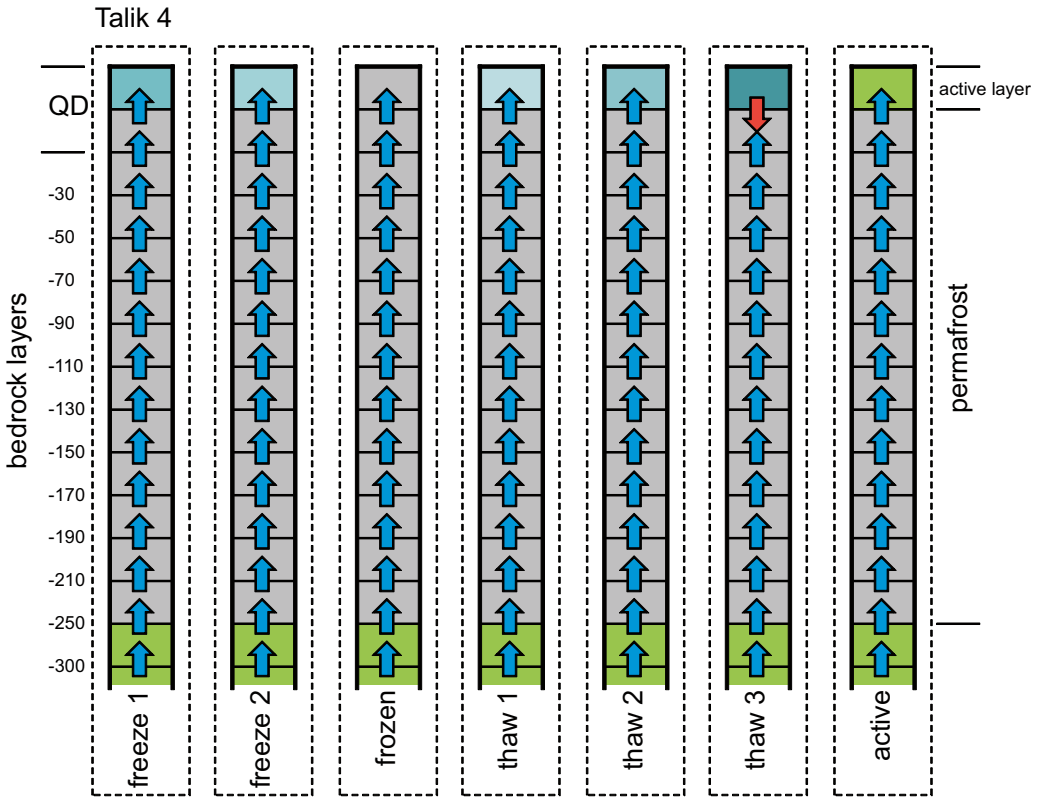

Figure 6-26. *Calculated mean vertical flow direction in talik 4 during the simulation periods with the 10000AD_10000QD model under permafrost conditions with a permafrost thickness of 240 m.*

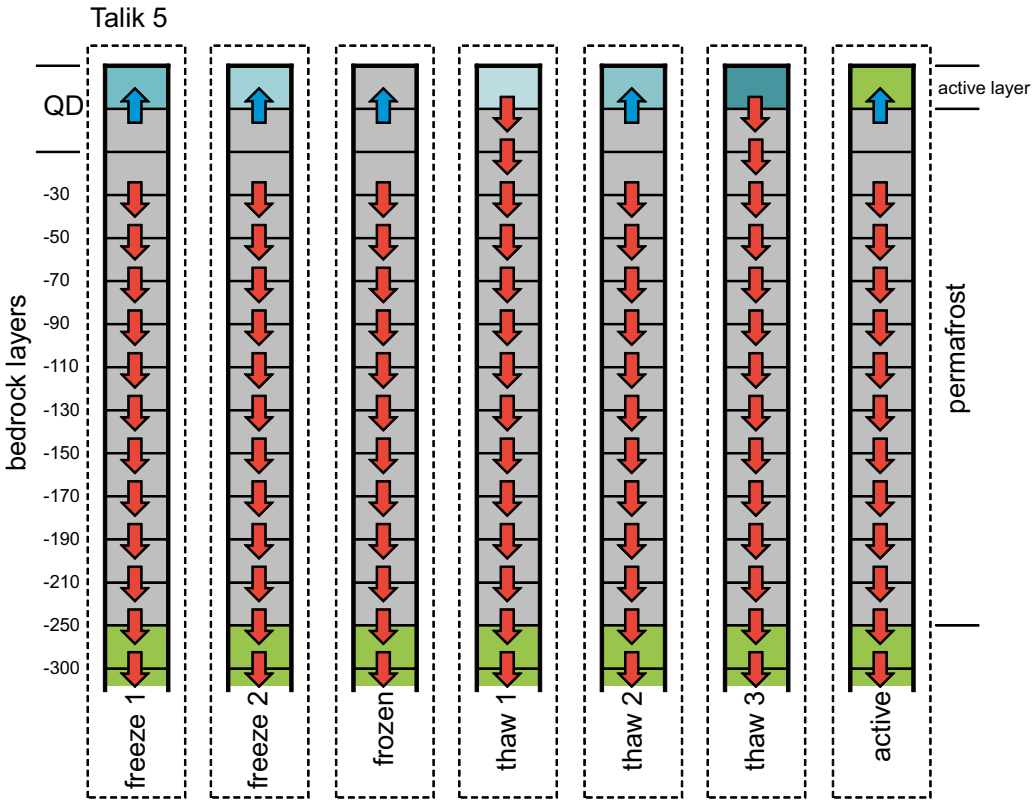

Figure 6-27. *Calculated mean vertical flow direction in talik 5 during the simulated periods with the 10000AD_10000QD model under permafrost conditions with a permafrost thickness of 240 m.*

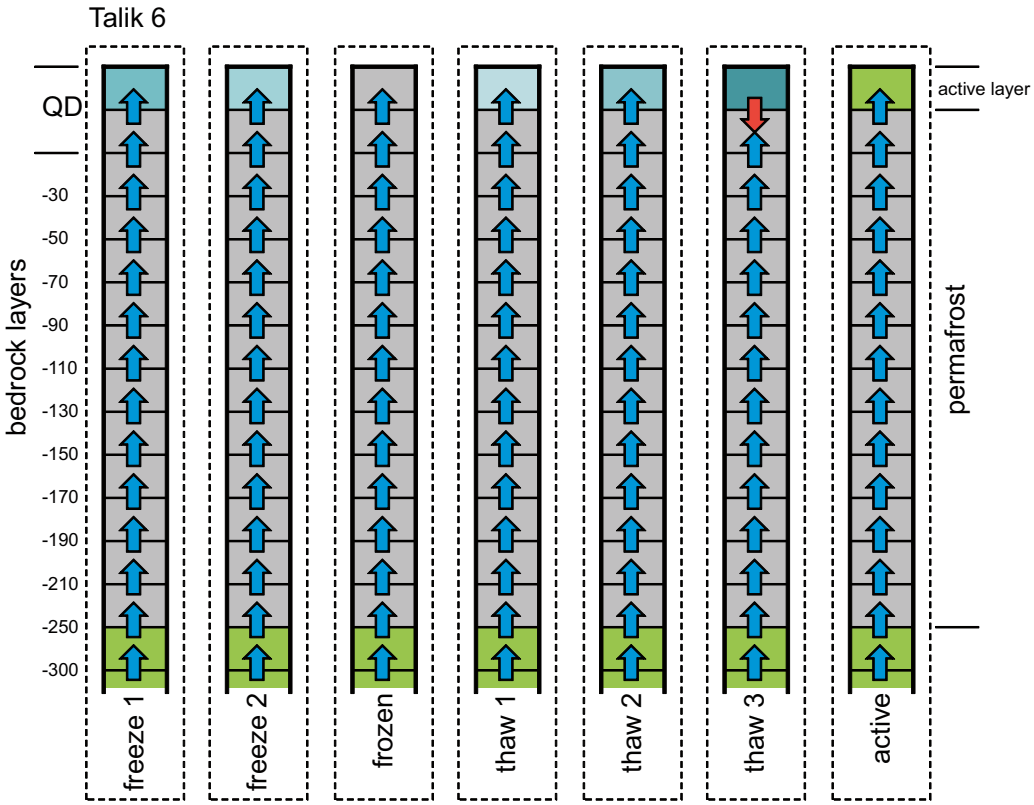

Figure 6-28. *Calculated mean vertical flow direction in talik 6 during the simulated periods with the 10000AD_10000QD model under permafrost conditions with a permafrost thickness of 240 m.*

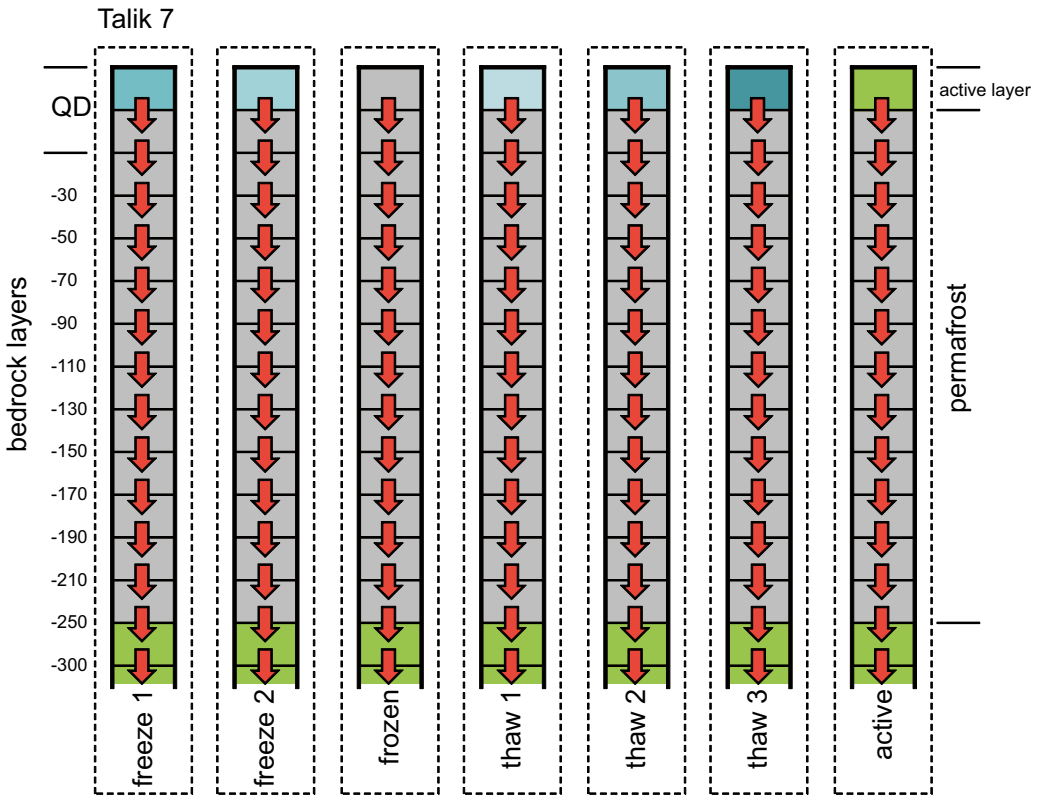

Figure 6-29. *Calculated mean vertical flow direction in talik 7 during the simulated periods with the 10000AD_10000QD model under permafrost conditions with a permafrost thickness of 240 m.*

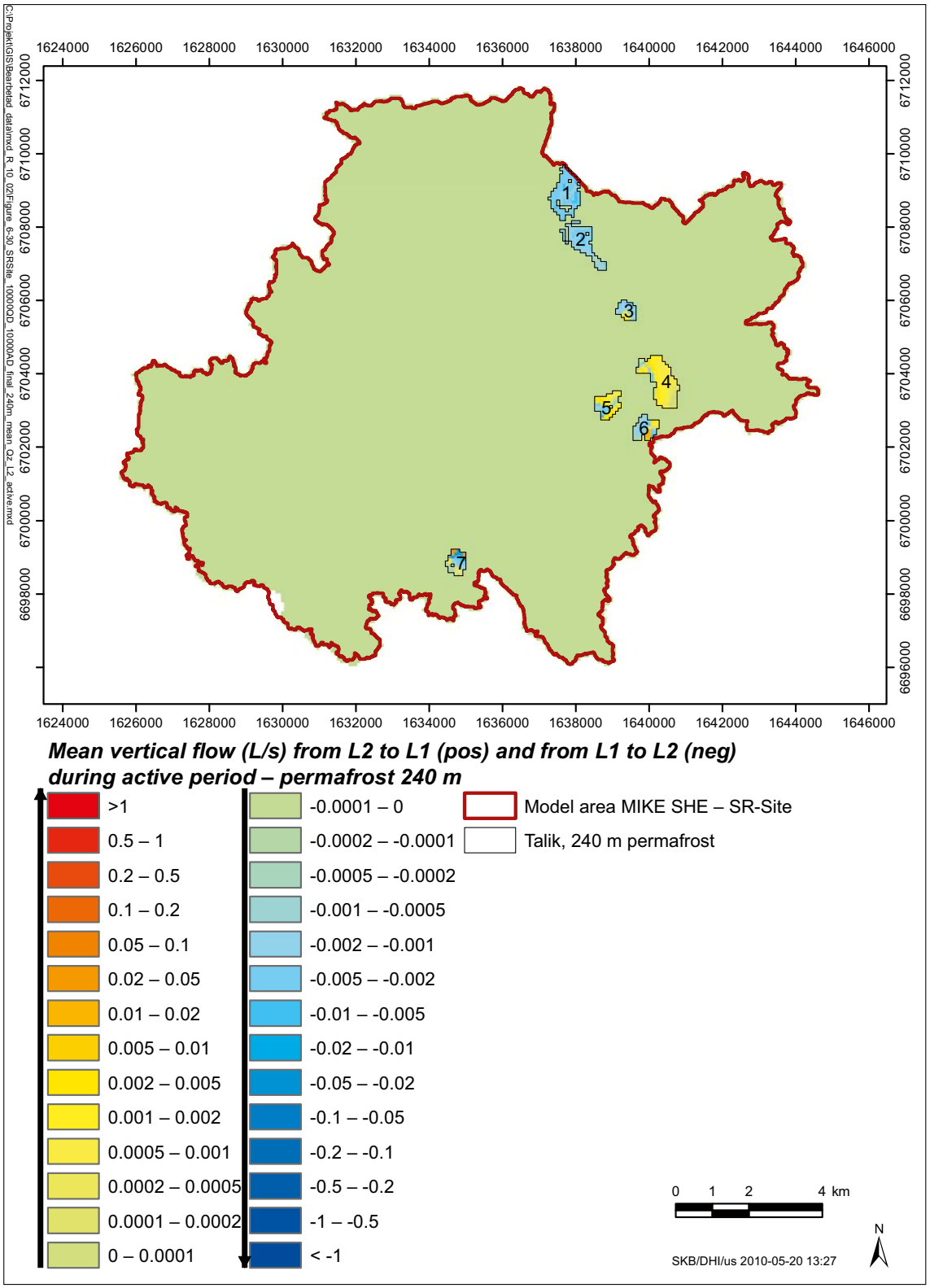

Figure 6-30. *Calculated mean vertical flow (units are in l/s) between the active layer and the top permafrost layer during the active period with a permafrost thickness of 240 m.*

6.2.2 Model with 100 m permafrost

Water balance

The water balances for the permafrost case with a permafrost thickness of 100 m are shown in Figures 6-31 and 6-32 and in Appendix 3 in Figures A3-23 to A3-29. Figure 6-31 illustrates the water balance for a one-year period. In Appendix 3 (Figures A3-23 to A3-29), the yearly water balance has been divided into partial balances for each permafrost simulation period, i.e. freeze 1, freeze 2, frozen, thaw 1, thaw 2, thaw 3 and active. The figures illustrate the water balance for the area constituting land at 10,000 AD. The accumulated water flow for each component within each model compartment is also illustrated as time series in Figures 6-33 to 6-36.

As described above, the precipitation used in the permafrost modelling is 412 mm, which is slightly lower than the precipitation used in the modelling based on the climate conditions. The calculated actual evapotranspiration is 194 mm and the runoff is 217 mm, which are the same results as obtained in the case with a permafrost thickness of 240 m. The distribution of the precipitated water is still approximately 50% runoff and 50% evapotranspirated water. This indicates that there are no changes in the amount of runoff or the internal distribution of water between runoff and evapotranspiration depending on the permafrost thicknesses applied.

The water balances in the two cases with different depths of permafrost are similar. The infiltration to the unsaturated zone decreases from 180 mm in the 240 m permafrost case to 169 mm in the 100 m permafrost case. The recharge is also slightly decreased from 89 mm to 80 mm. The only significant difference standing out is found in the exchange of water between overland and the saturated zone. The inflow to OL from SZ is reduced from 303 mm in the 240 m permafrost case to 193 mm in the 100 m permafrost case. The inflow from OL to SZ is also reduced, from 269 mm to 169 mm.

In Figure 6-32 a detailed water balance of the saturated zone is illustrated for the part of the model area constituting land at 10,000 AD, i.e. the sea-taliks 1 and 2 are not included. The recharge from the unsaturated zone to the saturated zone is c. 80 mm. Almost all of that water (approximately 99%) is removed from the saturated zone through the exchange with the overland water system (30%), through the streams (60%) and through evaporation (9%). Almost no water is left to percolate further down into the saturated zone resulting in very little water movement through the taliks, although more than in the 240 m permafrost case.

Studying the active layer (layer 1) and the top permafrost layer (layer 2) in detail, 0.40 mm is moving from layer 2 to layer 1 and 0.45 mm from layer 1 to layer 2. The vertical net flow is thus very small, but still approximately a factor 4 larger than the corresponding flow in the 240 m case. In the 100 m permafrost model, the mean flow is always downwards between layers 1 and 2.

The water balance varies between the seasons in the same way as in the 240 m permafrost case. The differences are very small and are focused to thaw 2, thaw 3 and the active period. The differences are found in the amount of runoff where the contribution of overland water to surface streams is included. Small differences are also found in the saturated zone storage. However, all of these differences are on a yearly basis equal to zero. The main differences in the water balance reflected in the yearly cycle are as described above the exchange of water between OL and SZ and the infiltration to UZ and recharge to SZ.

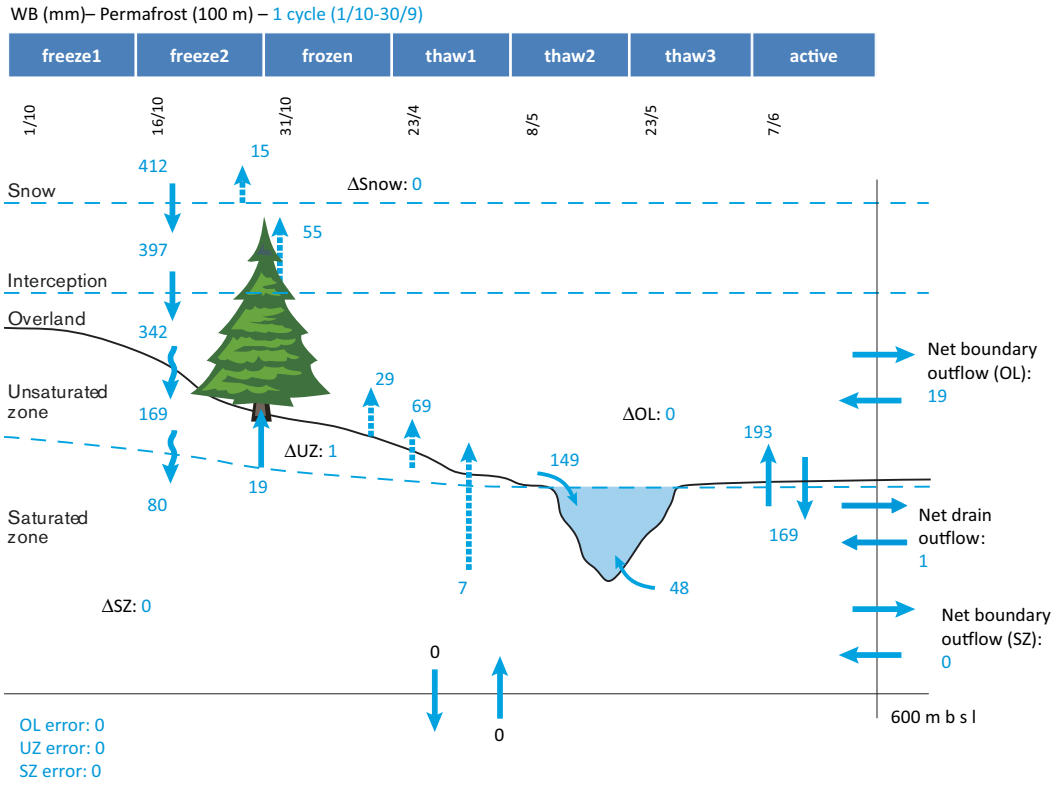

Figure 6-31. *Calculated one-year water balance (units in mm) for the 10000AD_10000QD-model under permafrost conditions with a permafrost thickness of 100 m for the area constituting land at 10,000 AD.*

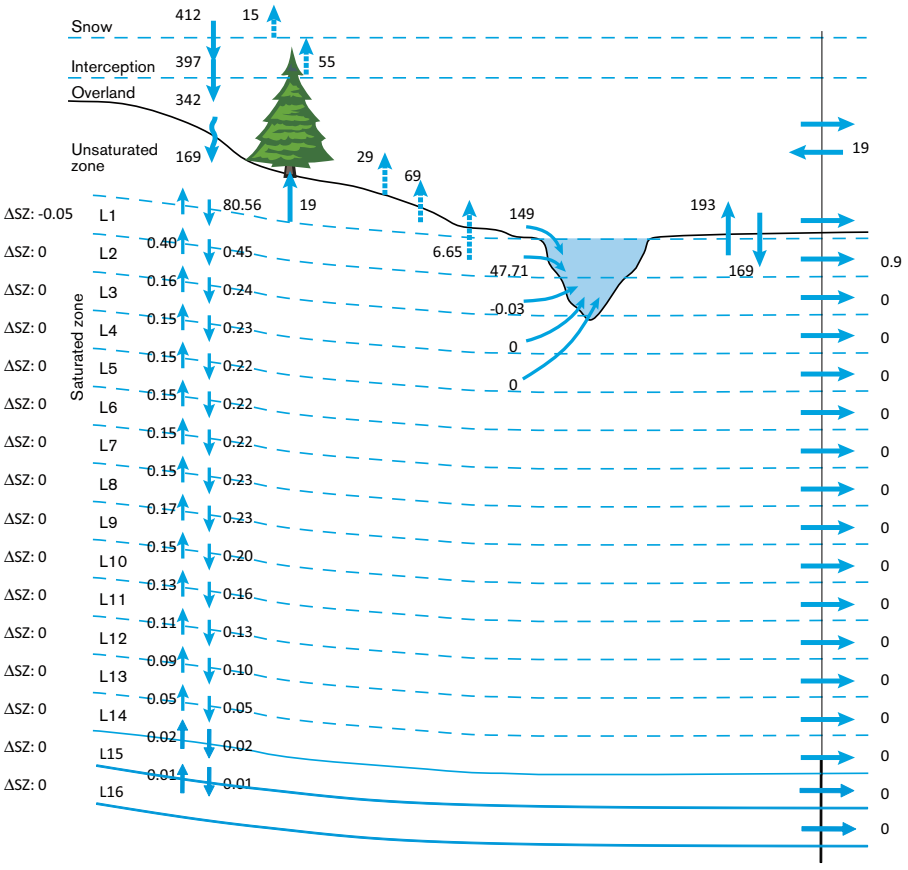

Figure 6-32. *Calculated detailed one-year water balance (units in mm) illustrating the exchange of water between layers in the saturated zone during the simulated year with a permafrost thickness of 100 m for the area constituting land at 10,000 AD. Permafrost is present in layers 2 through 13.*

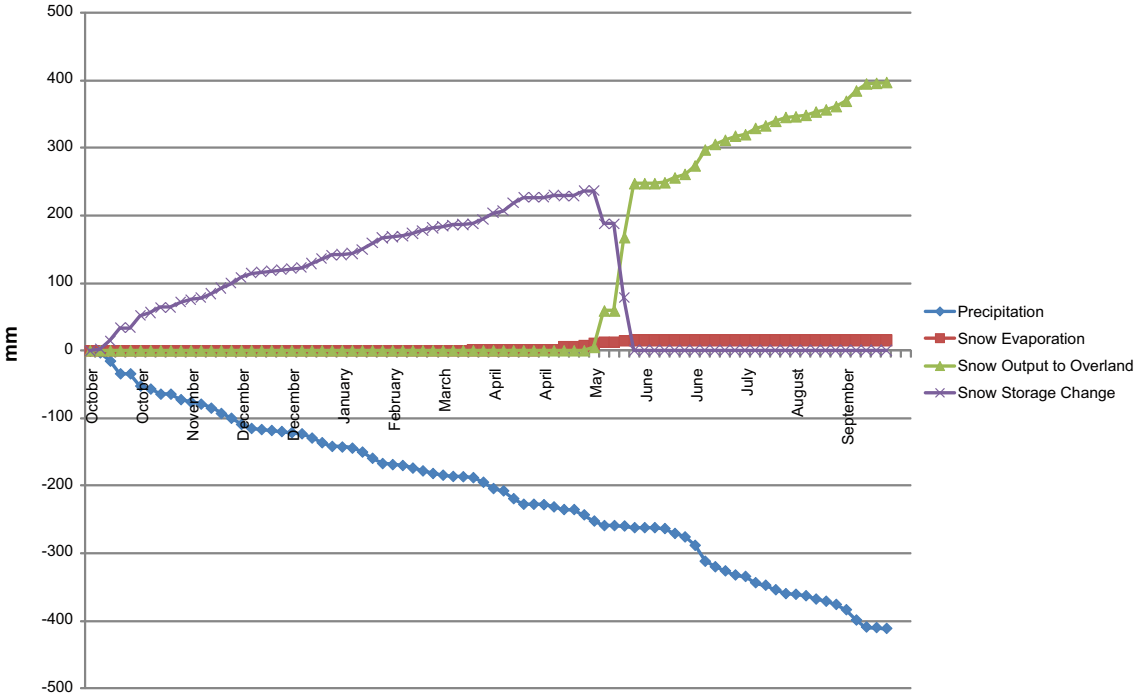

Figure 6-33. *Accumulated precipitation, snow evaporation, snow throughfall and change in snow storage during the simulated year with a permafrost thickness of 100 m for the area constituting land at 10,000 AD.*

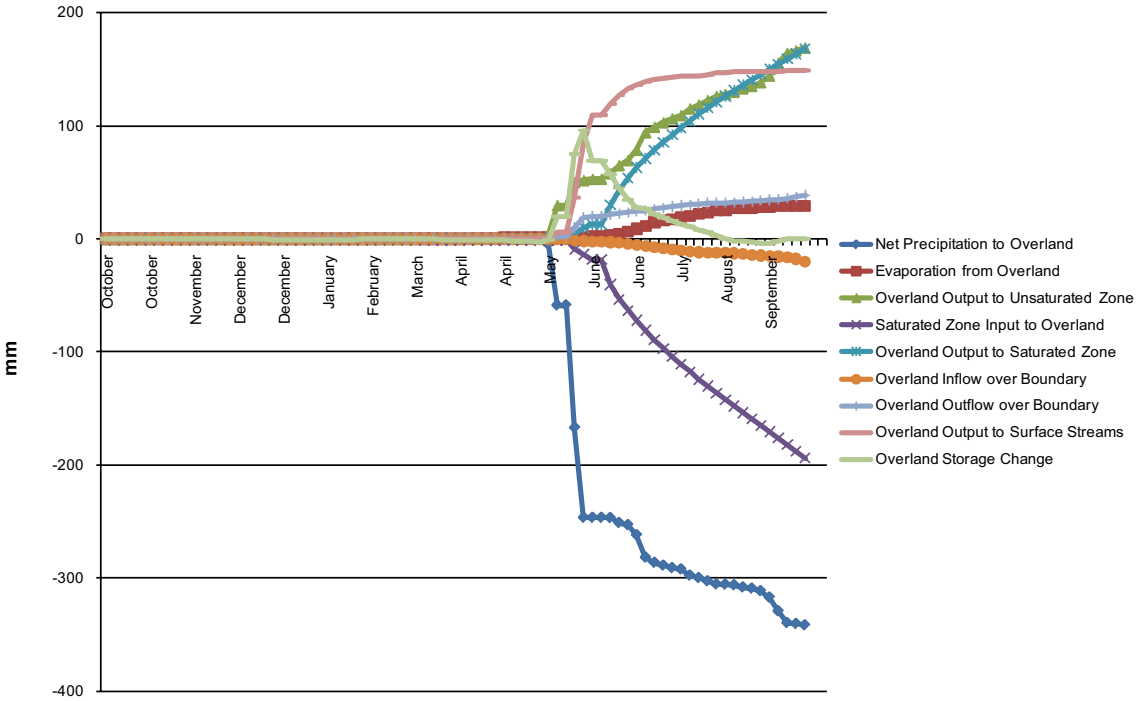

Figure 6-34. *Accumulated net precipitation to OL, evaporation from OL, infiltration to UZ from OL, exchange between OL and SZ, boundary inflow and outflow, OL water to streams and change in OL storage during the simulated year with a permafrost thickness of 100 m for the area constituting land at 10,000 AD.*

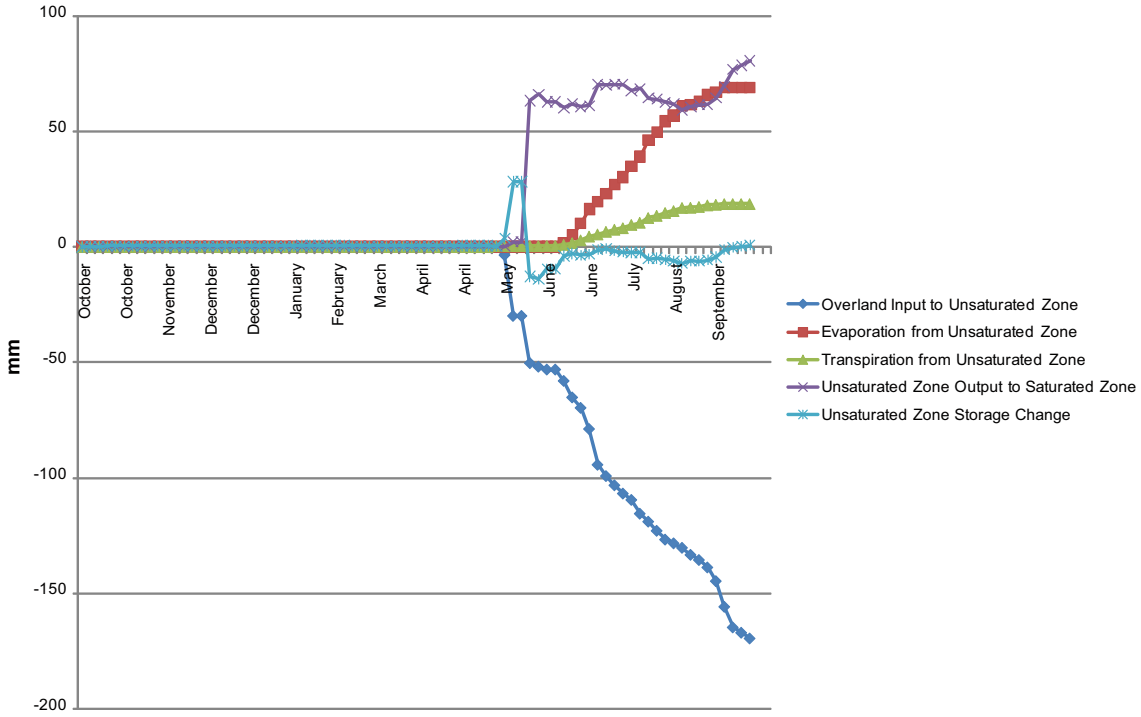

Figure 6-35. *Accumulated infiltration to UZ, evaporation from soil, plant transpiration, recharge to SZ from UZ and change in UZ storage during the simulated year with a permafrost thickness of 100 m for the area constituting land at 10,000 AD.*

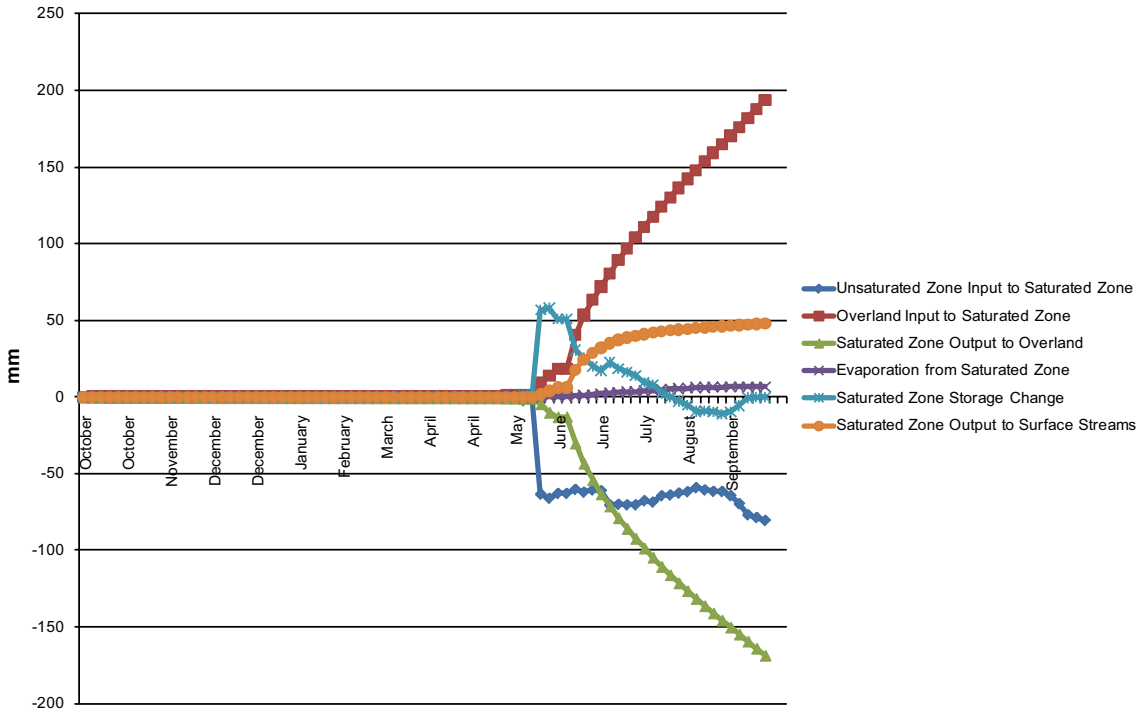

Figure 6-36. *Accumulated recharge to SZ, exchange between OL and SZ, evaporation from SZ, SZ drainage to streams and change in SZ storage during the simulated year with a permafrost thickness of 100 m for the area constituting land at 10,000 AD.*

Depth of overland water

The resulting overland water depths are very similar in the two permafrost cases. At the end of thaw 3 approximately 73% of the ground surface is covered with overland water. This is reduced to 56% at the end of the active period and 44% at the end of the frozen period. The mean depth of overland water is slightly larger than in the 240 m permafrost case.

This indicates that the depth of overland water is generally determined by the topography, the QD model and the thickness of the active layer, and not by the permafrost thickness or the distribution and number of taliks. In Figures 6-37 to 6-39 the depth of overland water is illustrated at the end of thaw 3, the active and the frozen period. During thaw 3 the major snow melt occurs and water is accumulating at the surface. The overland water depth has decreased at the end of the relatively dryer active period.

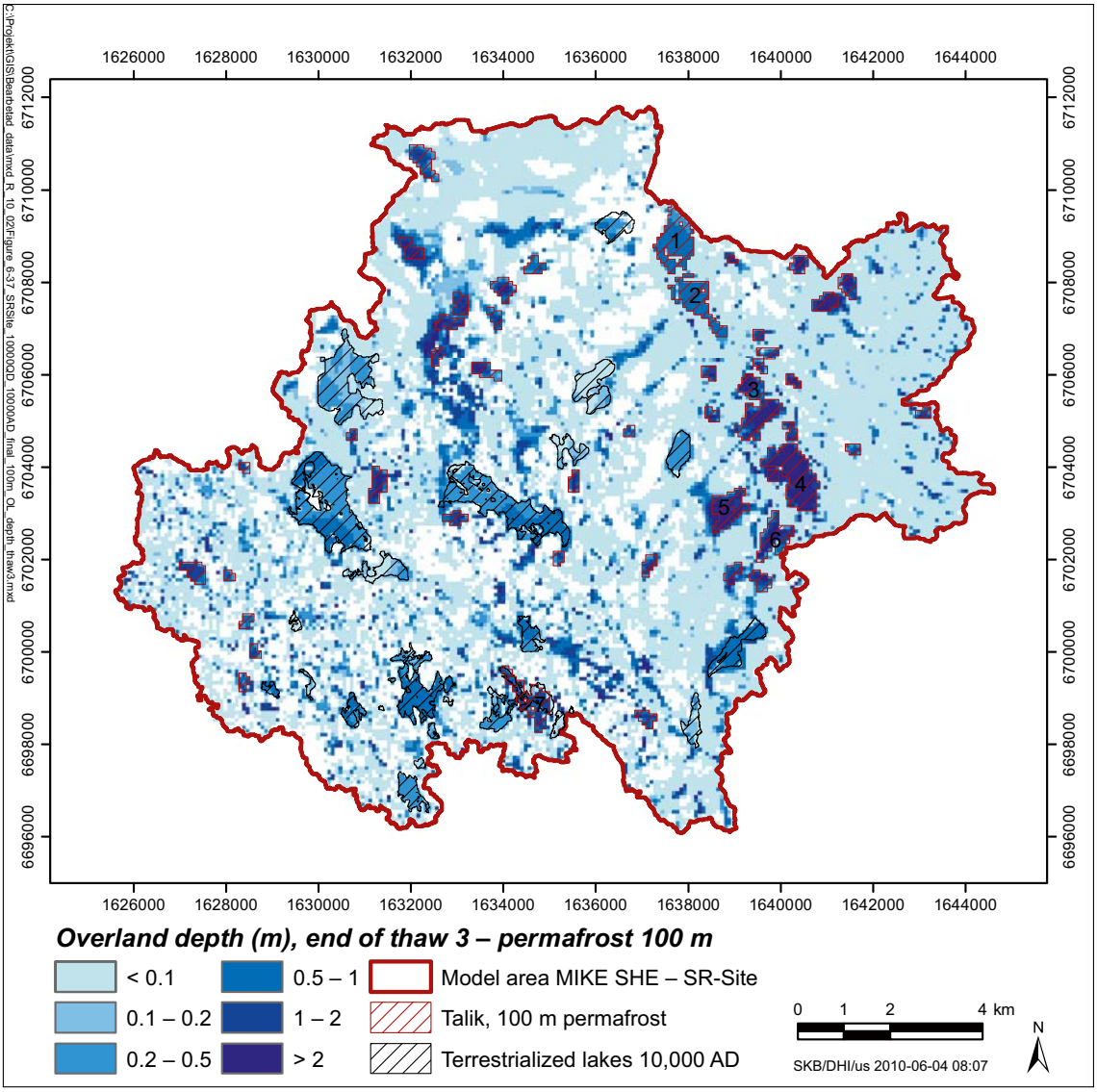

Figure 6-37. *Calculated depth of overland water from the 10000AD_10000QD model under permafrost conditions with a permafrost thickness of a 100 m. Results are extracted at the end of the thaw periods (thaw 3), when the areas is characterised by wet and semi-frozen conditions.*

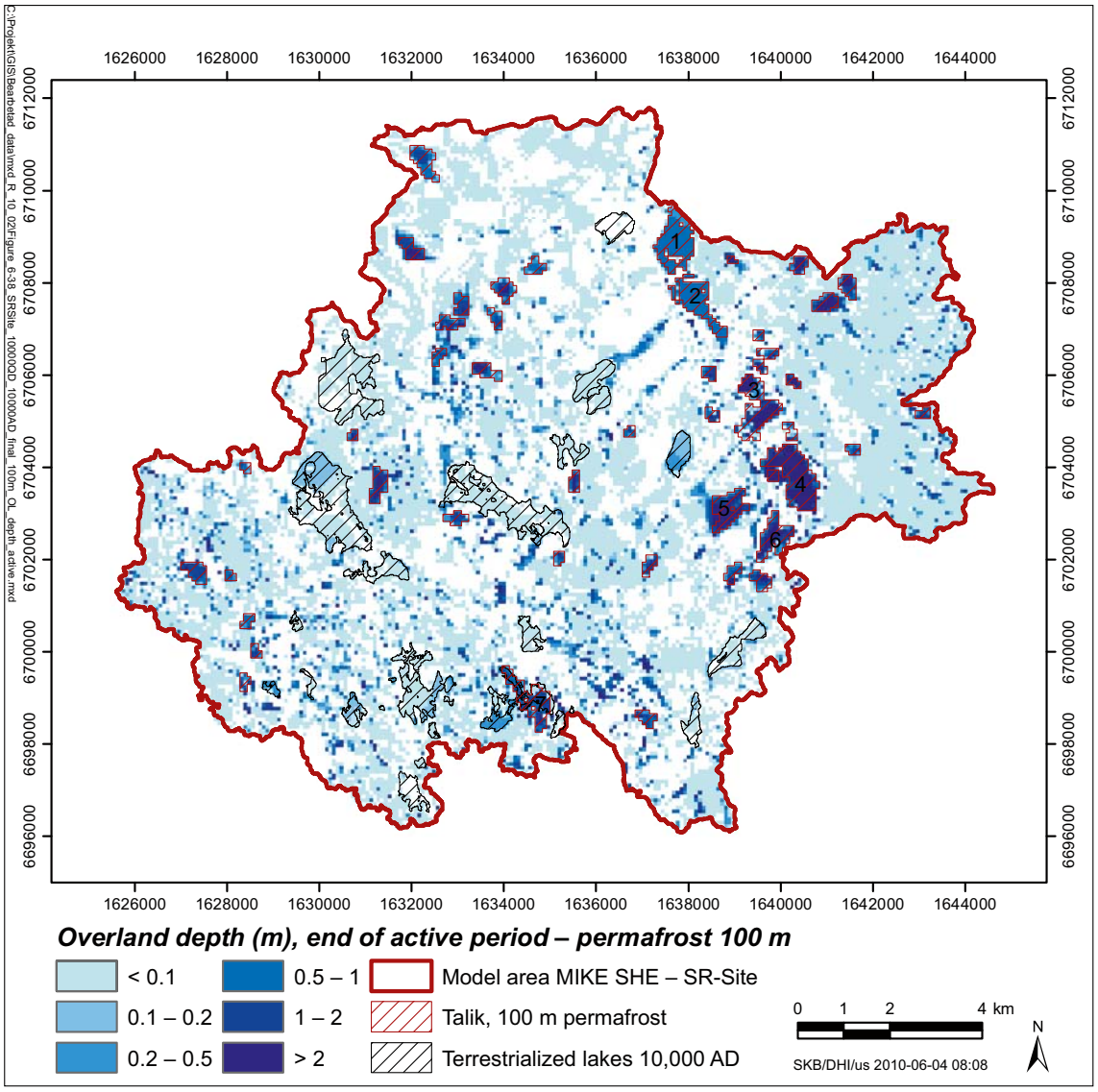

Figure 6-38. *Calculated depth of overland water from the 10000AD_10000QD model under permafrost conditions with a permafrost thickness of 100 m. Results are extracted at the end of the active period, when the area is characterised by dry and unfrozen conditions.*

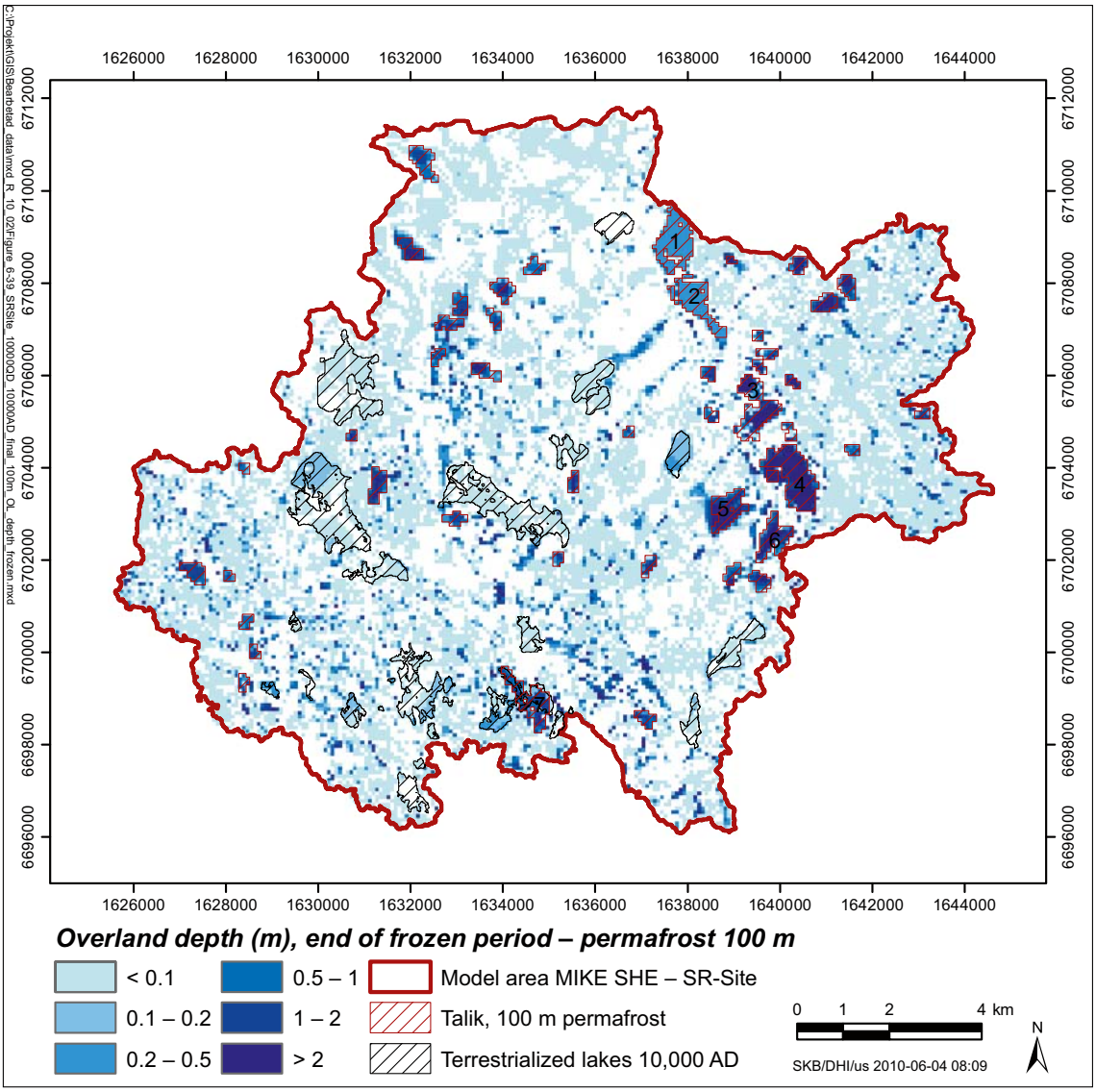

Figure 6-39. *Calculated depth of overland water from the 10000AD_10000QD model under permafrost conditions with a permafrost thickness of 100 m. Results are extracted at the end of the frozen period, i.e. after a long period of frozen conditions.*

Groundwater table depth

The depth of the groundwater table is limited to the bottom of the active layer, which is one metre below the ground surface in both permafrost depth cases. The fluctuations in the ground water table follow the same pattern for both permafrost cases, with a rise of the water table during thaw 3 and a fall during the active period.

Figure 6-40 illustrates the cumulative frequency distribution of the groundwater depth within the area constituting land at 10,000AD at the end of the simulation periods thaw 3, active and frozen. The mean groundwater depths are very similar in the two cases. The mean depth to the groundwater table is 0.46 m and 0.45 m at the end of the active period and the frozen period, respectively. The groundwater table at the end of thaw 3 is higher with a mean depth 0.11 m.

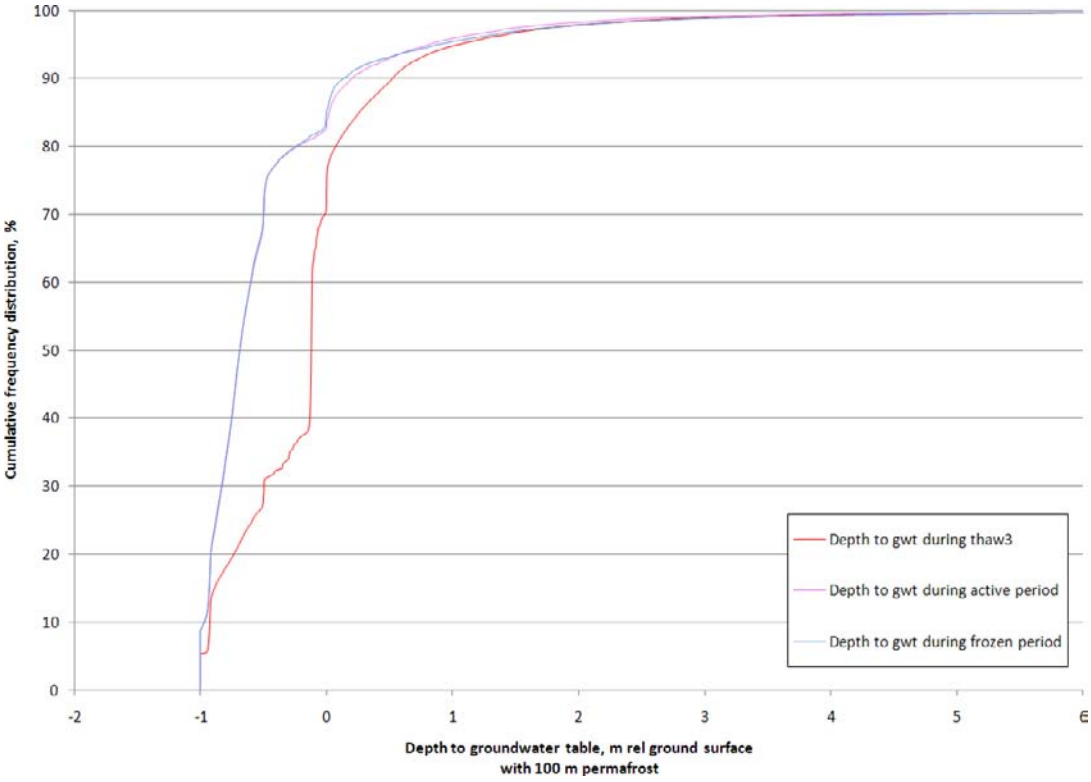

Figure 6-40. *Calculated cumulative frequency distribution of the depth to the groundwater table within the area constituting land at 10,000AD at the end of the thaw 3, active and frozen periods under permafrost conditions with a permafrost thickness of 100 m.*

Recharge and discharge areas

When the permafrost depth is reduced from 240 m to 100 m, the discharge areas increase due to the increased number of through taliks. The percentage of the model area occupied by through taliks has increased from 2% to 5% when comparing the 240 m and 100 m permafrost depth cases. As seen in the 240 m case, the recharge areas are stronger during thaw 3 due to intense snow melt. The extent of the discharge areas is largest during the frozen period.

As in the 240 m case the recharge and discharge areas in the upper and deeper bedrock are not influenced by the seasonal variations observed in the Quaternary deposits. The active recharge and discharge areas are also here focused to the through taliks, since the vertical flow is concentrated to them in a permafrost area. The spatial distributions of recharge and discharge areas in the QD for three different periods, thaw 3, the active period and the frozen period, are illustrated in Figures 6-41 to 6-43.

In Figure 6-44 the recharge and discharge areas for the active period in the upper bedrock containing the permafrost is shown and in Figure 6-45 the corresponding results for the layer below the permafrost are presented. The spatial distributions of recharge and discharge areas for all periods for the upper bedrock and the layer below the permafrost are presented in Appendix 3. The distributions of recharge and discharge areas in the different parts of the vertical profile are also reported in Table 6-3.

Table 6-3. Distribution (%) of recharge and discharge areas within the area constituting land at 10,000 AD under permafrost conditions with a permafrost thickness of a 100 m. The distributions are evaluated from the calculated mean head differences illustrated in Figures 6-22 to 6-30 (L1, L2 etc denote calculation layers in the MIKE SHE model).

Simulation period	Areas (%) of recharge/discharge L2–L1	Areas (%) of recharge/discharge L5–L4	Areas (%) of recharge/discharge L15–L14
thaw 3	94/6	2/3	62/35
active period	92/8	2/3	52/45
frozen period	88/12	2/3	53/44

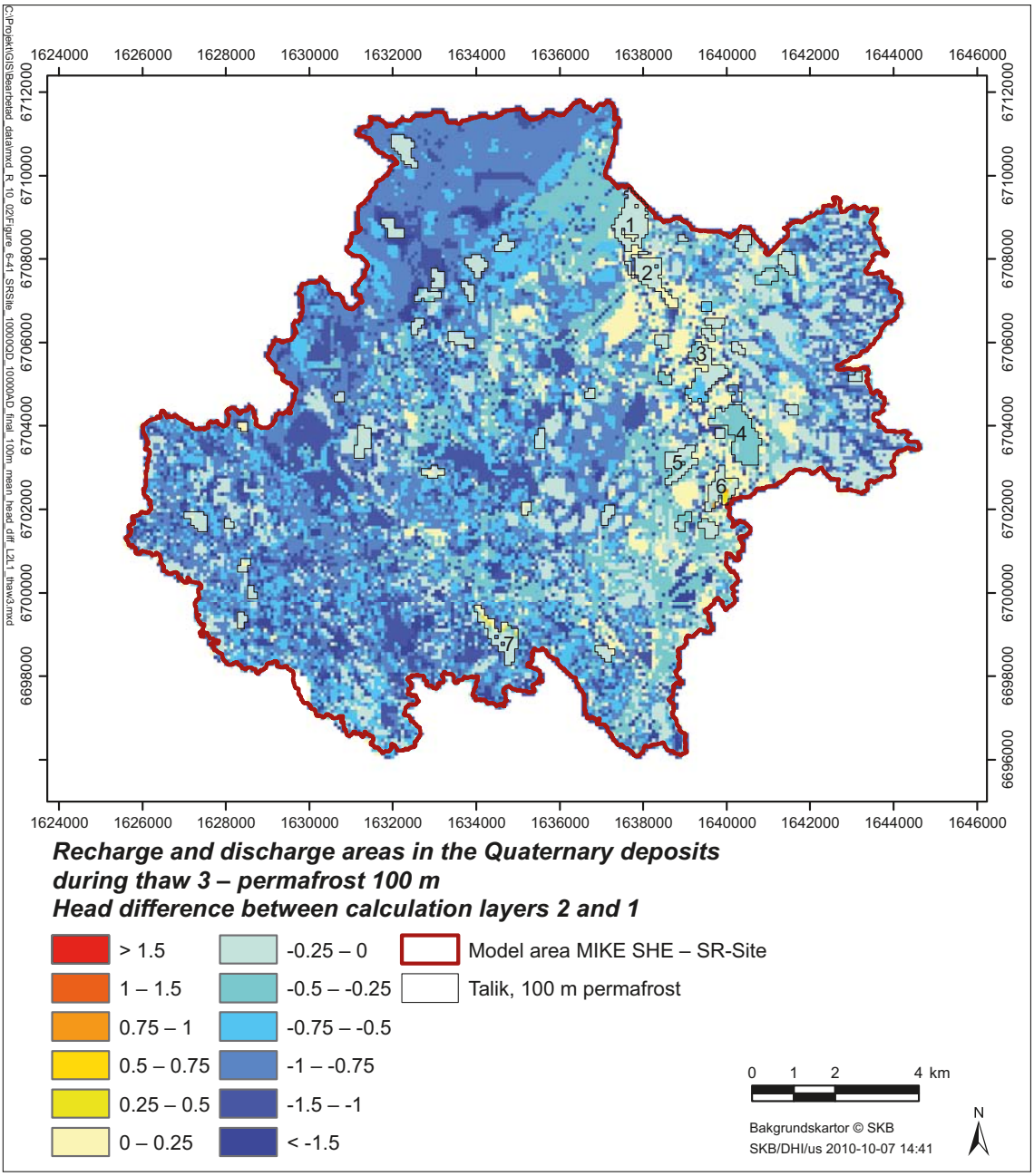

Figure 6-41. *The recharge (blue scale) and discharge (yellow to red scale) areas in the Quaternary deposits from the 10000AD_10000QD model under permafrost conditions with a permafrost thickness of a 100 m, calculated as the mean head difference between the two QD layers of the model during the last thaw period (thaw 3).*

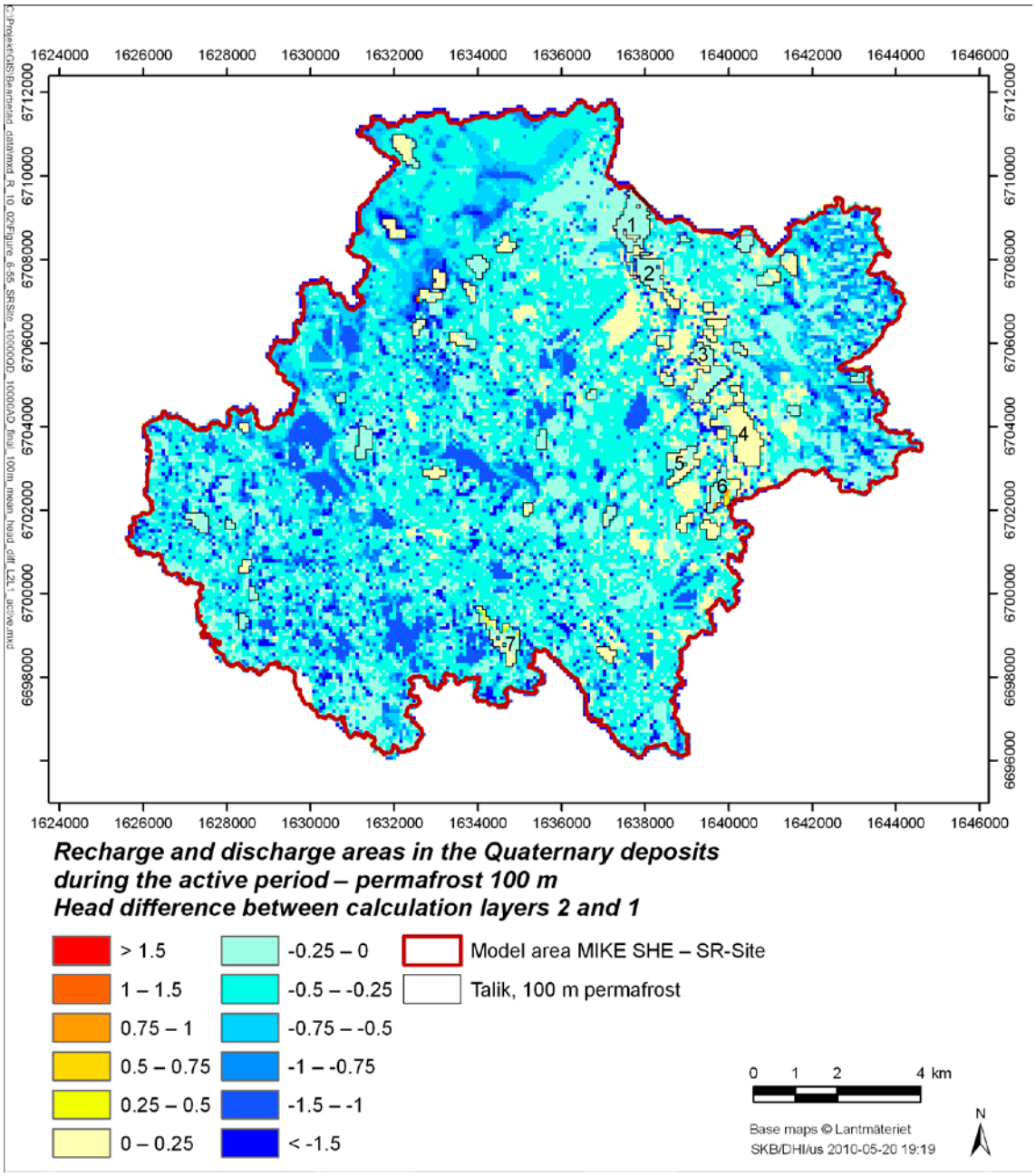

Figure 6-42. *The recharge (blue scale) and discharge (yellow to red scale) areas in the Quaternary deposits from the 10000AD_10000QD model under permafrost conditions with a permafrost thickness of a 100 m, calculated as the mean head difference between the two QD layers of the model during the active period.*

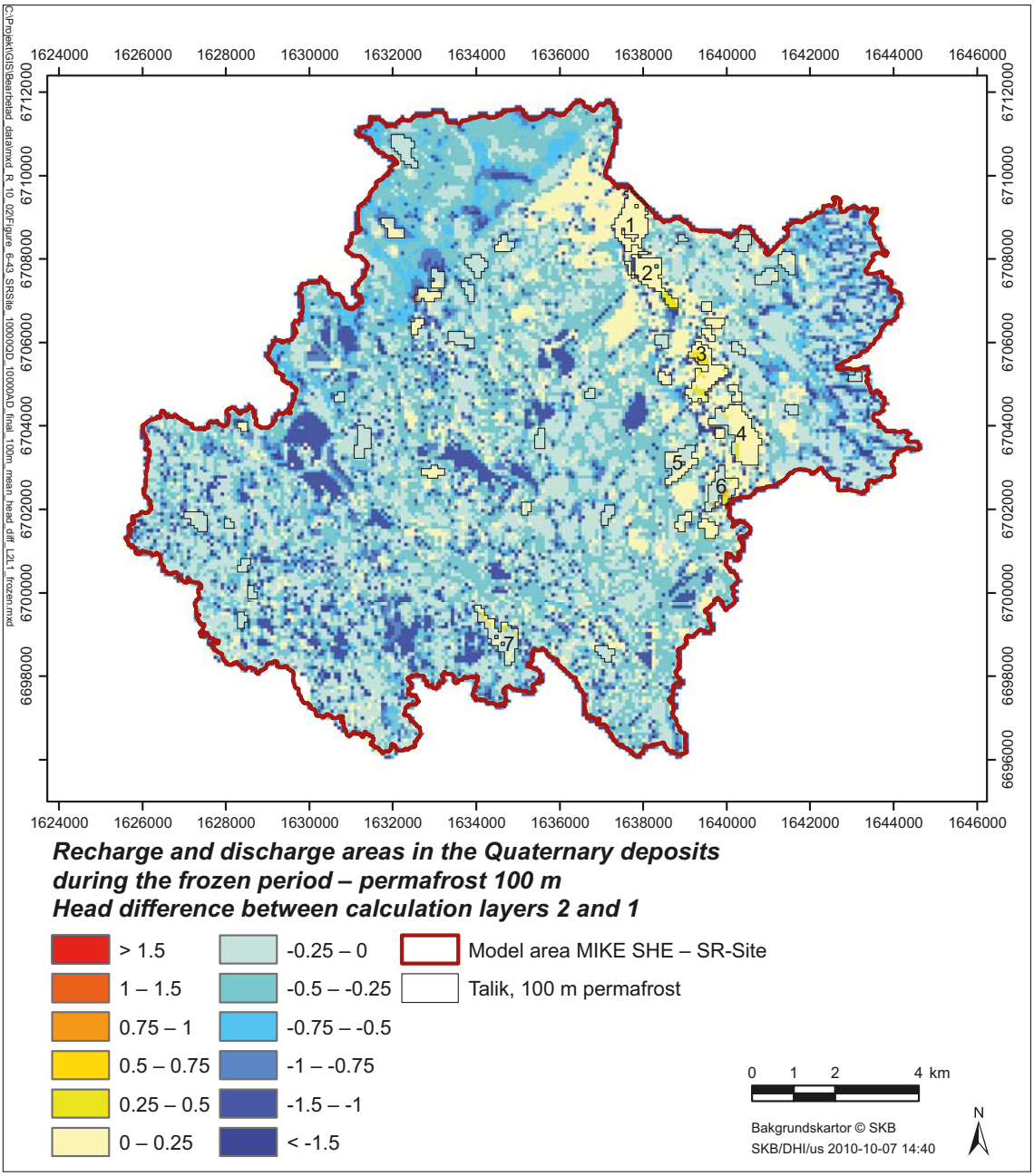

Figure 6-43. *The recharge (blue scale) and discharge (yellow to red scale) areas in the Quaternary deposits from the 10000AD_10000QD model under permafrost conditions with a permafrost thickness of a 100 m, calculated as the mean head difference between the two QD layers of the model during the frozen period.*

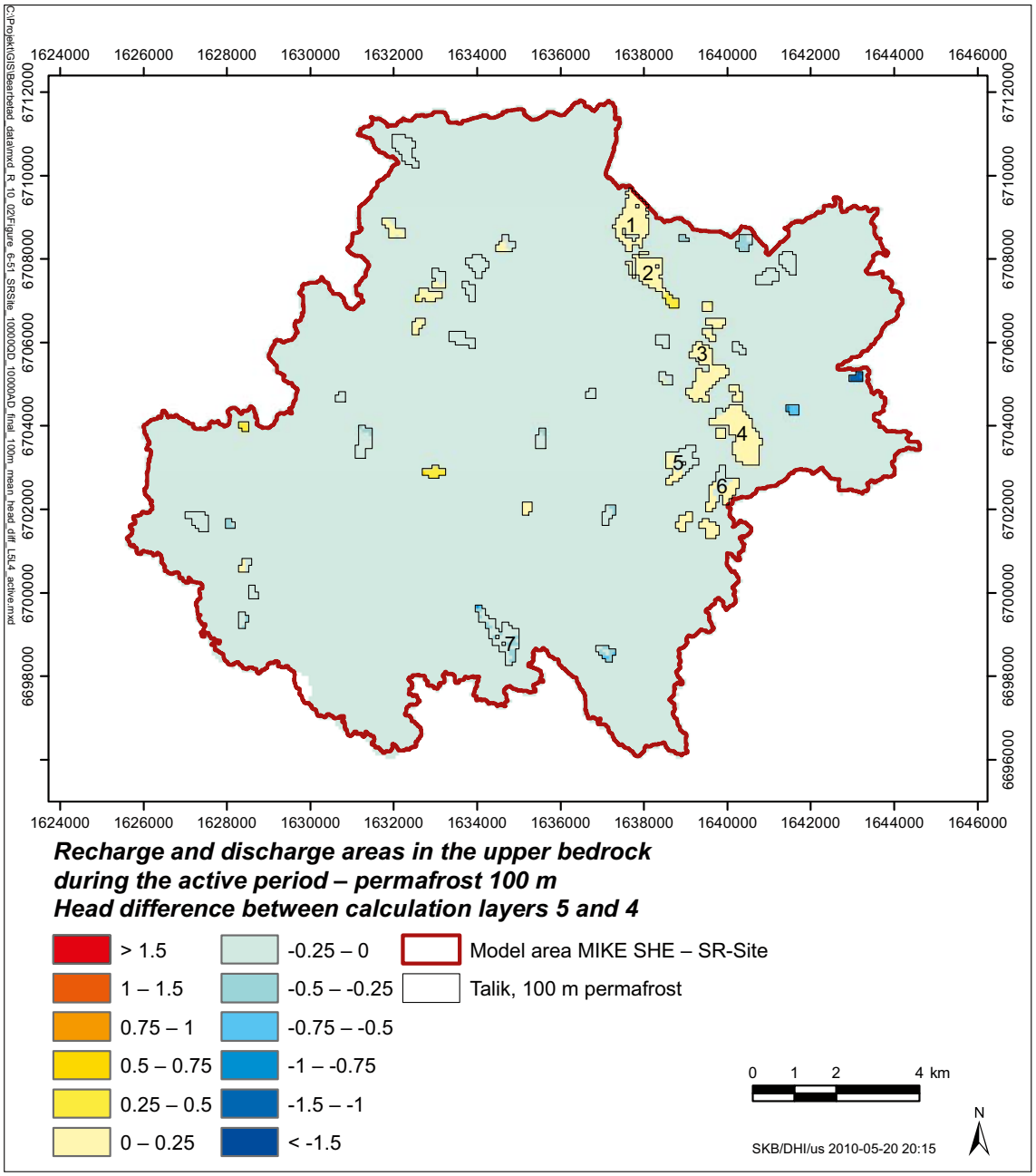

Figure 6-44. *The recharge (blue scale) and discharge (yellow to red scale) areas within the permafrost formation in the upper bedrock from the 10000AD_10000QD model under permafrost conditions with a permafrost thickness of a 100 m, calculated as the mean head difference between calculation layers 5 and 4 during the active period.*

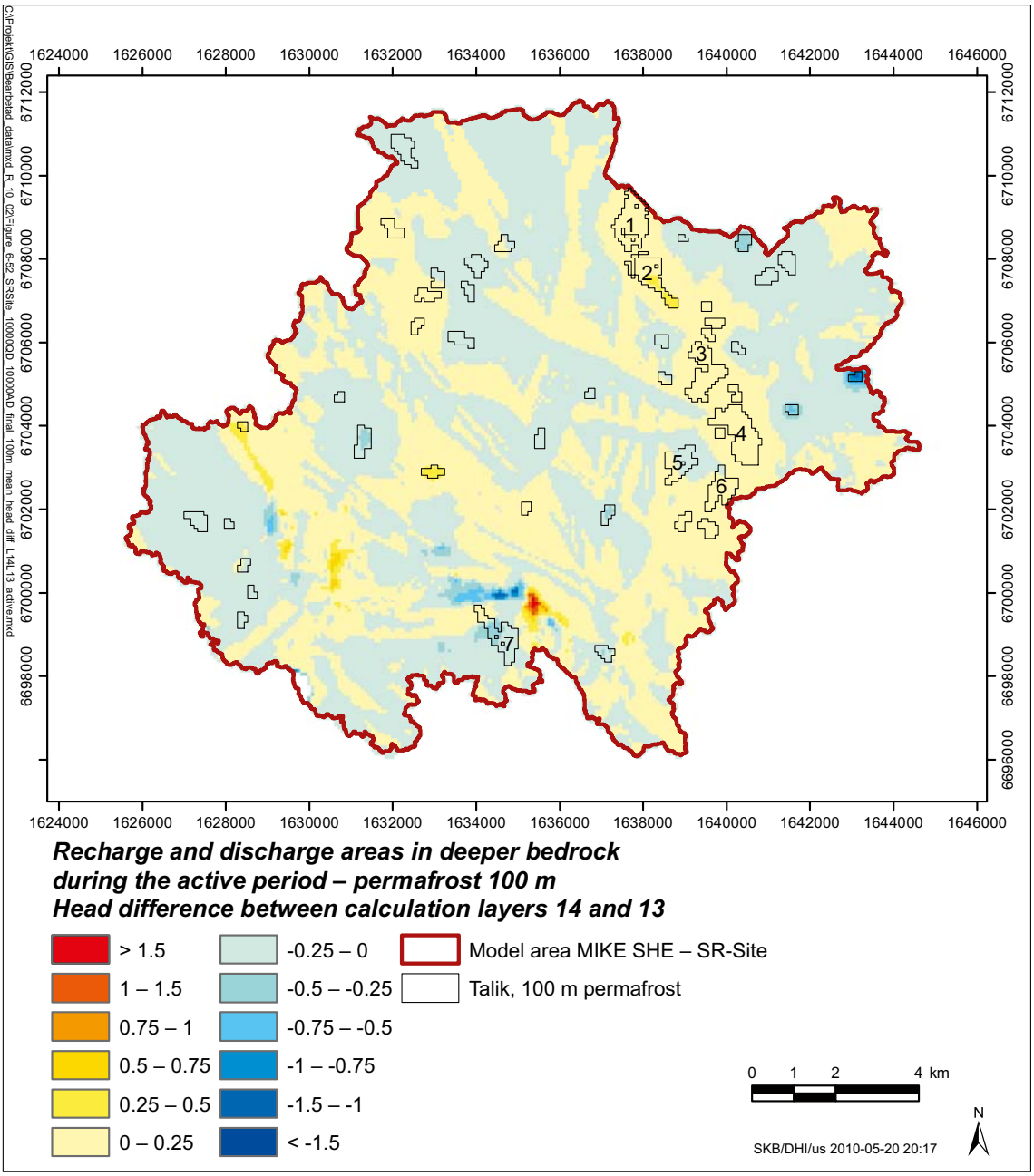

Figure 6-45. *The recharge (blue scale) and discharge (yellow to red scale) areas below the permafrost formation in the deeper bedrock from the 10000AD_10000QD model under permafrost conditions with a permafrost thickness of a 100 m, calculated as the mean head difference between calculation layers 14 and 13 during the active period.*

Vertical groundwater flow

This section presents the vertical groundwater flow calculated for each talik, see Figures 6-46 to 6-53. Since the number of taliks in the 100 m permafrost case is large (45), taliks with ID numbers from 8 to 45 have been lumped together and the mean flow for these taliks is presented in one figure. The locations of the taliks and their ID numbers are presented in Figure 6-5.

The vertical flow between the active layer and the upper permafrost layer during the active period is shown in Figure 6-54. There are changes in the direction of the vertical flow within each talik; a talik can have both an upward and a downward flow gradient depending on which cell column within each talik that is studied. This is further discussed in Section 6.3, which describes the results of the particle tracking simulations for periglacial conditions. The vertical flow between the active layer and the upper permafrost layer and the flow between the two upper permafrost layers for each talik and each period are illustrated in Appendix 3.

Just as in the 240 m permafrost case the general water movement in the model is from talik 7 towards the sea, i.e. taliks 1 and 2 which are discharge taliks. The surface water level of the sea is also transient during this simulation and the sea water level has an influence on the flow direction of the upper part of talik 1 but not on talik 2 as in the 240 m case.

Talik 3 has switched from a recharge talik in the 240 m permafrost case to a discharge talik in the 100 m permafrost case. The general flow direction is upwards with exception of the upper part where the flow direction turns downwards with the intense snow melt during thaw 3 and the active period. Talik 4 is a discharge talik with the same flow pattern as found in the 240 m permafrost case.

Talik 5 is a recharge talik in both cases, but with slightly different seasonal variations in the upper part of the talik. Talik 6 is also a discharge talik in both cases with the same flow pattern as talik 4. Talik 7 is located upstream and is in both cases the apparent recharge talik with a strong downward flow without the influence of seasonal variations in the upper part of the talik.

The mean flow in taliks 8 to 45 is downwards with exception of the upward flow occurring in the upper part during the active period. However, it should be emphasised that there are both recharge and discharge taliks represented, which is further illustrated in Figure 6-66 and Section 6.3 describing the results of the particle tracking simulations for periglacial conditions.

When comparing the flow conditions in the different layers of the saturated zone, it is apparent that there is less resistance for the water to flow through the taliks when the permafrost has a thickness of 100 m instead of 240 m. This is explained by shallower and more frequently occurring through taliks. However, although the vertical flow in the taliks increases with a thinner permafrost layer, the vertical flow is still very small and the amount of water from the surface that reaches the deeper parts below the permafrost layer is close to zero. Thus, with a greater permafrost thickness than 240 m it can be expected that the flow becomes even more limited, and with a thinner permafrost layer the flow will increase.

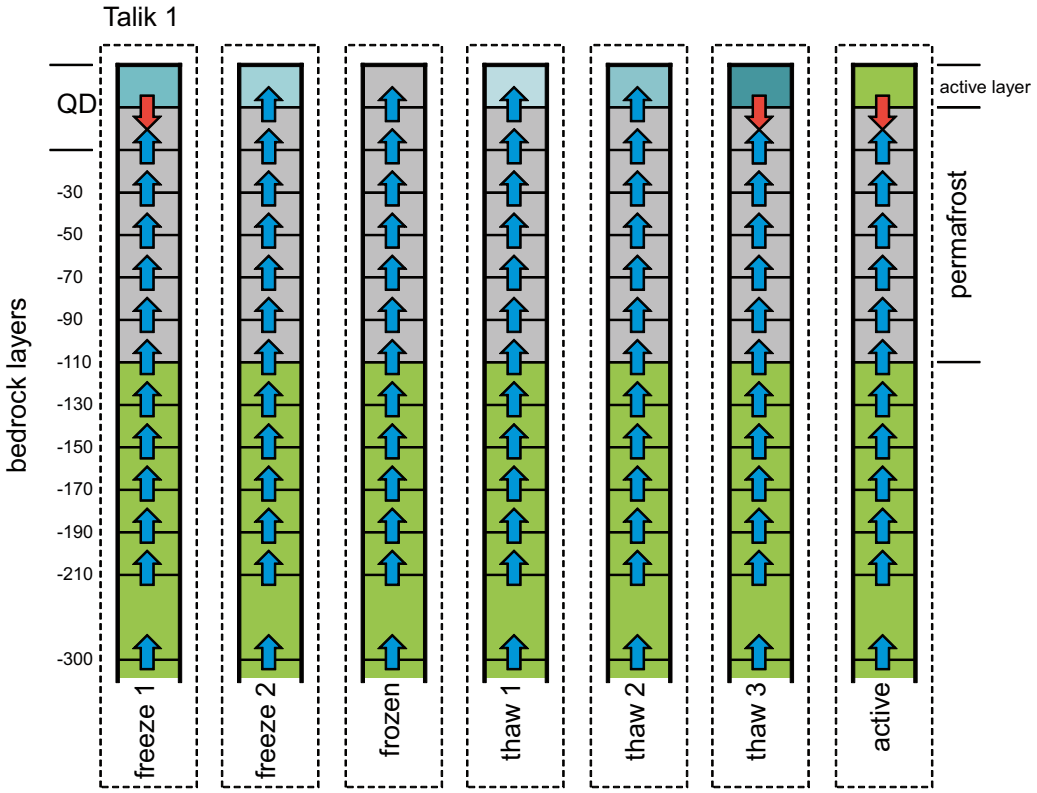

Figure 6-46. *Calculated mean vertical flow direction in talik 1 during the simulated periods with the 10000AD_10000QD model under permafrost conditions with a permafrost thickness of 100 m.*

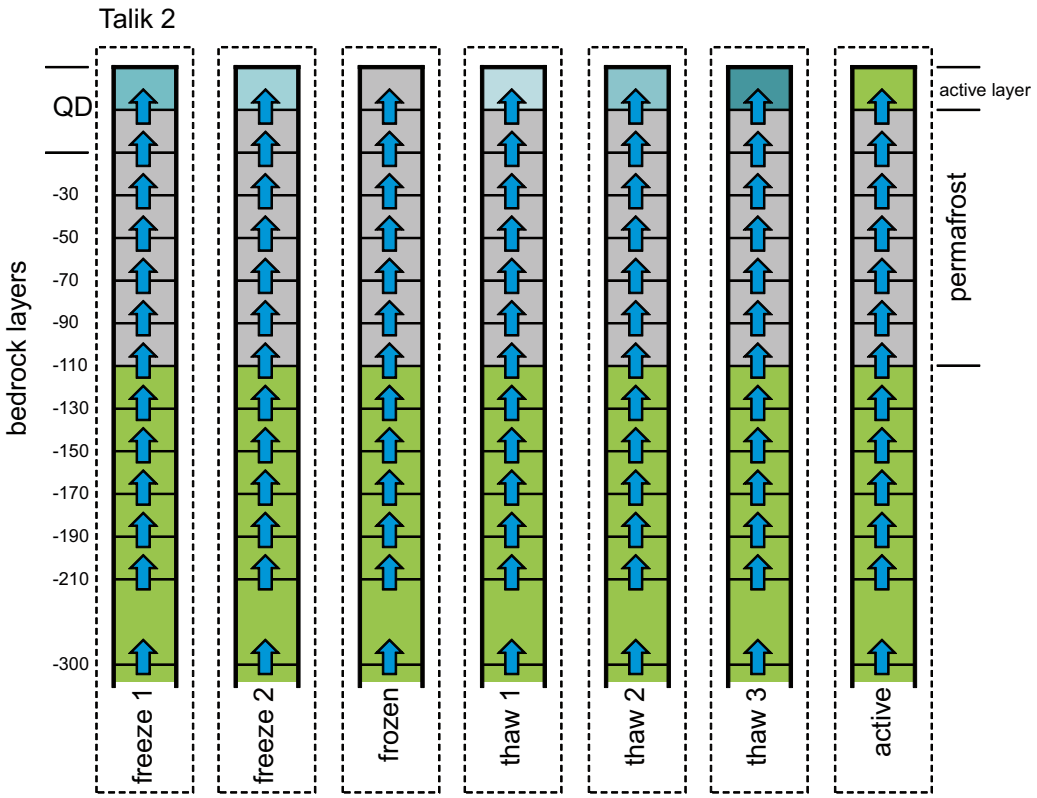

Figure 6-47. *Calculated mean vertical flow direction in talik 2 during the simulated periods with the 10000AD_10000QD model under permafrost conditions with a permafrost thickness of 100 m.*

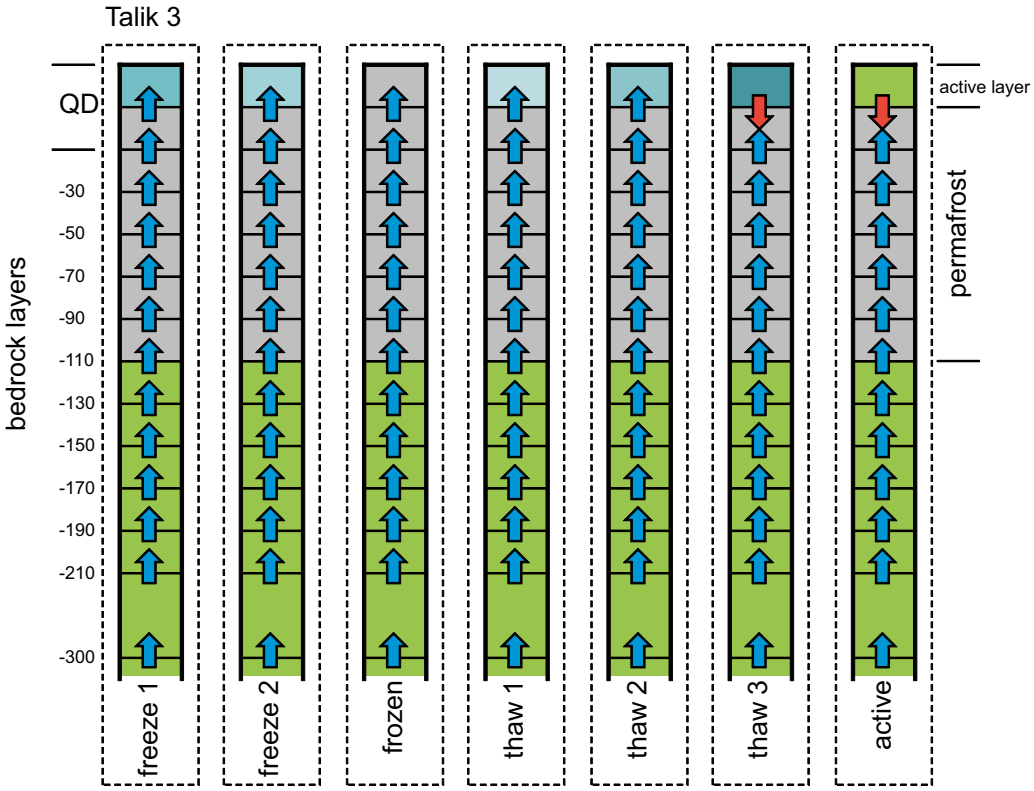

Figure 6-48. *Calculated mean vertical flow direction in talik 3 during the simulated periods with the 10000AD_10000QD model under permafrost conditions with a permafrost thickness of 100 m.*

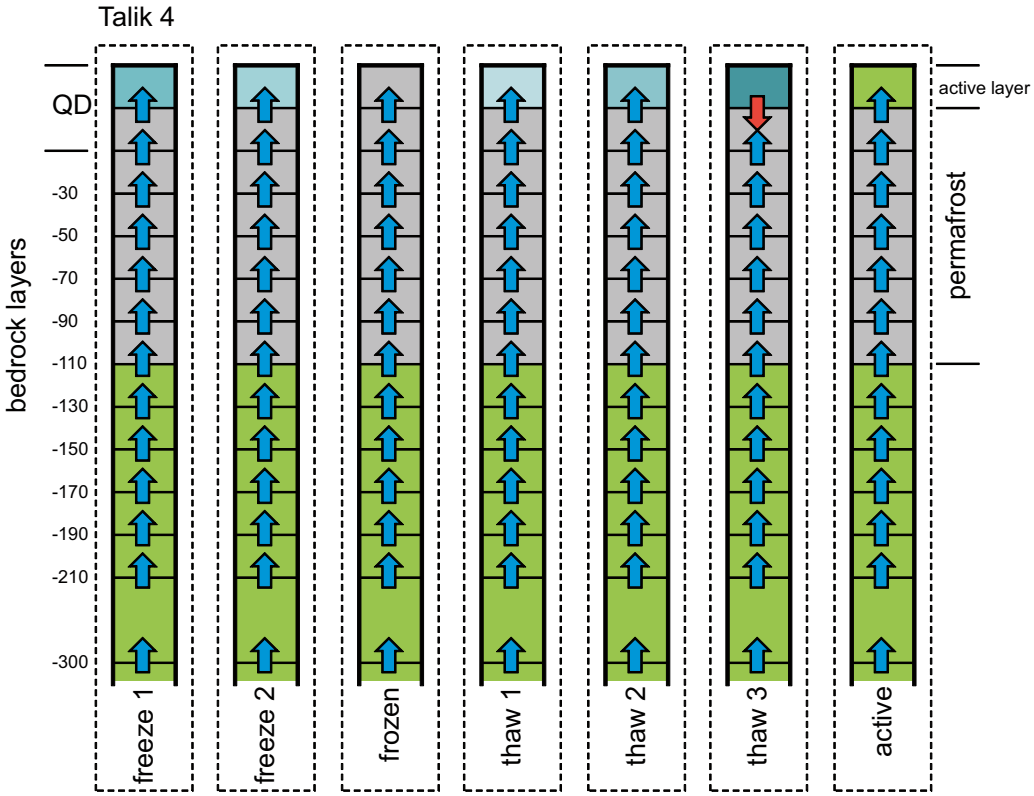

Figure 6-49. *Calculated mean vertical flow direction in talik 4 during the simulated periods with the 10000AD_10000QD model under permafrost conditions with a permafrost thickness of 100 m.*

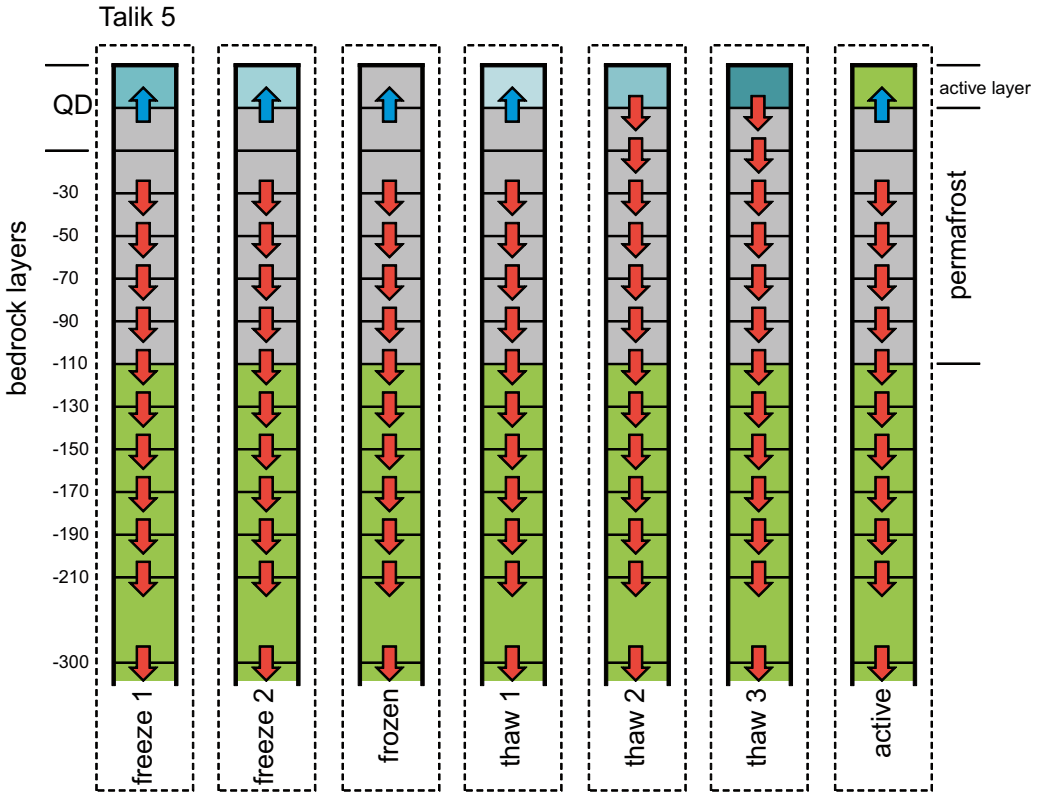

Figure 6-50. *Calculated mean vertical flow direction in talik 5 during the simulated periods with the 10000AD_10000QD model under permafrost conditions with a permafrost thickness of 100 m.*

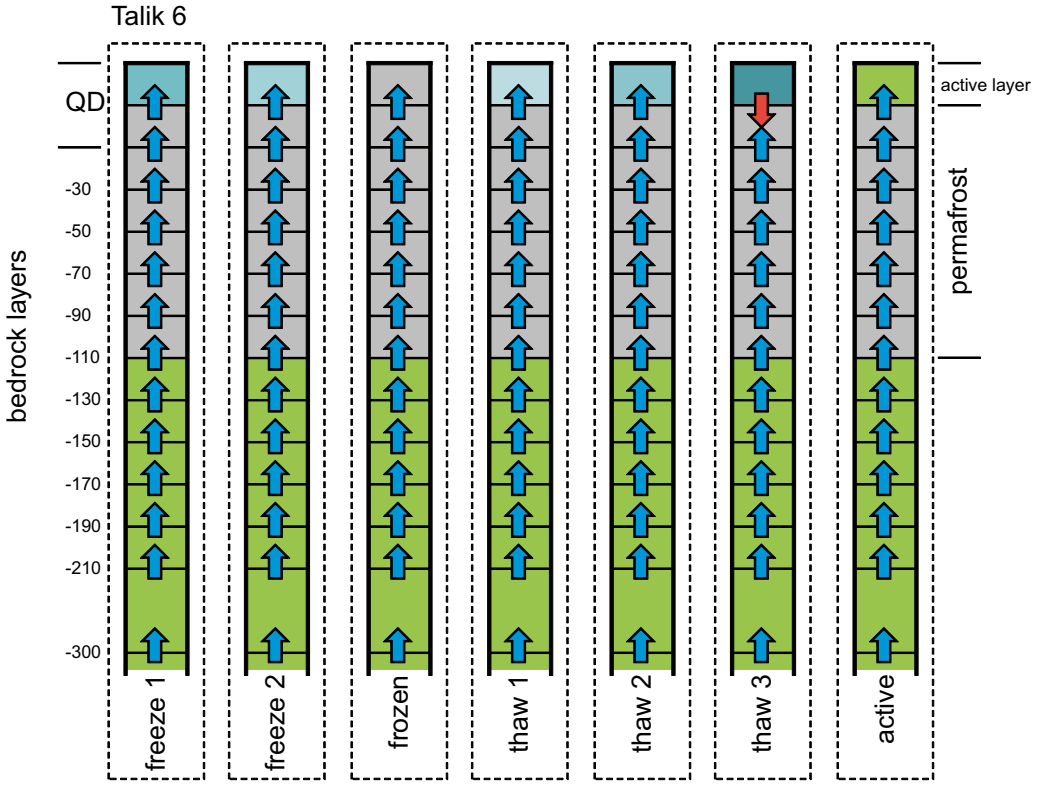

Figure 6-51. *Calculated mean vertical flow direction in talik 6 during the simulated periods with the 10000AD_10000QD model under permafrost conditions with a permafrost thickness of 100 m.*

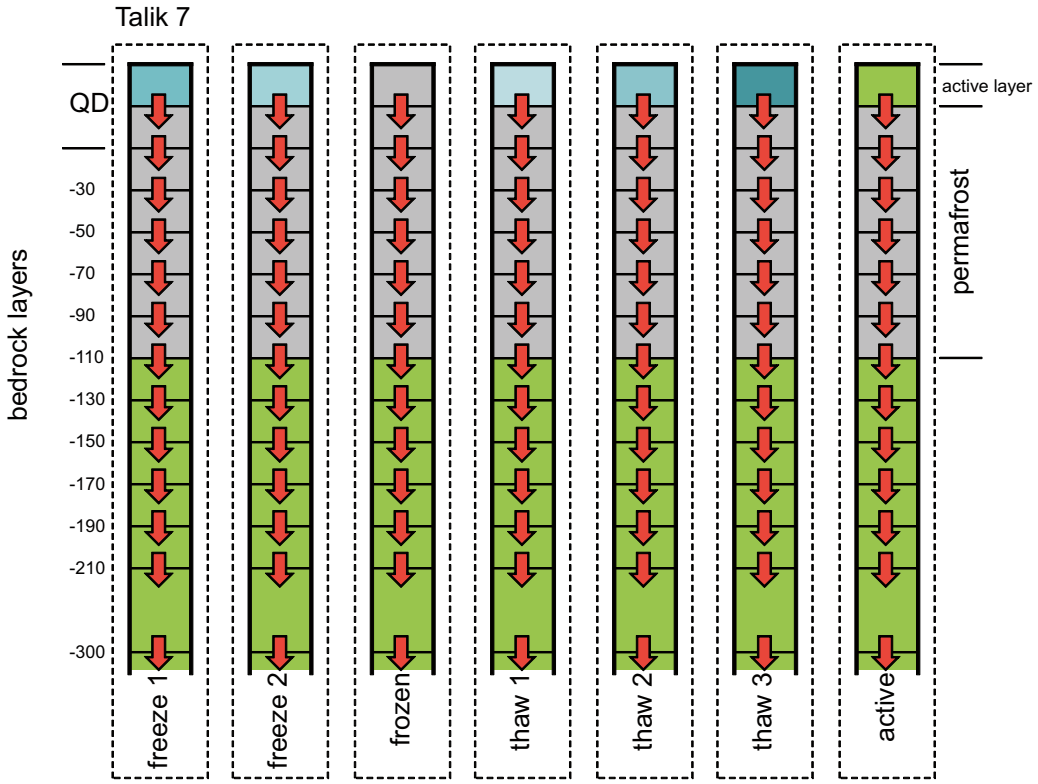

Figure 6-52. *Calculated mean vertical flow direction in talik 7 during the simulated periods with the 10000AD_10000QD model under permafrost conditions with a permafrost thickness of 100 m.*

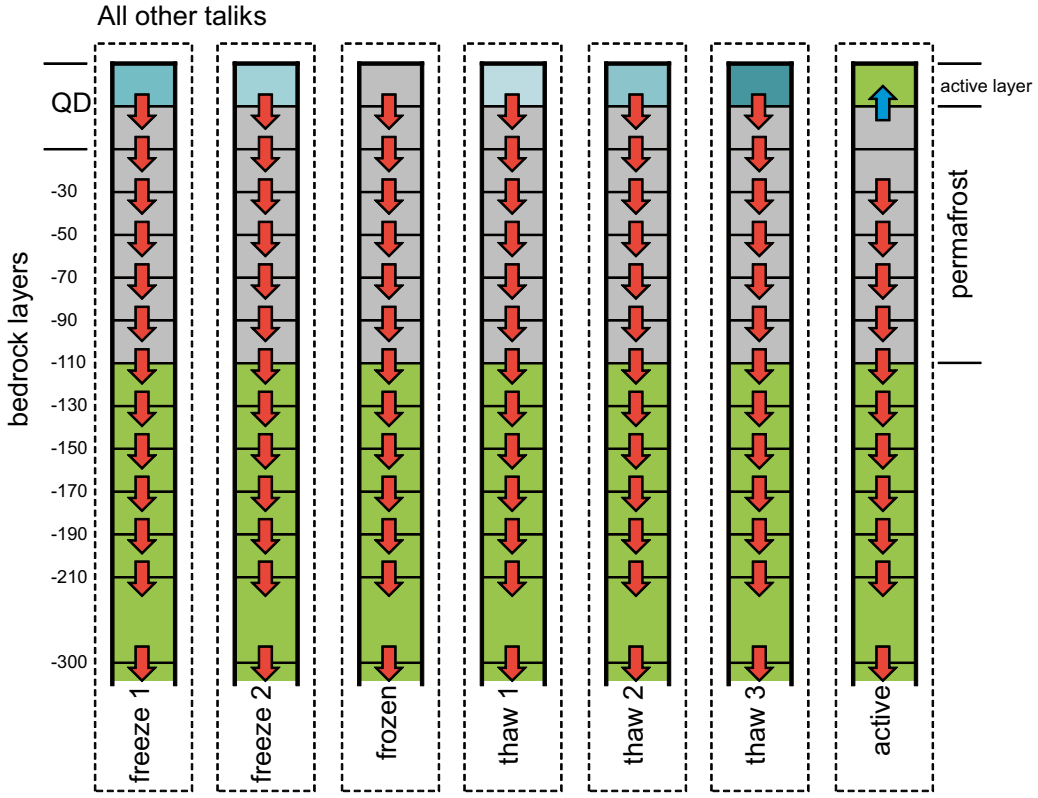

Figure 6-53. *Calculated mean vertical flow direction in taliks 8–45 during the simulated periods with the 10000AD_10000QD model under permafrost conditions with a permafrost thickness of 100 m.*

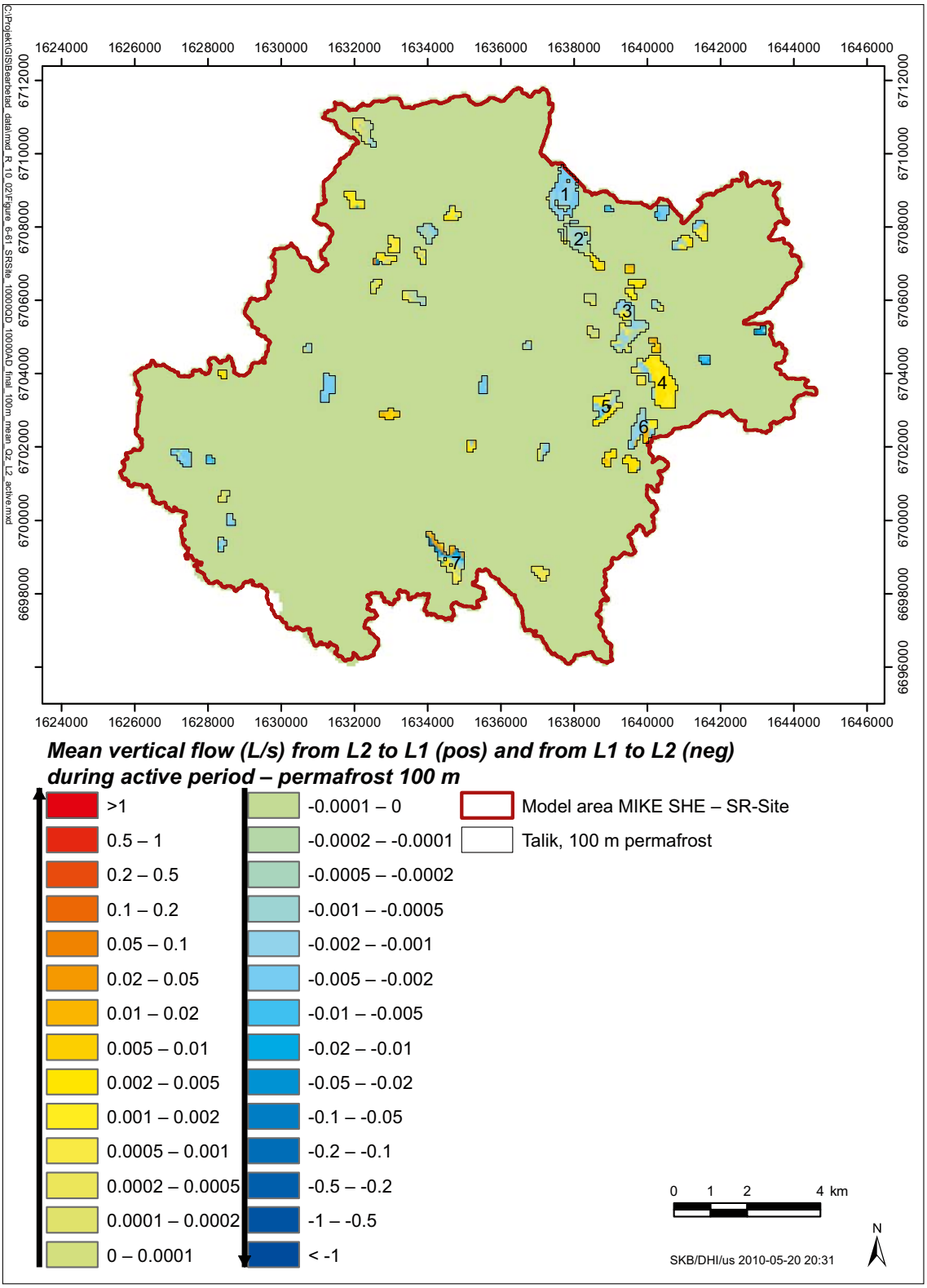

Figure 6-54. *Calculated mean vertical flow (units in l/s) between the active layer and the top permafrost layer during the active period with a permafrost thickness of 100 m.*

6.3 Solute transport under permafrost conditions

Since the MIKE SHE model code does not yet allow time varying spatial input data, the flow model simulating the permafrost conditions had to be performed by a step-by-step solution in which each year was divided into different periods identified as either freeze, frozen, thaw or active. The flow model was then run separately for each period with a "hotstart" from the previous period. As a consequence, the particle tracking (PT) simulations cannot be made for the entire yearly flow cycle. Instead, PT simulations were performed separately for the frozen and the active periods of the water movement simulations reported in Section 6.2. In this way, the PT simulations may be considered to represent the most and the least active periods with regard to the hydrological processes.

Based on the water flow field from the simulations with 100 m and 240 m deep permafrost, eight PT simulations were performed. In each case one particle per cell was introduced either in the bottom of the active layer or in the middle of the layer below the permafrost. All PT simulations were run for 5000 years, i.e. the frozen period or the active period was cycled for 5000 years and each year contains several active or frozen periods. Table 6-4 lists the different simulation cases. So-called registration zones were placed in the sediments under each lake defined as a talik. The registration zones make it possible to trace the birth locations of the particles moving into each registration zone.

6.3.1 Model with 240 m permafrost

Table 6-5 lists the different sinks to which the particles went in the different simulations. Also the numbers of particles left in the model after 5000 years of simulation time are listed for each case; all numbers are given in %. In the case *240mPf_frozen_belowpf,* 44.5% of the particles are still left in the model volume at the end of the simulation, which can be compared to 89% for the particles released during the active period (case *240mPf_active_belowpf).* Figures 6-55 and 6-56 show the locations and elevations of the particles left in the model at the end of the simulation from the cases *240mPf_active_belowpf* and *240mPf_frozen_belowpf*. The red and orange colours indicate a downward transport of particles. The elevations of these particles are lower than the level where they were released.

In Figure 6-55, illustrating the results from the frozen period, almost no particles are left in the sea bottom sediments in taliks 1 and 2. Only particles along the shoreline are still left in the model, whereas the rest have discharged to the sea. During the frozen period 44.7% of the particles leave the model volume via the sea, and this is the dominating sink for the frozen period. For the active period, almost all the particles leaving the model volume go to the unsaturated zone or the overland compartment of the model, see Table 6-5. Figure 6-56 shows the results from the active period; a lot of particles can be seen under the sea-taliks, i.e. taliks number 1 and 2.

During the active period no particles discharge to the sea. Due to the variation of the sea level during the active period, a downward gradient is built up in the uppermost layers of the sea-talik. The particles are stuck in the sediments during this period, whereas the gradient during the frozen period allows the particles to discharge to the sea. Approximately 53% of the particles that are left in the model for the active period are stuck in the sea bottom sediments. This means that 58% of the introduced particles for the active period have either left the model or are stuck in the sediments, while 42% are left in other parts of the model.

Consequently, when introducing the particles below the permafrost layer, the effect of having an active or frozen upper layer is small except for in the sea-taliks, which are dependent on the sea water level. The particles that are still left in the deeper parts of the model are still moving, and a longer simulation time would probably lead to more particles leaving the model through the taliks.

In the case *240mPf_frozen_activelayer* almost all particles are left in the model volume. The low hydraulic conductivity values in the active layer do not allow any longer transport distances during the simulation period. The majority of the particles are left at their starting positions. Approximately 15% of the particles have left the model volume. The dominating sink is the combined unsaturated zone/overland sink. The particles removed from the model volume are particles with a birth location close to a cell defined as a talik. For the active period almost all the particles leave the model volume after being introduced in the active layer. Only 13.8% are left in the model volume at the end of the simulation. The dominating sink is the combined unsaturated zone/overland sink.

Table 6-4. The different PT simulation cases for the permafrost simulations.

Permafrost depth, m	Water movement simulation period	Particle source	PT simulation name
100	active	1 particle/cell in the layer below permafrost	100mPf_active_belowpf
100	frozen	1 particle/cell in the layer below permafrost	100mPf_frozen_belowpf
100	active	1 particle/cell in the bottom of the active layer	100mPf_active_activelayer
100	frozen	1 particle/cell in the bottom of the active layer	100mPf_frozen_activelayer
240	active	1 particle/cell in the layer below permafrost	240mPf_active_belowpf
240	frozen	1 particle/cell in the layer below permafrost	240mPf_frozen_belowpf
240	active	1 particle/cell in the bottom of the active layer	240mPf_active_activelayer
240	frozen	1 particle/cell in the bottom of the active layer	240mPf_frozen_activelayer

Table 6-5. Particle balance data. Particles introduced in each case and the sinks for the particles that left the model are listed in the table, all number are given in %. The number of particles released is 27,828 for the cases with particle release in the active layer and 28,038 for the cases with particle release below the permafrost.

	Active period, particles released in active layer (%)	Frozen period, particles released in active layer (%)
Particles removed by sink:		
Particles gone with baseflow to streams	3.1	0.0
Particles gone with drain to streams	3.4	0.2
Particles gone with drain to boundary	0.1	0.0
Particles gone to UZ/OL	79.6	14.2
Particles gone to the sea	0.0	0.0
Total fraction of particles removed	86.2	14.4
Fraction of particles left in the model	13.8	85.6
Sum	100.0	100.0
	Active period, particles released in layer below permafrost (%)	**Frozen period, particles released in layer below permafrost (%)**
Particles removed by sink:		
Particles gone with baseflow to streams	0.9	2.1
Particles gone with drain to streams	0.0	0.0
Particles gone with drain to boundary	0.0	0.0
Particles gone to UZ/OL	9.8	8.7
Particles gone to the sea	0.0	44.7
Total fraction of particles removed	10.7	55.5
Fraction of particles left in the model	89.3	44.5
Sum	100.0	100.0

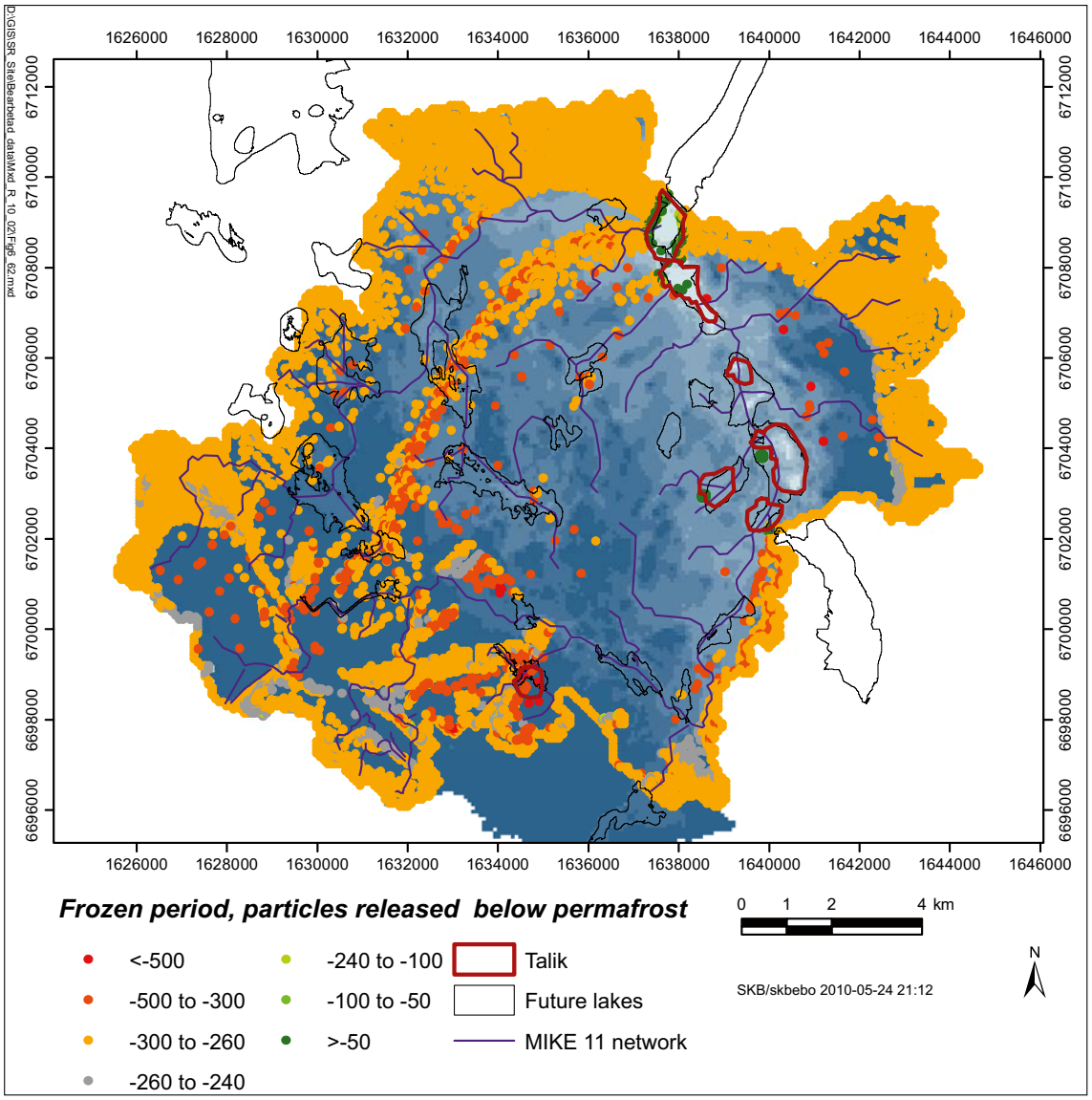

Figure 6-55. *Elevations and horizontal positions of the particles left in the model volume after 5000 years, results from the simulation 240mPf_frozen_belowpf.*

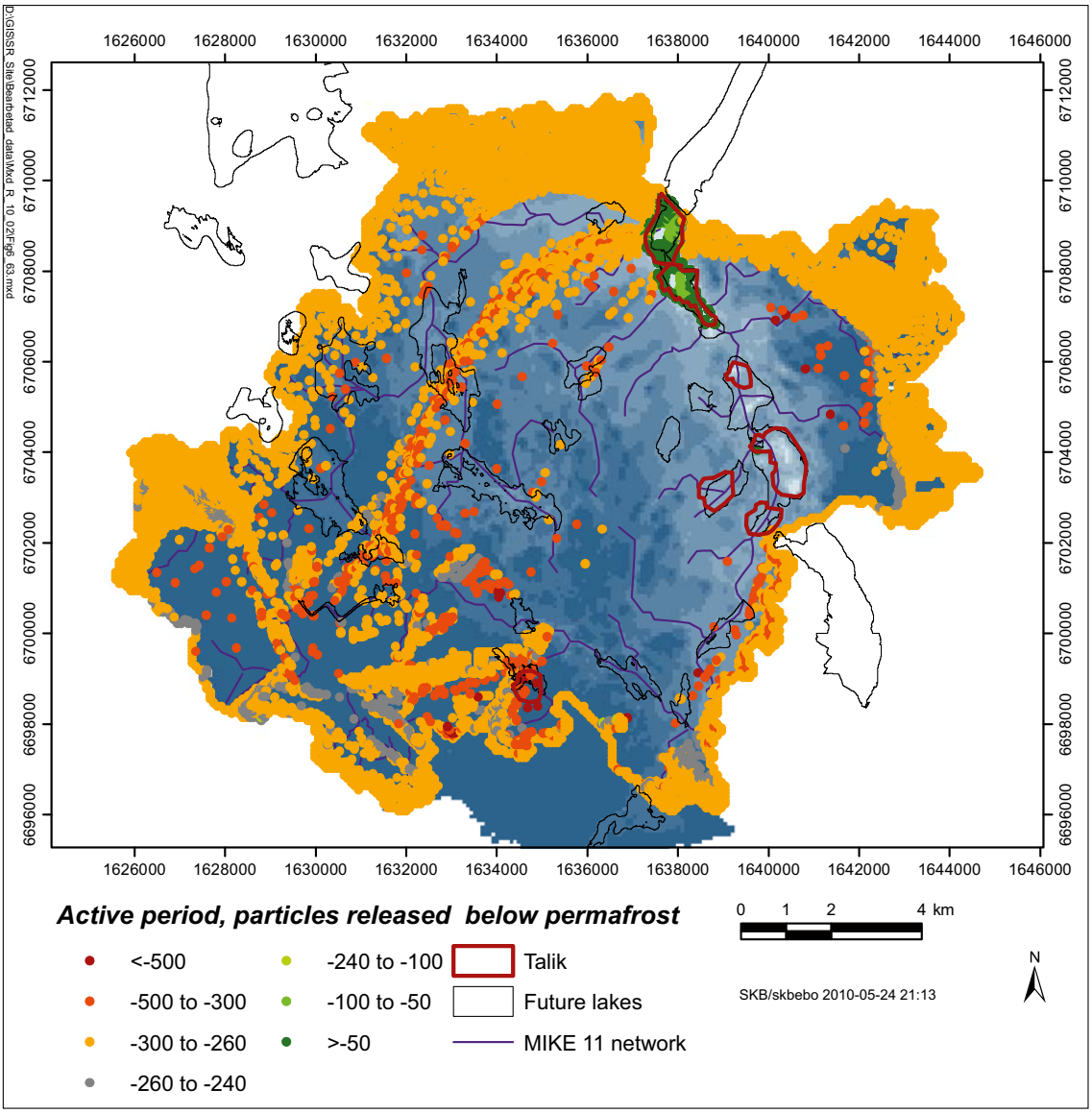

Figure 6-56. *Elevations and horizontal positions of the particles left in the model volume after 5000 years. Results from the simulation 240mPf_active_belowpf are shown; many particles are stuck in the sediments in the sea-taliks (taliks 1 and 2).*

When releasing particles in the calculation layer below the permafrost, the exit points at the ground surface are concentrated to the taliks, especially to the sea-taliks (number 1 and 2). During the active period the particles are stuck in the sediments below the sea due to the time-varying sea level. However, during the frozen period the gradient is directed upward within the sea-talik and the particles discharge to the sea. Some exit points are also found in the surface stream system close to the sea and a few exit points are found in taliks 4 and 6. The pattern of the exit points in the surface stream system in taliks 4 and 6 are the same during the frozen and active periods. The main difference between the two periods is the exit points in the sea appearing during the frozen period. The exit points for the case *240mPf_frozen_activelayer* are shown in Figure 6-57. The particles discharging at sea are concentrated to near-shore areas. No exit points are found in the middle of the sea-taliks.

The birth locations of the particles registered in the sediments below each talik are shown in Figure 6-58. Results are shown from the case *240mPf_active_belowpf*; however, the pattern is the same for the case *240mPf_frozen_belowpf*. It is seen that almost 50% of the model area is within the "flow field" contributing to any of the taliks in the model area. The taliks extract water from a large area. The particles move below the permafrost towards the taliks until they reach the talik area with higher conductivities and an upward transport takes place.

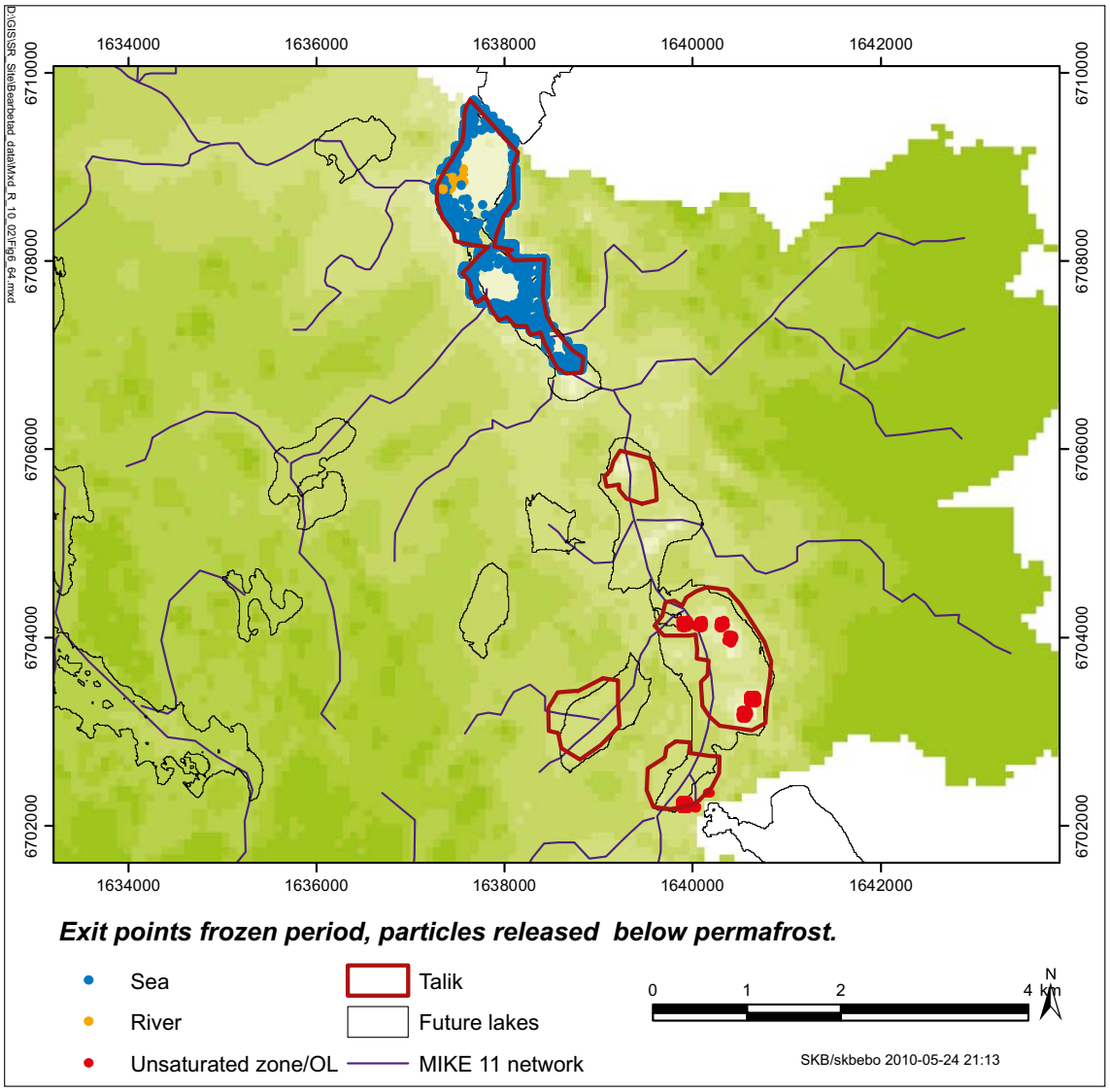

Figure 6-57. *Exit points at ground surface from the case 240mPf_frozen_belowpf. The different colours of the exit points indicate to which sinks the particles have gone; the dominating sink is the sea (blue points).*

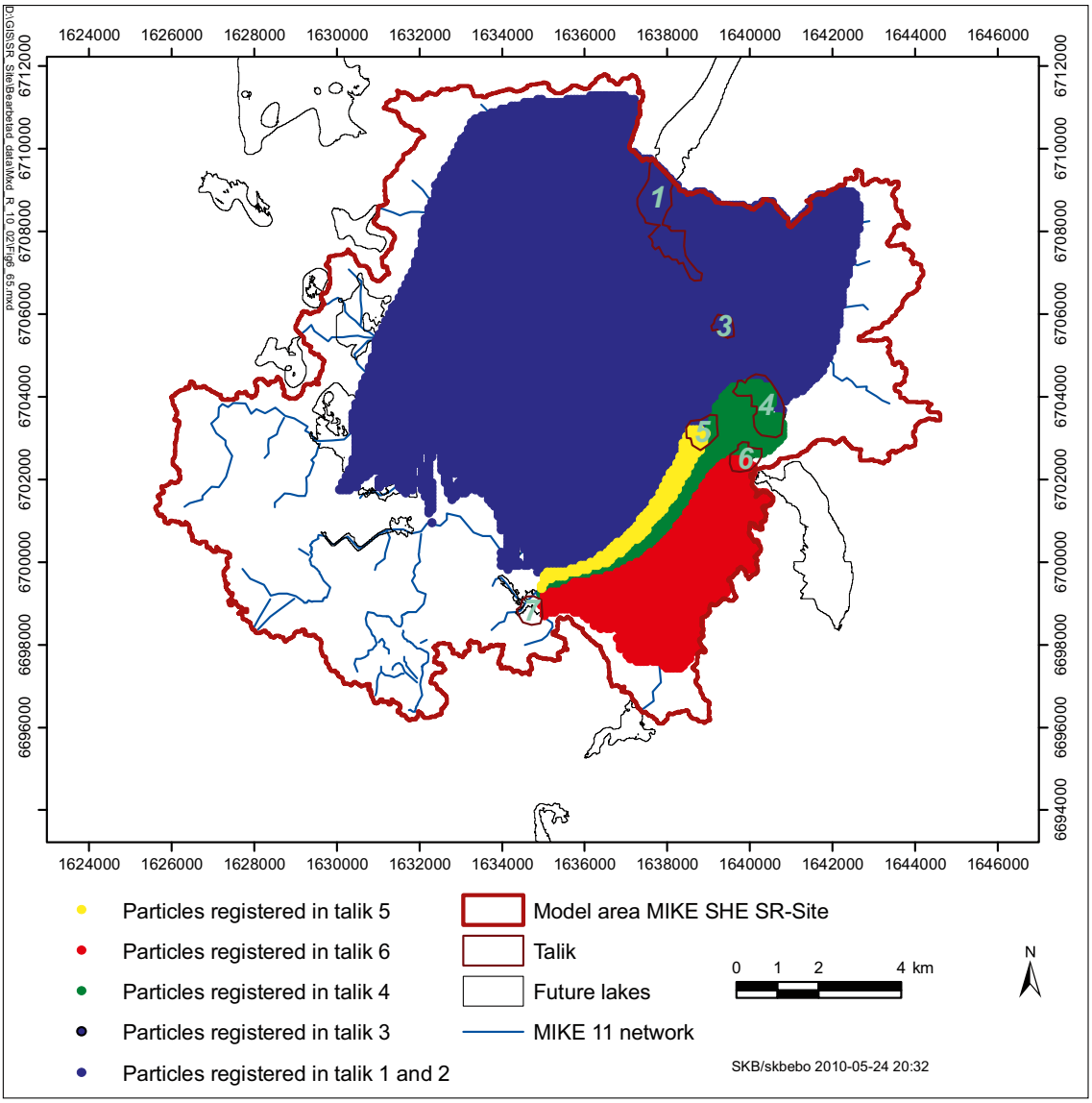

Figure 6-58. *Birth locations of particles registered in the sediments below different taliks.*

In Figure 6-58 it is seen that no particles travel towards talik number 3; this talik acts as a recharge area. This phenomenon is also illustrated in Figure 6-59, showing the particle flow paths in a 3D illustration. The particles are released below the permafrost and then move towards the taliks, which act as discharge areas. The colours of the flow paths indicate a slow transport below the permafrost and towards the taliks. Once the particles have reached the taliks, there is a fast upward transport until the particles reach the sediments of the lakes or the sea. The transport velocity is reduced when the particles enter the QD layers in the taliks.

When introducing particles in the active layer it is possible to identify transports between different taliks, i.e. to analyse if there is a downward transport of a particle through the permafrost layer in one talik and an upward transport of the same particle in a downstream talik. Figure 6-60 illustrates the flow paths between the different taliks within the model area. Talik number 7 acts as a recharge area, as well as parts of talik number 3, 5 and 6. Particles released in talik number 7 are transported downwards through the permafrost layer and flow below the permafrost towards talik 6 where the particles discharge. Parts of talik number 6 also act as a recharge area; a transport of particles from talik number 6 to talik number 4 can be seen in the figure. Both talik 3 and talik 5 are recharge areas contributing to the discharge in the sea-taliks (taliks 1 and 2). Figure 6-61 shows the same results as in 6-60, but in a horizontal view from above.

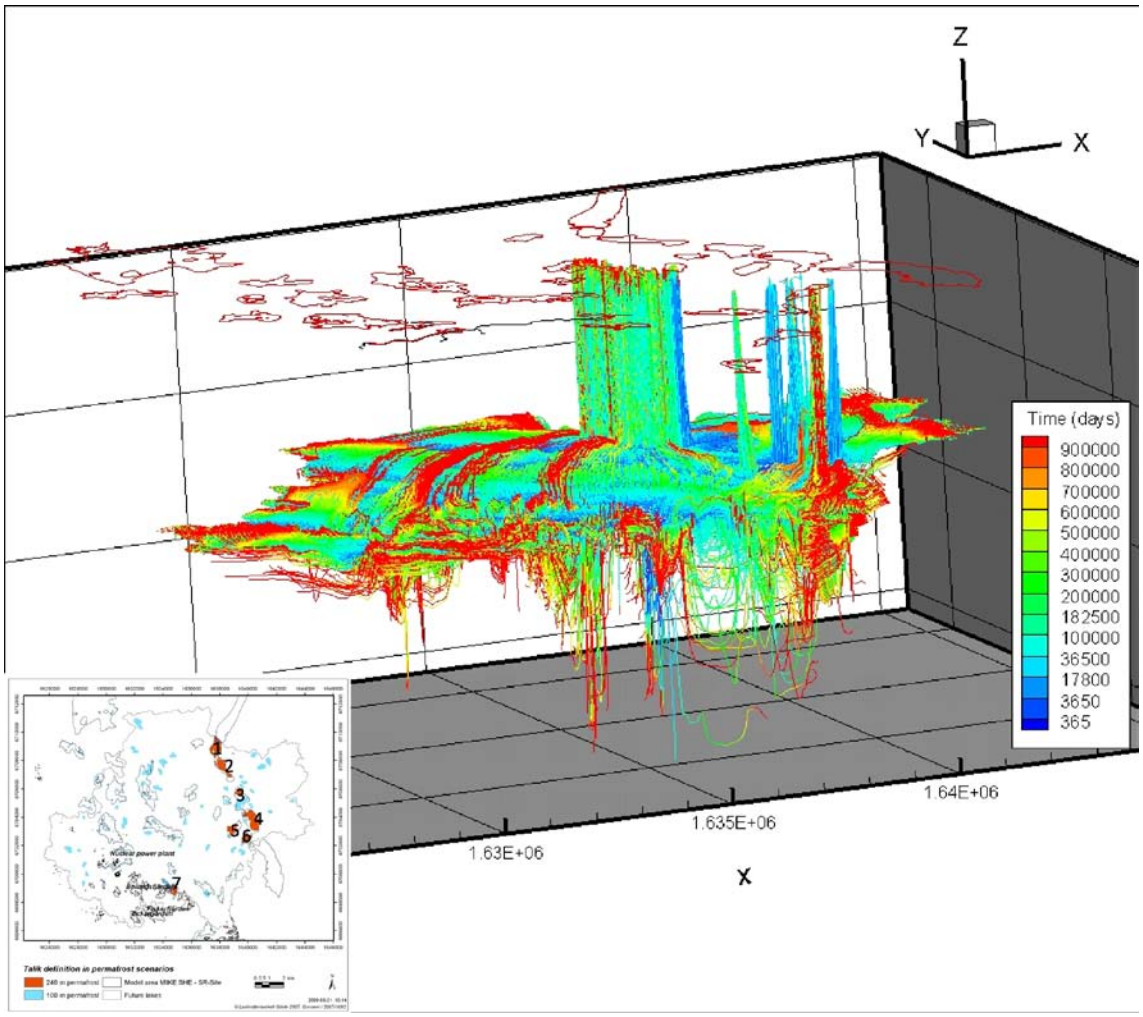

Figure 6-59. *Three-dimensional illustration of flow paths of particles released below the permafrost during the active period. The colour along each flow path shows the accumulated particle travel time in days. A map of the locations of the taliks is shown in Figure 6-5.*

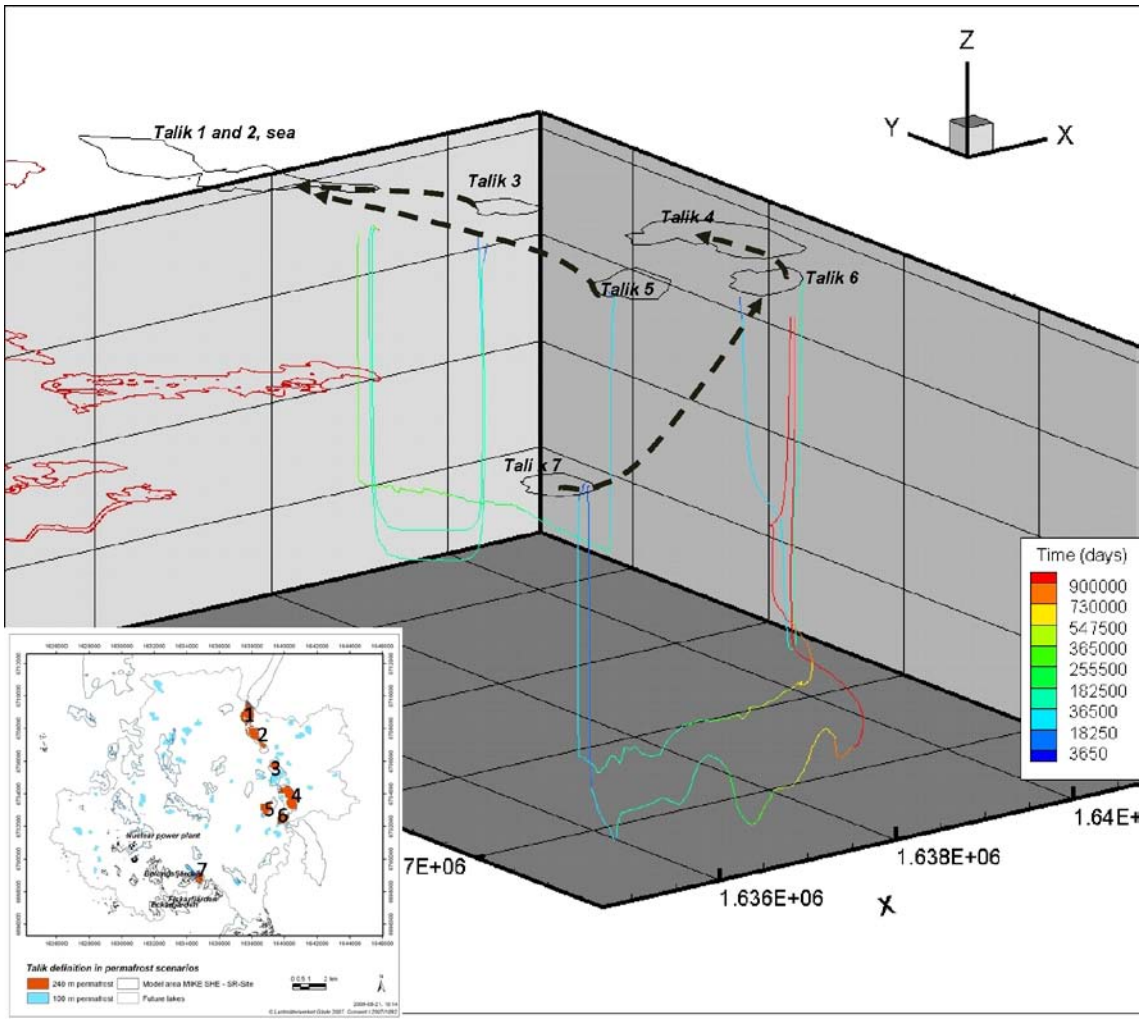

Figure 6-60. *Three-dimensional illustration of particle flow paths released in the active layer during the active period. Only the particles transported between different taliks are illustrated. The colour along each flow path shows the accumulated particle travel time in days. A map of the locations of the taliks is shown in Figure 6-5.*

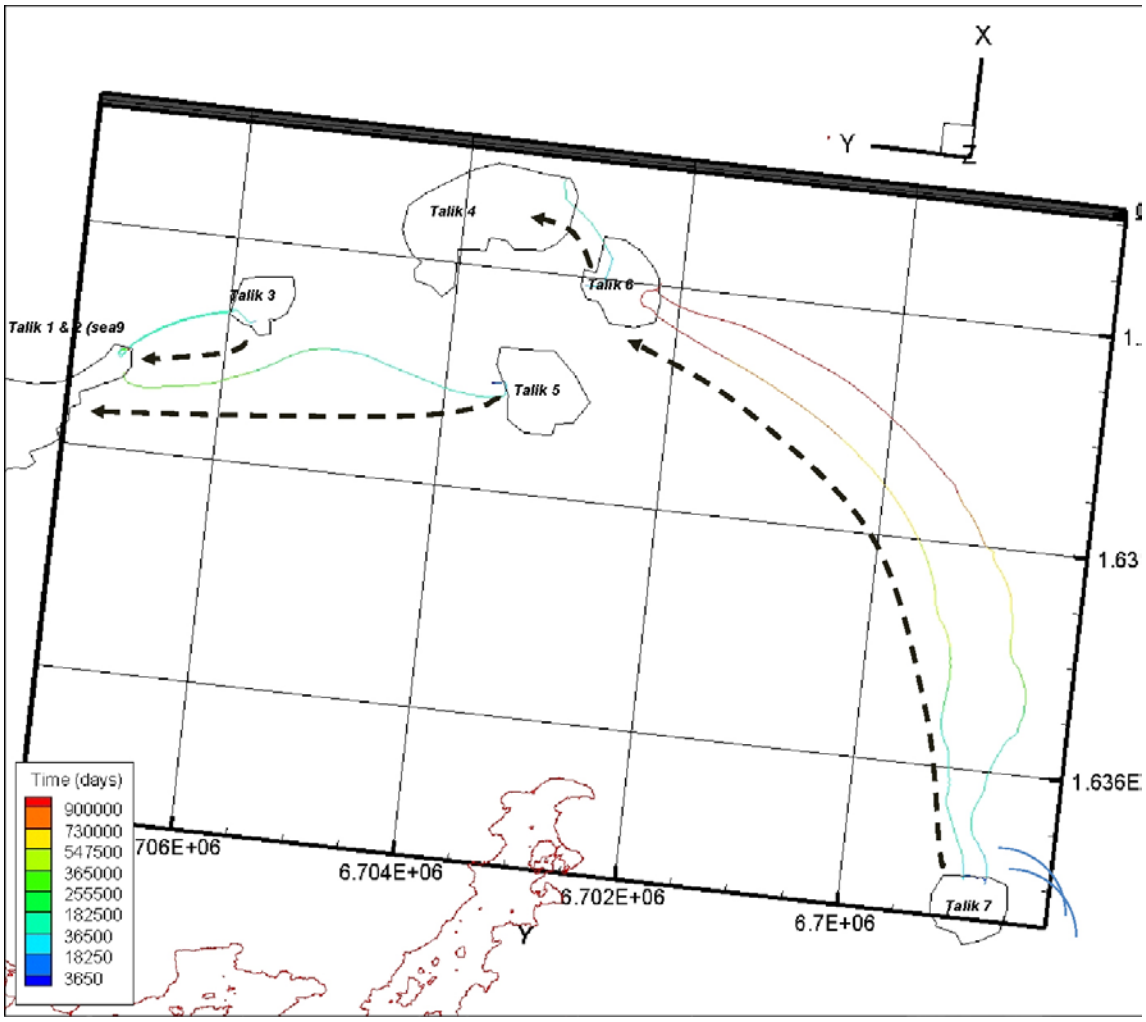

Figure 6-61. *Horizontal view from above of particle flow paths released in the active layer during the active period. Only the particles transported between different taliks are illustrated. The colour along each flow path shows the accumulated particle travel time in days.*

6.3.2 Model with 100 m permafrost

Table 6-6 lists the different sinks to which the particles went in the simulation with a 100 m thick permafrost layer. Also the numbers of particles left in the model after the 5000-year simulation are listed for each case; both the actual numbers of particles and the corresponding fractions (%) are shown. The horizontal locations and elevations of the particles left in the model at the end of simulations *100mPf_frozen_belowpf* and *100mPf_active_belowpf* are shown in Figures 6-62 and 6-63, respective. The red, orange and yellow colours indicate a downward transport of particles, which means that the final elevation of these particles is below the level where they were released.

In the case *100mPf_frozen_belowpf,* 16.1% of the particles are still left in the model volume at the end of the simulation, as compared to 45.6% of the particles released during the active period (*100mPf_active_belowpf*). The patterns are the same for the cases with 100 m deep permafrost and with 240 m deep permafrost. There are more particles left in the model volume for the active period than for the frozen period, and the major part of the particles left in the model at the end of the simulation are stuck in the sediments below the sea.

Due to the variation in the sea level during the active period a downward gradient is built up in the uppermost layers of the sea-talik also in this simulation case. The particles are stuck in the sediments during the active period whereas the gradient during the frozen period allows the particles to discharge to the sea. In Figure 6-63 a lot of particles can be seen under the sea-taliks (taliks 1 and 2) during the active period, whereas in Figure 6-62, which illustrates the results from the frozen period, no particles are left in the sea bottom sediments. During the frozen period 32.5% of the particles leave the model volume via the sea, whereas during the active period only 7.8% of the particles discharges to the sea. The dominating sink for the particles leaving the model volume during the active period is the combined unsaturated zone and overland water compartments. This is also the case for the frozen period, but the sea is also an important sink during this period.

Table 6-6. Particle balance data. The number of particles introduced in each case and the sinks for the particles that left the model are listed in the table.

	Active period, particles released in active layer		**Frozen period, particles released in active layer**	
	number	**%**	**number**	**%**
Particles removed by sink:				
Particles gone by baseflow to streams	809	2.9	21	0.1
Particles gone with drain to streams	1,685	6.1	0	0.0
Particles gone with drain to boundary	24	0.1	0	0.0
Particles gone to UZ/OL	22,392	80.5	2,756	9.9
Particles gone to the sea or to the boundary	28	0.1	213	0.8
Total number of particles removed	24,938	89.7	2,990	10.8
Particles left in the model	2,890	10.4	24,838	89.3
Total number of particles	27,828	100.0	27,828	100.0
	Active period, particles released in layer below permafrost		**Frozen period, particles released in layer below permafrost**	
	number	**%**	**number**	**%**
Particles removed by sink:				
Particles gone by baseflow to streams	192	0.7	125	0.4
Particles gone with drain to streams	360	1.3	0	0.0
Particles gone with drain to boundary	0	0.0	0	0.0
Particles gone to UZ/OL	12,504	44.6	14,298	51.0
Particles gone to the sea or to the boundary	2,187	7.8	9,102	32.5
Total number of particles removed	15,243	54.4	23,525	83.9
Particles left in the model	12,795	45.6	4,513	16.1
Total number of particles	28,038	100.0	28,038	100.0

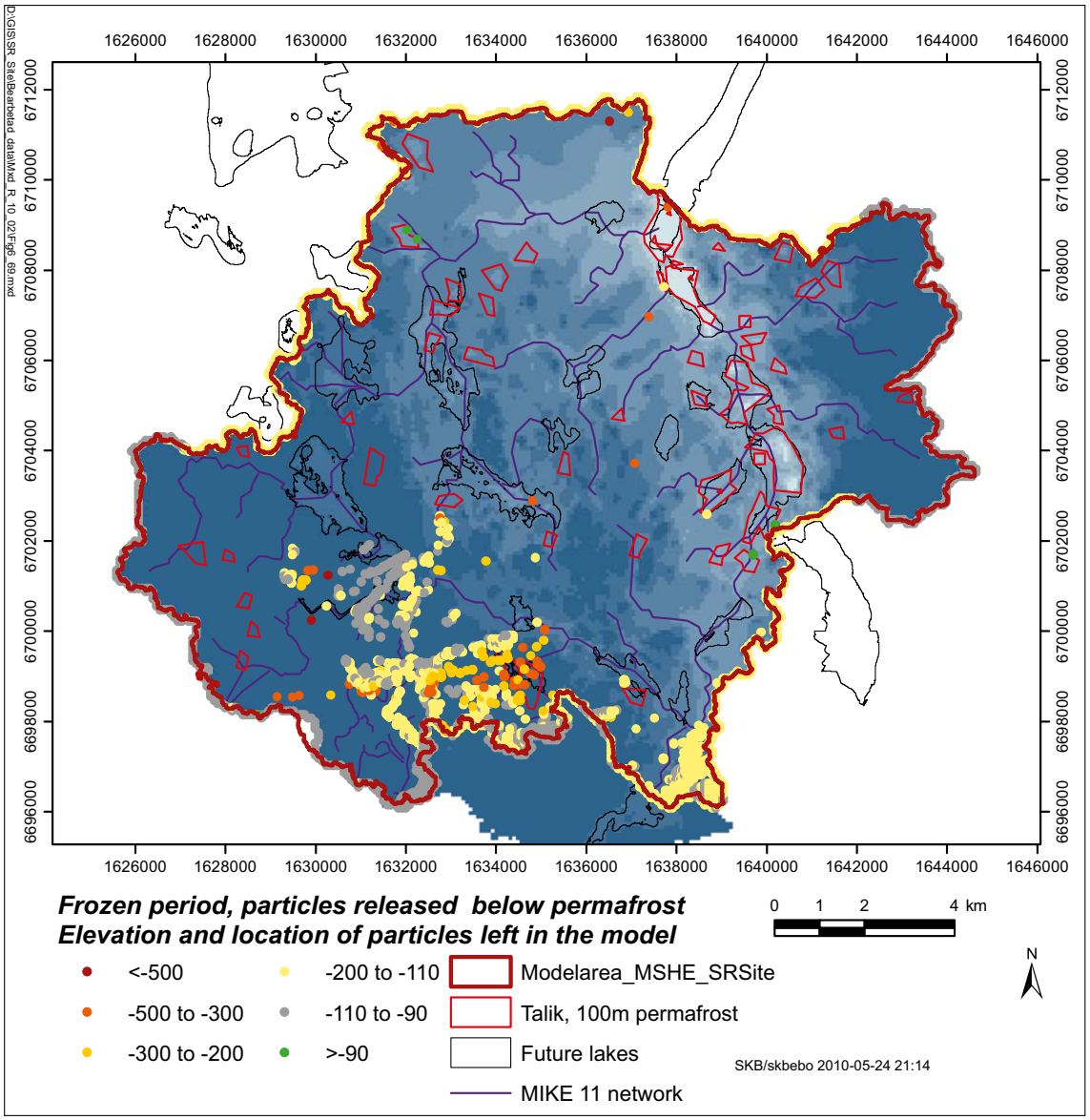

Figure 6-62. *Elevations and horizontal locations of the particles left in the model volume after 5,000 years, results from the simulation 100mPf_frozen_belowpf.*

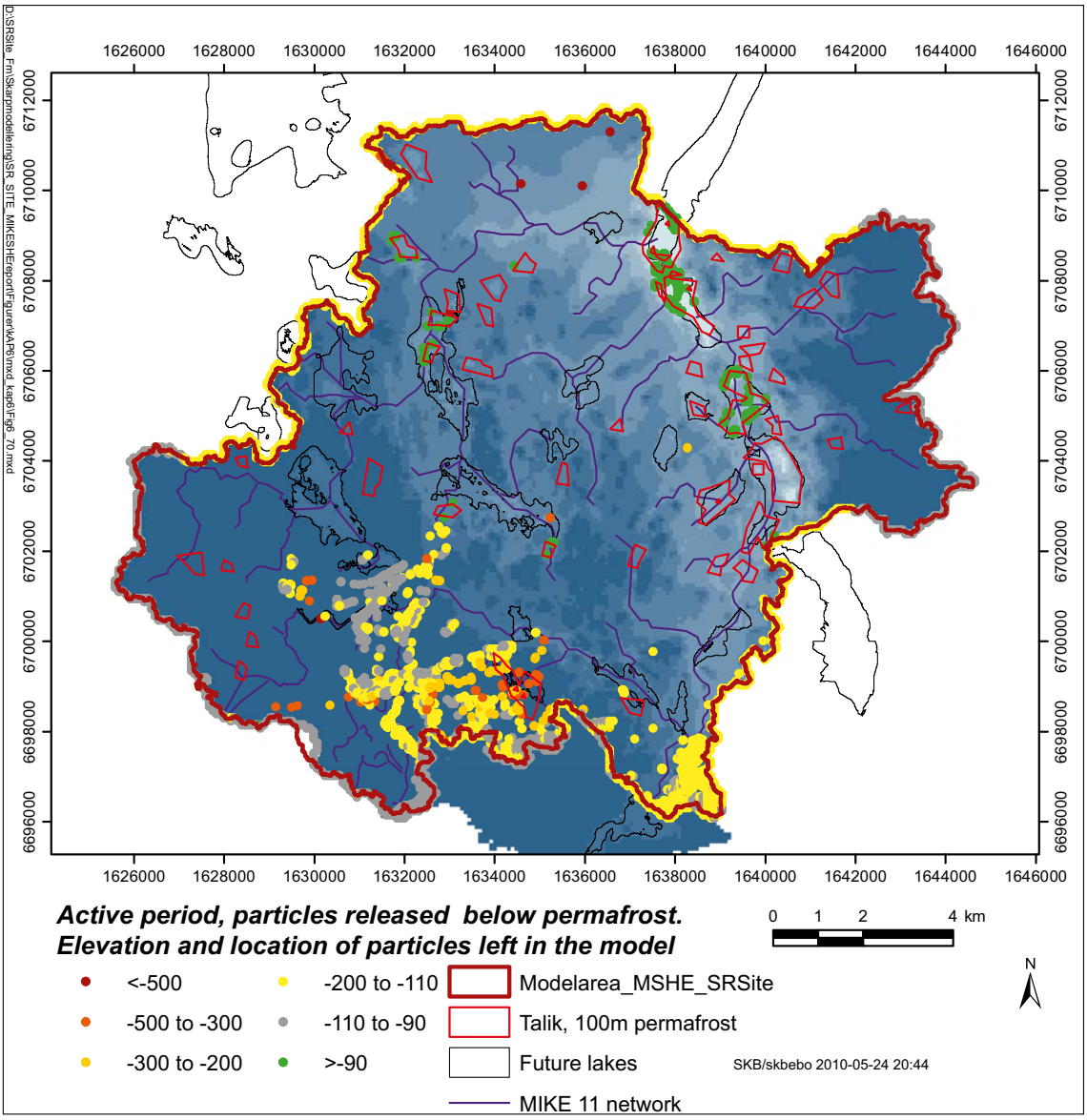

Figure 6-63. *Elevations and horizontal locations of the particles left in the model volume after 5,000 years, results from the simulation 100mPf_active_belowpf.*

For the two simulation cases with particle releases below the permafrost, the number of particles left in the model volume at the end of the simulations is less when applying the 100 m deep permafrost in the model than for the corresponding cases with a 240 m deep permafrost layer. The number of taliks is 45 with a 100 m deep permafrost layer, compared to only 7 taliks when the permafrost is 240 m deep. With an increased number of taliks the number of "windows" to the surface increases and a greater amount of particles leave the model volume.

In the case *100mPf_frozen_activelayer* almost all particles are left in the model volume. The low hydraulic conductivity values of the active layer do not allow longer transport distances. The majority of the particles are left at their birth locations. Approximately 10% of the particles have left the model volume. The dominating sink is the combined unsaturated zone/overland sink. The particles removed from the model volume are particles with birth locations close to a cell defined as a talik. For the active period simulation with particles introduced in the active layer, almost all particles leave the model volume; only 10.4% are left in the model volume at the end of the simulation. The dominating sink is the combined unsaturated zone/overland sink.

The exit points at the ground surface when releasing particles in the calculation layer below the permafrost are concentrated to the taliks, especially to the larger taliks. During the active period the particles are stuck in the sediments below the sea due to the time-varying sea level. The pattern of the exit points in the surface stream system and the inland taliks is the same during the frozen and the active period. The main difference between the two periods is the exit points in the sea appearing during the frozen period.

The exit points for the case *100mPf_frozen_activelayer* are shown in Figure 6-64. Figure 6-65 shows the particle flow paths for the particles discharging at the ground surface, i.e. the "exit points". The illustration is a horizontal view from above. The contributing flow field for each talik that is a discharge area is shown in the figure. The colours indicate the travel time for each particle; blue and green are relatively short travel times and red and yellow indicate longer travel times. The red arrows show the main transport directions of the particles. The increased number of taliks results in a more scattered pattern of recharge and discharge taliks compared to the simulation cases with the 240 m deep permafrost layer.

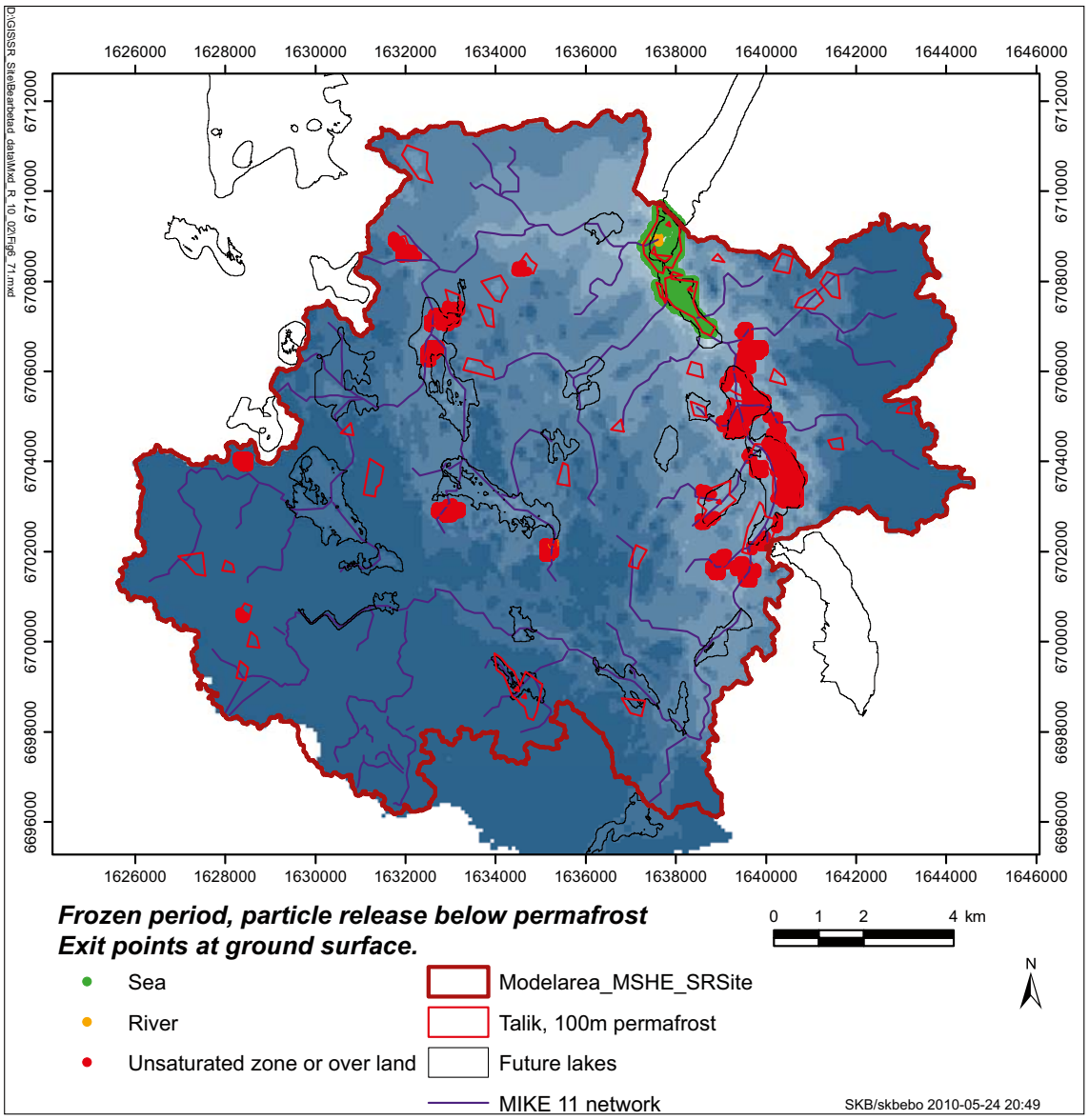

Figure 6-64. *Exit points at ground surface from the case 100mPf_frozen_belowpf. The different colours of the exit points indicate to which sink the particles have gone; the dominating sinks are the sea and the combined unsaturated zone/overland sink.*

Only the flow paths for particles that reaches ground surface, i.e an exit point, are illustrated.

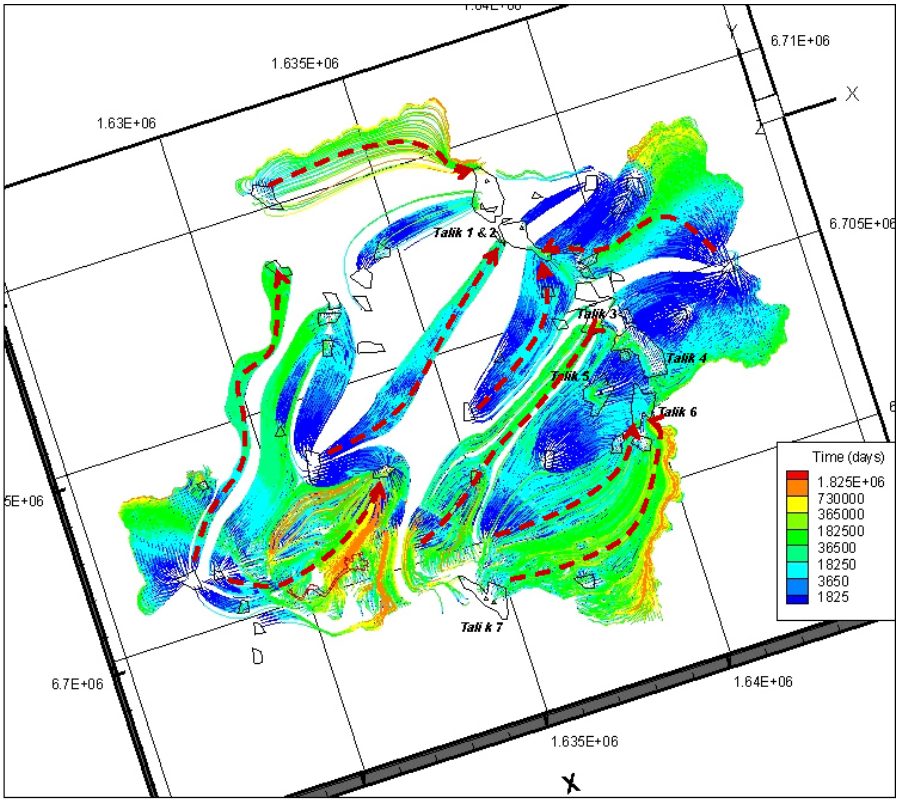

Figur 6-65. *Illustration of flow paths of particles released below the permafrost during the active period (case 100mPf_active_belowpf). The illustration is a horizontal view from above, and the colour along each flow path shows the accumulated particle travel time (in days).*

When introducing particles in the active layer in cases *100mPf_active_activelayer* and *100mPf_frozen_activelayer* a more scattered pattern of recharge and discharge areas are found compared to the simulation cases with 240 m deep permafrost and only 7 taliks. Figure 6-66 shows a 3D illustration of the transport between different taliks within the model area. The increased number of taliks allows more particles to travel between different taliks. There are more recharge and discharge areas compared to the cases with 240 m permafrost, resulting in more flow paths between taliks within the model area. The main flow directions are marked with black dotted arrows.

Figure 6-67 shows the same results as in 6-66, but in a horizontal view from above. In Figure 6-68 only the flow paths of the particles discharging to the sea (i.e. in taliks number 1 and 2) are illustrated. It is seen that areas within the part of the model area that constitutes land today (2000 AD) contribute to the discharge in the sea at 10,000 AD under permafrost conditions, given a 100 m thick permafrost layer.

The PT results for permafrost conditions are highly dependent of the number of taliks in the area. The only potential flow path for the particles through the permafrost is via the taliks. When the number of taliks within the model area increases, the number of "windows" to the surface increases. This results in an increased number of recharge and discharge areas and particle flow paths through the permafrost layer. The main transport of water within the model area takes place within or between the taliks. Thus the exit points are dependent on the number of and locations of the taliks. The patterns observed in the cases with different depths of the permafrost are similar. When releasing particles below the permafrost more particles are left within the model volume at the end of the simulation than in the simulation cases for the active period. However, fewer particles are left in the model volume when applying the 100 m deep permafrost layer due to more taliks and thus more potential areas/flow paths towards the surface where the particles can leave the model volume.

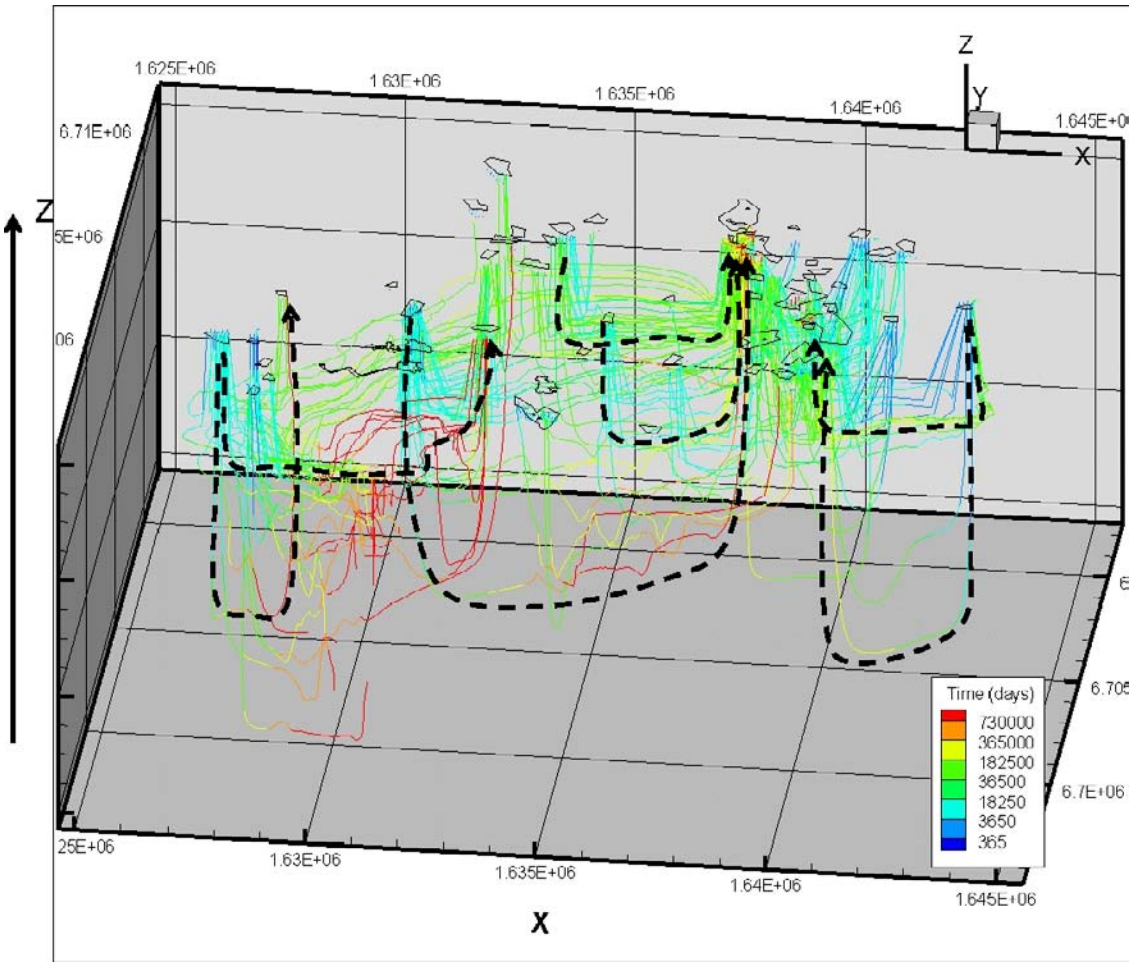

Figure 6-66. *Three-dimensional illustration of flow paths of particles released in the active layer during the active period (case 100mPf_active_activelayer). Transport between different taliks is marked with the black broken lines . The colour along each flow path shows the accumulated particle travel time in days.*

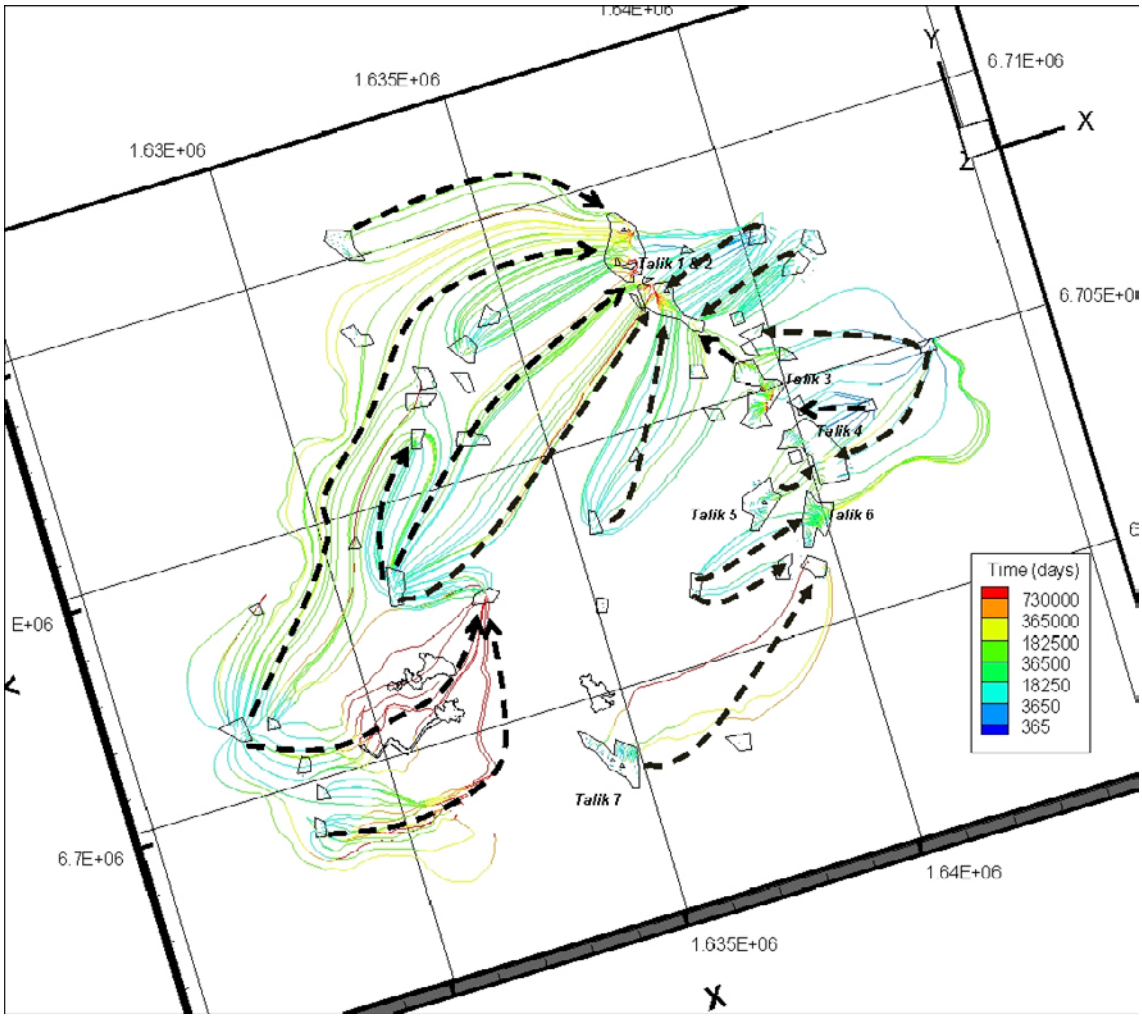

Figure 6-67. *Three-dimensional illustration of flow paths of particles released in the active layer during the active period (case 100mPf_active_activelayer). The transport between different taliks is shown from above and are illustrated by black broken lines). The colour along each flow path shows the accumulated particle travel time in days.*

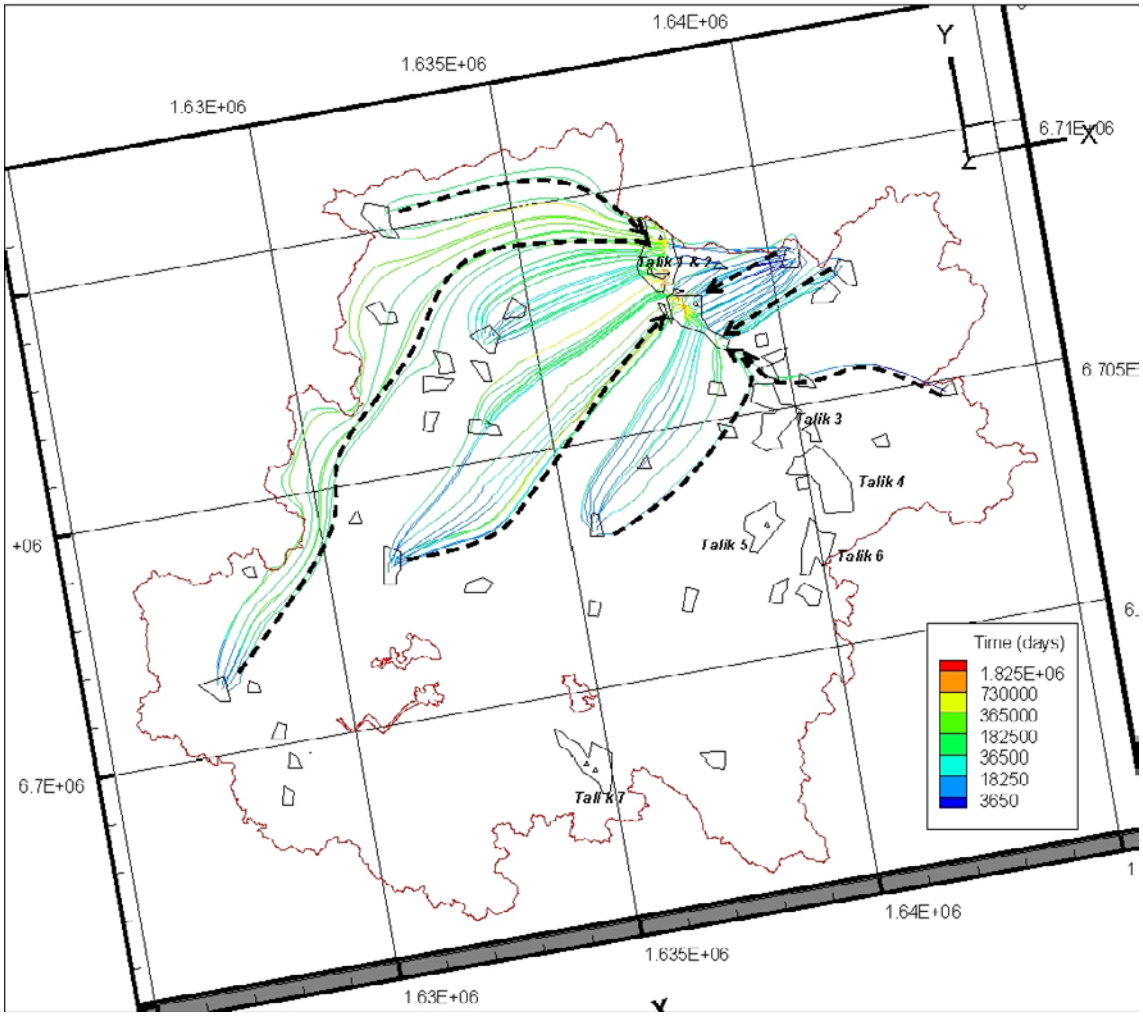

Figure 6-68. *Three-dimensional illustration of flow paths of particles released in the active layer during the active period (case 100mPf_active_activelayer). Only the flow paths of particles that discharge in taliks 1 and 2, i.e. in the sea, are shown. The colour along each flow path shows the accumulated particle travel time (in days).*

6.4 Summary of results from the regional models for wet or periglacial climate conditions

The main conclusions from the regional modelling with models based on climate data representing wet or periglacial conditions are summarised below.

- The wet climate conditions applied here include a mean yearly precipitation of 1,463 mm. When only studying the part of the model area that constitutes land today, the runoff corresponds to 20% of the precipitated water and 80% leaves the model volume as evapotranspiration. When taking the part of the model area constituting land 10,000 AD into consideration, the distribution is 25% runoff and 75% evapotranspiration. Due to the high evapotranspiration the amount of water leaving the model volume as runoff during wet climate is relatively lower than for temperate climate conditions. However, there is an absolute increase in yearly runoff from c.180 mm to c. 380 mm, i.e. the runoff increases with more than 100% due to the larger precipitation. The transpiration increases from approximately 145 mm with a normal temperate climate to approximately 470 mm under wet conditions. However, in all cases the transpiration is about 40% of the precipitation during the year.

- Due to the high evapotranspiration during periods of wet conditions, the depth to the groundwater table increases when applying a wet climate to the model, even though the infiltration increases. The increased precipitation, which is almost 3 times the precipitation used when modelling normal temperate conditions, does not cause higher groundwater levels in the area. This is because the precipitation increase is combined with a relatively larger evapotranspiration increase. In addition, the overland water runoff increases more than the infiltration, due to the more intense rainfalls.
- A significant change in the water balance appears under periglacial conditions, where the applied conditions include a yearly precipitation of 411 mm. When applying a periglacial climate and permafrost conditions to the model, the distribution of the precipitated water is approximately 50% runoff and 50% evapotranspiration. The relative increase of runoff is mainly explained by the short and intensive runoff period associated with snow melt. The transpiration constitutes only 10% of the total evapotranspiration, which is due to the combined effect of the poor vegetation cover and a smaller infiltration under periglacial conditions.
- With an increased runoff under periglacial conditions, the infiltration is subsequently reduced. The infiltration is also limited to unfrozen periods through the seasonal pattern of freeze and thaw periods occurring in the active layer. These seasonal changes in flow conditions are limited to the active layer and are not reflected in the upper and deeper bedrock.
- The percolation down to the deeper parts of the taliks and the unfrozen layers beneath the permafrost is almost non-existent. The vertical fluxes in the model increase with the number of through taliks since the taliks are the only possible flow path for groundwater to be transported from the unfrozen bedrock through the permafrost up to the surface. With a permafrost formation with a thickness of a 100 m the vertical flow percolating further down is reduced to approximately 1% of the water entering the saturated zone. Most of the water exits through an exchange with overland or the surface streams. When the permafrost thickness is increased to 240 m the vertical flow in the taliks is further reduced, since a thicker permafrost formation results in fewer taliks. However, the calculated vertical flows in the saturated zone (including the taliks) is in both permafrost cases in the same order of magnitude and are both very small in comparison to the flow conditions found under temperate climate conditions.
- Under periglacial conditions the through taliks function as either recharge or discharge taliks and have a consistent flow direction up or down, except for the vertical flow pattern and exchange between the active layer and the upper permafrost layer that fluctuate seasonally. The sea-taliks are the major discharge areas and the water movement in the model is towards these taliks. Some of the taliks are interconnected and with a permafrost thickness of 240 m water recharging in talik 7 (which is the strongest recharge talik for both permafrost thicknesses, and is located in the upstream part of the area) will discharge in talik 6. As talik 6 is a combined recharge and discharge area, water recharging there will discharge in talik 4. Both talik 3 and 5 contribute water to the sea-taliks. The presented particle migration patterns from the case with a permafrost thickness of a 100 m differ from the case with 240 m deep permafrost. This is due to both the permafrost thickness and the number and depth of the taliks, but also to the fact that the starting positions of the particles released below the permafrost differ in depth with approximately 140 m. The results are therefore not fully comparable, but it is clear that the flow pattern changes depending on the number and position of taliks.

7 Results from local models

7.1 Flow modelling

The main purpose of the local models is to make more detailed transport simulations for some of the lake objects, i.e. to study the transport patterns below and around the lakes. As a basis for the transport simulations, flow modelling must be performed using the same model setup. Results for the local flow models were extracted in the same way as for the regional model, see Chapter 5. However, since the focus of the simulations with the local models is on transport, the results from the flow modelling are presented only briefly in Sections 7.1.1 and 7.1.2 below, and only results that are relevant for the transport pattern are discussed. The local model A contains the three biosphere objects 118, 120 and 121, and the local model B contains object 116. The areas of the local models are shown in Figure 3-2.

7.1.1 Local model A

For local model A modelling was performed with the 10,000 AD shoreline and two different QD models, i.e. the QD model describing present conditions and the one for 10,000 AD. Thus, the two model setups considered were those referred to as 10000AD_2000QD and 10000AD_10000QD. Figures 7-1 to 7-4 show the overland water depths calculated with the two model setups for periods of wet conditions and dry conditions during the selected year. Both models show patterns similar to the overland depth for the corresponding regional models, see Figures 5-23 to 5-28.

The differences between the results for the two QD models are found in connection to the inlet canal, the area north of the inlet canal, as well as in the lake areas. The differences are explained by the differences in topography (cf. Figures 4-5 and 4-6). The QD model for 10,000 AD takes into account that the area has been exposed to erosion and sedimentation processes during another 8,000 years and that the presently existing lakes have been terrestrialised to wetlands in the at 10,000 AD. This is clearly seen in, for example, object 121_01 (see Figure 2-22), where there is a distinct lake area at 2000 AD and, according to the model, an area of only a very shallow overland water depth in the at 10,000 AD.

When connecting the MIKE SHE and MIKE 11 models, the water is always allowed to enter the surface water branches from the ground surface. However, in order to allow the water to flood from the MIKE 11 branch to the overland, the model option “allow overbank spilling” has to be included. In the present model version for local model A, the activation of the overbank spilling caused model instabilities due to the topography and, as a consequence, this option was not used.

This means that the water depth is probably underestimated in connection to MIKE 11 branches during the wet periods when the surface stream is flooded. For example, Figure 7-3 shows that the water depth in the lake in the northern part of the model area is very small. Including the overbank spilling option would probably lead to a larger water depth during wet periods. However, since the main objective of the local models was to run transport simulations and not to calibrate the surface water model, the results presented in Figures 7-1 to 7-4 were considered sufficiently accurate.

Figures 7-5 and 7-6 show the mean depth to the phreatic surface during the second year of simulation for the two different QD models used for the local model A. In the same way as for the surface water depth (Figures 7-1 to 7-4), the differences in topography between the 2000 QD and 10,000 QD models affect the results. Figure 7-7 shows the cumulative frequency distribution of the depth to the phreatic surface for the two different QD models. The figure indicates that the groundwater table is situated somewhat lower in relation to the ground surface in the QD model for present conditions than in the QD model for 10,000 AD. The reason may be that the present-day topography has more distinct heights, where the depth to the phreatic surface is greater.

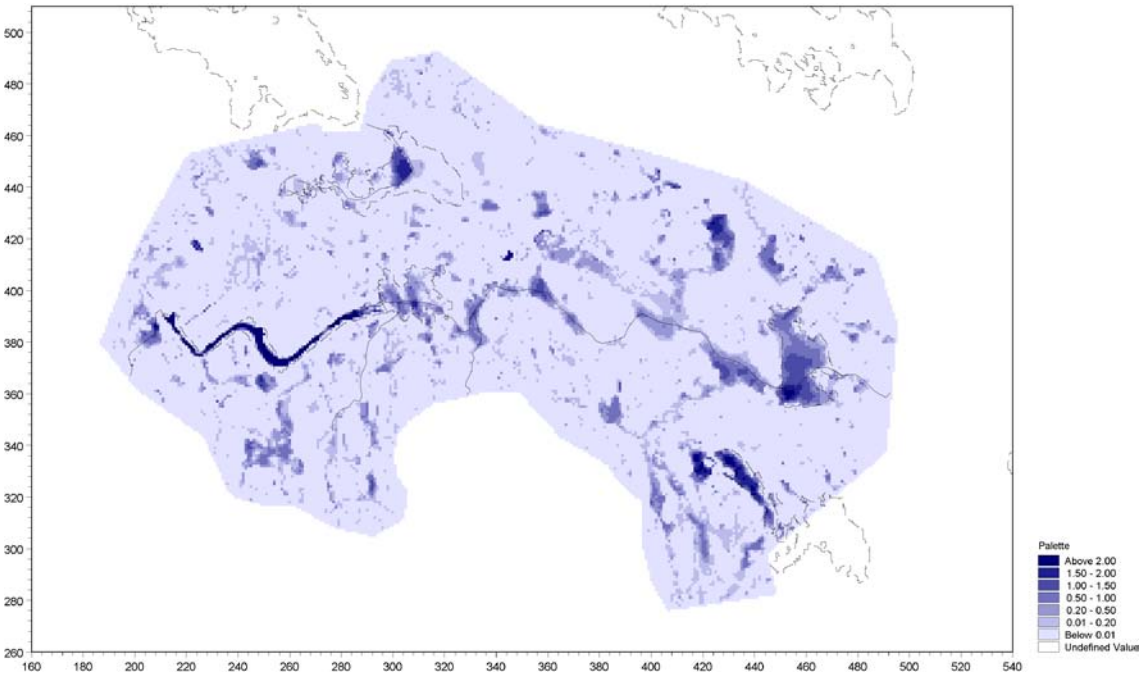

Figure 7-1. *Depth of overland water during wet period (March) for the 10000AD_2000QD version of local model A.*

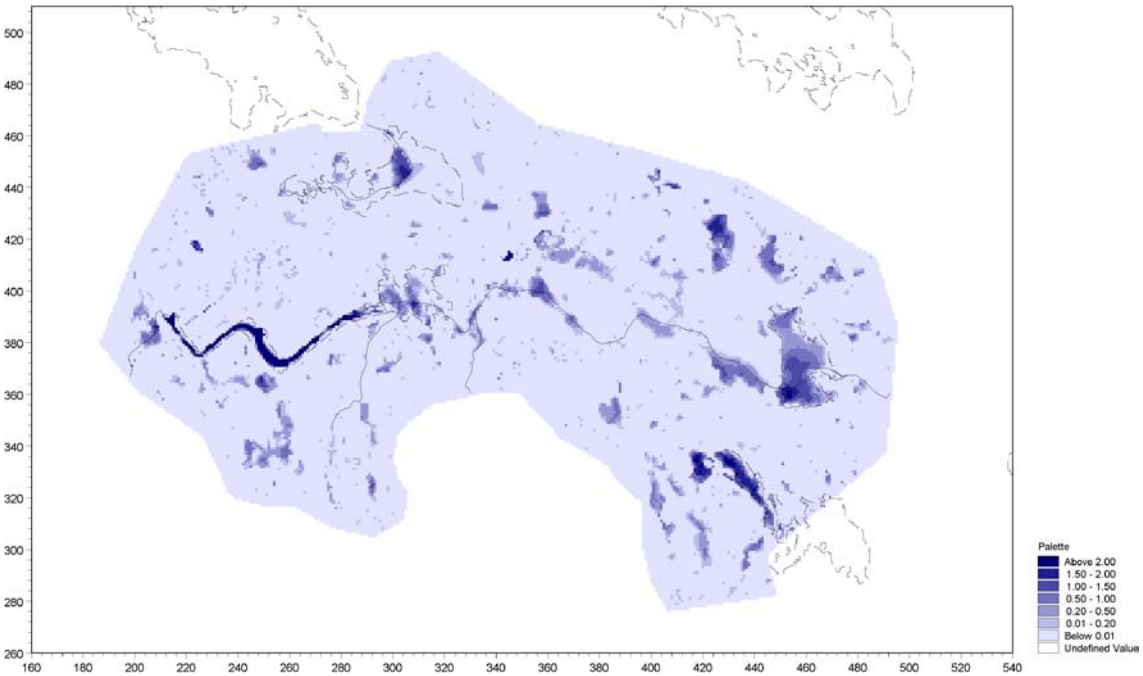

Figure 7-2. *Depth of overland water during dry period (July) for the 10000AD_2000QD version of local model A.*

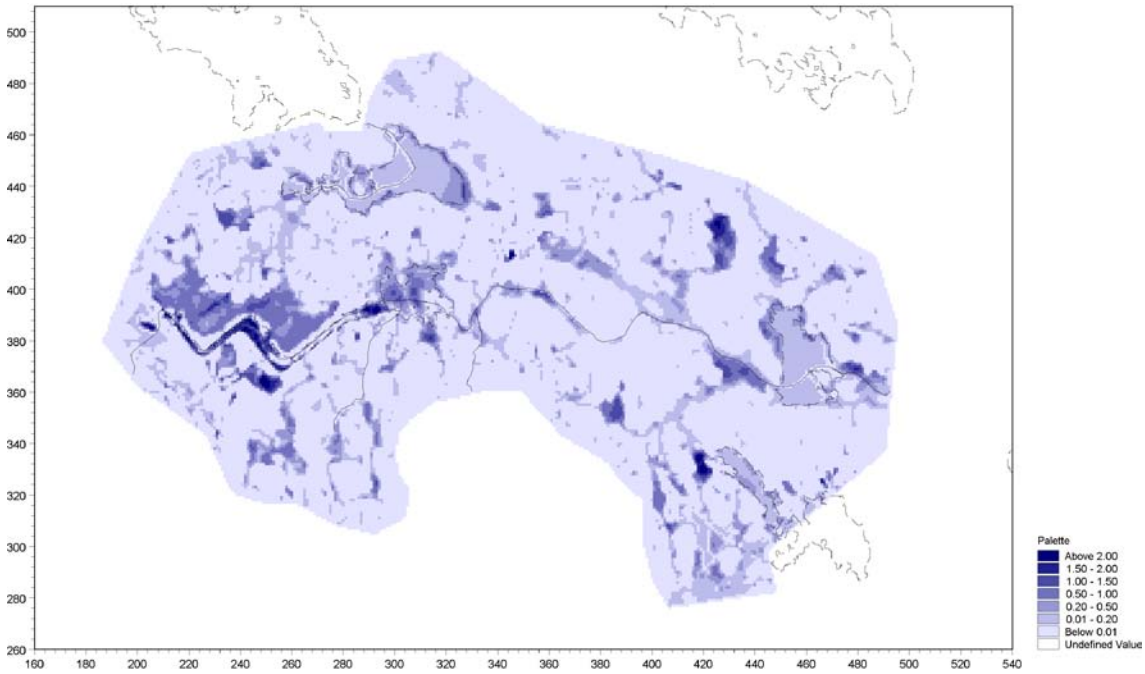

Figure 7-3. *Depth of overland water during wet period (March) for the 10000AD_10000QD version of local model A.*

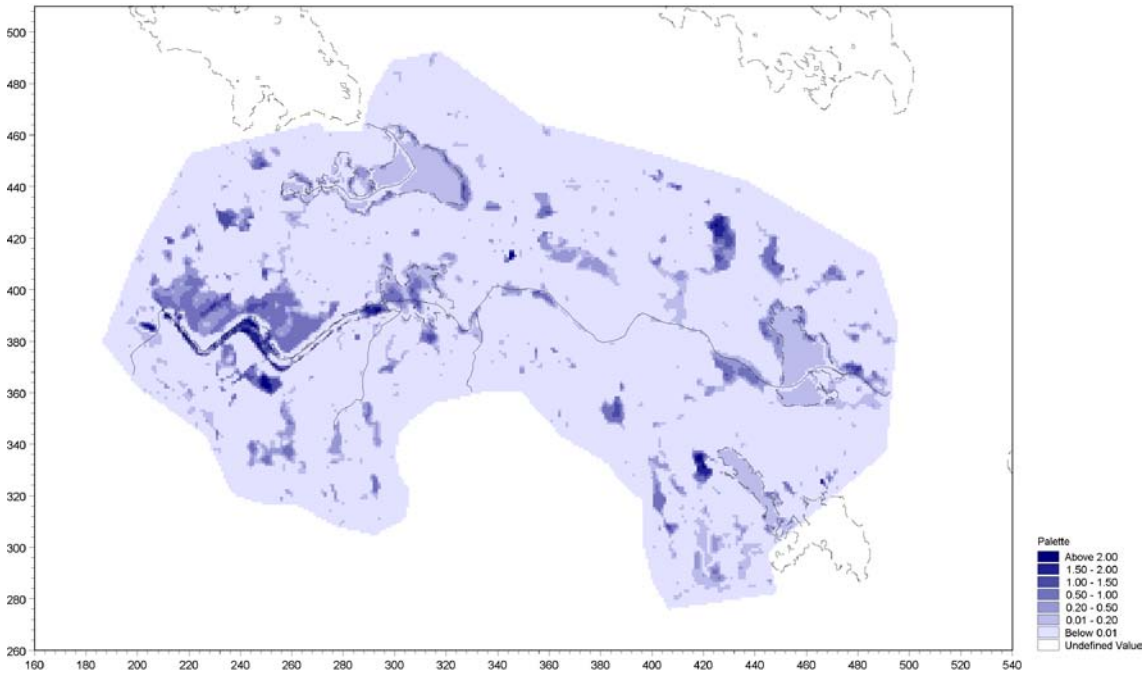

Figure 7-4. *Depth of overland water during dry period (July) for the 10000AD_10000QD version of local model A.*

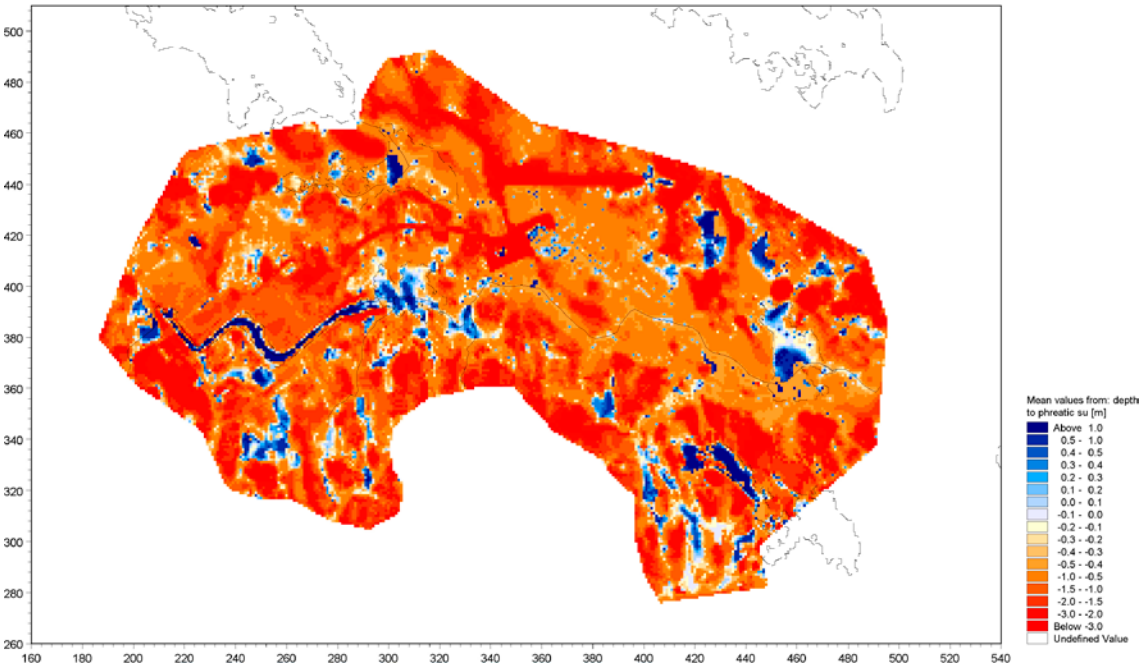

Figure 7-5. *Depth to the phreatic surface, calculated as the mean depth during the second year of the simulation, local model A 10000AD_2000QD.*

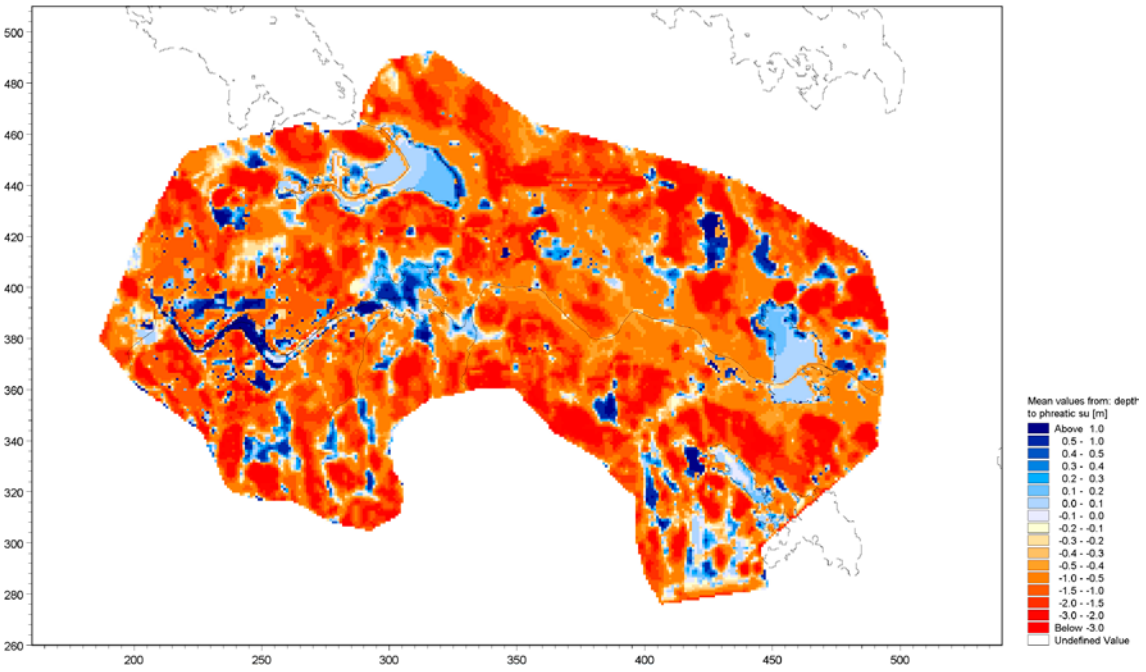

Figure 7-6. *Depth to the phreatic surface, calculated as the mean depth during the second year of the simulation, local model A 10000AD_10000QD.*

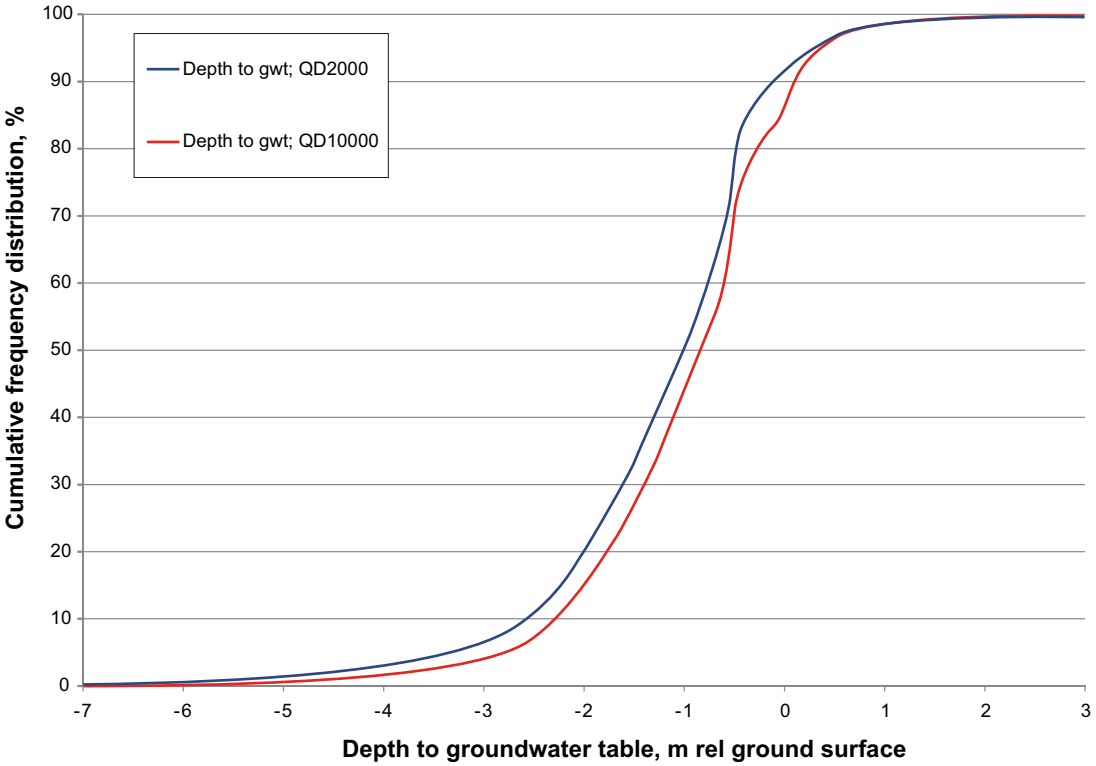

Figure 7-7. *Cumulative frequency of the depth to the phreatic surface (annual mean values) for the two different QD models used in local model A.*

Figures 7-8 to 7-11 illustrate the calculated recharge and discharge areas at two different depths for the two different QD models. Figure 7-8 and Figure 7-9 show the head differences between calculation layers L1 and L2, i.e. between the uppermost two QD layers, Figure 7-8 for the 10000AD_2000QD model and Figure 7-9 for the 10000AD_10000QD model. For the QD model describing present conditions, a comparison with the results for the regional model (Figure 5-32) and the local model shows that the general pattern is very similar with typically a small-scale pattern determined by the local topography. In the same way, a comparison between results from the regional model (Figure 5-34) and the local model results in Figure 7-9 for the 10000AD_10000QD case shows that the patterns are very similar also in this case.

Figures 7-10 and 7-11 show the head differences between two bedrock layers L11 and L12, situated at approximately 50 m.b.s.l. The recharge and discharge patterns are similar between the two models. The main difference is found in connection to the inlet canal and the area north of the inlet canal, which is also the area where the local surface topography, and consequently the thicknesses of the QD layers, differ the most.

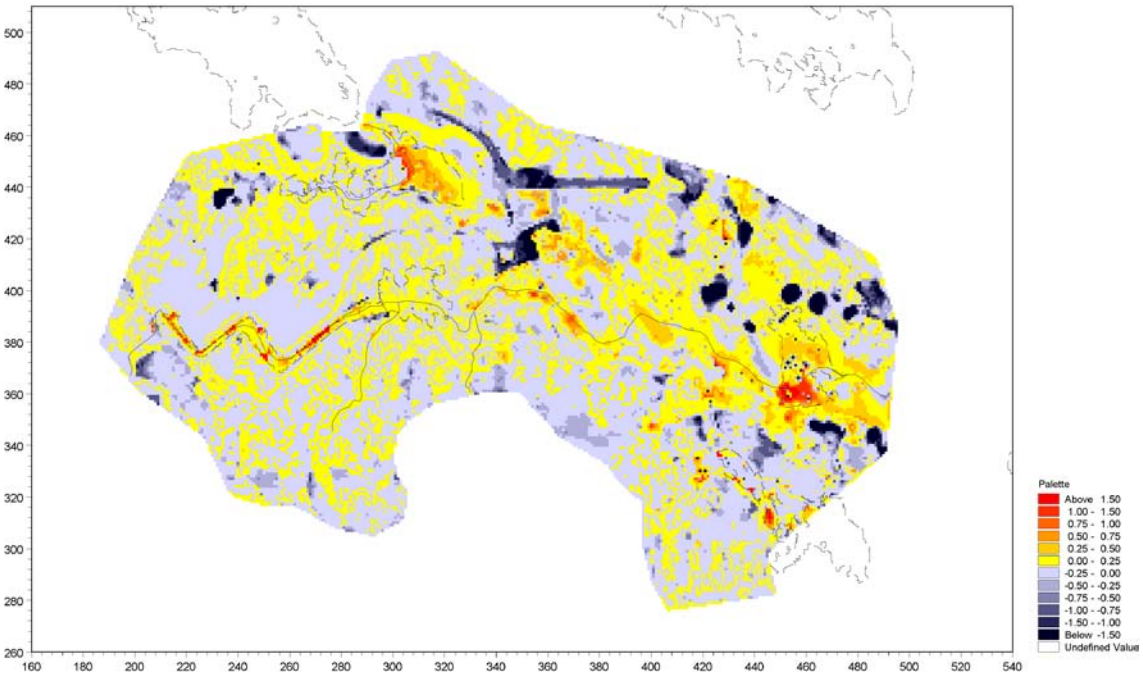

Figure 7-8. *Mean head difference between layers in the QD, i.e. recharge and discharge areas in the QD, for local model A 10000AD_2000QD.*

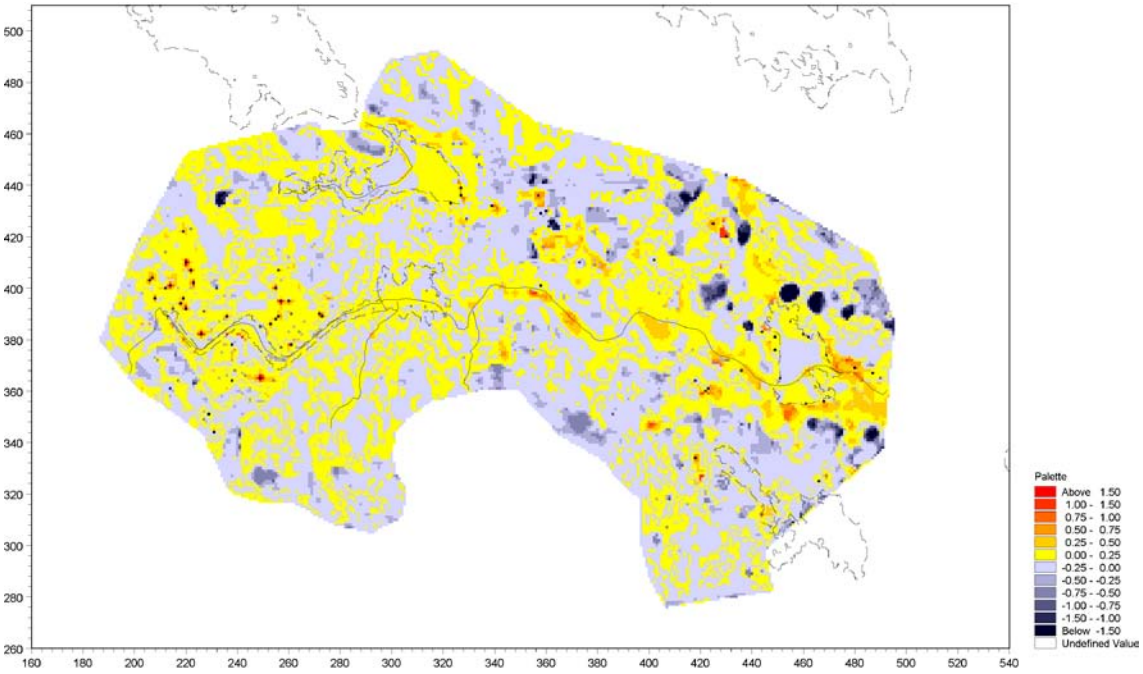

Figure 7-9. *Mean head difference between layers in the QD, i.e. recharge and discharge areas in the QD, for local model A 10000AD_10000QD.*

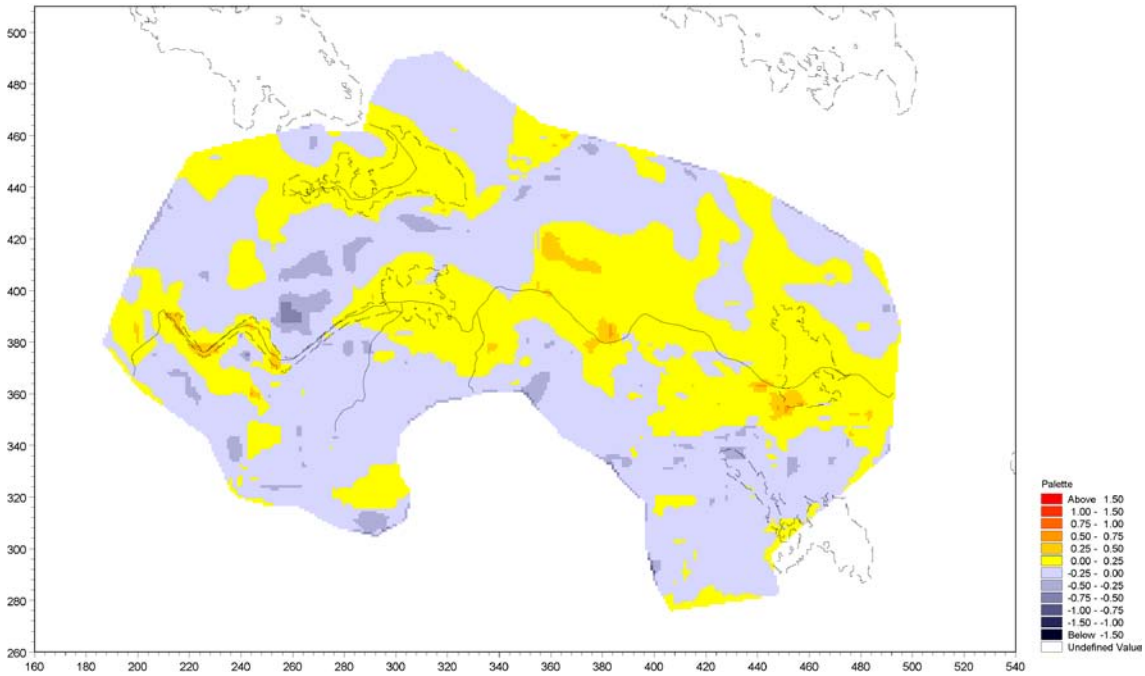

Figure 7-10. *Mean head difference between two bedrock layers at c. 50 m.b.s.l., i.e. recharge and discharge areas in the bedrock, for local model A 10000AD_2000QD.*

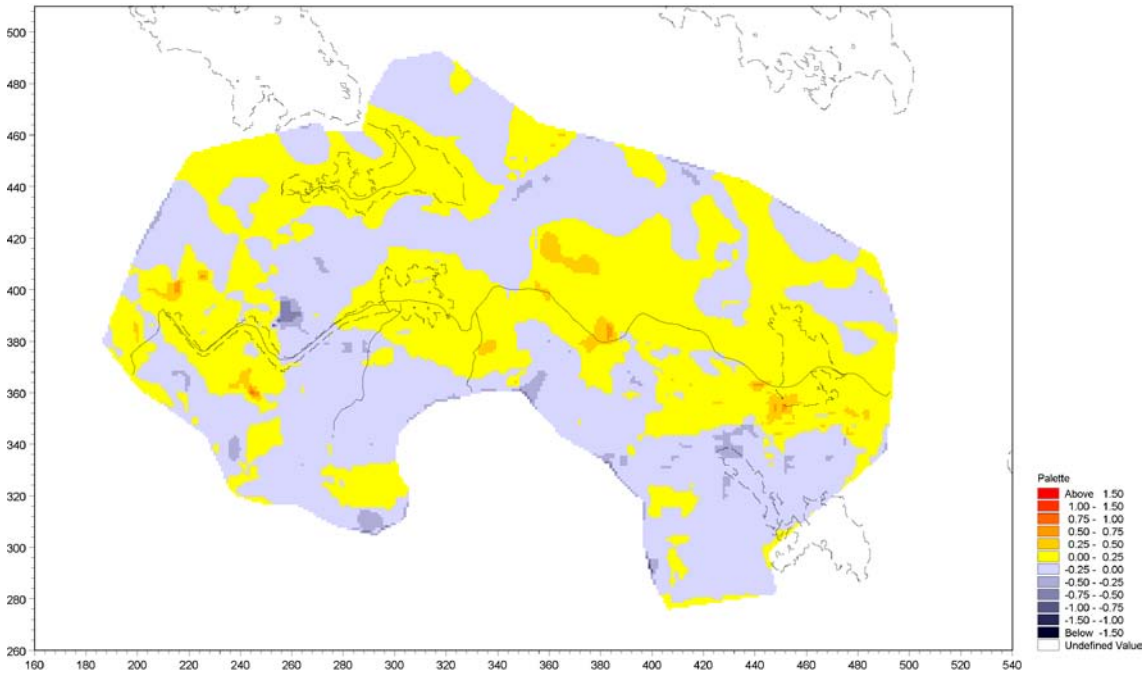

Figure 7-11. *Mean head difference between two bedrock layers at c. 50 m.b.s.l., i.e. recharge and discharge areas in the bedrock, for local model A 10000AD_10000QD.*

7.1.2 Local model B

Local model B is run with the QD model for 10,000 AD only. According to the model, the lake in object 116 is terrestrialised in the year 10,000 AD. For local model B, the MIKE 11 overbank spilling was activated, and consequently at a possible flooding event the water was allowed to flood from the MIKE 11 stream to the MIKE SHE model. Figures 7-12 and 7-13 show the calculated depths of overland water for a wet period, Figure 7-12, and a dry period, Figure 7-13. During the wet period the depth of overland water is up to a few decimetres in parts of object 116, while other parts of the object have almost no water depth at all. During the dry period, Figure 7-13, the overland water depth is close to zero all over the lake area.

Figure 7-14 shows the calculated depth to the phreatic surface, illustrated as the mean depth during the second year of simulation. Blue areas are areas in which the phreatic surface is above the ground surface, whereas in red areas the phreatic surface is located below the ground surface.

Figures 7-15 and 7-16 show the calculated head differences, i.e. the recharge and discharge areas, between two QD layers (calculation layers 2 and 3), and two bedrock layers (calculation layers 12 and 13). The differences are calculated as the mean head differences during the second year of simulation. Figure 7-15 shows the recharge and discharge areas in the QD layers. The results show that parts of the terrestrialised object 116 act as recharge areas while others are discharge areas. Figure 7-16 shows the recharge and discharge areas at approximately 70 m.b.s.l. in the bedrock, where the entire former lake area acts as a discharge area.

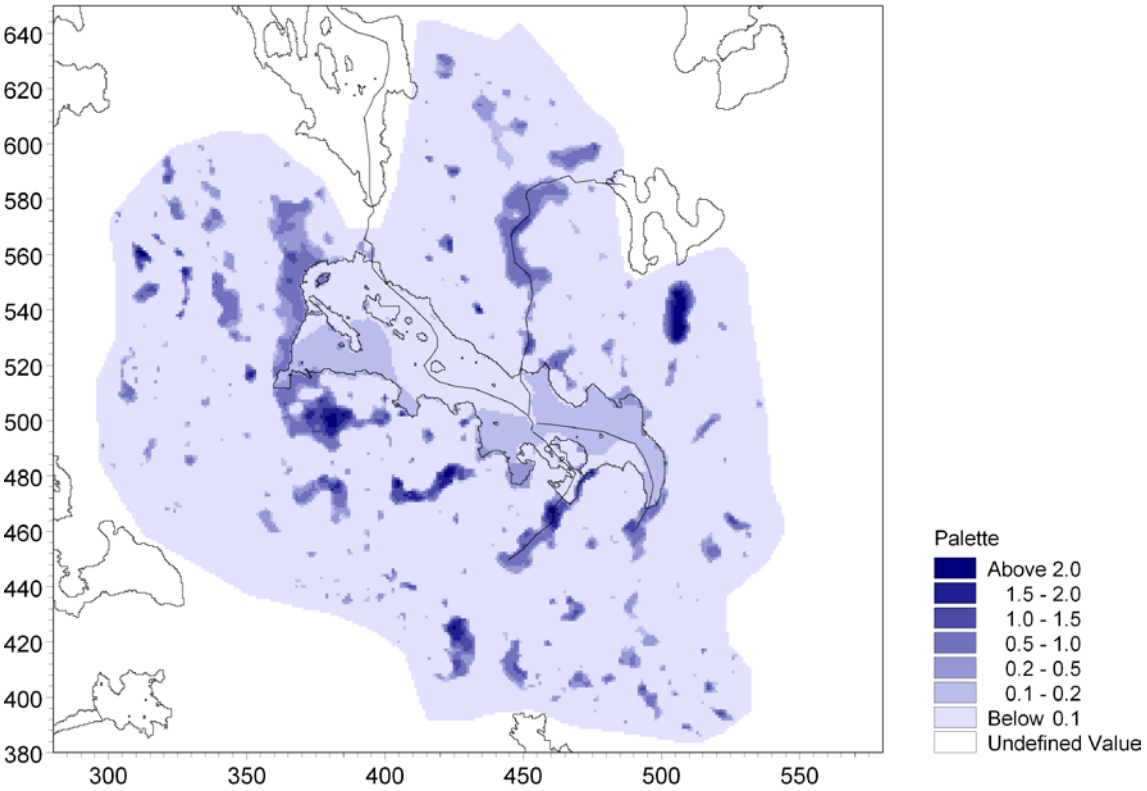

Figure 7-12. *Depth of overland water during a wet period (April) for local model B (based on 10000AD_10000QD).*

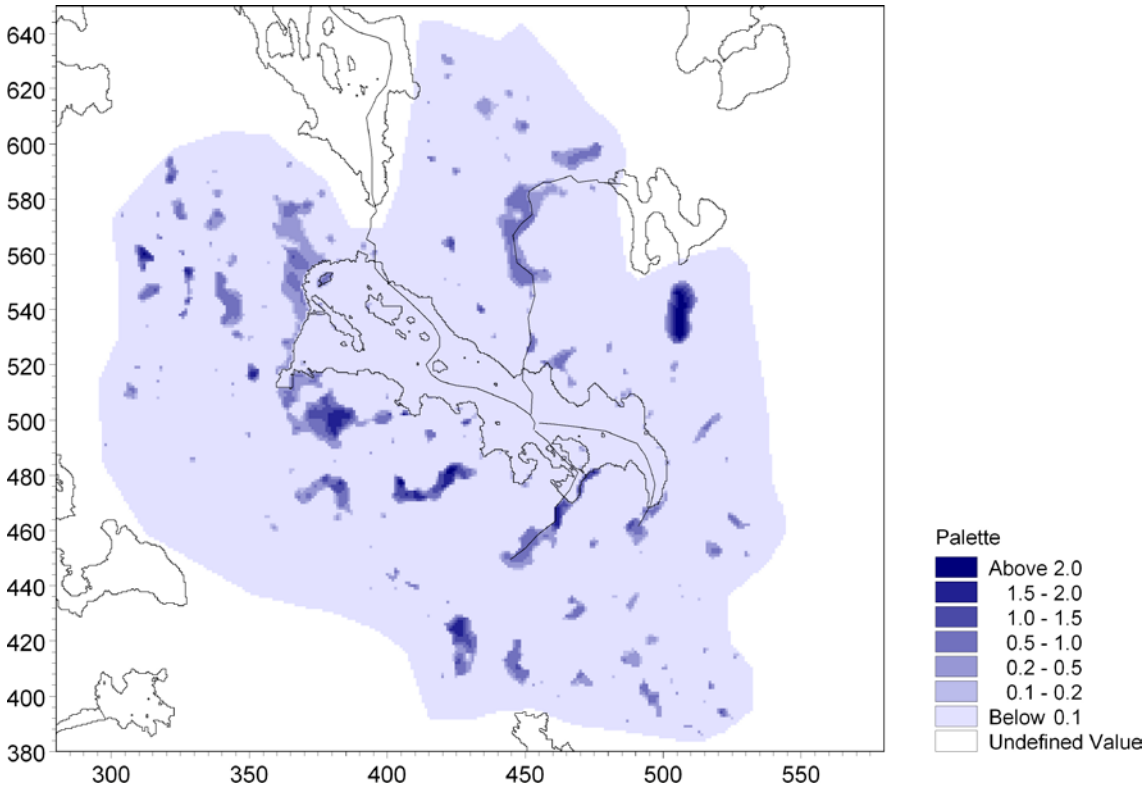

Figure 7-13. *Depth of overland water during a dry period (August) for local model B (based on 10000AD_10000QD).*

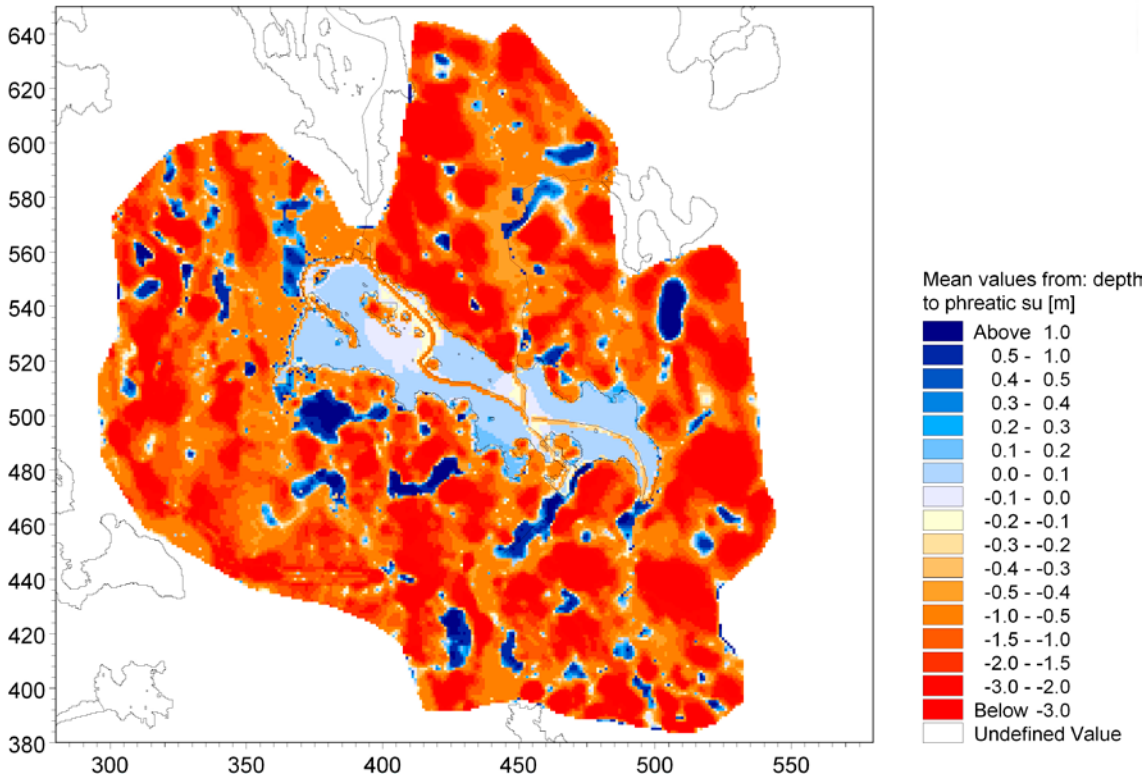

Figure 7-14. *Depth to the phreatic surface, calculated as the mean depth during the second year of the simulation for local model B (based on 10000AD_10000QD).*

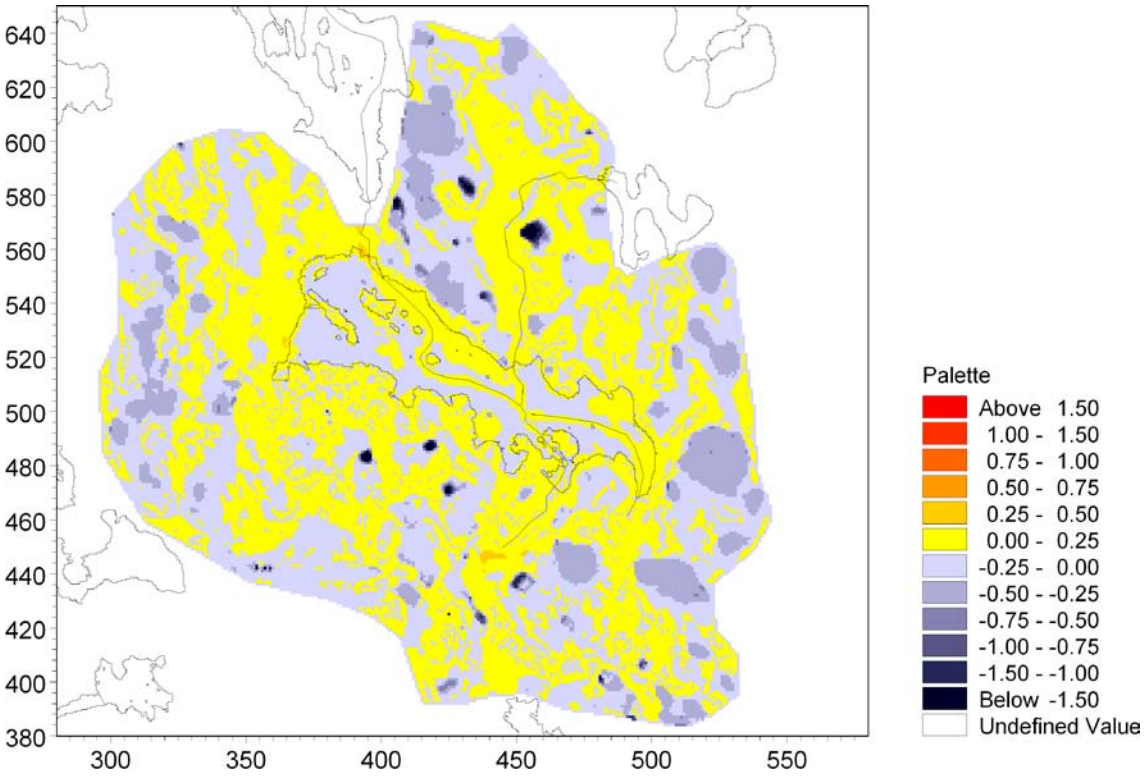

Figure 7-15. *Mean head difference between layers in the QD, i.e. recharge and discharge areas in the QD, for local model B (based on 10000AD_10000QD).*

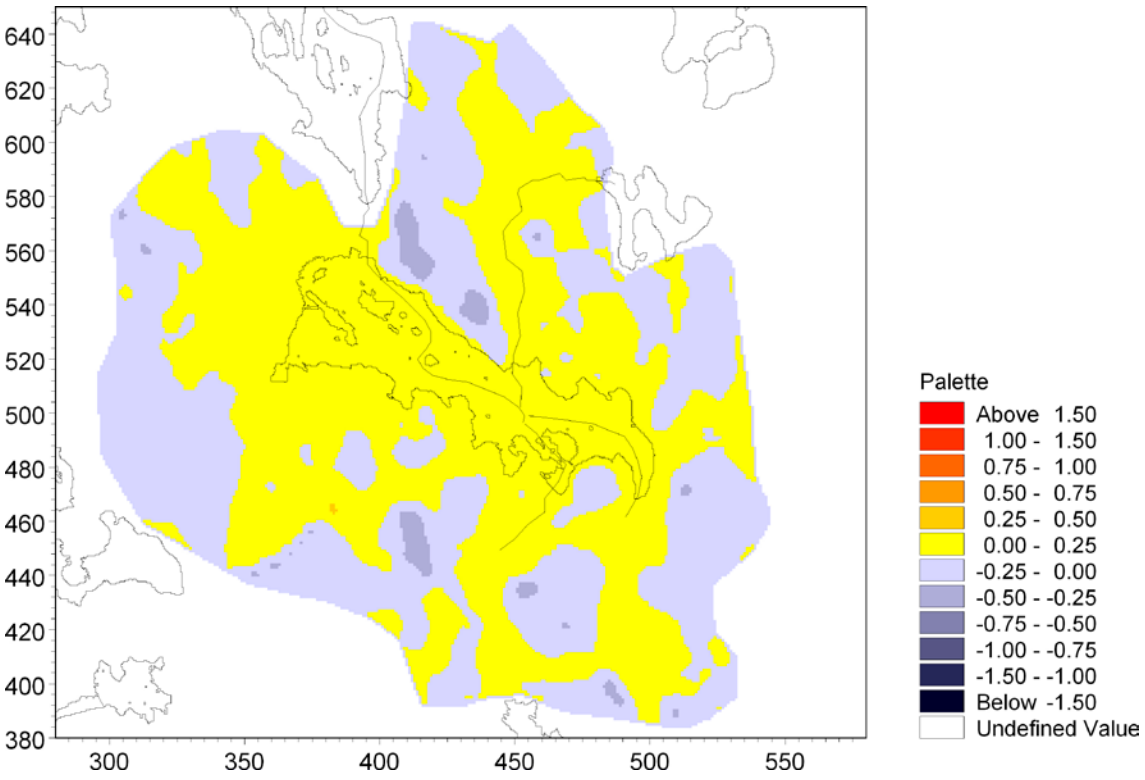

Figure 7-16. *Mean head difference between two bedrock layers at c. 70 m.b.s.l., i.e. recharge and discharge areas in the bedrock, for local model B (based on 10000AD_10000QD).*

7.2 Solute transport in local model A

7.2.1 Particle tracking

A simple way of estimating flow paths from one location to another is to make particle tracking simulations. Since the particle tracking, as performed in MIKE SHE, constitutes a purely advective transport simulation and is only active in the saturated zone, it is mainly used to investigate the flow directions from a specified release location to the corresponding exit location. However, since the simulations are based on results from the MIKE SHE flow model, surface processes that affect the saturated zone flow pattern will also affect the results of the particle tracking simulations.

Therefore, a particle tracking simulation made with the MIKE SHE module may give some additional information about the exit locations compared to the exit locations obtained from the ConnectFlow model used in the modelling focusing on bedrock hydrogeology, which has a more simplified description of the surface layers and processes. The main purposes with the particle tracking simulations made with local model A were to study the main transport pattern in the upper part of the model and to compare the exit locations with those from the ConnectFlow model.

Three different simulations with particle tracking (PT) were made for the local model A, see Table 3-5. In the first PT simulation, one particle per cell was released in the entire calculation layer, located at approximately 150 m.b.s.l. In the second PT simulation, the particles were released at a depth of c. 40 m.b.s.l. in positions obtained from the ConnectFlow model (Figure 3-7). Both of the first two PT simulations were run for a period of 1,000 years. The third PT simulation had the same particle release positions as the second one, but with a continuous release of particles. The third PT simulation was run for 100 years only, and the main purpose of the simulation was to compare the results to those from a simulation with the advection-dispersion (AD) module with the same source type, in order to see the effect of dispersion.

Table 7-1 shows the number of particles introduced to the model for the first two PT simulations and a summary of the sinks for the particles that have left the model. For the simulation with a release of one particle per cell at 150 m.b.s.l. a total number of 38,066 particles were released. After 1,000 years, 52% of the particles are still left in the model. Of the 48% that left the model, 27% went to the boundary, 23% to the MIKE 11 stream network, and 50% to the unsaturated zone or the overland water compartment.

In the simulation with a particle release at 40 m.b.s.l. a total number of 3,152 particles were introduced. After 1,000 years, 80% of the particles had left the model and 20% were still left within the model domain. For the particles that had been removed, 41% left the model through the MIKE 11 surface streams and 59% went to the unsaturated zone or the overland water. In both simulations, the dominating sink is the combined overland water/unsaturated zone compartments (which cannot be separated in the PT results). For the release at 40 m.b.s.l. no particles have gone to the vertical boundary.

Table 7-1. Number of particles introduced in PT simulations with the 10000AD_10000QD version of local model A, and distribution of particles on different sinks.

PT simulation for 1,000 years, local model A	Input at 150 m.b.s.l, 1 particle/cell	Input from ConnectFlow at 40 m.b.s.l
Number of introduced particles	38,066	3,152
Particles left in the model	52%	20%
Particles removed to sinks	48%	80%
Sinks:		
Boundary	27%	0%
MIKE 11 surface streams	23%	41%
Overland/unsaturated zone	50%	59%

Figure 7-17 illustrates the exit points for the PT simulation with particles released at a depth 40 m.b.s.l. at starting positions given by flow paths calculated with the ConnectFlow model. The red points are exit points and the green points are starting positions at 40 m.b.s.l. The figure illustrates that most particles are transported more or less vertically upwards to the surface, and that the particles are concentrated to the surface streams and along shorelines of the terrestrialised lakes as they reach the surface.

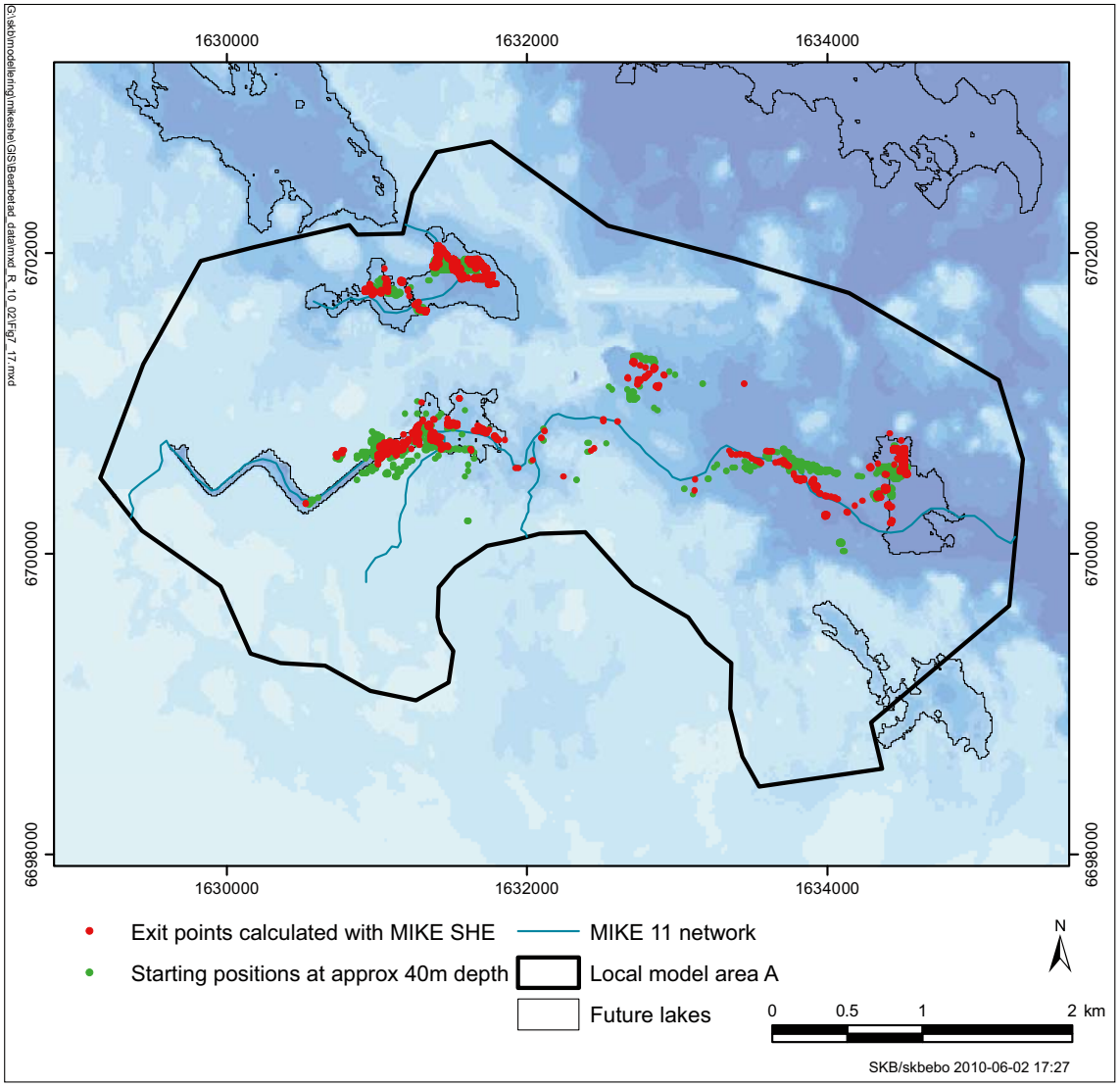

Figure 7-17. *Exit points calculated with MIKE SHE 10000AD_10000QD version of local model A (red dots) using starting positions from the ConnectFlow model at approximately 40 m.b.s.l. (green dots).*

Figure 7-18 compares exit points calculated with the MIKE SHE and ConnectFlow models. Since the starting positions of the particles in the MIKE SHE PT simulation were given by the ConnectFlow particle positions at 40 m.b.s.l. the particle positions are the same at this level. For the particles going to surface streams, the differences between the results from the two models are small. However, some differences can be observed in the lake areas. The particles leaving the MIKE SHE model tend to be more concentrated along the shorelines of the lakes, whereas the particles from the ConnectFlow model are appearing in the central parts of the lakes. This is illustrated in Figures 7-19 and 7-20.

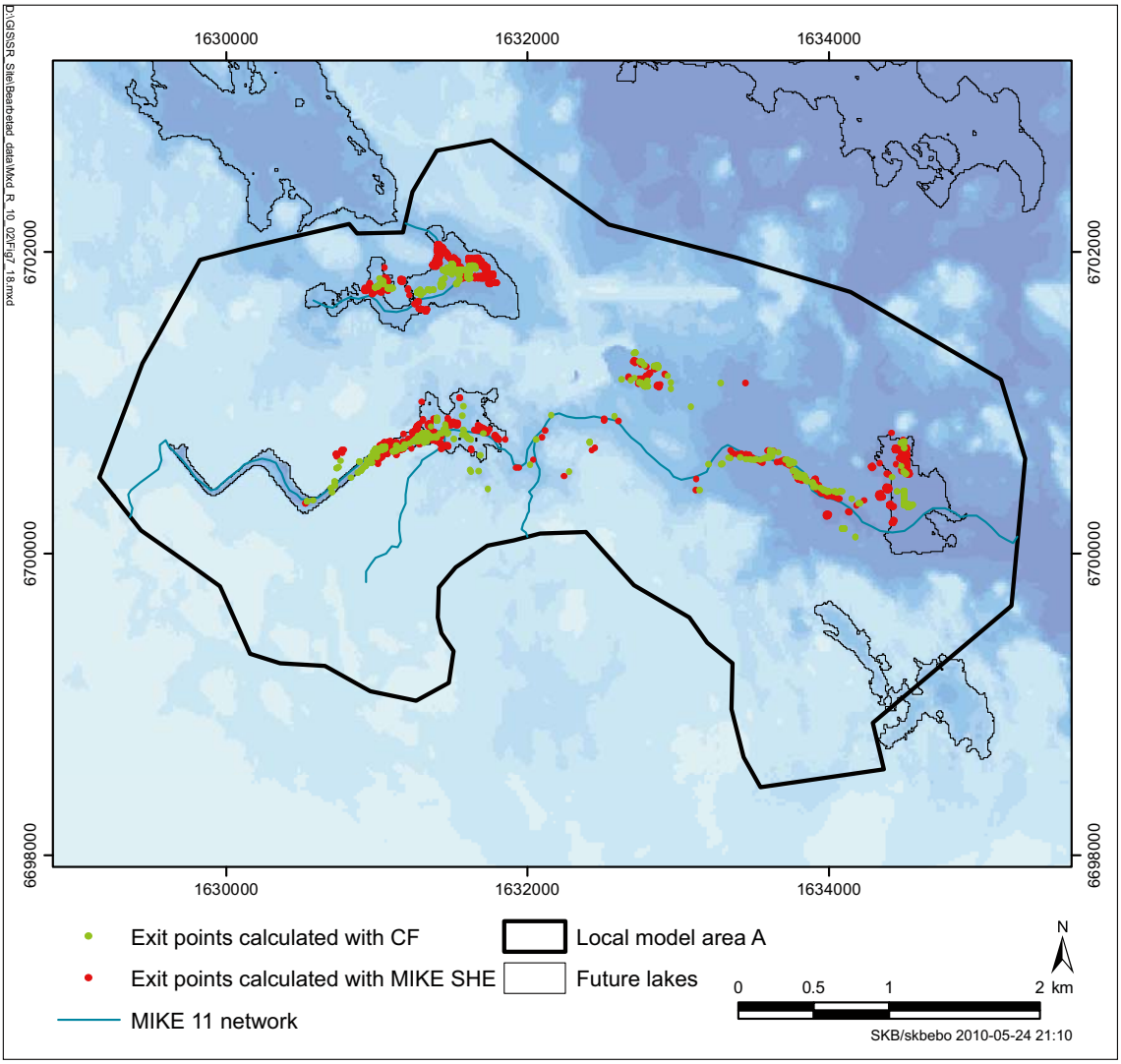

Figure 7-18. *Comparison of exit points in local model A, calculated with MIKE SHE (red dots) and ConnectFlow (CF, green dots).*

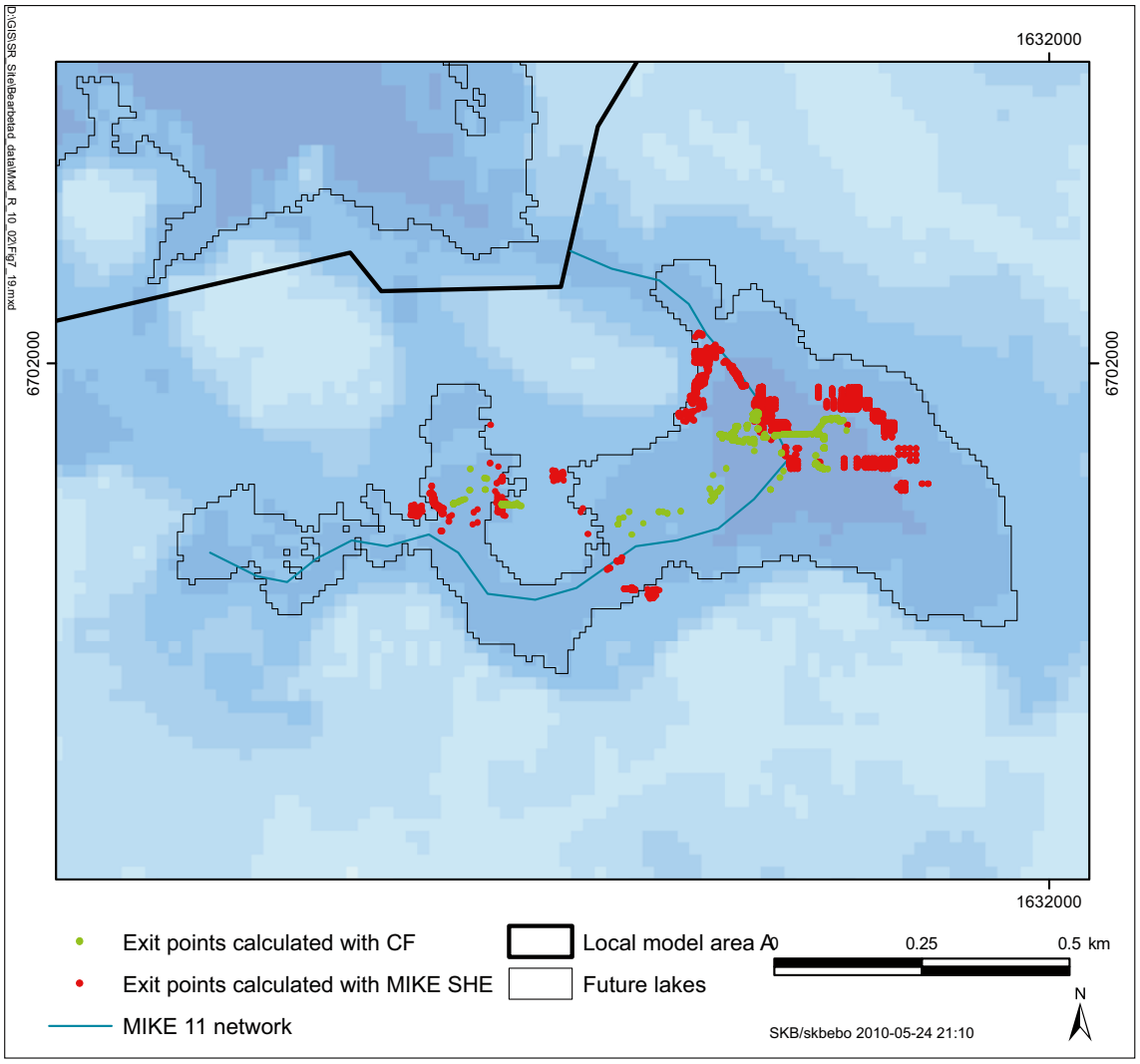

Figure 7-19. *Comparison of exit points of particles appearing in object 118, calculated with MIKE SHE (red dots) and ConnectFlow (CF, green dots).*

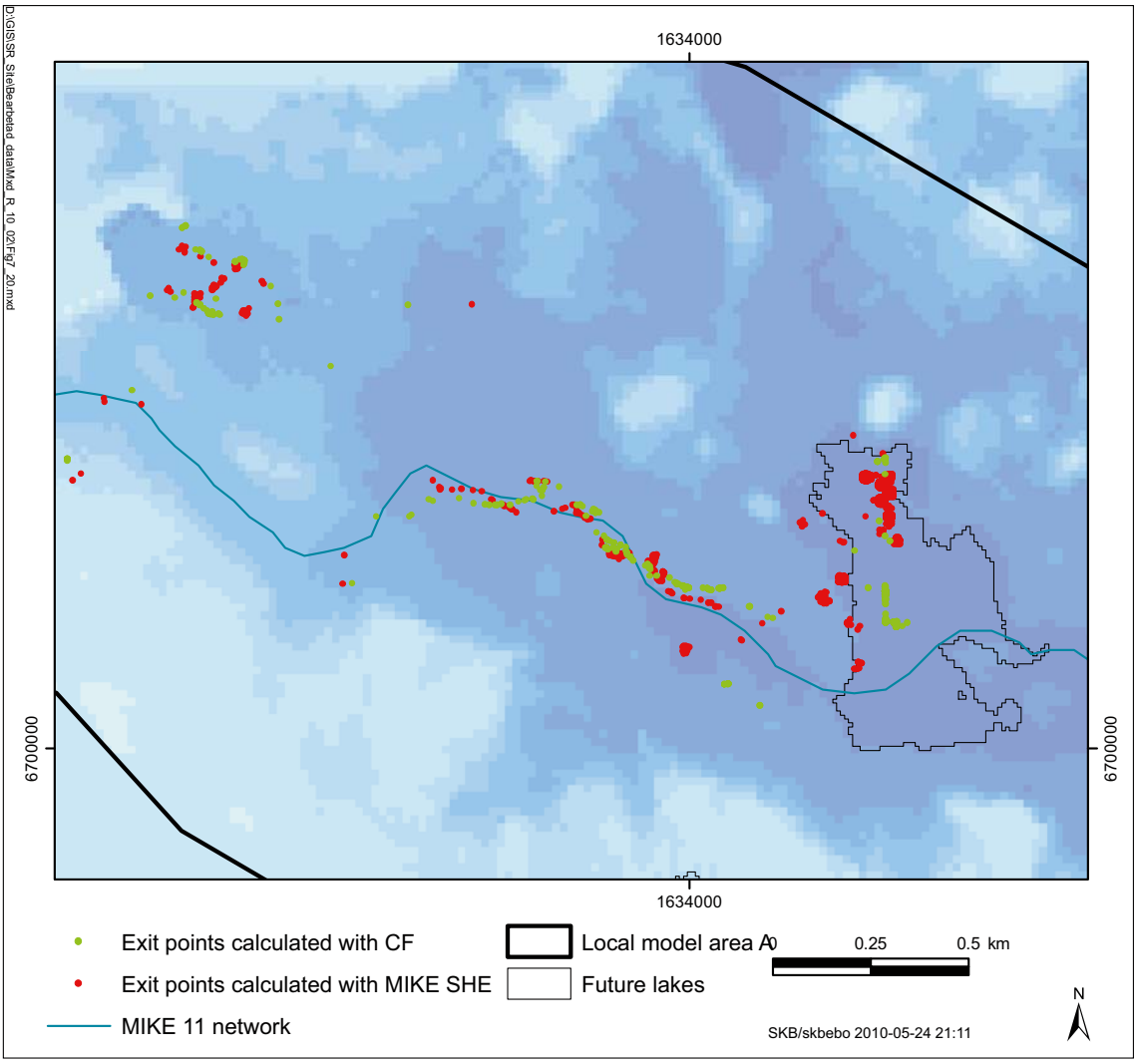

Figure 7-20. *Comparison of exit points of particles appearing in object 121_01, calculated with MIKE SHE (red dots) and ConnectFlow (CF, green dots).*

Figure 7-19 shows a more detailed view of the lake in the northern part of the model area (object 118). The figure shows how the ConnectFlow particles appear in the central part of the lake, while the MIKE SHE particles appear close to the shore and in connection to the surface stream going through the lake. Figure 7-20 shows a more detailed view of the lake in the eastern part of the model area (object 121_01). The same pattern is seen also for this lake; the particles from the ConnectFlow model are more concentrated to the lake centre, whereas the MIKE SHE particles are located along the lake shoreline.

One reason for the differences between the results from the ConnectFlow model and the MIKE SHE model may be that the extents and thicknesses of the lake sediments are described in more detail in the MIKE SHE model. Another reason is that the MIKE SHE model includes more surface processes than the ConnectFlow model. In connection to the lakes, the evapotranspiration along the lake shoreline decreases the groundwater head in the upper soil layers, creating un upward hydraulic gradient from the deeper layers, see /Bosson et al. 2008/.

Figure 7-21 shows the locations of the exit points for all particles introduced at 150 m.b.s.l. except those that have gone to the boundary. For the particles that have gone to the combined sink "unsaturated zone/overland", the main part has gone to the lake areas i.e overland. In the lake areas, the particles are concentrated to the lake shorelines, indicating either that the low-permeable lake sediments force the transport to go horizontally under the lakes and then vertically up along the shores or that the evapotranspiration along the lake shorelines creates an upward hydraulic gradient from the deeper layers. Almost all the particles that have gone to the streams have left the model in or close to object 118, object 121 and the inlet canal, i.e. in the same areas as the particles that go to overland water or the unsaturated zone.

A comparison between the exit locations for the two PT simulations illustrated in Figures 7-18 and 7-21 shows a few differences. For example, object 120 does not receive any particles at all during the 1,000 years of simulation when the particles are introduced at 150 m.b.s.l., whereas this object receives several particles in the simulation with the release points according to the ConnectFlow model. However, in the ConnectFlow model particles were released at positions located outside of the model domain for the local model A and the most probable explanation is that object 120 receives particles that are released at positions outside of local model A. Particles that are released at 150 m.b.s.l. within local model A are transported upwards until they reach a layer with a higher horizontal hydraulic conductivity, in which they are then transported mainly horizontally.

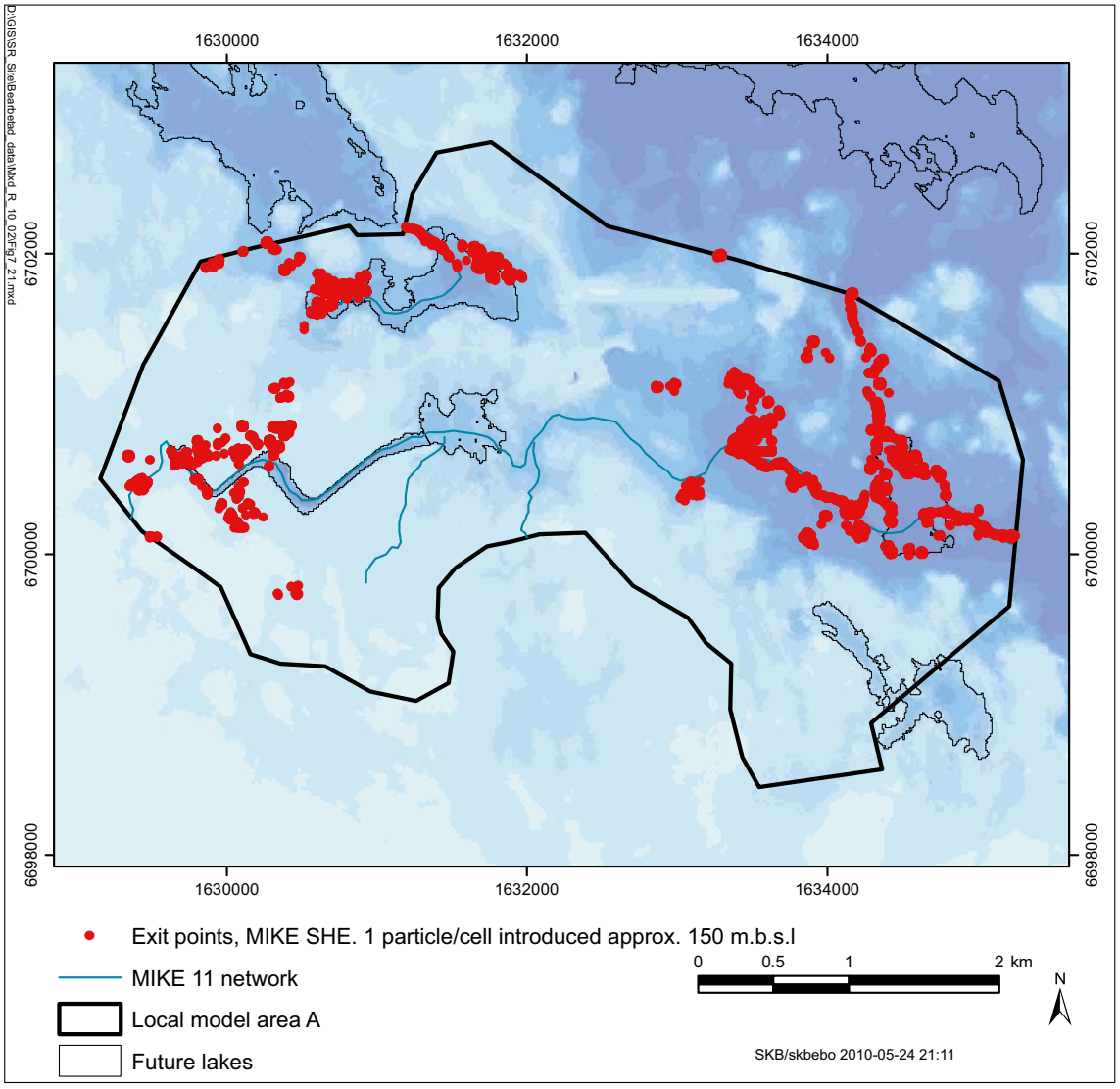

Figure 7-21. *Exit points in local model A after 1,000 years of MIKE SHE PT simulation with one particle per cell released at a depth of 150 m.b.s.l.*

Figure 7-22 shows the end locations for the particles still left in the model after 1,000 years of simulation. The colour of each point illustrates the depth of the particle at the end of the simulation; the darker red the deeper the particle is situated and the darker blue the closer to the surface. Particles illustrated by the grey colour are still within the layer in which they were released. Points that are orange or red have end locations situated at depths below the particle release layer, i.e. they are all particles that have been transported downwards in the model and after 1,000 years they are still located at depths greater than the initial release depth. The figure shows that the particles that are close to the surface are located close to the areas in which particles already have left the model.

Figure 7-23 shows a three-dimensional plot of the particle pathways for the case with one particle per cell released at 150 m.b.s.l. The depth is illustrated on the z-axis and the location of the lakes and surface water streams are indicated by black lines at the surface, i.e. at zero depth. The colour of each path-way shows the travel time for a particle. During the first month after the particle release, the travel path is dark blue but as the travel time increases the travel path changes colour. After 100 years the travel path is yellow and for travel times above 500 years the travel paths are shown in red colours.

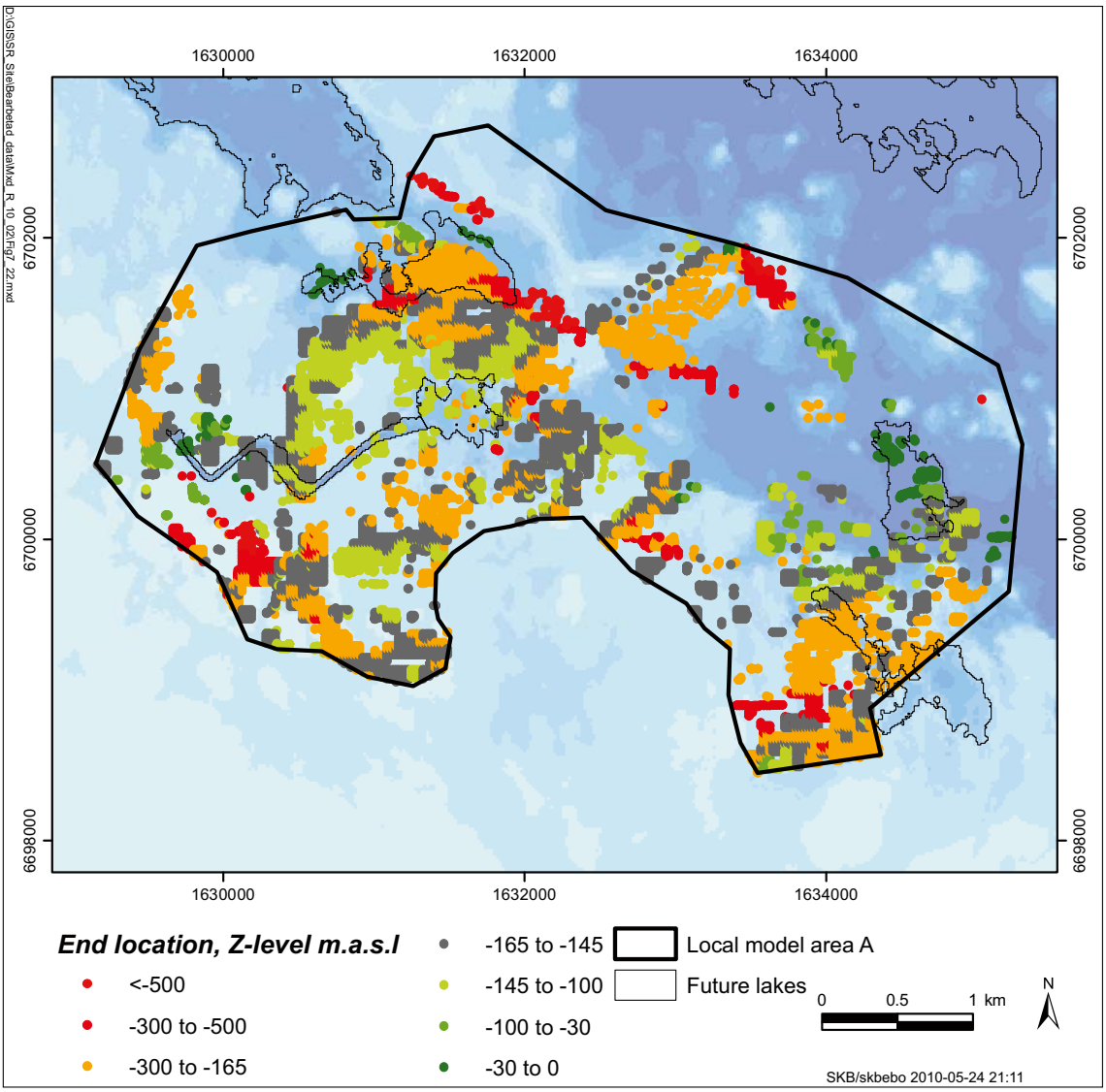

Figure 7-22. *Horizontal and vertical (colours) positions of particles left in local model A after 1,000 years of MIKE SHE PT simulation.*

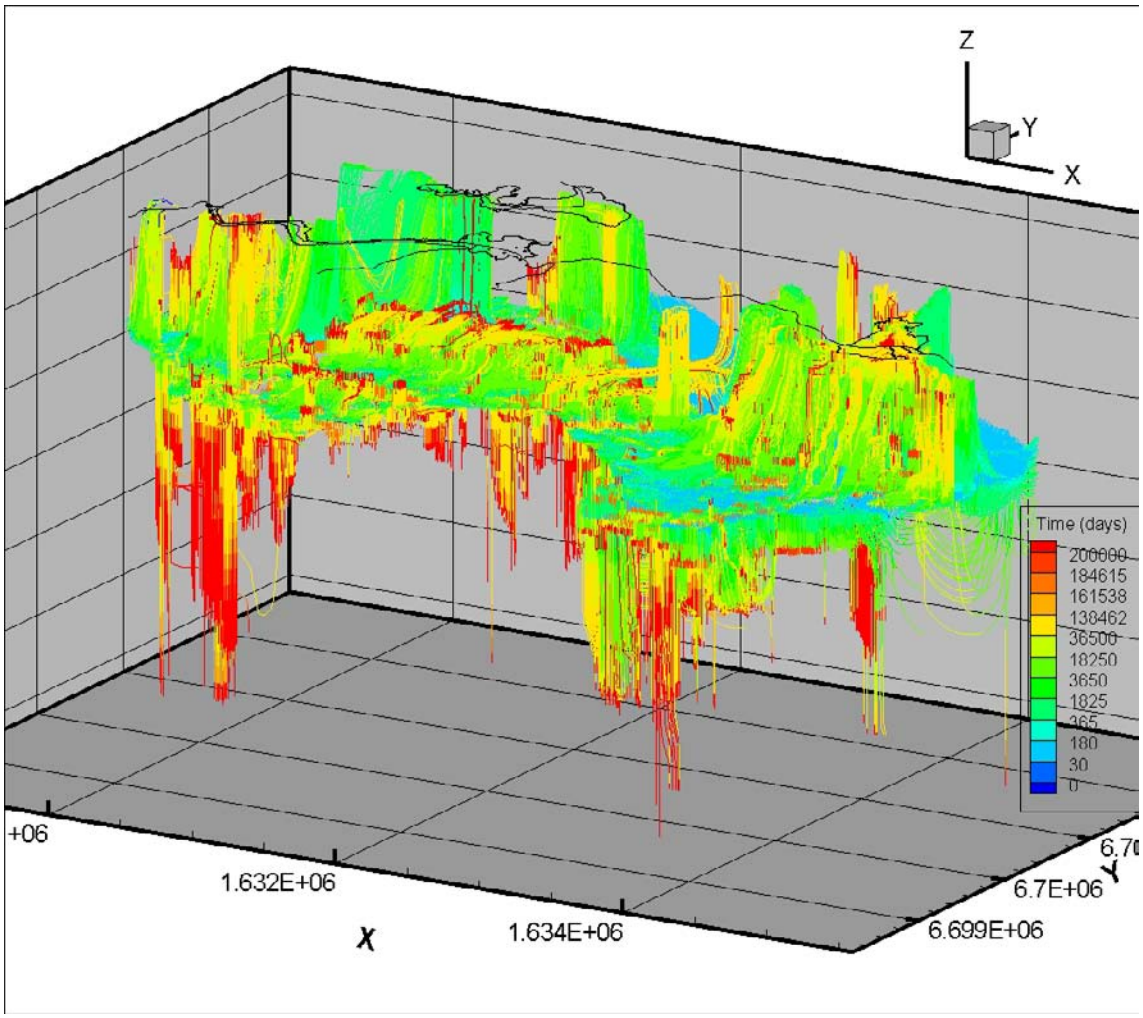

Figure 7-23. *Travel paths with colours indicating travel times for particles released at 150 m.b.s.l. within the area of the 10000AD_10000QD local model A. The colour of the travel times is changing along the flow paths, the accumulated travel time is illustrated in the figure.*

The figure shows that particles in some areas are transported almost vertically downwards. In other areas of the model domain, the particles are transported almost vertically upwards. The figure also shows that, due to the hydraulic gradient along the lake shoreline, the particles reach the lake shoreline before they reach the central parts of the lakes. For example, in object 118 the particles reaching the shoreline are indicated by green colours while the central part of the object is yellow. In the same way, for object 121_01 the shoreline is indicated by green or yellow colours, while the central part is red.

Figure 7-24 shows the pathways for all particles that have exit locations within object 118 and object 121_01. In the figure, the lake shorelines are illustrated by red lines, in the upper figure the shoreline of object 118 and in the lower figure the shoreline of object 121_01. It is seen that most of the particles with exit locations within object 121_01 have starting positions located more or less vertically below the lake area. For object 118, the same thing is seen for the eastern part of the lake. For the western part, however, the particles have starting positions much further away and the particles are being transported horizontally towards the north in layers with a high horizontal conductivity.

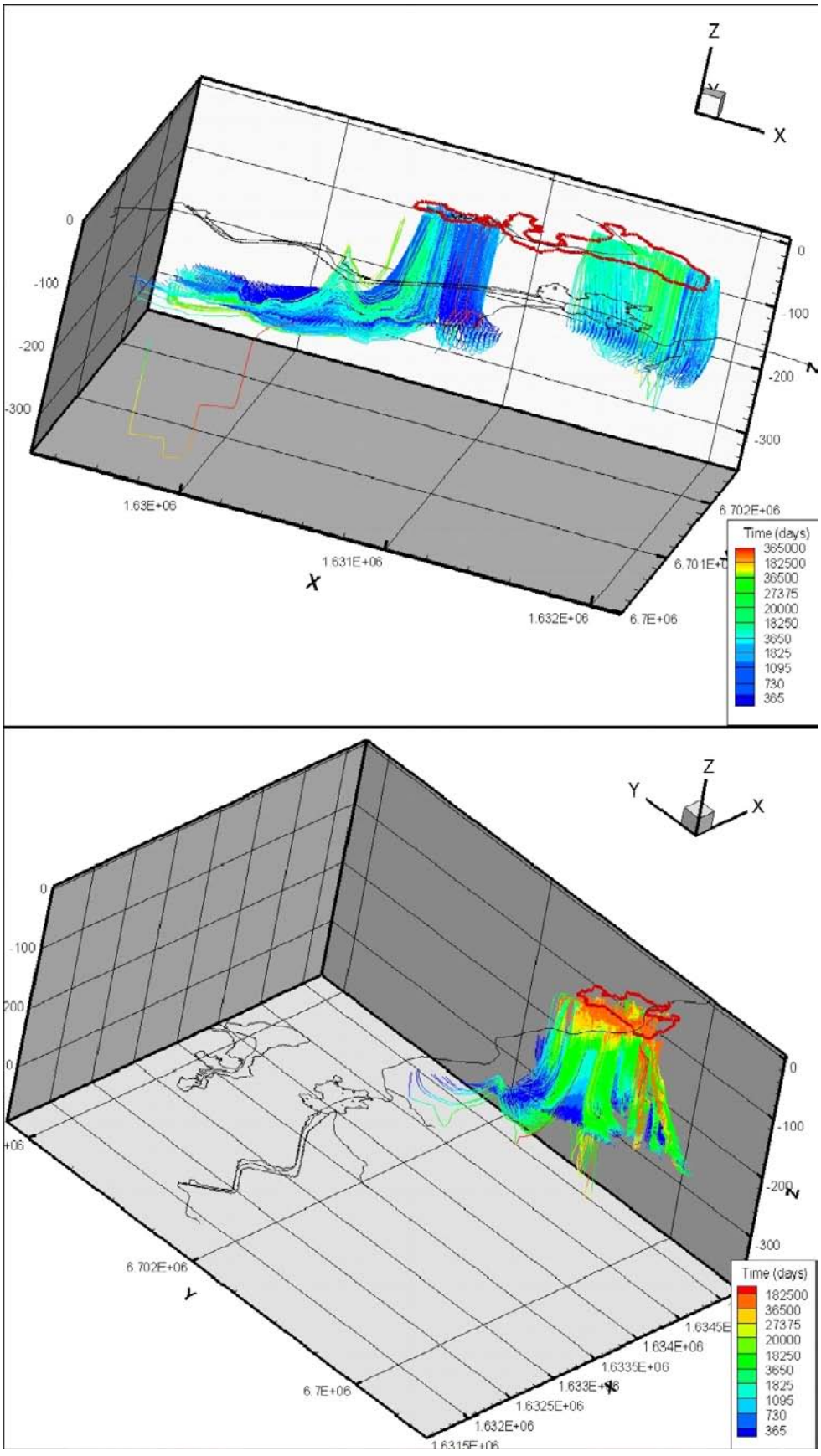

Figure 7-24. *Travel paths with colours indicating travel times for particles with exit locations within object 118 (upper figure) and object 121_01 (lower figure), based on a particle release at 150 m.b.s.l. in 10000AD_10000QD local model A.*

7.2.2 Advection-dispersion modelling

The main purpose with the advection-dispersion (AD) simulations is to investigate the transport pattern in and around the lake areas. The MIKE SHE model includes more surface processes than the ConnectFlow model used to define discharge locations in SR-Site, as well as more details in the description of the QD layers. As a consequence, the simulations made with the MIKE SHE AD transport module will give a better description of the transport pattern in the upper bedrock and in the QD layers.

In total, seven different simulations with the AD transport module were made for local model A, see Table 3-5. Two different types of input concentrations were used. Either the sources were continuous sources introduced at 40 m.b.s.l. at positions obtained from the ConnectFlow model (see Figure 3-7), or there was an initial concentration in a layer situated approximately 30 m.b.s.l. In all simulation cases the strength of the source is 1 g/m^3. The effect of using the AD module instead of the PT module was investigated. The simulations with the AD module were also used to investigate the effect of the different QD models for 2000 AD and 10,000 AD on the transport. Furthermore, simulations were made in order to study the effect of plant uptake and the hydraulic conductivities of the lake sediments.

Continuous injections along flow paths from the repository

Table 7-2 shows mass balance results for the simulations with the two different QD models, i.e. the model of the present QD and that describing the QD at 10,000 AD, and a continuous source at locations according to results from the ConnectFlow PT simulations (Figure 3-7) at 40 m.b.s.l. (i.e. in the saturated zone). Table 7-2 shows that for both models about 2/3 of the applied mass has left the model domain through some model sink. For the 10000AD_10000QD model the amount of mass that has left the model is a little larger than for the 10000AD_2000QD model. However, the amount of solute mass introduced is larger for the 10000AD_2000QD model, due to differences in the flow fields at the depth of the solute source. Table 7-2 also shows that in both simulations more than 90% goes to the surface stream while almost no solute reaches the boundary.

Figure 7-25 shows results from the AD simulation with a continuous source based on ConnectFlow particle positions at 40 m.b.s.l. Results are illustrated in terms of surface plots from the uppermost calculation layer for both QD models; results from the 10000AD_2000QD model are illustrated on the left side and those from the 10000AD_10000QD model on the right side. The figure shows that although the concentration patterns are similar for the two QD models, there are some differences.

For example, in the northern lake (object 118) the solute appears after shorter simulation time when using the QD model that represents present conditions. This is due to the fact that the 10,000 AD QD model contains more lake sediments, since the lake areas have been exposed to sedimentation for a longer period. This may also be seen in Figures 4-5 and 4-6, showing the topography of the two different local QD models. As time goes, however, the concentration patterns tend to be more similar for the two QD models and after 100 years of simulation the differences are rather small.

Table 7-2. Mass balances after 100 years of simulation for AD simulations in local model A with continuous sources at locations according ConnectFlow at the depth 40 m.b.s.l.

	10000AD_2000QD	10000AD_10000QD
Out from model (in % of applied mass)	**64.2**	**69.6**
To surface stream (in % of 'Out from model')	**91.2**	**93.6**
SZ drain to stream (in % of 'To surface stream')	0.4	3.4
SZ baseflow to stream (in % of 'To surface stream')	29.5	88.3
OL to stream (in % of 'To surface stream')	70.0	8.3
To boundary (in % of 'Out from model')	**0.0**	**1.0**
SZ flow to boundary (in % of 'To boundary')	100.0	0.1
SZ drain to boundary (in % of 'To boundary')	0.0	0.0
OL to boundary (in % of 'To boundary')	0.0	99.9
SZ to overland (in % of 'Out from model')	**8.5**	**5.4**

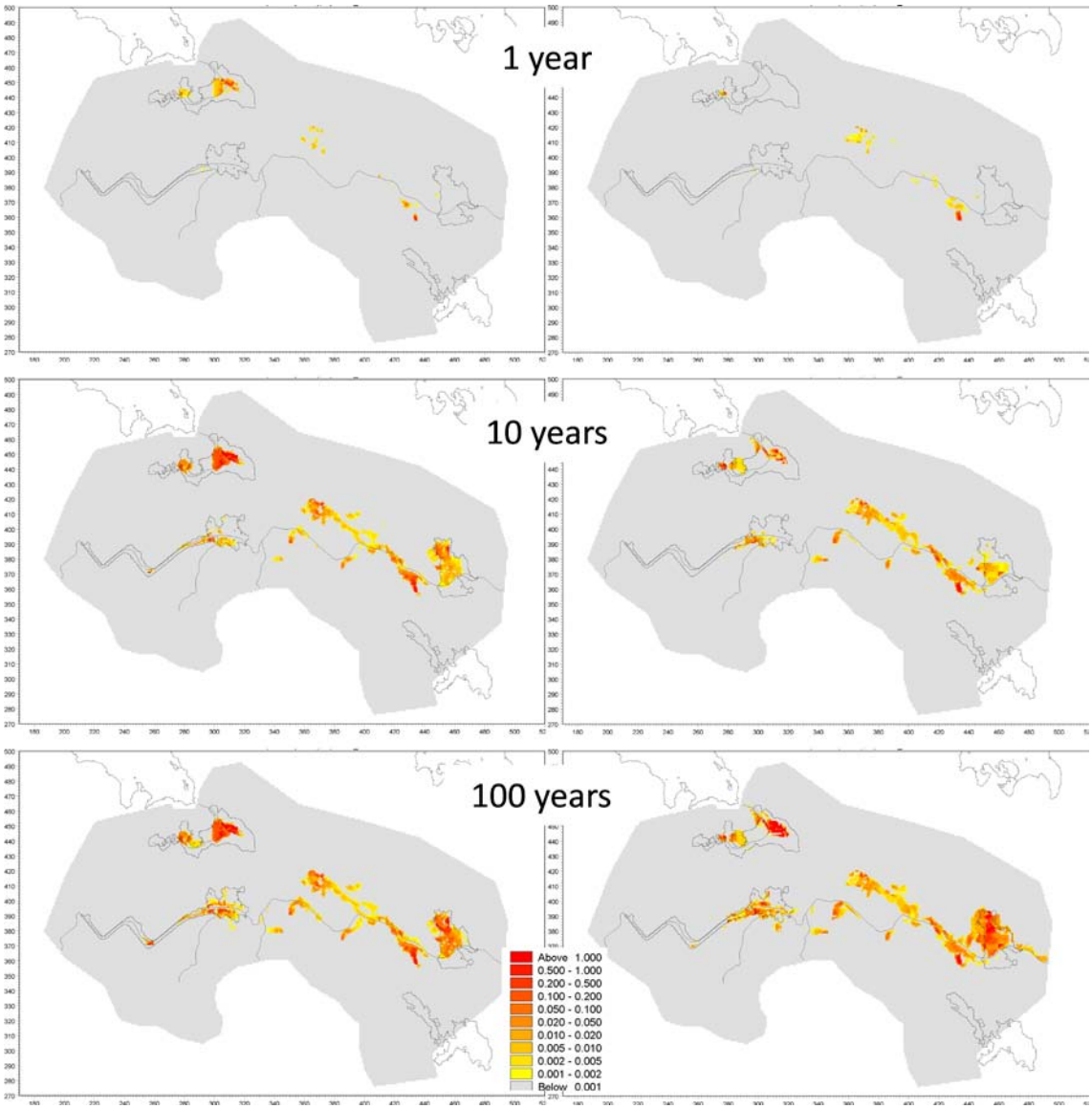

Figure 7-25. *Surface plots for the uppermost calculation layer for the local models based on the QD models describing present (2000 AD, on the left) and future (10,000 AD, on the right) QD distributions, in terms of solute concentrations after 1 year (upper), 10 years (middle) and 100 years (lower).*

Figure 7-26 shows a profile through object 118, for which solute concentrations are illustrated in Figure 7-27. The profile is taken from northeast to southwest. In the same way as in Figure 7-25, the concentration along the profile is illustrated for the 10000AD_2000QD model on the left side and for the 10000AD_10000QD model on the right side. Furthermore, the illustration is made for the same times as in Figure 7-25, i.e. 1, 10, and 100 years. The black lines indicate the lower levels of the MIKE SHE calculation layers. The bedrock layers are equal in both models, but there are differences for the QD layers, which are the upmost three calculation layers. The main difference is that in the 10,000 AD QD model the lake is terrestrialised and therefore the QD layers have a larger thickness there than the QD model describing the present conditions.

The different profiles show that after 1 year, the concentration in the 10000AD_2000QD model has already reached the surface at more than one location. In the northeast part of the lake the transport is almost vertical towards the surface. On the south-western part the concentration has reached the surface in a location outside of the profile and is spreading horizontally into the profile. After 100 years, the concentration has spread along almost the entire the profile.

When using the QD model for 10,000 AD, no solute has reached the surface along the profile after one year of simulation. After 10 years the concentration has reached the surface by an almost vertical transport. The horizontal transport that was seen in the 10000AD_2000QD model is not seen in the 10000AD_10000QD model. However, as time passes there is a horizontal movement of the concentration also in the 10,000 AD QD model. It appears that the solute is transported vertically in the north-eastern part of the lake and then spread horizontally towards the south-western part. The results discussed above are supported by the recharge and discharge areas illustrated in Figures 7-8 and 7-9, which show that the 10000AD_2000QD model has a stronger discharge pattern within object 118.

Figure 7-26. *Location of profile in object 118; the profile is taken from the north-eastern part of the lake towards the south-western part.*

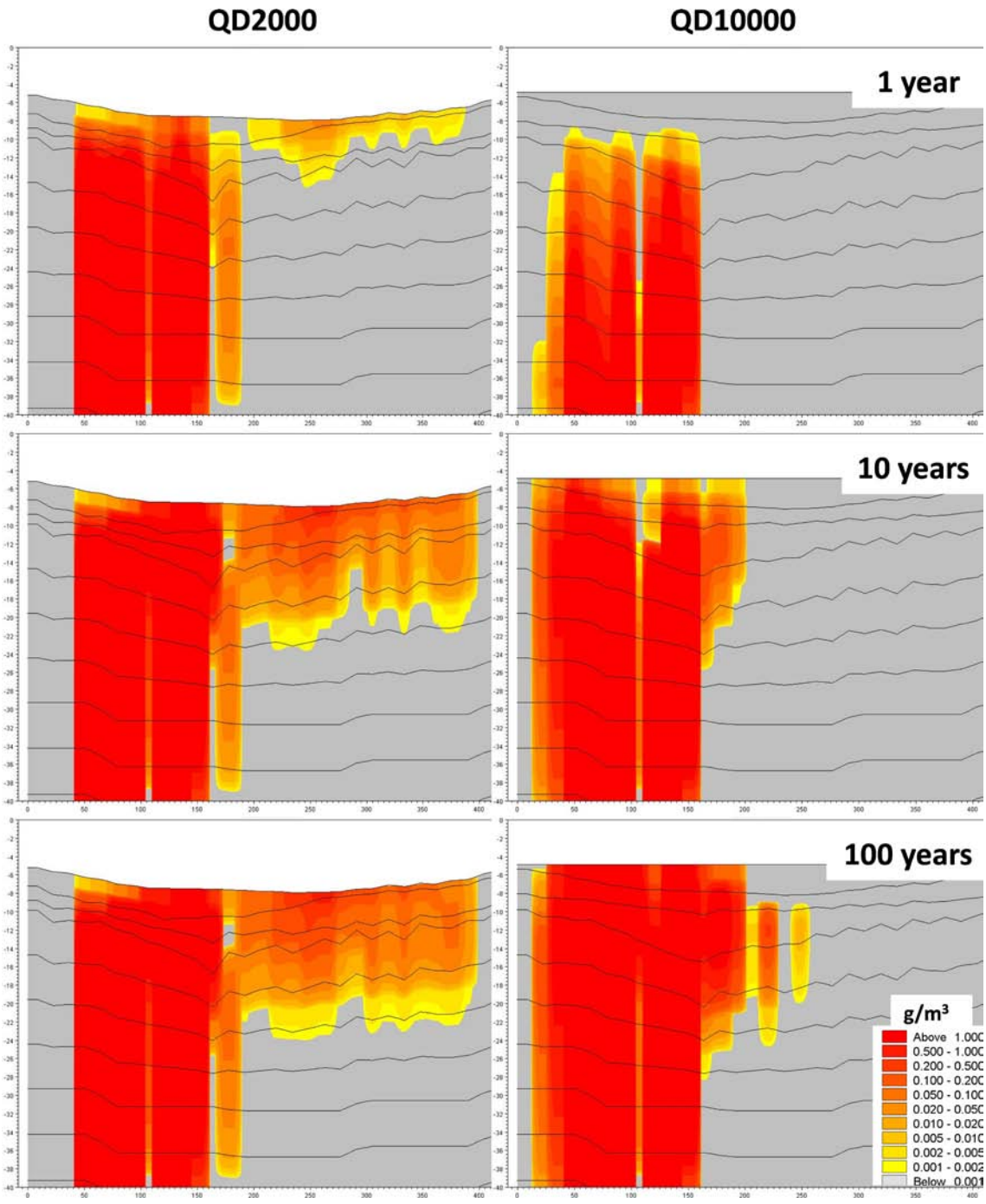

Figure 7-27. *Solute concentration along the profile across object 118. The profile is taken from north-east to south west. Results for the local 10000AD_2000QD model are illustrated on the left side of the figure and results from 10000AD_10000QD on the right side.*

Figure 7-28 shows concentration surface plots for different calculation layers for the simulation with the 10,000 QD model. Layer L1 is the uppermost calculation layer, which is a QD layer. Layer L4 is the uppermost bedrock layer. Layer L7 is located at a depth of c. 20–25 m.b.s.l. Layer L10 is located at the depth 35–40 m.b.s.l. and this is the layer in which most of the source is applied. Layer L14 is located at the depth 65–85 m.b.s.l. and layer 17 at c. 125–145 m.b.s.l. Layer L17 is the lowest layer in which solute with a concentration higher than 0.1 mg/m^3 was found. The figure illustrates that the solute is mainly transported vertically towards the surface. The solute reaches the surface along surface water streams and in connection to lake areas.

Figure 7-28 also shows that in parts of the model domain the solute is transported downwards. Figure 7-29 shows surface plots at layer 14 c. 65–85 m.b.s.l. after different times of simulation. After 10 years, the solute has reached layer 14 but it is still concentrated to the areas just below the source locations. After 25 years it is seen that the solute starts spreading towards the northeast. As time goes the solute is moving along layer 14 further north or northwest towards object 118.

To further examine the flow pattern in the area, two profiles were taken along the concentration plumes seen in layer 14. Figure 7-30 shows the location of the two profiles. In the figure, the blue dots are the locations of the sources. The sources are applied at the depth 40 m.b.s.l. The eastern profile is illustrated in Figure 7-31 and the western profile in Figure 7-32.

In Figure 7-31 it is seen that after 1 year of simulation the concentration is spreading downwards and in the layer situated just below the source, at a depth of about 40–50 m.b.s.l., the concentration starts spreading horizontally towards the north. After 10 years of simulation the concentration has spread a few meters further downwards and also somewhat further in the horizontal direction. After 25 years the solute has continued to spread downwards and has now reached a layer situated at c. 70 m.b.s.l., which is a layer with high horizontal hydraulic conductivity. As the solute reaches the layer it starts spreading horizontally within the layer towards the northeast. After 50 years the concentration plume is still moving within the layer towards the northwest and after 100 years the main part of the plume is still within the layer although the plume is also spreading to layers situated above.

Figure 7-32 shows results from the western profile. After 1 year the solute has started spreading downwards but a small portion of the solute is also moving horizontally in a layer situated at c. 45 m.b.s.l. After 10 years of simulation, the solute concentration plume has spread further downwards but also horizontally along two different layers, at c. 55 m.b.s.l. and c. 90 m.b.s.l. After 25 years the solute is mainly moving towards the north along the layer situated at 90 m.b.s.l. and this is seen also after 50 years and 100 years of simulation.

From most of the source locations the solute is transported upwards, towards lakes or surface water courses. Results from the particle tracking in Section 7.2.1 indicated that for the lake areas the solute appears along the lake shorelines, see Figure 7-17. However, in a PT simulation it is not possible to trace the particle once it has reached a sink, for example the unsaturated zone or the overland, because the particles are removed from the model. An AD simulation on the other hand, shows the spreading of the solute also after reaching the surface. To illustrate this for object 121_01, a profile is taken along the west-east direction, see Figure 7-33.

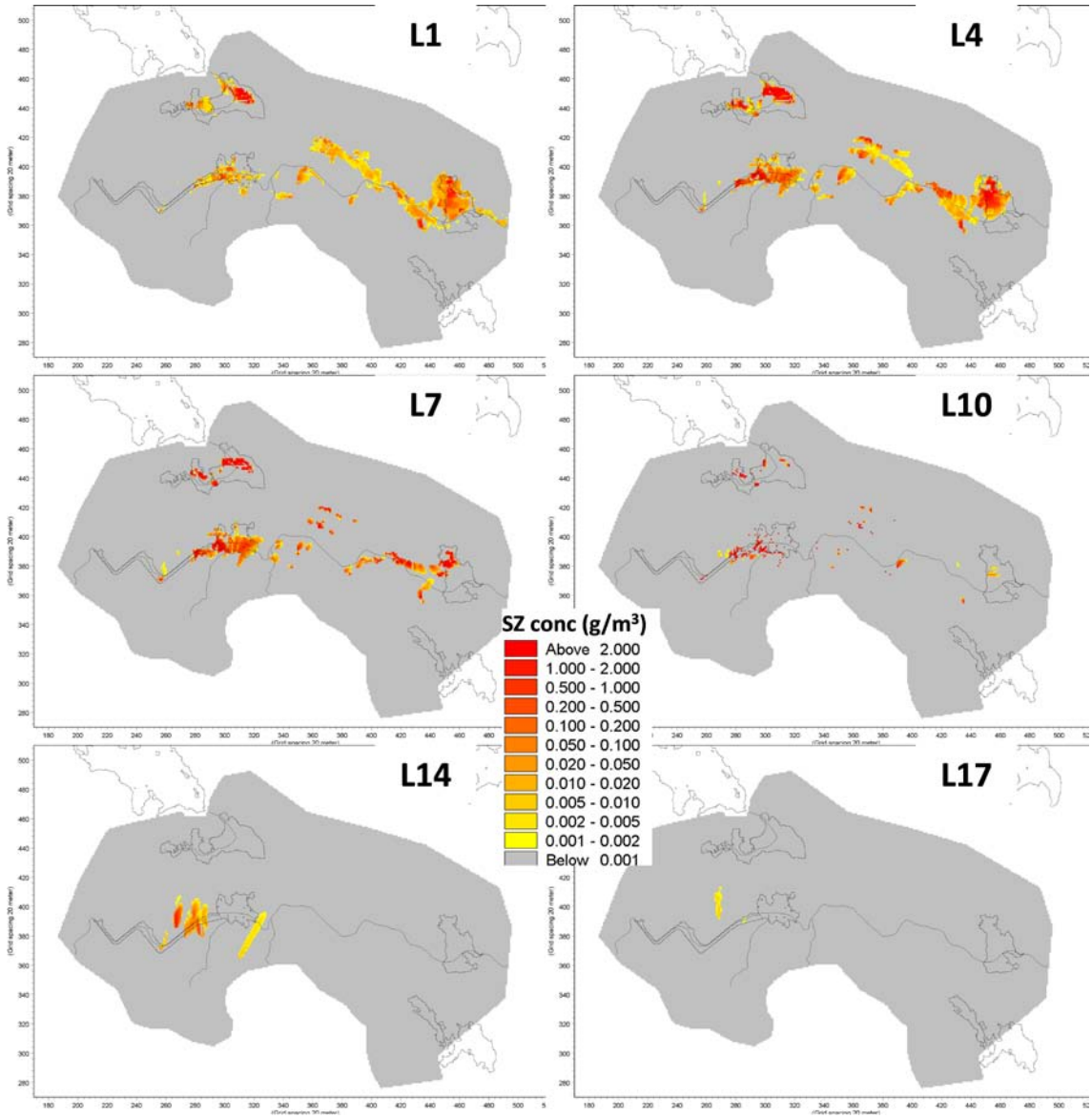

Figure 7-28. *Surface plots of concentrations in different calculation layers for the local 10000AD_10000QD model; all plots show results after 100 years of simulation.*

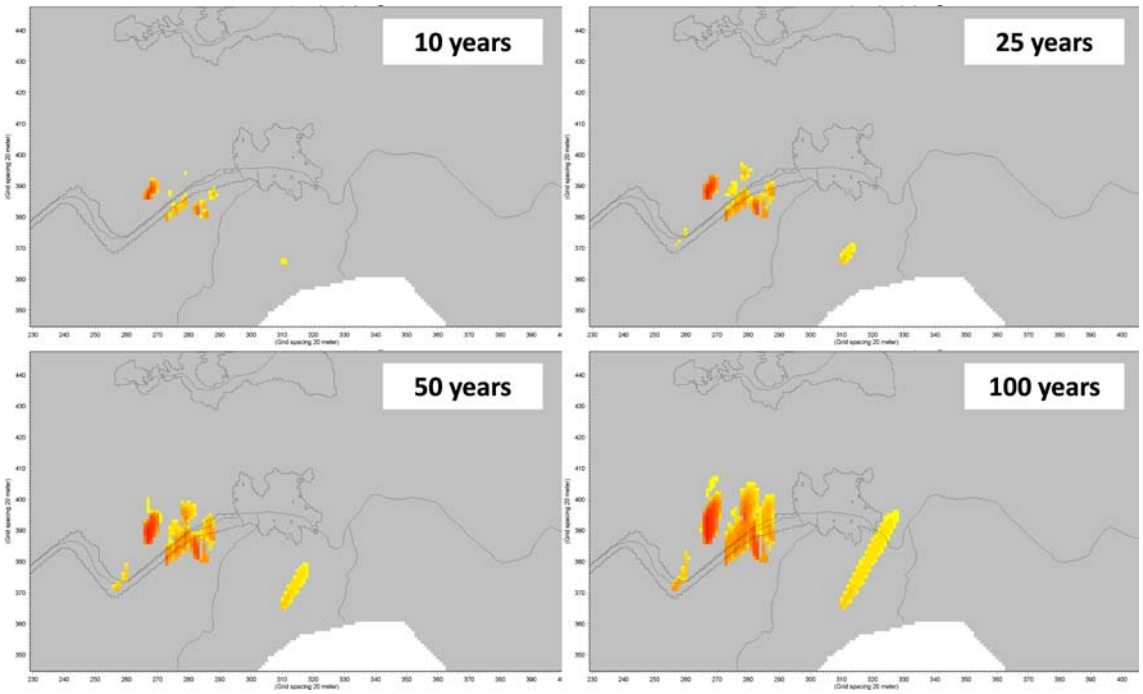

Figure 7-29. *Surface plots of solute concentrations in the central part of the 10000AD_10000QD version of local model A for calculation layer L14 situated at approximately 65–85 m.b.s.l., which is below the solute source.*

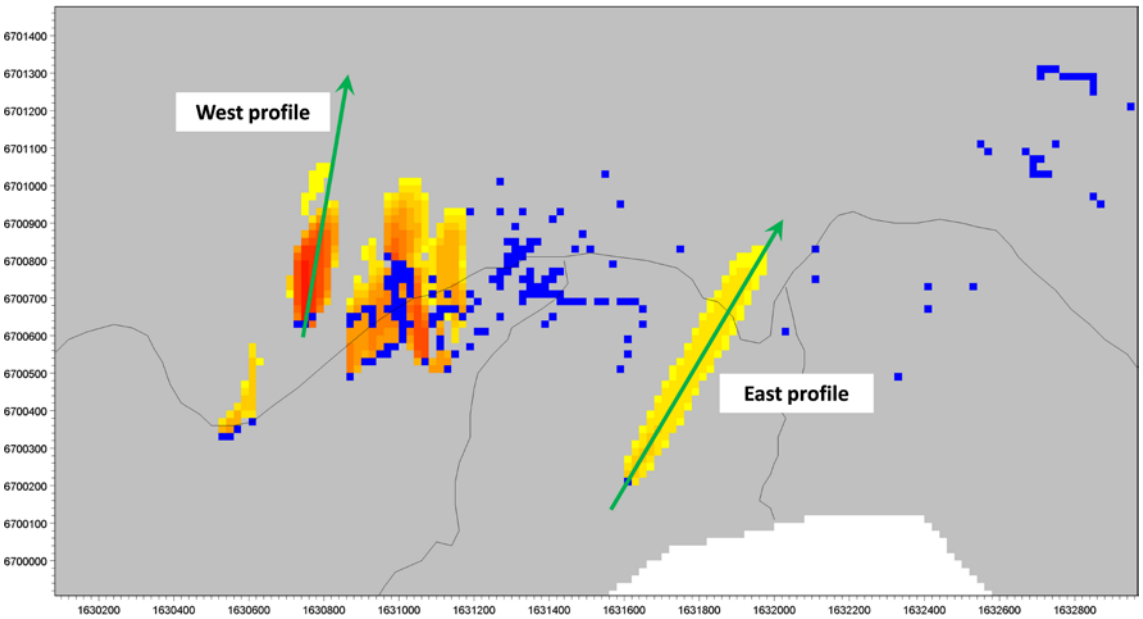

Figure 7-30. *Locations of the eastern and western profiles in 10000AD_10000QD local model A. The profiles are taken from the south towards the northern part of the model domain.*

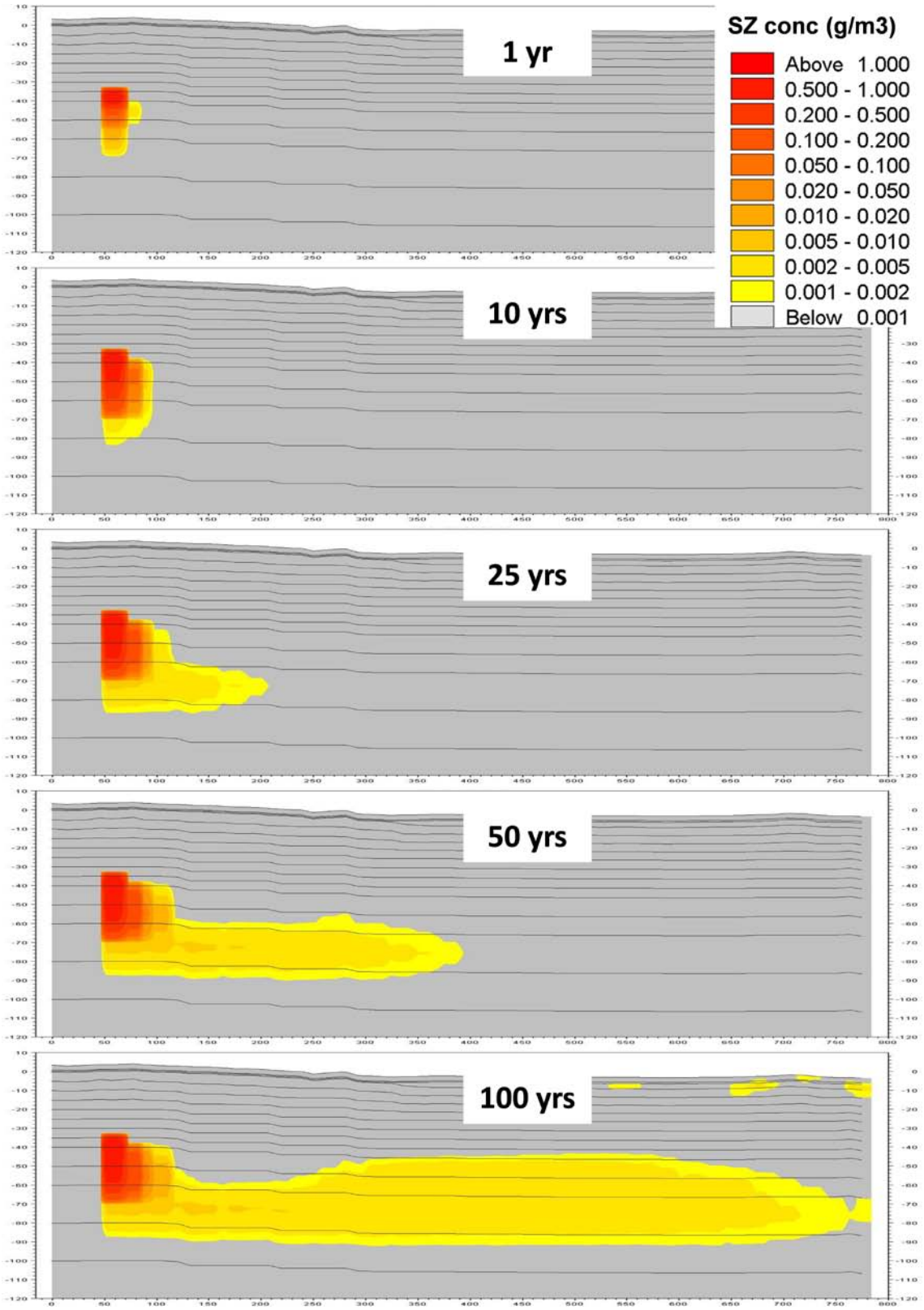

Figure 7-31. *Concentration along the eastern profile in Figure 7-30 after 1, 10, 25, 50 and 100 years of simulation.*

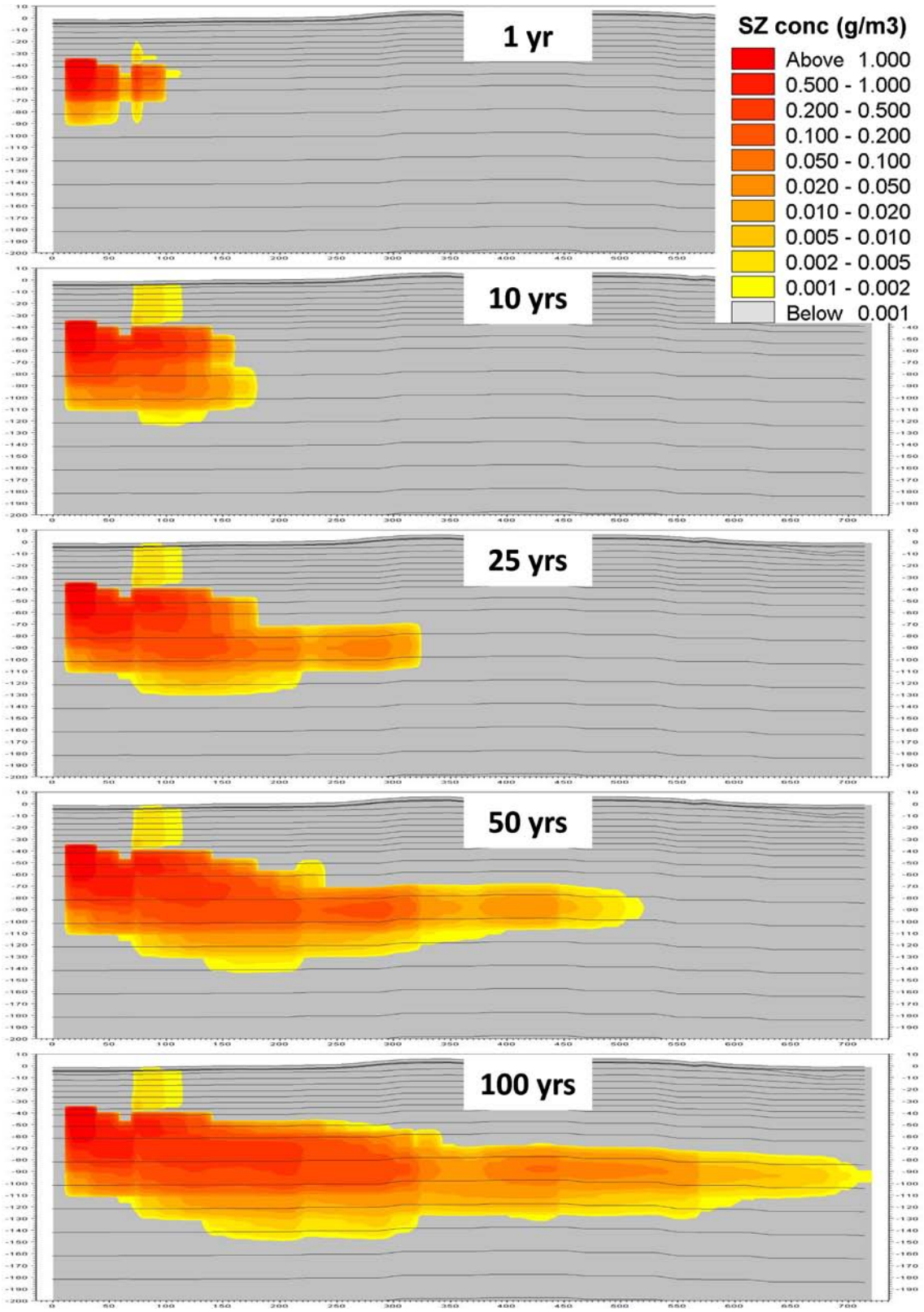

Figure 7-32. *Concentration along the western profile in Figure 7-30 after 1, 10, 25, 50 and 100 years of simulation.*

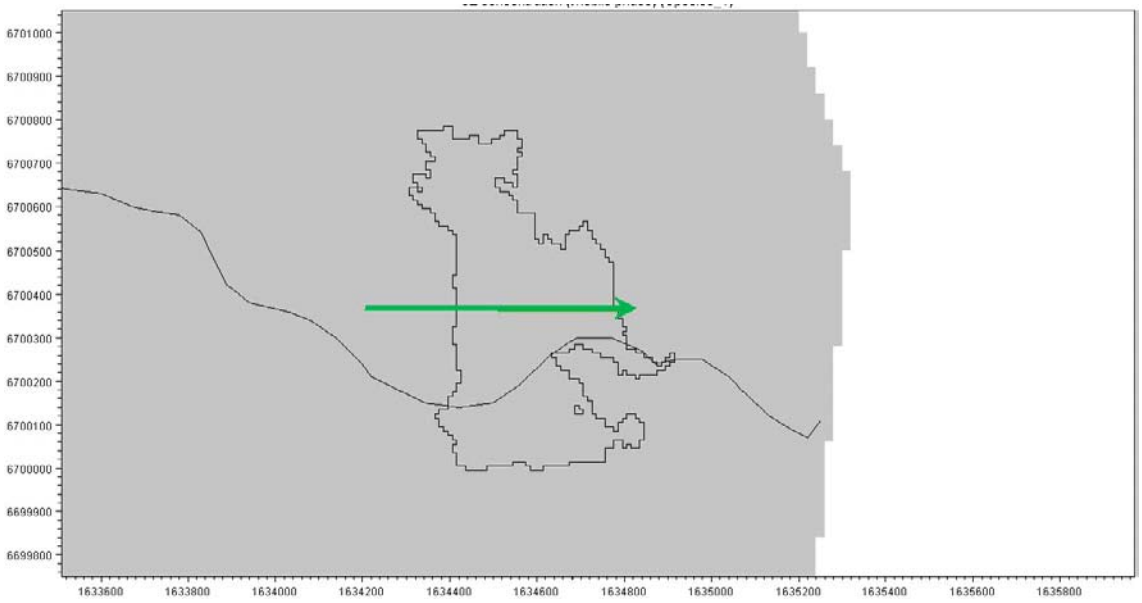

Figure 7-33. *Profile taken across object 121_01 in the 10000AD_10000QD local model A. The profile is taken from the west towards the east.*

Figure 7-34 shows the transport pattern for the profile. Since the source is based on the points obtained from the ConnectFlow model, see Figure 3-7, solute is applied only at a few locations. The figure indicates that the solute is mainly transported vertically upwards to the surface and then starts spreading horizontally in the top layers. As time goes, the solute that spreads horizontally starts to infiltrate and migrates downwards. However, some of the injected solute mass is also transported horizontally just below the depth of the source. This plume is transported towards the west and is only moving horizontally, at least for 100 years of simulation.

Comparison between advection-dispersion and particle tracking results

A PT simulation was made with the same source type as the AD simulation presented above, i.e. a continuous source at particle positions according to the ConnectFlow model at c. 40 m.b.s.l. (see Figure 3-7). The purpose of the simulation was to study the effect of dispersion on the transport results, since the particle tracking is a purely advective transport simulation.

In the PT simulation, only the saturated zone is included for particle transport and particles are removed from the model as soon as they reach a sink, for example the unsaturated zone or a surface stream. Therefore, it is not obvious which layer to use in the comparison between the PT and AD simulations. Figure 7-35 shows the accumulated particle count after 100 years of the PT simulation in calculation layers 1 to 4, i.e. all three QD layers and the uppermost bedrock layer. The figure shows that layer 3 has the largest amount of accumulated particles.

Figure 7-36 shows the numbers of particles that are present in the uppermost four calculation layers after 100 years of simulation. Since the source is continuous, there are still several particles left in the model after 100 years of simulation. However, the differences in the number of particles, compared to the accumulated particle count in Figure 7-35, show that many particles have left the model.

Figure 7-37 shows the results of the PT simulation to be compared with the results from the AD simulation with the same type of sources. Results are compared in the third calculation layer since particles are removed from the PT simulation in the uppermost two calculation layers. The figure shows that the PT simulation results in more concentrated areas with a higher solute concentration than the AD simulation. The reason is that the PT simulation does not include any dispersion or diffusion.

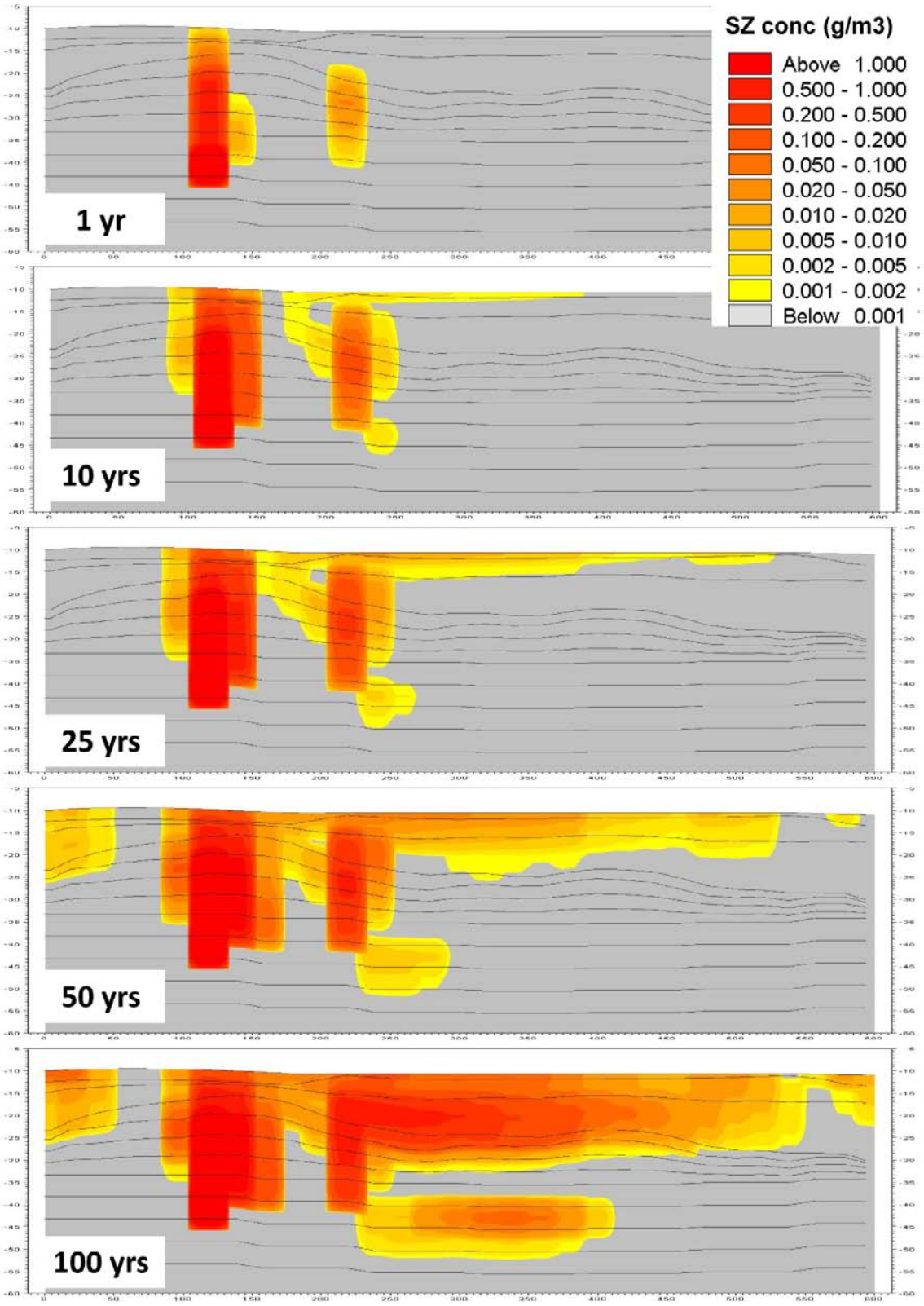

Figure 7-34. *Concentration along the profile across object 121_01 in Figure 7-33 after 1, 10, 25, 50 and 100 years of simulation.*

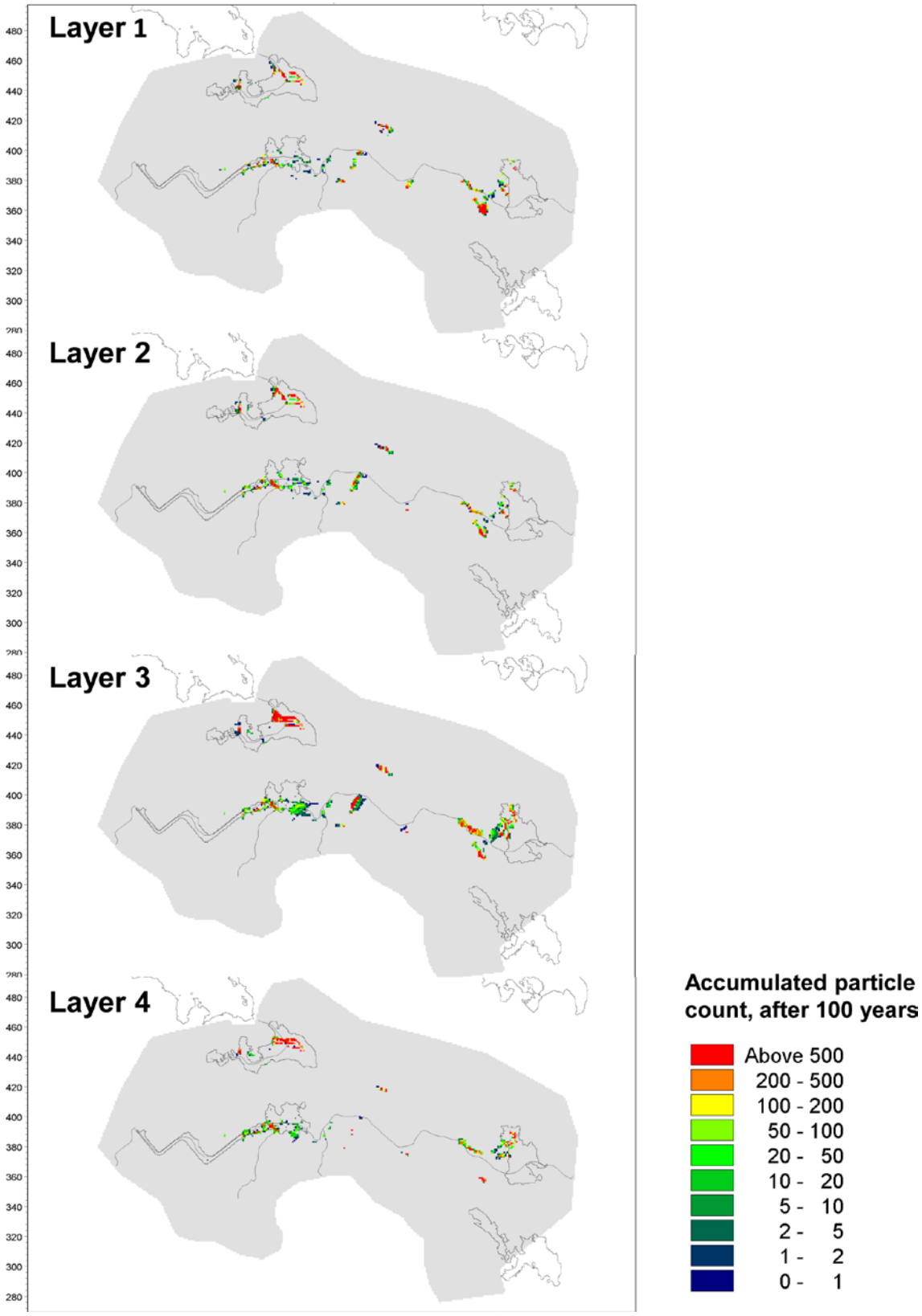

Figure 7-35. *Accumulated particle count after 100 years for a PT simulation with local model A with continuous sources in positions obtained from the ConnectFlow model.*

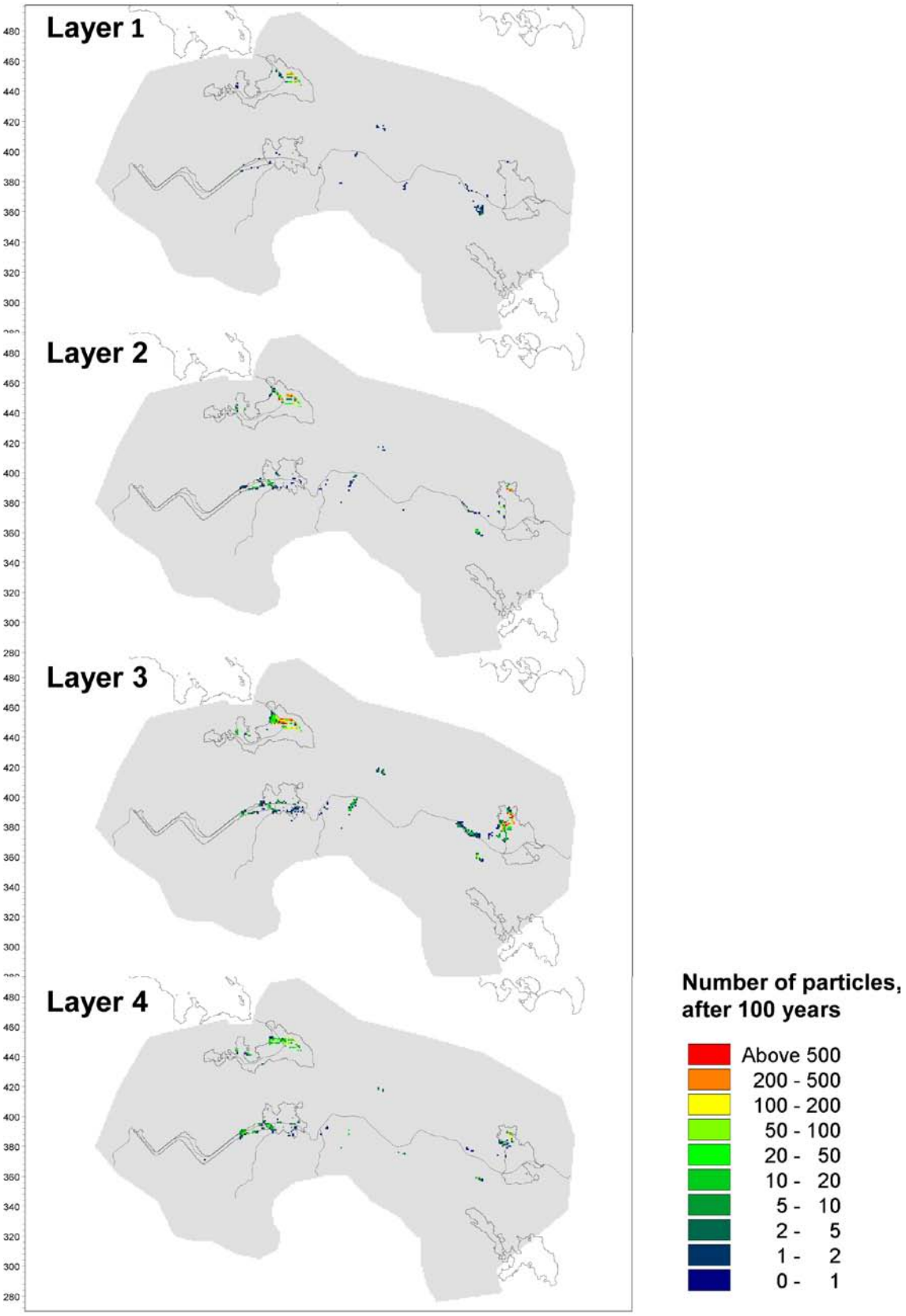

Figure 7-36. *Numbers of particles present in layers 1–4 after 100 years of PT simulation with local model A with continuous sources in positions obtained from the ConnectFlow model.*

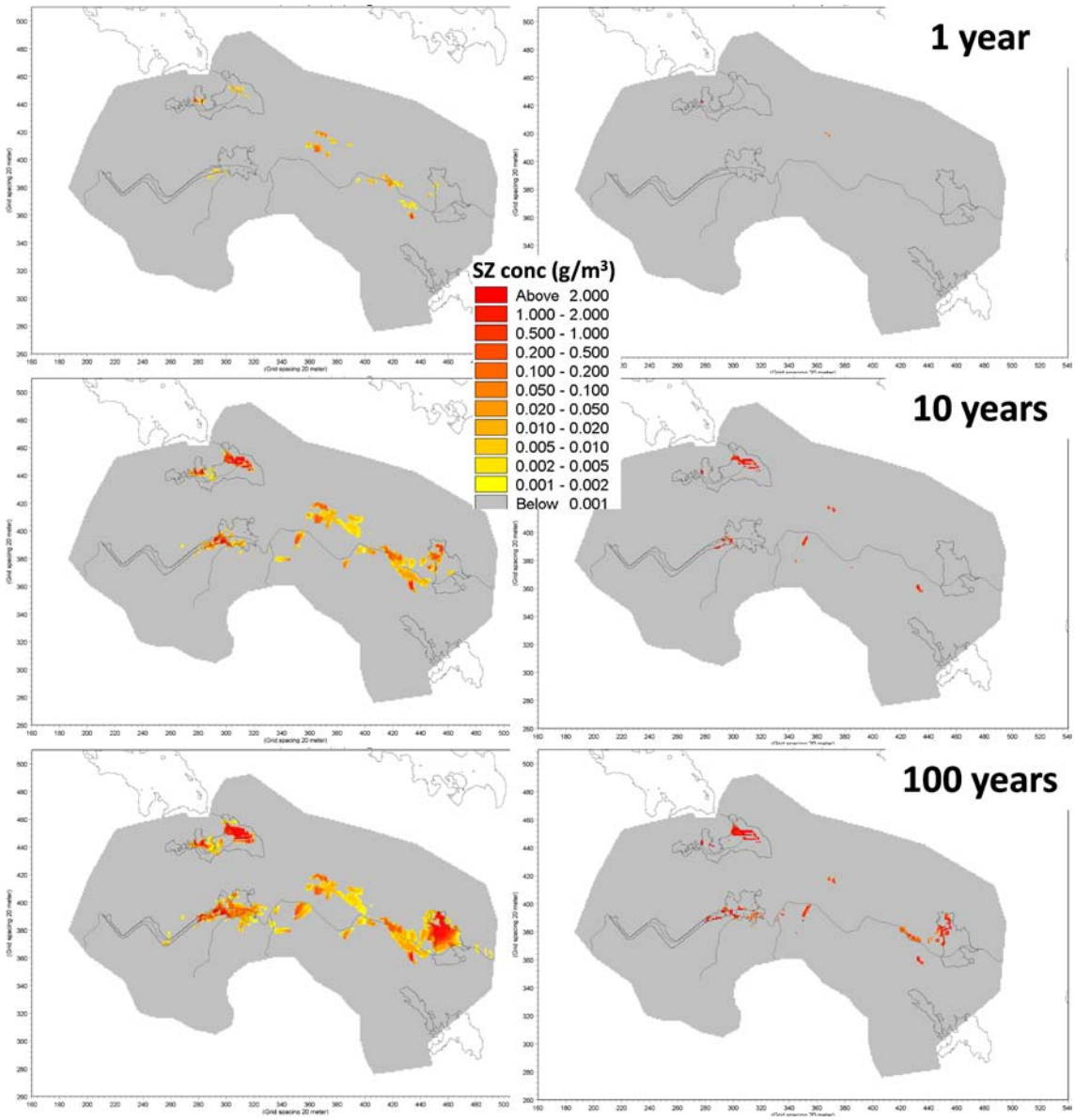

Figure 7-37. *Comparison between simulation results based on the 10000AD_10000QD local model A with the AD module (left side) and the PT module (right side) with the same type of source; results are illustrated as surface plots for calculation layer L3.*

Figure 7-37 also shows that there are some areas that do not receive any solute at all in the PT simulation, whereas the AD simulation shows apparent areas with solute concentration, for example in the area between object 118 and object 121_01. The reason for this is that the number of particles produced in the particle tracking simulation depends on the given concentration. The mass of a particle is given in the model setup and based on the concentration, the groundwater flow and the particle mass, a number of particles are produced. If the concentration is low and the particle mass high, no particles are produced.

By lowering the particle mass, more particles are produced, but this also makes the simulation more time and computer memory consuming. Figure 7-38 shows the locations of the particles produced in MIKE SHE compared to the input locations according to positions delivered from the ConnectFlow model for a part of the model domain. Figure 7-38 illustrates that there are some areas in which the concentration and/or the groundwater flow is too low to yield particles for the PT simulation. For the AD simulation however, a concentration is given at all ConnectFlow positions.

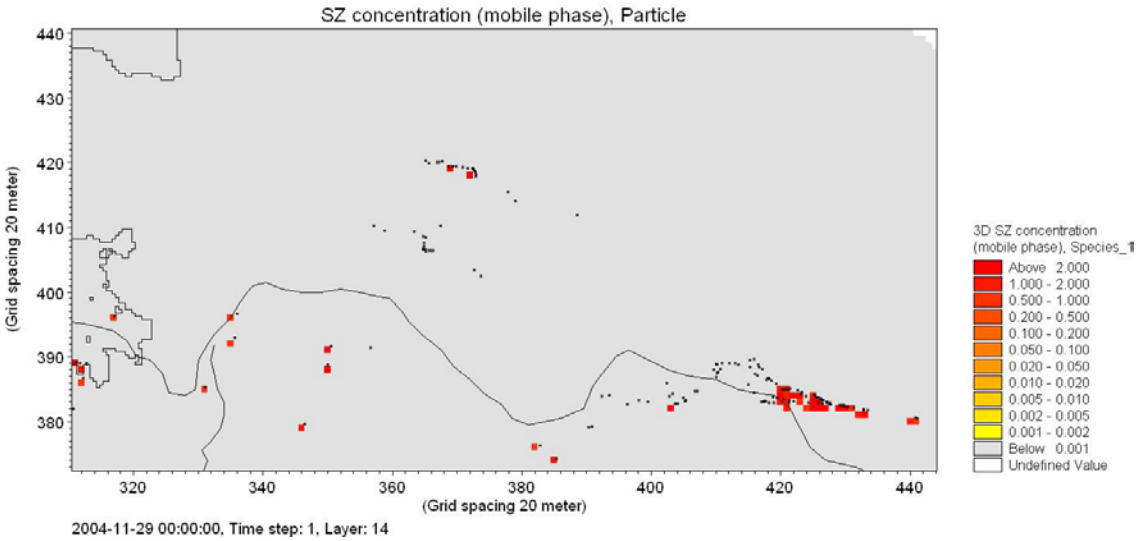

Figure 7-38. *Locations of produced particles in the particle tracking (red dots) and locations of the original input positions obtained from the ConnectFlow model (black dots).*

Effects of plant uptake

In the AD simulations presented above, the effect of plant uptake was not considered, i.e. the "plant uptake factor" in MIKE SHE was set to zero. The plant uptake factor is the factor that determines the rate at which plants will remove the mobile solute from the water. When the plant uptake factor is equal to zero, the solute is accumulated in the upper layers until leaving the model through either a surface stream or a boundary. Therefore, a simulation with no plant uptake will result in concentrations that are higher than expected close to the surface.

The plant uptake factor is an empirical factor that determines to what extent the available solute is taken up by the plants. Different roots have different capabilities when it comes to filtering out various solutes. The plant uptake is a passive transport coupled to the transpiration and is expressed as a function of the solute concentration in the liquid phase. The plant uptake is calculated according to

$$R_r = f_c \, S_r \, c$$

Where R_r (g/m^3/s) is the sink term in the AD equation, f_c (-) is the plant uptake factor, S_r (/s) is the root water uptake, and c (g/m^3) is the solute concentration.

The areas in which the solute appears on the surface are mainly wetland areas with vegetation. To make a sensitivity analysis of the effects of plant uptake, a simulation with a full plant water uptake in the whole model area was made, i.e. a case in which the plant uptake factor was set to one was modelled. In this way the two extremes with regard to plant uptake were investigated. In the MIKE SHE model, the plant uptake is a sink term, which means that once the concentration has been extracted by the plants it will disappear from the model volume. In reality, this would represent a situation where the plants are being removed from the surface, e.g. harvested, so that the concentration disappears from the system. However, if the plants are not removed the plant will decompose and the solute concentration will remain on the soil surface and is allowed to infiltrate again. So, even if the sensitivity cases represent two extremes with regard to the plant uptake, it is not obvious which the most realistic case is since it depends on how the soil and the plants are being used.

A comparison between the results in terms of solute concentration in the saturated zone, with no or full plant water uptake, is shown as surface plots in Figure 7-39. Shown on the left side are the results from the simulation with no plant uptake and on the right side those obtained with full plant uptake. The difference between the two cases is seen as time goes and the concentration appears in the lake areas. Especially for object 121_01 the difference between the results is distinct. After 10 years of simulation almost no concentration is seen within the lake area for the case with full plant uptake, while a large part of the lake is covered for the case with no plant uptake. After 100 years of simulation there is still a large difference between the two simulations for object 121_01.

For the case with no plant uptake almost the entire lake area is covered by solute, while only the lake shoreline is covered for the case with full plant uptake. In the year 10,000 AD, object 121_01 is a wetland area covered by vegetation, but since the plant uptake removes the solute from the water, the difference is larger for the lake area, and smaller for the lake shoreline. The pattern illustrated in Figure 7-39 is similar if looking at the concentration in the unsaturated zone.

To further illustrate the effect of the plant uptake in object 121_01, the profile in Figure 7-33 is shown also for the case with full plant uptake, Figure 7-40. A comparison with the results based on no plant uptake, presented in Figure 7-34, shows that the horizontal spreading in the lake sediments is significantly reduced when plant uptake is considered. In Figure 7-34 it is illustrated that after 25 years almost the entire upper layer is covered by solute in the uppermost layer, while in Figure 7-40 only the vertical transport is seen in the figure. This is because the plants remove the solute from the uppermost layer at that time. As time goes, there is still a spreading along the profile in Figure 7-40, although the spreading mainly takes place in the third layer, which is the deepest of the QD layers.

Looking at the concentration curves in a single cell column in object 121_01 further illustrates the plant uptake in areas with vegetation. Figure 7-41 shows the location of the selected cell column and Figure 7-42 shows the concentration curves in calculation layers L1 to L4. In the upper figure the curves are illustrated for the case with no plant uptake and in the lower figure with full plant uptake. For layer 4, which is a bedrock layer, and layer 3, which is the deepest QD layer, there is no difference between the two simulations. For layer 2 the concentration is somewhat lower for the case with full plant uptake. The big difference in the results is for calculation layer L1, which is the uppermost layer in which the plant processes are active. After 100 years of simulation, the concentration in the simulation without plant uptake is just above 1 g/m^3, while the concentration for the simulation with full plant uptake is close to zero.

Figure 7-43 shows the total plant uptake from the unsaturated (red line) and saturated (blue line) zone during the 100 years of simulation. The plant uptake from the unsaturated zone is much smaller than the uptake from the saturated zone, approximately 15–20% of the uptake from the saturated zone. The reason is that most of the solute appears on the surface in areas which are saturated or close to saturated, i.e. in the lake areas and in connection to surface water courses.

Figure 7-44 shows how the plant uptake is distributed over the year. The figure is taken for a year after c. 50 years of simulation. The figure illustrates that the plant uptake is active from March to August. The total yearly plant uptake from the saturated zone is approximately 3–3.5 kg/year for the entire model domain, based on a continuous source with a concentration of 1 g/m^3. The plant uptake from the unsaturated zone is approximately 0.5 kg/year.

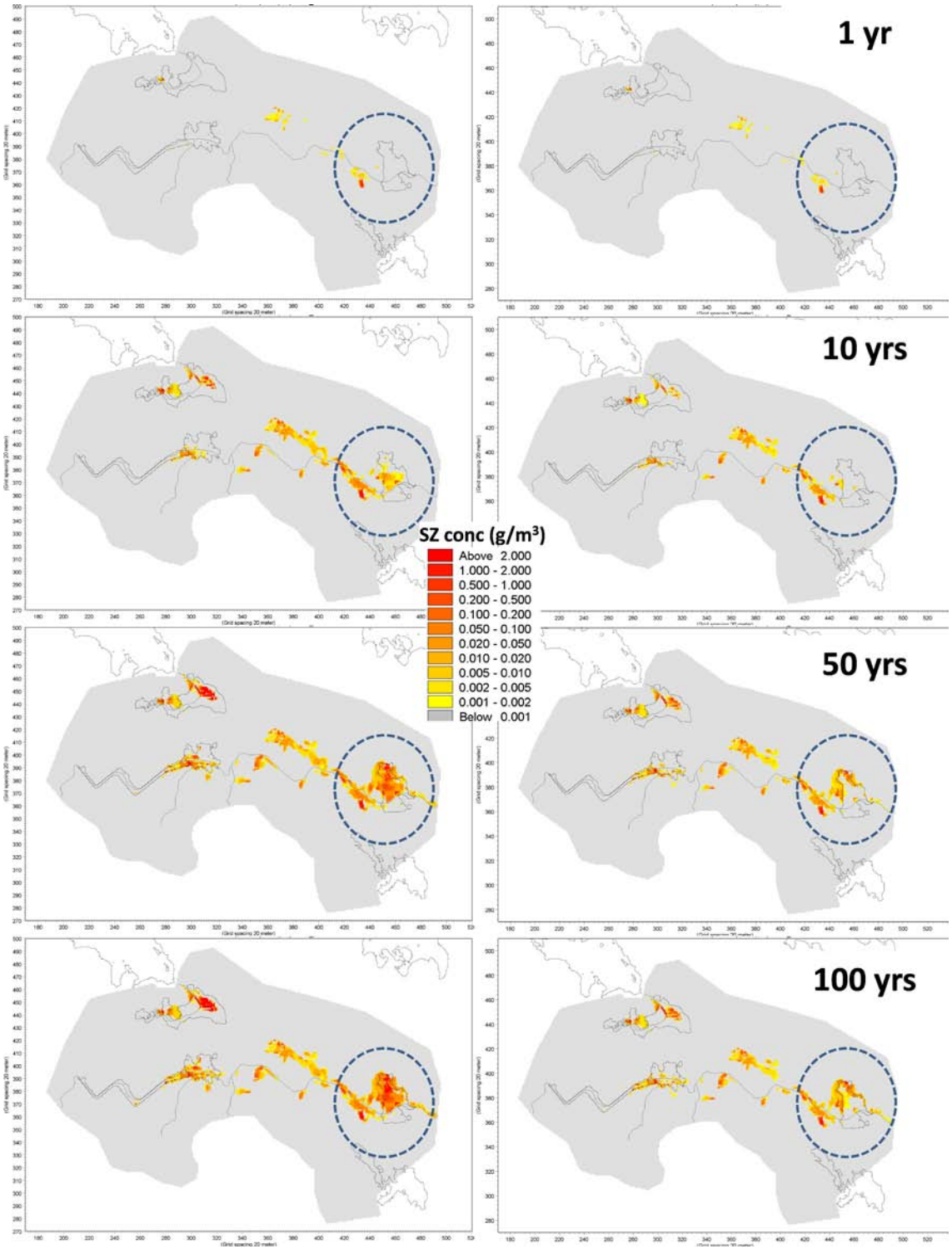

Figure 7-39. *Effect of plant uptake in the saturated zone for local model A. On the left side results are illustrated for the case with no plant uptake and on the right side with full plant uptake. Both simulations are based on the 10000AD_10000QD version of the model.*

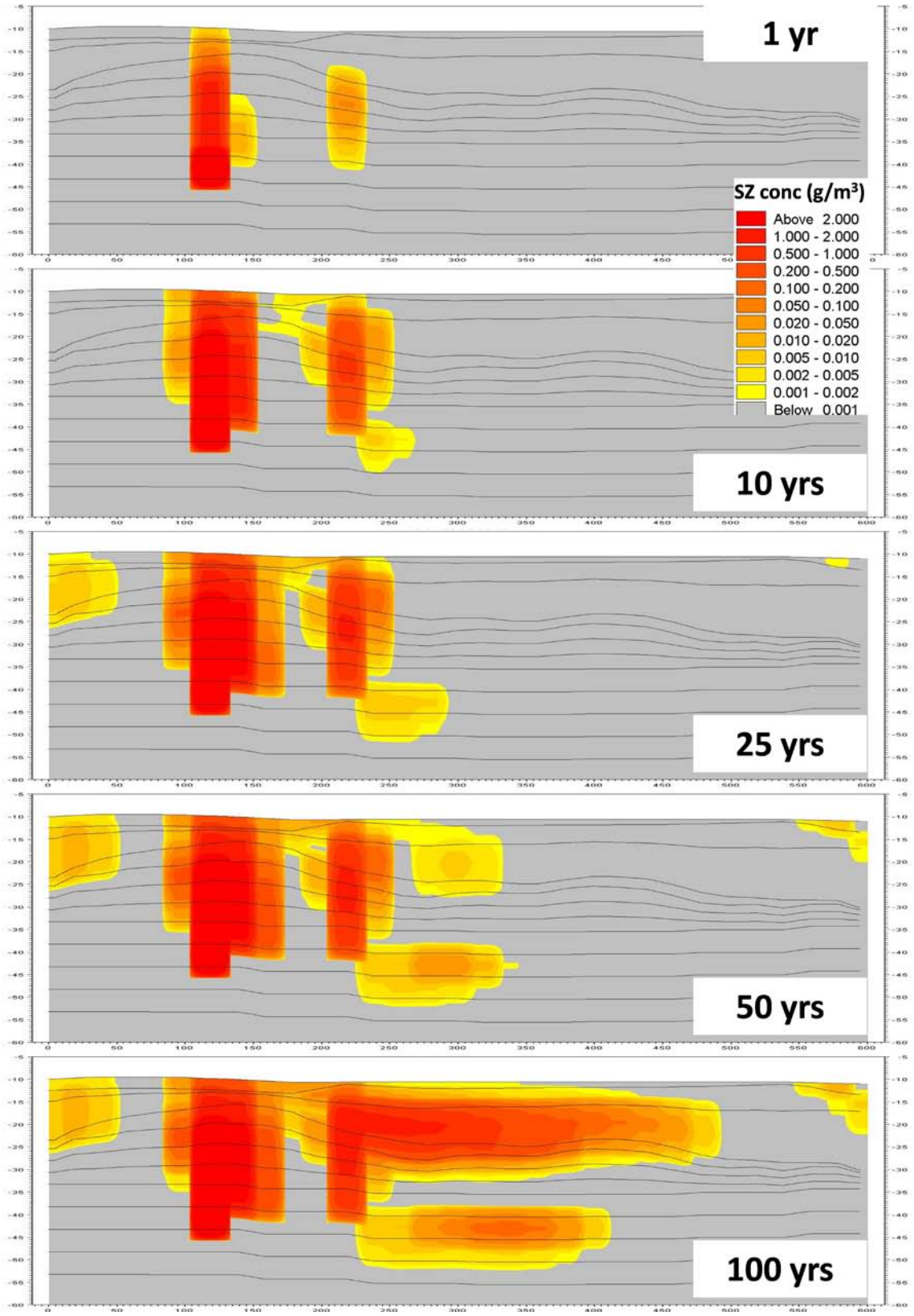

Figure 7-40. *Concentration plots along the profile across object 121_01 illustrated in Figure 7-33 after 1, 10, 25, 50 and 100 years of simulation.*

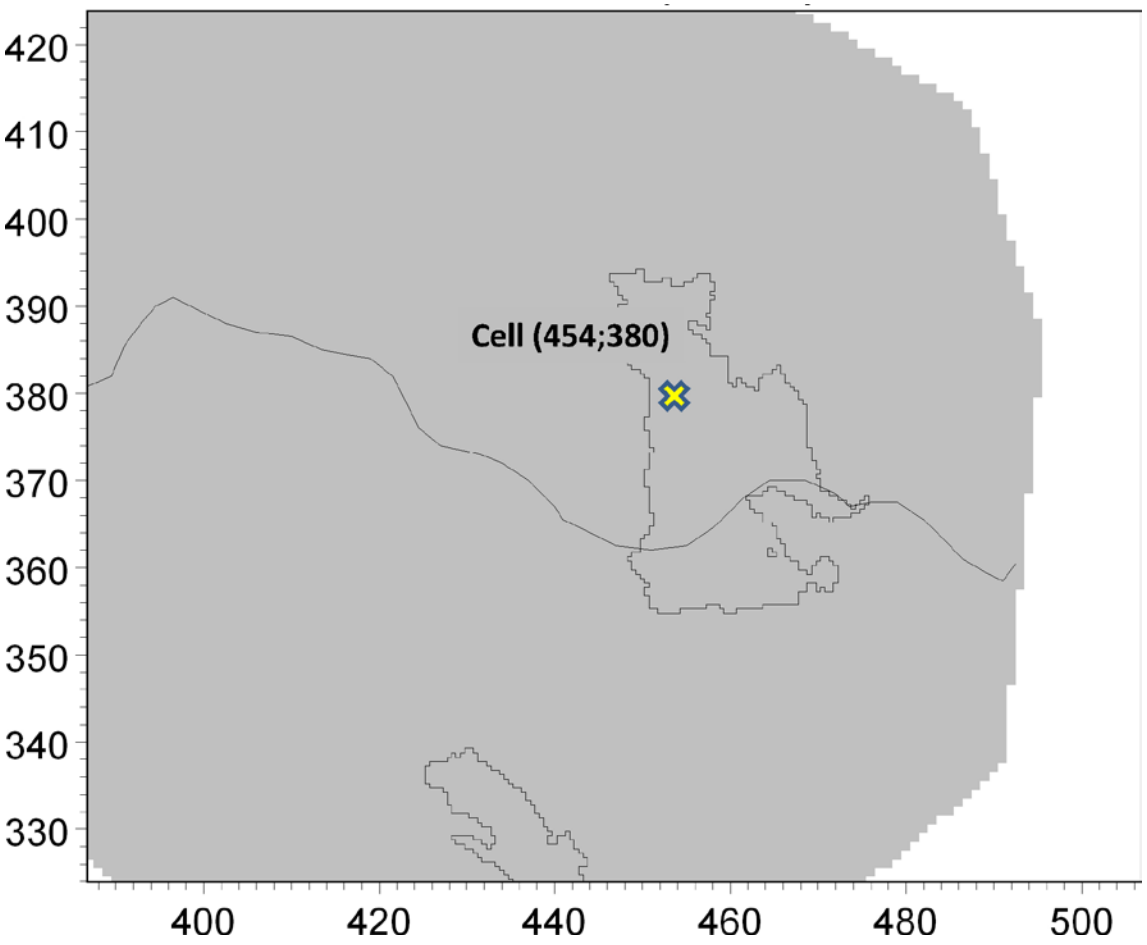

Figure 7-41. *Location of cell (454;380) within object 121_01.*

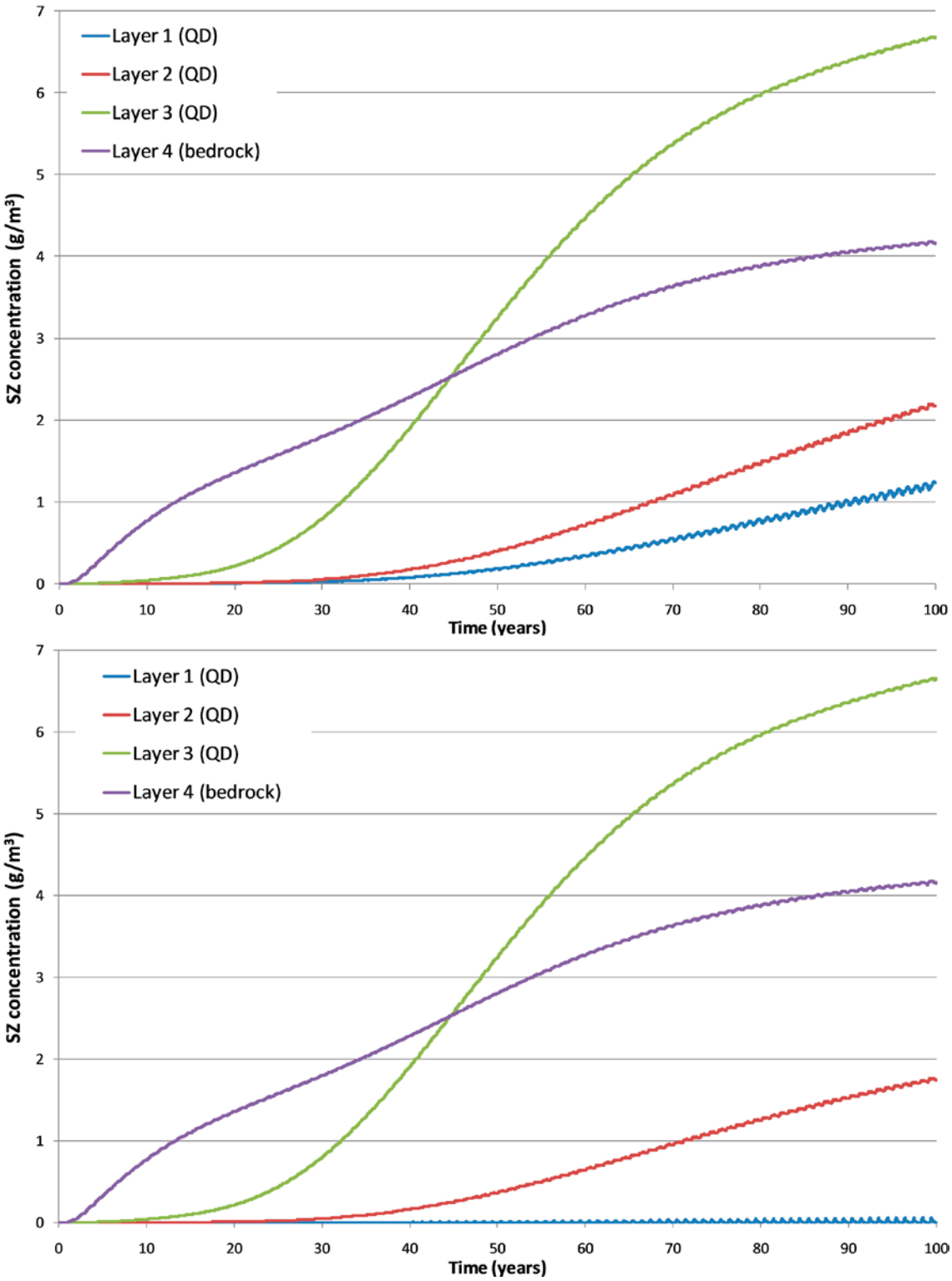

Figure 7-42. *Illustration of plant uptake from the uppermost 4 calculation layers in cell column (454;380). The upper figure is from a simulation with no plant uptake and the lower figure with full plant uptake. Both simulations are based on the 10000AD_10000QD local model A.*

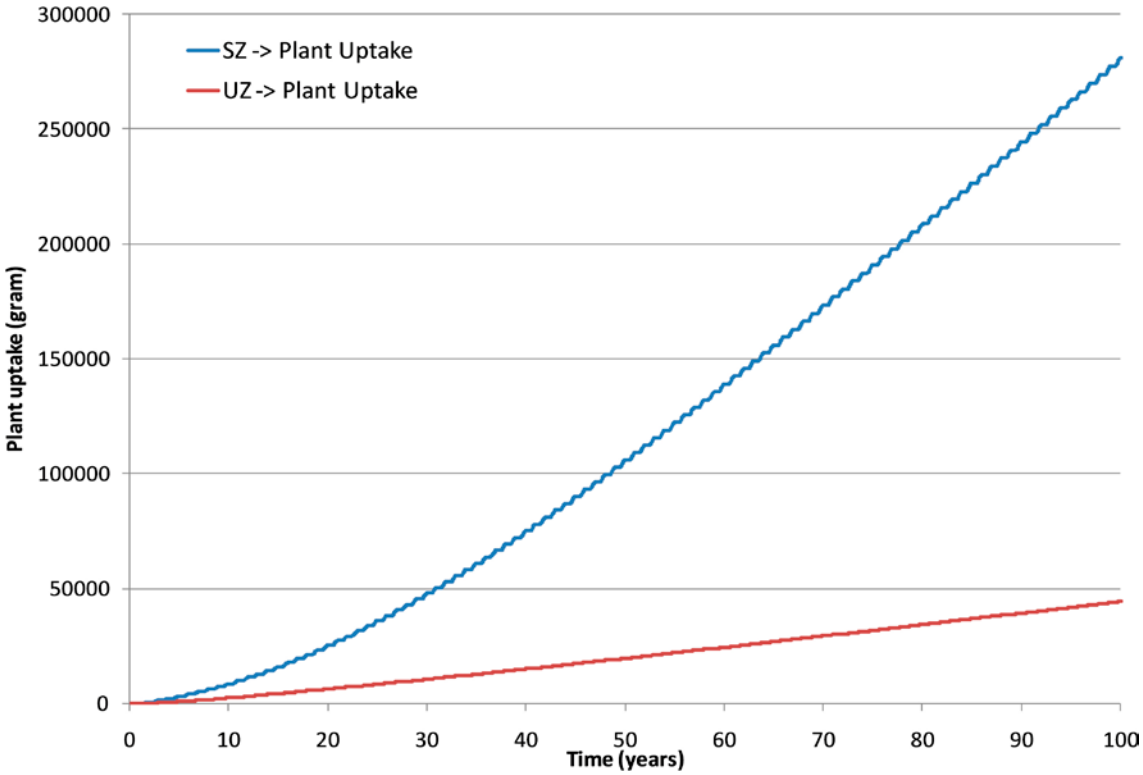

Figure 7-43. *Plant uptake from the saturated zone (blue line) and the unsaturated zone (red line) for the 10000AD_10000QD local model A.*

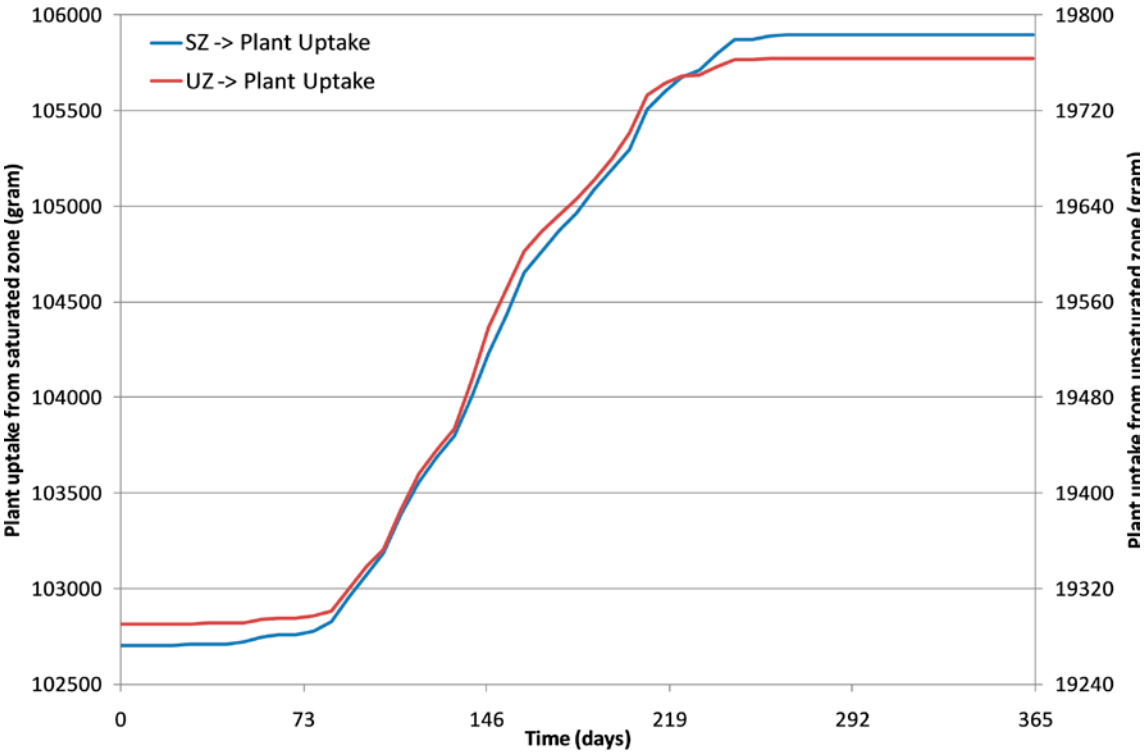

Figure 7-44. *Cumulative plant uptake from the saturated (SZ, blue line) and unsaturated (UZ, red line) zones during the year; example results for year 50 after simulation start.*

Specified initial concentration in a whole model layer

Besides the simulations with a continuous source at 40 m.b.s.l., simulations were made with a uniform initial concentration in a calculation layer situated at c. 30 m.b.s.l. The main purpose of these simulations was to further investigate the transport pattern in the lake areas. With an initial concentration the concentration is set to 1 g/m^3 in every cell within the layer at the start of the simulation. Simulations were made with models based on both the 10000AD_2000QD and the 10000AD_10000QD combinations of shoreline and QD model.

Table 7-3 shows a summary of the mass balance for the two simulations. The table shows that less than 60% of the solute has left the model, which is a little lower than in Table 7-2. The solute leaves the model mainly through the surface streams, although a larger portion goes to the boundary than what was seen in Table 7-2. Since the solute is applied all over the model area, a larger fraction of the solute goes to the vertical boundaries, either through the saturated zone or the overland model compartment.

Figure 7-45 shows surface plots for the uppermost QD layer for both the present-day QD model and that for 10,000 AD. The plots show results extracted after 1 year, 10 years, and 100 years of simulation. The main pattern is the same for the two models, although there are a few differences. For both models the solute is concentrated to lake areas and surface water courses. In the QD model for present conditions, the areas with solute on the ground surface are somewhat smaller than for the future (10,000 AD) QD model. The reason may be that the present topography is less flat than that at 10,000 AD, which gives more distinct discharge areas.

A comparison between the results in Figure 7-45 with the results in Figure 7-25 shows that the overall pattern is the same in both figures. The largest difference between the two simulations is that the simulation with an initial concentration in the entire layer yields non-zero concentration in some additional discharge areas on the surface.

To further compare the results from the two different QD models, a profile is taken along the model area according to Figure 7-46. The profile is taken from the south to the north and Figure 7-47 shows the results after 1, 10 and 100 years of simulation. On the left side the results from the QD model for 2000 AD are illustrated and on the right side the results from the 10,000 QD model. The results are similar and the main pattern is the same for the two models, although some local differences are found. Since the differences are rather small and the model taking QD development into account is considered is the most probable QD model, only results from simulations based on the 10000AD_10000QD model are discussed in the following.

Table 7-3. Mass balance parameters for AD simulation with a uniform initial concentration in a bedrock layer at 30 m.b.s.l.

	10000AD_2000QD	10000AD_10000QD
Out from model (in % of applied mass)	**59.5**	**54.6**
To surface stream (in % of 'Out from model')	**77.6**	**82.9**
SZ drain to stream (in % of 'To surface stream')	1.5	2.0
SZ baseflow to stream (in % of 'To surface stream')	66.4	89.0
OL to stream (in % of 'To surface stream')	32.1	9.0
To boundary (in % of 'Out from model')	**22.4**	**17.1**
SZ flow to boundary (in % of 'To boundary')	82.5	58.1
SZ drain to boundary (in % of 'To boundary')	0.3	6.9
OL to boundary (in % of 'To boundary')	17.1	35.0

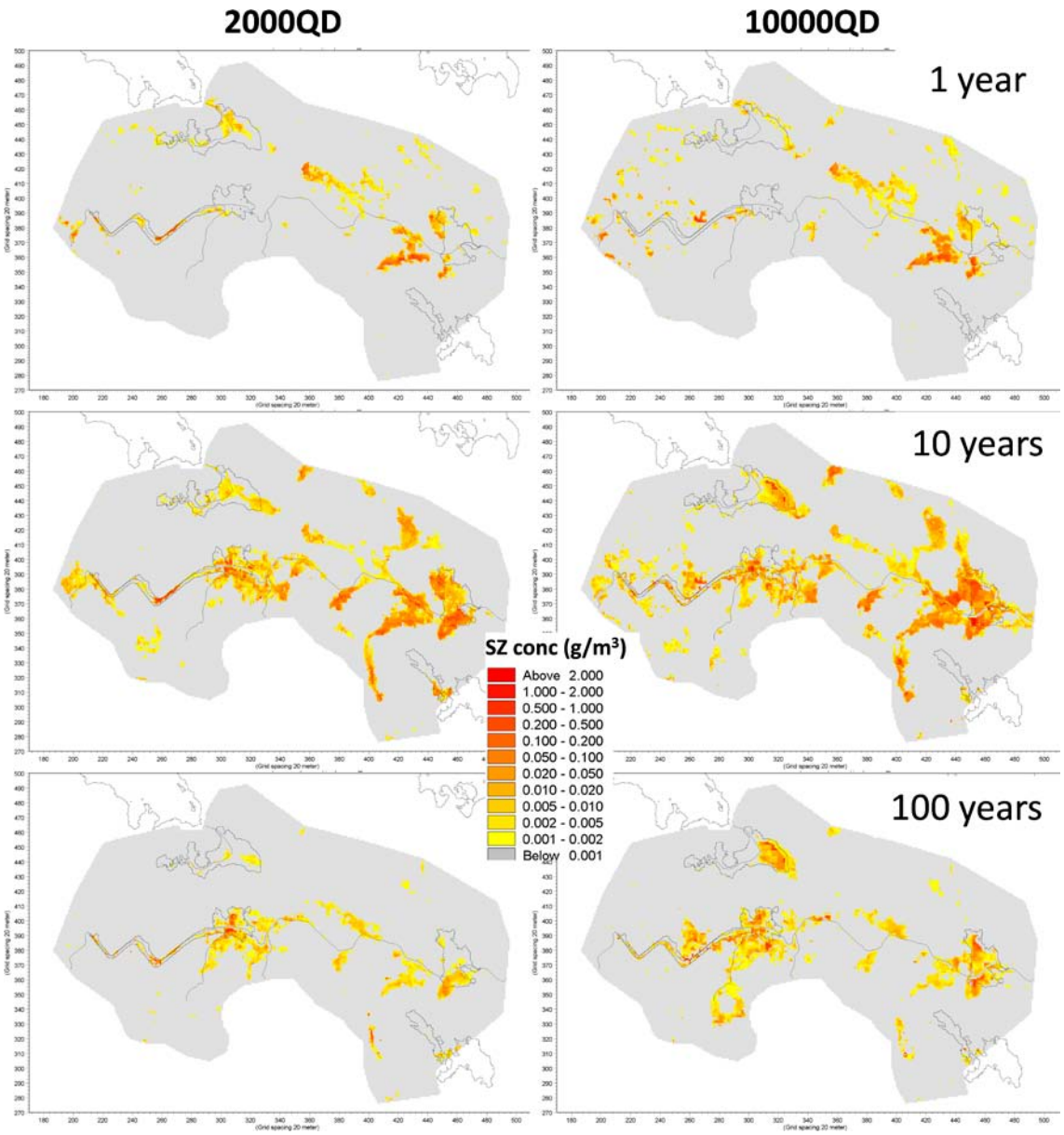

Figure 7-45. *Surface plots for the uppermost calculation layer for local model A based on the 10000AD_2000QD (left side) and 10000AD_10000QD (right side) setups for the simulation with a uniform initial concentration applied at 30 m.b.s.l.*

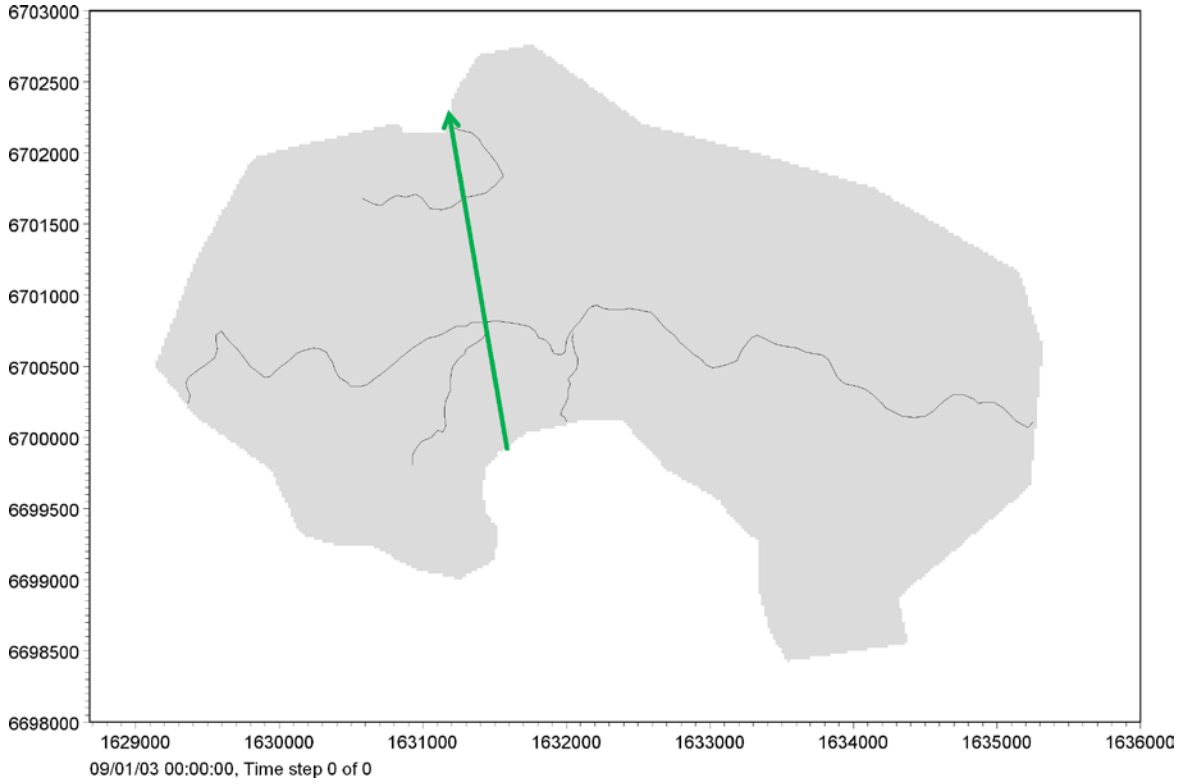

Figure 7-46. *Location of profile from south to north in local model A.*

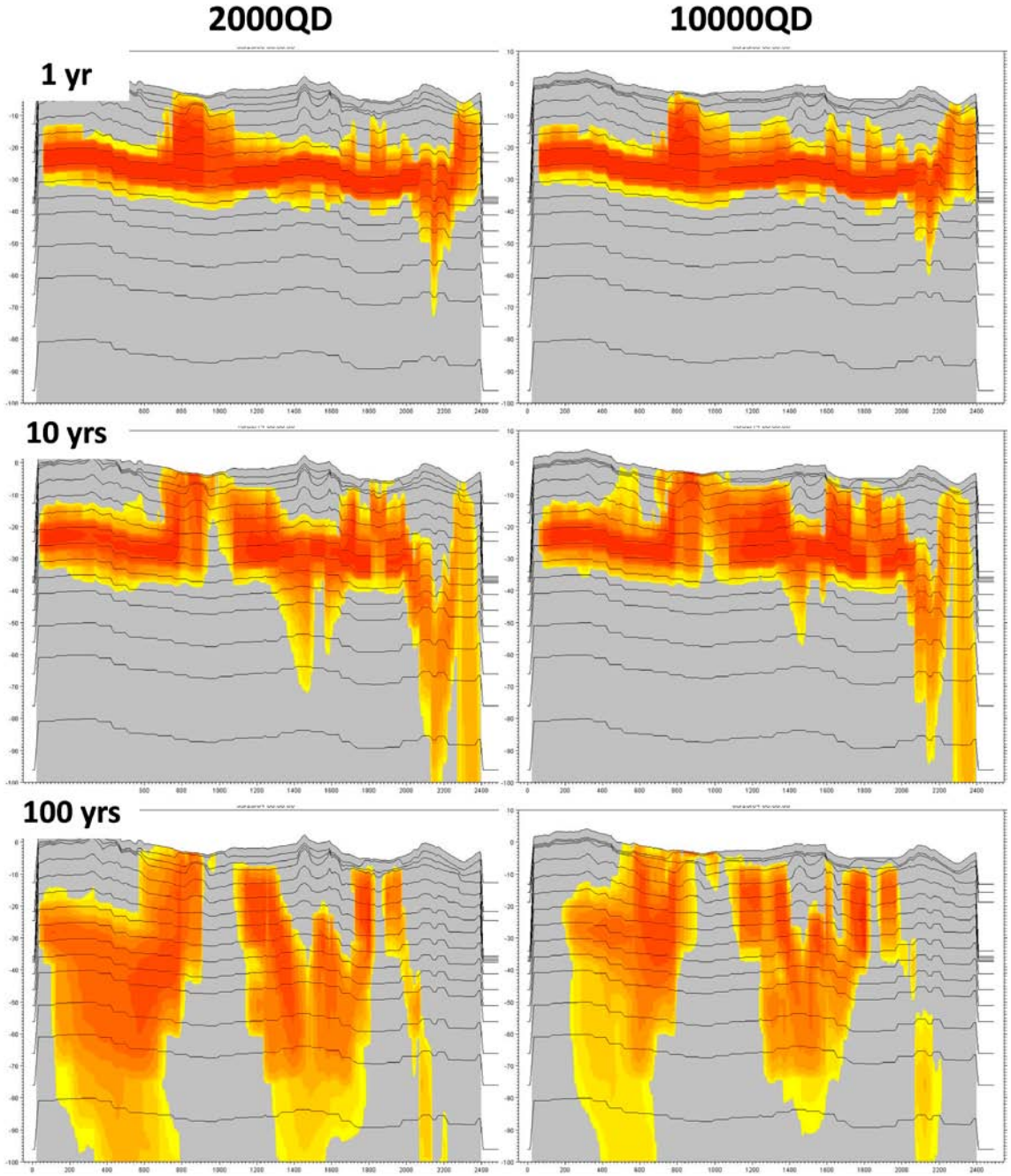

Figure 7-47. *Comparison of concentrations obtained with the QD models for present (2000 AD, left side) and future (10,000 AD, right side) conditions along the profile in Figure 7-46 for a simulation with an initial concentration in the layer at c. 30 m.b.s.l.*

Since one of the main objectives with the local models is to investigate the transport pattern in connection to the lakes areas, two profiles are drawn for each of the objects object 118 and object 121_01. Figure 7-48 shows the locations of the two profiles in object 118. Figures 7-49 and 7-50 show the resulting profiles for object 118.

Figure 7-49 is the profile taken in the north-south direction along the lake. The uppermost figure on the left side shows the layer with the initial concentration, situated at c. 30 m.b.s.l. After 6 months the concentration has already reached the surface at the lake shorelines, while the concentration is still below the QD layers in the central part of the lake. As times goes, the concentration moves further upwards but also a horizontal transport at the surface is seen in the figure showing the profile after 2 years. After 10 years solute is found in almost the whole lake area.

Since the higher-altitude areas around the lake are recharge areas, the solute is not being transported upwards in those areas. Instead, the solute is being transported downwards and then towards the lake shorelines. The figure shows that after 100 years, solute from the higher area on the right side of the figure is still moving from below towards to the lake shoreline. Solute transport is going from adjacent cells towards the lake shorelines. After 100 years of simulation most of the solute mass has left the model and under the central part of the lake the concentration is observed in the upper layers only. However, there is still some vertical solute transport to the southern part of the lake from other parts of the model.

Figure 7-50 shows the results for the profile along the east-west direction. In the same way as for the profile in the north-south direction, the concentration reaches the surface after only a few months, however, only on the eastern side of the lake. Under the lake the solute is transported more slowly, and after 2 years a horizontal spreading is seen in the upper calculation layer. As time goes, the solute is gradually removed from the model but remains in the lake sediments. In the western part of the lake, solute is still transported towards the lake after 100 years of simulation.

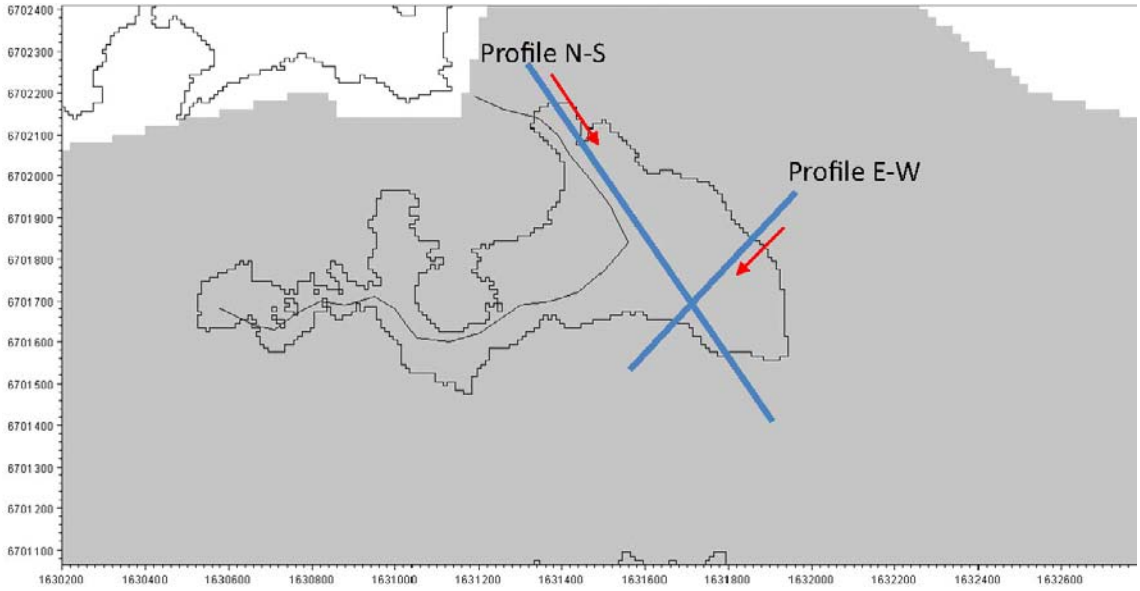

Figure 7-48. *Locations of the two profiles across object 118.*

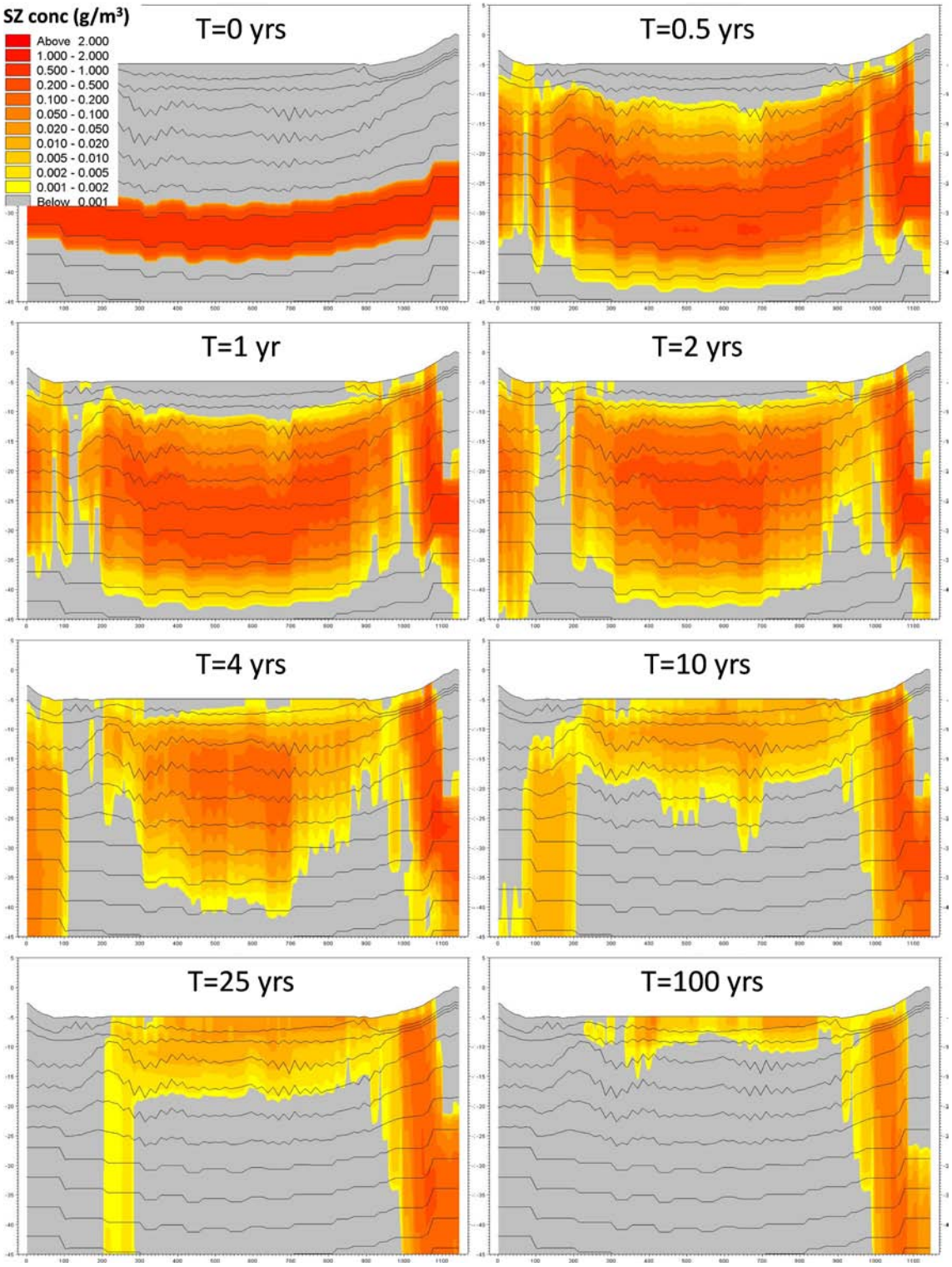

Figure 7-49. *Concentrations in the N-S profile across object 118 (Figure 7-48) from a simulation with an initial concentration applied at a depth of approximately 30 m.b.s.l. in the 10000AD_10000QD local model A.*

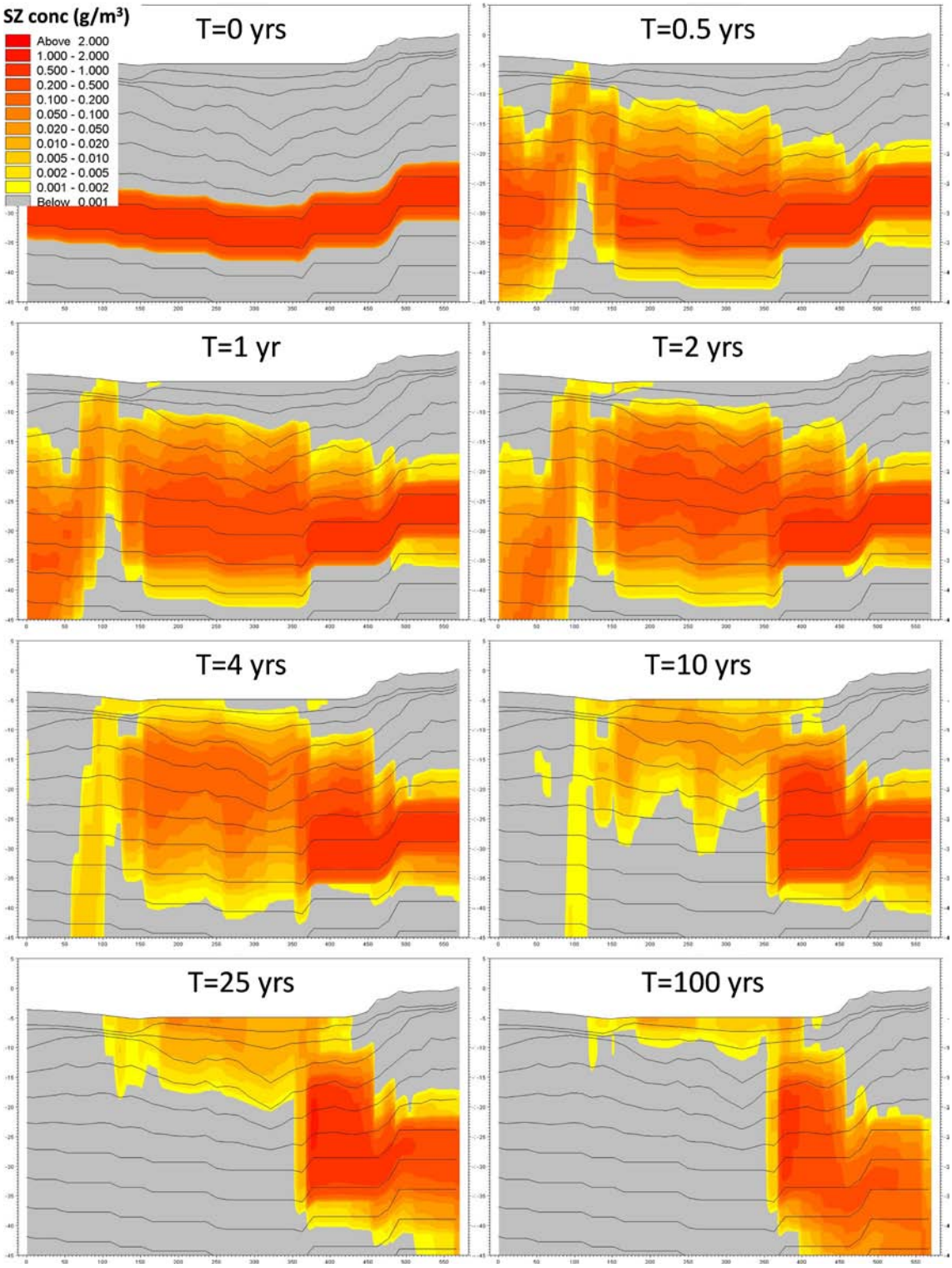

Figure 7-50. *Concentrations in the E-W profile across object 118 (Figure 7-48) from a simulation with an initial concentration applied at a depth of approximately 30 m.b.s.l. in the 10000AD_10000QD local model A.*

Figure 7-51 shows the locations of the two profiles across object 121_01. The profile in the west-east direction is the same profile as in Figure 7-33. The results are presented in Figures 7-52 and 7-53.

Figure 7-52 shows the profile taken from the north to the south. The figure shows that the solute is rapidly transported up to the southern lake shoreline and that it starts spreading horizontally in the uppermost layers towards the centre of the lake. The concentration seen close to the surface in the centre of the lake after 1-2 years is being transported horizontally into the profile from adjacent grid cells. Furthermore, in the results after 1 year and 2 years it is seen how the solute is delayed in the areas with thick QD layers. At the end of the simulation the entire lake bottom has a concentration above 1 mg/m^3 and the solute is detained in the QD layers.

Figure 7-53 shows the same profile as Figure 7-34, although the contamination source is different. In this case the solute is applied as an initial concentration instead of a continuous source and it is applied in a layer approximately 10 m above the source in Figure 7-34. However, the solute reaches the surface approximately at the same locations as in Figure 7-34. Also for the case with the initial concentration, the horizontal transport in the upper layer is seen. The vertical transport upwards in the centre of the lake was not seen in Figure 7-34 since the source was not located under the entire lake. After 100 years of simulation the solute is still left in the lake sediments.

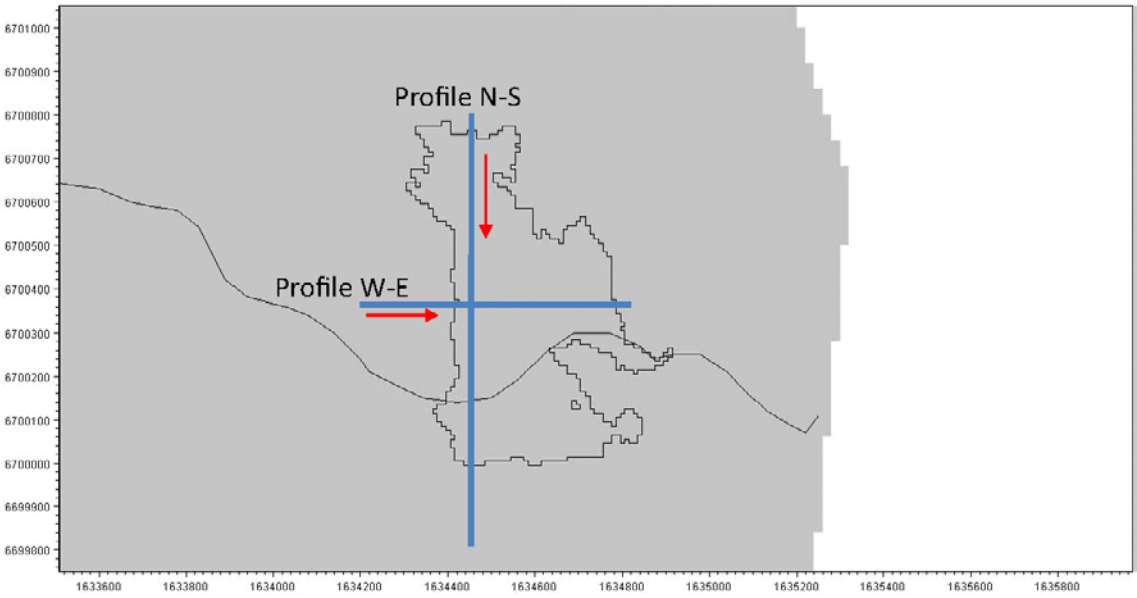

Figure 7-51. *Locations of profiles across object 121_01.*

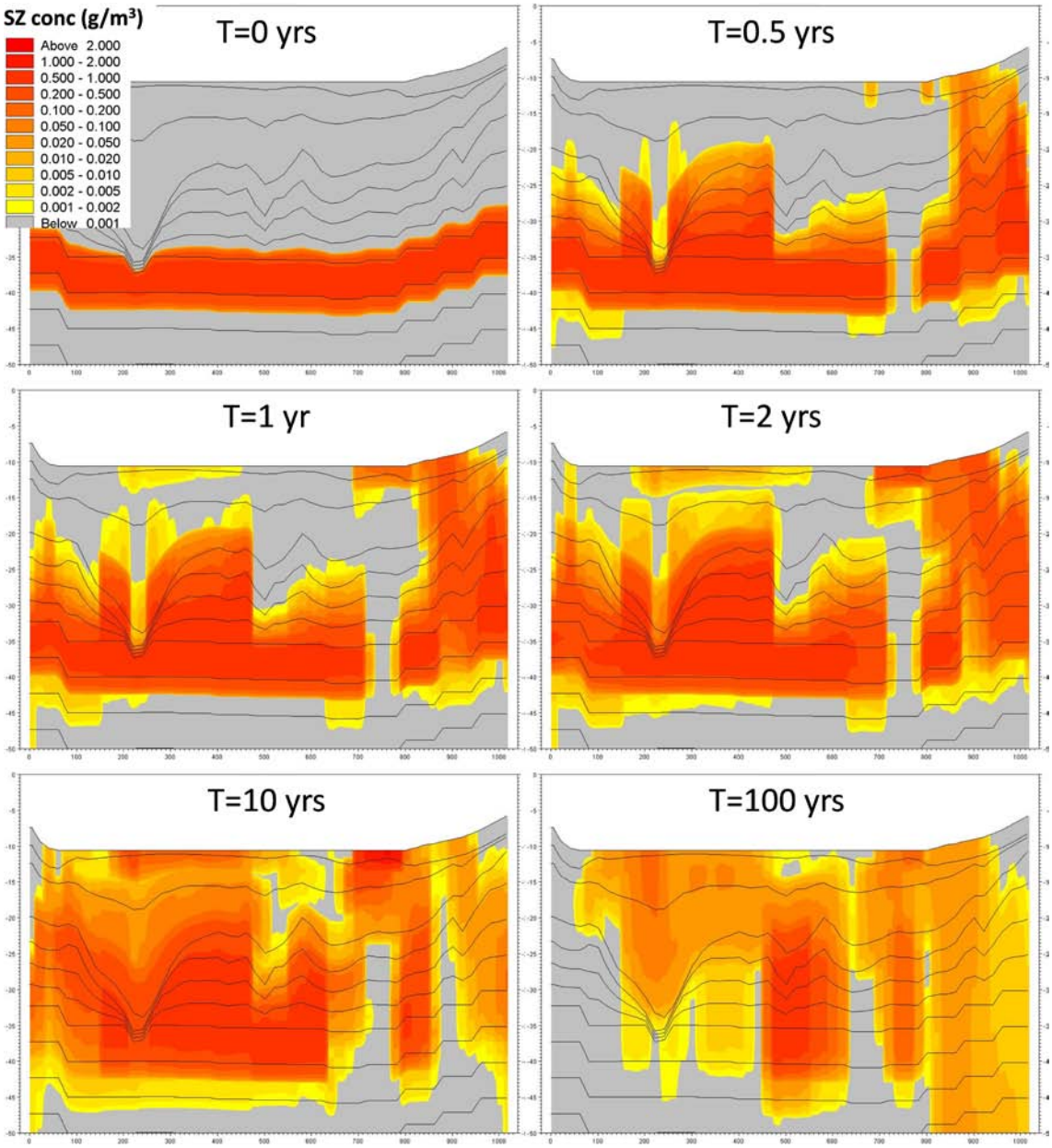

Figure 7-52. *Concentrations in the N-S profile across object 121_01 (Figure 7-51) from a simulation with an initial concentration applied at a depth of approximately 30 m.b.s.l. in the 10000AD_10000QD local model A.*

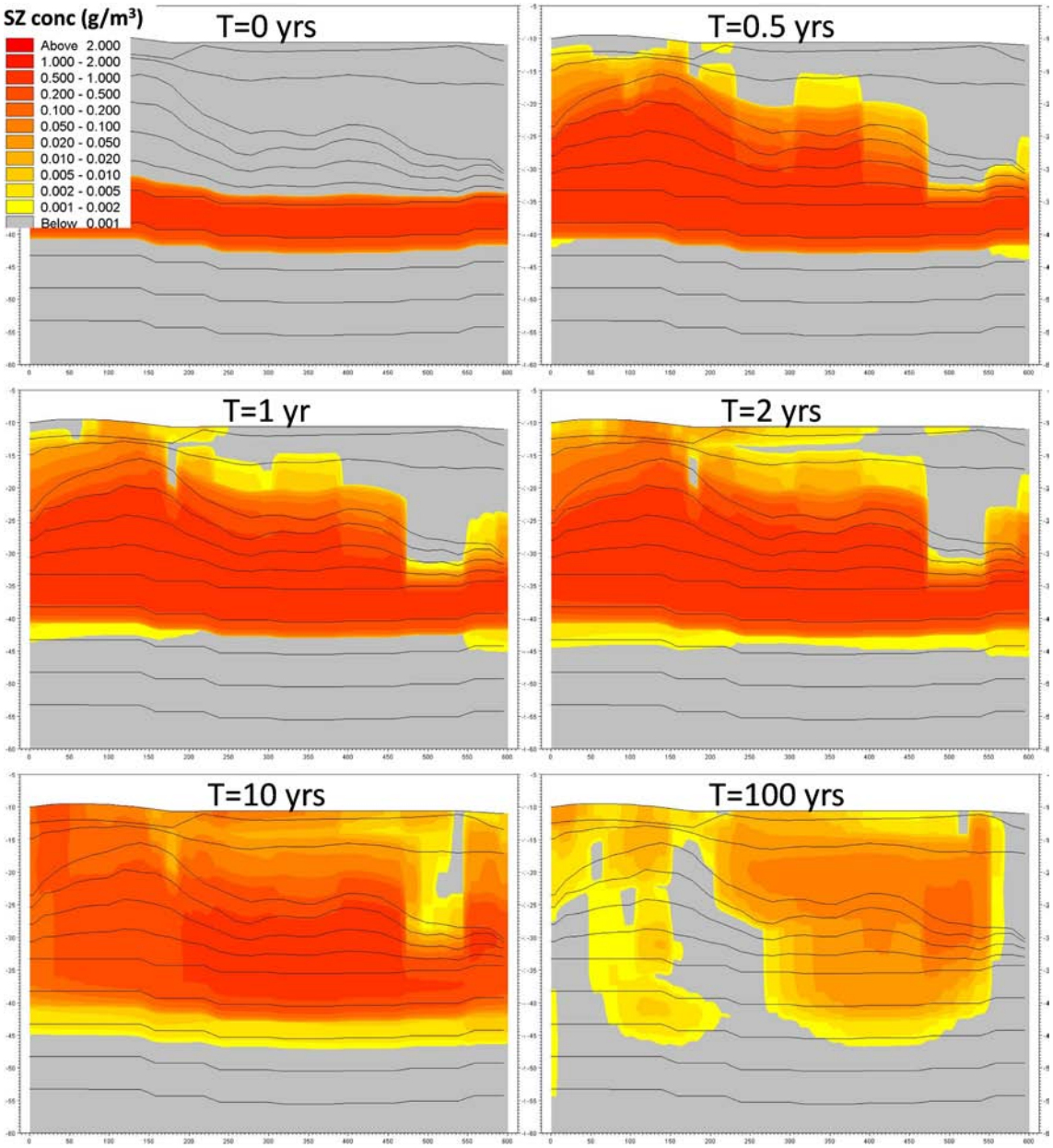

Figure 7-53. *Concentrations in the W-E profile across object 121_01 (Figure 7-51) from a simulation with an initial concentration applied at a depth of approximately 30 m.b.s.l. in the 10000AD_10000QD local model A.*

Effects of dispersivities and sediment hydraulic conductivities

Since the main purpose of the transport simulations is to investigate the transport pattern in and around the lakes, a sensitivity simulation with regard to the hydraulic conductivities in the lake sediments was made. For the simulation with an initial source, the hydraulic conductivities were reduced by a factor of 100 in all sediments.

Figure 7-54 shows surface plots for the concentration in calculation layer L1 for both the case with the original conductivities (on the left side) and the reduced conductivities (on the right side). After 1 year of simulation the difference between the two cases is not very large. After 10 years the differences in the lake areas become larger and there is less concentration in the lake areas in the case with the lower conductivities in the lake sediments. After 100 years the concentration in the lake areas is higher for the case with the lower conductivities. The low hydraulic conductivity retains the solute in the sediments.

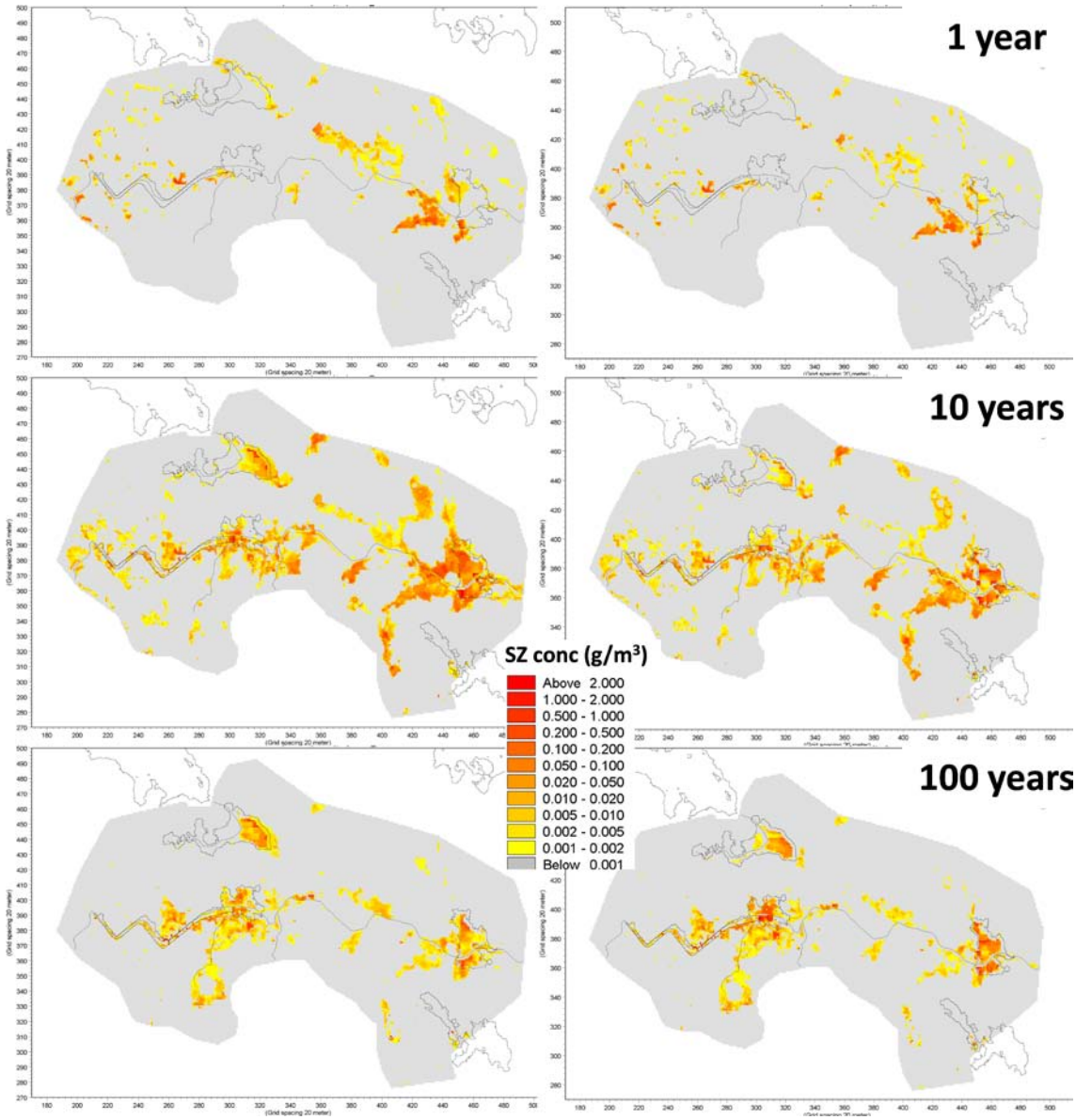

Figure 7-54. *Comparison of concentrations in the upper QD layer in terms of surface plots for the sensitivity analysis with hydraulic conductivities in the lake sediments reduced by a factor 100. On the left side results with the original conductivities are presented and on the right side the results for the reduced conductivities; both cases are based on the 10000AD_10000QD local model A.*

Concentration time series in the cell shown in Figure 7-55 are presented in Figure 7-56. This grid cell is located below one of the future lakes in the area within object 120, see Figure 2-22. The concentration curves are illustrated for the uppermost 4 calculation layers in the model. Layers 1–3 are QD layers, whereas layer 4 is the uppermost bedrock layer. The graphs show that for the lower two layers the difference in the results is small, while for the upper two layers there is a significant delay in the peak concentration arrival. This is caused by the low hydraulic conductivity in the lake sediment layers. The time series also show that the seasonal variations in vegetation and climatic data affect the solute concentration in the upper layers.

Figures 7-57 to 7-60 show the results for the simulation case with reduced hydraulic conductivities in the sediments for the profiles illustrated in Figures 7-48 and 7-51. For the two profiles across object 118, Figures 7-57 and 7-58, there is a distinct delay in the transport for the case with the reduced hydraulic conductivities. Furthermore, the solute is retained in the sediments for a longer period when the conductivities are reduced.

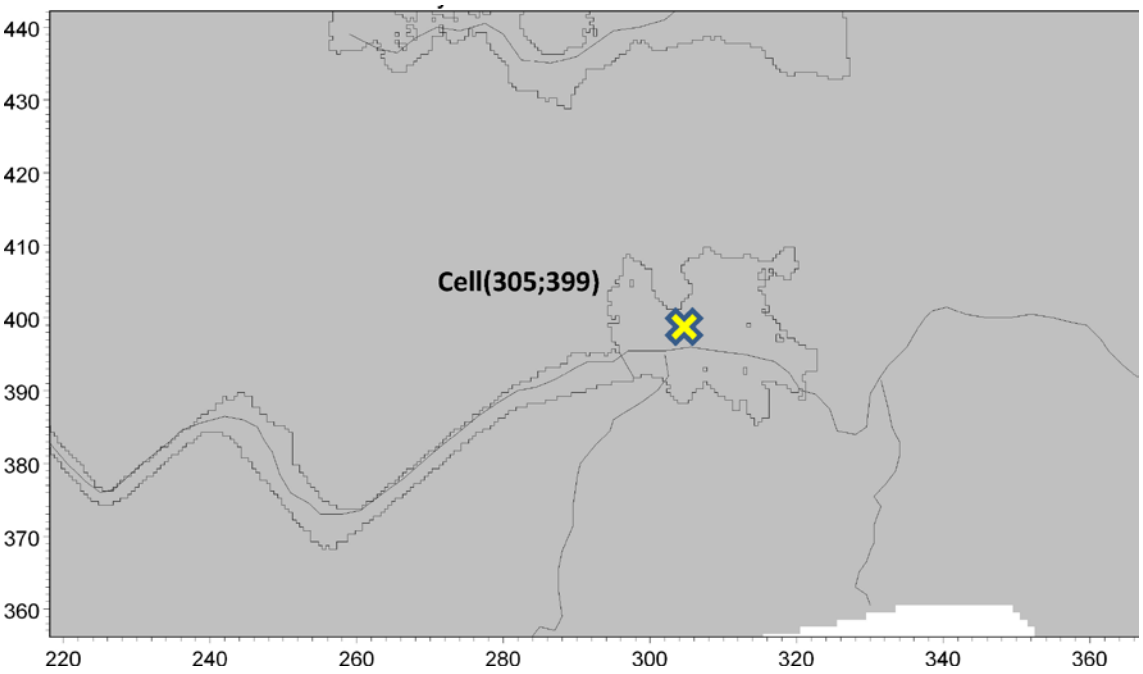

Figure 7-55. *Location of cell (305;399 in object 120).*

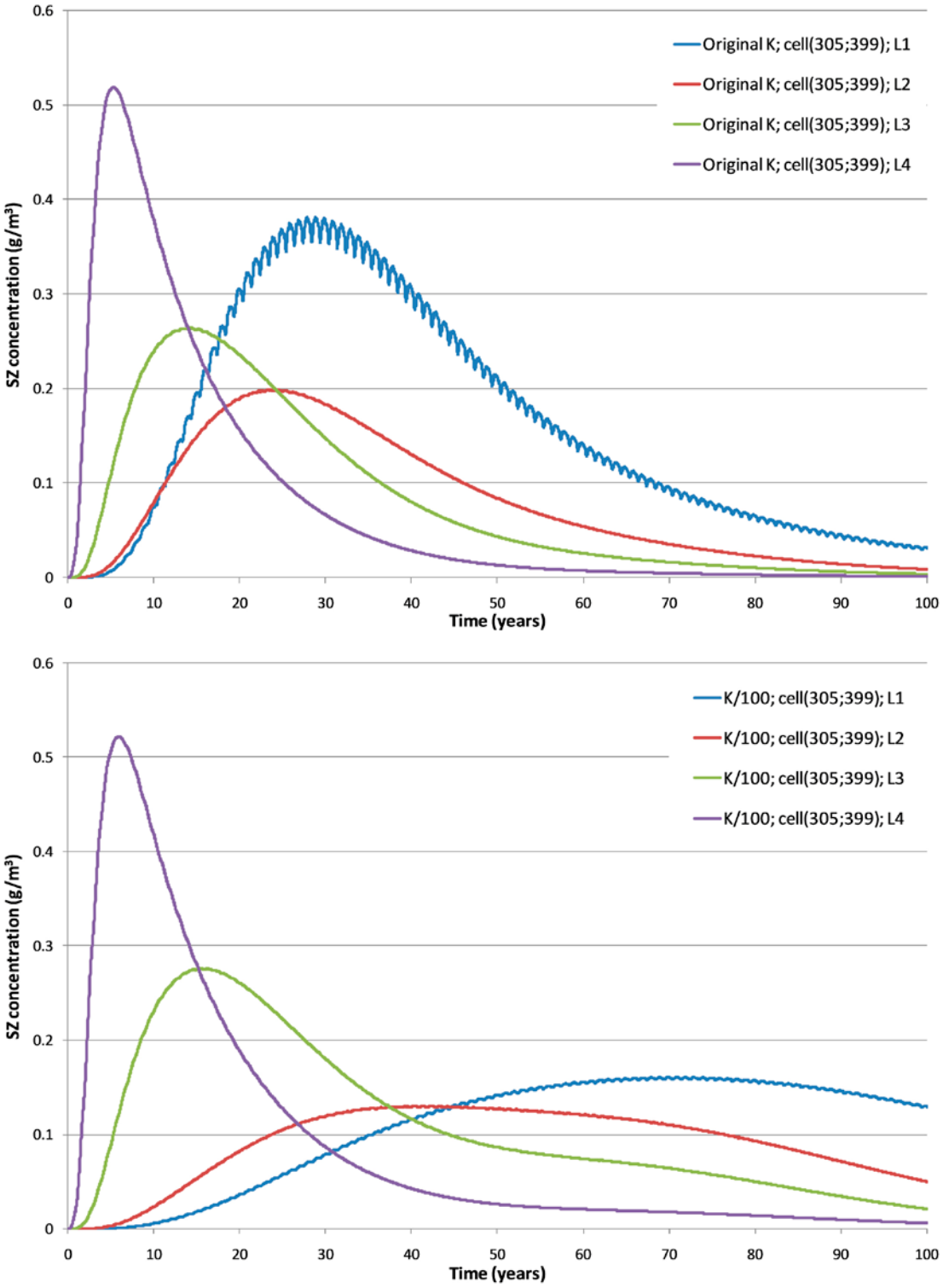

Figure 7-56. *Time series in cell (305;399) for original K in lake sediments (upper figure) and K/100 in lake sediments (lower figure), in simulations based on the 10000AD_10000QD local model A.*

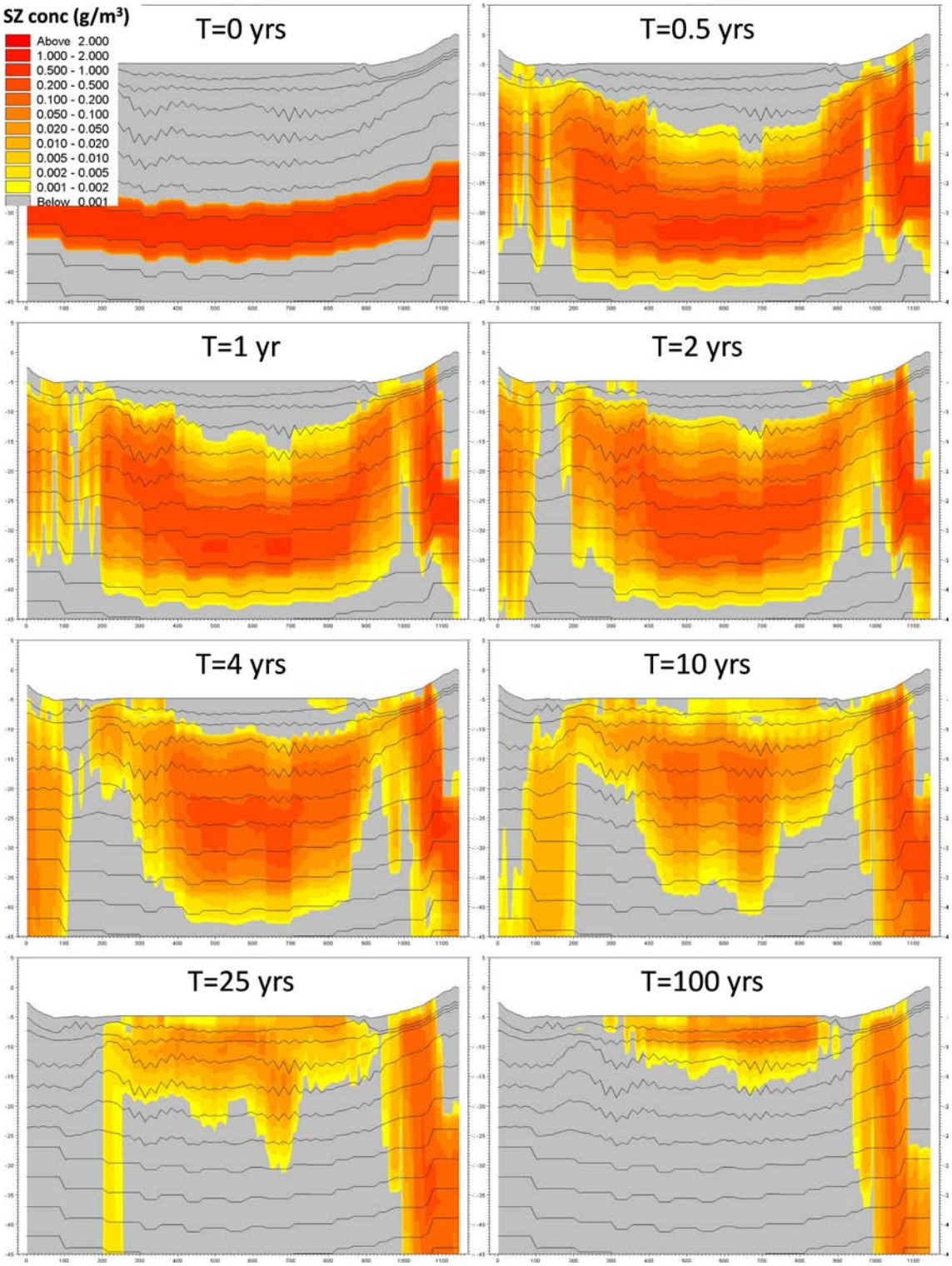

Figure 7-57. *Concentrations in the N-S profile across object 118 (Figure 7-48) from the sensitivity simulation with hydraulic conductivities in the lake sediments reduced by a factor of 100 in the 10000AD_10000QD local model A.*

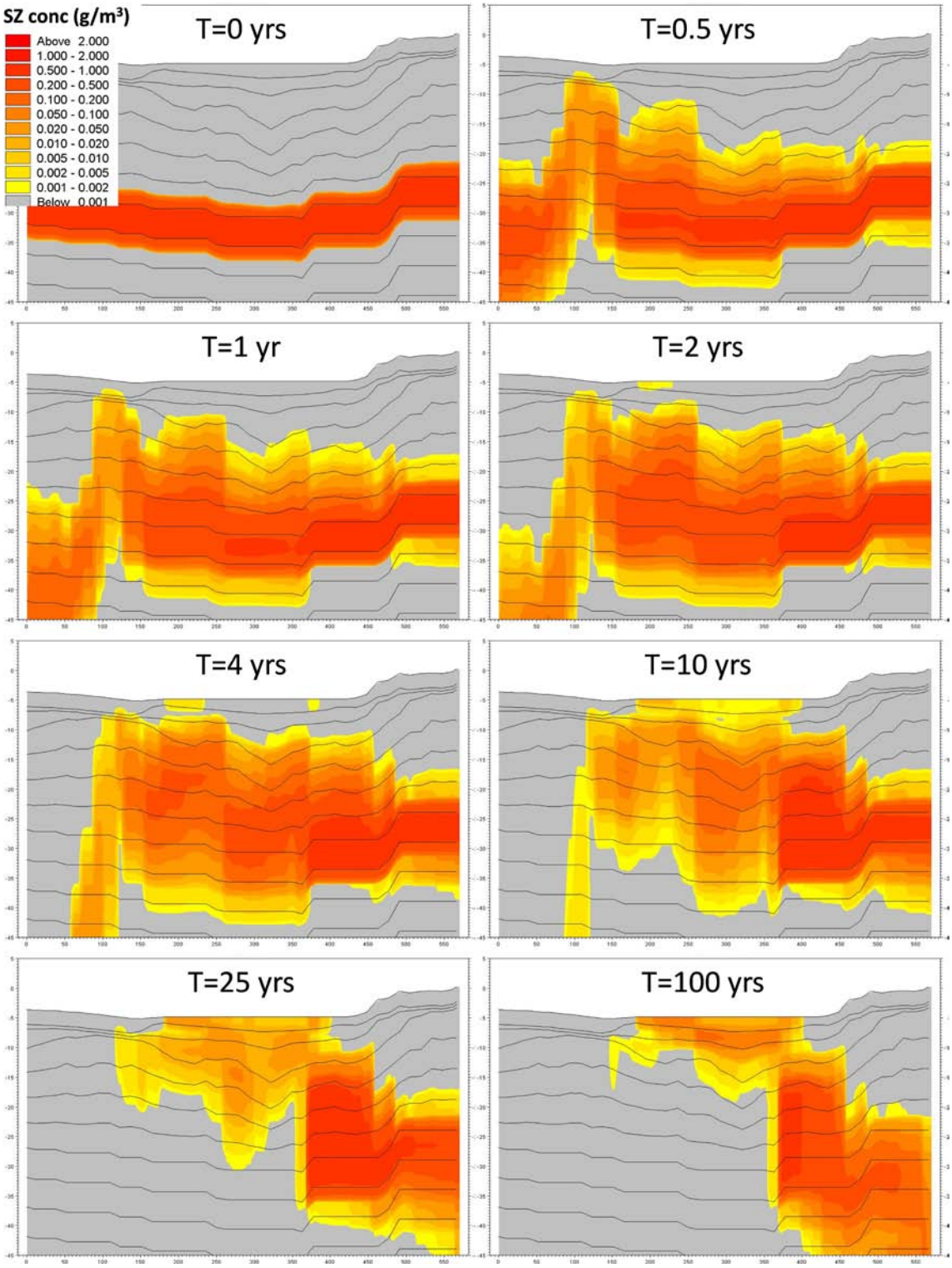

Figure 7-58. *Concentrations in the E-W profile across object 118 (Figure 7-48) from the sensitivity simulation with hydraulic conductivities in the lake sediments reduced by a factor of 100 in the 10000AD_10000QD local model A.*

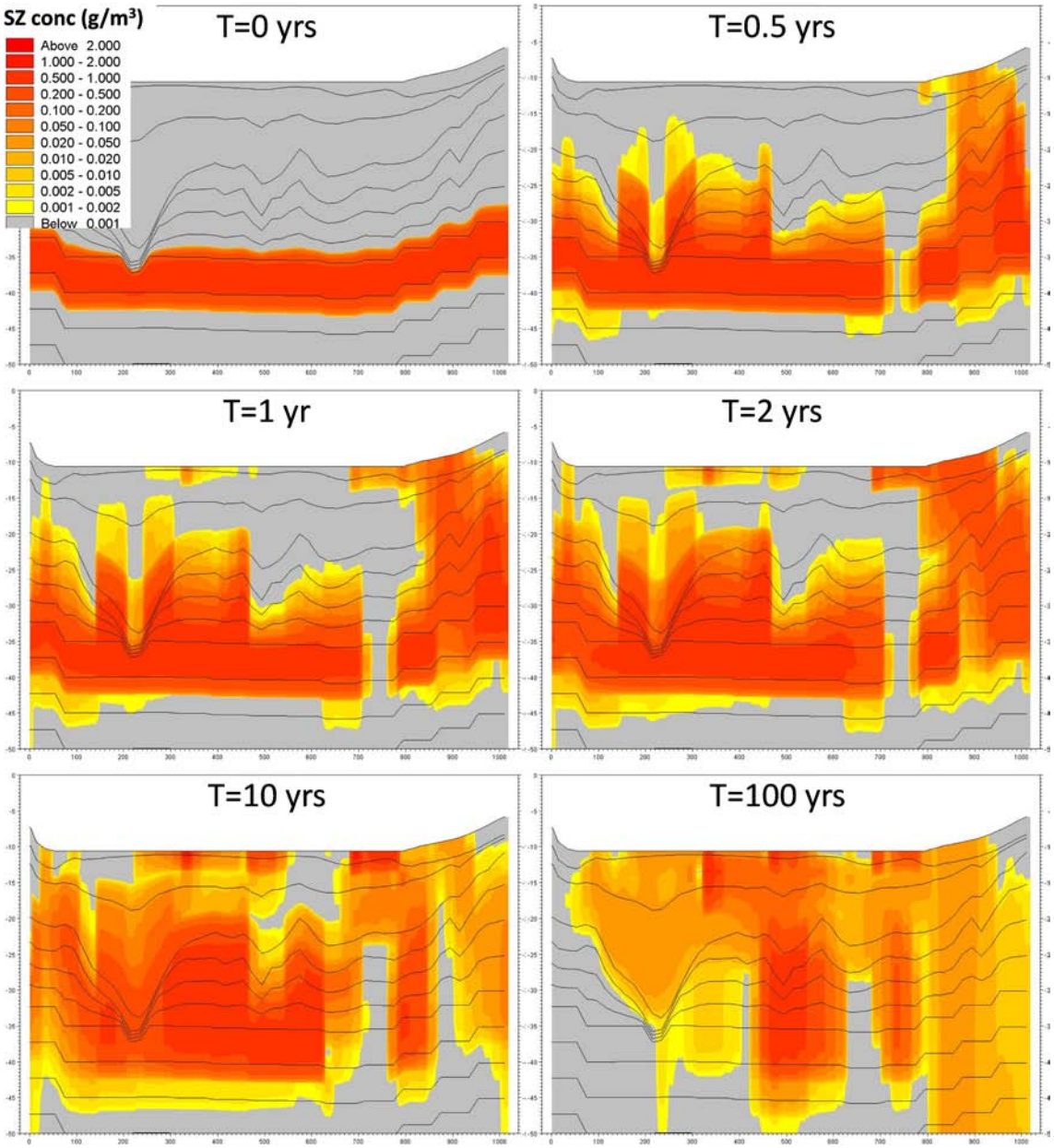

Figure 7-59. *Concentrations in the N-S profile across object 121_01 (Figure 7-51) from the sensitivity simulation with hydraulic conductivities in the lake sediments reduced by a factor of 100 in the 10000AD_10000QD local model A.*

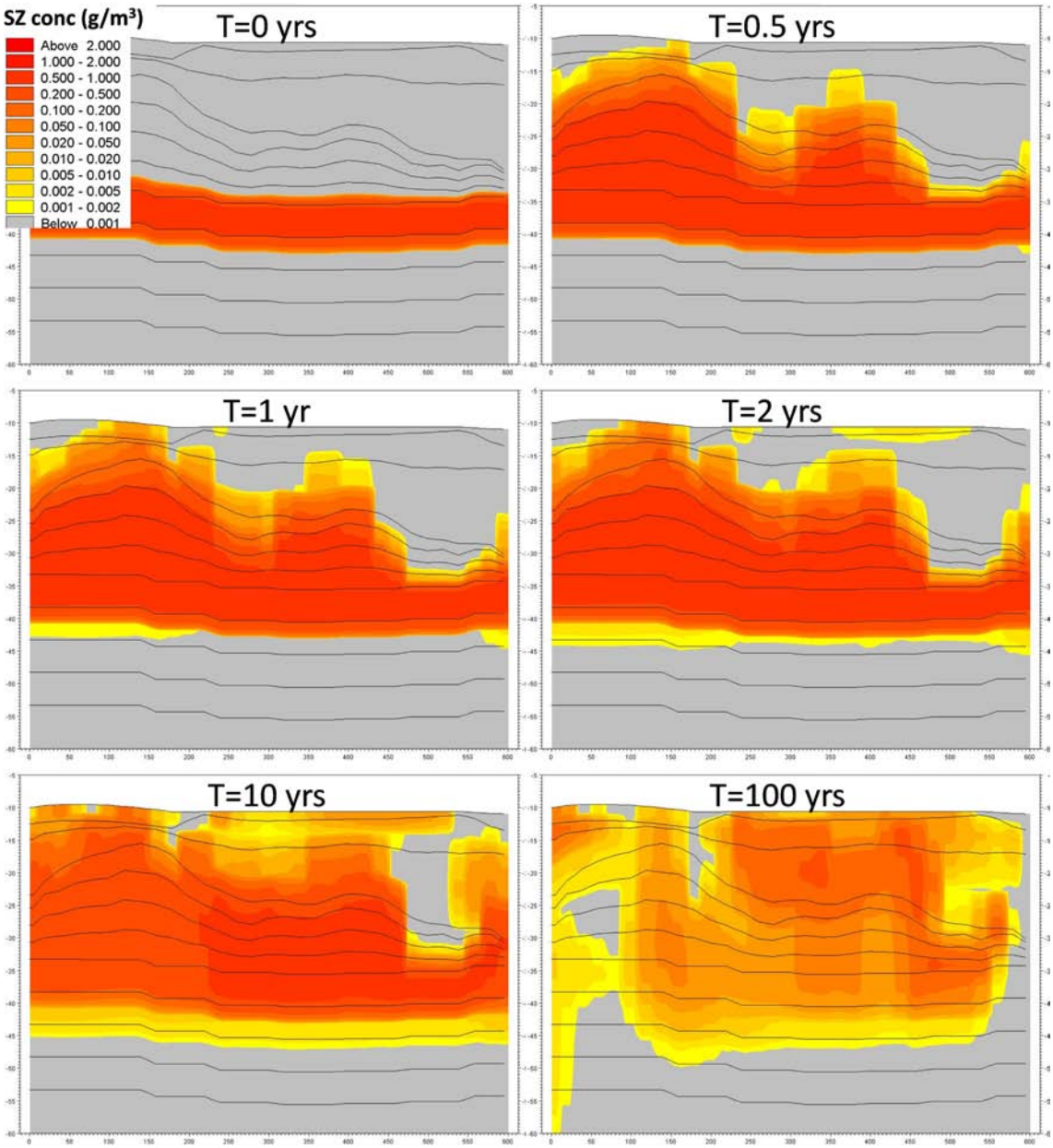

Figure 7-60. *Concentrations in the W-E profile across object 121_01 (Figure 7-51) from the sensitivity simulation with hydraulic conductivities in the lake sediments reduced by a factor of 100 in the 10000AD_10000QD local model A.*

For the profiles across object 121_01, illustrated in Figures 7-59 and 7-60, the effect is the same as in Figures 7-57 and 7-58, although a bit more difficult to see because larger parts of the profile are covered by solute. However, it is seen that after the first year of simulation the spreading towards the surface is slower when the hydraulic conductivities are reduced. The results also show that the horizontal spreading along the surface is reduced both in the horizontal and the vertical direction when the conductivities are reduced.

Numerical dispersion is a phenomenon that arises when the numerical resolution, i.e. grid cells and/or time steps, are too large for the considered processes to be modelled with sufficient accuracy by the numerical model. If a model is affected by numerical dispersion there will be solute dispersion in the results even if the model dispersivities are set to zero. In the transport modelling for SDM-Site, reported in /Gustafsson et al. 2008/, a sensitivity analysis with regard to numerical dispersion was made. For the model that was concluded to be sufficiently accurate, the grid sizes were larger than in the present model, both in the horizontal and vertical directions. Therefore, it is assumed here that the impact of numerical dispersion in the present model is small.

Since dispersion coefficients are difficult to estimate, a sensitivity simulation with regard to the dispersion coefficients of the QD layers was made. The original simulation has low dispersion coefficients both in the QD layers and in the bedrock layers. The longitudinal dispersivity is 0.2 m and the transverse dispersivity is 0.01 m. In the sensitivity simulation the longitudinal dispersivity of the QD layers was 20 m and the transverse 0.2 m; the dispersivities in the bedrock layers were not changed. Figure 7-61 shows surface plots for the uppermost QD layer for both the simulation with low dispersion (on the left side) and the simulation with high dispersion in the QD (right side). The figure shows that the differences between the two cases are not very large, although the solute indeed is somewhat more dispersed in the case with the higher dispersion.

The profiles in Figures 7-62 and 7-63 are the same as in Figures 7-49 and 7-50, and the profiles in Figures 7-64 and 7-65 are the same as Figure 7-52 and 7-53. The figures show that for the higher dispersion case the surface layer is covered by the solute faster than with the low dispersion. Since both simulations have the same dispersion coefficients in the bedrock layers, the difference is only seen in the QD layers.

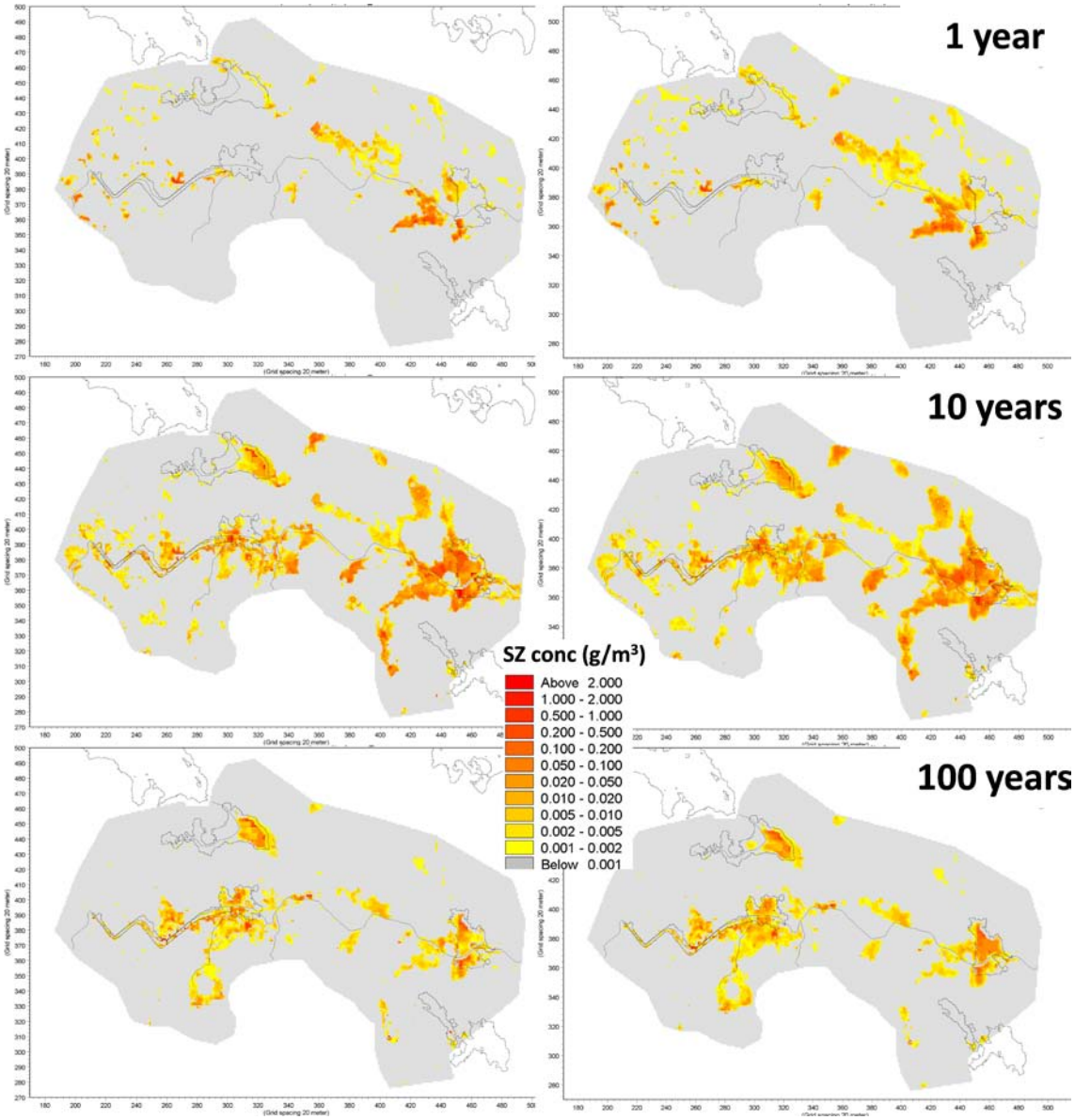

Figure 7-61. *Comparison of concentrations in the uppermost QD layer in terms of surface plots for the sensitivity analysis of the dispersion coefficients of the QD layers. On the left side results with the original (low) dispersion are presented and on the right side the results for the case with high dispersion; the simulations are based on the 10000AD_10000QD local model A.*

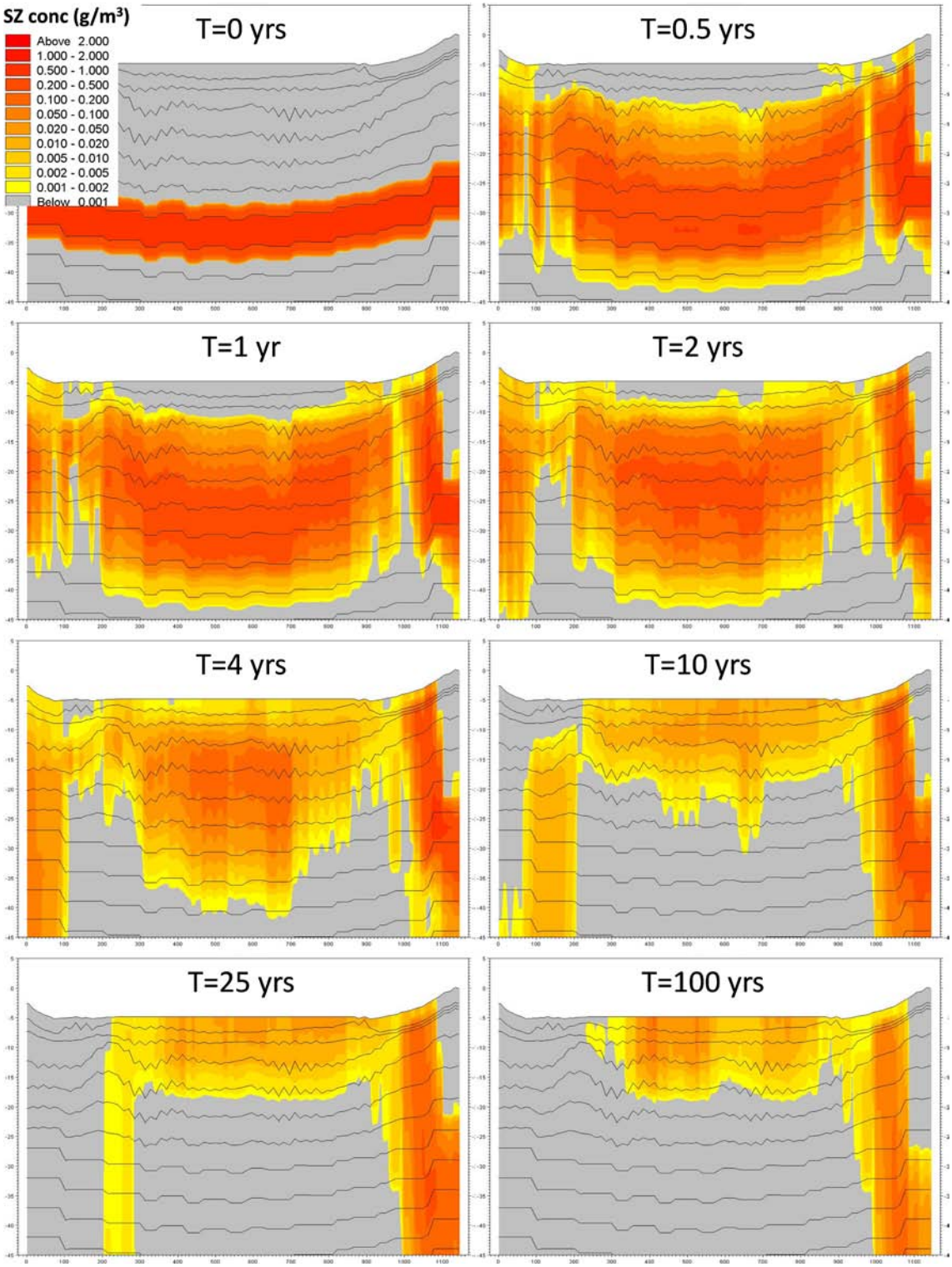

Figure 7-62. *Concentrations in the N-S profile across object 118 (Figure 7-48) from the sensitivity simulation with higher dispersion in the QD layers in the 10000AD_10000QD local model A.*

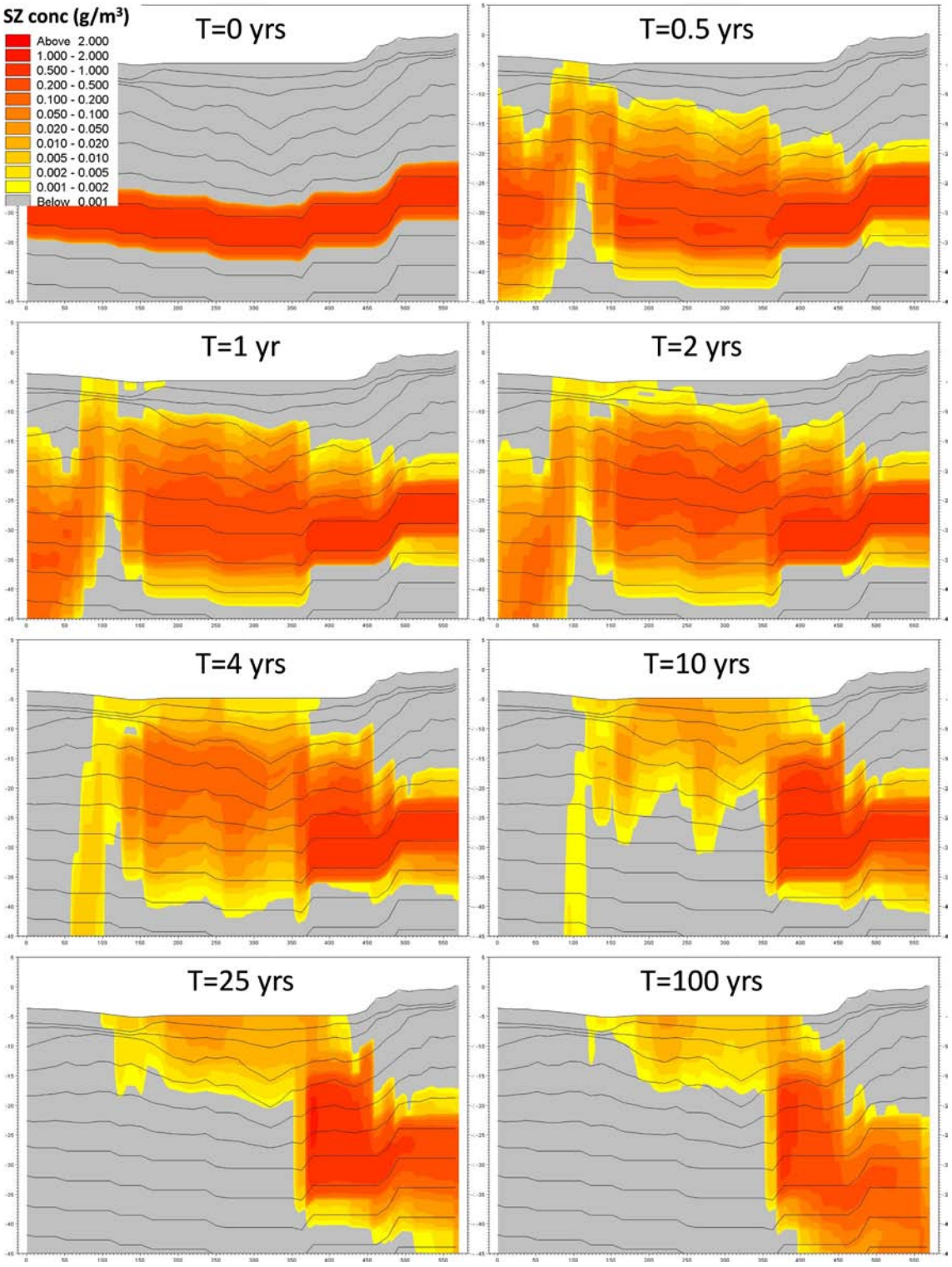

Figure 7-63. *Concentrations in the E-W profile across object 118 (Figure 7-48) from the sensitivity simulation with higher dispersion in the QD layers in the 10000AD_10000QD local model A.*

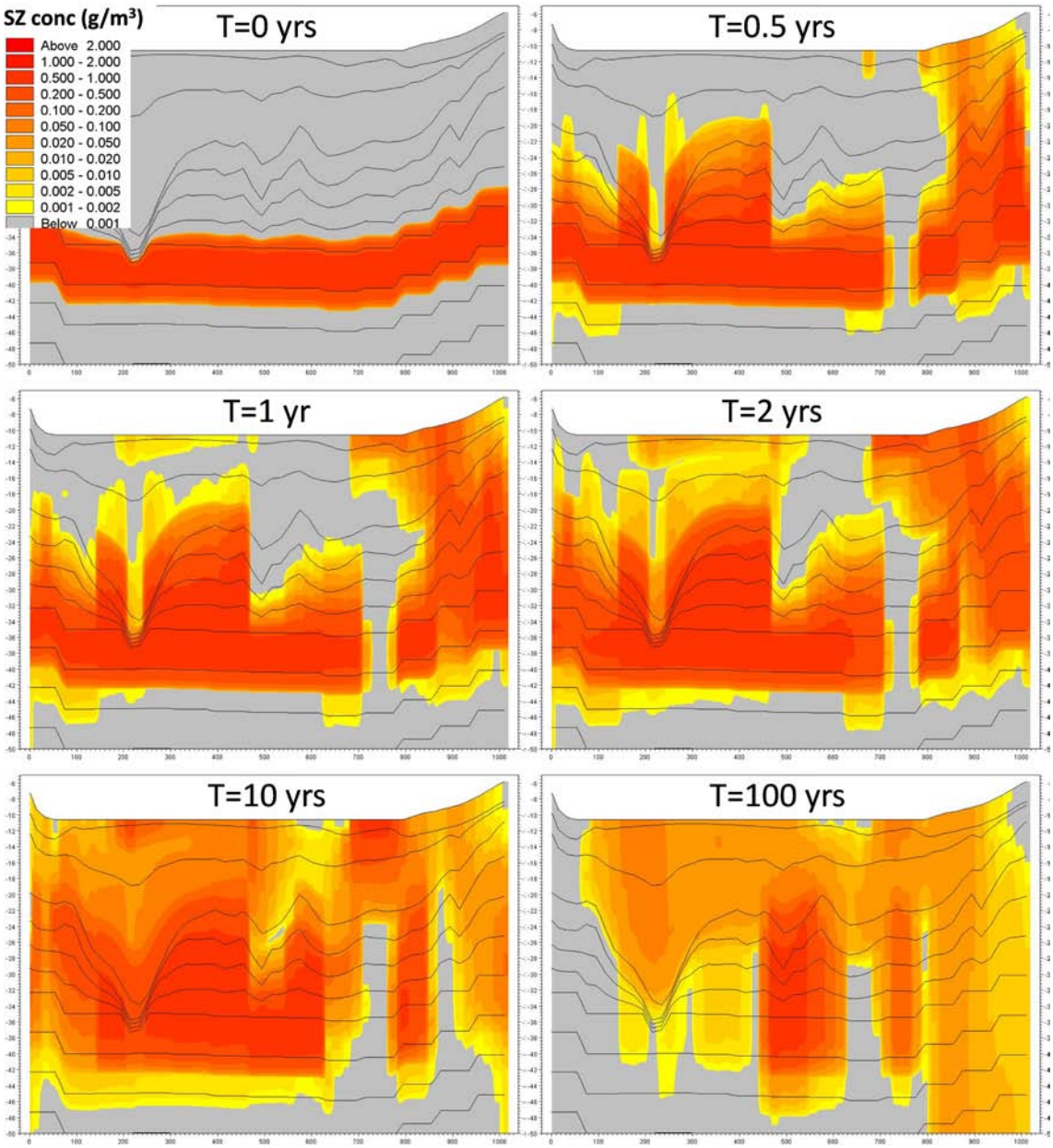

Figure 7-64. *Concentrations in the N-S profile across object 121_01 (Figure 7-51) from the sensitivity simulation with higher dispersion in the QD layers in the 10000AD_10000QD local model A.*

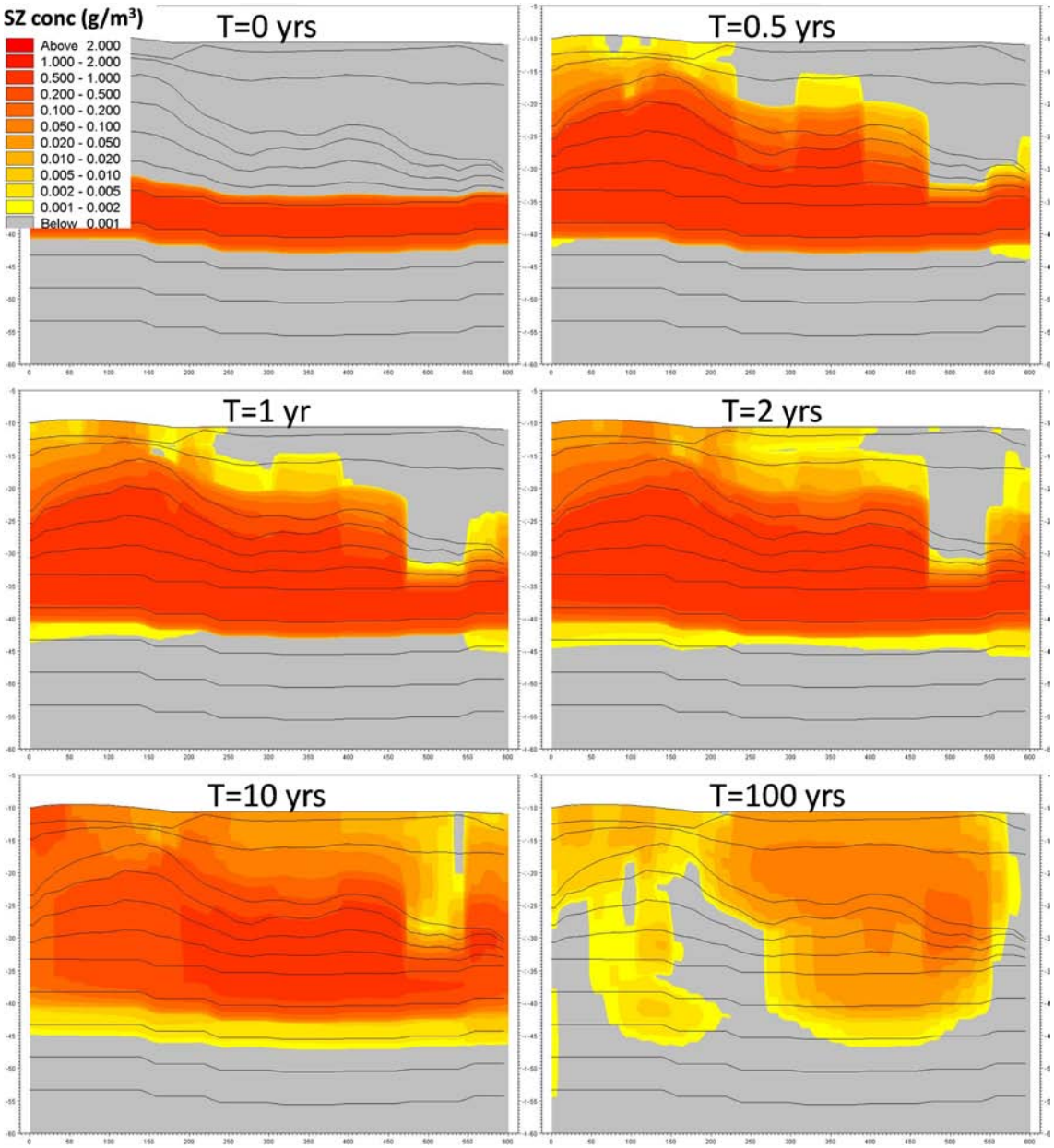

Figure 7-65. *Concentrations in the W-E profile across object 121_01 (Figure 7-51) from the sensitivity simulation with higher dispersion in the QD layers in the 10000AD_10000QD local model A.*

7.3 Solute transport in local model B

For the local model including object 116, model B, no particle tracking simulations were carried out. Two simulations with the advection-dispersion (AD) module were made. In both simulations an initial solute concentration was applied all over a calculation layer situated at c. 40 m.b.s.l. In the first simulation the dispersion coefficients were low in all layers, while the dispersion coefficients in the second simulation were high in the QD layers. The initial concentration was 1 g/m^3. Both simulations were based on the 10000AD_10000QD combination of shoreline and QD model.

7.3.1 Transport pattern and mass balance

Figures 7-66 to 7-68 illustrate the mass balance parameters for the AD simulation with low dispersion coefficients in all layers. Figure 7-66 shows the amount of solute contained in the model during the 100 years of simulation. Since there is no continuous source, but only an initial solute concentration at 40 m.b.s.l., the amount decreases with time. After 100 years less than 5% of the initial mass is left within the model volume. Figure 7-66 also shows the amount of solute stored in the unsaturated zone and the overland compartment, which both increase during the first 10 years and then start to decrease again. The reason is that the solute accumulates in the unsaturated zone and the overland before either a surface stream or the overland is reached.

Figure 7-67 shows the sinks through which solute mass leaves the model. About 88% of the solute goes to the surface stream network and 12% to the vertical boundary. Figure 7-68 shows that more than 90% of the amount of solute mass that discharges to the surface streams goes from the overland compartment to the streams, and less than 10% directly from the saturated zone to the streams. The graphs in Figure 7-68 also show that the solute that goes directly to the streams from the saturated zone does it in the first few years after the simulation starts. The transport from the saturated zone via overland to the surface streams takes longer time due to longer pathways.

Figure 7-68 also shows that more than 60% of the amount of solute that goes to the boundary comes from the overland compartment, whereas c. 20% comes from the saturated zone flow and another 20% from the saturated zone through drainage.

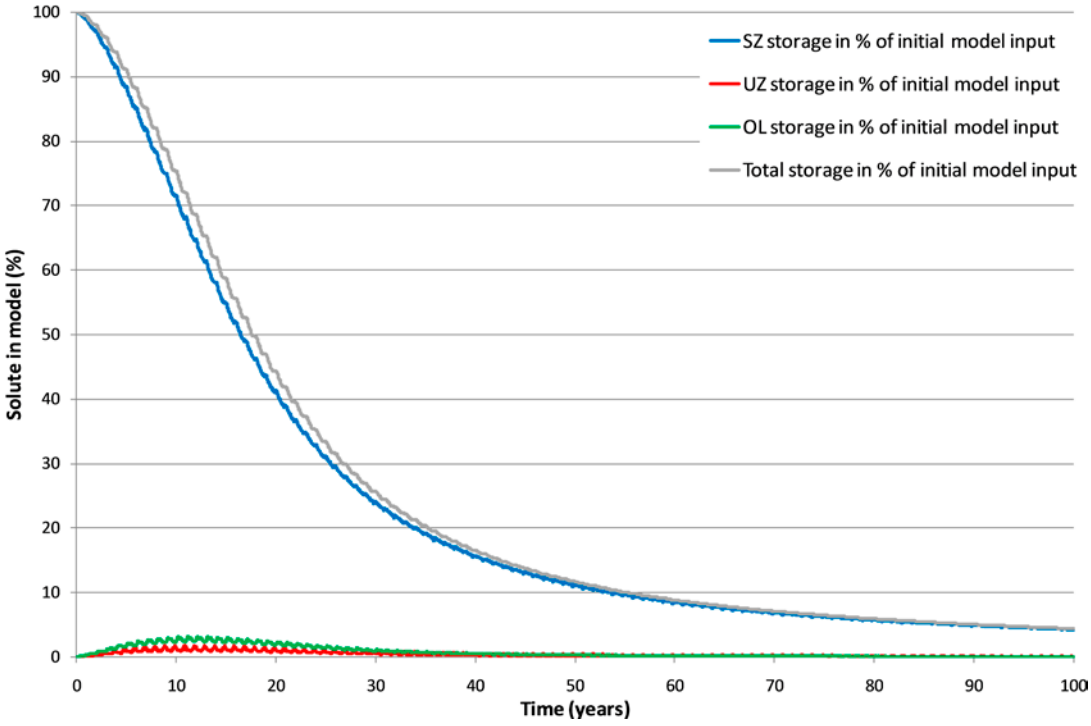

Figure 7-66. *Storage of solute in local model B (based on 10000AD_10000QD) during the 100 years of simulation. The grey line is the total storage in the model volume, the blue line is the storage in the saturated zone, the red line is the storage in the unsaturated zone and the green line is the storage in the overland compartment.*

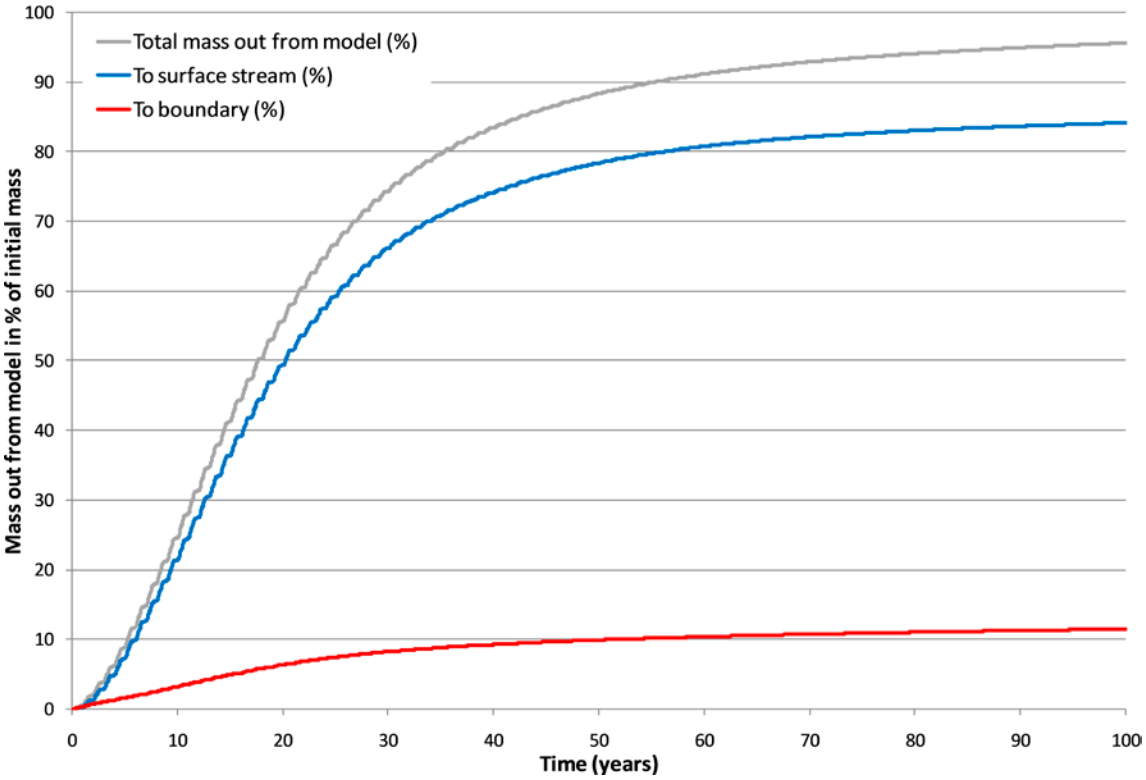

Figure 7-67. *Solute sinks for local model B (based on 10000AD_10000QD) during 100 years of simulation. The grey line is the total amount in % of the applied mass that leaves the model, the blue line is the total amount of the applied mass that goes to the MIKE 11 streams, and the red line is the total amount of the applied mass that goes to the boundary.*

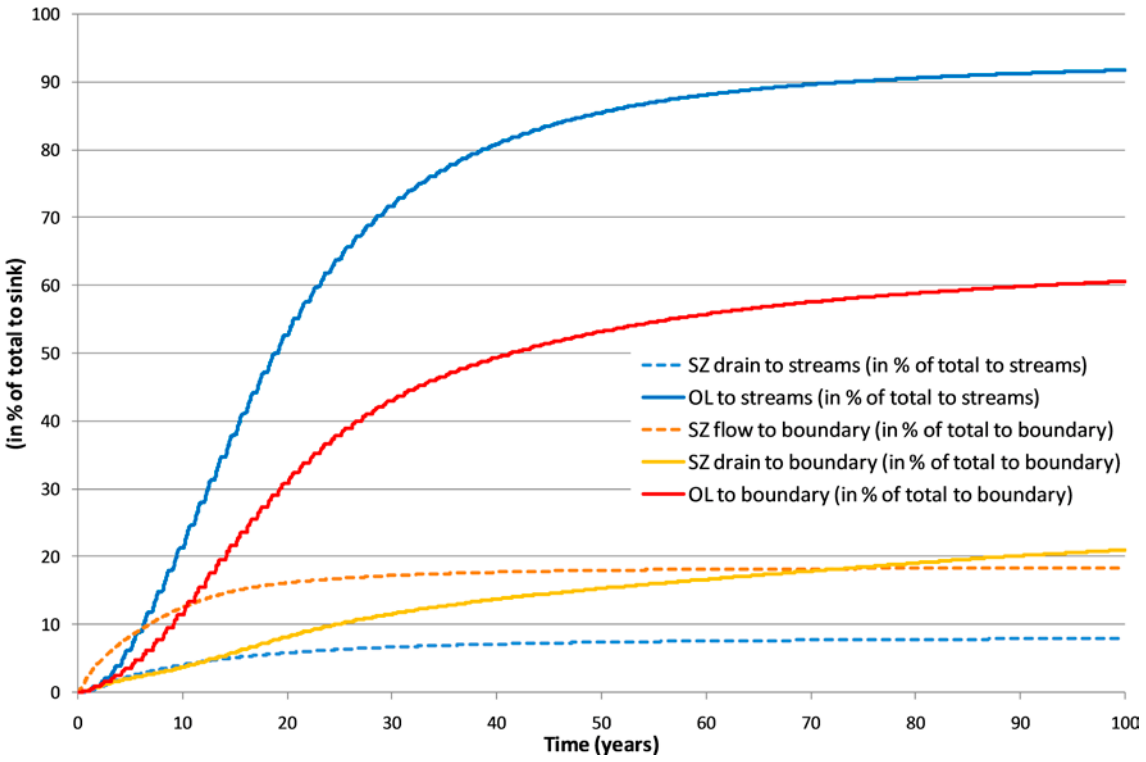

Figure 7-68. *Distribution of mass to different model sinks for local model B (based on 10000AD_10000QD). The blue lines show the distribution of the mass going to the streams the red and orange lines the distribution of mass going to the boundary.*

Figure 7-69 shows surface plots for the simulation with low dispersion coefficients in all layers. Results are illustrated for six different layers after one year of simulation. Layer L2 is a QD layer, L4 is the uppermost bedrock layer, L9 is the layer with the initial concentration source and is situated at c. 40 m.b.s.l. Layers 12, 15 and 20 are all bedrock layers and are situated at c. 60, 100 and 200 m.b.s.l., respectively. The figure shows that solute mainly reaches the surface along the lake shoreline and the MIKE 11 surface streams. In the first bedrock layer, L4, the solute is more spread out over the surface; thus, the pattern in L2 is a reflection of the transport pattern in the QD. In layer L9 the fractures in the bedrock are clearly seen. In layer L20 concentration is seen in the areas which are strong recharge areas according to Figure 7-16.

Figure 7-70 shows surface plots for layer L2, which is in the middle of the three QD layers in the model, at different times after the simulation start. The figure shows that the transport in most areas is rather fast and already after one year of simulation the main transport pattern is seen. After 50 years of simulation the solute concentration has decreased in most areas and the concentration is mainly left in areas located within some distance from the surface streams.

Figures 7-72 and 7-73 show the concentration along the profile illustrated in Figure 7-71 at different times after the start of the simulation. At the start of the simulation, the concentration is located in layer L9 at c. 40 m.b.s.l. After one year, the solute concentration has started to move upwards in discharge areas and downwards in recharge areas. As time goes, the solute moves further downwards in the recharge areas. However, deeper down the solute starts moving towards the former lake areas and as it reaches a discharge area it turn upwards. After 5 years of simulation, the solute is mainly located under the lake areas and it is moving upwards towards the lake shoreline. After 100 years of simulation almost no solute is seen along the profile.

Figures 7-75 and 7-76 show the concentration along the profile illustrated in Figure 7-74 at different times after the start of the simulation. In the same way as for the profile illustrated in Figures 7-71 to 7-73, the solute is moving downwards in recharge areas and upwards under the lake and stream areas. As time goes, the solute moves towards the lake areas and then upwards. After 100 years of simulation only small fractions of the solute mass are left along the profile.

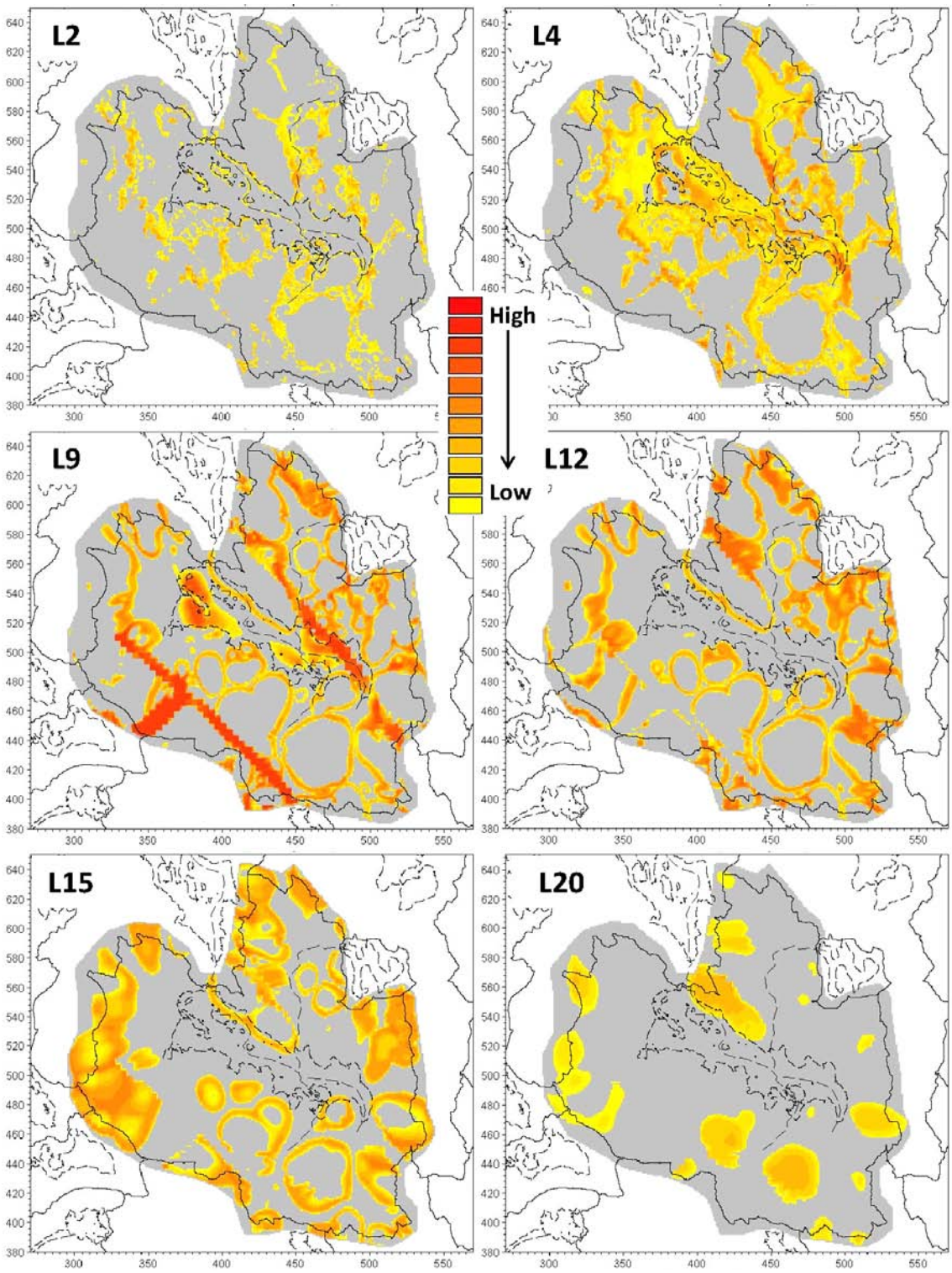

Figure 7-69. *Surface plots of calculated concentrations for local model B (based on 10000AD_10000QD) in six different layers after one year of AD simulation with low dispersion coefficients in all layers.*

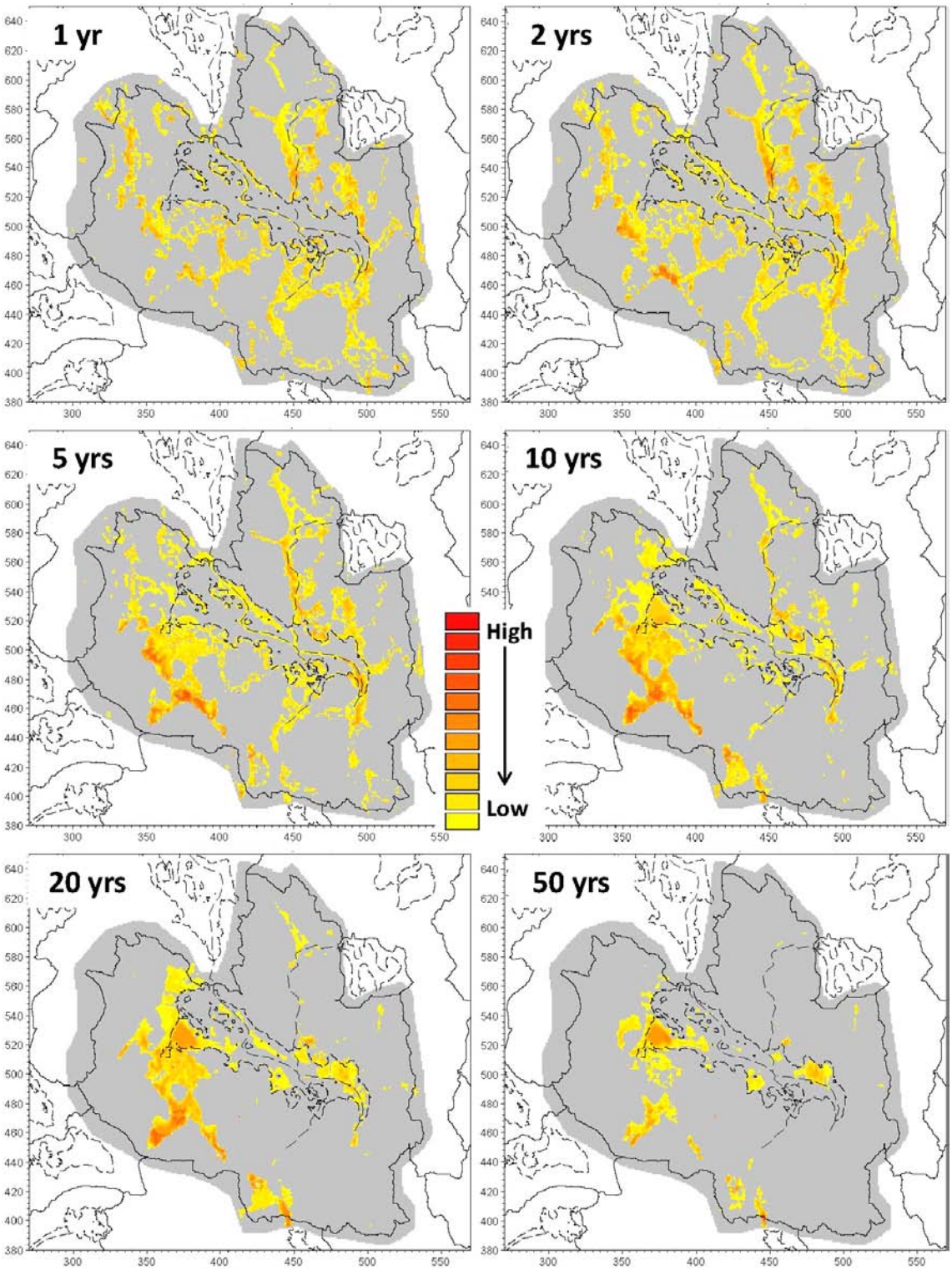

Figure 7-70. *Surface plots of calculated concentrations in layer L2 in local model B (based on 10000AD_10000QD) after 1, 2, 5, 10, 20 and 50 years of AD simulation with low dispersion coefficients in all layers.*

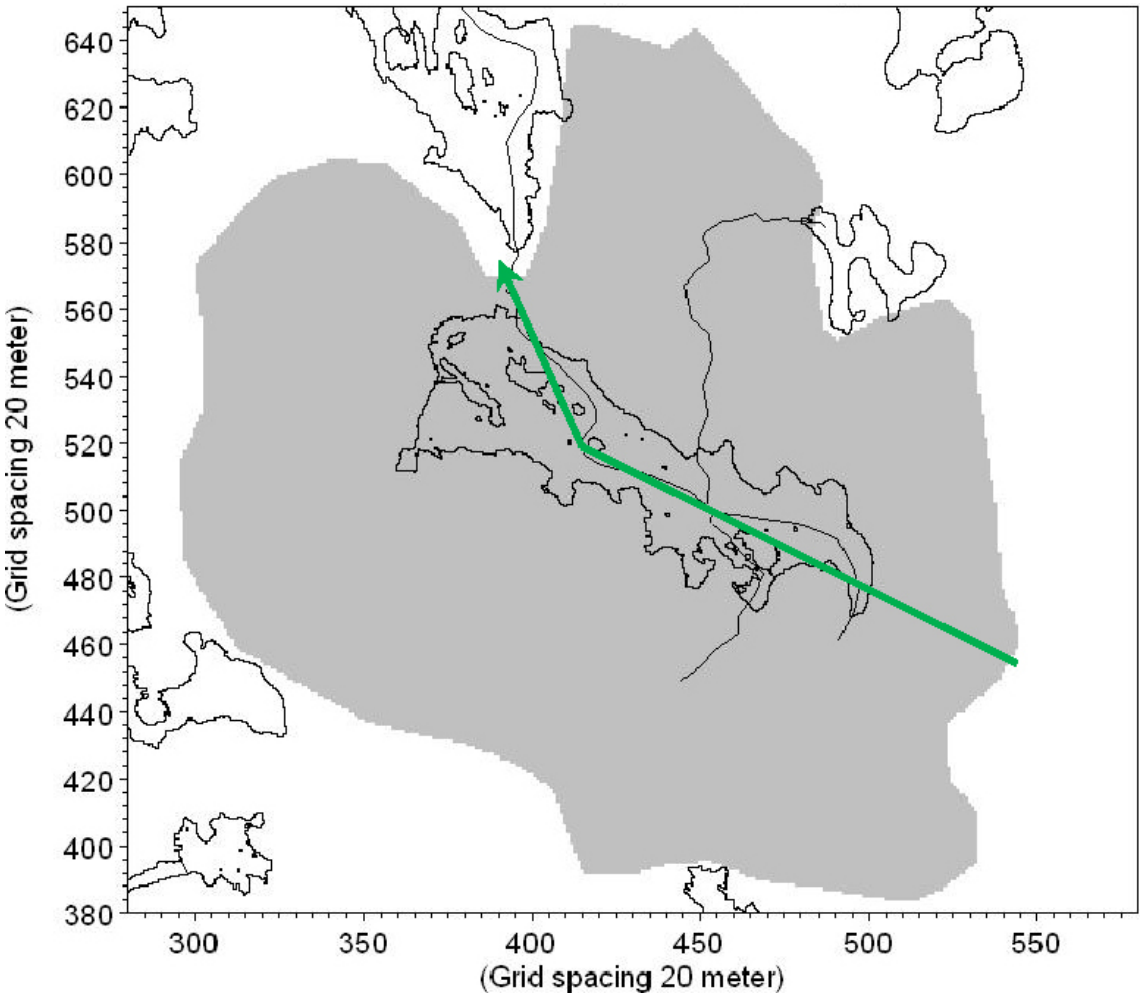

Figure 7-71. *Location of profile in the SE-NW direction across local model B.*

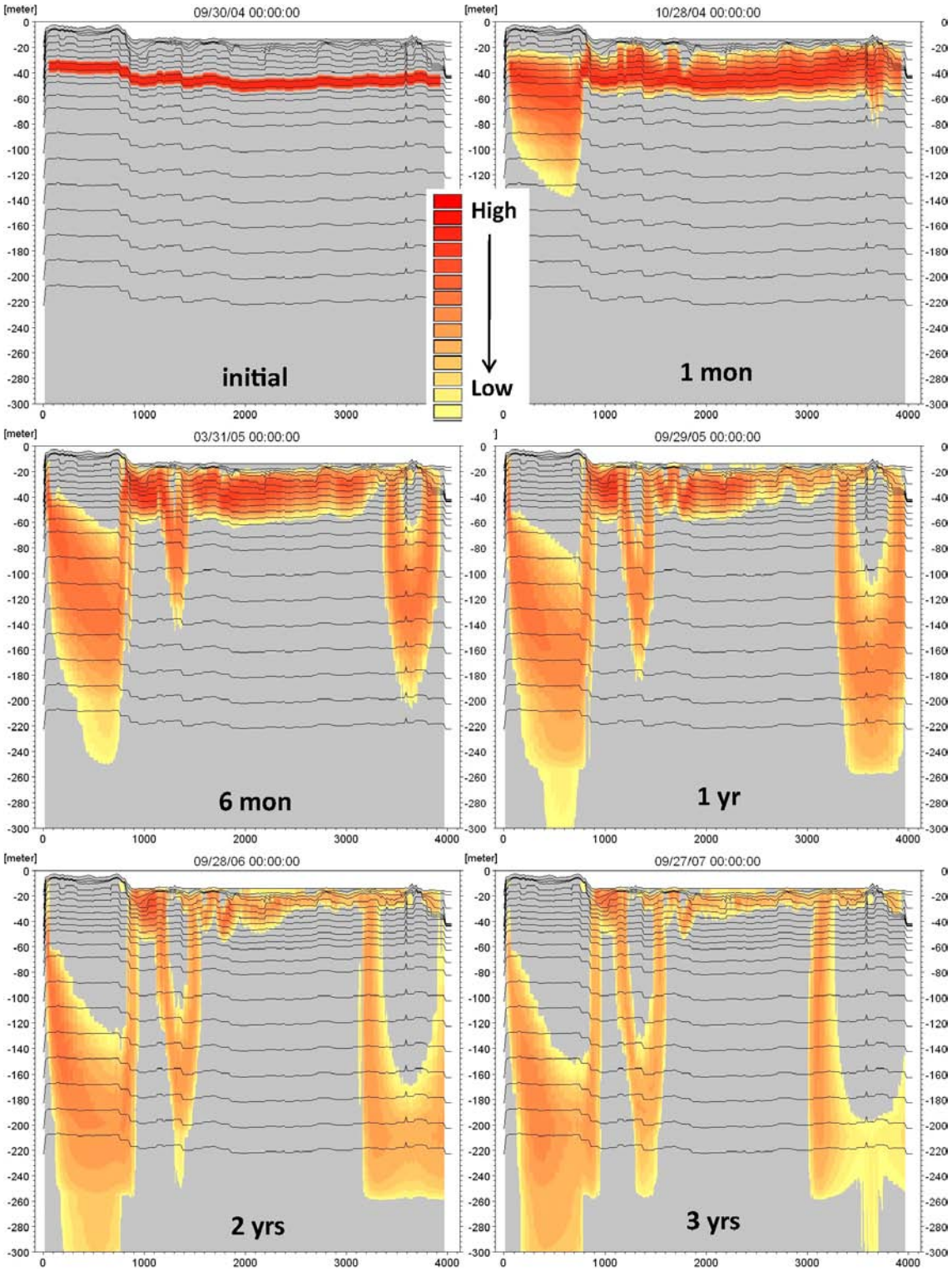

Figure 7-72. *Concentrations at different times up to three years of simulation along profile through local model B (based on 10000AD_10000QD) with location shown in Figure 7-71.*

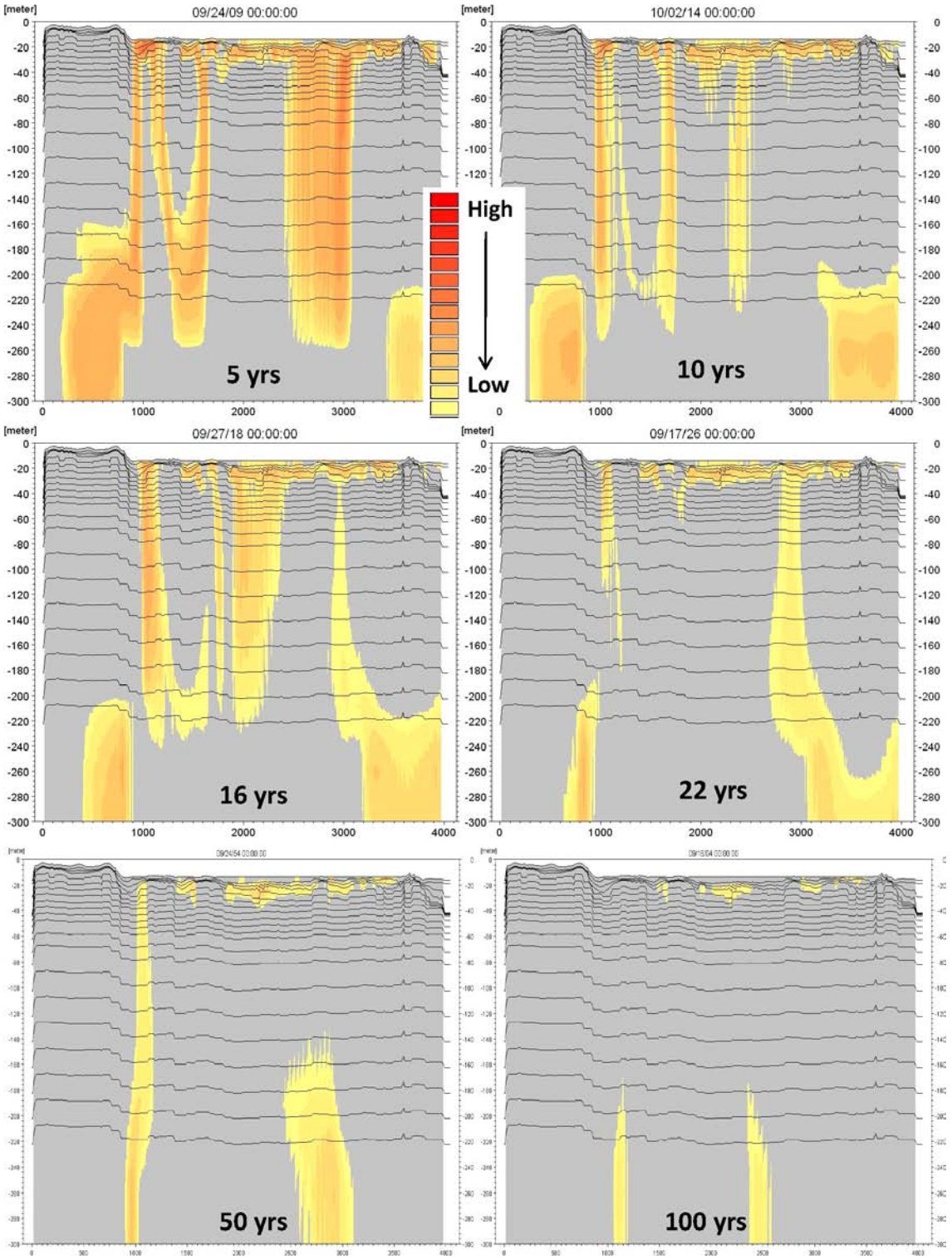

Figure 7-73. *Concentrations at different times between 3 years and 100 years of simulation along profile through local model B (based on 10000AD_10000QD) with location shown in Figure 7-71.*

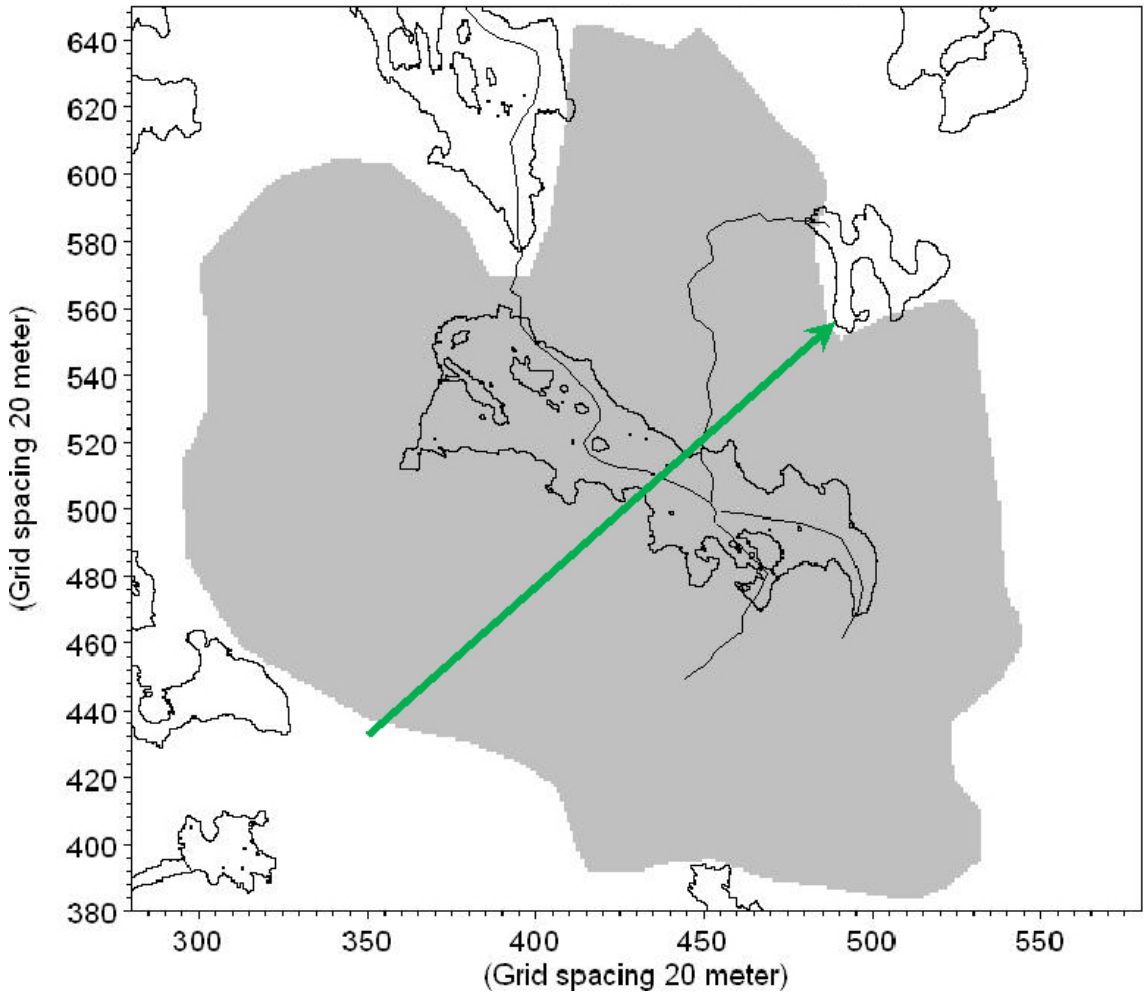

Figure 7-74. *Location of profile in the SW-NE direction across local model B.*

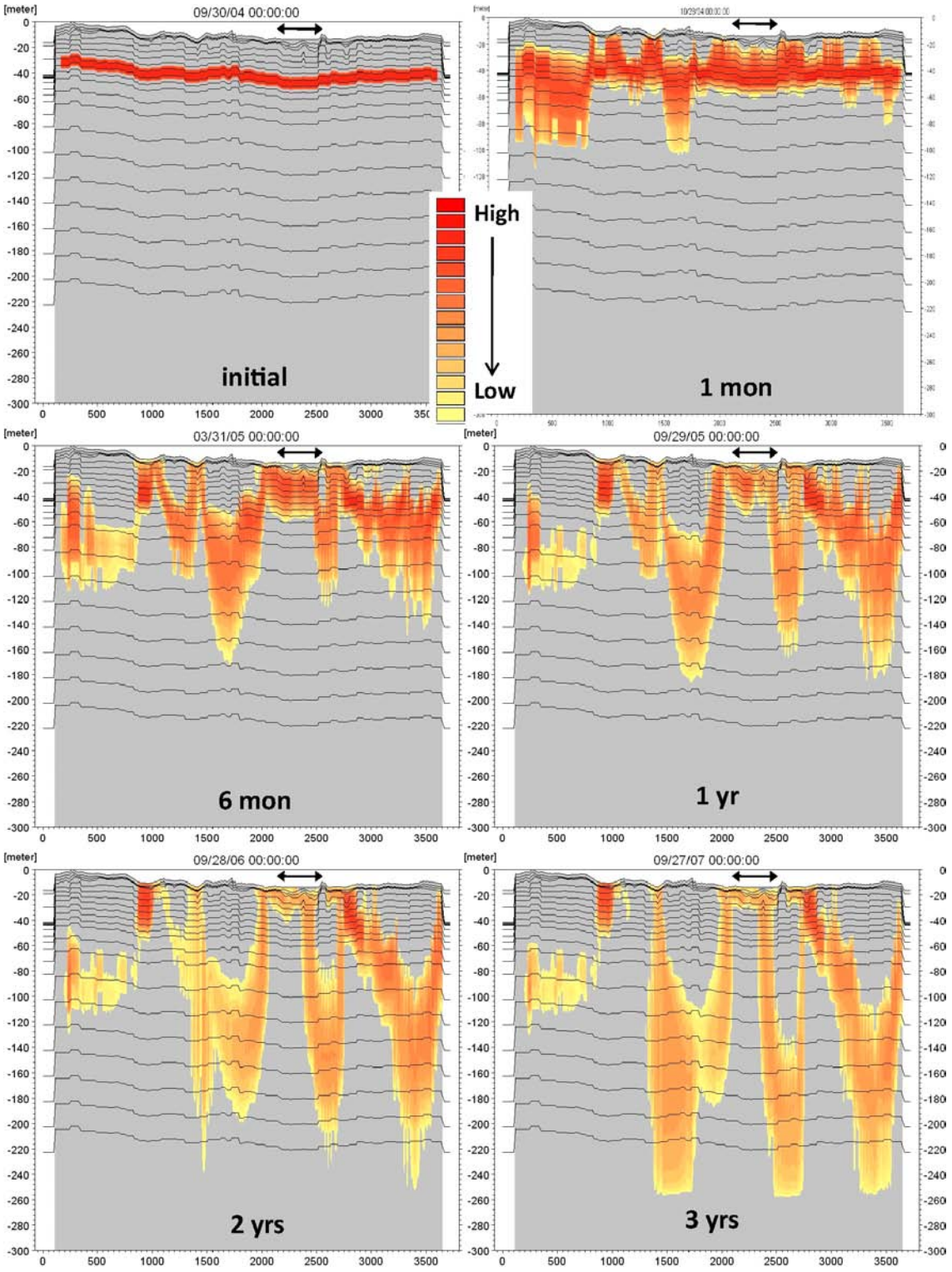

Figure 7-75. *Concentrations at different times up to three years of simulation along profile through local model B (based on 10000AD_10000QD) with location shown in Figure 7-74. The arrow above the ground surface shows the location of the terrestrialised lake.*

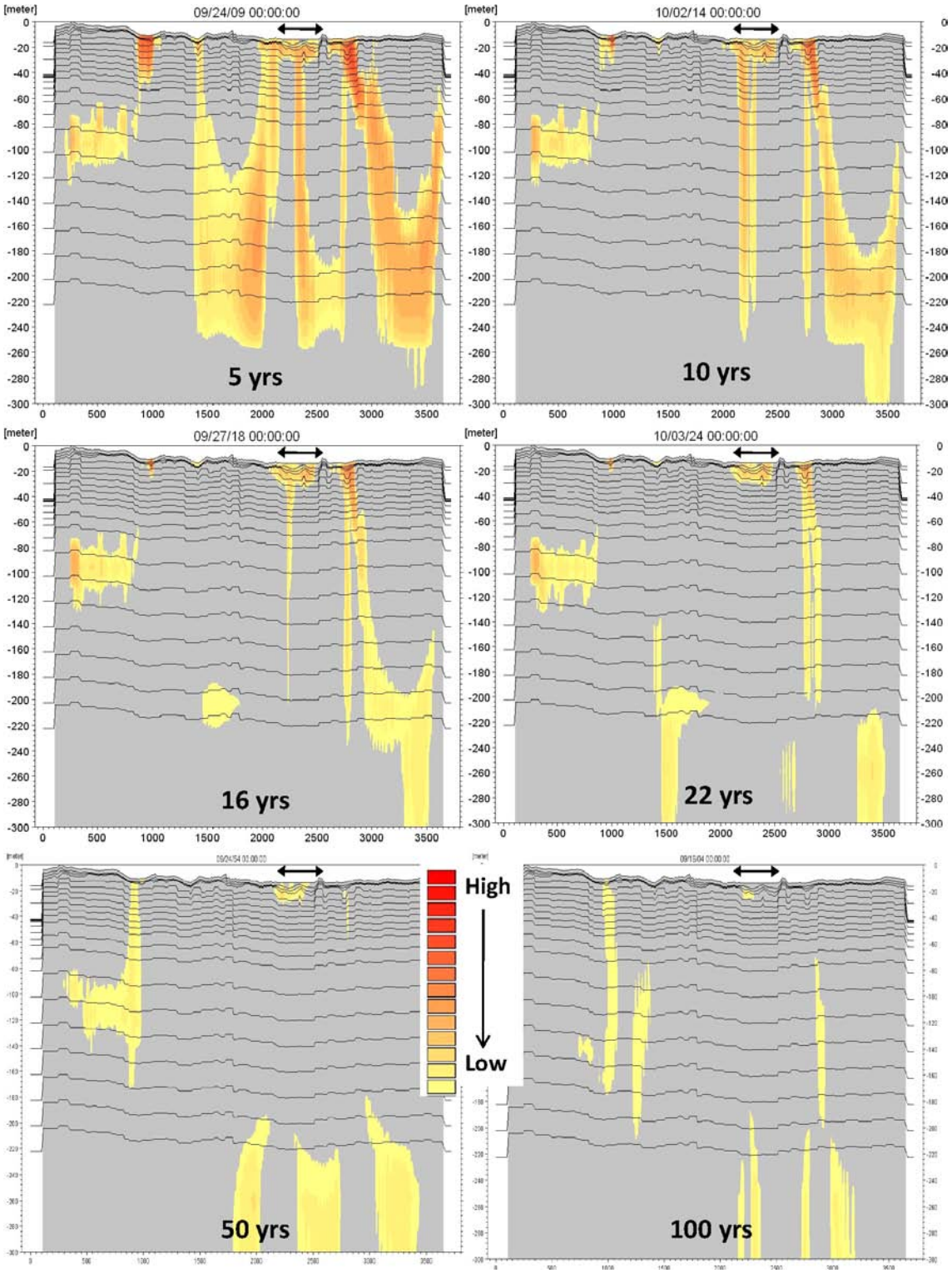

Figure 7-76. *Concentrations at different times between 3 years and 100 years of simulation along profile though local model B (based on 10000AD_10000QD) with location shown in Figure 7-74. The arrow above the ground surface shows the location of the terrestrialised lake.*

7.3.2 Sensitivity to dispersion parameters

In the second local model B simulation with the AD transport module, the dispersion coefficients in the QD layers were increased. The longitudinal dispersivity was changed from 0.2 m to 20 m and the transverse from 0.01 m to 0.2 m. No changes were made in the bedrock layers.

Table 7-4 compares the mass balance parameters for the two AD simulations made for the local model B. The differences are very small. The largest differences are found in the parameters quantifying the amounts of mass going to the boundary. The portion of solute going from the saturated zone to the boundary is somewhat larger for the case with higher dispersion and, consequently, the amount going from the overland to the boundary is smaller. The reason is that the higher dispersion causes more spreading in the saturated zone and thus more solute reaches the boundary.

Figure 7-77 compares surface plots for layer L2 at different times for the two simulations with different dispersion coefficients. On the left side results from the simulation with low dispersion coefficients in all layers are shown, and on the right results from the simulation with stronger dispersion in the QD. The results are very similar although, as expected, the solute is more dispersed on the right side.

Figure 7-78 compares results from the two AD simulations down to the depth 30 m.b.s.l. along the profile in Figure 7-71. Results are illustrated after 1, 5 and 20 years of simulation. The figure shows that in the case with the higher dispersion in the QD a larger part of the lake area is covered by solute.

Figure 7-79 compares results from the two AD simulations down to the depth 30 m.b.s.l. along the profile in Figure 7-74. Results after 1, 5 and 20 years of simulation are illustrated. In the same way as in Figure 7-78, Figure 7-79 shows that in the case with the higher dispersion in the QD a larger part of the terrestrialised lake area is underlain by solute. Furthermore, the figure shows that the concentration is also more widely spread in the valleys on the left side of the profile.

Table 7-4. Mass balance parameter for two cases with different dispersion coefficients. SZ is the saturated zone, OL is the overland compartment. Simulations are based on the 10000AD_10000QD combination of shoreline and QD model.

	Low dispersion coefficients QD (%)	High dispersion coefficients QD (%)
Out from model (in % of initial mass)	**95.7**	**95.9**
To surface stream (in % of 'Out from model')	**88.0**	**88.1**
SZ drain to stream (in % of 'To surface stream')	8.0	8.0
SZ baseflow to stream (in % of 'To surface stream')	0.2	0.2
OL to stream (in % of 'To surface stream')	91.8	91.8
To boundary (in % of 'Out from model')	**12.0**	**11.9**
SZ flow to boundary (in % of 'To boundary')	18.4	18.9
SZ drain to boundary (in % of 'To boundary')	21.0	22.2
OL to boundary (in % of 'To boundary')	60.6	58.9

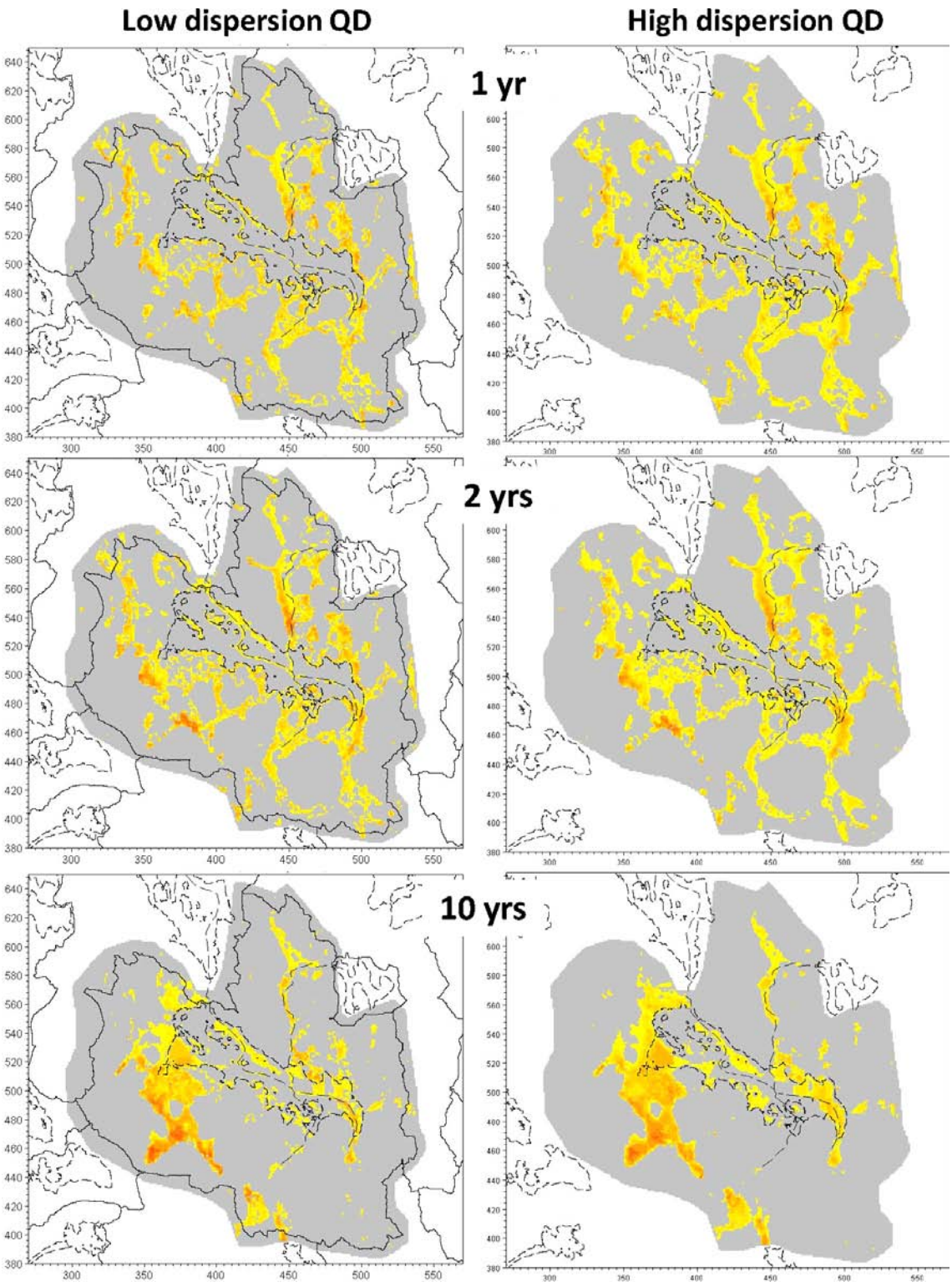

Figure 7-77. *Surface plots of calculated concentrations (local model B 10000AD_10000QD) in layer L2 in the QD after 1, 5 and 20 years of AD simulation with low dispersion (left side) and high dispersion (right side) in the QD.*

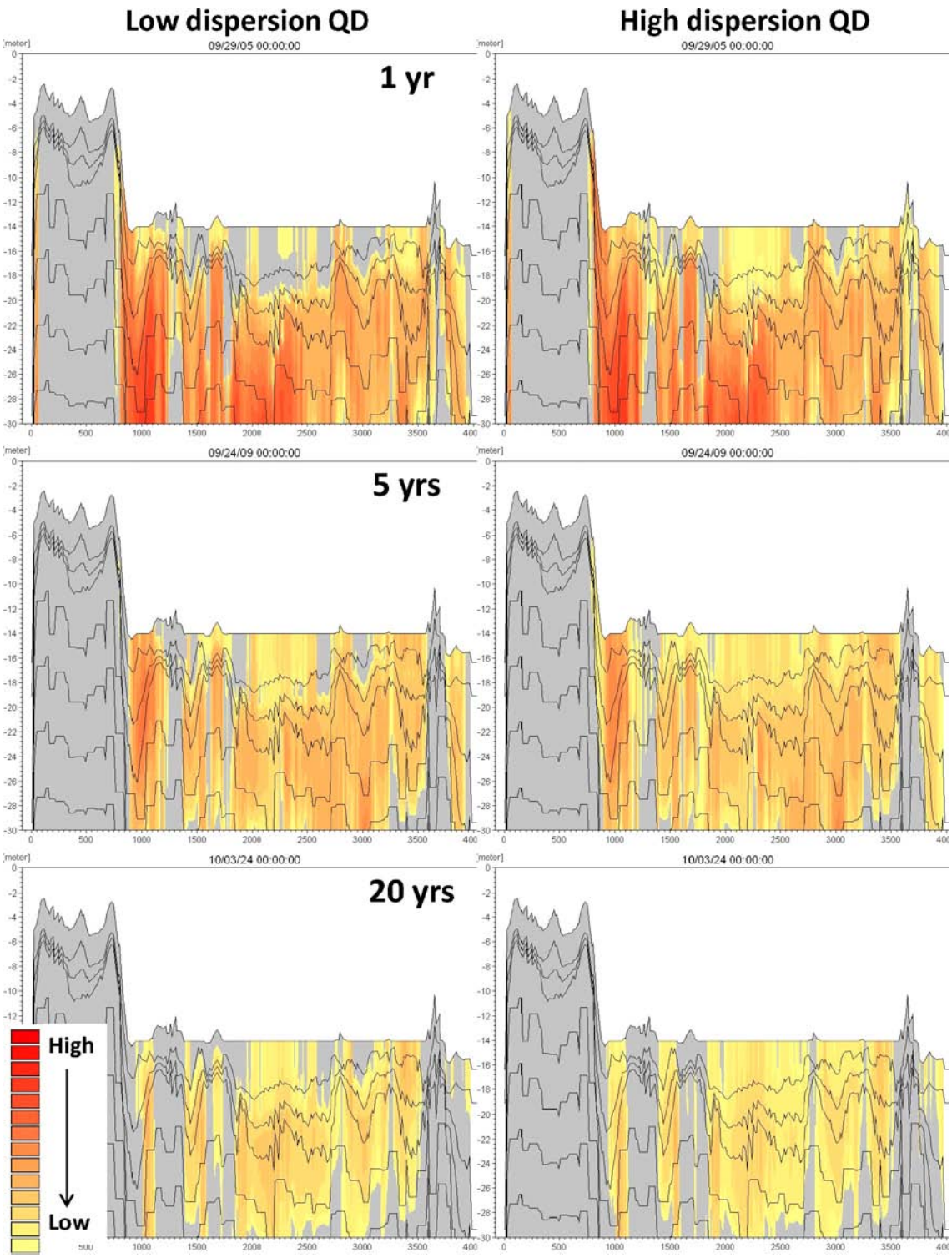

Figure 7-78. *Calculated concentrations along profile through local model B (based on 10000AD_10000QD) shown in Figure 7-71 for the upper 30 meters after 1, 5 and 20 years of AD simulation with low dispersion (left side) and high dispersion (right side) in the QD.*

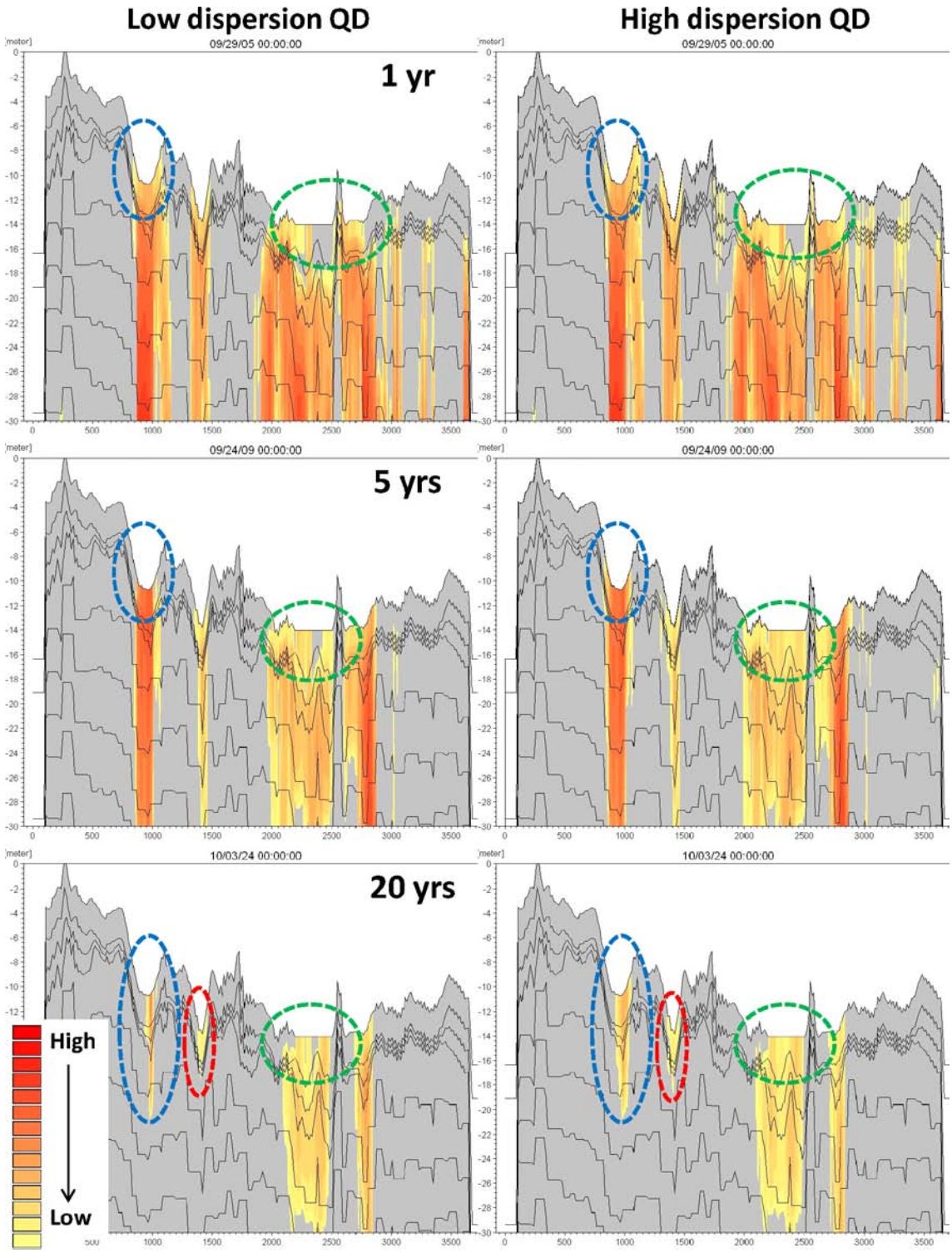

Figure 7-79. *Calculated concentrations along profile through local model B (based on 10000AD_10000QD) shown in Figure 7-74 for the upper 30 meters after 1, 5 and 20 years of AD simulation with low dispersion (left side) and high dispersion (right side) in the QD. Areas for which the main differences are noted are marked in the figure.*

7.4 Solute transport from selected deposition holes

Based on the calculated discharge points presented in /Joyce et al. 2010/, ten canister positions in the repository with relatively high groundwater flow rates in the deposition holes and short travel times to the ground surface were selected. The flow paths from the ten canisters are a subset of the flow paths discussed earlier in this report. Using the ConnectFlow particle tracking simulations of flow paths from the repository, the positions at 40 m.b.s.l. along the flow paths associated with the ten selected deposition holes were identified and then used as source locations in transport modelling with MIKE SHE.

Separate transport simulations were made for each of the ten source locations using the advection-dispersion (AD) module in MIKE SHE. The purpose of these simulations was to study near-surface solute transport associated with canister positions and flow paths of particular interest for the safety assessment. The results for local models A and B are discussed below in Section 7.4.1 and Section 7.4.2, respectively.

7.4.1 Local model A

For the local model A, including objects 118, 120, and 121, flow paths from seven different deposition holes, or canisters, were identified within the model domain. Figure 7-80 shows the locations of the flow paths at 40 m.b.s.l. Within object 118, only the flow path from canister 1978 is located. Also for object 120 there is only one flow path, from canister 411. In object 121 five different flow paths are located, based on releases from the canisters with numbers 5756, 5757, 5758, 5761 and 6875.

In the grid cells corresponding to each position illustrated in Figure 7-80, a continuous concentration source was set in a MIKE SHE AD simulation. The source in each cell was given the same number as the canister from which the flow path originated. The strength of each source was 1 g/m^3 and the sources were located at 40 m.b.s.l. However, since the groundwater flow velocity varies in the model area, the solute mass produced by the sources may differ substantially. Therefore, the results should mainly be used to indicate the directions of the spreading from the different sources. Furthermore, as the simulations are very time-consuming it was not possible to run the simulations for more than approximately 65 years. For some of the sources, this period was too short for the solute to reach the ground surface or other model boundaries.

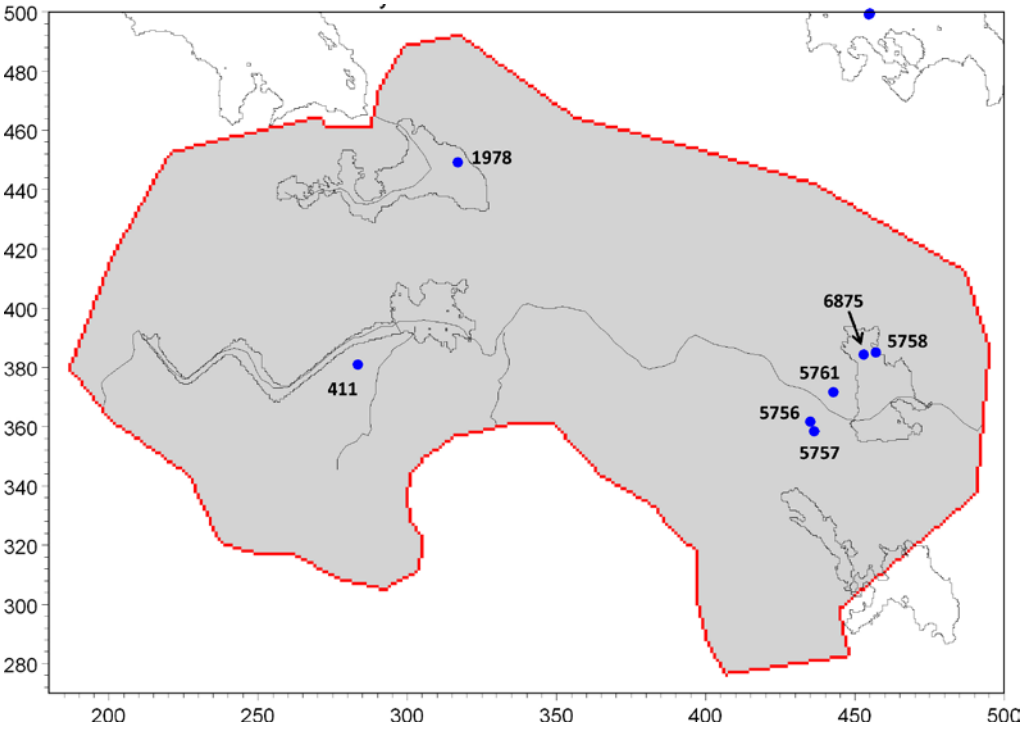

Figure 7-80. Starting positions at 40 m.b.s.l. within local model A for AD simulation with MIKE SHE. The positions are identified based on flow paths from hypothetical releases from selected deposition holes in the repository.

Canister 1978 (object 118)

Figure 7-81 shows the mass balance parameters for source 1978. The red line is the cumulative solute mass introduced in the model domain. The black line is the storage of the solute in the saturated zone. During the first 20 years, all introduced solute mass stays in the saturate zone. After c. 20 years, the solute has reached the overland water and starts to leave the model domain through the MIKE 11 surface stream system. After 65 years (i.e. at the end of the simulation) the saturated zone storage starts to converge to a steady state, where the amount of solute leaving the model equals the amount entering the model domain. All solute mass that leaves the model domain is transported by the surface streams. In the model, the stream is only included as a model sink and it is not possible to trace the solute after it has entered the stream.

Figure 7-82 shows a surface plot for object 118. The upper figure shows the location of the source at 40 m.b.s.l. and the lower figure shows the extent of the saturated zone concentration plume in the upper calculation layer. The strength of the source at 40 m.b.s.l. is 1 g/m^3 but the concentration at the surface is very low except directly above the concentration source. In Figure 7-82, all concentrations higher than 10^{-14} g/m^3 are illustrated; the scale is logarithmic. Figure 7-82 shows that the concentration is mainly transported directly to the MIKE 11 stream. However, part of the solute mass is being spread horizontally over a larger area.

Figure 7-83 shows the concentration along a profile in object 118; the scale for the concentration is the same as in Figure 7-82. The location and direction of the profile are illustrated in Figure 7-82. The concentration along the profile is illustrated after 1, 10 and 65 years of simulation. The figures show that the solute is mainly transported vertically upwards to the surface and when it has reached the surface it starts spreading in the horizontal direction in the top layer. From the top layer the solute spreads both horizontally and vertically.

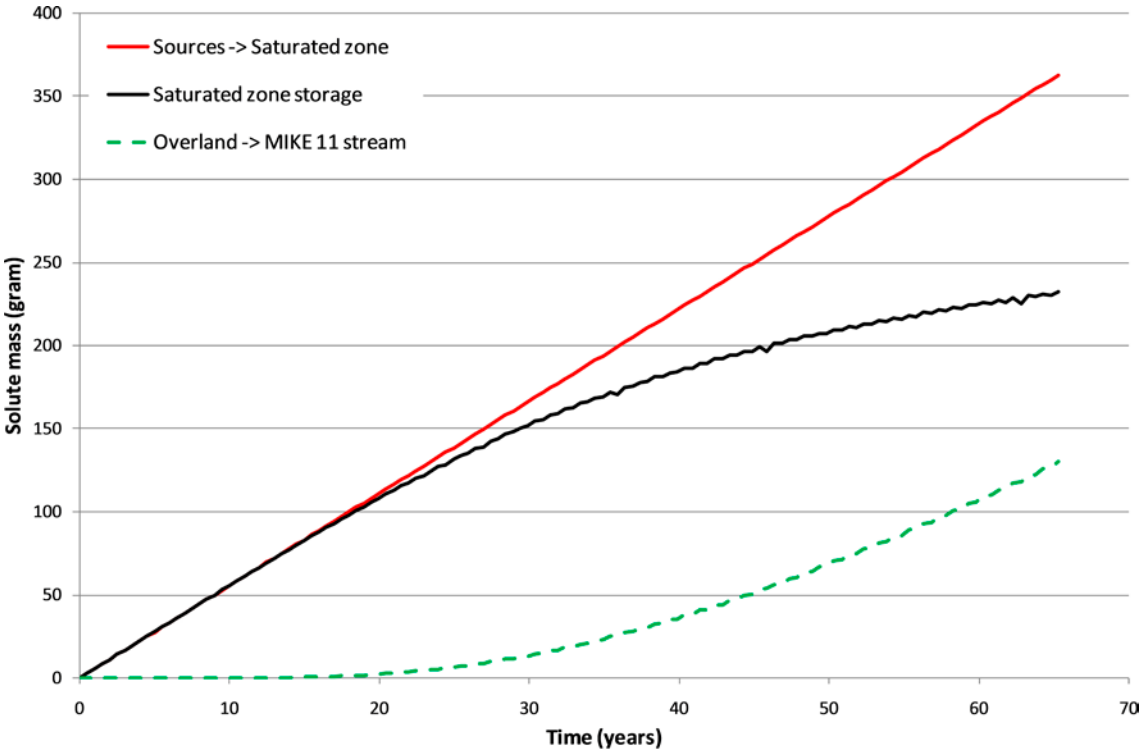

Figure 7-81. *Mass balance parameters for AD simulation with local model A based on 10000AD_10000QD and starting position 1978.*

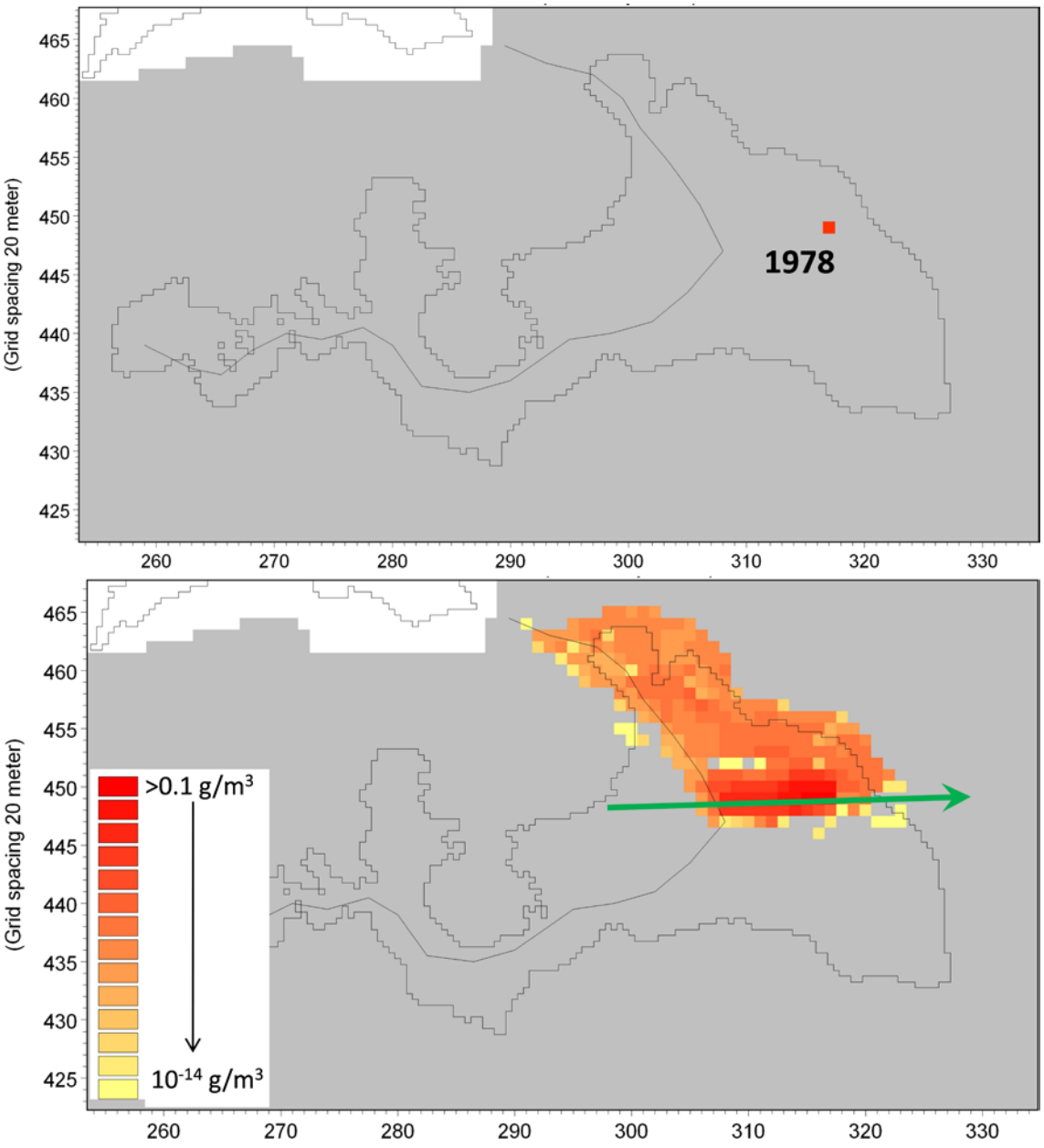

Figure 7-82. *Surface plots of object 118. The upper figure shows the location of source 1978 and the lower figure the extent of the concentration plume in the uppermost layer. The lower figure also shows the location and direction of the profiles illustrated in Figure 7-83. The simulation is based on the 10000AD_10000QD combination of shoreline and QD model.*

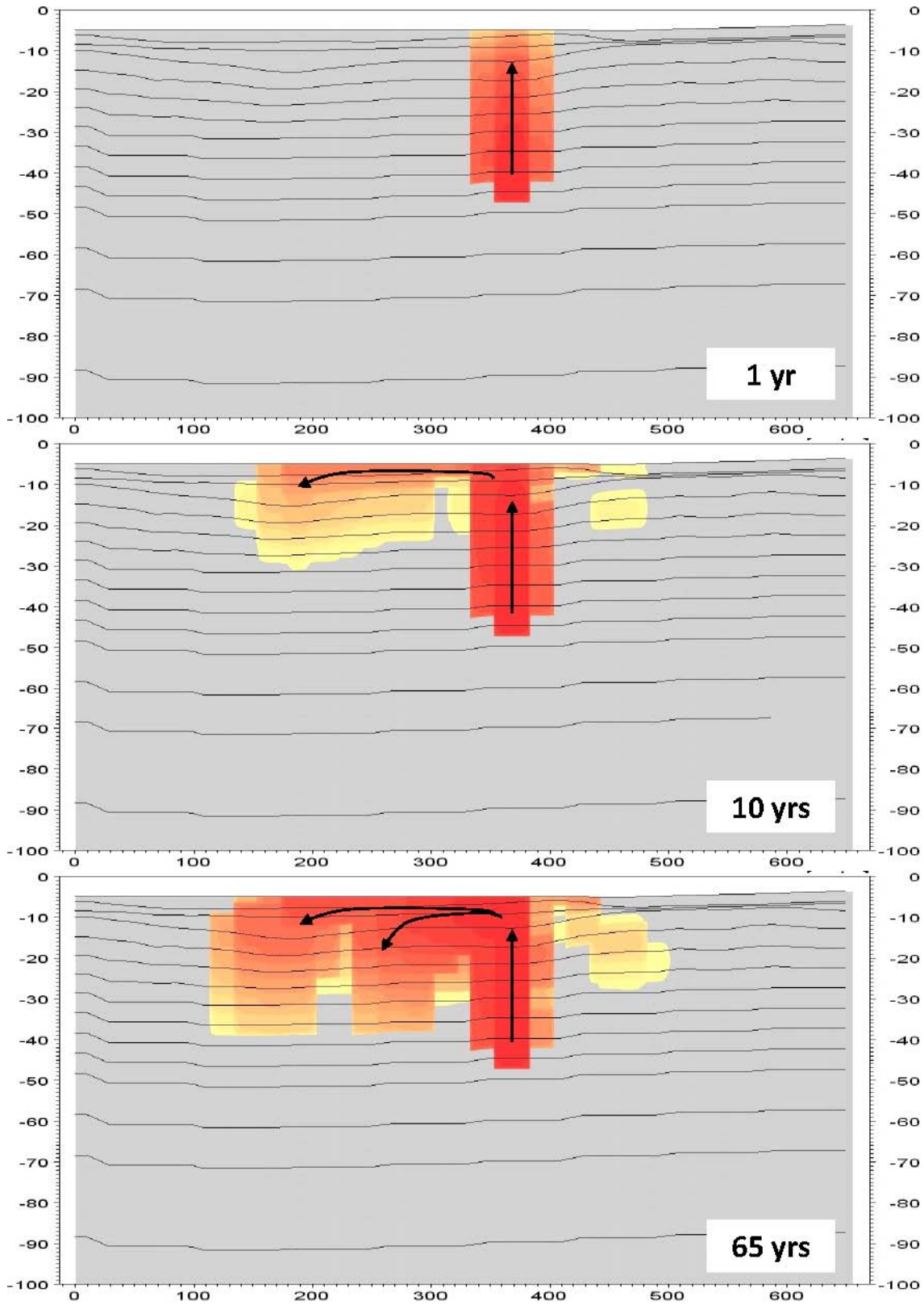

Figure 7-83. *Concentrations along profile shown in Figure 7-82, results after 1, 10 and 65 years of simulation.*

Canister 411 (object 120)

Figure 7-84 shows the mass balance parameters for source 411. The figure shows that all of the mass introduced to the model volume is still stored in the saturated zone after 65 years of simulation. The location of the source was obtained from the ConnectFlow model and it was defined as an exit point based in their model. In the MIKE SHE model, source 411 is located in a recharge area. The difference between the two models are probably due to that the MIKE SHE model includes more surface processes and a more detailed description of the QD layers, which may lead to local differences in the recharge and discharge patterns. In the area around source 411, a small-scale pattern of recharge and discharge areas is observed, and at short distances from source 411 discharge areas are found also in the MIKE SHE model.

Besides being located in a recharge area, source 411 is also connected to layers with high horizontal conductivities. This is further discussed in Section 7.2, see Figures 7-28 to 7-32. For source 411 no solute is observed in the upper layers. Figure 7-86 shows a profile across the area of source 411. The location and direction of the profile are illustrated in Figure 7-85; since no concentration is seen in the upper layers, Figure 7-85 shows the concentration plume in a bedrock layer located below the source. Figure 7-86 shows how the solute is transported downwards and then starts spreading in the horizontal direction as it reaches a layer with high horizontal conductivity. This is the same pattern as seen in Figures 7-31 and 7-32.

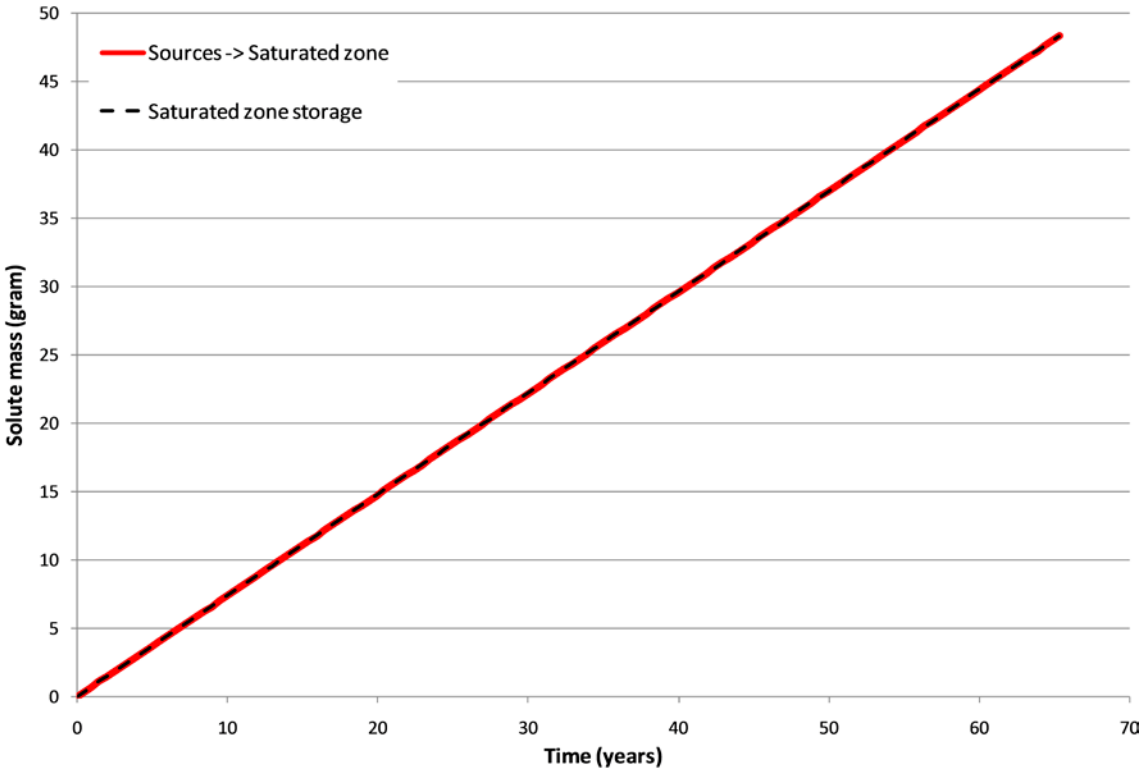

Figure 7-84. *Mass balance parameters for AD simulation with local model A based on the 10000AD_10000QD model and starting position 411.*

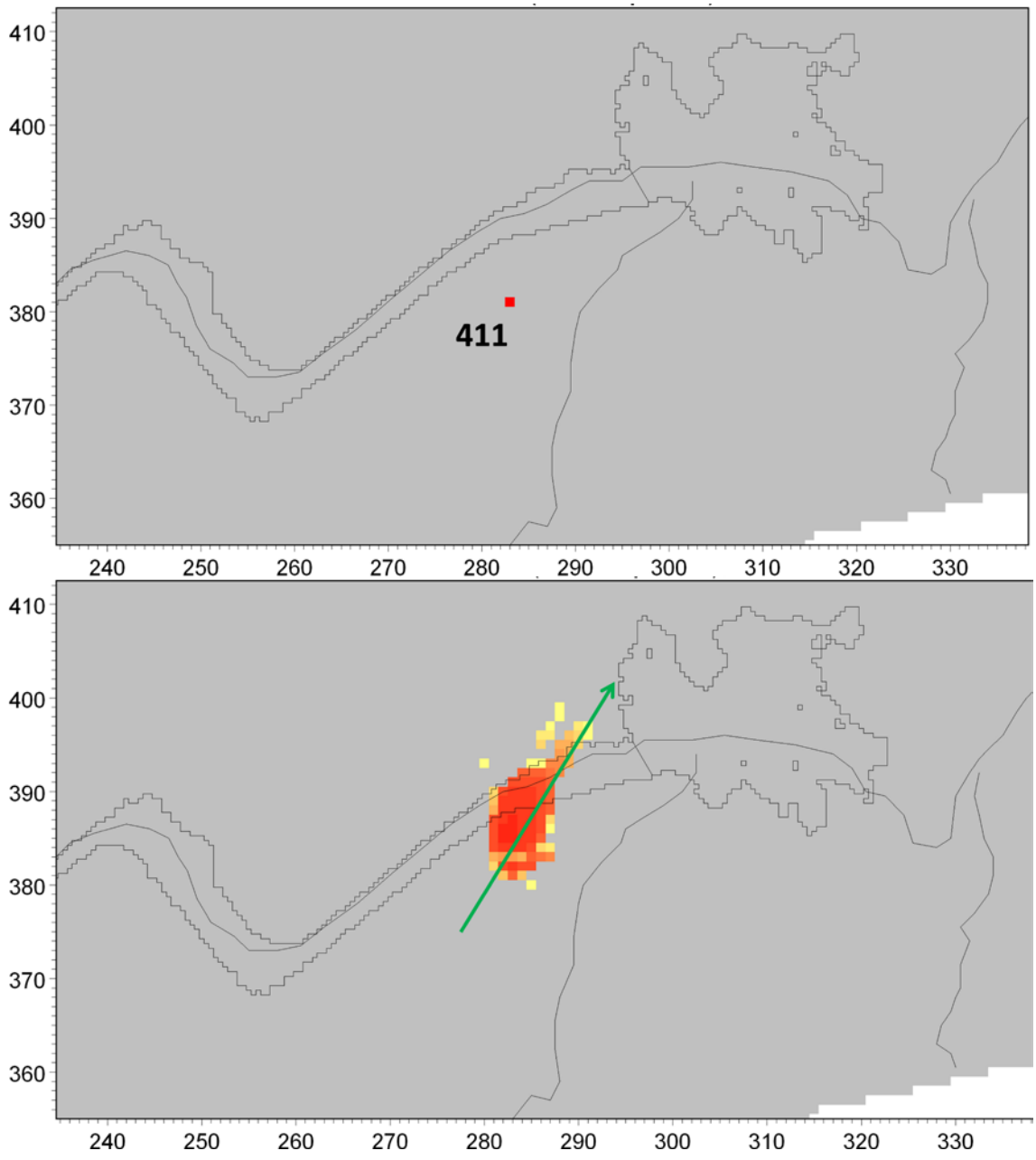

Figure 7-85. *The upper figure shows the location of source 411 and the lower figure the direction of the profile through source 411 illustrated in Figure 7-86. The concentration distribution shown in the figure is from a layer located below the source. The simulation is based on the 10000AD_10000QD model.*

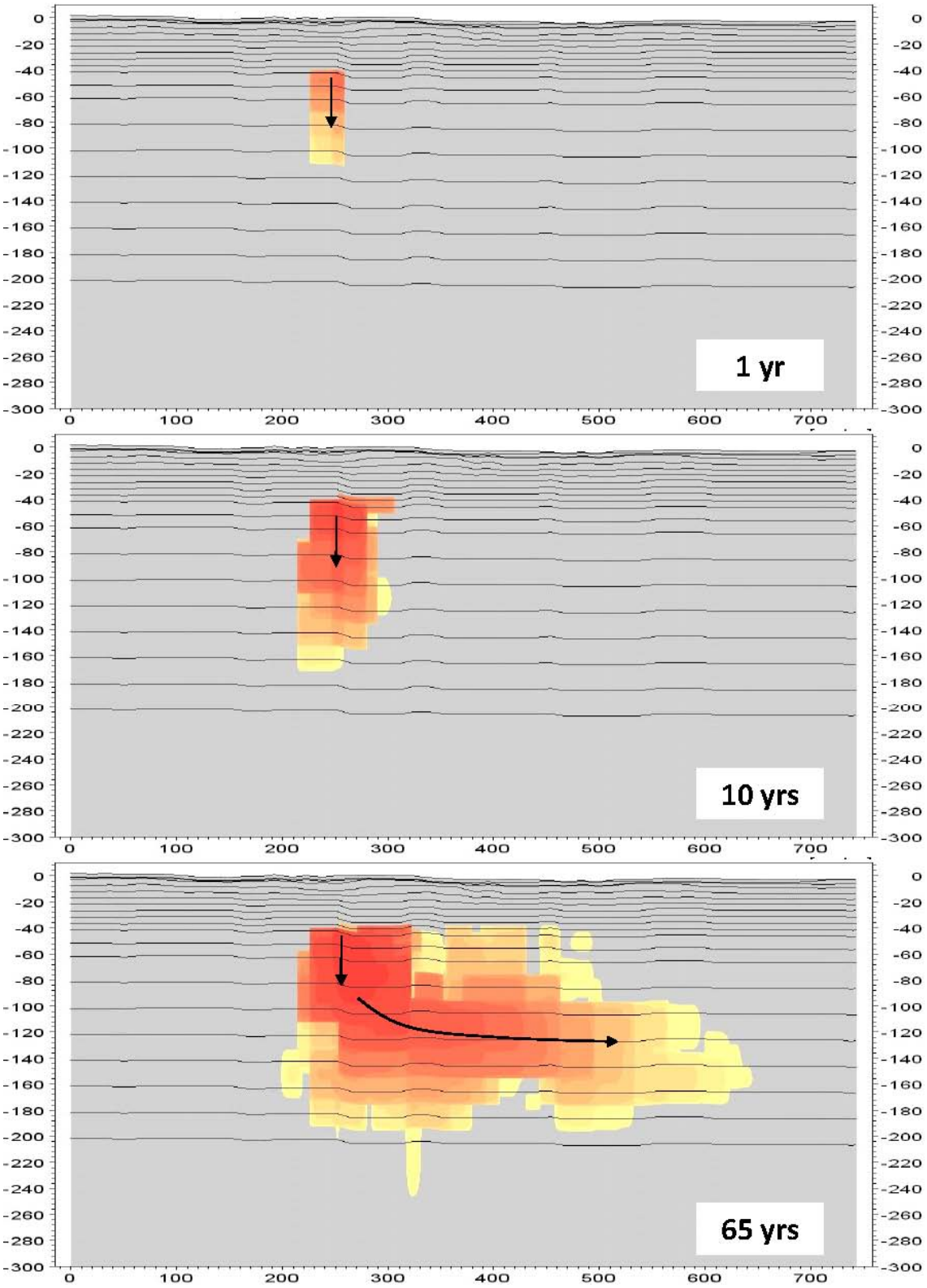

Figure 7-86. *Concentrations along the profile illustrated in Figure 7-85, results after 1, 10, and 65 years of simulation.*

Canister 5756 (object 121)

Figure 7-87 shows the mass balance parameters for the simulation based on source 5756. The source is located southwest of object 121_01, see the upper graph in Figure 7-88. After 65 years of simulation, about 90% of the applied solute mass is still left in the saturated zone. Most of the solute that has reached the surface stream has been transported to the stream by a subsurface drainage at a shallow depth in the highly conductive top layer, and only a very small portion has reached the stream via overland water. However, since the transport is significantly slower when going via the overland compartment, it is likely that the relative portion of solute leaving the model domain through overland will increase with time.

Figure 7-88 shows the location of solute source 5756 and a surface plot of the concentration in the upper QD layer after 65 years of simulation. The figure shows that the solute reaches the surface and spreads mainly along the surface stream. A small portion of the solute is however also spread towards the terrestrialised lake area.

A profile along the concentration plume that is transported towards the former lake area, Profile 1 in the figure, is illustrated in Figure 7-89. The profile shows that although the solute is transported vertically upwards rather quickly, the concentration that reaches the surface is very low and the solute is also transported horizontally towards the terrestrialised lake area in the bedrock layers. The lower figure in Figure 7-89 shows that after 65 years of simulation the main concentration plume is moving towards the former lake in the bedrock layers.

Figure 7-90 shows the concentration profile along Profile 2 in Figure 7-88. In this direction, the solute starts spreading vertically towards the surface and as the concentration reaches the QD layers it spreads in the horizontal direction in the upper layers. After 65 years of simulation the solute is spread along almost the entire profile and the solute starts reaching the stream.

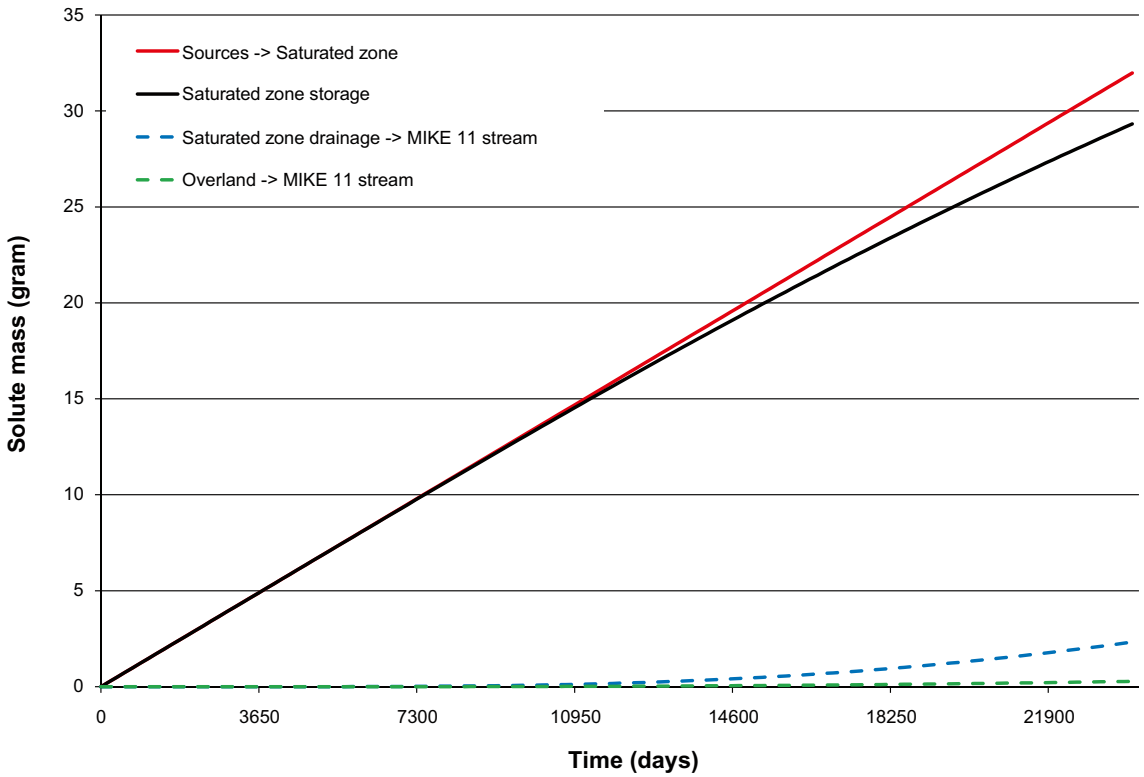

Figure 7-87. *Mass balance parameters for AD simulation with local model A based on the 10000AD_10000QD model and starting position 5756.*

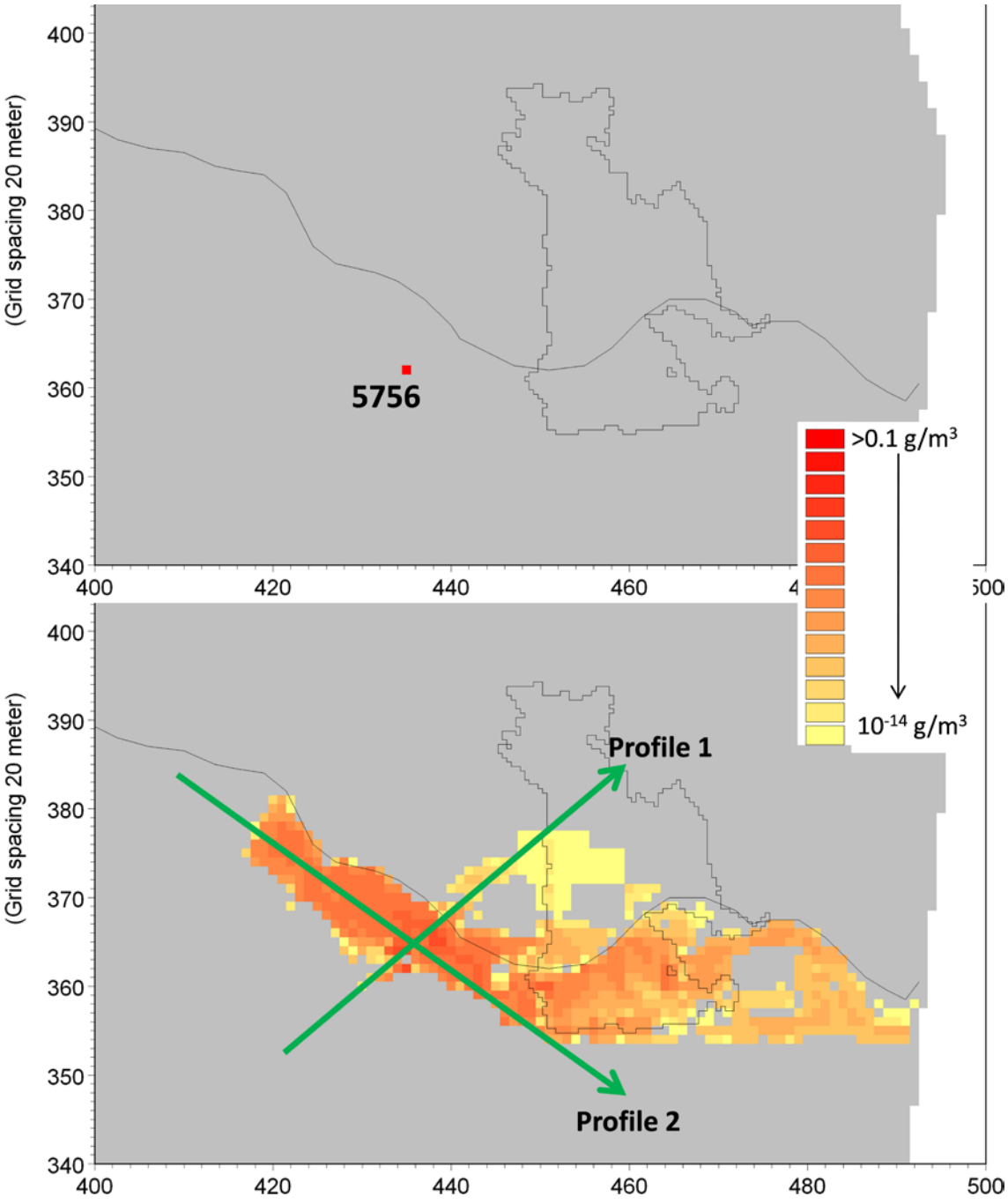

Figure 7-88. *Surface plot for object 121_01. The upper figure shows the location of source 5756 and the lower figure shows the extent of the concentration plume in the uppermost layer. The lower figure also shows the locations and directions of the profiles illustrated in Figure 7-89 and 7-90. The simulation is based on the 10000AD_10000QD model.*

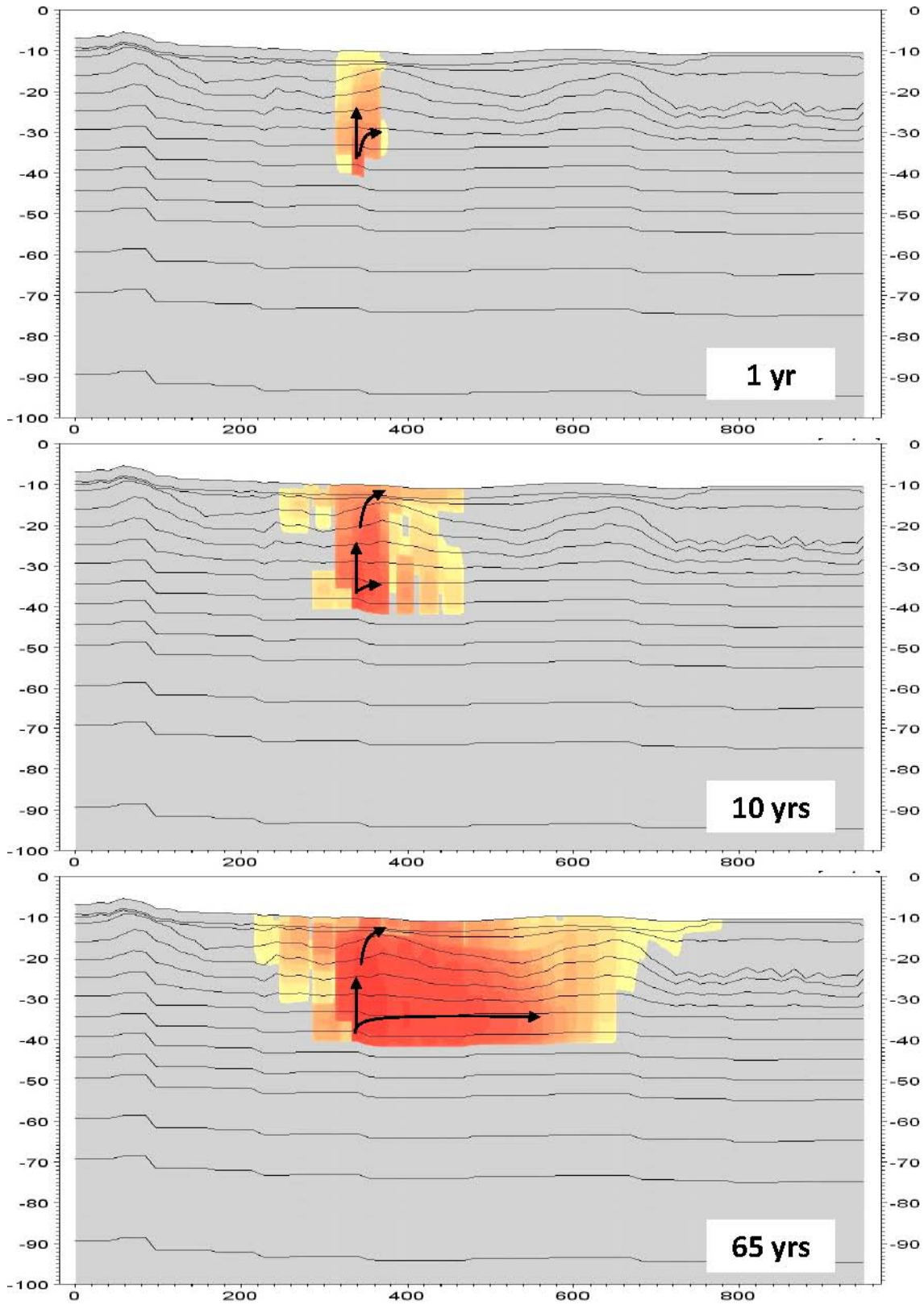

Figure 7-89. *Concentrations along Profile 1 illustrated in Figure 7-88, results after 1, 10 and 65 years of simulation.*

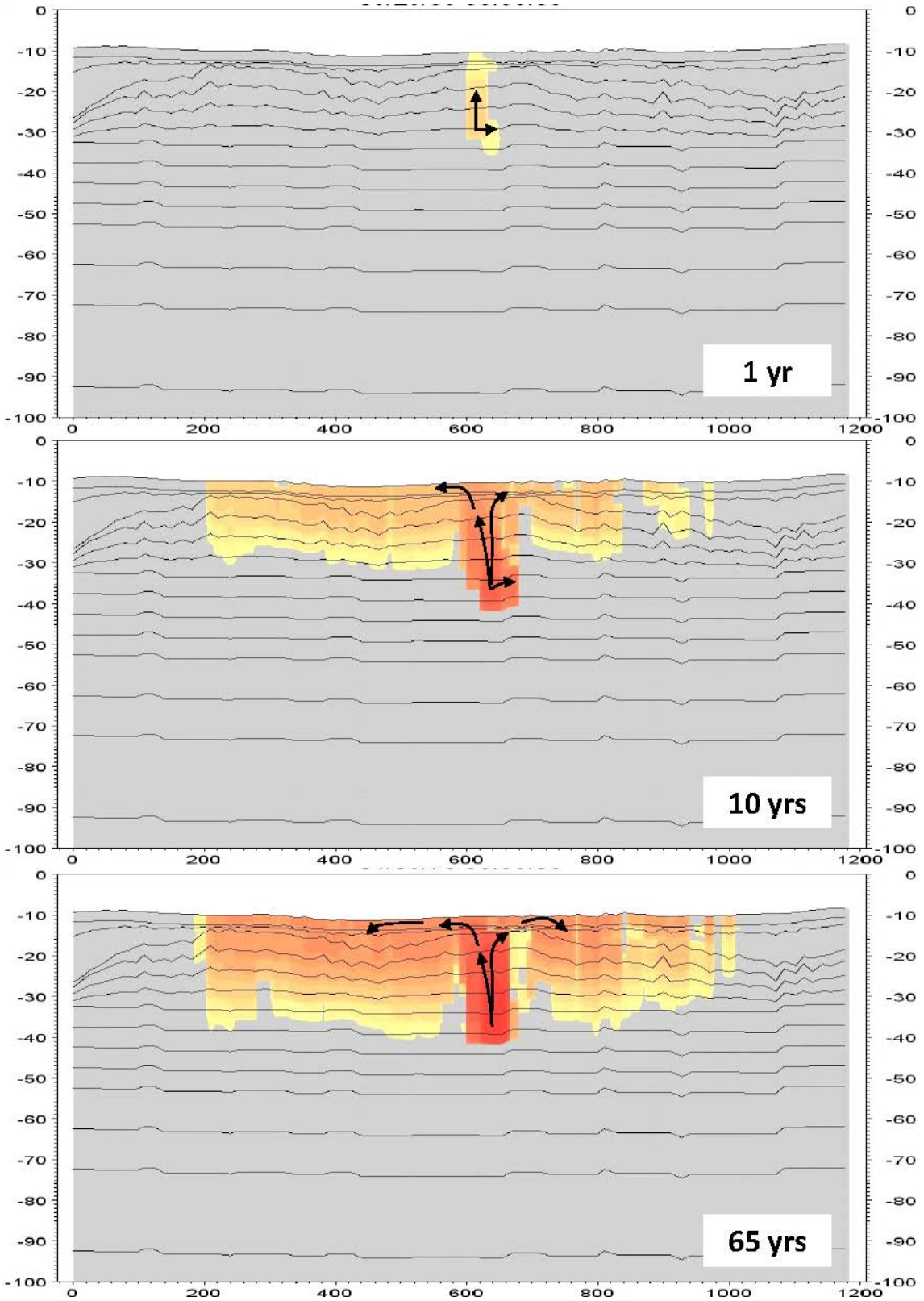

Figure 7-90. *Concentrations along Profile 2 illustrated in Figure 7-88, results after 1, 10 and 65 years of simulation.*

Canister 5757 (object 121)

Figure 7-91 shows the mass balance graphs for source 5757. The location of 5757 is illustrated in the upper graph in Figure 7-92. Figure 7-91 shows that the saturated zone storage is small for source 5657, and most of the solute is transported to the MIKE 11 surface stream system. However, the figure shows that most of the solute mass is transported to the surface stream through drainage flow from the saturated zone, although the amount of solute reaching the stream through the overland compartment is increasing with time.

Figure 7-92 shows a surface plot for the uppermost layer after 65 years of simulation. The extent of the concentration plume is very similar to what was seen for source 5756 (Figure 7-88). The spreading on the surface is mainly in connection to the surface stream.

Figure 7-93 shows the concentration distribution along Profile 1 in Figure 7-92. The figure illustrates that the concentration is moving rather quickly in the vertical direction up to the surface, where it is spread towards the stream. In the upper layers the solute is also spread vertically downwards again.

Figure 7-94 shows the concentration profile in Profile 2 in Figure 7-92. Also this plot illustrates that the solute is first transported rapidly in the vertical direction up to the surface before it starts spreading horizontally in the upper layers, and then vertically downwards again.

Although sources 5756 and 5757 are located close to each other, the results differ significantly. The extent of the concentration plume (observing the horizontal view) is almost the same. However, the introduced mass differs significantly, which is a result of the differences in the flow fields (i.e. in the velocities in the source cells). Also the transport patterns along the profiles in the south-north direction differs due to the local topography, see Figure 7-89 and 7-93. Figure 7-95 shows the recharge and discharge areas in the QD layers for object 121_01. The figure shows that source 5756 is located in a recharge area in the QD, while 5757 is located in a discharge area; this can be an explanation of the differences in the results. In the bedrock, however, both sources are located in discharge areas, see Figure 7-96.

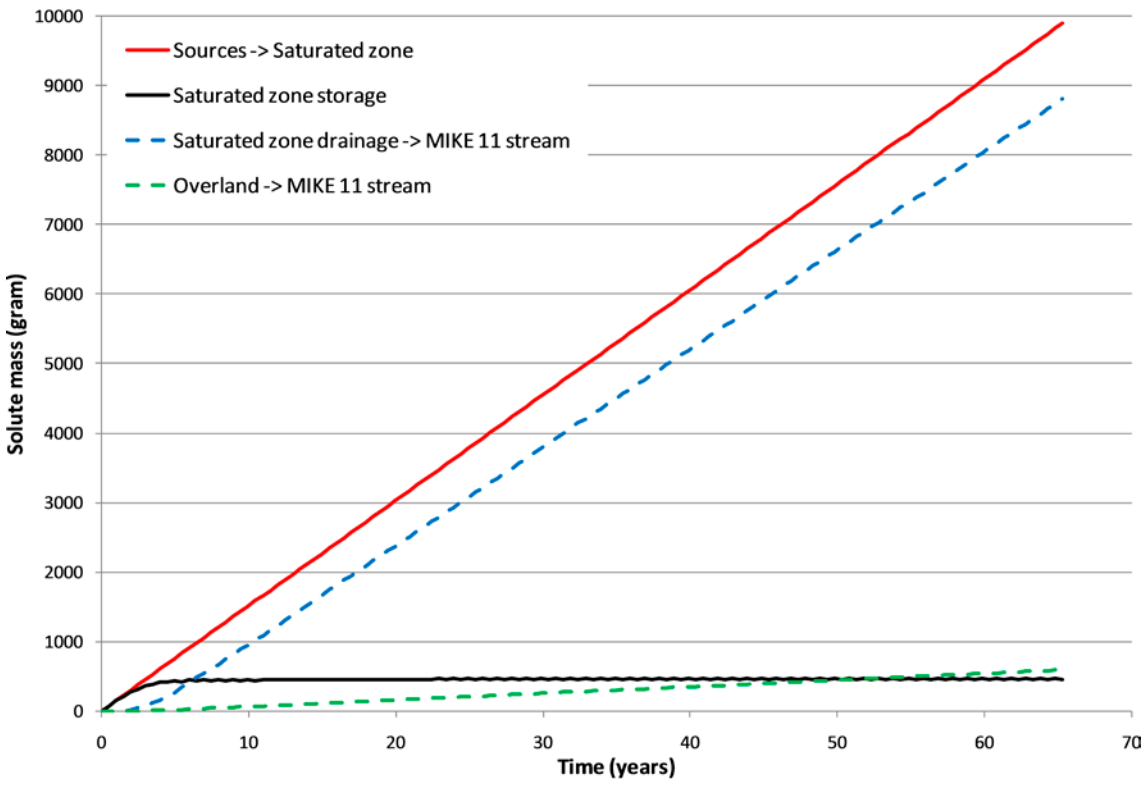

Figure 7-91. *Mass balance parameters for AD simulation with local model A based on the 10000AD_10000QD model and starting position 5757.*

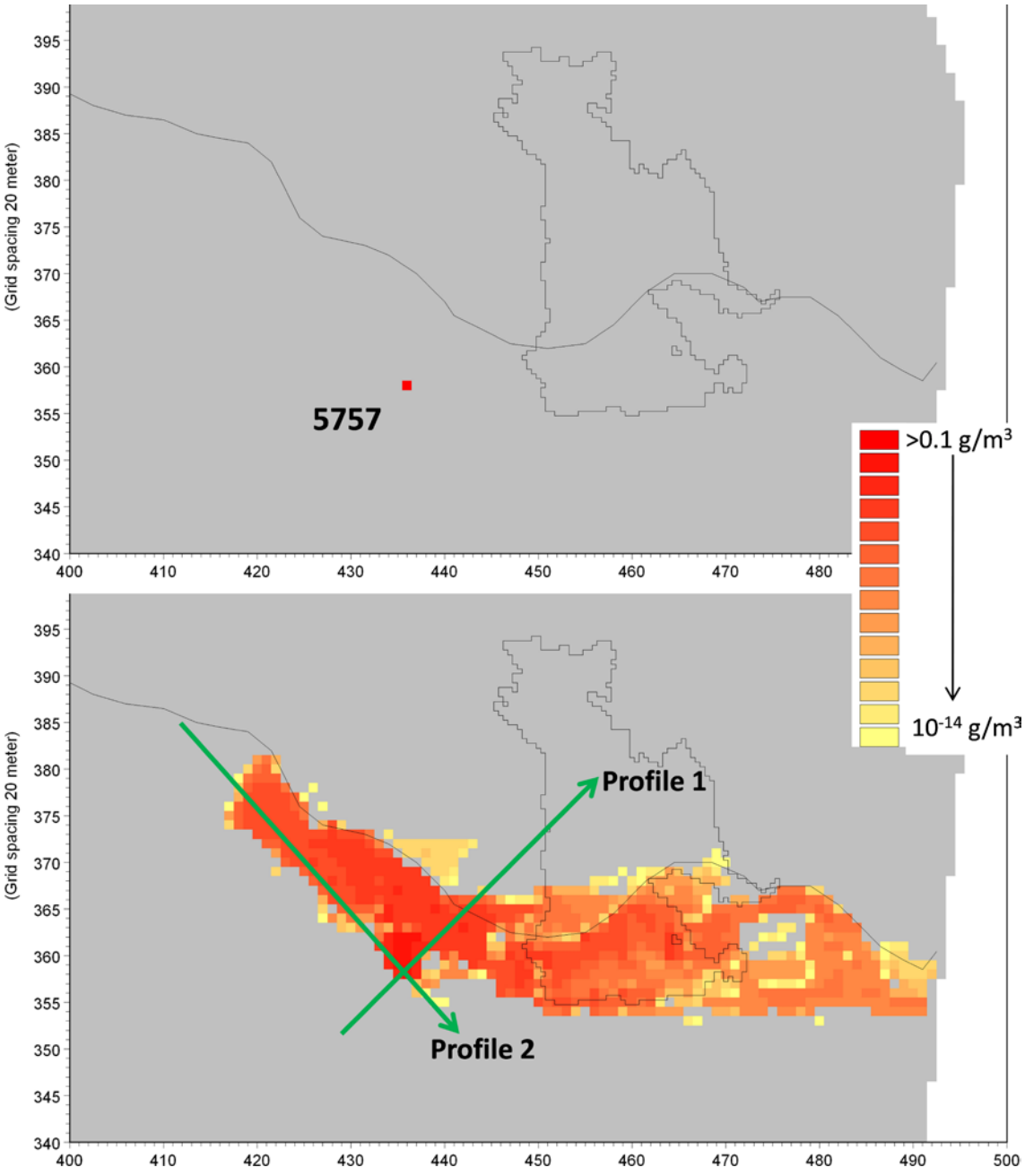

Figure 7-92. *Surface plot for object 121_01. The upper figure shows the location of source 5757 and the lower figure the extent of the concentration plume in the uppermost layer. The lower figure also shows the locations and directions of the profiles illustrated in Figure 7-93 and 7-94. The simulation is based on the 10000AD_10000QD model.*

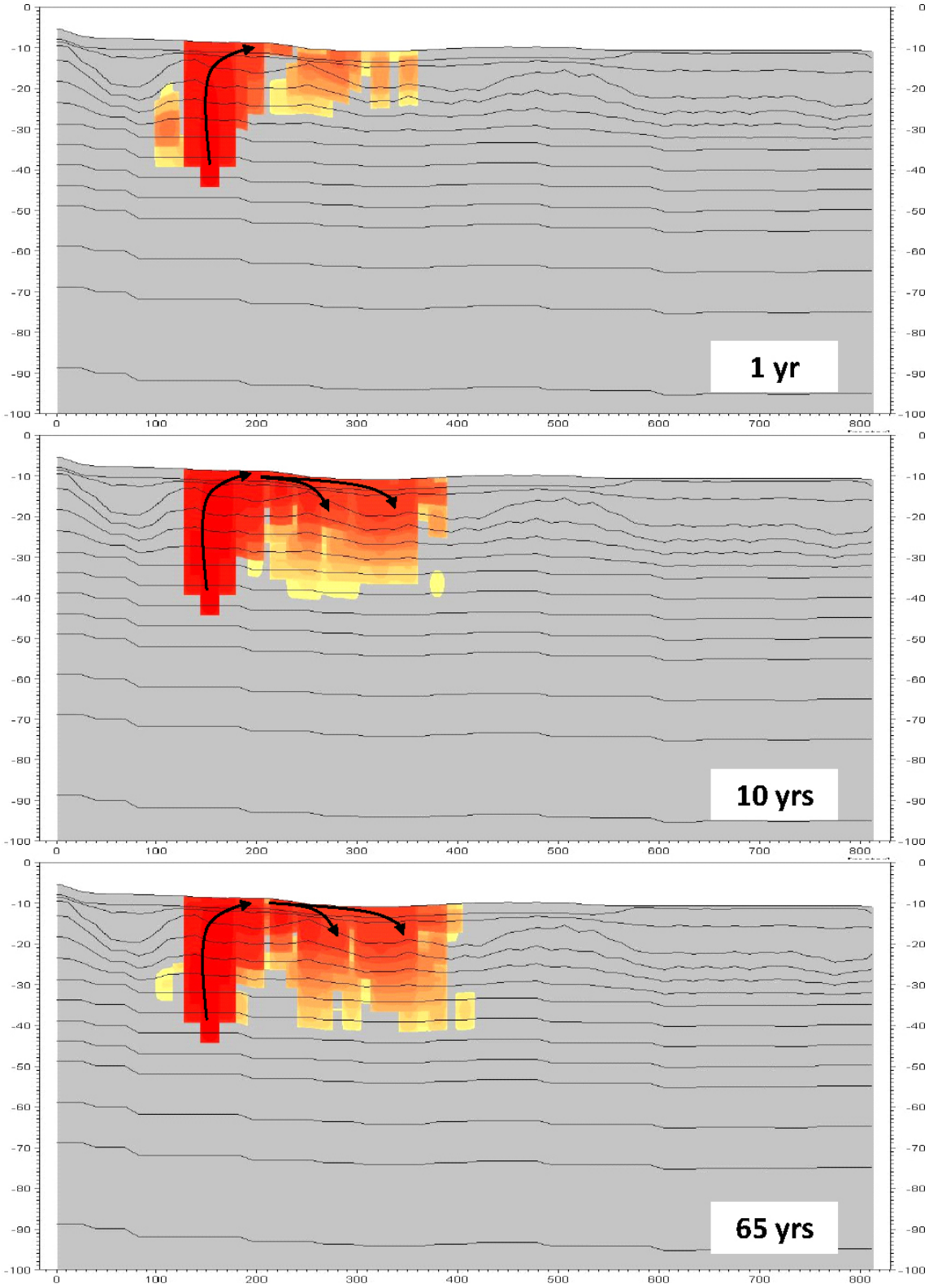

Figure 7-93. *Concentrations along Profile 1 shown in Figure 7-92, results after 1, 10 and 65 years of simulation.*

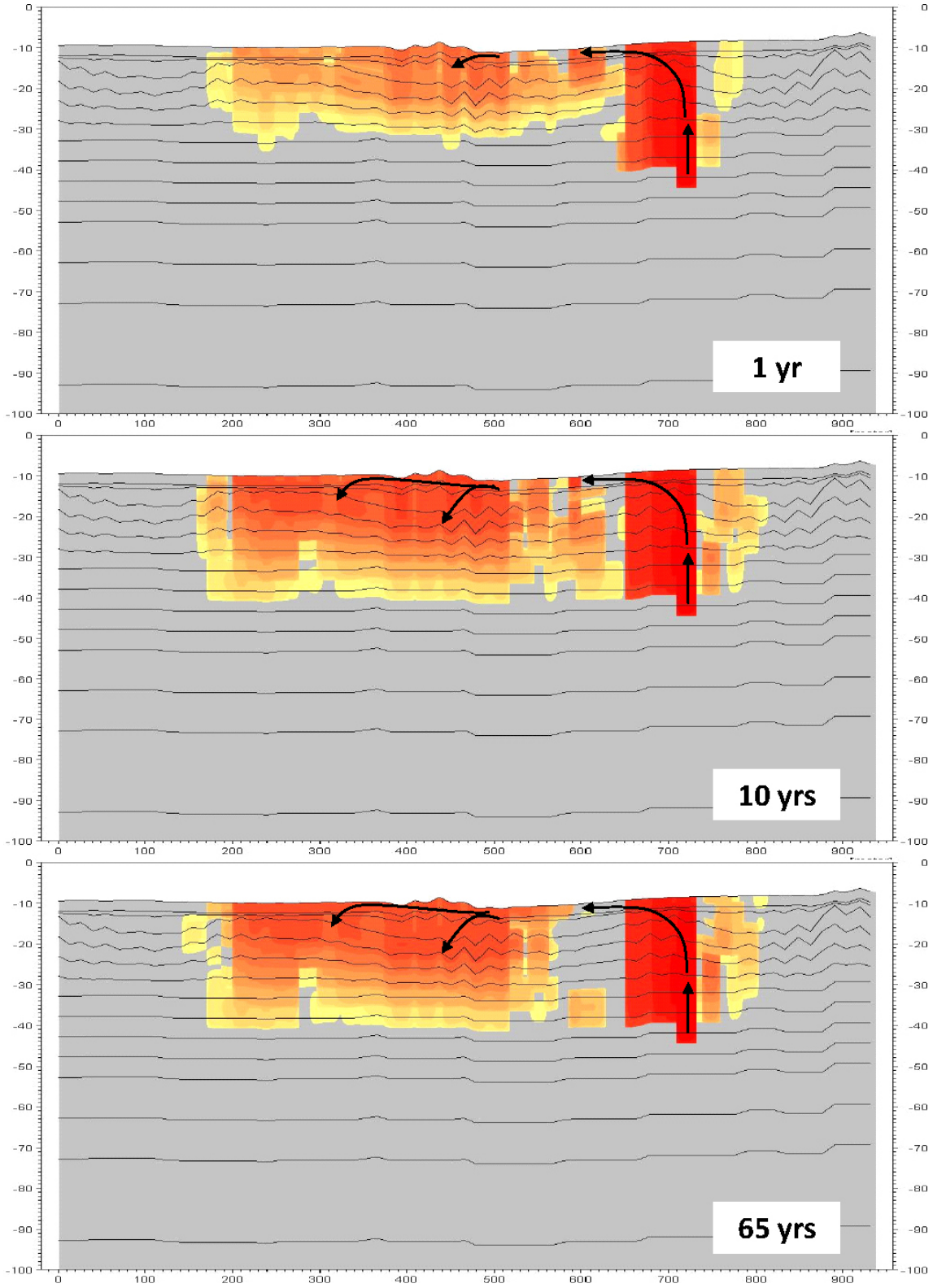

Figure 7-94. *Concentrations along Profile 2 shown in Figure 7-92, results after 1, 10 and 65 years of simulation.*

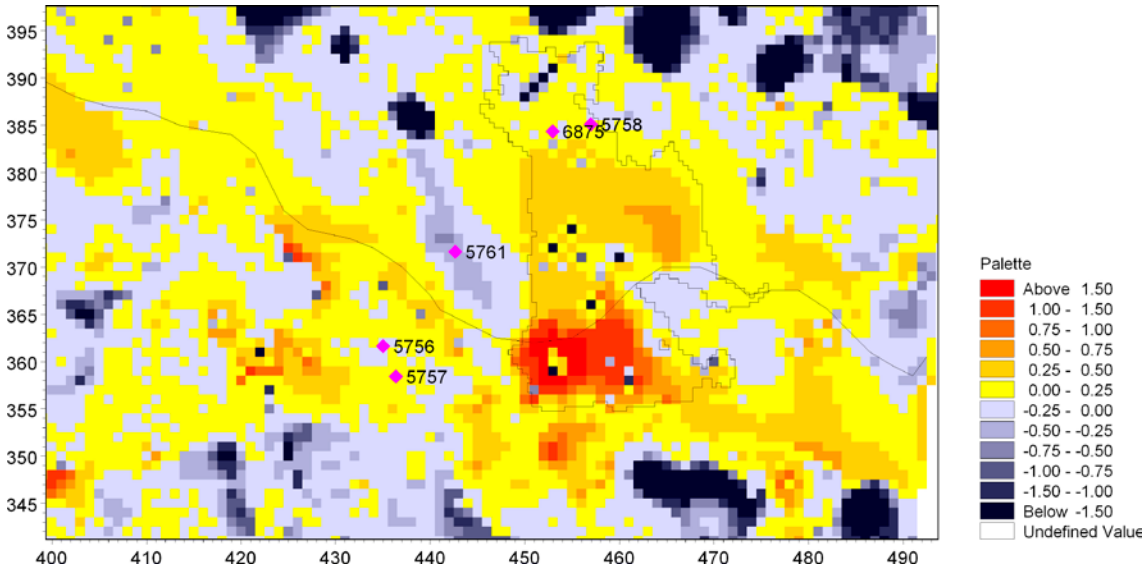

Figure 7-95. *Recharge and discharge areas in the QD layers in object 121_01 based on a simulation with local model A (10000AD_10000QD). Results are illustrated as yearly mean values; blue areas are recharge areas and yellow/red areas are discharge areas.*

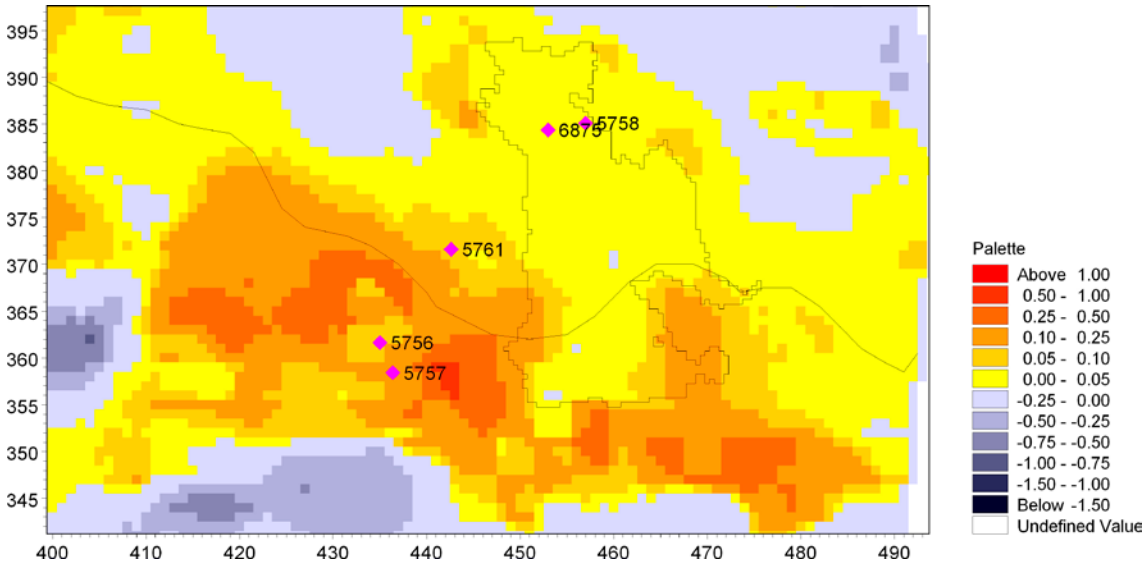

Figure 7-96. *Recharge and discharge areas in the bedrock at c. 25 m.b.sl. in object 121_01 based on a simulation with local model A (10000AD_10000QD). Results are illustrated as yearly mean values; blue areas are recharge areas and yellow/red areas are discharge areas.*

Canister 5758 (object 121)

Figure 7-97 shows the mass balance parameters for source 5758. The location of source 5758 is illustrated in the upper figure in Figure 7-98. After 65 years of simulation about 45% of the applied solute is still stored in the saturated zone. For this source, solute is also stored in the overland compartment; after 65 years, 11% of the applied solute is stored in the overland. Of the solute that has left the model, about 80% has gone via drainage flow to the surface streams and the other 20% has gone through the overland to the boundary.

Figure 7-98 shows a concentration surface plot for source 5758. The plot is shown for the uppermost layer and after 65 years of simulation. The solute is mainly transported along the shoreline of the terrestrialised lake and then along the surface stream towards the model boundary. Figure 7-99 shows the concentrations along the profile shown in the lower graph in Figure 7-98. The solute is transported up to the QD layers and then spreads horizontally. The thicknesses of the QD layers are large along the whole profile.

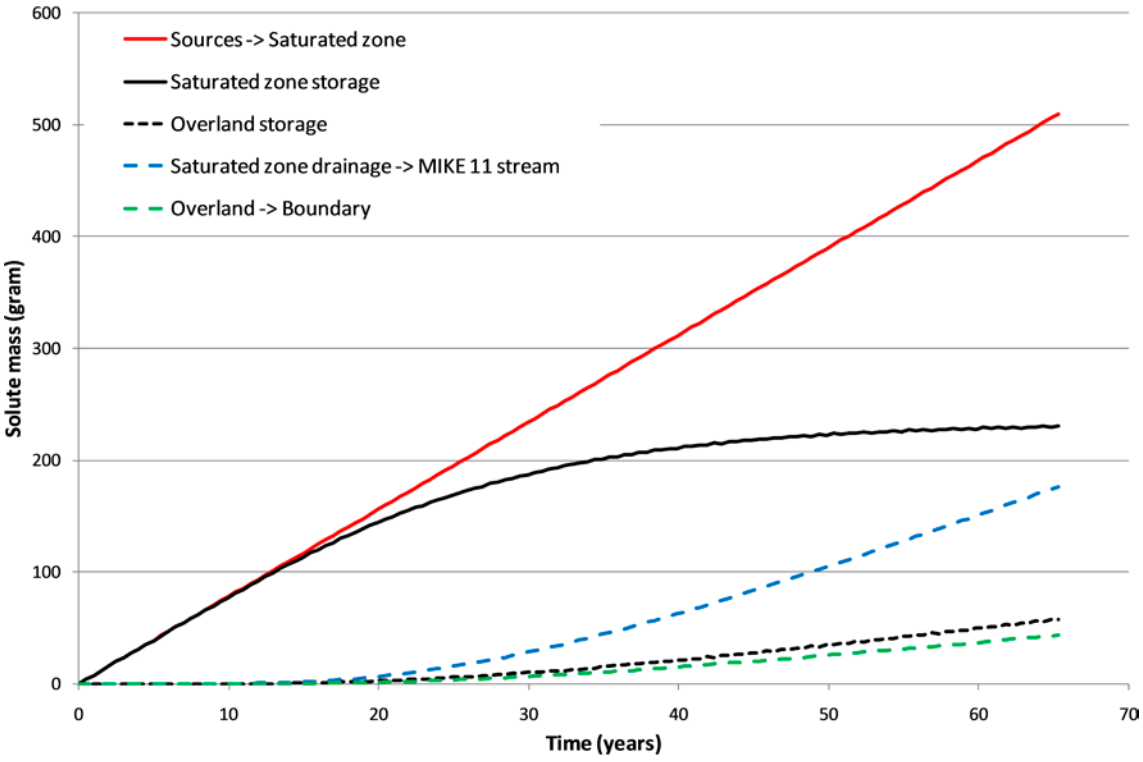

Figure 7-97. *Mass balance parameters for AD simulation with local model A based on the 10000AD_10000QD model and starting position 5758.*

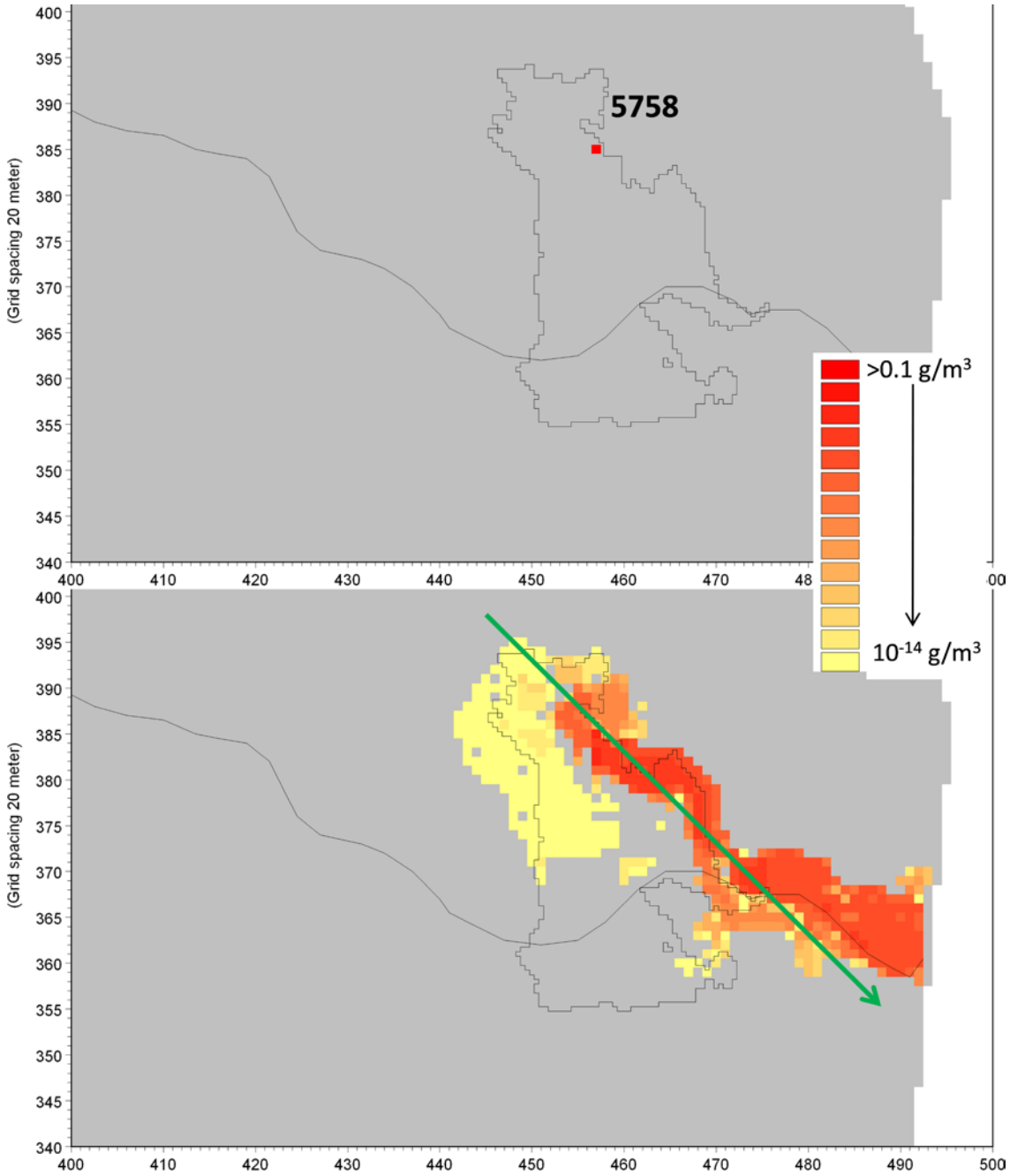

Figure 7-98. *Surface plot for object 121_01. The upper figure shows the location of source 5758 and the lower figure shows the extent of the concentration plume in the uppermost layer. The lower figure also shows the location and direction of the profile shown in Figure 7-99. The simulation is based on the 10000AD_10000QD model.*

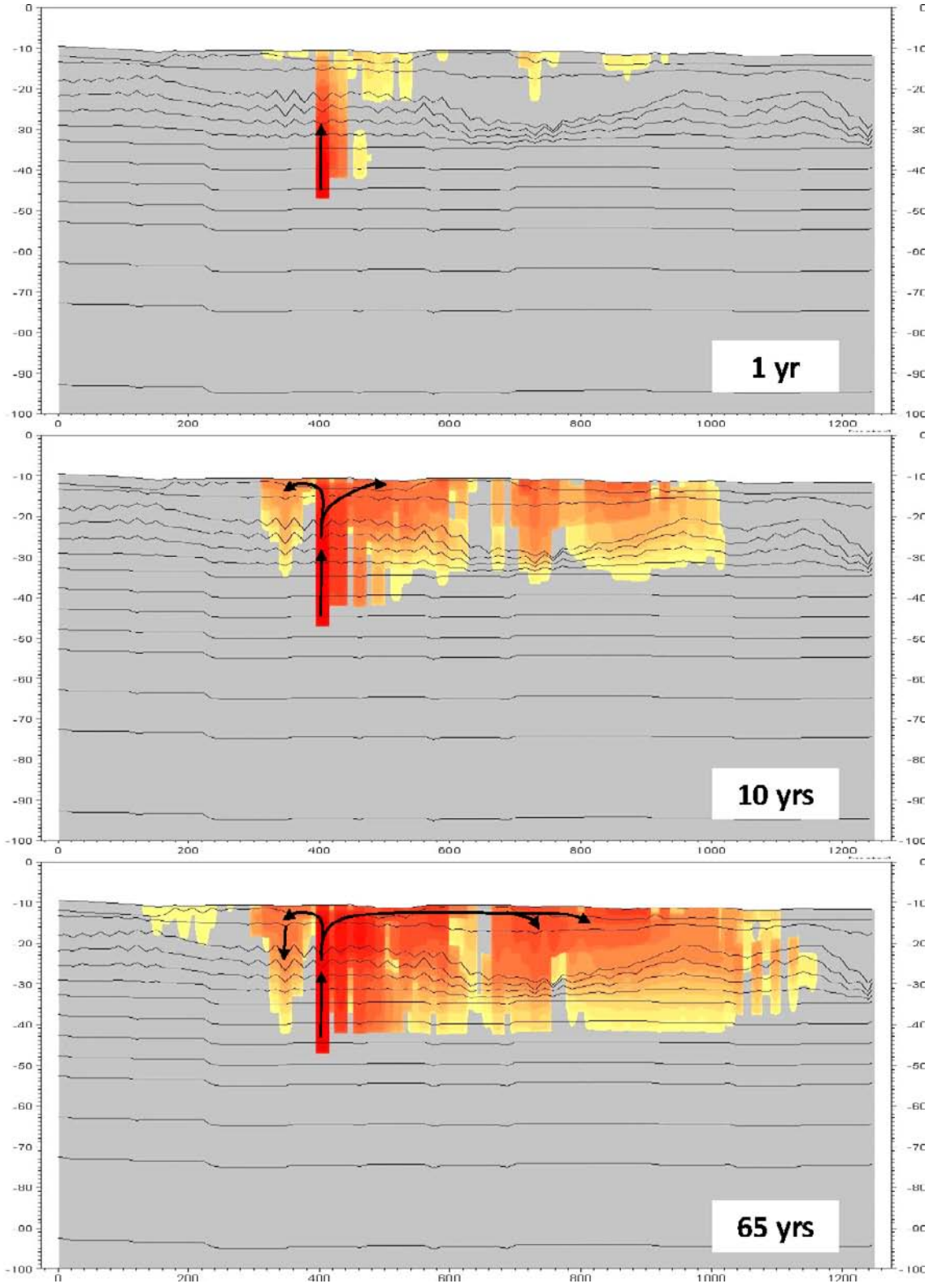

Figure 7-99. *Concentrations along profile illustrated in Figure 7-98, results after 1, 10 and 65 years of simulation.*

Canister 5761 (object 121)

Figure 7-100 shows the mass balance components for source 5761. The location of the source is illustrated in the upper figure in Figure 7-101. After 65 years of simulation about 28% of the applied solute is left in the saturated zone. Almost all of the solute that has left the model has gone to the MIKE 11 stream through drainage flow. During the last years of the simulation period the solute starts reaching the stream also through the overland compartment; however, the amount is still very small after 65 years.

Figure 7-101 shows a surface plot of the saturated zone concentration after 65 years. Almost the entire area of the former lake is covered by solute. Solute is also being transported along the surface stream. Figures 7-102 and 7-103 show the concentration profiles according to Profile 1 and Profile 2 in the lower figure in Figure 7-101.

In Figure 7-102 it is illustrated that the solute is transported both upwards to the upper layers but also horizontally in some of the layers. The solute then spreads both towards the terrestrialised lake area and the surface stream. The major part of the solute mass moves towards the stream. Figure 7-103 shows the concentration distribution in Profile 2 in Figure 7-101 and illustrates the spreading towards the former lake area. The solute is moving towards the surface and then spreads along the surface and into the deeper layers.

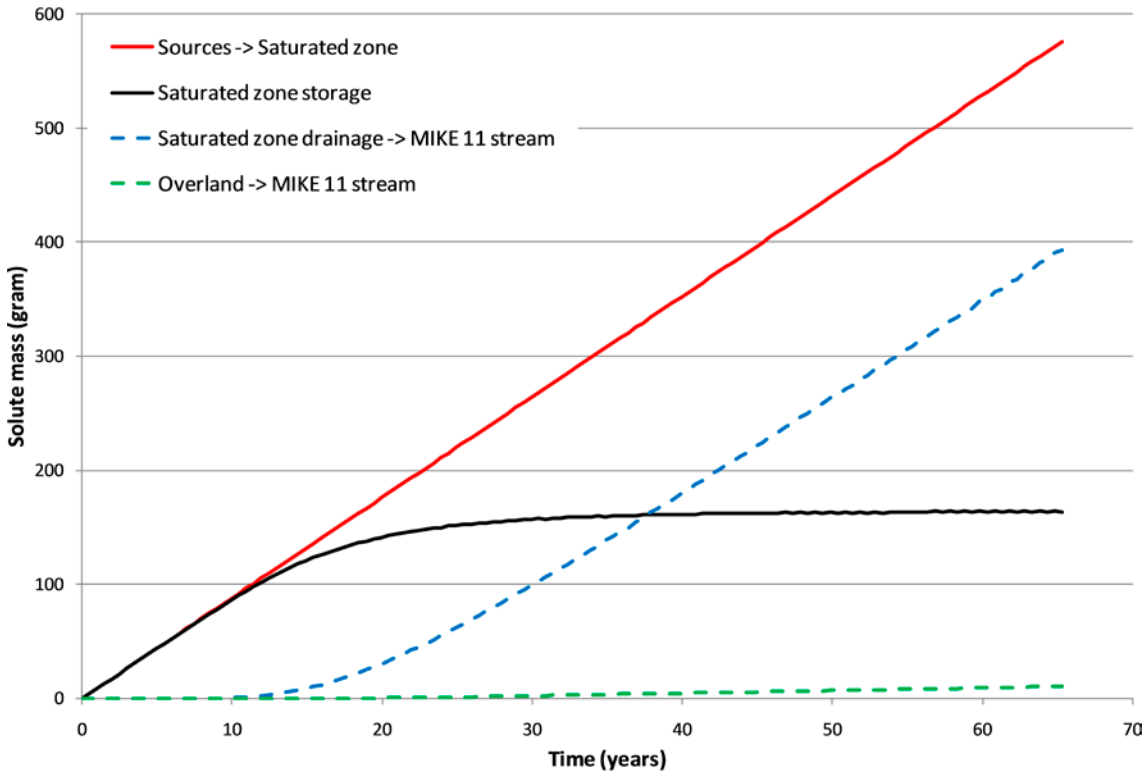

Figure 7-100. *Mass balance parameters for AD simulation with local model A based on the 10000AD_10000QD model and starting position 5761.*

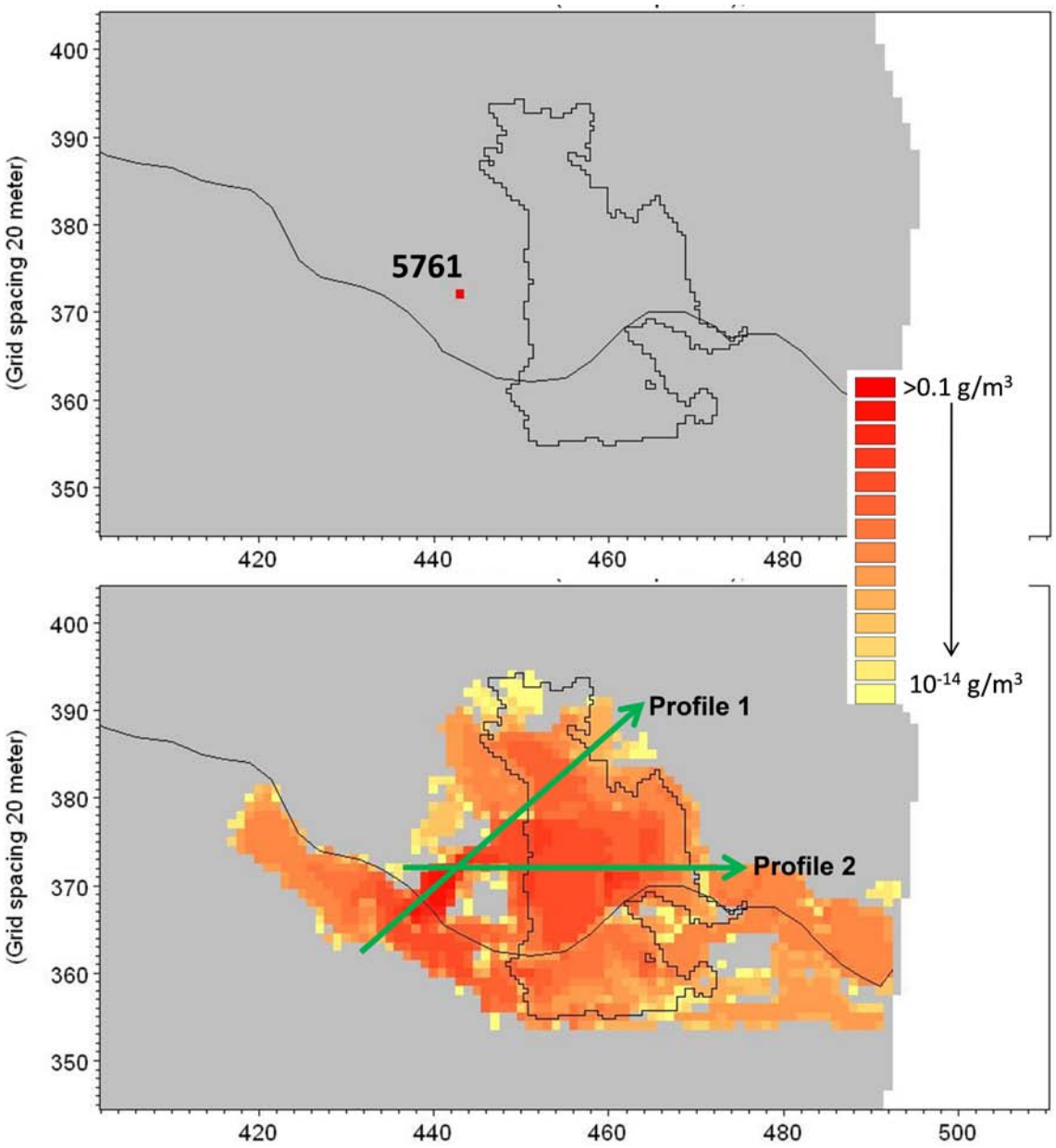

Figure 7-101. *Surface plot for object 121_01. The upper figure shows the location of source 5761 and the lower figure shows the extent of the concentration plume in the uppermost layer after 65 years of simulation. The lower figure also shows the locations and directions of the profiles illustrated in Figures 7-102 and 7-103. The simulation is based on the 10000AD_10000QD model.*

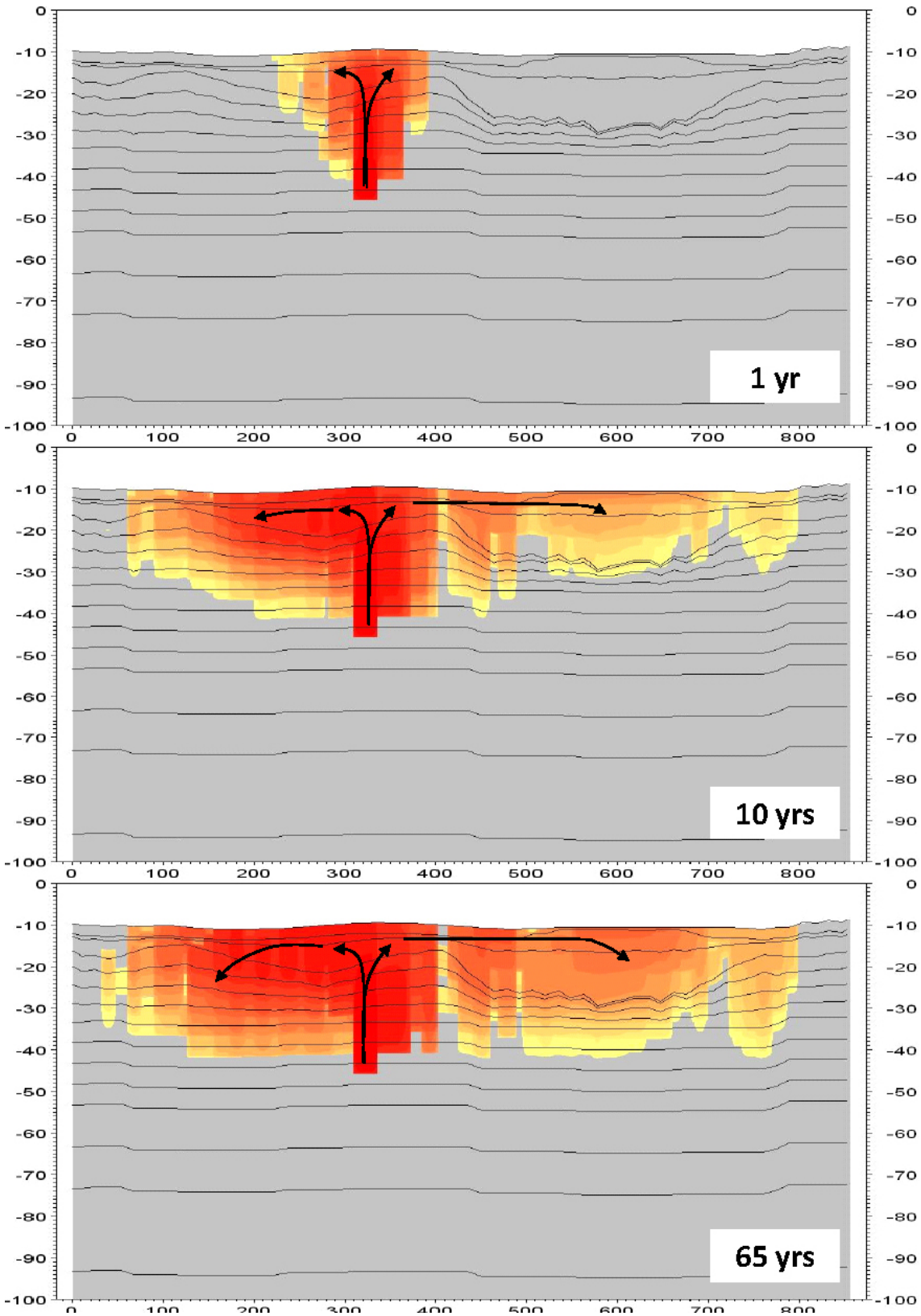

Figure 7-102. *Concentrations along Profile 1 shown in Figure 7-101, results after 1, 10 and 65 years of simulation.*

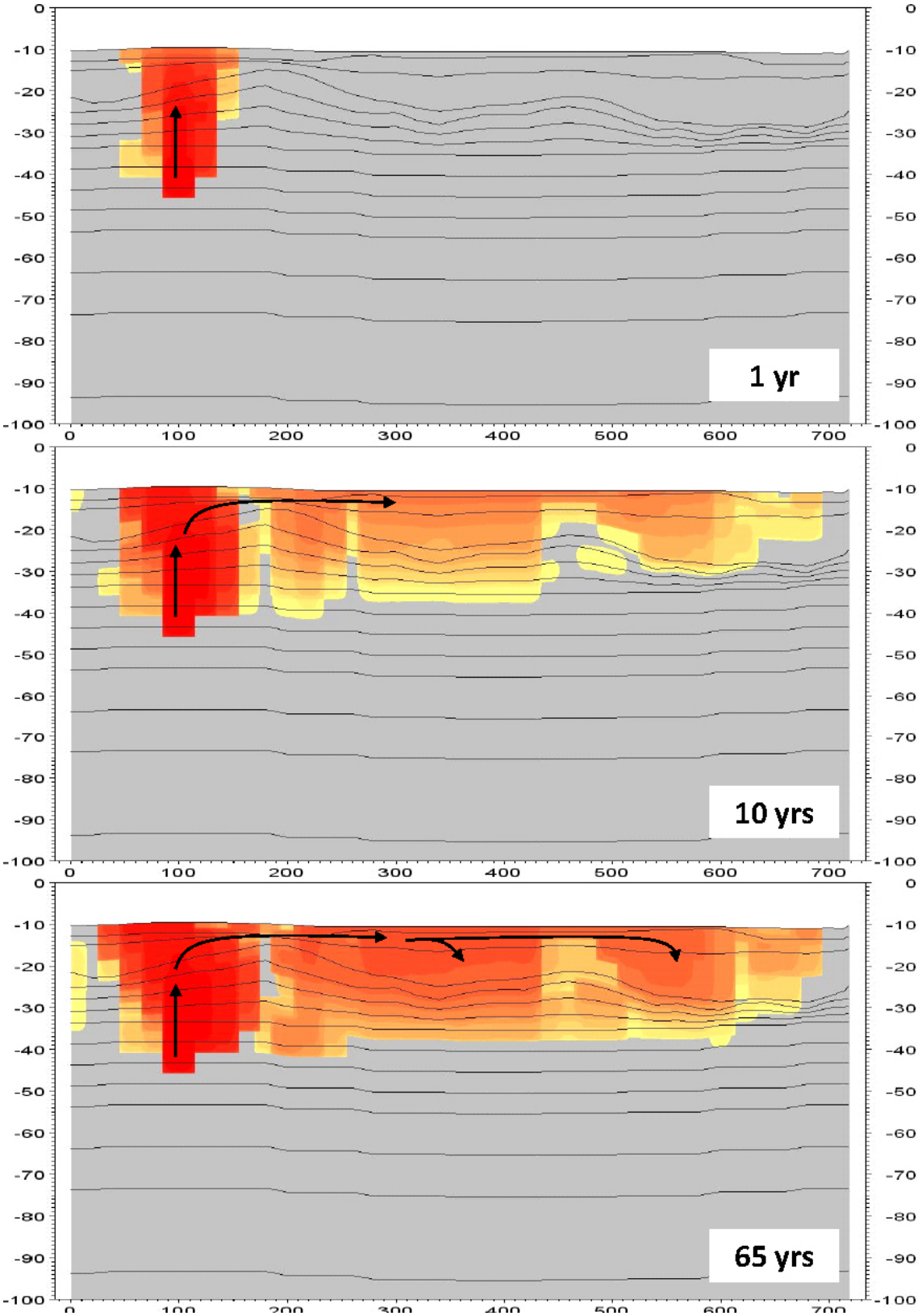

Figure 7-103. *Concentrations along Profile 2 shown in Figure 7-101, results after 1, 10 and 65 years of simulation.*

Canister 6875 (object 121)

Figure 7-104 shows the mass balance parameters for source 6875. The location of the source is shown in the upper graph in Figure 7-105. The mass balance parameters show that almost no solute has left the saturated zone. In fact, only 0.15% of the applied mass has left the saturated zone after 65 years.

Figure 7-105 shows the saturated zone concentration in the uppermost layer at the end of the simulation. The transport pattern is very similar to what was seen for source 5758, which is located close to source 6875. Also the profile in Figure 7-106 is similar to the profile for source 5758. However, although the pattern of the profiles and surface plots are similar, there is a large difference with regard to the mass balances. For source 5758 more than 50% of the solute has left the model volume after 65 years of simulation, as compared to only a very small amount for source 6875. The reason for this is that source 6875 is located in an area with significantly lower hydraulic conductivities in the upper QD layers, which leads to slow solute transport. The concentrations along the profiles in Figure 7-106 are significantly lower than the concentrations in Figure 7-99.

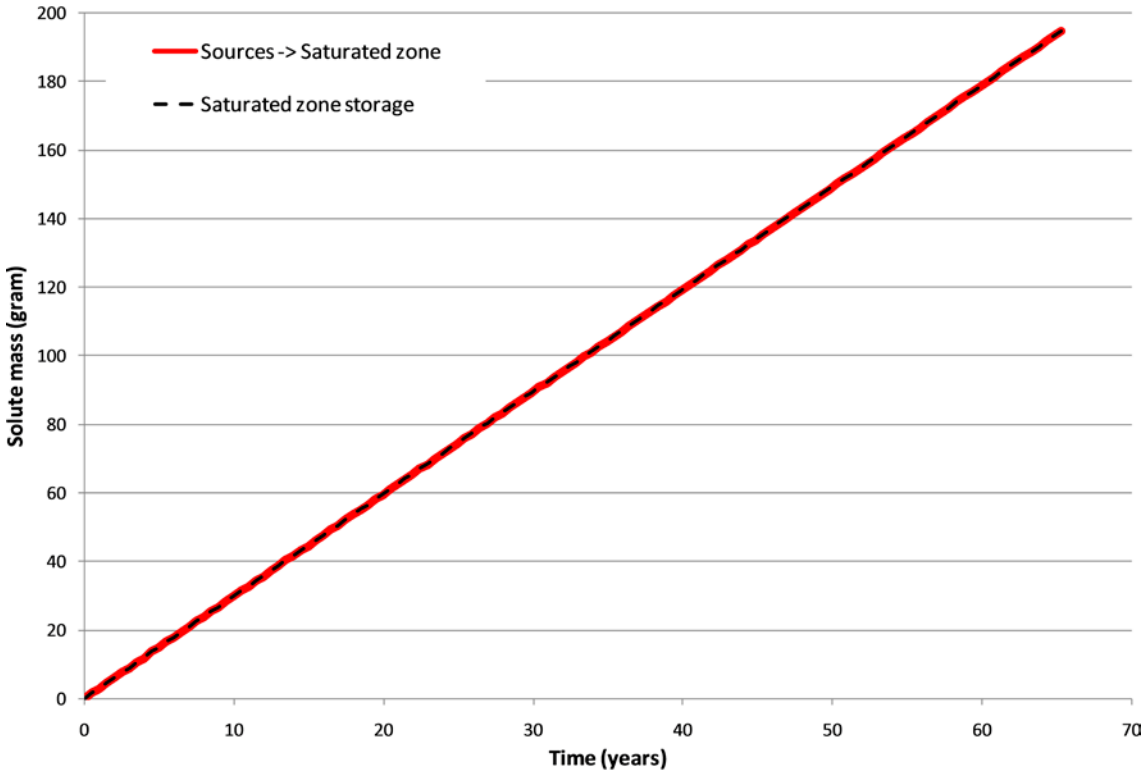

Figure 7-104. *Mass balance parameters for AD simulation with local model A based on the 10000AD_10000QD model and starting position 6875.*

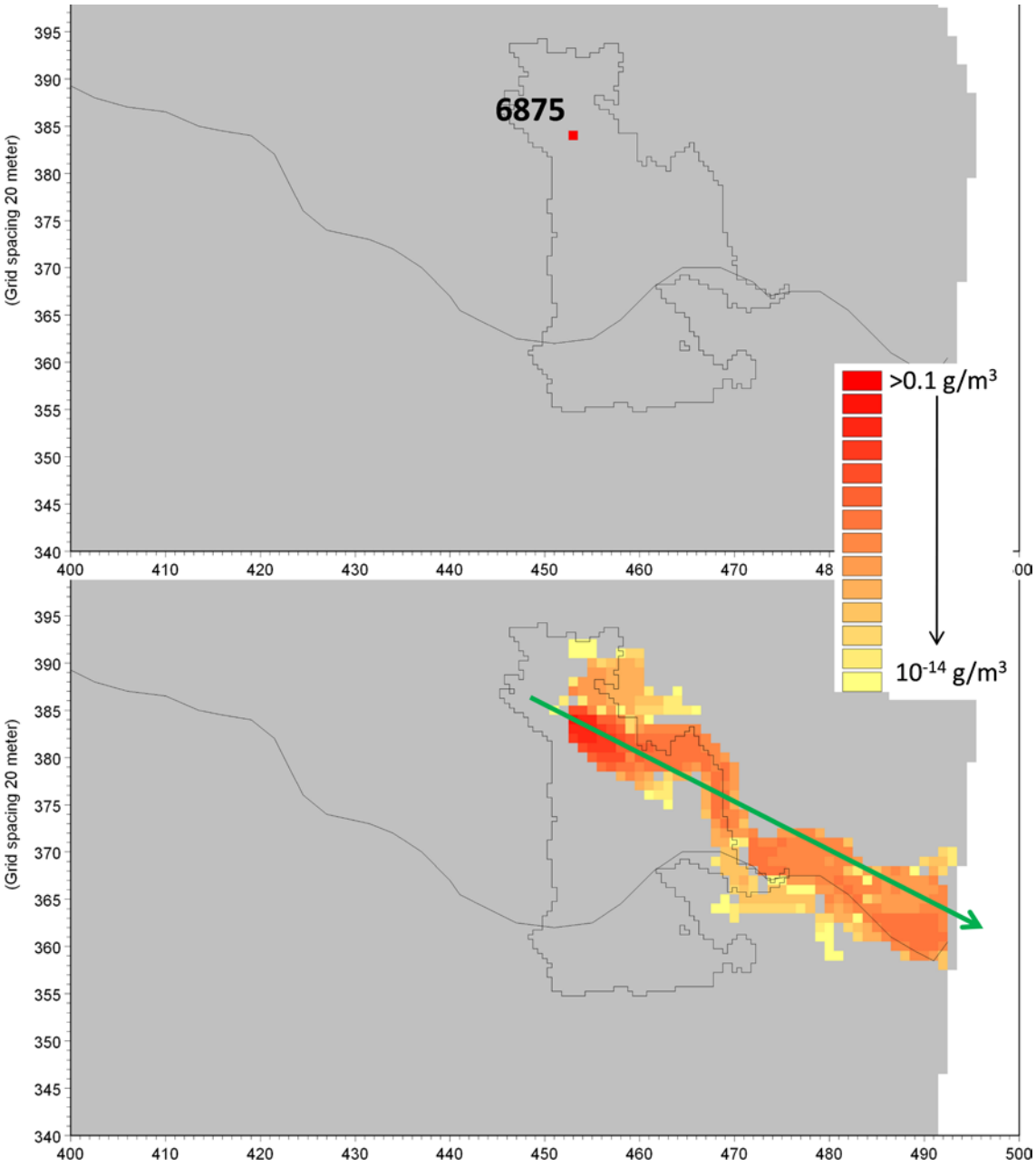

Figure 7-105. *Surface plot for object 121_01. The upper figure shows the location of source 6875 and the lower figure the extent of the concentration plume in the uppermost layer. The lower figure also shows the locations and directions of the profiles illustrated in Figure 7-106. The simulation is based on the 10000AD_10000QD model.*

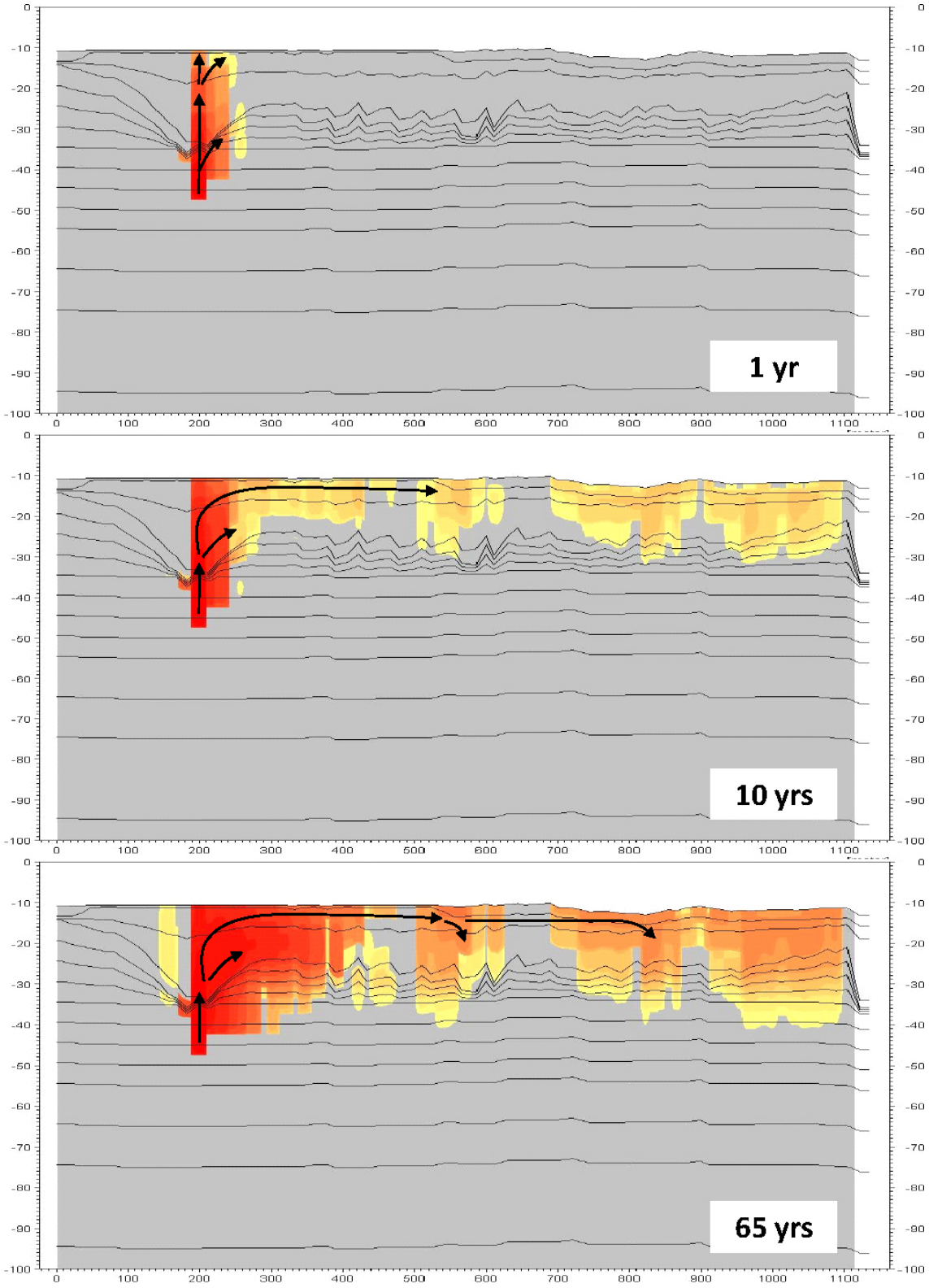

Figure 7-106. *Concentrations along the profile shown in Figure 7-104, results after 1, 10 and 65 years of simulation.*

7.4.2 Local model B

For local model B, which contains object 116, flow paths from three of the selected deposition holes were identified within the model domain. The numbers of the corresponding canisters are 3897, 5759 and 5760. However, two of the flow paths, those from canister 5759 and 5760, were situated very close to each other and within the same grid cell in the MIKE SHE model. Therefore, the source strength in that cell is 2 g/m³ instead of 1 g/m³ for all cells with one flow path. Figure 7-107 shows the locations of the flow paths from the three canisters. The sources are located at 40 m.b.s.l. For local model B, the AD simulations were run for approximately 70 years, i.e. somewhat longer than for local model A. This was possible because the model B simulations were running slightly faster than those with model A.

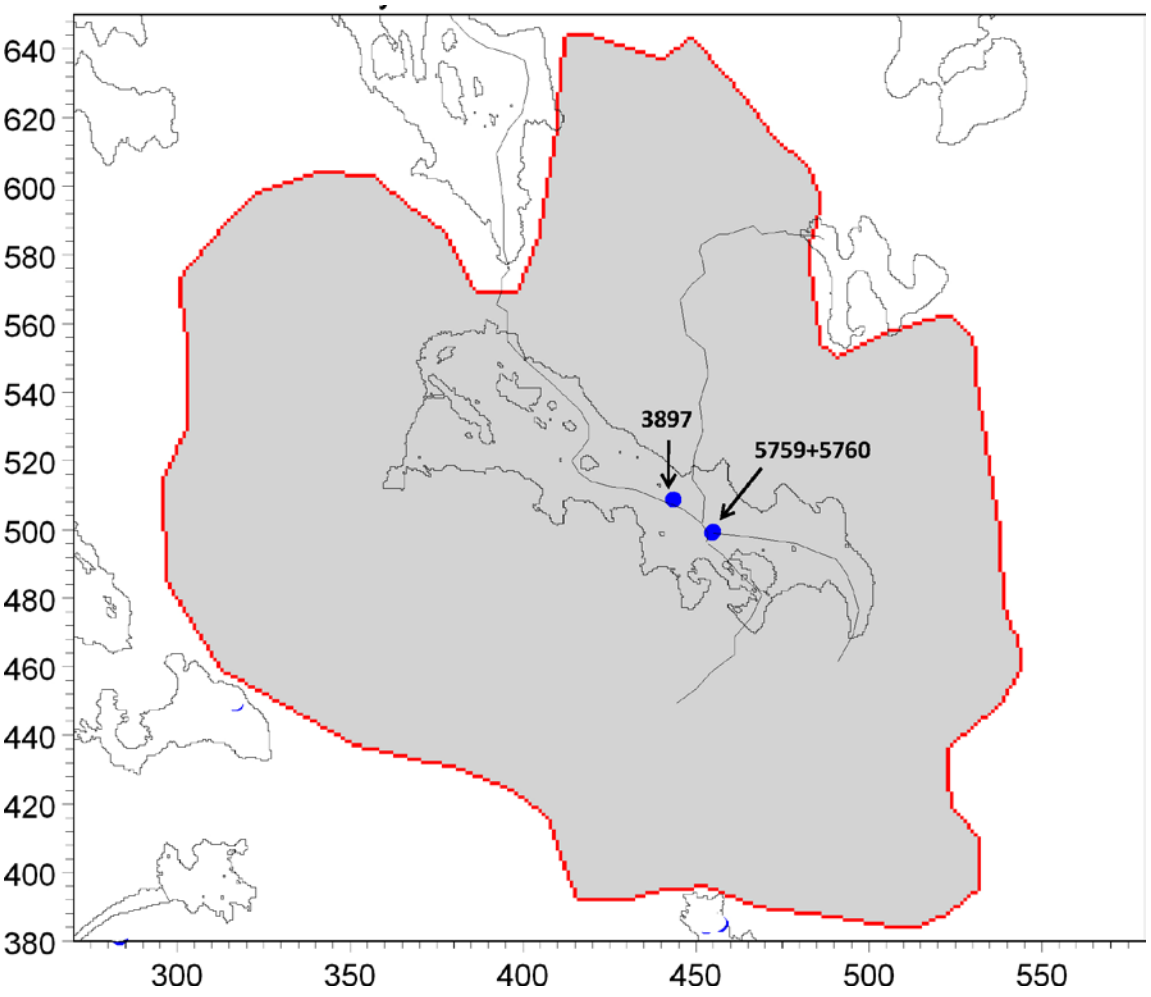

Figure 7-107. *Starting positions at 40 m.b.s.l. within the local model B for AD simulation with MIKE SHE. Positions are based on flow paths from hypothetical releases from selected canisters within the repository.*

Canister 3897

Figure 7-108 shows the mass balance parameters for the simulation based on source 3897. The source is located within the terrestrialised lake area and in the vicinity of the MIKE 11 stream running through the former lake. Initially, the storage in the saturated zone increases, but already after approximately 20 years of simulation the accumulation in the saturated zone storage has ceased. All solute mass that leaves the model goes to the MIKE 11 stream system.

Figure 7-109 shows a surface plot for source 3897. The upper figure shows the location of the source at 40 m.b.s.l. The red square illustrates the extent of the area magnified in the lower figure. The lower figure shows the saturated zone concentration in the uppermost calculation layer after c. 70 years of simulation. Figure 7-109 shows that the spreading of the solute is small for source 3897. The reason is that the source is located directly under the surface stream. Once the solute has entered the stream it is considered to have left the model domain since the stream is a model sink. At present, it is not possible to follow the solute after it has reached a MIKE 11 surface stream.

Figure 7-110 shows the concentration distribution in the profile illustrated in Figure 7-109. The concentrations are shown after 1, 10, and 50 years of simulation. The solute is moving vertically up to the surface, but also directly up towards the surface stream, which is located on the left side of the source. The differences between the three profiles are not very large, since the transport is fast and the spreading of the solute is small.

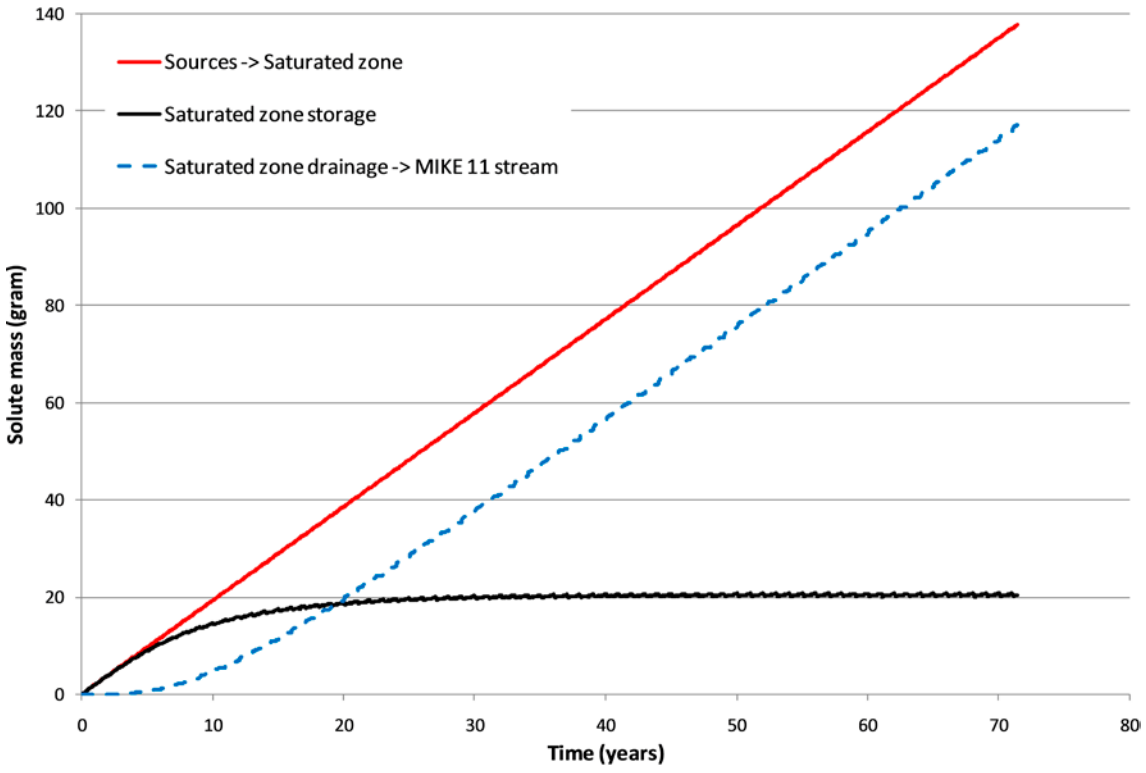

Figure 7-108. *Mass balance parameters for AD simulation with local model B based on the 10000AD_10000QD model and starting position 3897.*

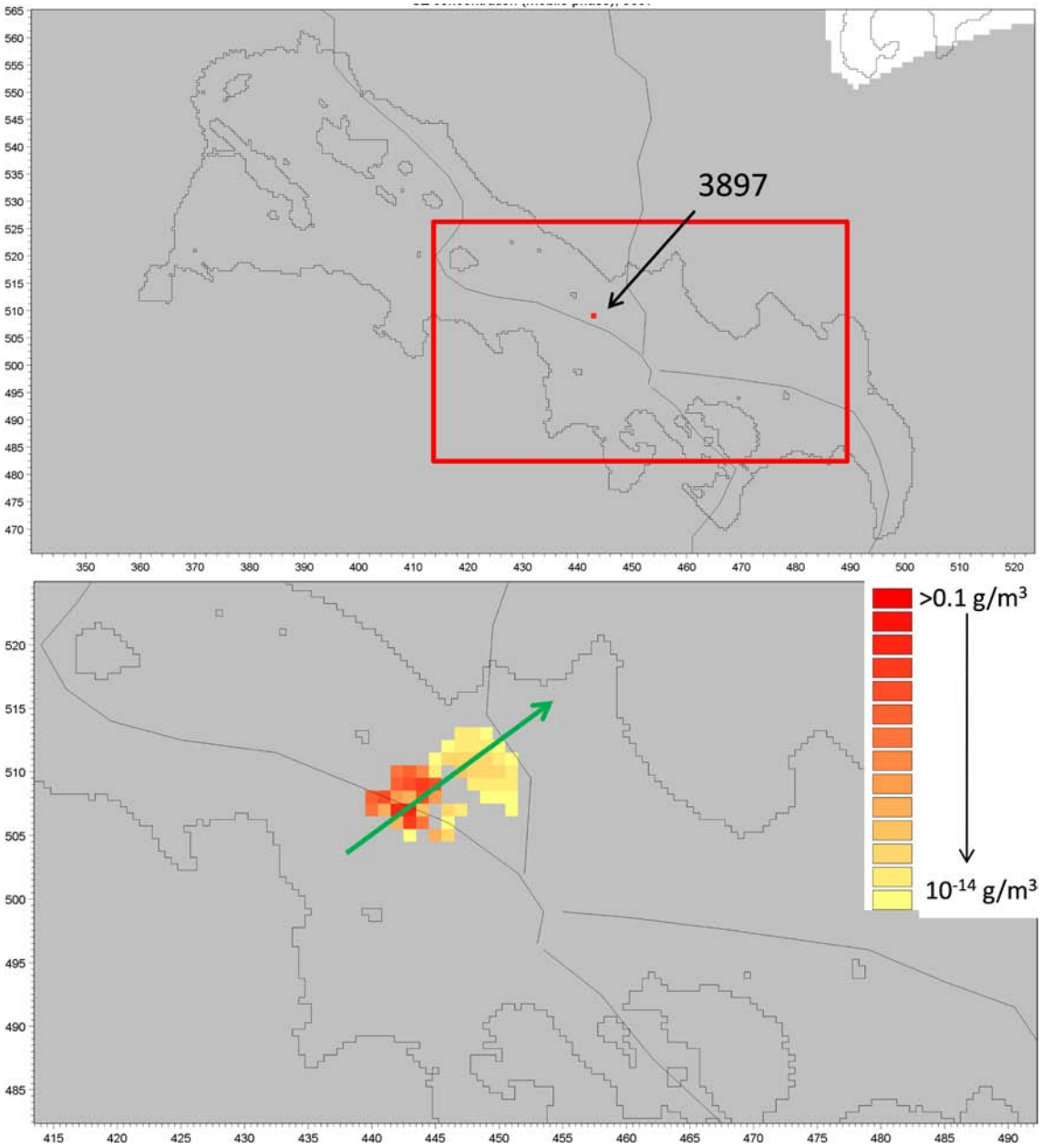

Figure 7-109. *Surface plot for source 3897 based on the 10000AD_10000QD local model B. The upper figure shows the location of the source and the extent of the area illustrated in the lower figure. The lower figure shows the saturated zone concentration plume in the top layer after c. 70 years of simulation. The arrow shows the direction and location of the profile illustrated in Figure 7-110.*

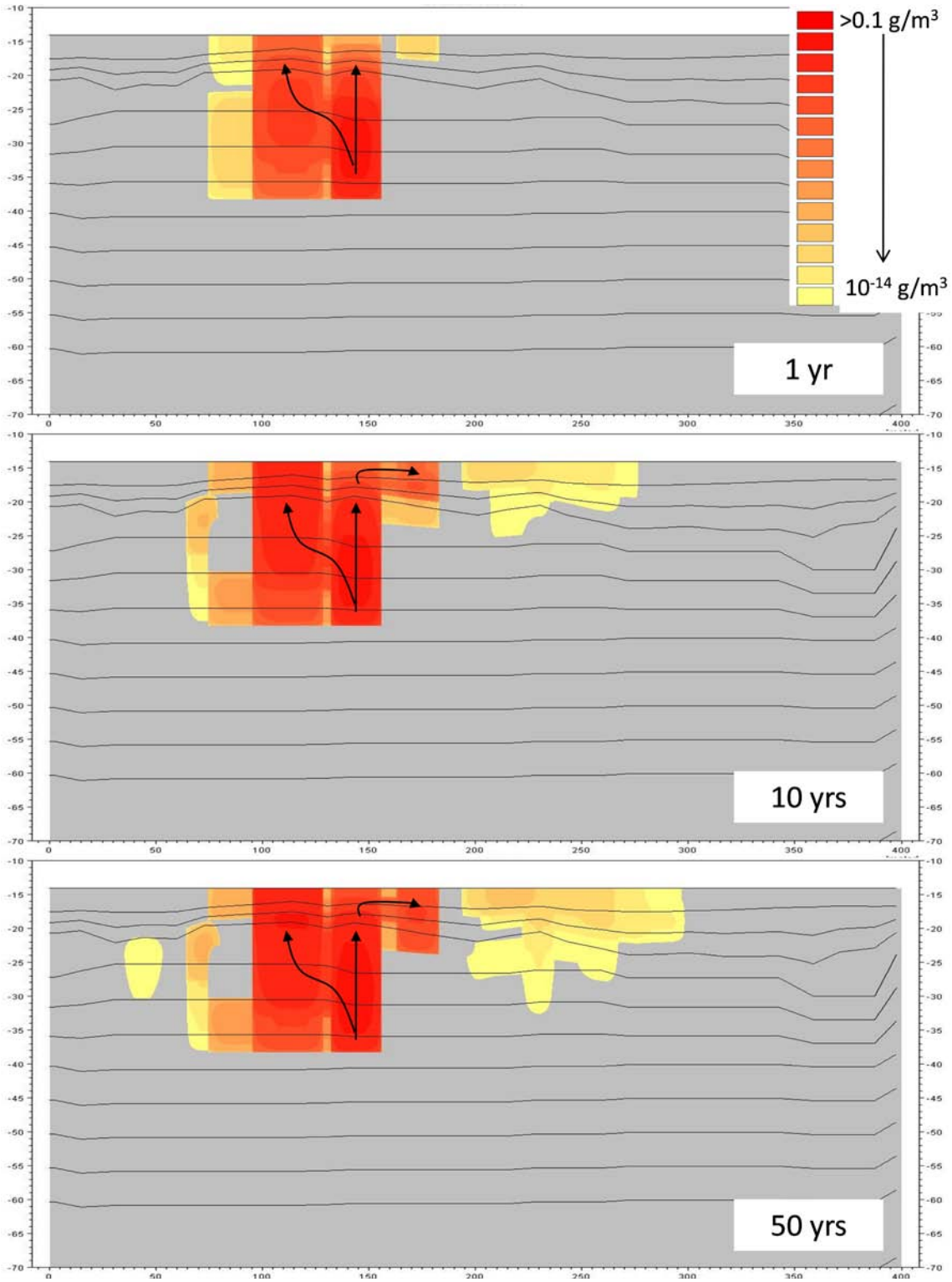

Figure 7-110. *Concentrations along the profile shown in Figure 7-109, results after 1, 10, and 50 years of simulation.*

Canisters 5759 and 5760

Figure 7-111 shows the mass balance parameters for the combined 5759 and 5760 sources. The results are the same as for source 3897, i.e. the saturated zone storage increased just during the first years and all of the solute that leaves the model goes to the MIKE 11 surface stream. The reason is that also this source is located directly under the surface stream flowing through the terrestrialised lake area.

Figure 7-112 shows the surface plot for sources 5759 and 5760. The upper figure shows the location of the source at 40 m.b.s.l. The red square illustrates the extent of the area in the lower figure. The lower figure shows the saturated zone concentration in the upper calculation layer after c. 70 years of simulation. The spreading of the solute is limited to the area close to the surface streams.

Figure 7-113 shows the concentrations along the profile shown in Figure 7-112. Concentration profiles after 1, 10, and 50 years of simulation are illustrated. The solute is moving vertically up towards the streams on the surface. All three profiles are similar because the spreading is fast and does not increase significantly over time.

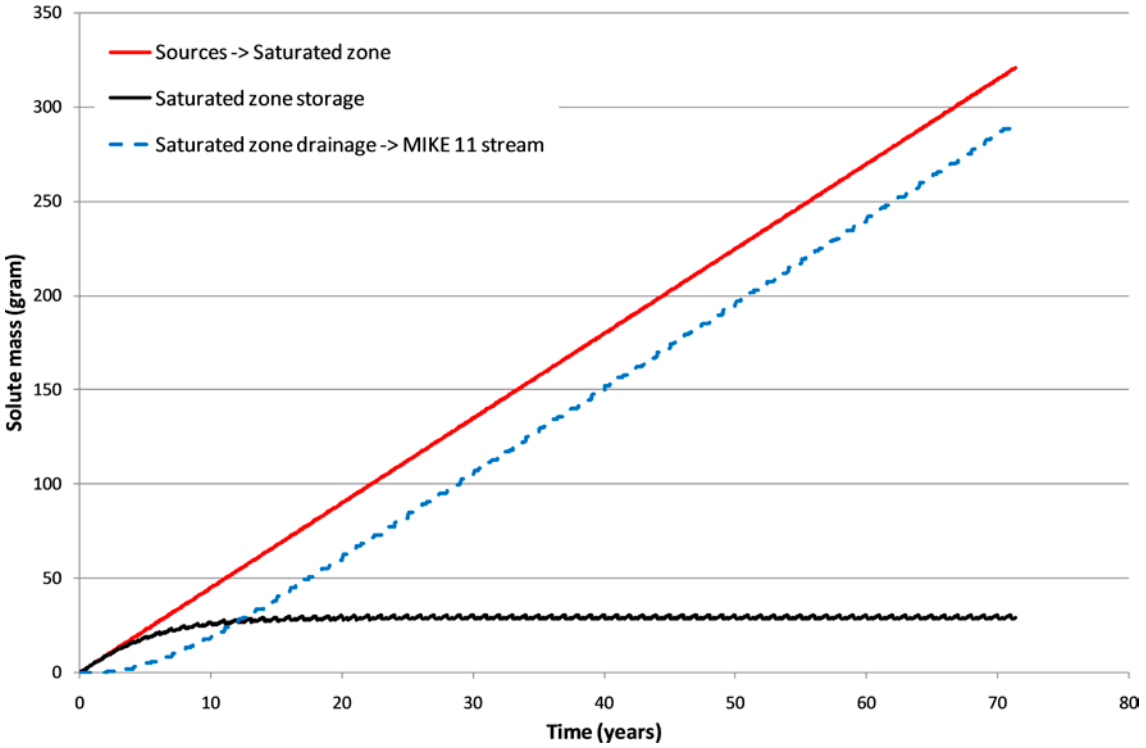

Figure 7-111. *Mass balance parameters for AD simulation with local model B based on the 10000AD_10000QD model and starting positions 5759 and 5760.*

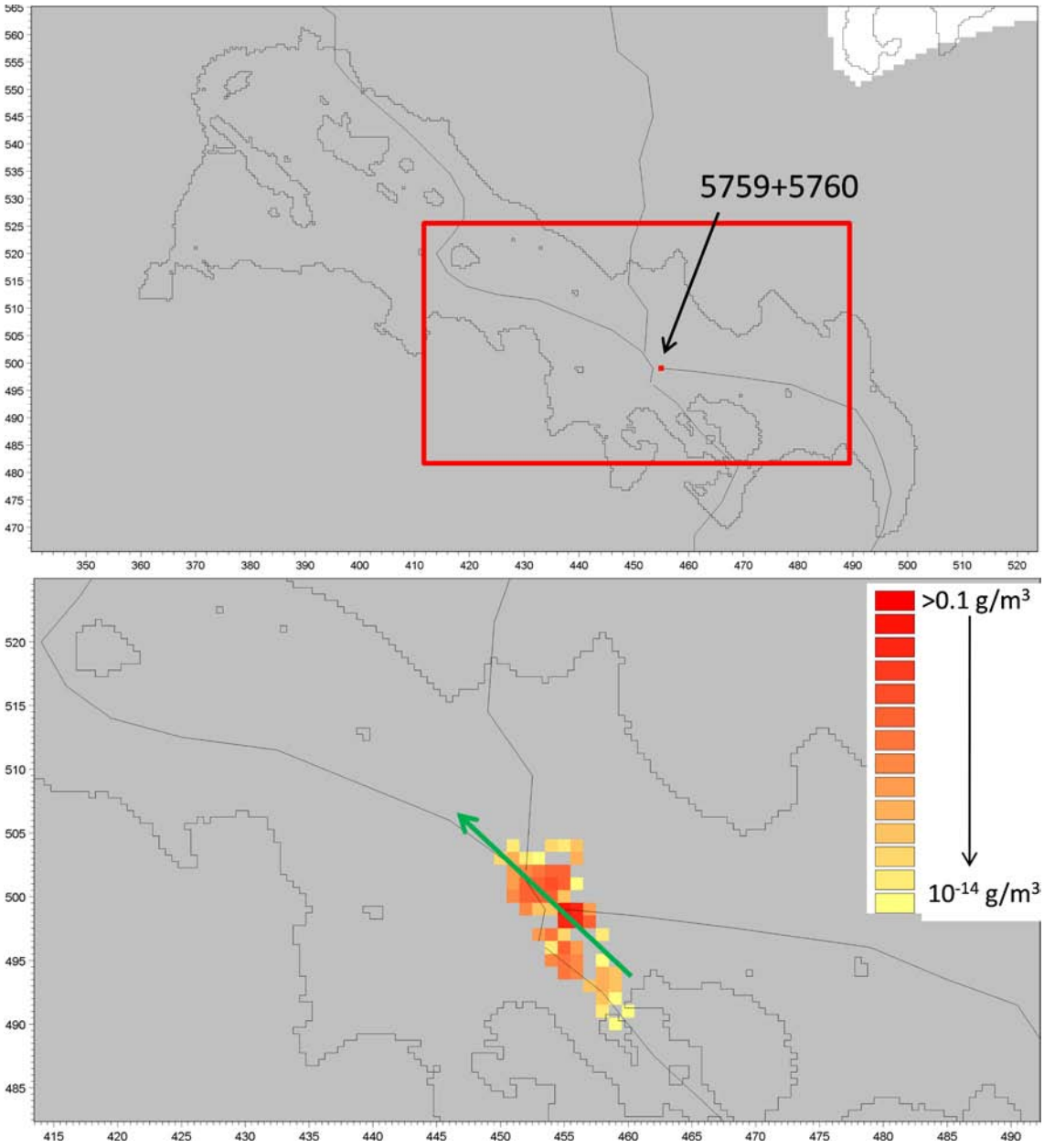

Figure 7-112. *Surface plot for the combined 5759 and 5760 sources. The upper figure shows the location of the source and the extent of the area illustrated in the lower figure. The lower figure shows the saturated zone concentration plume in the top layer after c. 70 years of simulation. The arrow shows the direction and location of the profile illustrated in Figure 7-113. The simulation is based on the 10000AD_10000QD model.*

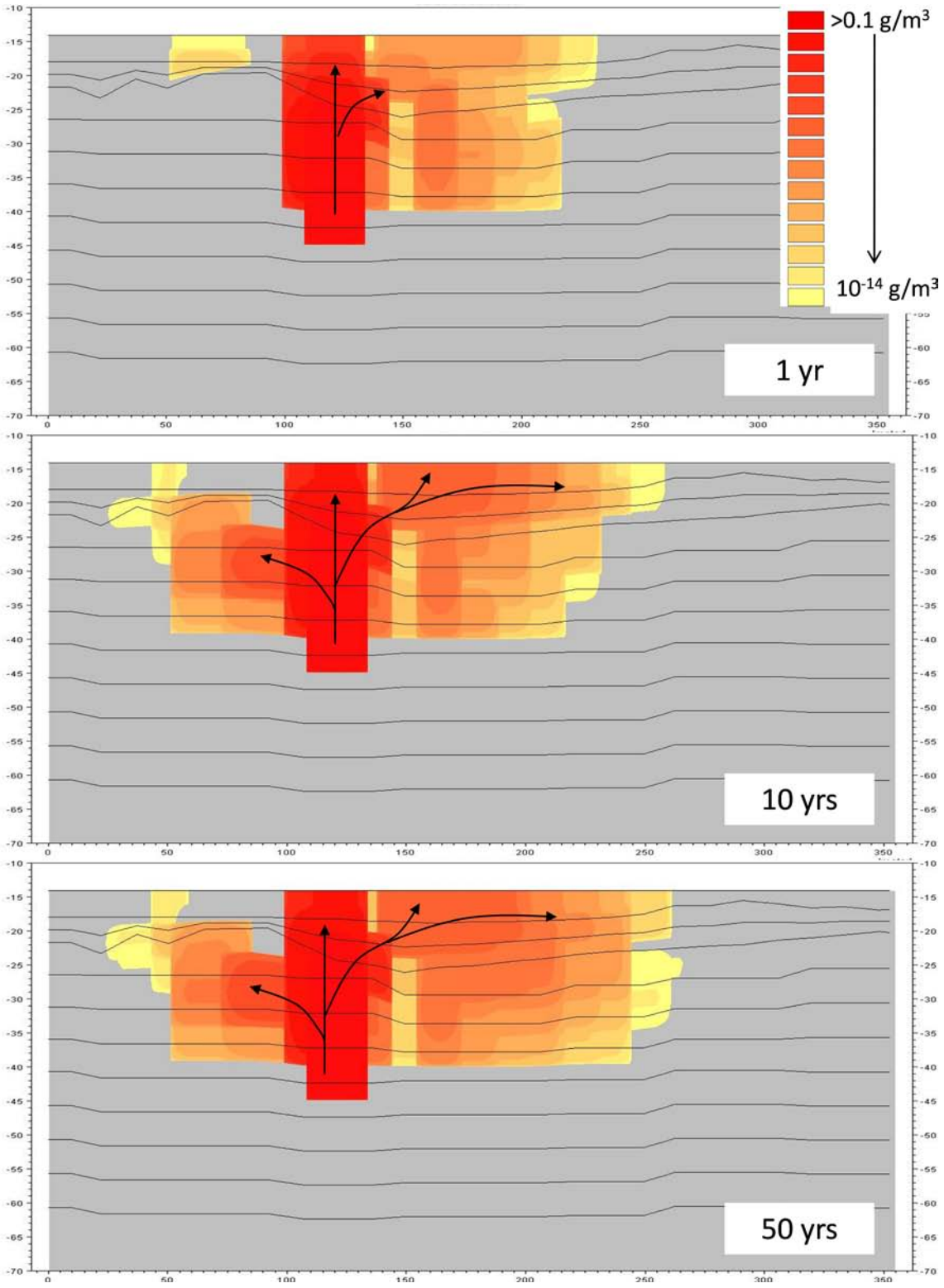

Figure 7-113. *Concentrations along the profile illustrated in Figure 7-112, results after 1, 10, and 50 years of simulation.*

7.5 Summary of results from the local models

For local model A, which contains objects 118, 120, and 121, transport simulations were conducted with both the particle tracking (PT) module and the advection-dispersion (AD) module. For local model B, containing object 116, only AD simulations were made. All of the AD simulations are limited to transport of a conservative solute in the saturated zone; no sorption or degradation processes are included in the present analysis. The main conclusions of the transport simulations based on the local models are summarised below.

- A particle release at c. 150 m.b.s.l. in the whole model area showed that after 1,000 years of simulation, more than 50% of the introduced particles are still left in the model. If instead the particles are introduced at 40 m.b.s.l. more than 80% leave the model within 1,000 years of simulation.
- Particles that are released at 40 m.b.s.l. are transported more or less vertically upwards to the ground surface, and the exit locations are concentrated to the surface streams and lake areas.
- A comparison between exit point obtained from the ConnectFlow modelling and the MIKE SHE modelling shows that there are few differences. For the lake areas, the particles leaving the MIKE SHE model tend to be more concentrated along the shorelines of the lakes, whereas the particles from the ConnectFlow model are appearing in the central parts of the lakes. For the particles going to surface streams, the differences between the results from the two models are small.
- Particles are concentrated to the lake shorelines, rather than the central parts of the lakes. One important reason for this is probably that because the lake sediments are less hydraulically conductive the particles are forced to move towards the shorelines instead of through the sediments. Another explanation is that the evapotranspiration, mainly the transpiration from plants along the shoreline and in surrounding areas, creates an upward hydraulic gradient from the deeper layers.
- Particles that are released at c. 150 m.b.s.l. also appear in lake and stream areas. However, when the particles are released at c. 150 m.b.s.l. no particles are found in object 120. The reason is that object 120 is underlain by layers with a high horizontal conductivity. The sheet joints in the upper part of the bedrock in Forsmark have a large influence on solute transport from the deeper bedrock towards the surface. Once the particles enter a layer with a high horizontal conductivity, they are transported horizontally towards the northern part of the model domain, i.e. towards object 118.
- A comparison between results based on the two different QD models indicates that the main transport pattern is the same, although there are some local differences. The main difference is that solute is observed in the lakes after shorter simulation times, especially in object 118, when using the QD model describing present conditions. One explanation for this is that the sediment layers in the lake areas are thinner in the model for the present QD than in the QD model for 10,000 AD.
- Profiles across object 121_01 indicate that when the solute is applied based on input locations from the ConnectFlow model, the solute is transported vertically upwards towards the lake shoreline and then starts spreading in the lake area in the uppermost calculation layers.
- When applying plant uptake of solute in the model, the solute concentration is strongly reduced in the central parts of the lakes. Since plant uptake is a sink term in the model it implies that the solute taken up by plants is then removed from the model. In reality, this would be the case if the vegetation is removed from the lake at the end of the season. However, if the vegetation is not removed but is allowed to decompose at the site, the solute will not disappear from the site, instead it will be able to infiltrate again. So whether to use plant uptake or not in the model depend on the case to study. Since the case with no plant uptake will result in the highest concentration in the QD layers it may be seen as a worst case.
- Plant uptake from the saturated zone is the dominant plant uptake factor. The reason for this is that most of the solute appears in lake areas and in connection to the surface water courses, i.e. in areas that are saturated or close to saturated. The plant uptake from the unsaturated zone is about 15–20% of the uptake from the saturated zone.

- Decreasing the hydraulic conductivity in the lake sediments by a factor of 100 does not change the transport pattern significantly, but causes a delay of the transport through the sediments.
- The dominating sink in the AD simulations is the surface stream system. Once the solute reached a MIKE 11 surface stream branch, it was not possible to follow the continued mass transport in the stream system. This was due to practical project-specific limitations on simulation times. In theory, also the streams could have been included in the AD simulations. However, with the large number of grid cells and the temporal resolution required in the present modelling, simulation times would have been prohibitive.
- Increasing the dispersion coefficients of the QD layers causes a faster spreading of the solute in the uppermost layers, although the differences are not very large. This is consistent with the results found in /Gustafsson et al. 2008/.

8 Complementary transport modelling and delivery of results to dose calculations

8.1 Delivery to dose calculations

8.1.1 Background and methodology

Before the final delivery of all input files for the SR-Site modelling, a preliminary SR-Site model was set up and calibrated during winter 2008/2009. The preliminary model was based on the SDM-Site model /Bosson et al. 2008/, but the model area was extended as shown in Figure 8-1. The main reasons for performing this "pre-modelling" were to develop a technique for the SR-Site modelling and to identify potential problems and unforeseen difficulties. The modelling considered three different times, i.e. 2000 AD, 3000 AD and 5000 AD, which, as in the modelling described above, corresponded to different shorelines and distributions of sea and land areas within the model area. The models for the three times are all based on a QD model representing 2000AD. Different climates were simulated, but the results that were extracted and delivered to the dose calculations are all based on the selected year representing a temperate climate.

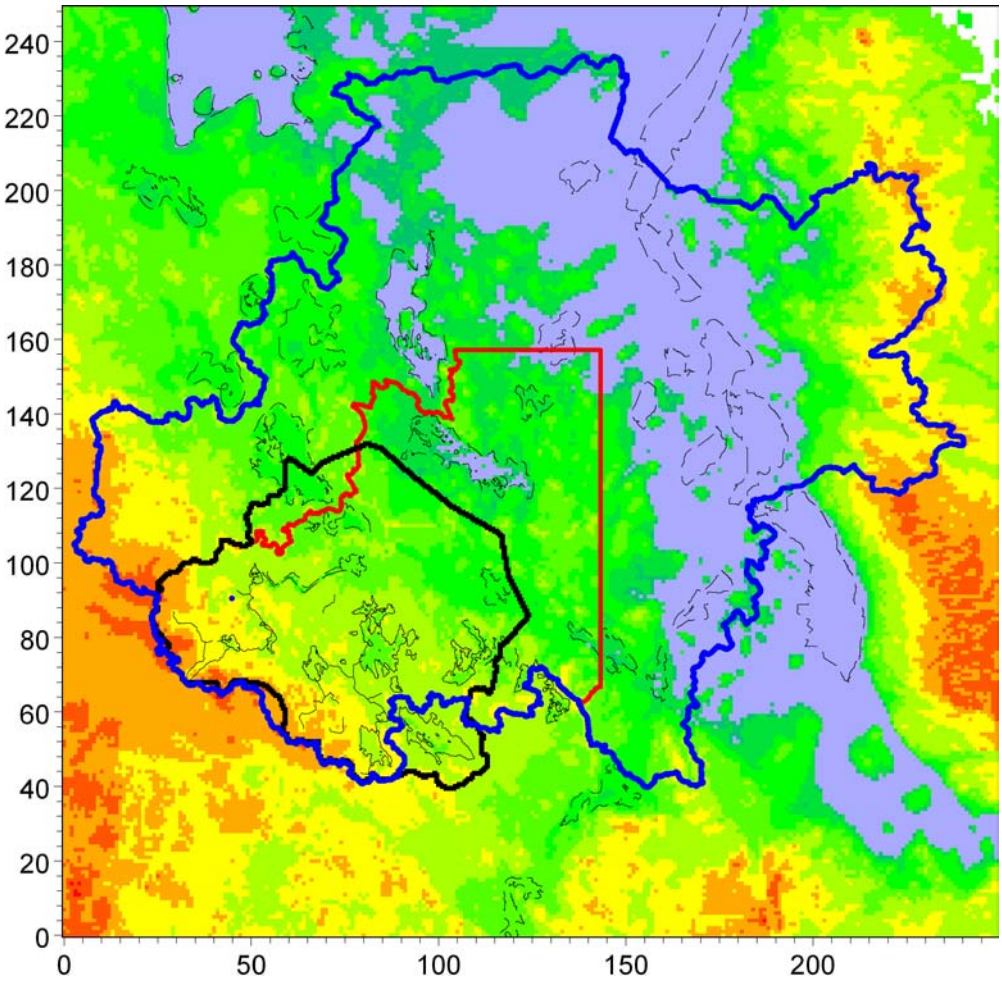

Figure 8-1. *MIKE SHE model area in the "pre-modelling" (red line) shown together with the SDM-Site MIKE SHE model area (black line) and the final SR-Site regional model area (blue line) considered in the modelling presented in Chapters 5 and 6 of this report.*

Results from the MIKE SHE "pre-modelling" in terms of water fluxes between different model compartments and calculation layers were needed as input data to the radionuclide modelling, which is the modelling that calculates the doses to humans in the different biosphere objects. The radionuclide modelling is performed using the Pandora tool /Ekström 2011/, which is a development of Tensit /Jones et al. 2004/ and an extension of Matlab© and Simulink© from Mathworks. Pandora simplifies the development of models that contain large systems of differential equations. Radionuclide decay chains can be handled.

The Pandora tool comprises a library of blocks that facilitates the creation of compartment models and a stand-alone toolbox for management of input parameters and probabilistic simulations. The decay and in growth of radionuclides in a chain is handled with the help of the Pandora Radionuclide block. The activity concentrations and doses were calculated from the amount of activity in different compartments.

MIKE SHE flow modelling results in terms of water fluxes between and within lake and mire areas were required for the radionuclide modelling. Since the final MIKE SHE SR-Site modelling was not yet conducted at the time when the radionuclide modelling was initiated, results from the "pre-modelling" described in this chapter were delivered in June 2009 and used as input to the SR-Site radionuclide modelling. Specifically, results from the 5000 AD model were used.

Six different lake areas were selected for the calculations providing input to the radionuclide modelling, see Figure 8-2. In the figure, the grey area is the MIKE SHE model area. All of the six selected lakes are existing at present. The main reason for choosing existing lakes is that the data are more extensive and the lakes are better described in the model. The six lakes represent different types of lakes within the model area. The lakes are of different sizes, with different types of vegetation and different thicknesses of underlying sediments. Therefore, the average values for the six lakes were thought to be representative for an "average lake area" in Forsmark.

For each one of the six lakes, water balances were calculated using the MIKE SHE model setup for 5000 AD. Each water balance is calculated for one year, i.e. the results are yearly mean values. Three different water balances were calculated for each selected area, one for the lake area, one for the mire area and one for the total area (lake + mire), resulting in totally 18 water balances. Figure 8-3 shows the distribution of lake versus mire areas for the six lakes. The outer line (black) is the total area (lake + mire) and the inner line (blue) represents the lake area. The boundaries for the lake and mire areas were defined based on site investigations of the littorial and pelagial zones of the lakes in the Forsmark area /Brunberg et al. 2004/ The green area is the mire area in the MIKE SHE model (grid size: 40 m × 40 m), and thus the white area inside the green area is the lake area in the model. The size of each lake and mire area is given in Table 8-1, together with the number of numerical grid cells for which each water balance was calculated.

Table 8-1. Areas and number of grid cells used in each water balance.

		No of cells (40×40m)	Area (km^2)
Bolundsfjärden	Lake	246	0.39360
	Mire	139	0.22240
	Lake+Mire	385	0.61600
Fiskarfjärden	Lake	252	0.40320
	Mire	247	0.39520
	Lake+Mire	499	0.79840
Gunnarsboträsket	Lake	13	0.02080
	Mire	31	0.04960
	Lake+Mire	44	0.07040
Gällsboträsket	Lake	10	0.01600
	Mire	120	0.19200
	Lake+Mire	130	0.20800
Puttan	Lake	16	0.02560
	Mire	41	0.06560
	Lake+Mire	57	0.09120
Stocksjön	Lake	5	0.00800
	Mire	20	0.03200
	Lake+Mire	25	0.04000

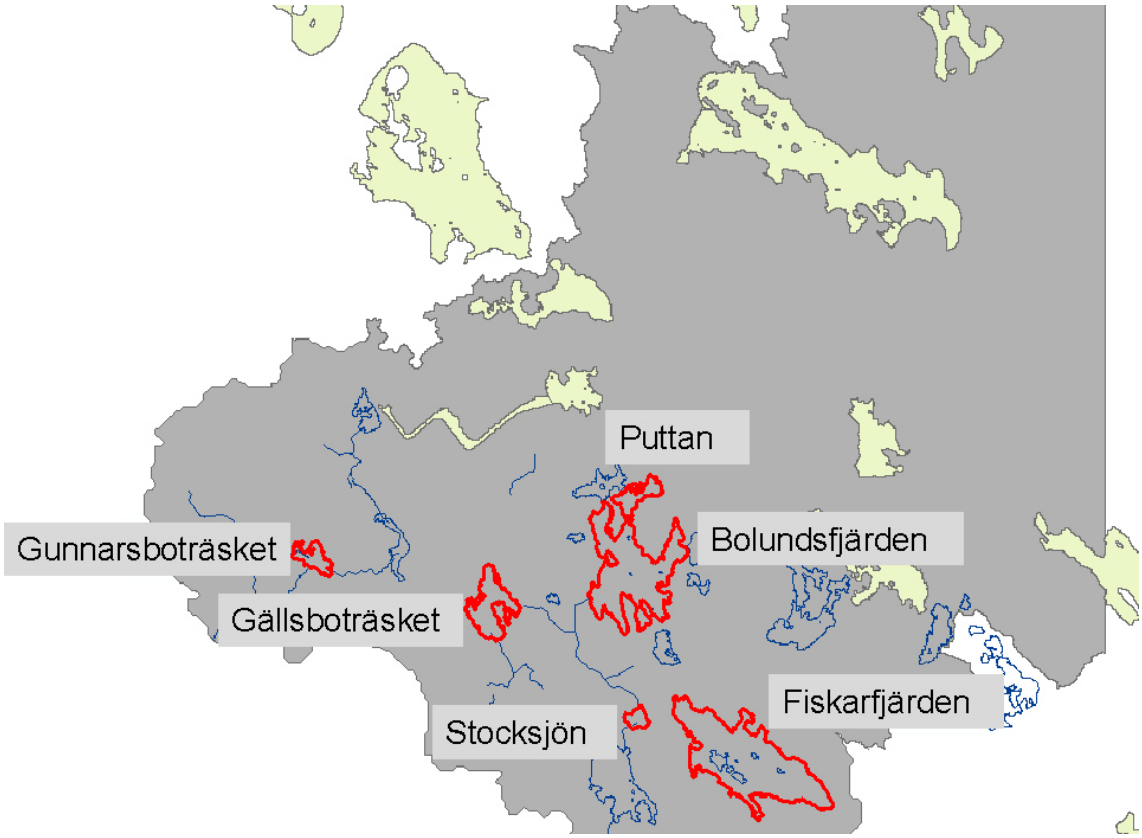

Figure 8-2. *Lakes included in the calculations. Note that Lake Puttan and Lake Bolundsfjärden are treated as two different objects in the modelling.*

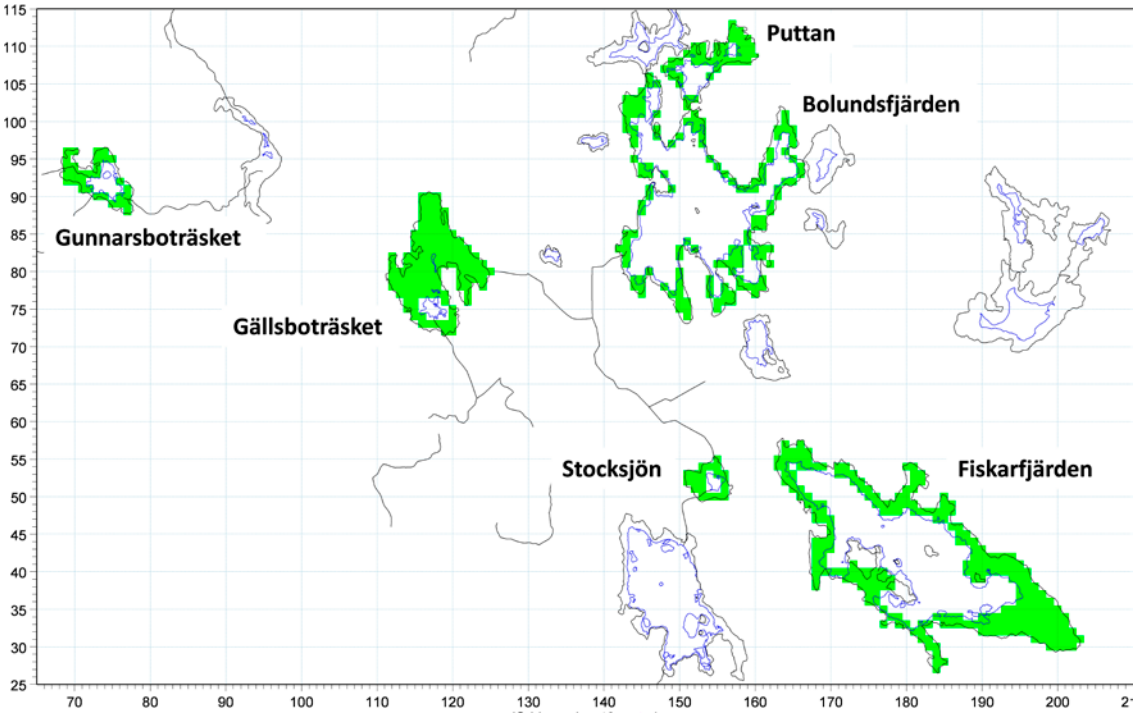

Figure 8-3. *Illustration of the distribution of lakes and mires for the six lake-mire areas. Green areas are mire areas surrounding the lakes. Note that Lake Puttan and Lake Bolundsfjärden are treated as two different objects (Figure 8-2).*

The water balance utility in MIKE SHE is a post-processing tool for generating water balance summaries from MIKE SHE simulations. Water balance output can include area normalised flows (storage depths), storage changes, and model errors for individual model components (e.g. the unsaturated zone evapotranspiration components). A water balance can be generated at a variety of spatial and temporal scales. Figure 8-4 shows a schematic description of the parameters that were considered in the lake/mire water balances.

The blue arrows are parameters obtained from the water balance for the lake area, the green arrows are obtained from the mire water balance, and the red arrows are obtained from the water balance in which both lakes and mires are included. After the calculations, all values are normalised with respect to the total area, i.e. the area for lake+mire, to make them comparable.

In Figure 8-4, OL is short for overland, i.e. water on the ground surface. Furthermore, L1 is the uppermost calculation layer in MIKE SHE, L2 is the second layer and, consequently, L3 is the third layer. In the MIKE SHE model for Forsmark, L1 and L2 represent the Quaternary deposits, whereas L3 is a bedrock layer. Layer L1 consists mainly of lake sediments and layer L2 is a till layer.

For the lake areas, values for the vertical water fluxes between the overland and the sediment layers are calculated; they are denoted as 'OL to L1' and 'L1 to OL' in the figure. In the same way, water fluxes between the sediment layer and the till layer, 'L1 to L2' and 'L2 to L1', and between the till layer and the bedrock, 'L2 to L3' and 'L3 to L2', are calculated. For the mire areas, the vertical fluxes are calculated in the same way as for the lake areas.

The horizontal fluxes between the lake and the mire are obtained from the water balance for the lake area. The water exchange terms between the two compartments at the surface are OLin (from the mire to the lake) and OLout (flux from the lake to the mire). In the same way, the horizontal fluxes between lake and mire are calculated for the two layers with Quaternary deposits. The red arrows are horizontal fluxes into and out from the total lake-mire areas.

The net precipitation is included in the figure just in order to get a water balance in each compartment; it is not a parameter used in the Pandora model. The net precipitation is calculated as the precipitation minus all evaporation and transpiration components in the model.

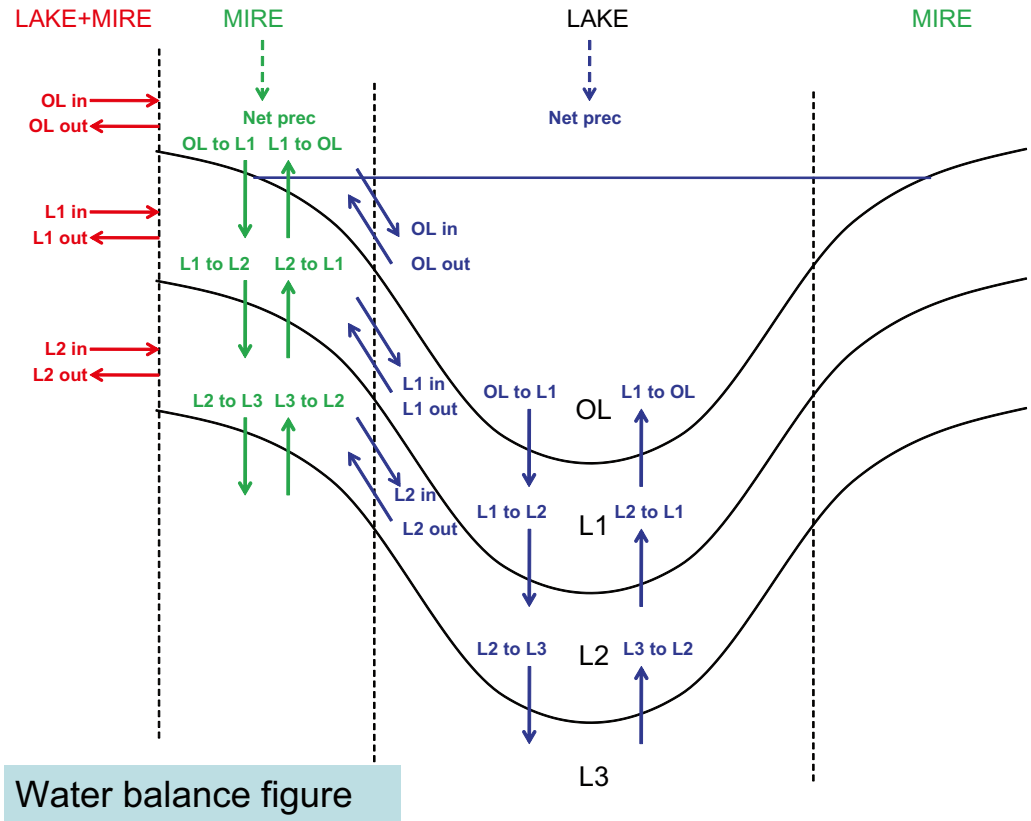

Figure 8-4. *Schematic figure showing parameters calculated in water balances for lake and mire areas in Forsmark.*

8.1.2 Delivered output data

Transforming the MIKE SHE water balance parameters to the Pandora box model gives a model according to Figure 8-5. For more details on the Pandora box model, see /Avila et al. 2010/. The numbers illustrated in the figure are mean values for all six lakes included in the analysis. The boxes in the figure have denotations according to the Pandora model and correspond to the different calculation layers in the MIKE SHE model.

All parameter names starting with "Aqu_" refer to the lake area in MIKE SHE and all names starting with "Ter_" refer to the mire area. The name "_regoLow" corresponds to layer L2 in MIKE SHE and the name "_regoMid" to layer L1. Furthermore, the "Aqu_Water" box refers to the OL lake area in MIKE SHE. The "Ter_Water" box is a fictive box, which does not exist in the Pandora model. It is however necessary to include the "Ter_Water" box for the results from the MIKE SHE model in order to get a correct water balance for each box and for the entire model.

In MIKE SHE the upper box contains the overland compartment. This box might be dry if the studied area is not saturated. For the mire area, the water depth varies significantly depending on seasonal changes. The releases to the lakes and the mires are estimated as the net vertical water flux from the bedrock to the till layer in MIKE SHE, i.e. the difference between the 'L3 to L2' and 'L2 to L3' flows.

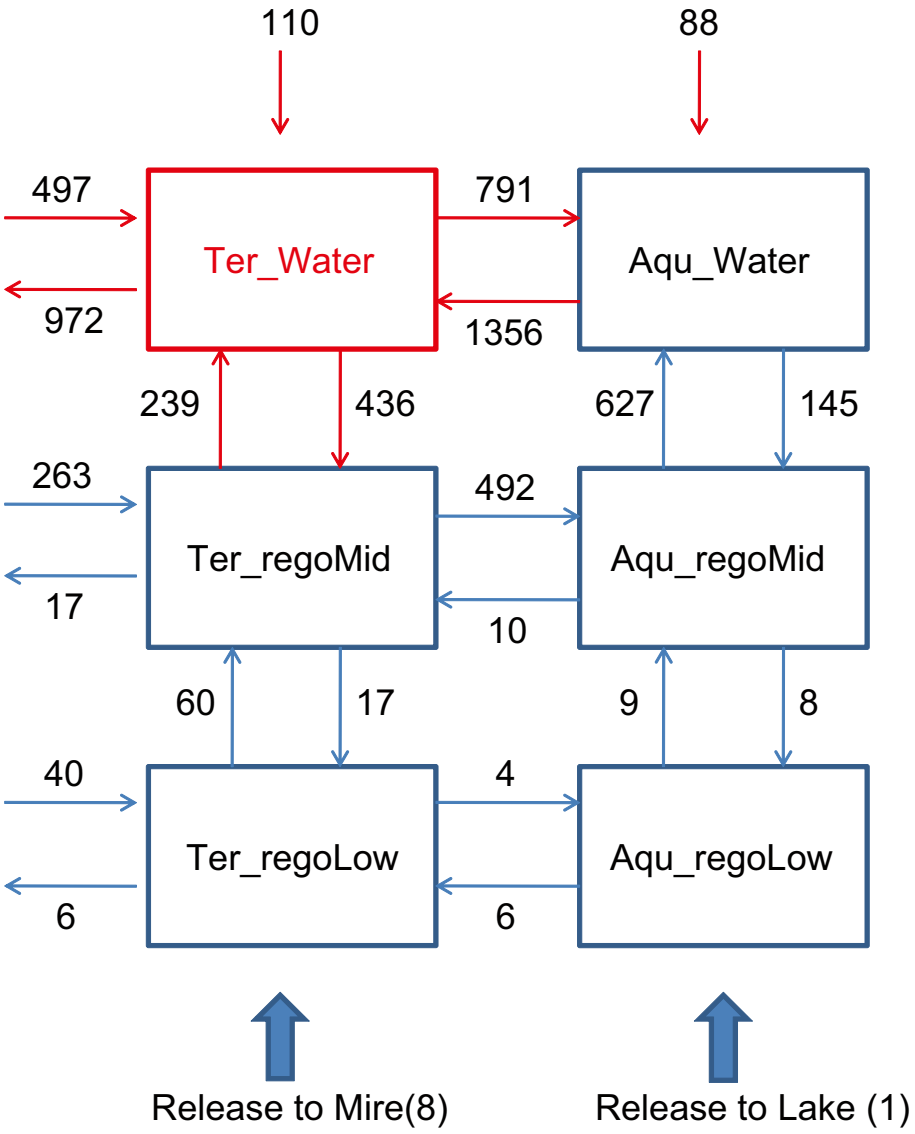

Figure 8-5. *Advective fluxes (units in mm y^{-1}) for an average lake-mire object obtained from the MIKE SHE simulations and transformed to a box model.*

Groundwater discharge to the sea

The groundwater discharge from the bedrock to the sea bottom sediments is also an input parameter to the Pandora model. To estimate the water fluxes below the sea, a water balance for the area constituting sea in the 2000AD_2000QD model was calculated. The reason to use the 2000AD_2000QD MIKE SHE model is that a large part of the model area is covered by sea at 2000 AD, which means that data for the majority of the sea basins could be extracted.

In the Pandora model, it is assumed that there is a net upward flux through the QD-layers, equal to the flux from the geosphere to the lowest QD-layer. This flux is assumed constant through the "regoLow", "regoMid" and "regoUp" boxes, because there is no influence of the lateral surface fluxes appearing in the models of the lake and terrestrial systems /SKB 2009/. In order to have a conservative estimate, the maximum net upward flux in the marine basins of the 2000AD_2000QD model was used. The maximum net flux value, 8 mm/year calculated for basin 121_2, was used for all marine biosphere objects during all time steps. The fluxes to and from the bedrock in each basin are listed in Table 8-2 and the location of each basin is shown in Figure 8-6.

Table 8-2. Flow rates below the sea, mm/year, from the bedrock to the QD. The maximum net upward flux 8 mm/y is found in basin 121_2.

	Basin 101		**Basin 108**		**Basin 107**	
	Up	Down	Up	Down	Up	Down
Bedrock, to/from QD	0.77	0.85	1.55	1.35	2.13	2.59
	Basin 116		**Basin 117**		**Basin 118**	
	Up	Down	Up	Down	Up	Down
Bedrock, to/from QD	1.37	1.28	1.30	1.06	3.04	0.36
	Basin 121_3		**Basin 121_1**		**Basin 121_2**	
	Up	Down	Up	Down	Up	Down
Bedrock, to/from QD	5.31	0.05	5.31	1.25	7.99	0.01
	Basin 123		**Basin 146**		**Basin 126**	
Bedrock, to/from QD	Up	Down	Up	Down	Up	Down
	1.01	0.98	0.28	0.18	1.29	1.02
	Basin 120		**Basin 105**		**Basin 114**	
Bedrock, to/from QD	Up	Down	Up	Down	Up	Down
	3.70	0.04	1.38	1.32	1.48	1.05

Up = Upward flow, from the current layer to the layer above (mm/y)

Down = Downward flow, from the layer above to the current layer (mm/y)

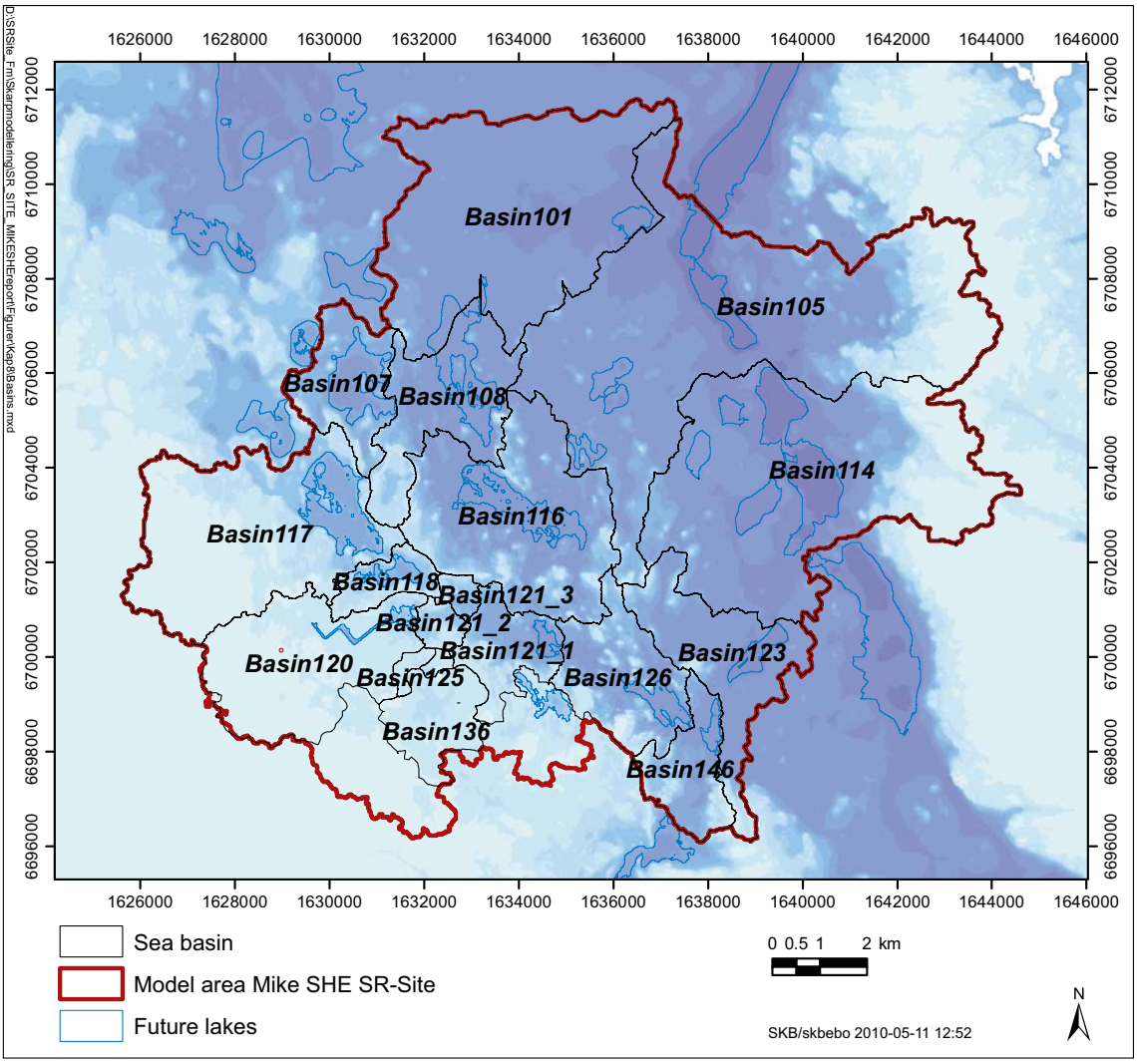

Figure 8-6. *The different sea basins in the Forsmark area.*

The Pandora model is also used for calculating radionuclide transport and doses to humans during a cold period with permafrost. The MIKE SHE permafrost simulation for the case with a permafrost layer down to a depth of 240 m.b.s.l. was used in the calculation (see Section 6.2.1). Water balances were extracted for object 114 in the same way as for the lake and mire objects, i.e. one water balance for the talik area, one for the mire area around the talik, and one water balance for both the talik and mire area. Figure 8-7 shows the extent of the areas for the talik and the mire. The talik area within object 114 consists of two separate taliks, taliks number 3 and 4 according to Figure 6-5. The total number of grid cells for the talik area within object 114 is 118, corresponding to an area of 1.16 km^2. The mire area consists of 277 grid cells with an area of 1.77 km^2. Consequently, the entire talik plus mire area consists of 458 grid cells with a total area of 2.93 km^2.

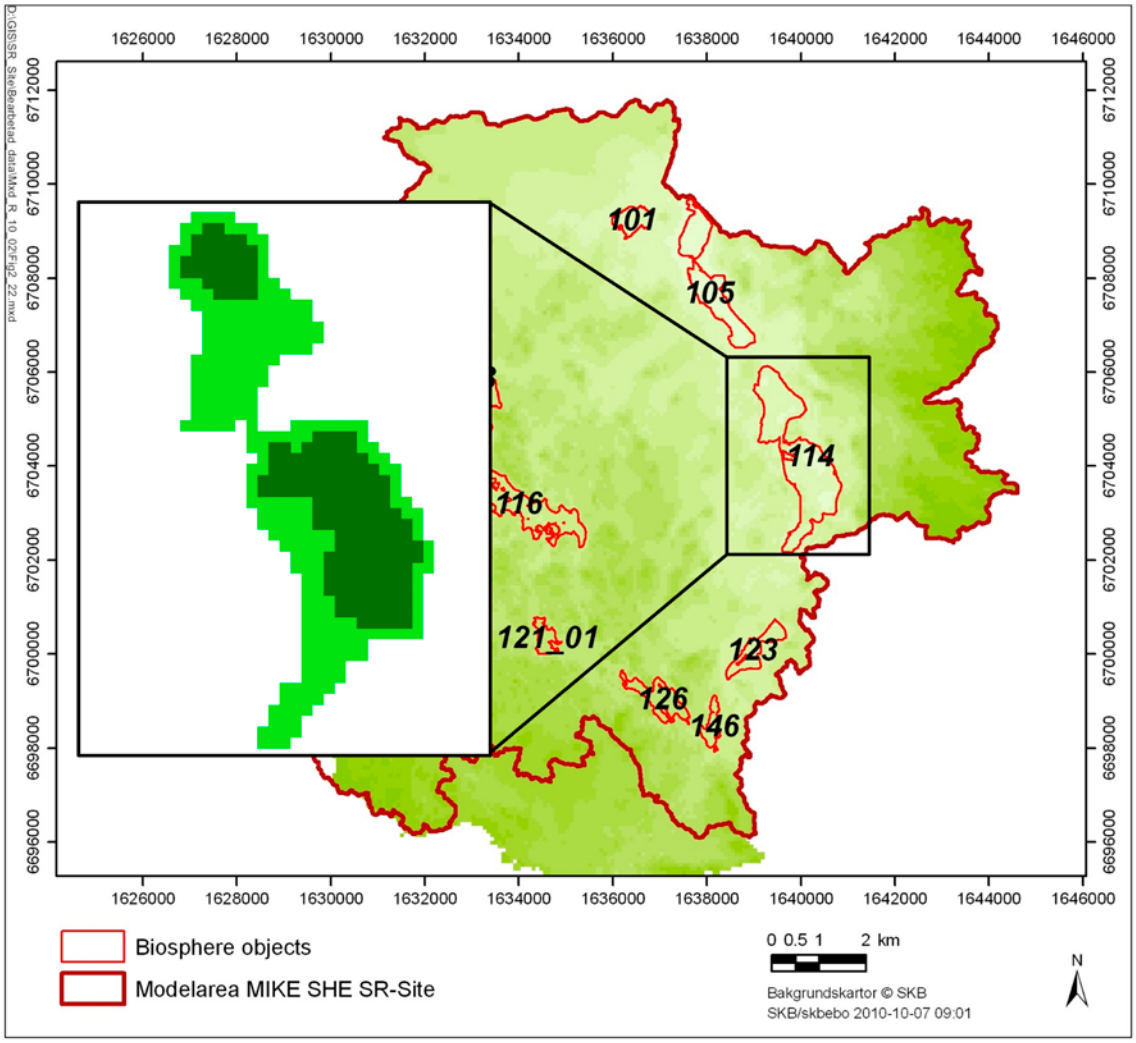

Figure 8-7. *Definition of talik and lake areas used in extraction of water balances for the MIKE SHE permafrost simulation with a permafrost layer down to a depth of 240 m.b.s.l. The upper talik is referred to as talik number 3 and the lower talik as number 4.*

The extracted results are presented in Figure 8-8. The definitions of the different model boxes are the same as for the lake-mire water balances presented above (Figure 8-5). The general pattern of the net fluxes between the different model compartments is the same for the permafrost case as for the temperate climate, although the individual fluxes are very different in most compartments. All values are yearly mean values, which for the permafrost simulation means that the presented values include all periods throughout the year, i.e. the freezing period, the frozen period, the thawing and the active periods.

The transport from the underlying bedrock to the "regoLow" compartment is very small. The net flux from the bedrock to the mire is directed upwards while the net flux to the talik is directed downwards. The reason for the small net fluxes and a net flux directed downwards in the talik area is that parts of the talik act as recharge areas while other parts act as discharge areas. Based on the permafrost simulations presented in Section 6.2.1 it was concluded that talik number 3 is mainly a recharge talik, while talik number 4 is a discharge talik.

Furthermore, all horizontal fluxes between the boxes in the QD layers, i.e. the "regoMid" and "regoLow" boxes, are significantly smaller for the permafrost case since the soil is frozen during long periods and the active layer is only 1 m deep. Most of the water in the model is circulated in the uppermost parts of the model.

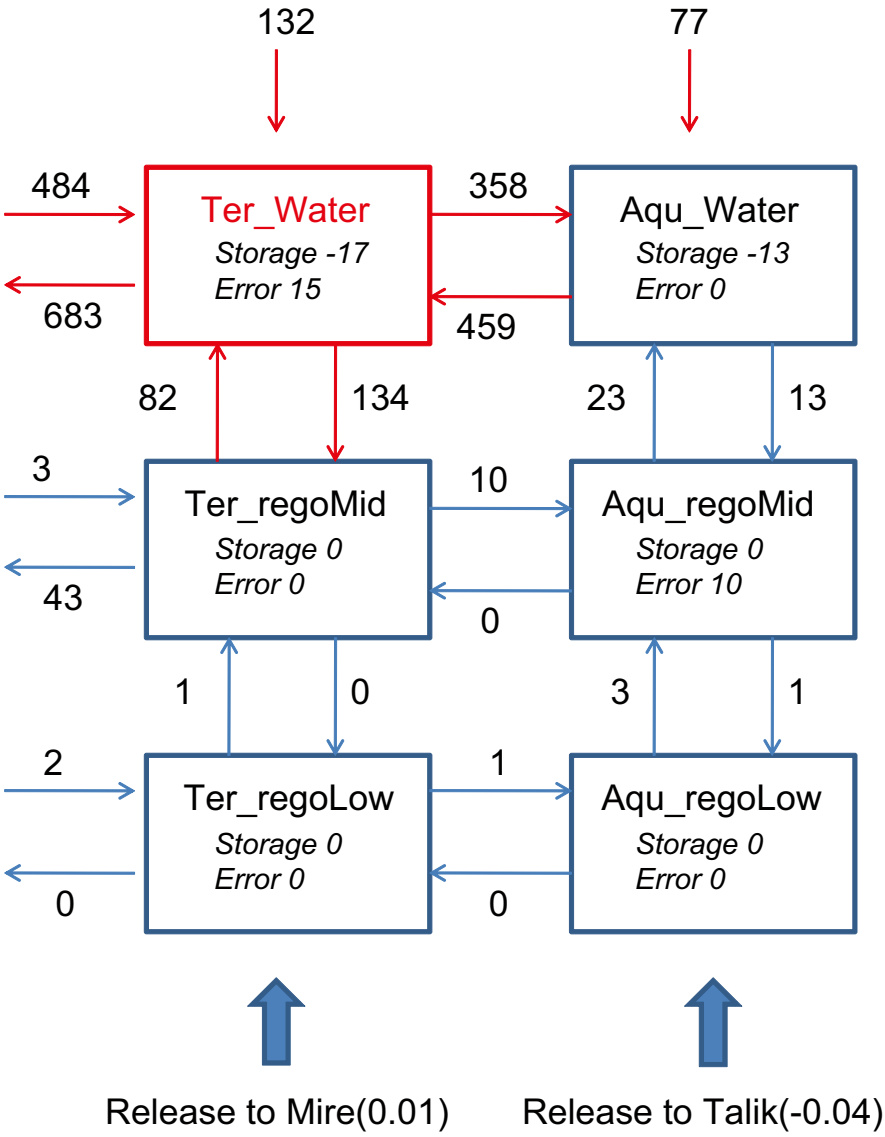

Figure 8-8. *Advective fluxes (units in mm y^{-1}) for object 114 obtained from the MIKE SHE permafrost simulation and transformed to a box model.*

8.2 Particle tracking simulations for different climate conditions

One of the conclusions from the flow and transport modelling described in Section 5-7 is that the climate has a large influence on the recharge and discharge pattern in the model area. Therefore, particle tracking simulations with the three studied climate cases (wet, periglacial and temperate) were performed in order to study the influence of the climate on the flow paths from repository depth to the ground surface. In the MIKE SHE transport simulations described in Chapters 5 to 7, no case with the source at repository depth was considered. The only cases with sources associated with the repository volume were those where particles from the ConnectFlow model were further traced in the MIKE SHE model to analyse how the flow paths were influenced by the details of the QD and the near-surface processes.

In all PT simulations described in this section, the conditions at 10,000 AD were modelled. Particles were introduced within the volume hosting the repository. This means that the particles were not released at the exact positions of the depositions holes, but in all cells contained by the outer boundary of the planned repository. The simulations were run for 16,000 years, which means that the transient flow during the year evaluated in each case (normal or wet temperate, or periglacial) was cycled 16,000 times. For the periglacial simulations the active period was cycled, since it is not possible to simulate a whole annual cycle in the same PT simulation in MIKE SHE. For periglacial climate conditions, PT simulations were performed for permafrost depths of both 100 m and 240 m. All four simulations cases and their related flow results are listed in Table 8-3.

In total, 2,375 particles were released, and most of the particles were still left in the model volume after 16,000 years of simulation. Under normal (present) temperate conditions, only 45 particles reached the QD layers, and under wet climate conditions only 39 particles entered the QD layers. The flow paths obtained for the normal and wet temperate cases are almost the same. In the model for periglacial conditions, more particles reached the QD layers, and the flow paths also differed from those in the temperate cases. The number of particles reaching the QD layers depended on the depth of the permafrost, and consequently on the number of taliks. When the permafrost was 100 m thick, 405 particles entered the QD layers, whereas 187 entered the QD layers when the permafrost was 240 m thick.

The exit points, in this case defined as the positions where the particles enter the QD layers, are illustrated in Figure 8-9. The 3D flow paths from the repository towards ground surface for each case are illustrated in Figures 8-10 and 8-11. The flow paths are almost the same for the normal and wet temperate cases (Figure 8-10). In both cases the particles in the eastern part of the repository have the fastest flow paths and are moving up towards object 121. Object 121 is also the only object receiving particles in the temperate simulation cases. There are also particles moving up towards the inlet canal (object 120), but these particles do not reach the QD layers within the 16,000 years of simulation.

When applying a periglacial climate to the model, the flow paths converge towards the talik areas, which are the only possible transport pathways through the permafrost (Figure 8-11). When the permafrost is 240 m deep, the flow paths converge to the sea-talik, object 105, which is the only talik attracting particles and also the only object with exit points after 16,000 years of simulation. In the case with 100 m deep permafrost, more taliks attract particles and exit points are identified in objects 105 and 114 and in the vicinity of object 116. All these objects are taliks in the simulation case with 100 m permafrost.

Table 8-3. PT simulation cases with particle released within the volume contained by the planned repository.

PT simulation case	Based on flow field from model	Flow results described in chapter
Temperate	10000AD_10000QD	5.3
Wet	Wet	6.1
Periglacial_100m	Periglacial, 100 m permafrost, active period	6.2.1
Periglacial_240m	Periglacial, 240 m permafrost, active period	6.2.2

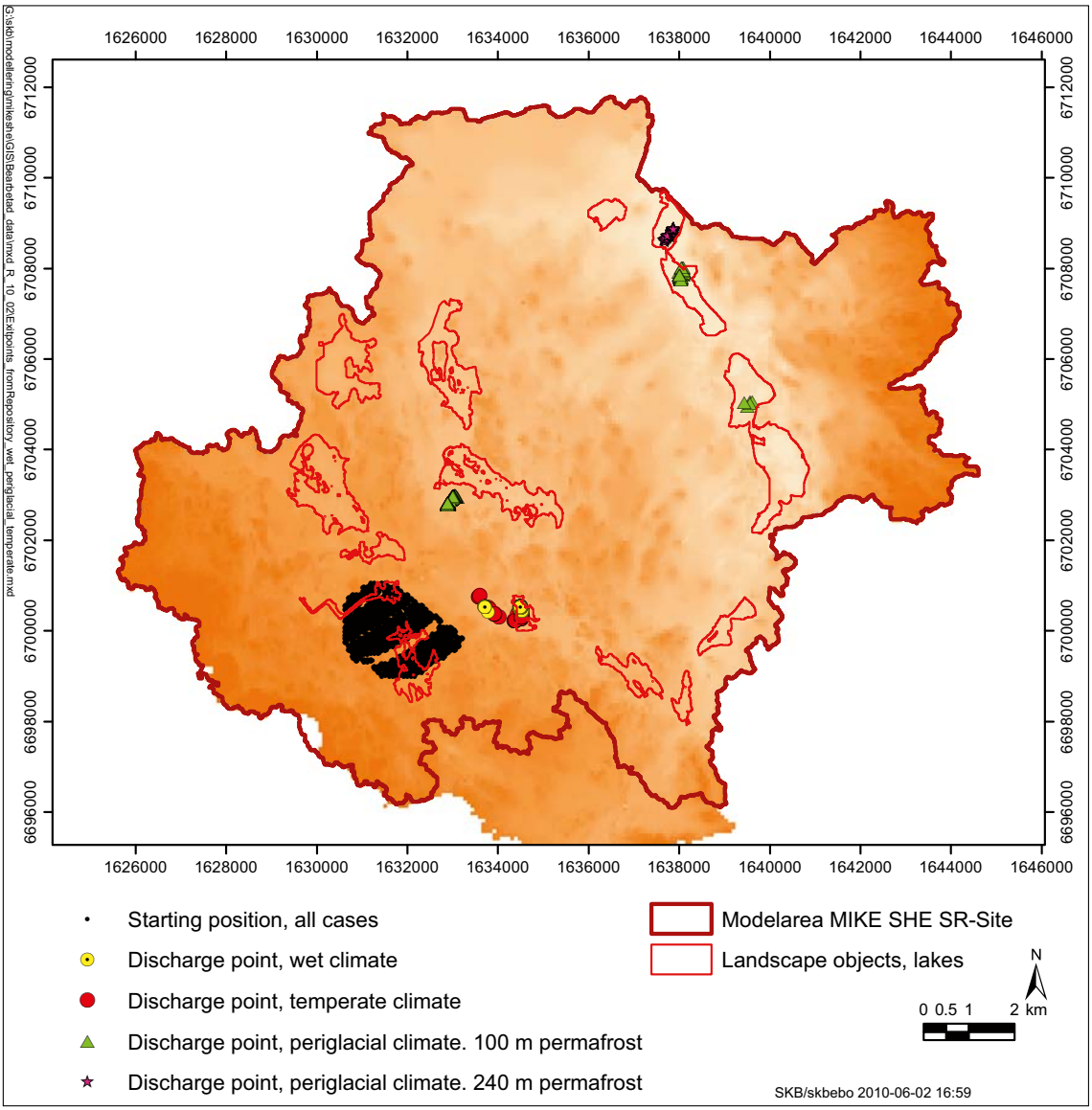

Figure 8-9. Positions where the particles in each simulation case enter the QD layers.

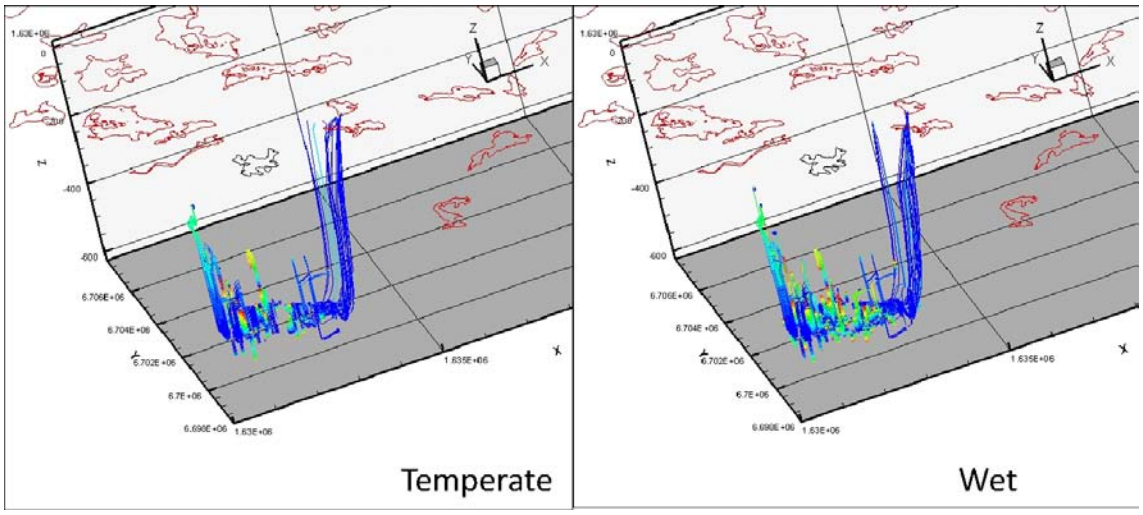

Figure 8-10. *Three-dimensional flow paths from the repository volume towards ground surface from the normal temperate (left) and wet (right) simulation cases.*

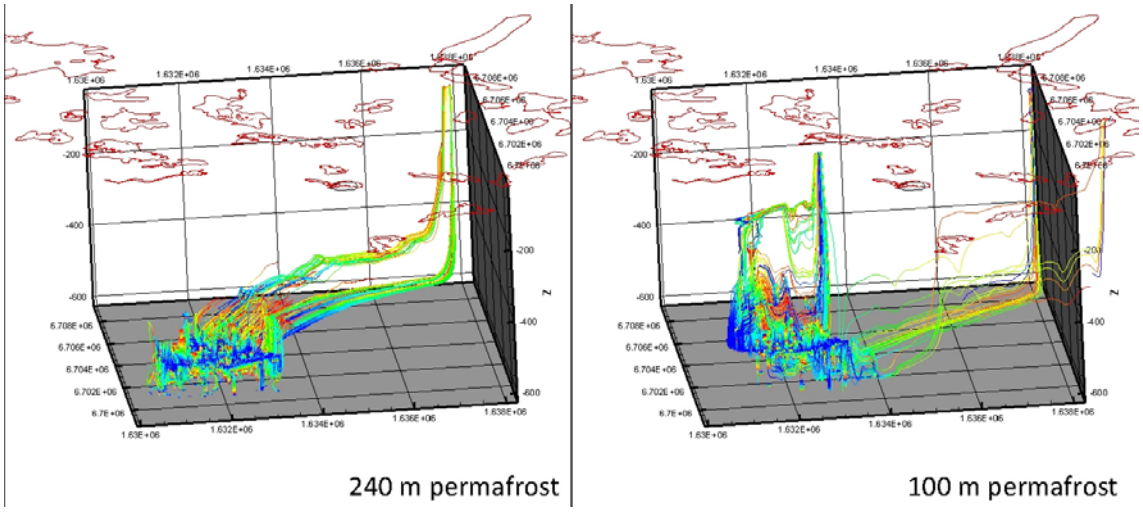

Figure 8-11. *Three-dimensional flow paths from the repository volume towards ground surface from the periglacial simulation cases with 240 m (left) and 100 m (right) permafrost thickness.*

9 Discussion and conclusions

The development of the landscape in a hydrological perspective has been analysed by studying the effects of shoreline displacement, development of the QD layers and vegetation cover, and the effects of different climates. Numerical models describing present and future conditions have been developed and applied in order to answer questions about the future hydrology in Forsmark. Present conditions regarding meteorology, surface water levels and discharges, groundwater levels in QD and bedrock, and locations of recharge and discharge areas have been investigated during the site investigations. Data from site investigations have been used when calibrating and testing the numerical models describing the present hydrological situation at the Forsmark site. The knowledge gained from the site investigations and the site descriptive modelling has been the basis for the models describing possible futures in Forsmark. Simulations have been performed for normal and wet temperate climates, and for a cold climate. For the studied cases with a cold climate a continuous permafrost formation interrupted by through taliks was assumed to be present in the area.

The present water balance in the area, estimated from long-term regional measurements and local measurements with a precipitation of approximately 560 mm/y, an evapotranspiration of 400–410 mm and a runoff of 150–160 mm is supported by the numerical modelling. The water balances calculated in the numerical modelling with future shorelines do not differ from the measured or calculated water balances for present conditions. When studying only the effects of the shoreline displacement on the overall water balance, no major changes from present conditions can be noticed. The different flows between different model compartments differ less than 10% in all the studied cases. The internal distribution of the precipitated water is approximately 70% evapotranspiration and 30% runoff independently of the shoreline position and hence of the land area considered (present or future land).

The largest change in the internal flows within the system appears when changing the QD model as the land is rising, i.e. when studying the combined effect of the shoreline displacement and the development of the QD layers (which is considered the most realistic case). The QD model influences the infiltration capacity; the applied models for future QD result in a lower infiltration of water from the surface to the unsaturated zone. Still the changes in the amount of water infiltrating the soil in the different studied cases are less than 10% and the internal distribution of the precipitated water is approximately 70% evapotranspiration and 30% runoff independently of the applied QD-model. With a different vegetation cover the potential for transpiration changes and thus the internal distribution of the total actual evapotranspiration is affected. However, the total evapotranspiration is almost the same as long as a temperate climate is applied to the model.

Two water balances for two sub-areas, the catchment area of Lake Bolundsfjärden situated on land 2000 AD and the catchment area of object 116, a future lake, have been studied separately. The lake percentages in the two catchment areas are almost the same, 8% in the catchment area of Lake Bolundsfjärden is covered by open water compared to 11% in the catchment area of object 116. The area of open water affects the actual evapotranspiration in the area since the actual evapotranspiration equals the potential evapotranspiration in flooded areas. Thus, the two areas are similar concerning lake percentage and they are both “lake centred” catchment areas with a relative flat topography.

It is of interest to analyse the dynamics within the two catchment areas for different shoreline positions and development stages of the QD. When studying the two different catchment areas, the differences in the overall water balance are very small. The runoff and evapotranspiration within the two catchments are almost the same. Also, the water balance for the catchment area of Lake Bolundsfjärden is almost the same at 2000 AD and 10,000 AD.

When applying a wet climate, with an annual average precipitation of 1463 mm, to the model the internal distribution of the precipitated water changes. For a wet climate the runoff is approximately 20% of the applied precipitation and the evapotranspiration is 80%. Due to the high evapotranspiration, the part of the precipitated water leaving the model volume as runoff under wet climate conditions is relatively lower than for normal temperate climate conditions. However, there is an absolute increase in runoff from c.180 mm to c. 360 mm. The transpiration increases from approximately 145 mm during temperate climate to approximately 475 mm under wet conditions. In both cases the transpiration is about 40% of the precipitated water. The fact that the water demand of the plants in the area always is supplied, due to the high precipitation, may affect the uptake of radionuclides to the vegetation.

The largest change in the overall water balance is observed when modelling periglacial climate conditions. The internal distribution of the precipitated water is 50% runoff and 50% evapotranspiration. The water demand from the vegetation is very low, due to both a poor vegetation cover, but also because the active period is short. Even during the active period the temperature is quite low; thus, there is no driving force for an effective evapotranspiration. The precipitation under cold conditions is lower than for temperate weather conditions. The applied precipitation in the MIKE SHE model decreases from 533 mm to 412 mm.

Since the evapotranspiration is very low the runoff leaving the system via the surface water streams is larger for the cold climate than under temperate climate conditions, even if the applied precipitation is lower. This is also a result of the fact that a large portion of the precipitation is snow, which gives a relatively short and intensive runoff during the snow melt when the evapotranspiration is still relatively small. The infiltration capacity under permafrost conditions is low resulting in a larger amount of direct runoff from the surface to the streams. The total amount of water transported to the streams via the saturated zone is the same under temperate and cold conditions with permafrost.

The increased runoff under wet climate conditions affects the turnover and residence times of water in lakes and streams, which influence the transport of matter within and between the different ecosystems in the landscape. The effect of dilution of a hypothetical release from the repository on the surface might be higher under wet climate conditions due to the higher amount of water circulating in the surface system. Studying the discharge in the streams and the depth of overland water in the area it is likely that the streams have enough capacity to transport the water further downstream. No larger flooded areas have been seen in the model results with an applied wet climate. This implies that radionuclides that have reached the surface stream network will follow the same flow paths as under temperate climate conditions.

In summary, as long as a temperate climate governs the hydrology at the Forsmark site no major changes will occur in the water balance. The internal distribution of the precipitated water might change somewhat. The available models indicate that there will be minor changes, all of them within 10% of the present water balance at the site. Under different climate conditions changes in the overall water balance will occur. Under wet conditions, a larger amount of water will contribute to the runoff with shorter residence times of water as a result.

Under periglacial climate conditions with a permafrost formation the infiltration will be strongly reduced. Also the annual variation and dynamics in the hydrology deviate from the temperate conditions. The main part of the turnover of the water takes place under the relative short active period of the year, with an initial intensive snow melt runoff. During the frozen period, all precipitation is accumulated on the ground surface; almost no water infiltrates due to the frozen soil. Only the talik areas are unfrozen and an exchange of water through the taliks may occur. This is further discussed below.

The overall pattern of recharge and discharge areas is the same for the different time periods studied. A scattered pattern governed by the local topography is found in the QD independently of the shoreline position, the vegetation or the applied QD model. In the bedrock the discharge areas are concentrated to areas under the lakes and stream valleys. Changing QD model from the one representing the present conditions to the ones reflecting the QD development up to 5000 AD or 10,000 AD does not have a strong influence on the pattern of recharge and discharge areas. It has an impact on the strengths of the recharge or discharge areas (i.e. on the sizes of the upward or downward fluxes), but areas with an upward or downward gradient in the 2000 AD QD model still have the same directions of the flow gradients when applying the models for future QD.

There are some exceptions, but in general the overall recharge-discharge pattern seems to be governed by the topography, and not so much by the stratigraphy, thickness or type of QD. However, the distribution of recharge and discharge areas under some specific objects might change when a lake turns from a lake to a wetland.

The water flow paths from the deep bedrock do not change with different QD models or vegetation cover. Studying the particle tracking results from different time periods, almost the same discharge points can be seen for the area constituting land at present. The areas receiving particles at present are also discharge areas in the future models as long as a temperate climate is applied. More particles are reaching the ground surface as the shoreline is moving and new land areas are created. The low gradients below the sea cause very small flow velocities and many particles released below the sea in the model for present conditions are stuck in the model volume. The local topography at the former sea bottom creates gradients that become driving forces for new recharge and discharge areas. Thus, a hypothetical release of radionuclides from the repository will be more easily transported towards the surface as the land is rising.

As described above, most of the lakes act as discharge areas and the transport under the lakes is dominated by the vertical component as long as the transport takes place in the bedrock. One exception is areas with sheet joints, in these areas the transport is dominated by the horisontal component. The transport in the QD under and around the lakes is dominated by the horizontal component. The low conductive lake sediments reduce the vertical flow through the lake bottom and the main discharge of groundwater is seen along the shores of the lakes and wetlands.

The same pattern as described above is found when a wet climate is applied to the model. Under cold conditions with continuous permafrost the pattern of recharge and discharge areas changes dramatically. During the present temperate period, the local topography has a strong influence on the location of recharge and discharge areas, whereas the recharge and discharge areas are concentrated to the through taliks under permafrost conditions. The taliks provide the only available pathways for the water, and consequently also for matter transported by water, to be transported up or down through the permafrost.

Some taliks act as recharge areas and some as discharge areas. Thus, the periglacial flow paths from the repository towards the surface will deviate from the flow paths developed under present climate conditions. Many of the areas defined as taliks are discharge areas also under present conditions. However, the radionuclide concentrations might be higher in the talik areas during a period of continuous permafrost, which could affect doses calculated for this and subsequent time periods.

The shallow groundwater table at present will prevail also under future conditions. However, a lowering of the water table within the area above the planned repository can be noticed when taking the shoreline displacement and the development of the QD into consideration. At present, the main part of the area has a groundwater table less than one metre below ground surface. Under future conditions with a more distant shoreline, the depth to the groundwater will increase somewhat. Specifically, the model results indicate that the part of the model area having depths between 1 and 3 m below ground surface will increase.

With a lower groundwater table the amount of water transported in the upper part of the profile, which has a high transport capacity, will decrease. Thus, the fast transport of water to the surface stream network after a rain event might be reduced. A larger portion of the water will infiltrate to the deeper part of the QD profile and the water will be transported in the saturated zone towards the streams. This phenomenon can be seen when studying the future water balances discussed above, the contribution from the subsurface saturated zone to the runoff increases as the land rises, whereas the contribution from the overland part of the model decreases.

The processes and changes in the landscape identified as important for the description of the future hydrology in Forsmark are summarised below.

- The variation of the climate is important to describe. The climate is the parameter that has the strongest influence on the water balance in the area. The estimation of the potential evapotranspiration coupled to each climate case is also of great importance within the numerical modelling, since the PET has a large influence on the calculated actual evapotranspiration. Thus, the PET applied in the future model cases is an uncertainty. The estimated PET is also of importance because the groundwater table in the Forsmark area is so close to the ground surface, and a lot of water is available for evapotranspiration. The overall water balance is affected by climate changes, even though the relative distribution of the precipitated water on different water balance components is less sensitive to the applied climate. Especially, the permafrost has a strong influence on the temporal variations and the distribution of the water exchange in the area. The locations of recharge and discharge areas are not affected by the climate except from in the case with a permafrost landscape. The spatial distribution of recharge and discharge areas under periglacial conditions deviates from the distribution under wet and temperate conditions.
- The location of future streams and lake thresholds is important and also a large uncertainty in the description of the future hydrology. The locations and properties of the streams are important to describe to reach a proper runoff and prevent the forming of flooded areas in the model that will not appear in reality. The lake thresholds are difficult to determine due to their sensitivity to erosion and sedimentation processes, but the locations and elevations of the thresholds have large influence on the local recharge and discharge pattern.
- The description of the future topography is important. The topography together with the climate are the most important driving forces for the hydrology. The details of the QD model used together with the topographical model are less important for the overall water balance and the pattern of regional recharge and discharge areas. However, the stratigraphy and thickness of the QD have an influence on the local distribution of recharge and discharge areas in the near-surface system. Since most of the recharge areas of deep groundwater are concentrated to present or future lakes and/or wetlands, the distribution of the QD in these areas can have a strong impact on the details of the transport of radionuclides there, in case of a future release from the repository.
- Vegetation development has an influence on the hydrology when large changes in the vegetation occur, for example due to climate changes. Small changes in the internal distributions of different vegetation types do not have a large impact in the hydrology in the area. During a period of cold climate conditions, very poor vegetation is developed with a low transpiration as a result. This affects the distribution of the different evapotranspiration components of the area. However, “climate induced vegetation changes” appear to have small effects on the hydrology compared to changes in the climate itself.

10 References

SKB's (Svensk Kärnbränslehantering AB) publications can be found at www.skb.se/publications

Aneljung M, Gustafsson L-G, 2007. Sensitivity analysis and development of calibration methodology for near-surface hydrogeology model of Forsmark. SKB R-07-27, Svensk Kärnbränslehantering AB.

Avila R, Ekström P-A, Åstrand P-G, 2010. Landscape dose conversion factors used in the safety assessment SR-Site. SKB TR-10-06, Svensk Kärnbränslehantering AB.

Bosson E, Berglund S, 2006. Near-surface hydrogeological model of Forsmark. Open repository and solute transport applications – Forsmark 1.2. SKB R-06-52, Svensk Kärnbränslehantering AB.

Bosson E, Gustafsson L-G, Sassner M, 2008. Numerical modelling of surface hydrology and near-surface hydrogeology at Forsmark. Site descriptive modelling, SDM-Site Forsmark. SKB R-08-09, Svensk Kärnbränslehantering AB.

Brunberg A-K, Carlsson T, Blomqvist P, Brydsten L, Strömgren M, 2004 (revised 2007). Forsmark site investigation. Identification of catchments, lake-related drainage parameters and lake habitats. SKB P-04-25, Svensk Kärnbränslehantering AB.

Brydsten L, Strömgren M, 2004. Forsmark site investigation. Measurements of brook gradients and lake thresholds. SKB P-04-141, Svensk Kärnbränslehantering AB.

Brydsten L, Strömgren M, 2010. A coupled regolith-lake development model applied to the Forsmark site. SKB TR-10-56, Svensk Kärnbränslehantering AB.

Canadell J, Jackson R B, Ehleringer B, Mooney H A, Sala O E, Schulze E-D, 1996. Maximum rooting depth of vegetation types at the global scale. Oecologia, 108, pp 583–595.

DHI Software, 2007. MIKE SHE: user manual. DHI Water & Environment, Hørsholm, Denmark.

DHI Software, 2009. MIKE SHE: user manual. DHI Water & Environment, Hørsholm, Denmark.

Ekström P-A, 2011. Pandora – a simulation tool for safety assessments. Technical description and user's guide. SR-Site Biosphere. SKB R-11-01, Svensk Kärnbränslehantering AB.

Follin S, 2008. Bedrock hydrogeology Forsmark. Site descriptive modelling, SDM-Site Forsmark. SKB R-08-95, Svensk Kärnbränslehantering AB.

French H M, 2007. The periglacial environment. 3rd ed. Chichester: John Wiley and Sons.

Graham D N, Butts M B, 2005. Flexible, integrated watershed modelling with MIKE SHE. In: Singh V P, Frevert D K (eds). Watershed models. Boca Raton: CRC Press, pp 245–272.

Gustafsson L-G, Gustafsson A-M, Aneljung M, Sabel U, 2009. Effects on surface hydrology and near-surface hydrogeology of an open repository in Forsmark. Results of modelling with MIKE SHE. SKB R-08-121, Svensk Kärnbränslehantering AB.

Gustafsson L-G, Sassner M, Bosson E, 2008. Numerical modelling of solute transport at Forsmark with MIKE SHE. Site descriptive modelling, SDM-Site Forsmark. SKB R-08-106, Svensk Kärnbränslehantering AB.

Hedenström A, Sohlenius G, 2008. Description of the regolith at Forsmark. Site descriptive modelling, SDM-Site Forsmark. SKB R-08-04, Svensk Kärnbränslehantering AB.

Hedenström A, Sohlenius G, Strömgren M, Brydsten L, Nyman H, 2008. Depth and stratigraphy of regolith at Forsmark. Site descriptive modelling, SDM-Site Forsmark. SKB R-08-07, Svensk Kärnbränslehantering AB.

Johansson P-O, 2008. Description of surface hydrology and near-surface hydrogeology at Forsmark. Site descriptive modelling, SDM-Site Forsmark. SKB R-08-08**,** Svensk Kärnbränslehantering AB.

Johansson P-O, Öhman, J, 2008. Presentation of meteorological, hydrological and hydrogeological monitoring data from Forsmark. Site descriptive modelling, SDM-Site Forsmark. SKB R-08-10, Svensk Kärnbränslehantering AB.

Jones J, Vahlund F, Kautsky U, 2004. Tensit - a novel probabilistic simulation tool for safety assessments. Tests and verifications using biosphere models. SKB TR-04-07, Svensk Kärnbränslehantering AB.

Joyce S, Simpson T, Hartley L, Applegate D, Hoek J, Jackson P, Swan D, Marsic N, Follin S, 2010. Groundwater flow modelling of periods with temperate climate conditions – Forsmark. SKB R-09-20, Svensk Kärnbränslehantering AB.

Kellner E, 2003. Wetlands - different types, their properties and functions. SKB TR-04-08, Svensk Kärnbränslehantering AB.

Kjellström E, Strandberg G, Brandefelt J, Näslund J-O, Smith B, Wohlfarth B, 2009. Climate conditions in Sweden in a 100,000-year time perspective. SKB TR-09-04, Svensk Kärnbränslehantering AB.

Kristensen K J, Jensen S E, 1975. A model for estimating actual evapotranspiration from potential evapotranspiration. Nordic Hydrology, 6, pp 170–188.

Larsson-McCann S, Karlsson A, Nord M, Sjögren J, Johansson L, Ivarsson M, Kindell S, 2002. Meteorological, hydrological and oceanographical information and data for the site investigation program in the communities of Östhammar and Tierp in the northern part of Uppland. SKB TR-02-02, Svensk Kärnbränslehantering AB.

Lindborg T (ed), 2008. Surface system Forsmark. Site descriptive modelling. SDM-Site Forsmark. SKB R-08-11. Svensk Kärnbränslehantering AB.

Lindborg T (ed), 2010. Landscape Forsmark, Data, methodology and results for SR-Site. SKB TR-10-05, Svensk Kärnbränslehantering AB.

Löfgren A (ed), 2010. The terrestrial ecosystems at Forsmark and Laxemar-Simpevarp. SR-Site Biosphere. SKB TR-10-01, Svensk Kärnbränslehantering AB.

SKB, 2006. Climate and climate-related issues for the safety assessment SR-Can. SKB TR-06-23, Svensk Kärnbränslehantering AB.

SKB, 2009. Site description of Laxemar at completion of the site investigation phase. SDM-Site Laxemar. SKB TR-09-01, Svensk Kärnbränslehantering AB.

SKB, 2010a. Biosphere analyses for the safety assessment SR-Site – synthesis and summary of results. SKB TR-10-09, Svensk Kärnbränslehantering AB.

SKB, 2010b. Comparative analysis of safety related site characteristics. SKB TR-10-54, Svensk Kärnbränslehantering AB.

SMHI, 2009. Havsvattenstånd vid svenska kusten. Faktablad nr 41, Sveriges Meteorologiska och Hydrologiska Institut.

Spadavecchia L, Williams M, Bell R, Stoy P C, Huntley B, Van Wijk M T, 2008. Topographic controls on the leaf area index and plant functional type of a tundra ecosystem. Journal of Ecology, 96, pp 1238–1251.

SSM 2008. Strålsäkerhetsmyndighetens föreskrifter och allmänna råd om skydd av människors hälsa och miljön vid slutligt omhändertagande av använt kärnbränsle och kärnavfall. (The Swedish Radiation Safety Authority's Regulations on the Protection of Human Health and the Environment in connection with the Final Management of Spent Nuclear Fuel and Nuclear Waste) (in Swedish). Stockholm: Strålsäkerhetsmyndigheten (Swedish Radiation Safety Authority). (SSMFS 2008:37)

Summerfield M A, 1991. Global geomorphology: an introduction to the study of landforms. Singapore: Longman Singapore Publishers, pp 293–294.

Werner K, Bosson E, Berglund S, 2005. Description of climate, surface hydrology, and near-surface hydrogeology. Simpevarp 1.2. SKB R-05-04, Svensk Kärnbränslehantering AB.

Werner K, Johansson P-O, 2003. Forsmark site investigation. Slug tests in groundwater monitoring wells in soil. SKB P-03-65, Svensk Kärnbränslehantering AB.

Appendix 1

Identification of through taliks

The general prerequisites for maintaining an open talik beneath a lake are described in Section 3.5.2. However, an exact criterion was developed for each simulation case with 240 m or 100 m depth of permafrost, to be applied to the overland water at the surface generated in the 10000AD_10000QD model.

For the case with a permafrost thickness of 240 m the following criteria were applied.

- A minimum overland depth of 0.01 m.
- A minimum number of 8 cells in a cluster.
- An average lake radius of 240 m corresponding to a diameter of 480 m or 6 cells where the average overland depth is greater than 0.5 m.
- An average lake radius of 144 m corresponding to a diameter of 288 m or 3.6 cells where the average overland depth is greater than 4 m.
- Also the shape of the potential talik is considered. If, for example, 2×4 cells are aligned, then it will not qualify as a talik, although the number of cells is 8. The reason is that if the minimum radius of the talik is too small the talik will not be able to stay open. An elongated talik will only be included if it is large enough and has a minimum radius of 140 m.
- Sometimes a cluster of cells does not qualify as a talik, i.e. the average overland depth is smaller than 0.5 m. The border of cells has then sometimes been excluded and the core cells of the lake will then qualify as a talik.
- Streams are not defined as taliks.
- The sea is considered to be a through talik.

For the case with a permafrost thickness of 100 m the following criteria were applied.

- A minimum overland depth of 0.01 m.
- An average lake radius of 100 m corresponding to a diameter of 200 m or 2.5 cells where the average overland depth is greater than 0.5 m.
- An average lake radius of 60 m corresponding to a diameter of 180 m or 1.5 cells where the average overland depth is greater than 4 m.
- Sometimes a cluster of cells does not qualify as a talik, i.e. the average overland depth is smaller than 0.5 m. The border of cells has then sometimes been excluded and the core cells of the lake will then qualify as a talik.
- Streams are not defined as taliks.
- The sea is considered to be a through talik.

The inlet canal does not qualify as a talik in any of the cases above. The inlet canal is not defined as a talik although it is approximately 12 m metres deep. The width of the inlet canal is too small and therefore the canal will freeze according to the selection criteria applied in this study.

Describing permafrost processes in MIKE SHE

The MIKE SHE parameters identified to be of particular importance when simulating the processes associated with permafrost conditions are listed and described in Table A1-1 below.

Parameters describing snow melt, snow accumulation and evapotranspiration processes are generally not manually altered when describing freezing and thawing processes throughout the year. One exception is the initial settings of the parameters describing melting of snow in response to the heat content of rain as well as snow sublimation from dry snow. These parameters have to be changed manually in order to describe the initial conditions of each period of the year.

The leaf area index (LAI) and the potential evapotranspiration (PET) are time series input to the model, and describe time varying conditions adapted to a periglacial climate. The overland-ground-water leakage (LC-OL) coefficient, the Manning number (M), the saturated hydraulic conductivity (Ks), the horizontal and vertical hydraulic conductivities (K) and the drain time constant (TC) are all parameters that are changed manually step-by-step between the simulations periods making up the one-year cycle.

Table A1-1. Modelled periglacial processes and identified key parameters in the permafrost cases.

Process	Process in MIKE SHE	MIKE SHE parameter
Snow melt	**Thermal melting of snow in response to the heat content of rain** The heat released from liquid rain as it cools is an important contributor to snow melt. Energy melting occurs only if the air temperature is above the threshold melting temperature. The temperature of the rain is assumed to be the same as the air temperature. MIKE SHE includes an energy melting coefficient, which is a constant value for the entire model and describes the relationship between the energy in the rain and the energy required to turn snow into water.	Energy melting coefficient
Evapotranspiration	**Snow sublimation from dry snow** The ET (evapotranspiration) module will remove water from snow storage before any other ET water is removed. ET is removed first from wet snow as evaporation because the energy requirements for evaporation are lower than sublimation. The ET is removed from wet snow at the full rate, assuming that wet snow can be treated in the same way as ponded water. If there is no wet snow (either because it is too cold or that all the wet snow has been evaporated), then ET will be removed from dry snow as sublimation. However, sublimation has a higher energy requirement than evaporation, so MIKE SHE includes a user defined reduction factor for sublimation. The sublimation factor simply reduces the available ET rate from the snow.	Snow sublimation factor
	Interception ET from interception is controlled by the leaf area index (LAI). No ET from intercepted water occurs when LAI is zero.	Leaf area index (LAI)
	Transpiration The transpiration from the vegetation depends on the density of the crop green material, the leaf area index (LAI), the soil moisture content in the root zone and the root density.	Leaf area index (LAI), Kc, root depth
	Ponded water ET from ponded water is active although T<0, if the evaporative demand remains according to PET.	Potential evapotranspiration (PET)
	Upper soil ET from soil is inactive as long as there is snow. Without snow cover, ET from the soil is active although T<0, if the evaporative demand remains according to PET.	Potential evapotranspiration (PET)

Process	Process in MIKE SHE	MIKE SHE parameter
Overland flow	**Infiltration at ground surface** When the net rainfall rate exceeds the infiltration capacity of the soil, water is ponded on the ground surface as overland water. The overland-groundwater leakage coefficient reduces the infiltration rate at the ground surface. It works in both directions. That is, it reduces both the infiltration rate and the seepage outflow rate across the ground surface. By reducing the leakage coefficient, LC, the overland water cannot flow on the surface and is accumulating on the ground. The reduction of the LC imitates the accumulation of ice on the ground surface. Overland flow occurs when T>0 and continues although T<0. But this can be controlled by the given Mannings M, see below. It is assumed that overland water freezes in a two week period.	Overland-groundwater leakage coefficient (LC-OL)
	Surface runoff When overland water is ponded on the ground surface the water is available as surface runoff, to be routed downhill towards the river system. The exact route and quantity is determined by the topography and flow resistance, as well as the losses due to evaporation and infiltration along the flow path. By reducing the value of Mannings M the surface water runoff will be reduced or stopped, which is the method of simulating frozen surface water.. Overland flow occurs when T>0 and continues although T<0. It is assumed that overland water freezes in a two week period.	Manning number (M)
Unsaturated flow	**Infiltration to the soil** Infiltration into the unsaturated zone (UZ) is controlled by the LC-OL coefficient. By reducing the leakage coefficient, a frozen lid on the surface is modelled, which also affects the infiltration to the UZ. The water content remains at field capacity when the transpiration is switched off.	Overland-groundwater leakage coefficient (LC-OL)
	Capillary transport The water content, the soil moisture retention curve and the hydraulic conductivity function (where Ks is a parameter) govern the capillary transport in the unsaturated zone (UZ). Equilibrium exits at field capacity, but if the water content becomes less there will be a transport towards lower pressure heads. This transport is ruled by the head gradients (decided by retention curve and water content) and the hydraulic conductivity at the current water content. The conductivity will drop with a reduced water content. The capillary transport in the UZ can be controlled and repressed by reducing Ks. However Ks should not be reduced to zero due to probable numerical stability problems. It is assumed that the soil drains to field capacity before it freezes.	Saturated hydraulic conductivity (Ks)
Saturated flow	**Saturated flow in the active layer** For a given gradient, flow is determined by the hydraulic conductivity. By lowering the horizontal and vertical conductivity, flow resistance is added. During the freeze periods the conductivity is gradually reduced. During ground frost the conductivity is set to a very low value to achieve frozen no-flow conditions (with exception of the taliks where conditions in the saturated zone always are kept unfrozen). When the thaw period commences the conductivity is gradually increased to allow more flow.	Horizontal and vertical hydraulic conductivity (K)
	Saturated flow in the permafrost Flow is active according to the given hydraulic conductivity. The permafrost deposits are kept frozen by a constant very low hydraulic conductivity (except in through taliks where the conductivity is kept unchanged).	Horizontal and vertical hydraulic conductivity (K)
	Saturated flow in the taliks Through taliks are present both in the active layer and in the permafrost. The conditions in the taliks are always unfrozen and consequently the conductivities are never changed from the 10000AD_10000QD model.	Horizontal and vertical hydraulic conductivity (K)
	Saturated flow in the unfrozen layers below the permafrost The unfrozen layers in the permafrost are never frozen and the conductivities are kept unchanged from the 10000AD_10000QD model,	Horizontal and vertical hydraulic conductivity (K)
	Groundwater drainage The drain time constant is a factor used to regulate how quickly the water in the saturated zone above the drain level flows, when using the drain function to simulate the higher conductivities in the uppermost soil layer. By changing it the same way as the conductivity, the drainage water can freeze and thaw. No drain is active in the taliks.	Drain time constant (TC)

Water balances for different time periods

The following four figures, Figures A2-1 to A2-4, illustrate the water balances for the regional model simulation cases 5000AD_2000QD, 5000AD_5000AD, 10000AD_2000QD and 10000AD_10000QD for a normal temperate climate. The water balances are calculated for the area constituting land at 2000 AD. The water balances for the model cases with different QD models and shoreline positions are described in Section 5.3.1.

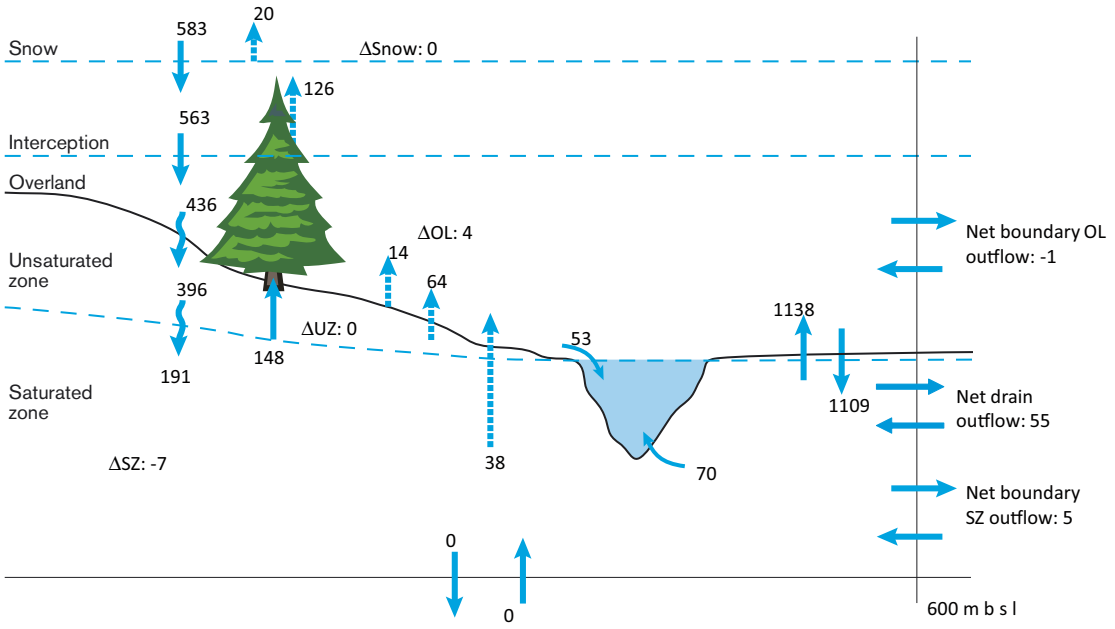

Figure A2-1. *Water balance from the 5000AD_2000QD regional model case for the area constituting land at 2000 AD.*

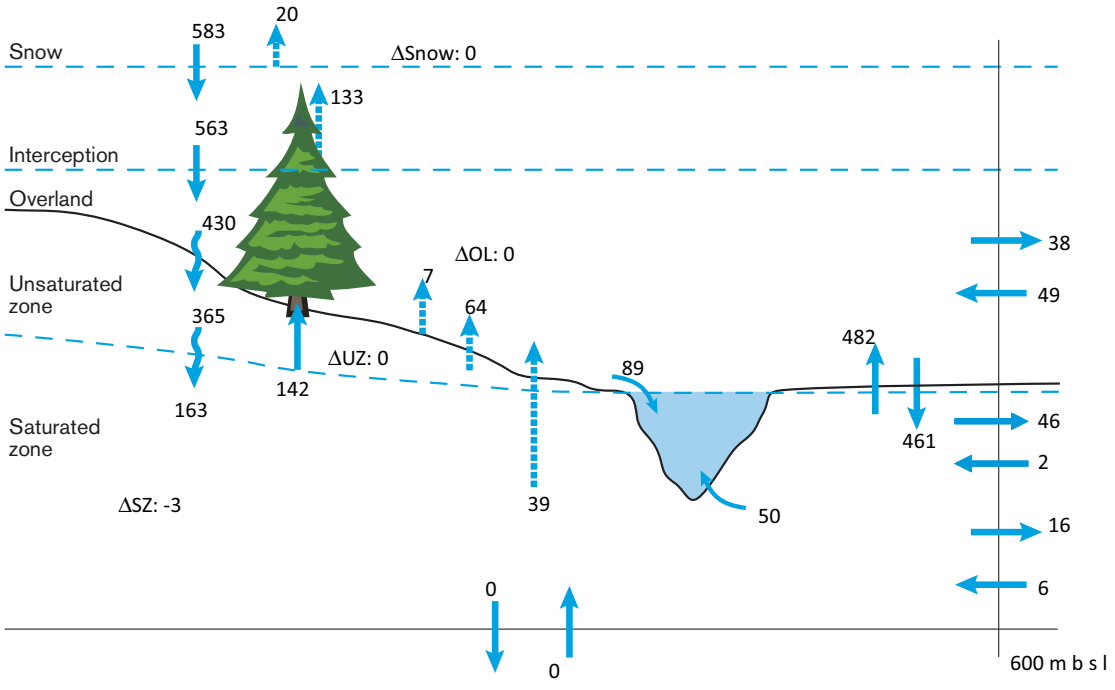

Figure A2-2. *Water balance from the 5000AD_5000QD regional model case for the area constituting land at 2000 AD.*

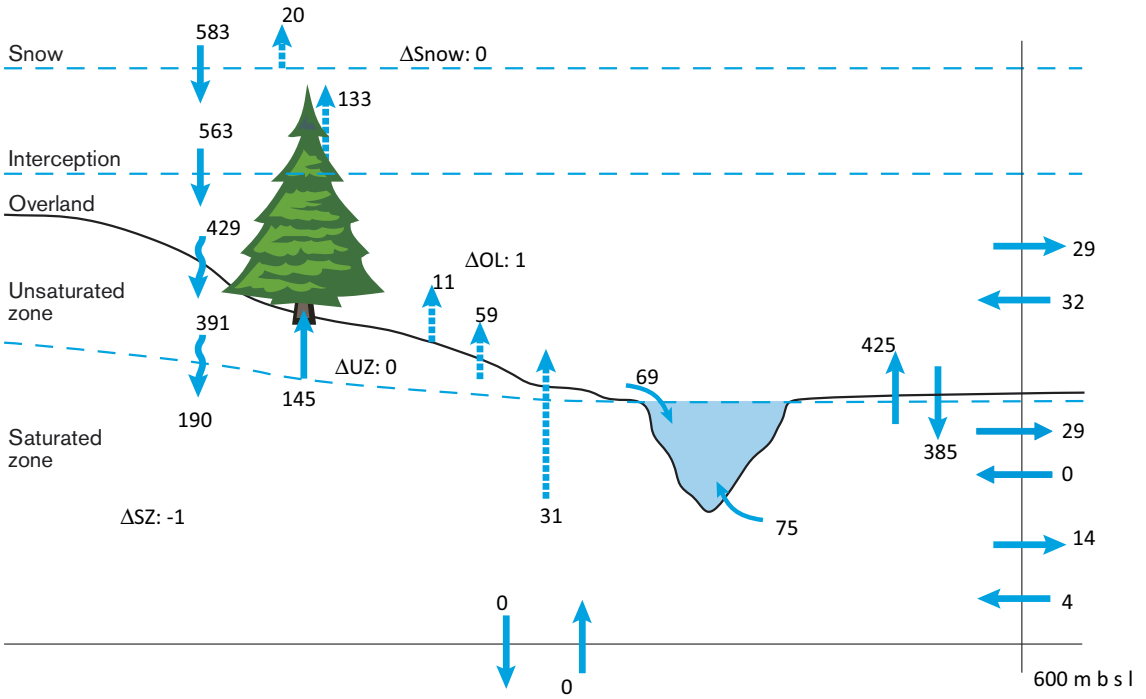

Figure A2-3. *Water balance from the 10000AD_2000QD regional model case for the area constituting land at 2000 AD.*

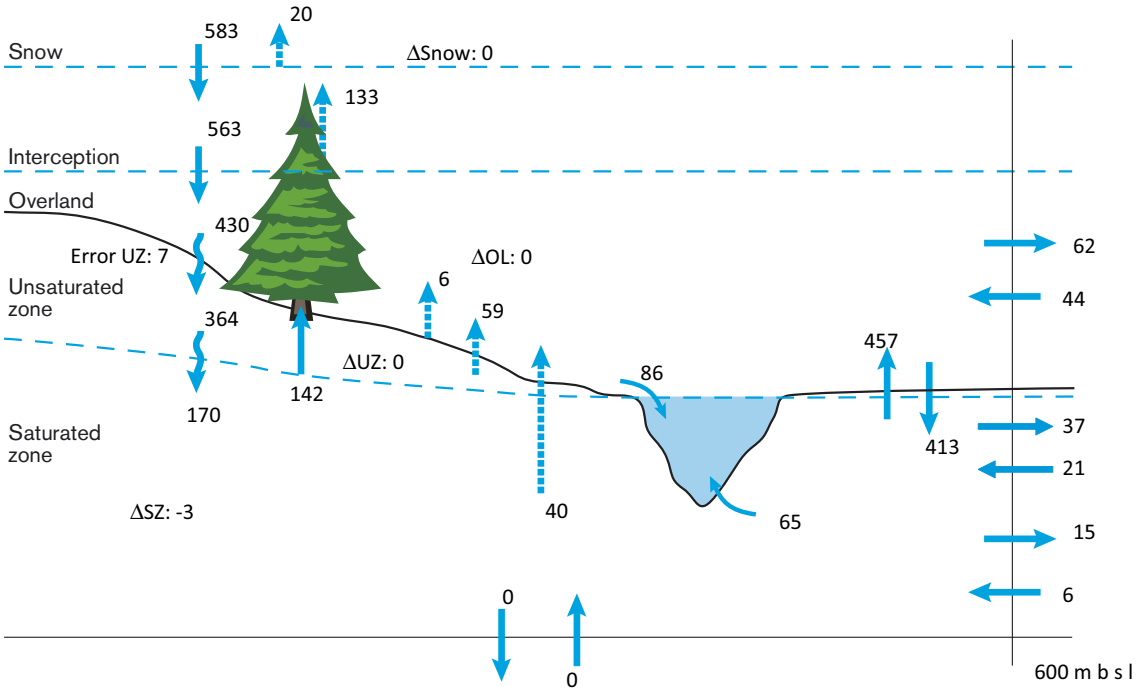

Figure A2-4. *Water balance from the 10000AD_10000QD regional model case for the area constituting land at 2000 AD.*

The following four figures, Figures A2-5 to A2-8, illustrate the water balances for the simulation cases 5000AD_2000QD, 5000AD_5000AD, 10000AD_2000QD and 10000AD_10000QD. The water balances are calculated for the area constituting land at each point of time considered, i.e. 5000 AD and 10,000 AD. The water balances for the model cases with different QD models and shorelines are described in Section 5.3.1.

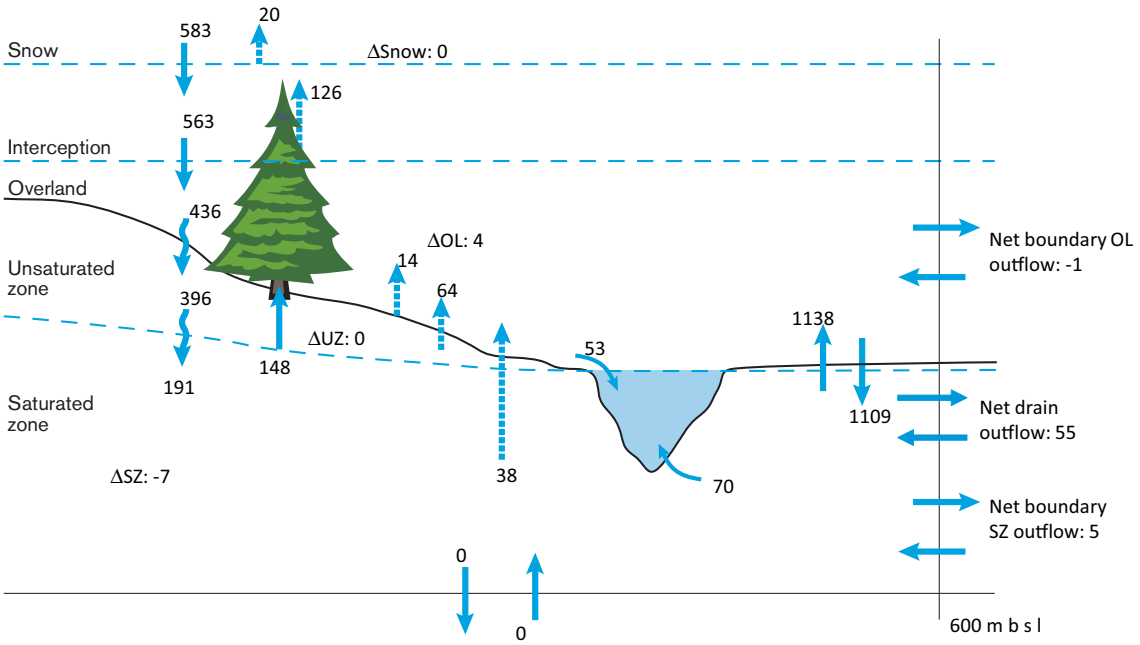

Figure A2-5. *Water balance from the 5000AD_2000QD regional model case for the area constituting land at 5000 AD.*

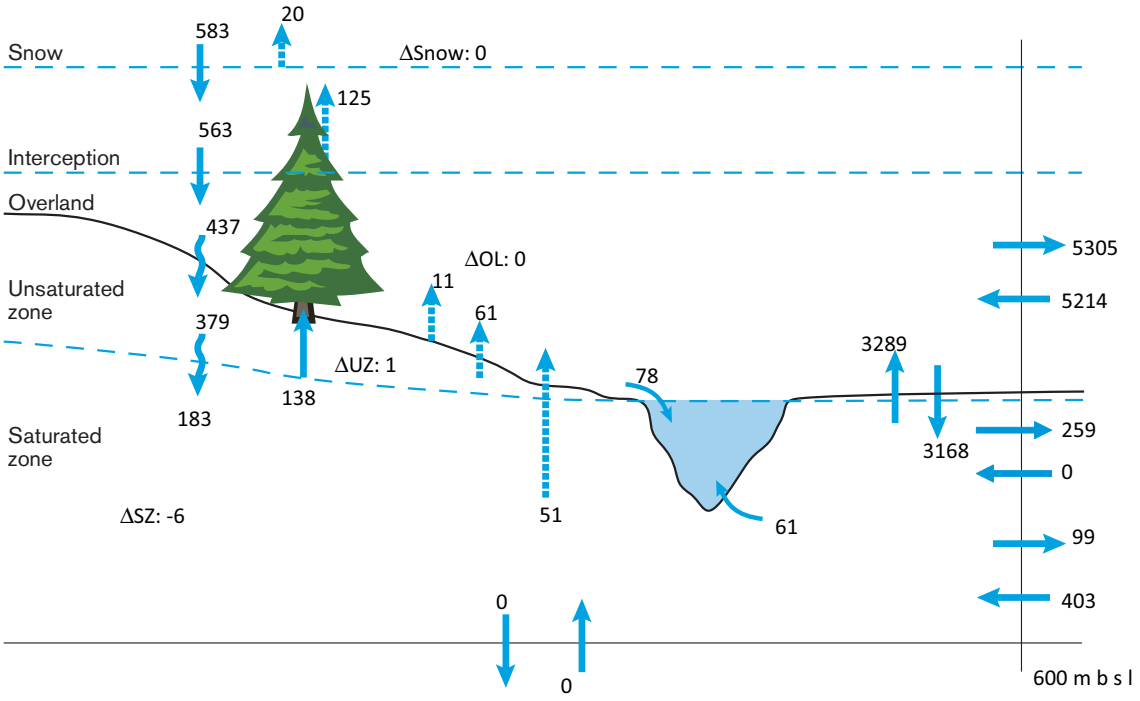

Figure A2-6. *Water balance from the 5000AD_5000QD regional model case for the area constituting land at 5000 AD.*

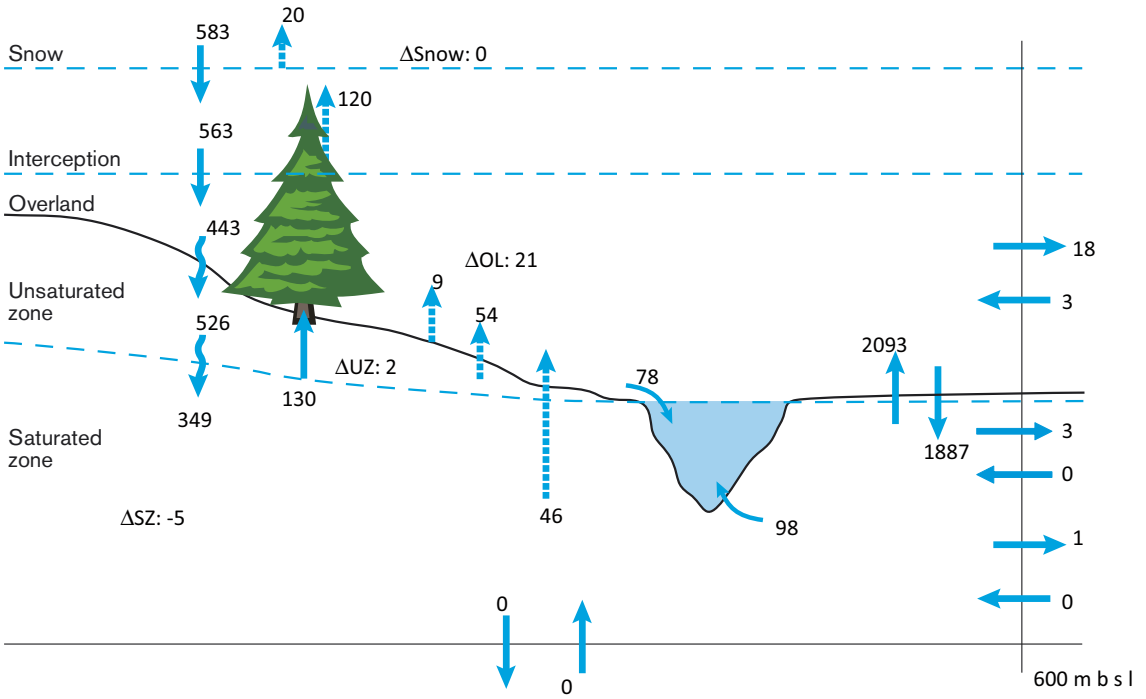

Figure A2-7. *Water balance from the 10000AD_2000QD regional model case for the area constituting land at 10,000 AD.*

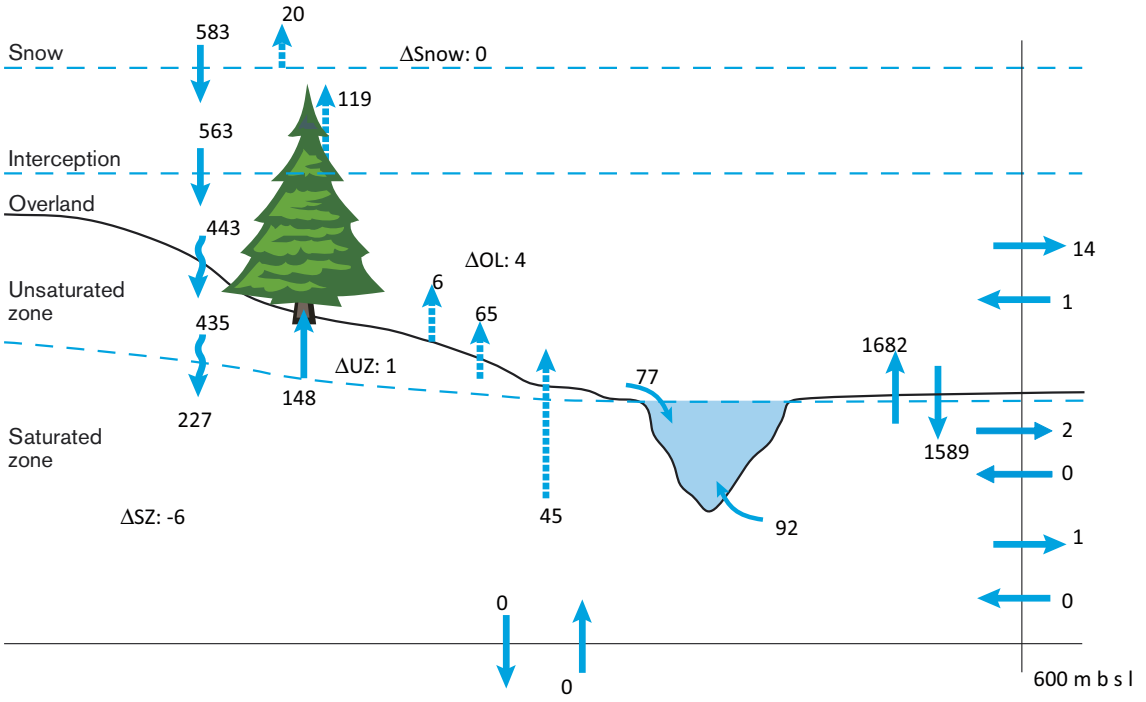

Figure A2-8. *Water balance from the 10000AD_10000QD regional model case for the area constituting land at 10,000 AD.*

Appendix 3

Water balances, recharge and discharge areas and vertical groundwater flow under periglacial conditions

Appendix 3 includes additional results from the simulations with permafrost under periglacial conditions presented in Section 6.2.1 and 6.2.2. Figures A3-1 to A3-22 show results from the case with 240 m of permafrost, whereas Figures A3-23 to A3-44 show results from the case with 100 m of permafrost.

Figures A3-1 to A3-7 and A3-23 to A3-29 illustrate water balance results where the yearly water balances have been divided into partial balances for each simulation period, i.e. the freeze 1, freeze 2, frozen, thaw 1, thaw 2, thaw 3 and active periods. The figures illustrate the water balances for the area constituting land at 10,000AD.

Figures A3-8 to A3-11 and A3-30 to A3-33 illustrate the recharge and discharge areas within and below the permafrost. Figures A3-12 to A3-22 and A3-34 to A3-44 illustrate the mean vertical groundwater flow during the frozen, thaw3 and active periods at different depths above, within or below the permafrost.

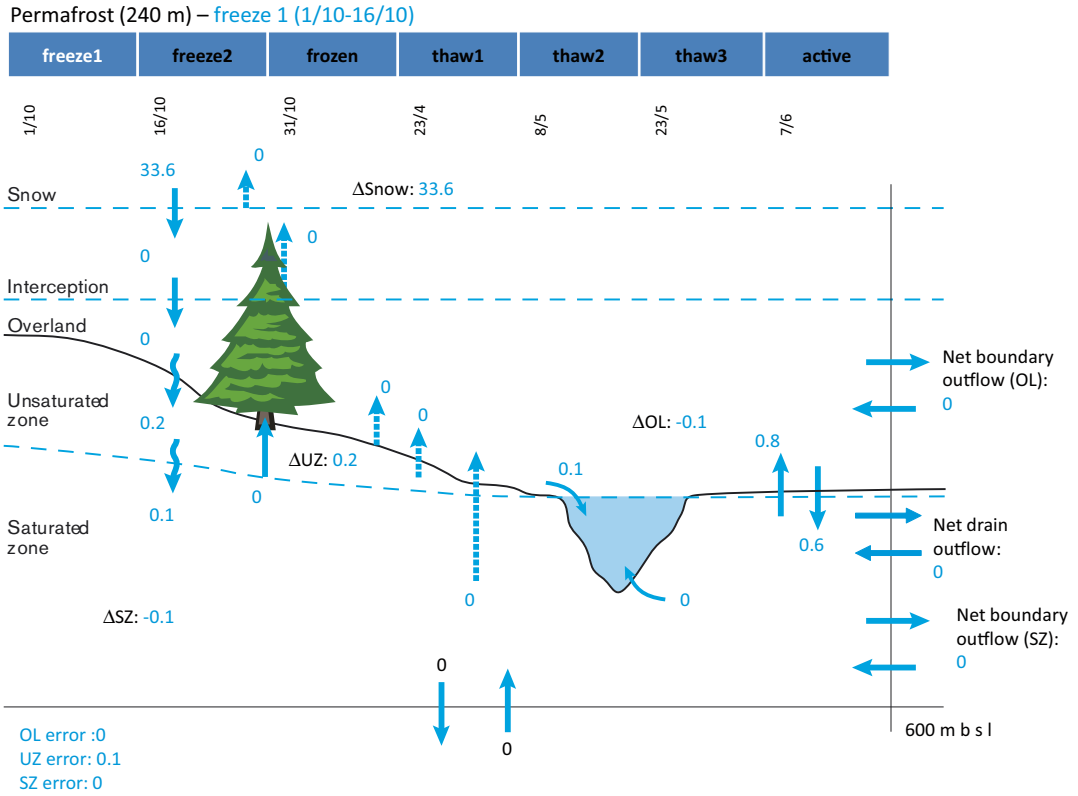

Figure A3-1. *Calculated water balance for the period freeze 1 from the 10000AD_10000QD model for permafrost conditions with a permafrost thickness of 240 m for the area constituting land at 10,000 AD.*

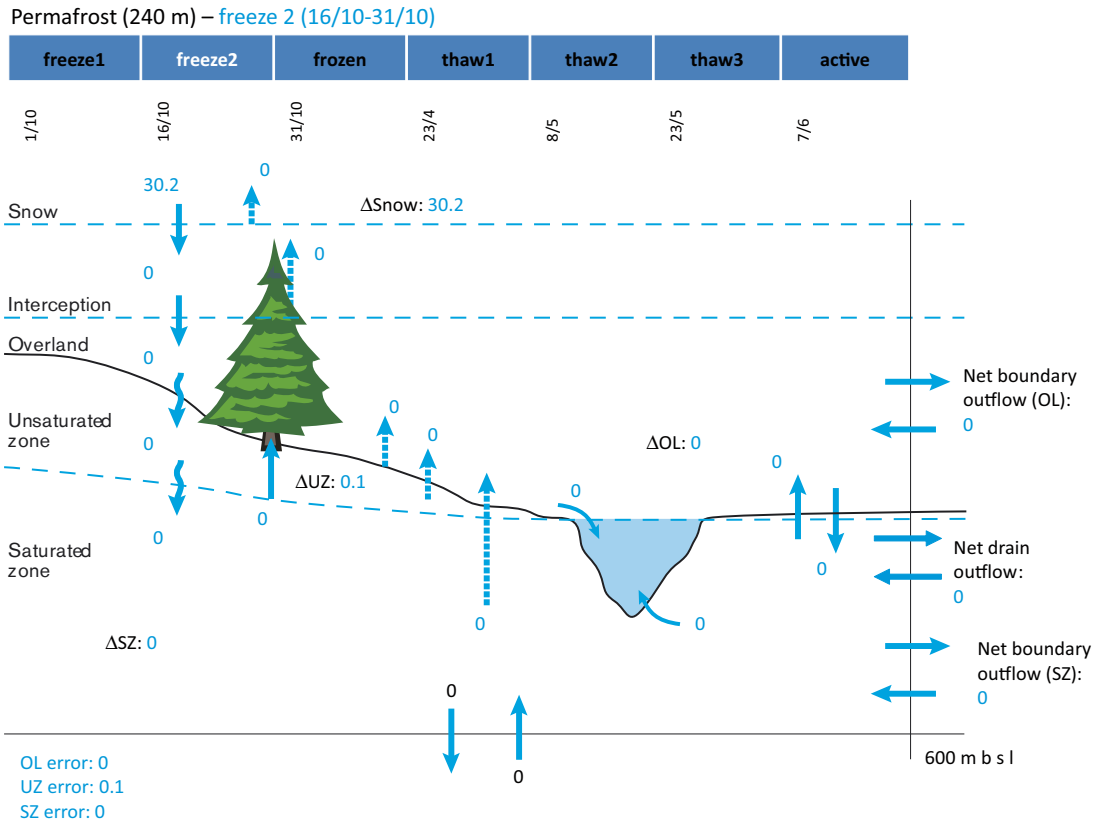

Figure A3-2. *Calculated water balance for the period freeze 2 from the 10000AD_10000QD model for permafrost conditions, with a permafrost thickness of 240 m for the area constituting land at 10,000 AD.*

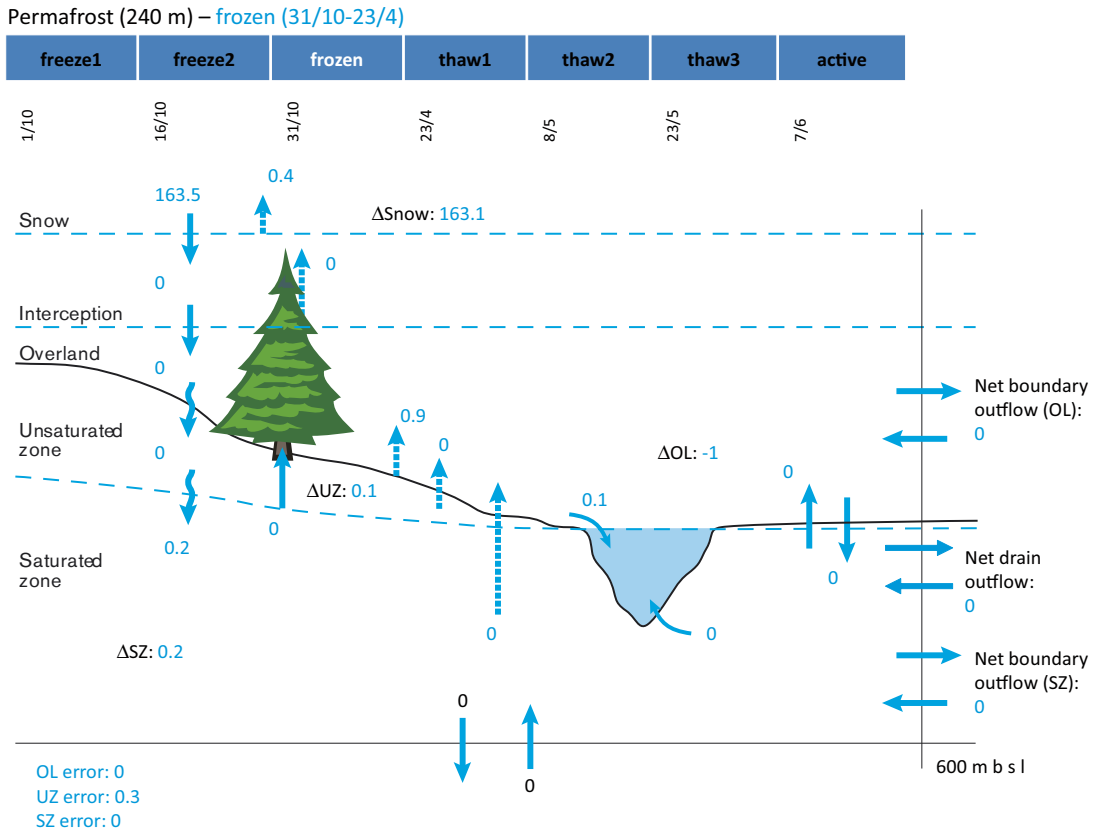

Figure A3-3. *Calculated water balance for the frozen period from the 10000AD_10000QD model for permafrost conditions, with a permafrost thickness of 240 m for the area constituting land at 10,000 AD.*

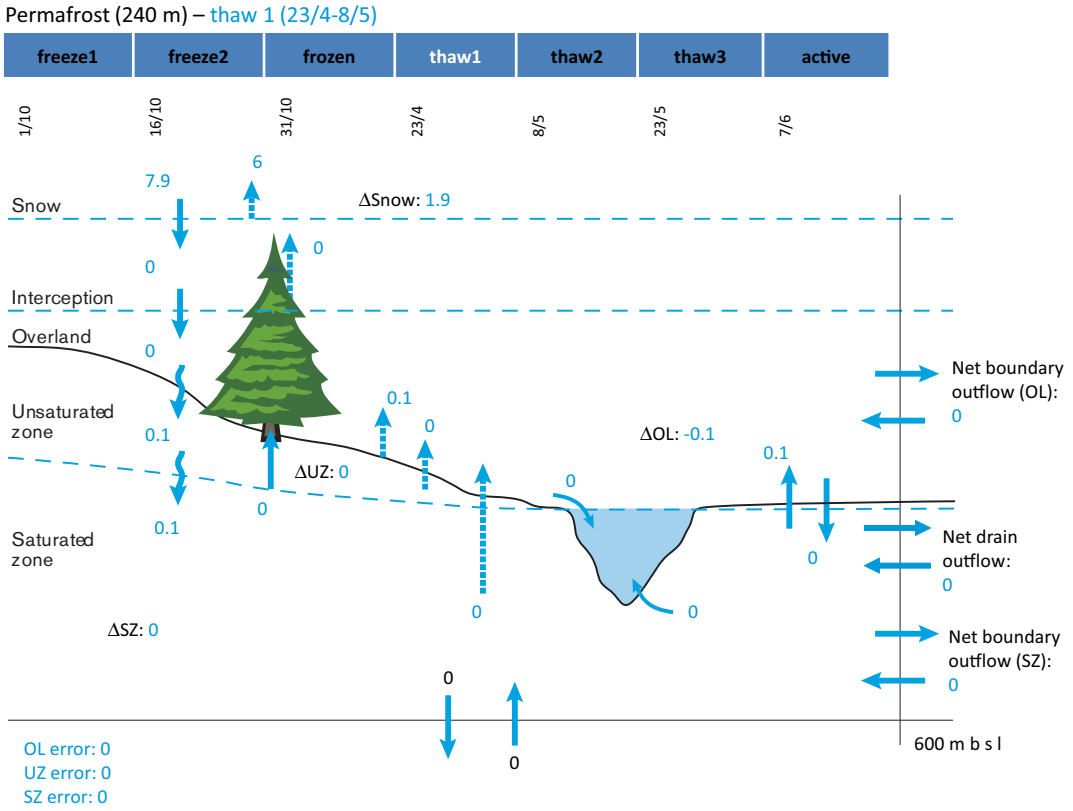

Figure A3-4. *Calculated water balance for the period thaw 1 from the 10000AD_10000QD model for permafrost conditions, with a permafrost thickness of 240 m for the area constituting land at 10,000 AD.*

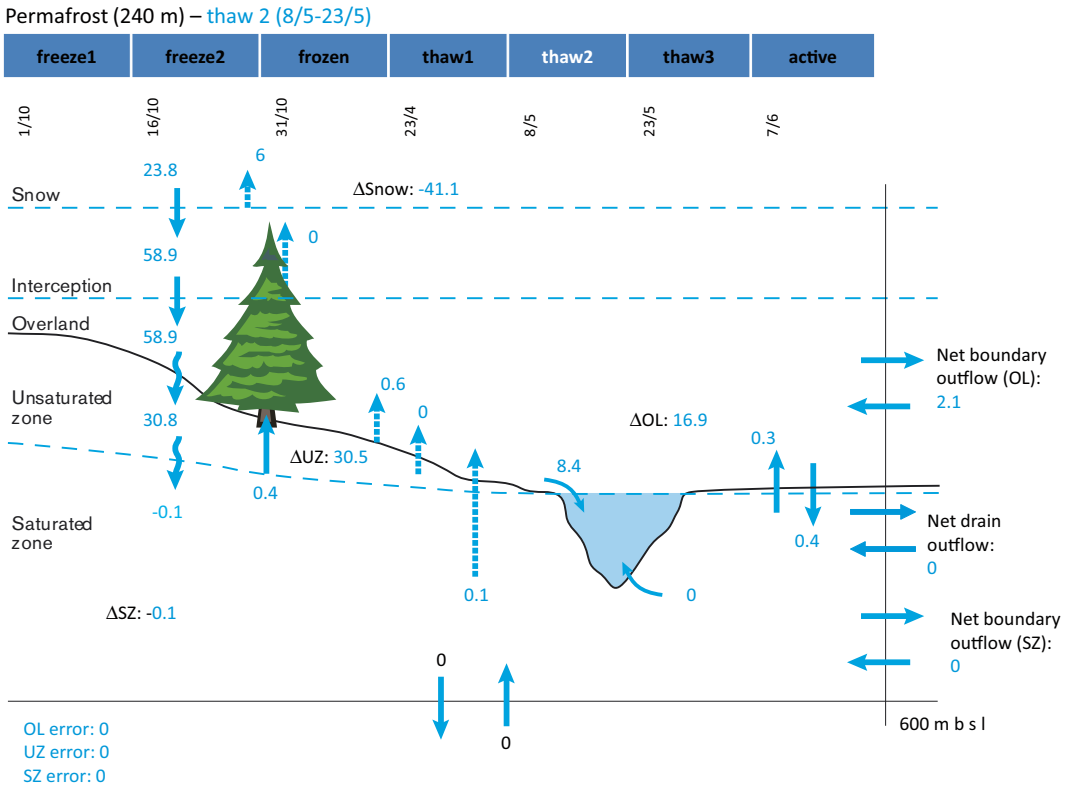

Figure A3-5. *Calculated water balance for the period thaw 2 from the 10000AD_10000QD model for permafrost conditions, with a permafrost thickness of 240 m for the area constituting land at 10,000AD.*

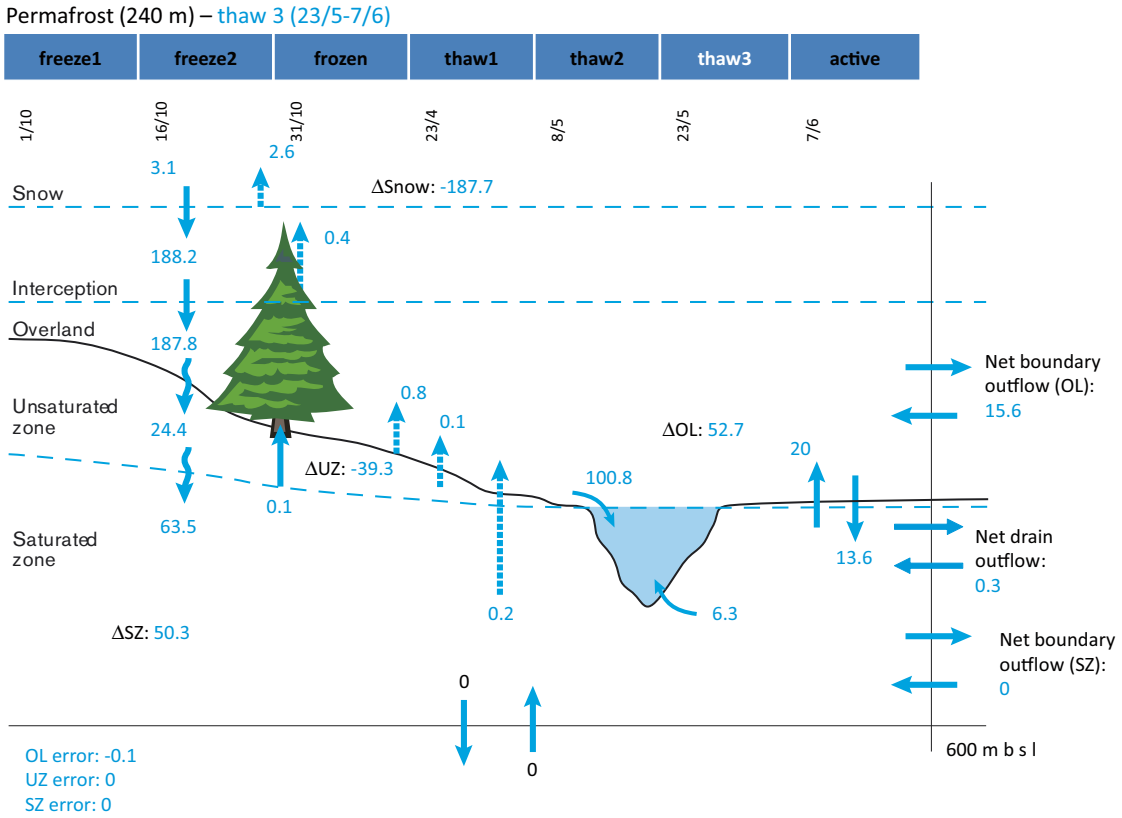

Figure A3-6. *Calculated water balance for the period thaw 3 from the 10000AD_10000QD model for permafrost conditions, with a permafrost thickness of 240 m for the area constituting land at 10,000 AD.*

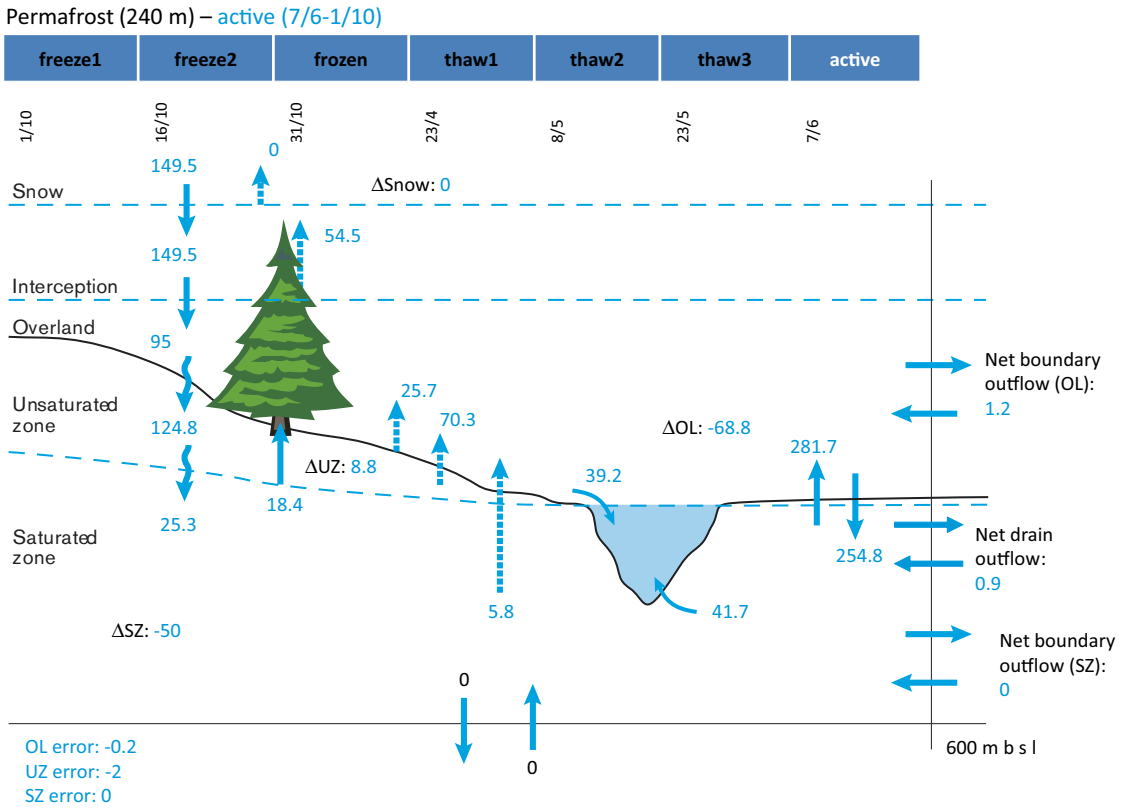

Figure A3-7. *Calculated water balance for the active period from the 10000AD_10000QD model for permafrost conditions with a permafrost thickness of 240 m for the area constituting land at 10,000 AD.*

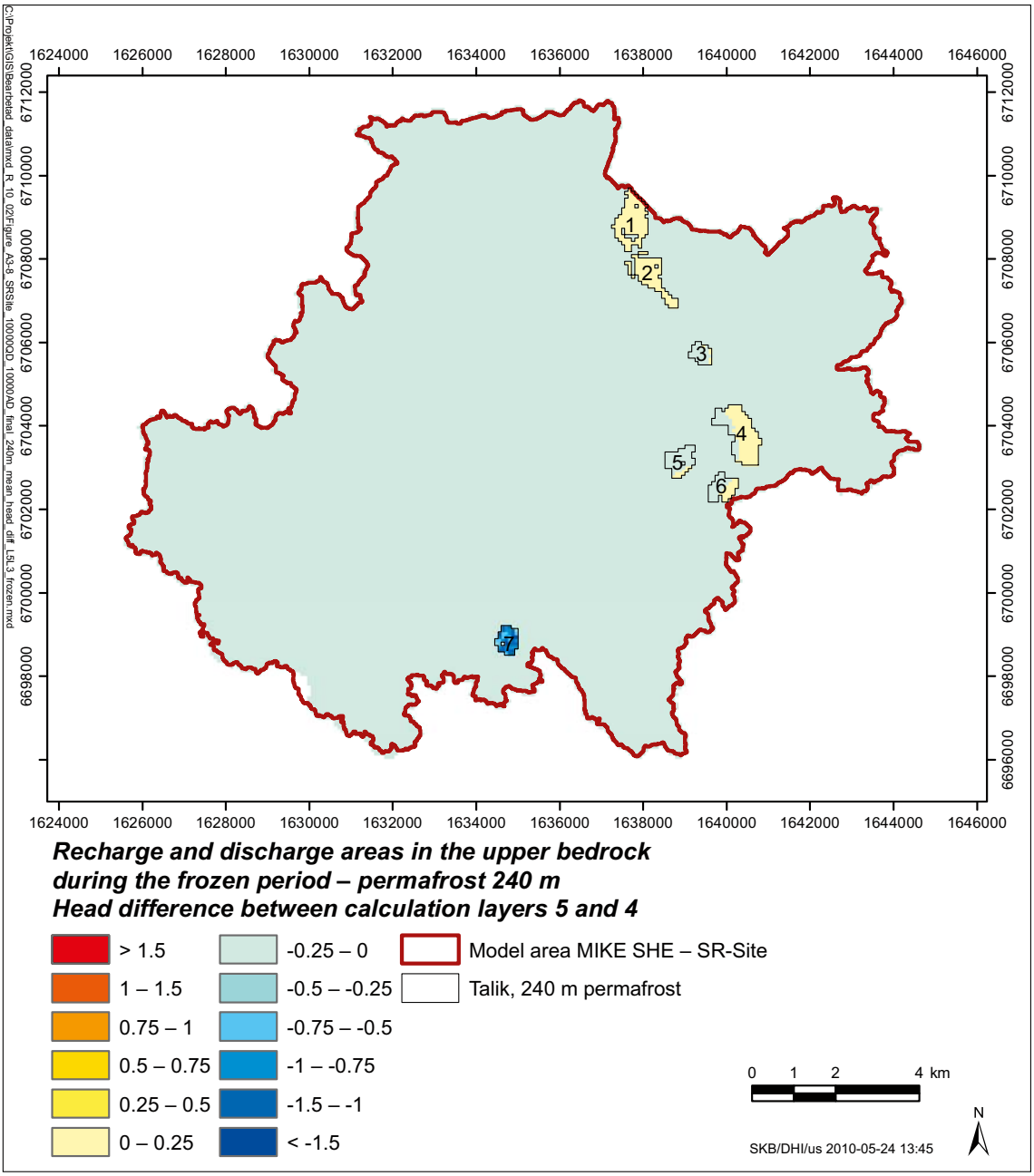

Figure A3-8. *The recharge (blue scale) and discharge (red scale) areas within the permafrost formation in the upper bedrock from the 10000AD_10000QD model for permafrost conditions with a permafrost thickness of 240 m, calculated as the mean head difference between calculation layers 5 and 4 during the frozen period.*

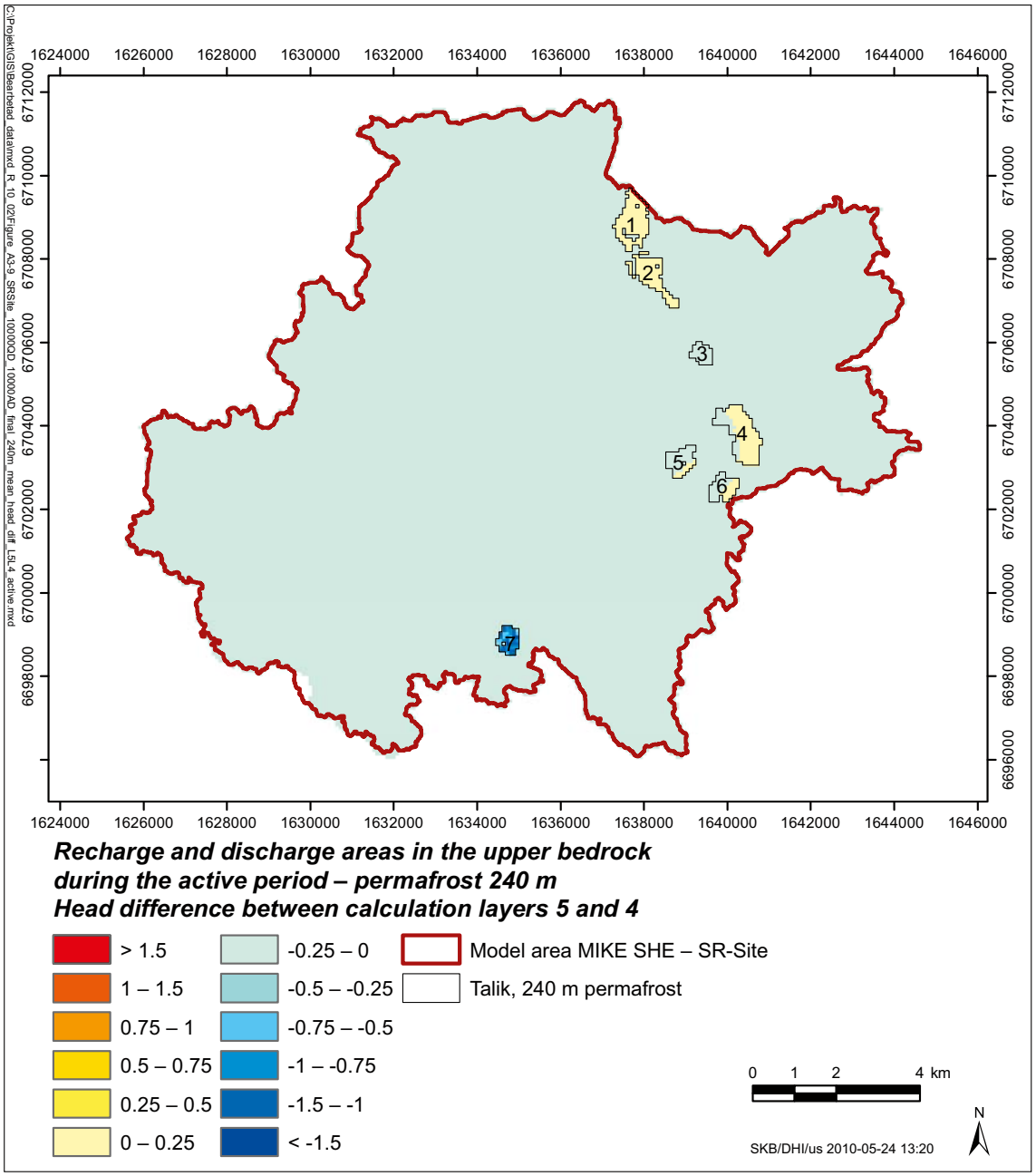

Figure A3-9. *The recharge (blue scale) and discharge (red scale) areas within the permafrost formation in the upper bedrock from the 10000AD_10000QD model for permafrost conditions with a permafrost thickness of 240 m, calculated as the mean head difference between calculation layers 5 and 4 during the active period.*

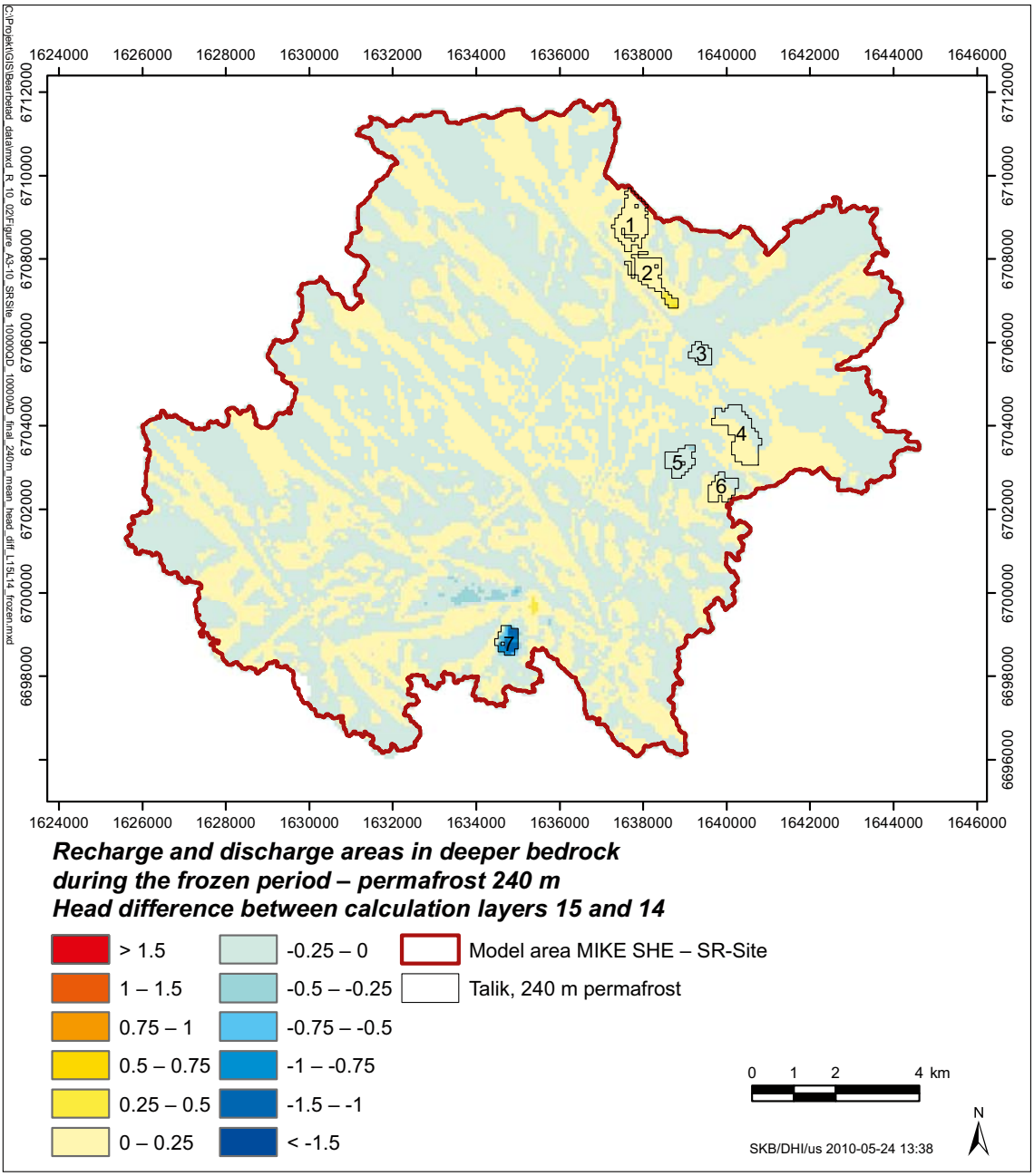

Figure A3-10. *The recharge (blue scale) and discharge(red scale) areas below the permafrost formation in the deeper bedrock from the 10000AD_10000QD model for permafrost conditions with a permafrost thickness of 240 m, calculated as the mean head difference between calculation layers 15 and 14 during the frozen period.*

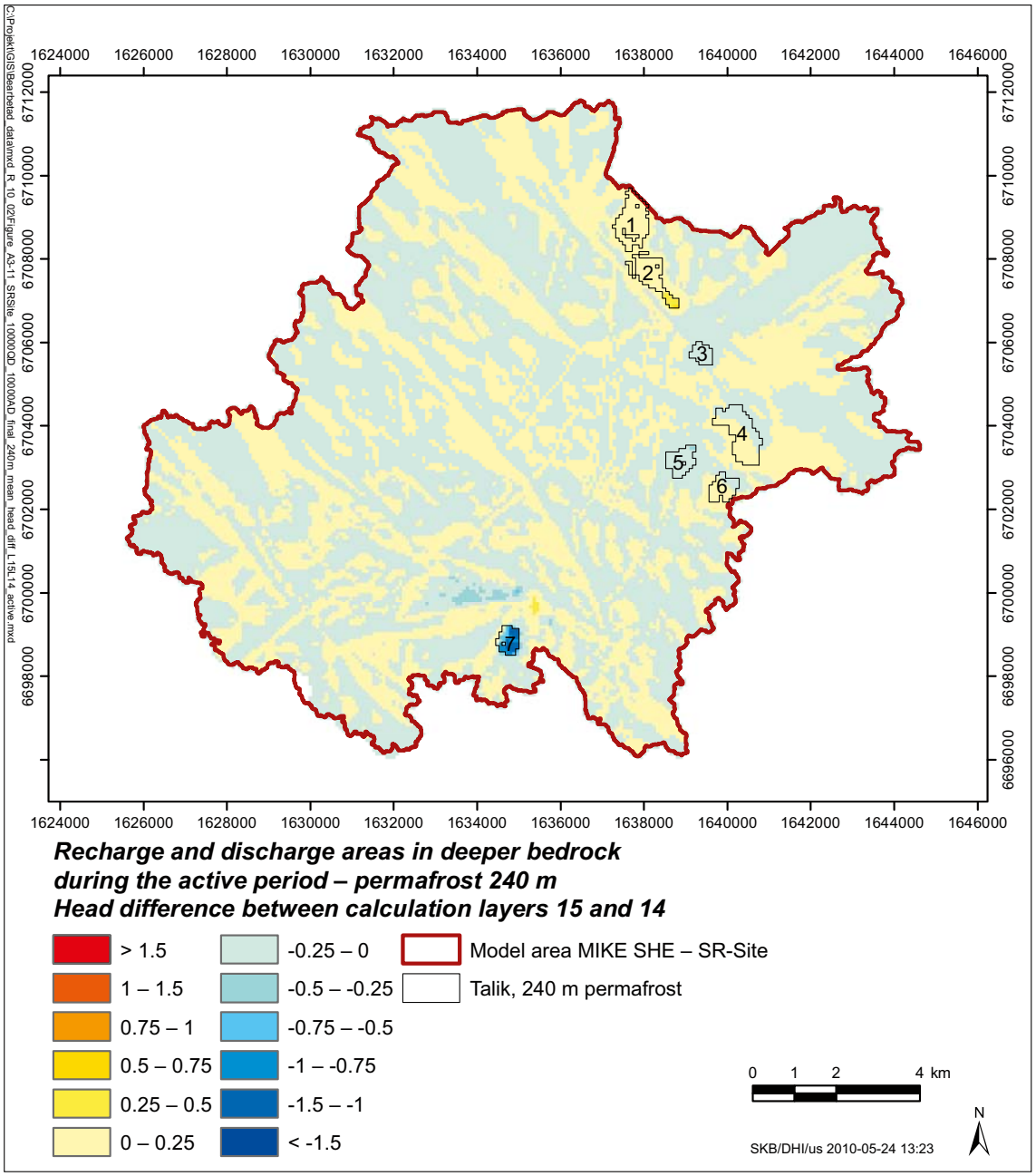

Figure A3-11. *The recharge (blue scale) and discharge(red scale) areas below the permafrost formation in the deeper bedrock from the 10000AD_10000QD model for permafrost conditions with a permafrost thickness of 240 m, calculated as the mean head difference between calculation layers 15 and 14 during the active period.*

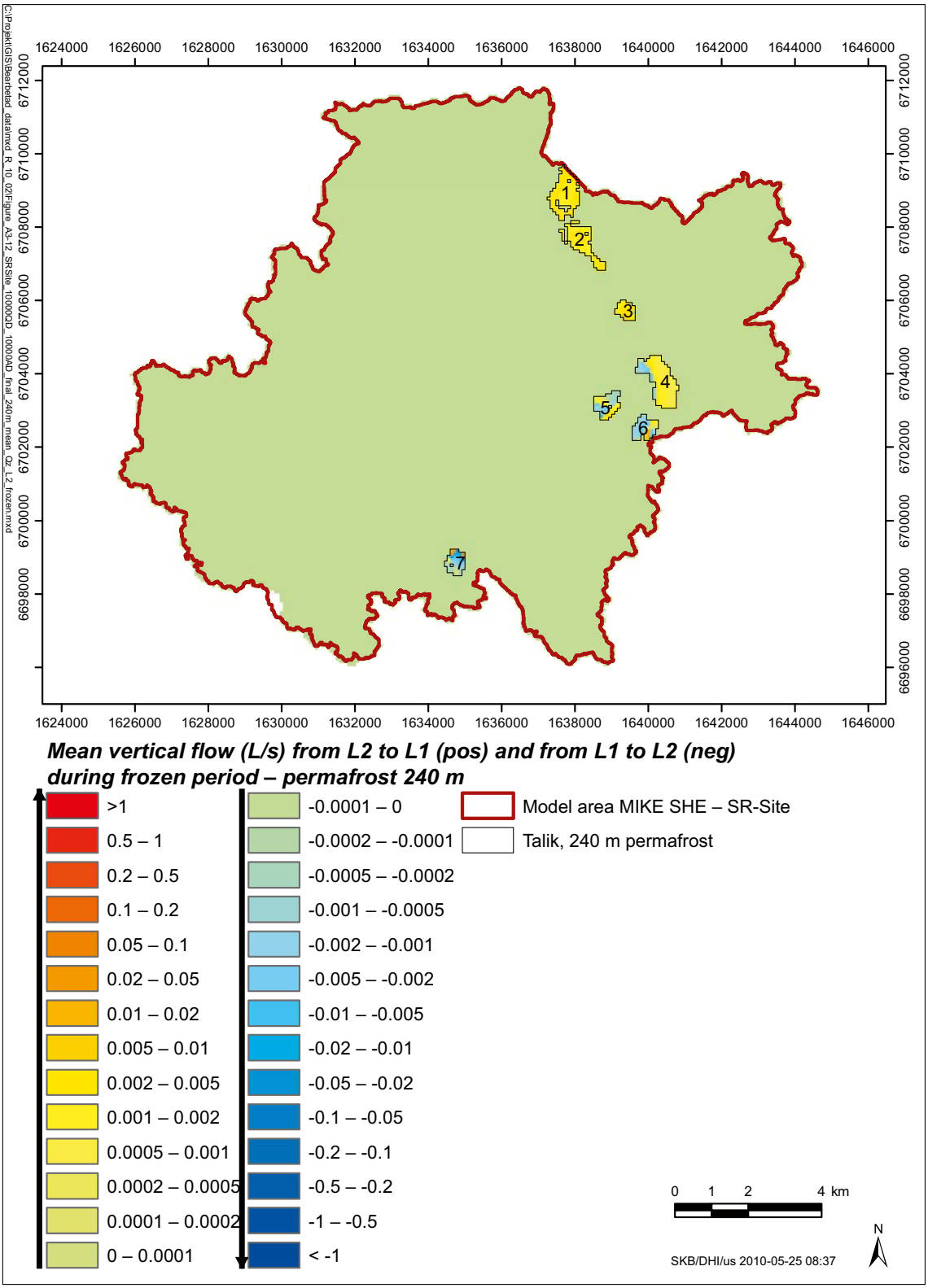

Figure A3-12. *Calculated mean vertical flow (units in l/s) between the active layer and the top permafrost layer during the frozen period with a permafrost thickness of 240 m.*

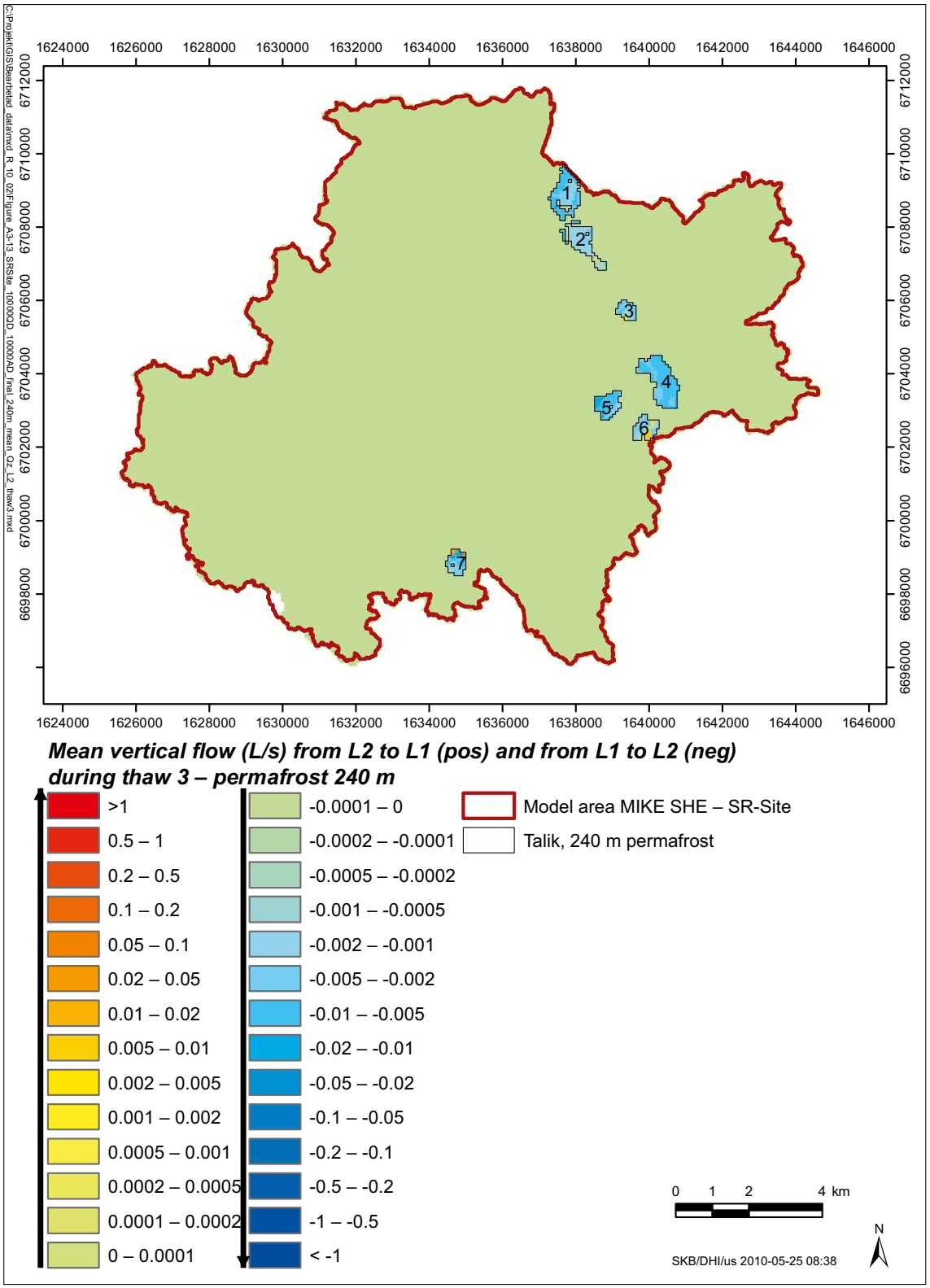

Figure A3-13. *Calculated mean vertical flow (units in l/s) between the active layer and the top permafrost layer during the thaw 3 period with a permafrost thickness of 240 m.*

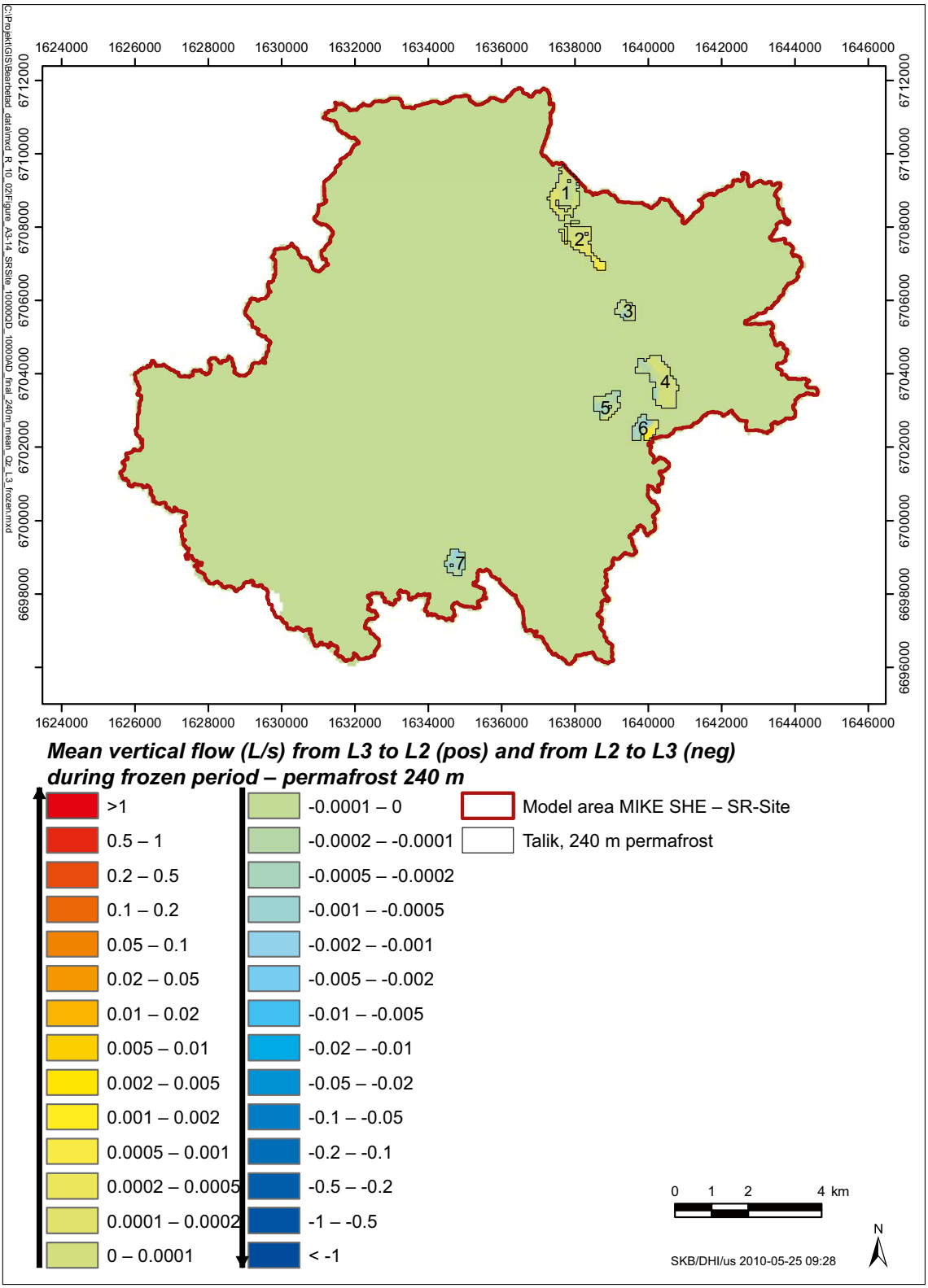

Figure A3-14. *Calculated mean vertical flow (units in l/s) between the two upper permafrost layers during the frozen period with a permafrost thickness of 240 m.*

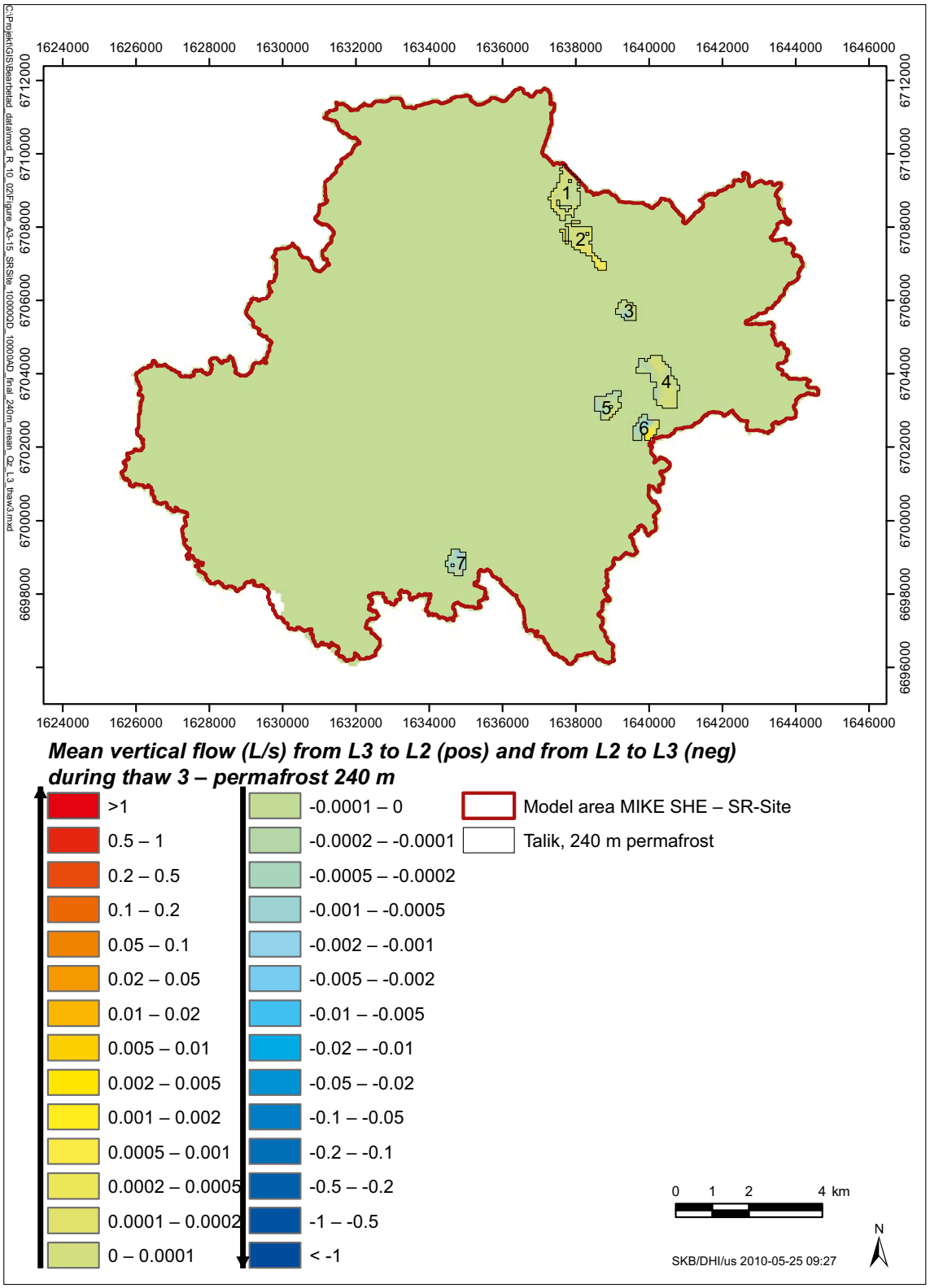

Figure A3-15. *Calculated mean vertical flow (units in l/s) between the two upper permafrost layers during the thaw 3 period with a permafrost thickness of 240 m.*

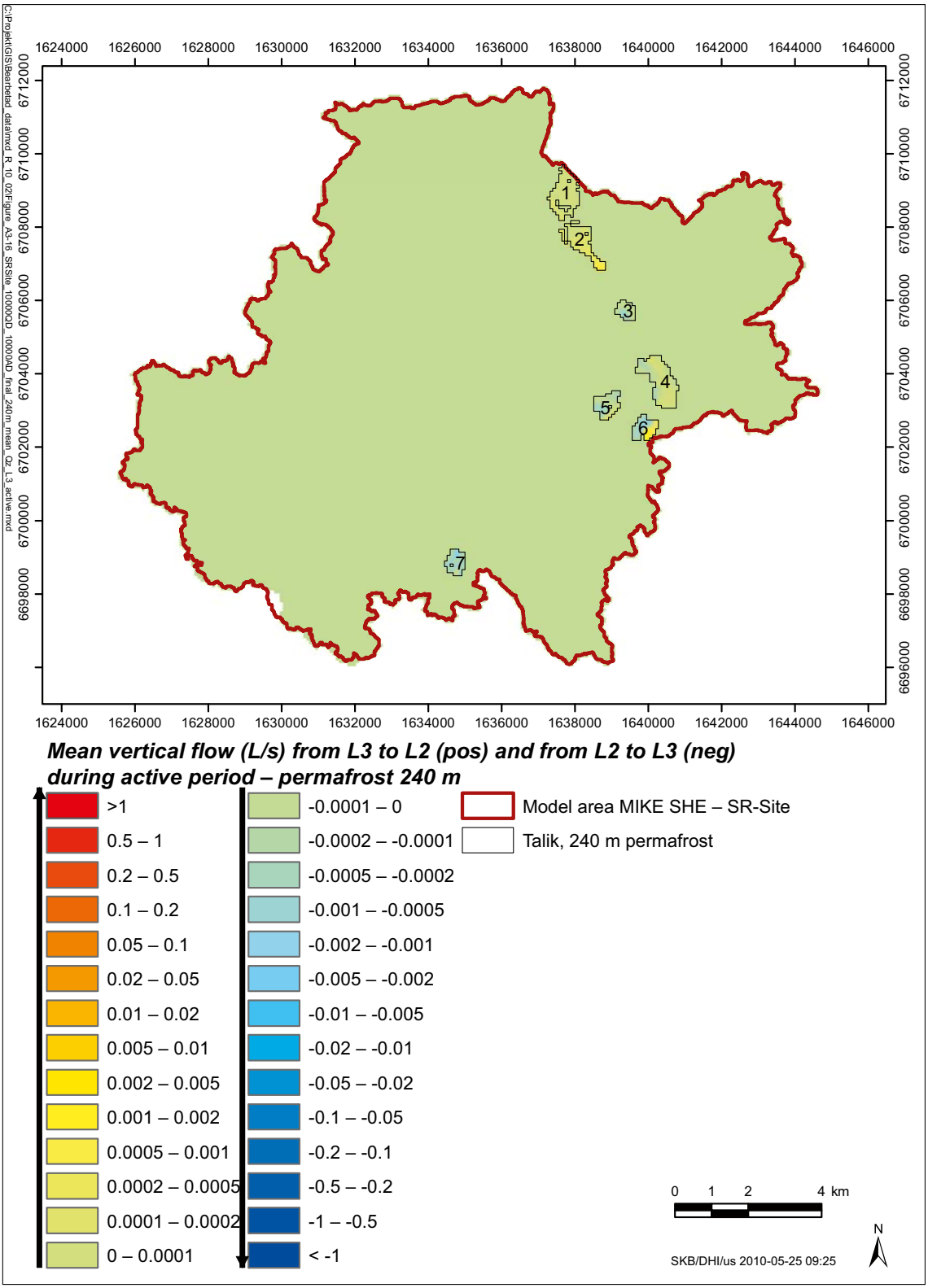

Figure A3-16. *Calculated mean vertical flow (units in l/s) between two upper permafrost layers during the active period with a permafrost thickness of 240 m.*

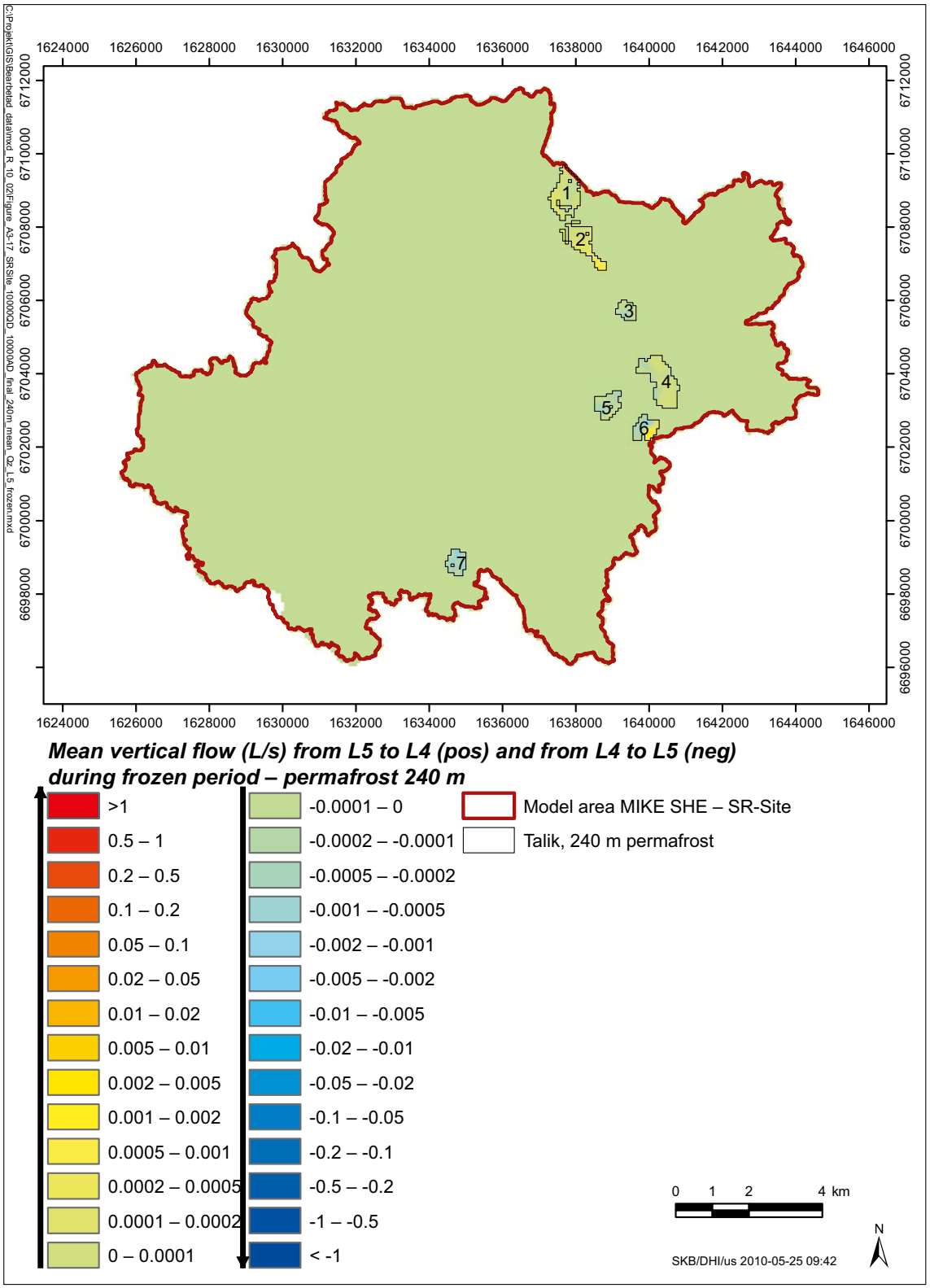

Figure A3-17. *Calculated mean vertical flow (units in l/s) between two middle permafrost layers during the frozen period with a permafrost thickness of 240 m.*

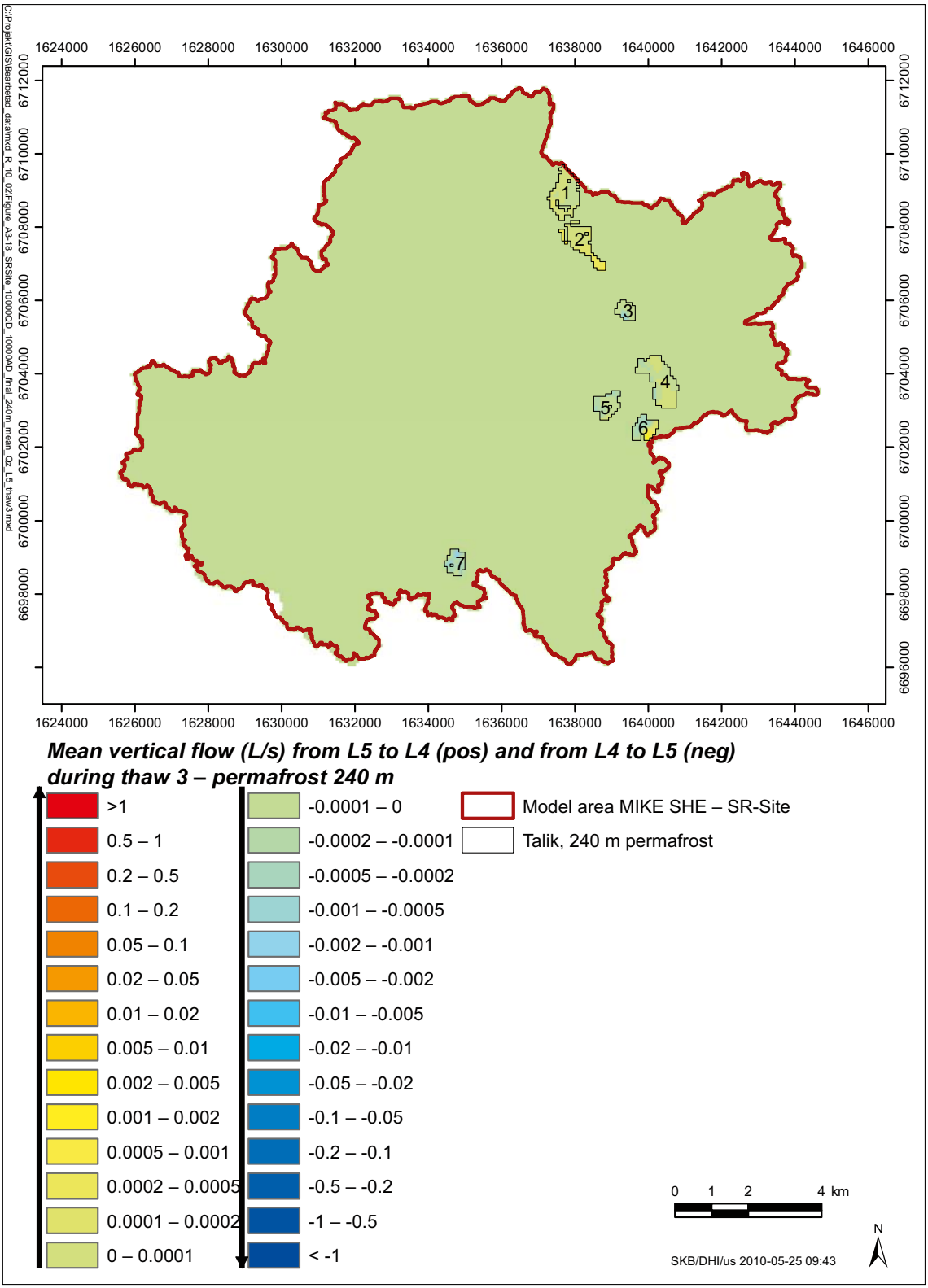

Figure A3-18. *Calculated mean vertical flow (units are in l/s) between two middle permafrost layers during the thaw3 period with a permafrost thickness of 240 m.*

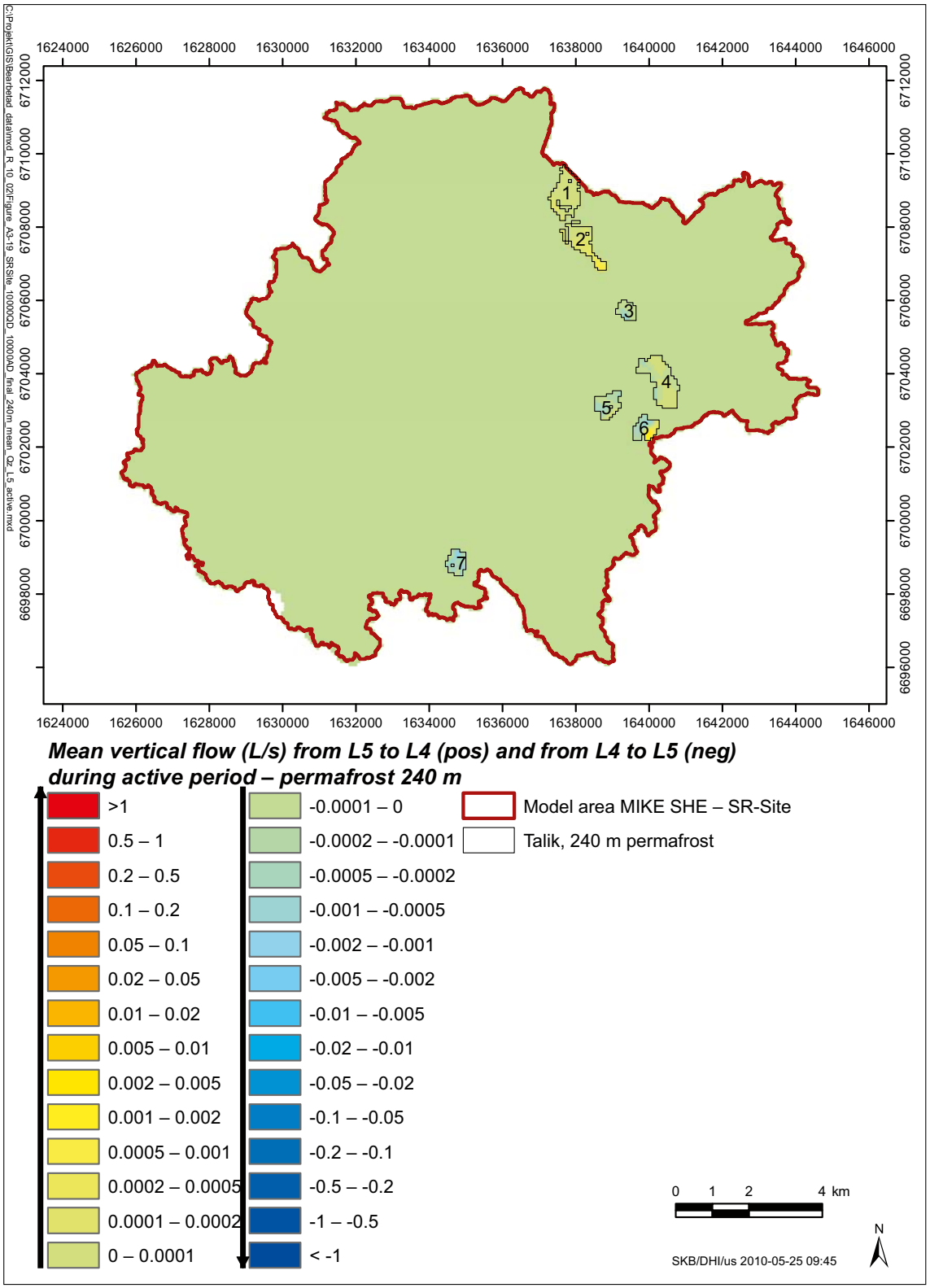

Figure A3-19. *Calculated mean vertical flow (units in l/s) between two middle permafrost layers during the active period with a permafrost thickness of 240 m.*

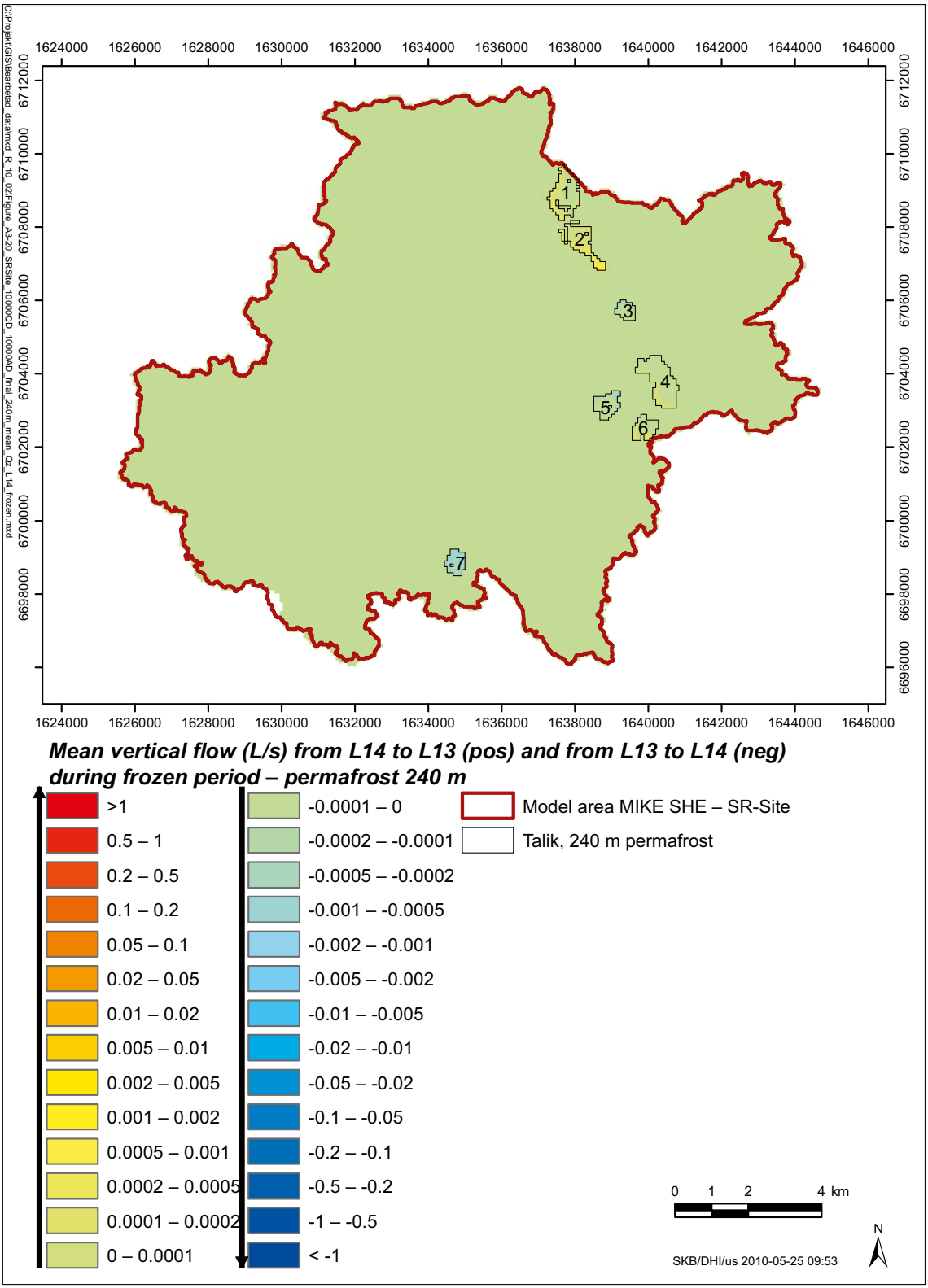

Figure A3-20. *Calculated mean vertical flow (units in l/s) between the deepest permafrost layer and the unfrozen layer below during the frozen period with a permafrost thickness of 240 m.*

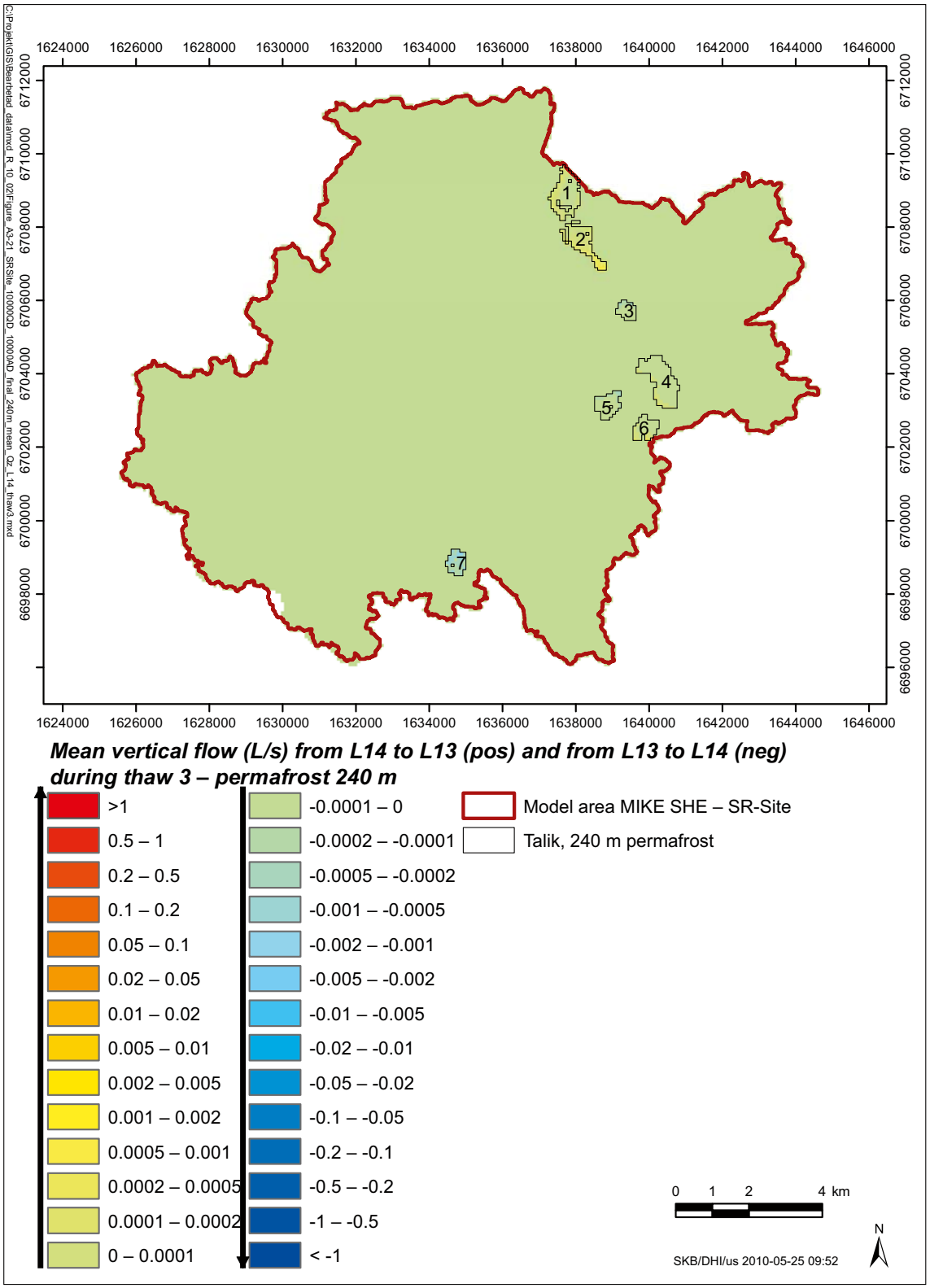

Figure A3-21. *Calculated mean vertical flow (units in l/s) between the deepest permafrost layer and the unfrozen layer below during the thaw3 period with a permafrost thickness of 240 m.*

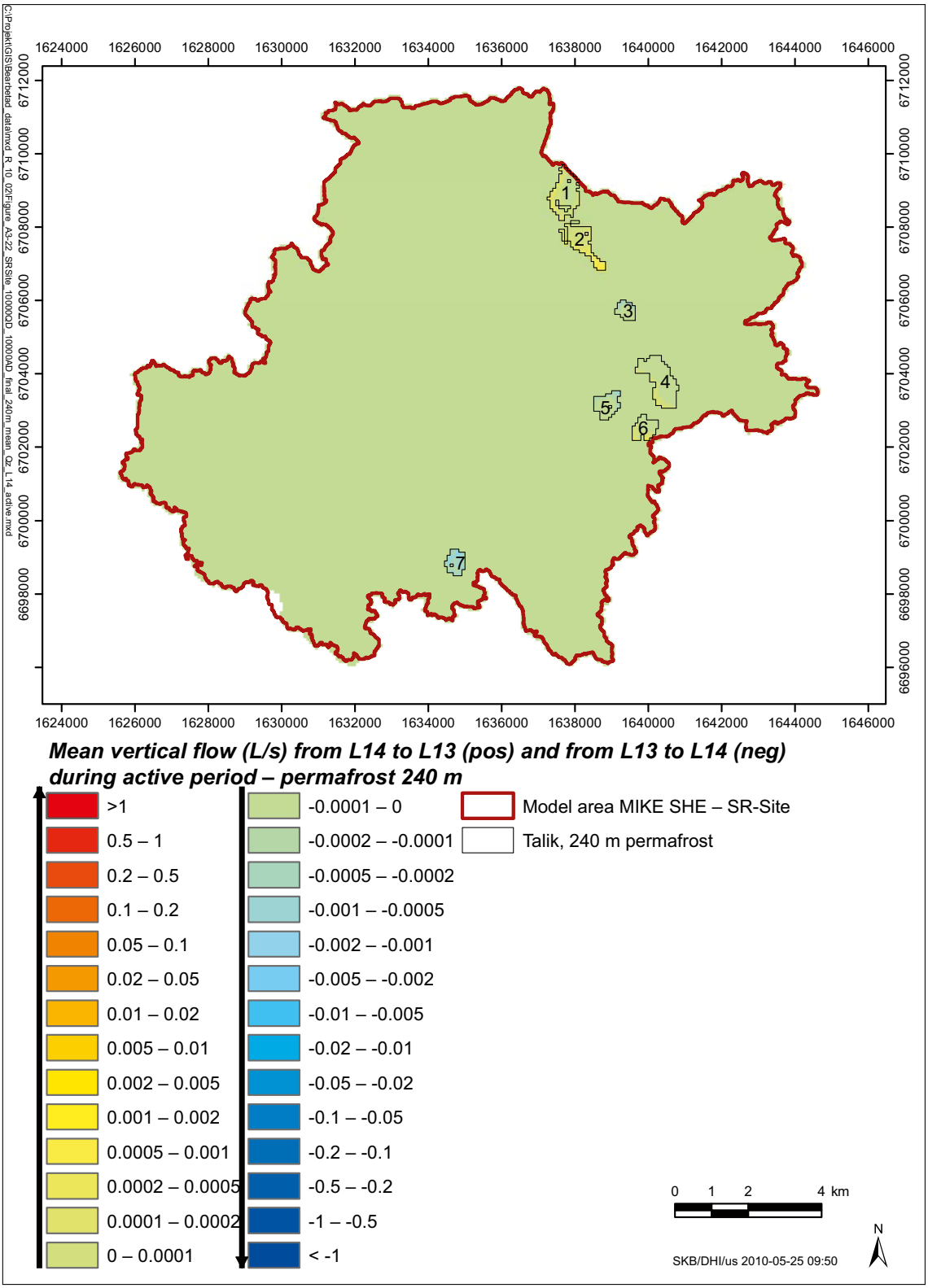

Figure A3-22. *Calculated mean vertical flow (units in l/s) between the deepest permafrost layer and the unfrozen layer below during the active period with a permafrost thickness of 240 m.*

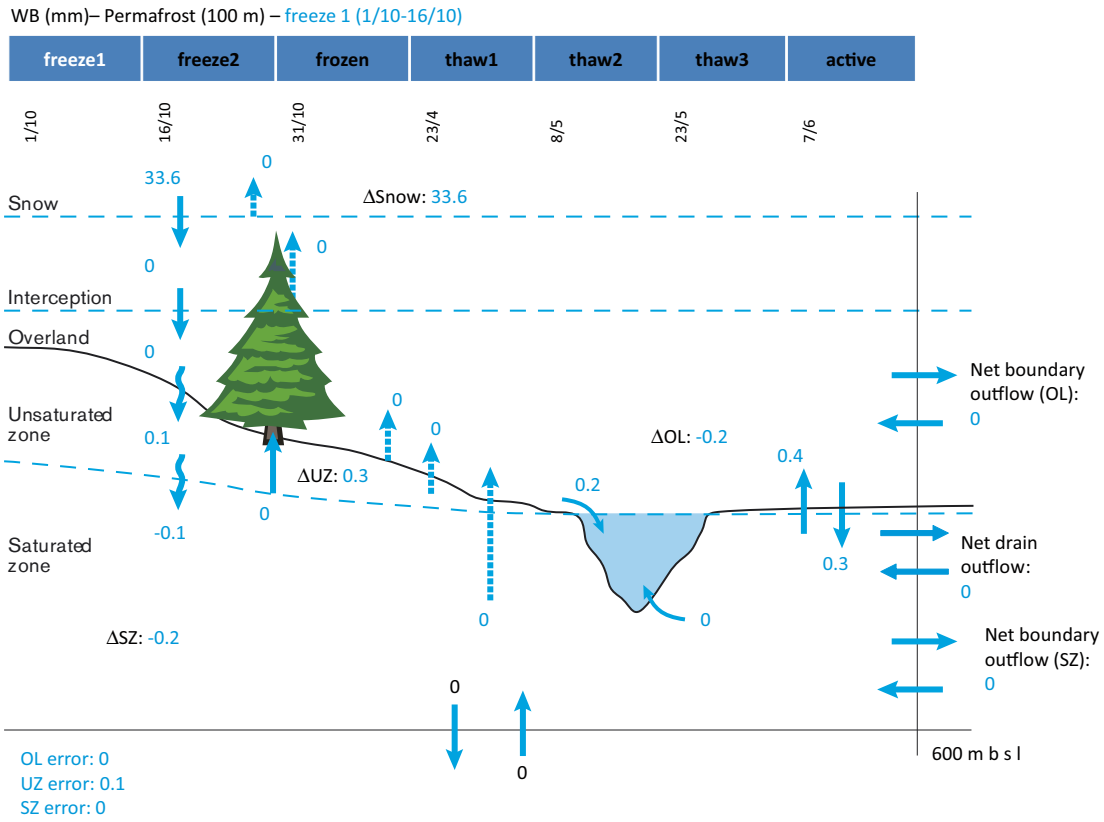

Figure A3-23. *Calculated water balance for the period freeze 1 from the 10000AD_10000QD model for permafrost conditions with a permafrost thickness of 100 m for the area constituting land at 10,000 AD.*

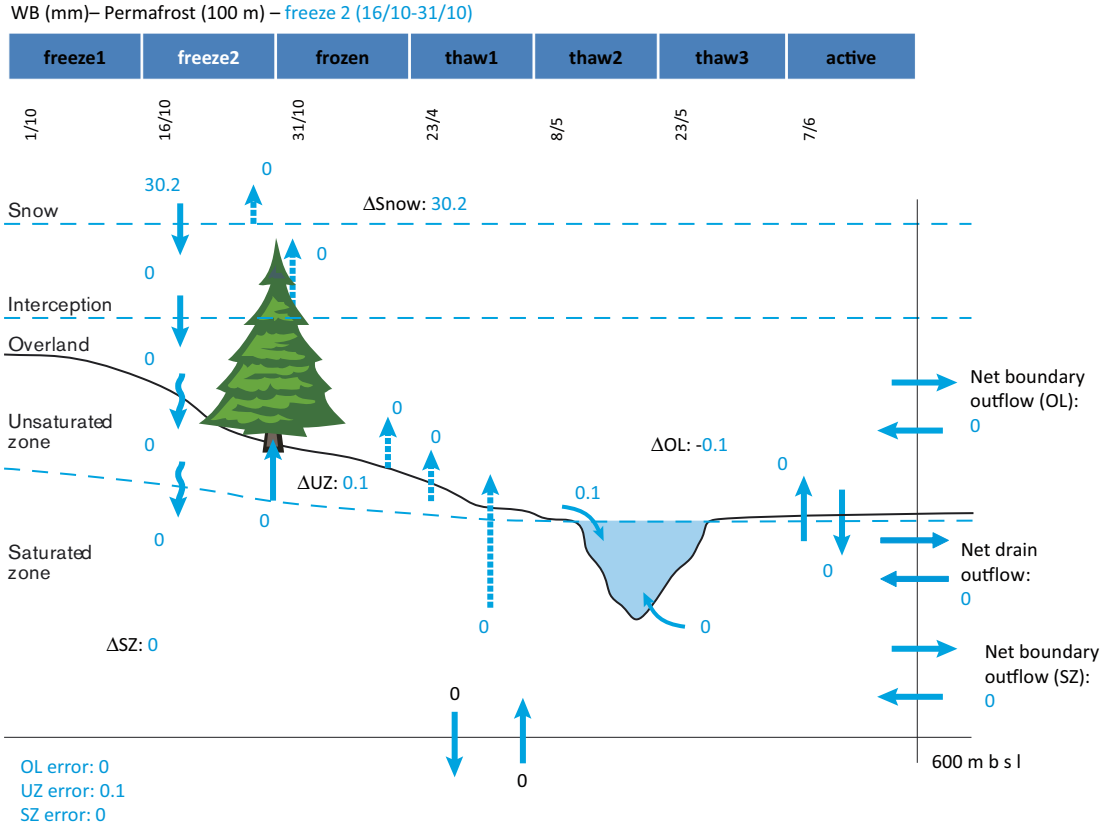

Figure A3-24. *Calculated water balance for the period freeze 2 from the 10000AD_10000QD model for permafrost conditions, with a permafrost thickness of 100 m for the area constituting land at 10,000 AD.*

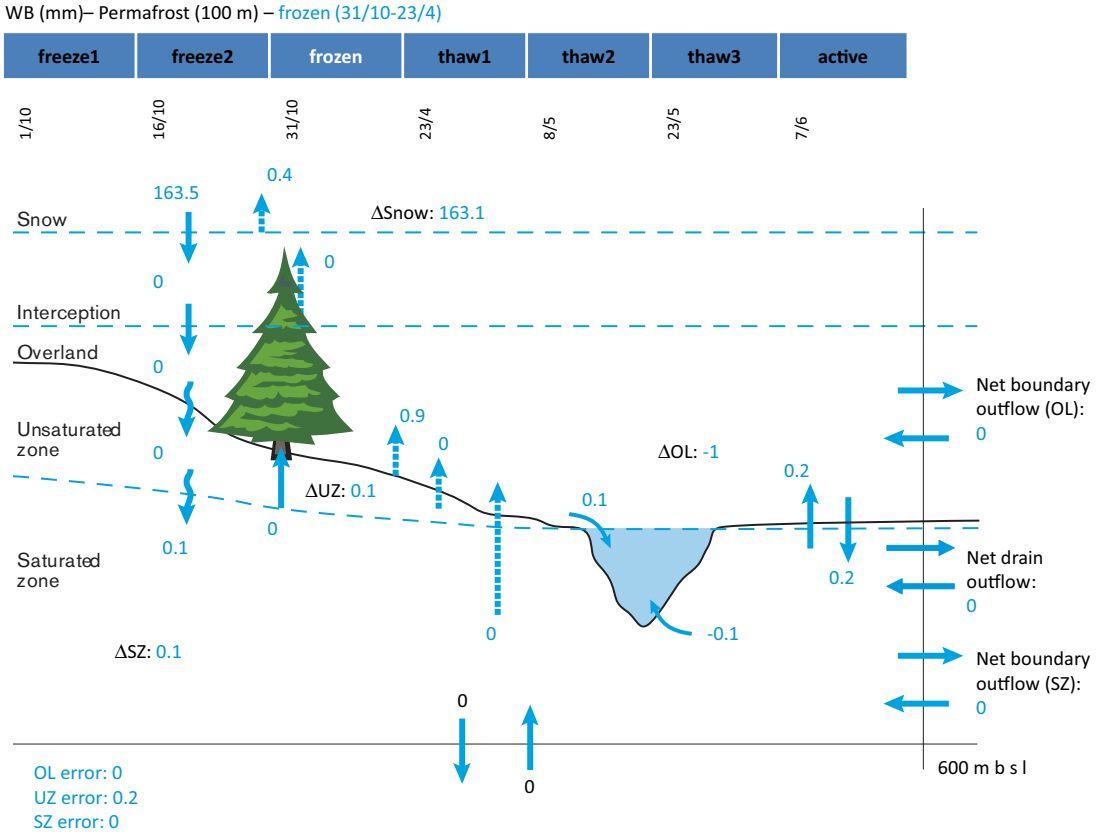

Figure A3-25. *Calculated water balance for the frozen period from the 10000AD_10000QD model for permafrost conditions, with a permafrost thickness of 100 m for the area constituting land at 10,000 AD.*

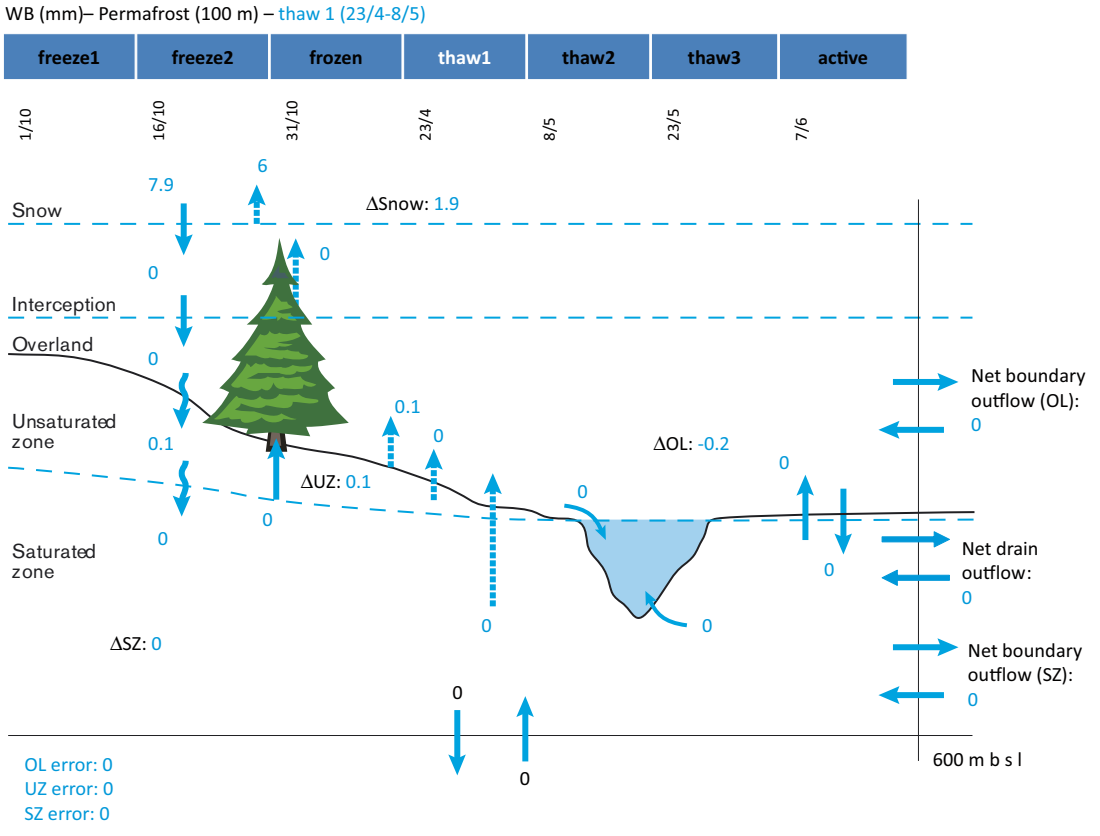

Figure A3-26. *Calculated water balance for the period thaw 1 from the 10000AD_10000QD model for permafrost conditions, with a permafrost thickness of 100 m for the area constituting land at 10,000 AD.*

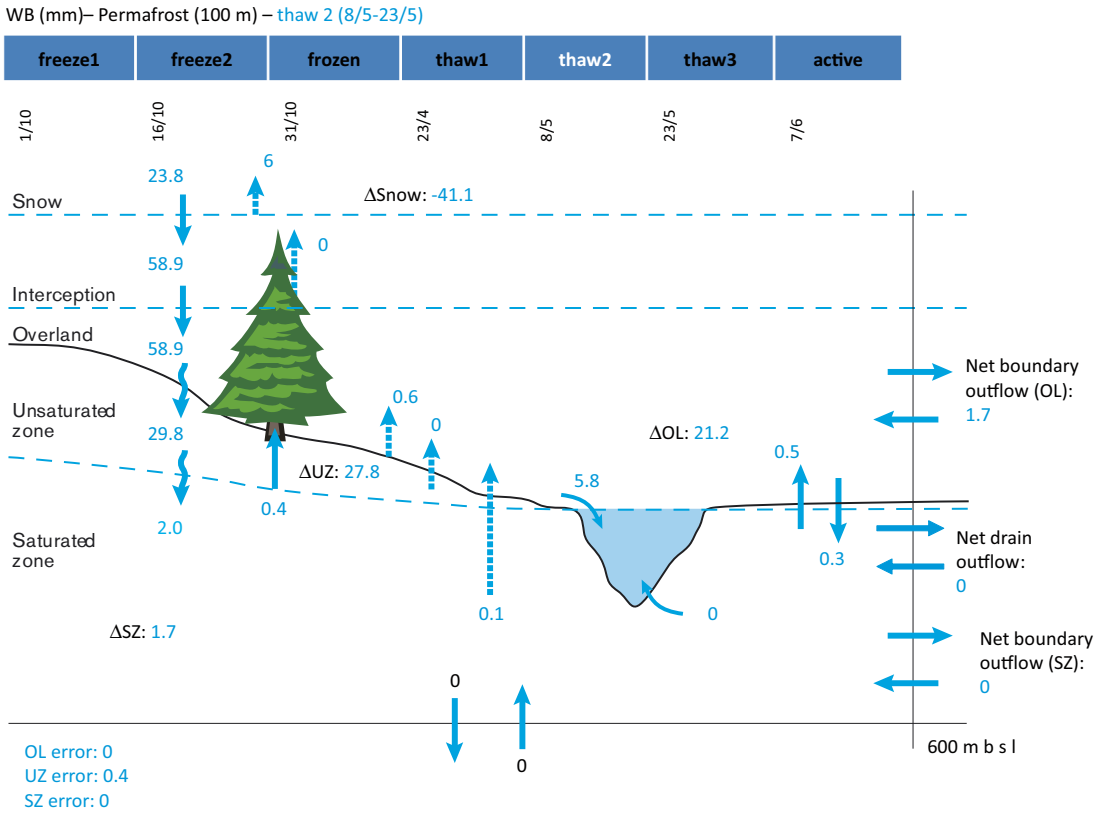

Figure A3-27. *Calculated water balance for the period thaw 2 from the 10000AD_10000QD model for permafrost conditions, with a permafrost thickness of 100 m for the area constituting land at 10,000 AD.*

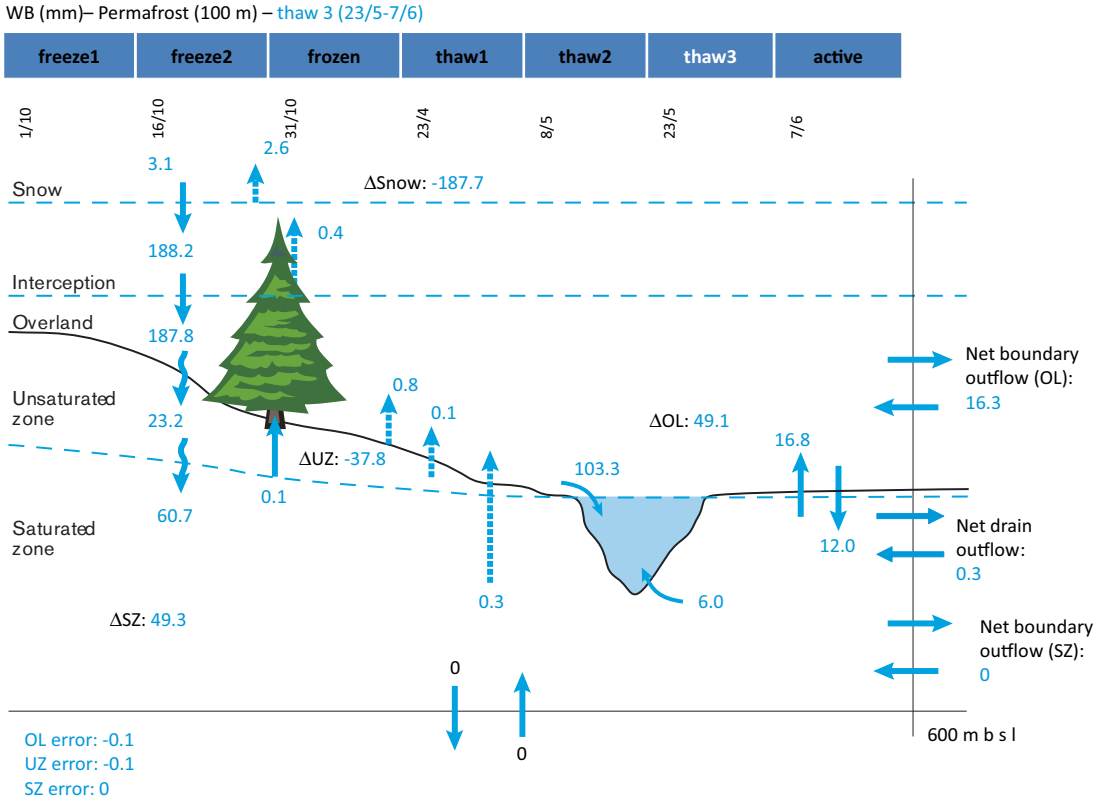

Figure A3-28. *Calculated water balance for the period thaw 3 from the 10000AD_10000QD model for permafrost conditions, with a permafrost thickness of 100 m for the area constituting land at 10,000 AD.*

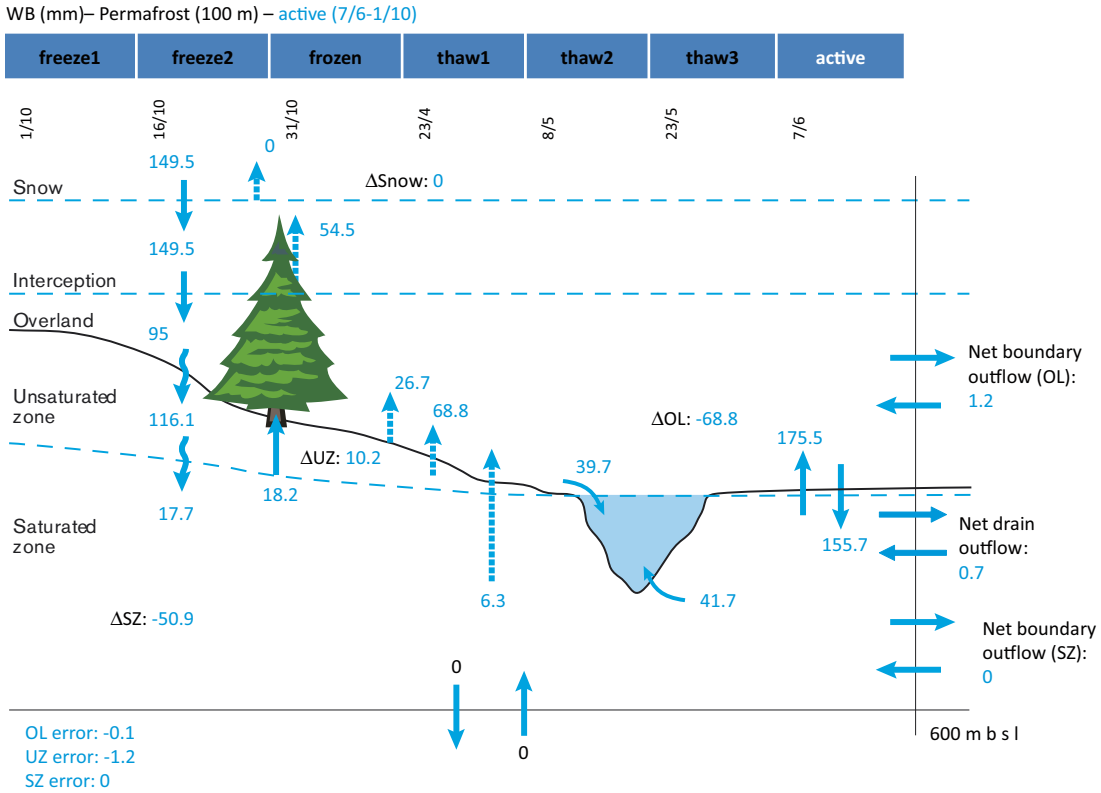

Figure A3-29. *Calculated water balance for the active period from the 10000AD_10000QD model for permafrost conditions with a permafrost thickness of 100 m for the area constituting land at 10,000 AD.*

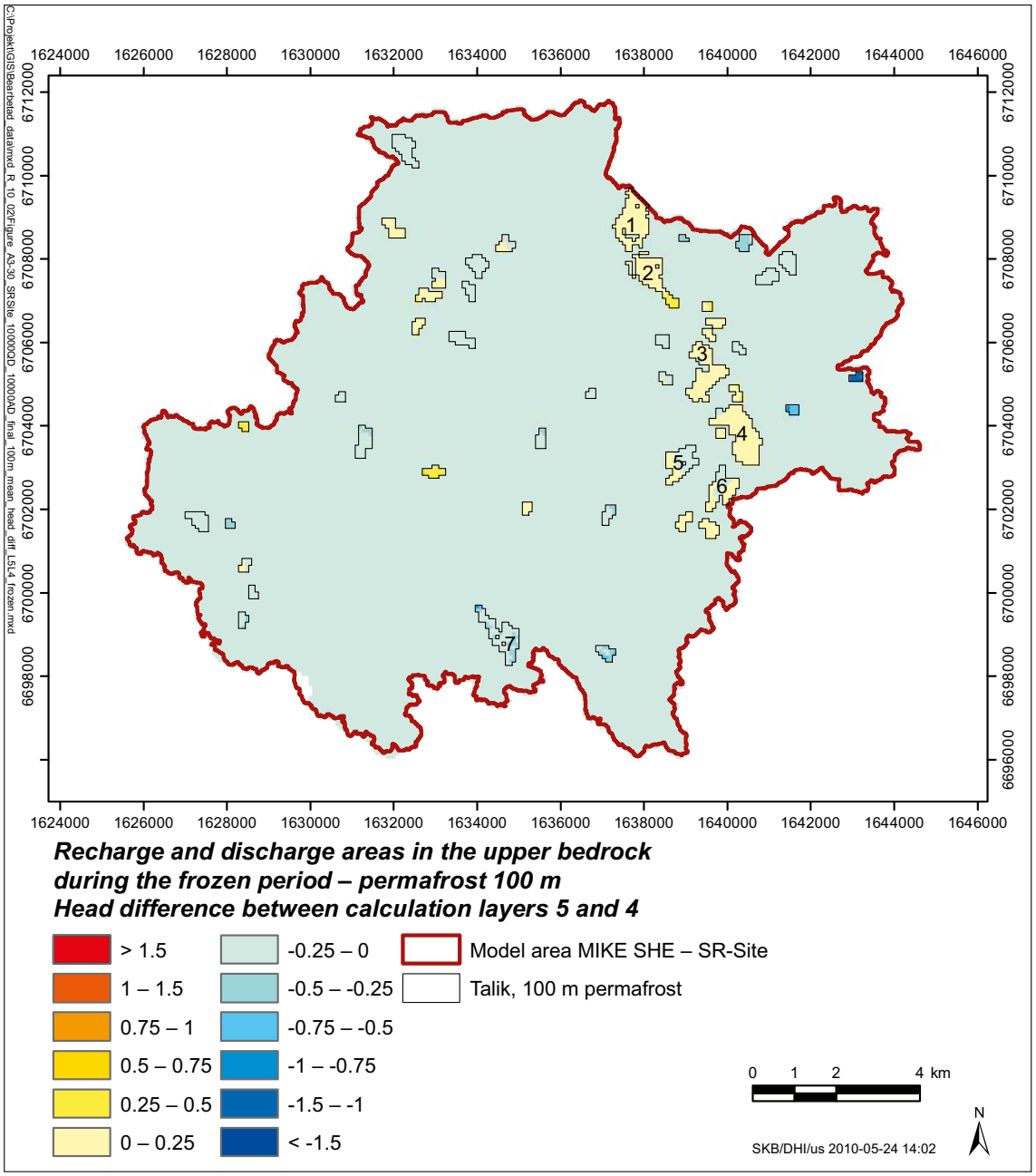

Figure A3-30. *The recharge (blue scale) and discharge (red scale) areas within the permafrost formation in the upper bedrock from the 10000AD_10000QD model for permafrost conditions with a permafrost thickness of 100 m, calculated as the mean head difference between calculation layers 5 and 4 during the frozen period.*

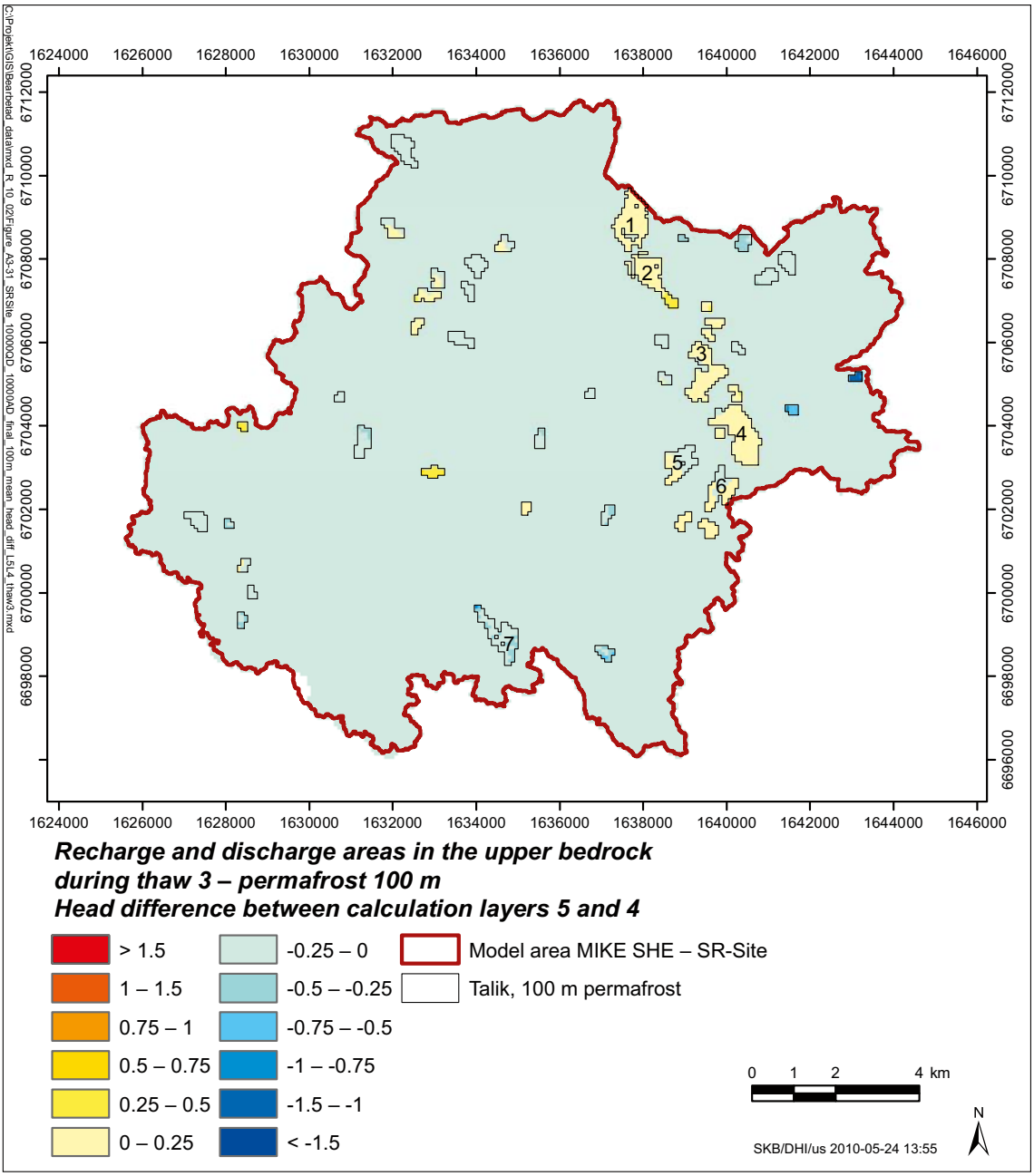

Figure A3-31. *The recharge (blue scale) and discharge (red scale) areas within the permafrost formation in the upper bedrock from the 10000AD_10000QD model for permafrost conditions with a permafrost thickness of 100 m, calculated as the mean head difference between calculation layers 5 and 4 during the thaw 3 period.*

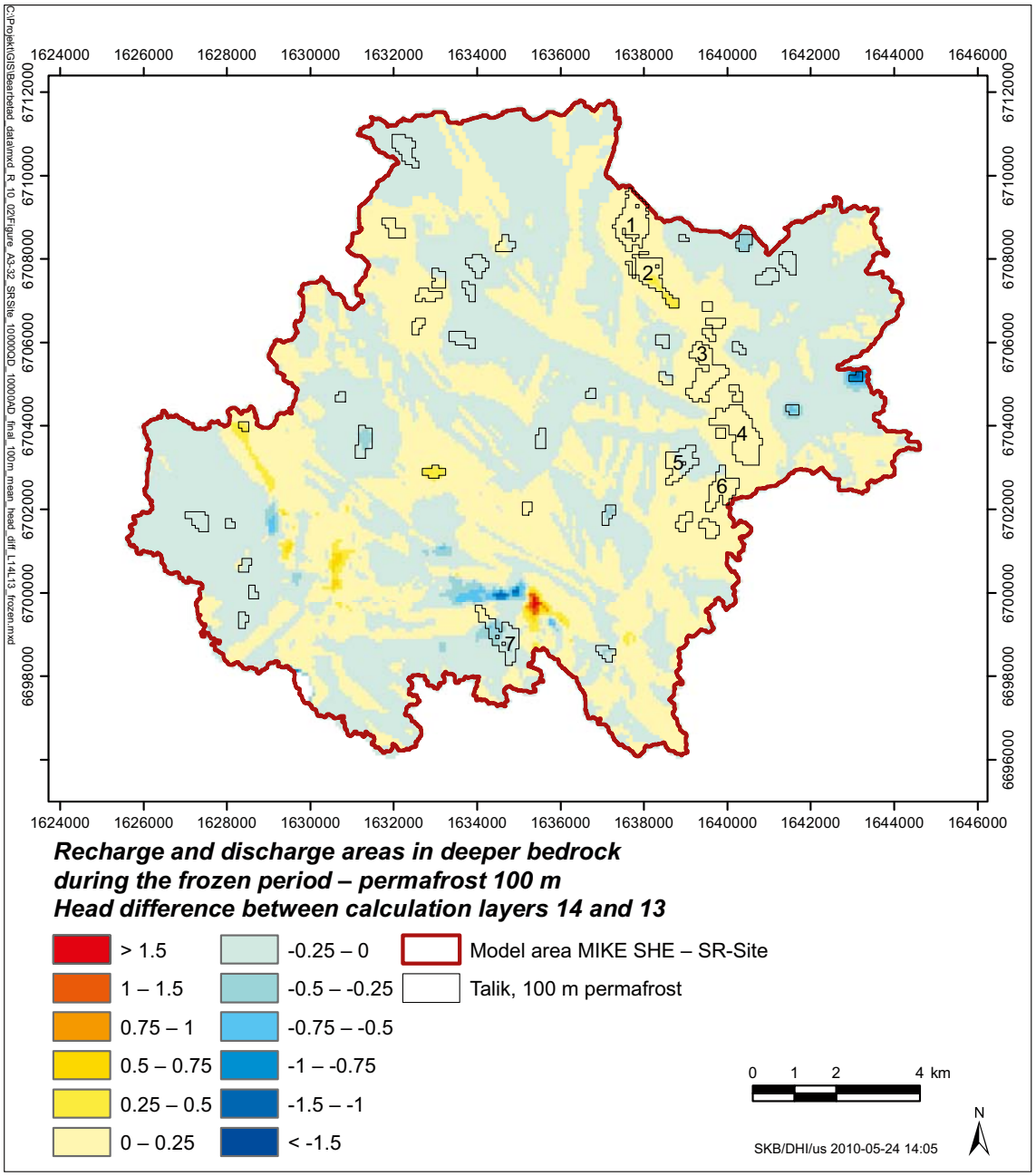

Figure A3-32. *The recharge (blue scale) and discharge(red scale) areas below the permafrost formation in the deeper bedrock from the 10000AD_10000QD model for permafrost conditions with a permafrost thickness of 100 m, calculated as the mean head difference between calculation layers 14 and 13 during the frozen period.*

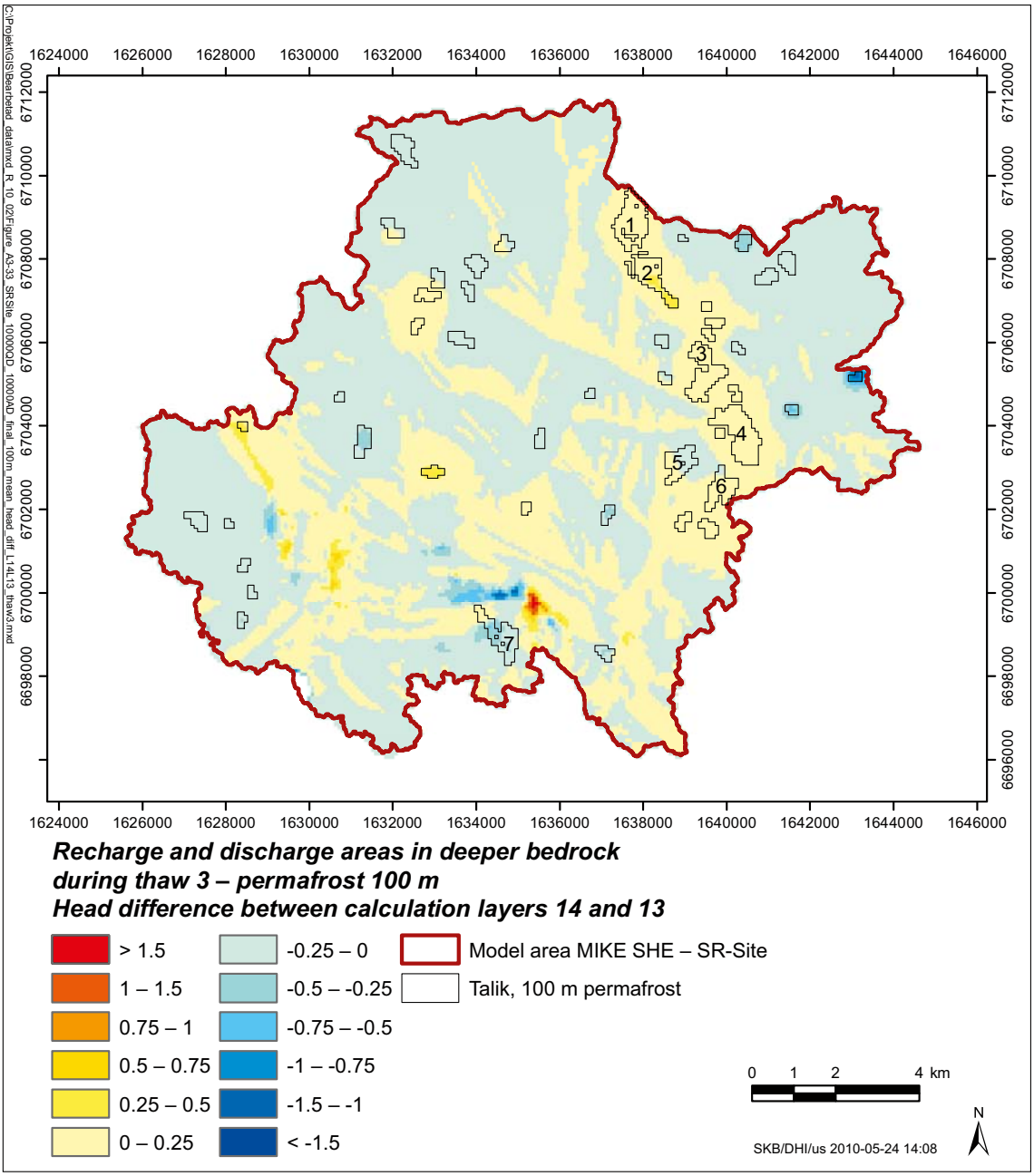

Figure A3-33. *The recharge (blue scale) and discharge(red scale) areas below the permafrost formation in the deeper bedrock from the 10000AD_10000QD model for permafrost conditions with a permafrost thickness of 100 m, calculated as the mean head difference between calculation layers 14 and 13 during the thaw 3 period.*

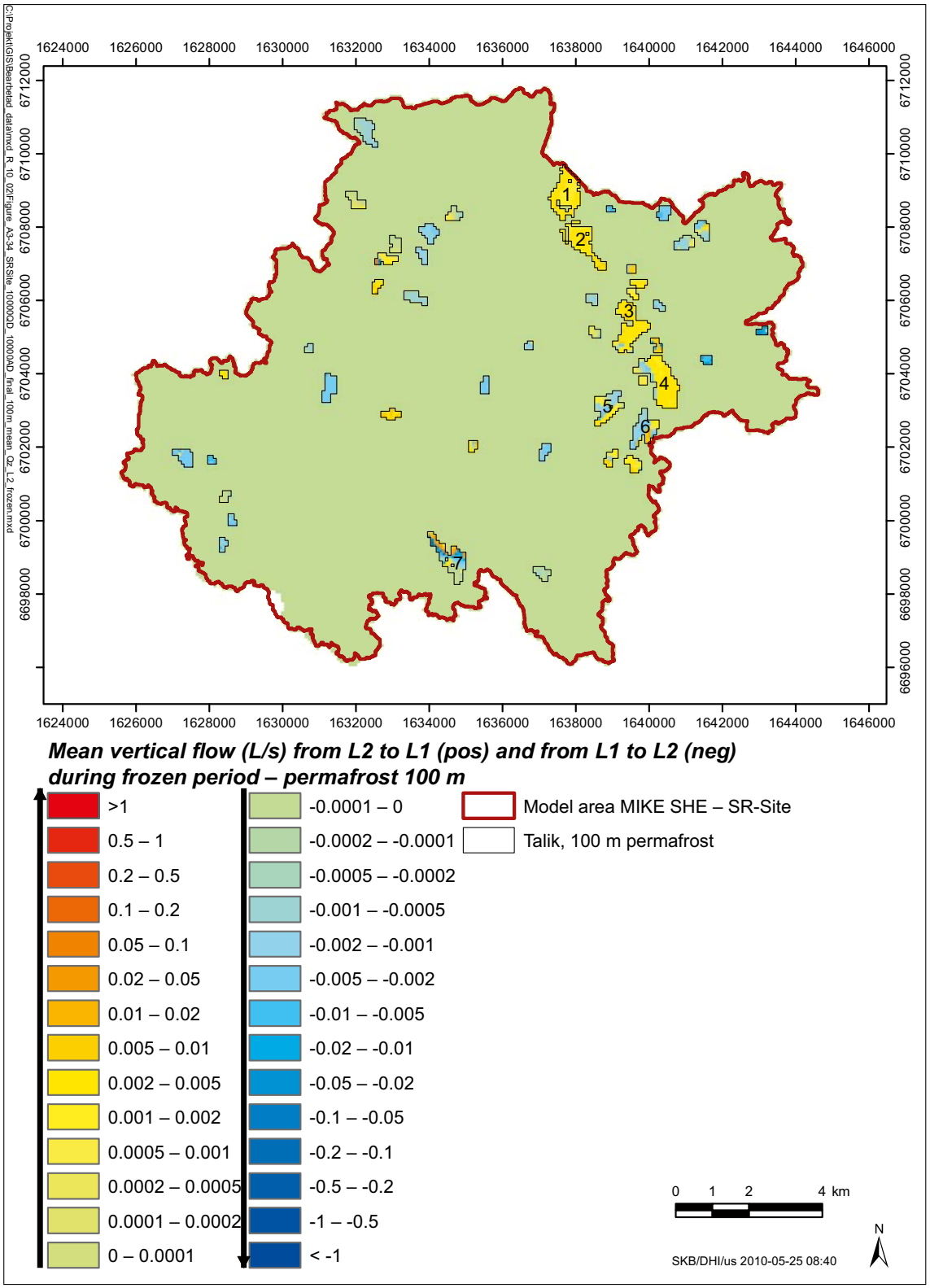

Figure A3-34. *Calculated mean vertical flow (units in l/s) between the active layer and the top permafrost layer during the frozen period with a permafrost thickness of 100 m.*

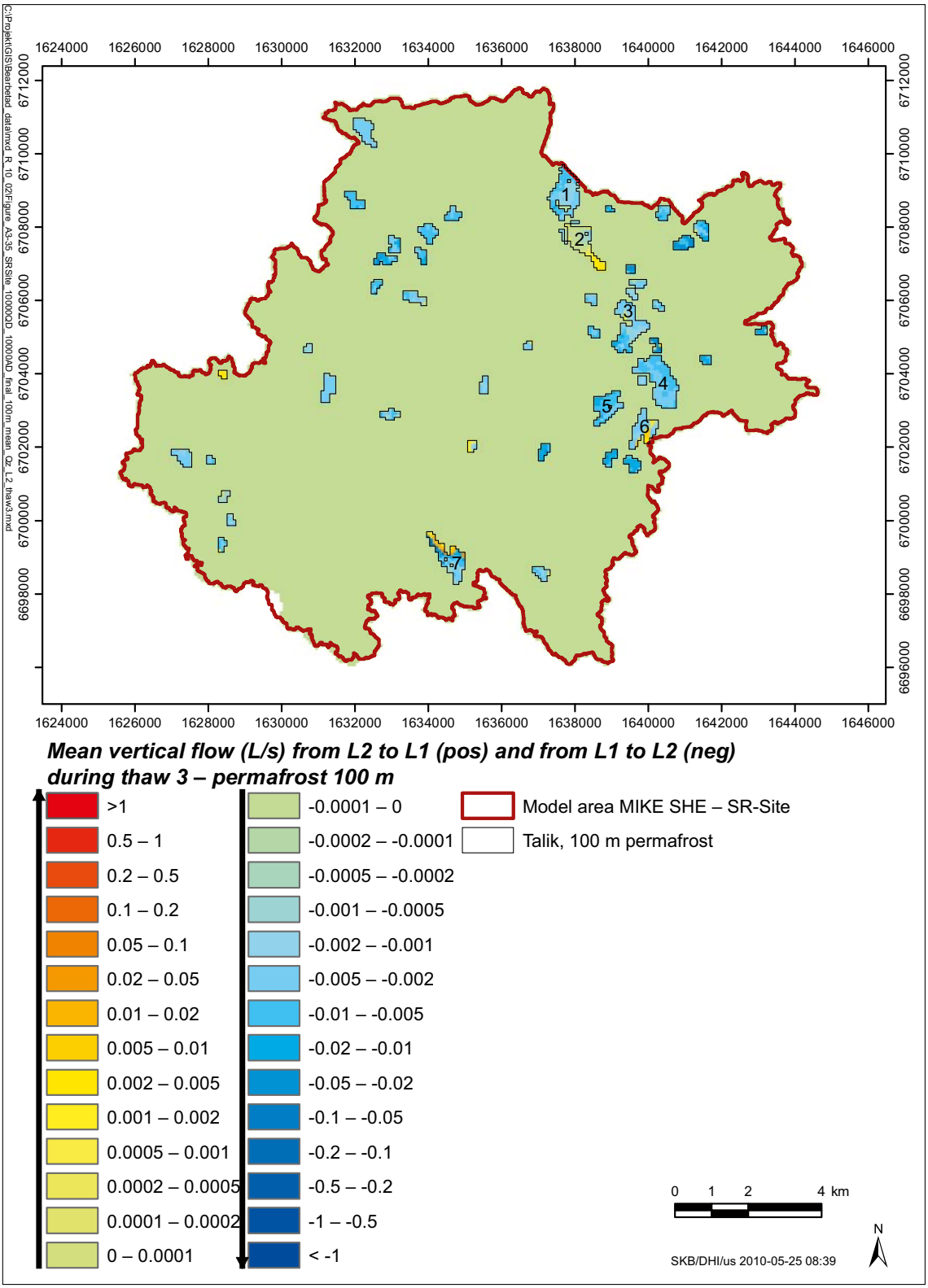

Figure A3-35. *Calculated mean vertical flow (units in l/s) between the active layer and the top permafrost layer during the thaw3 period with a permafrost thickness of 100 m.*

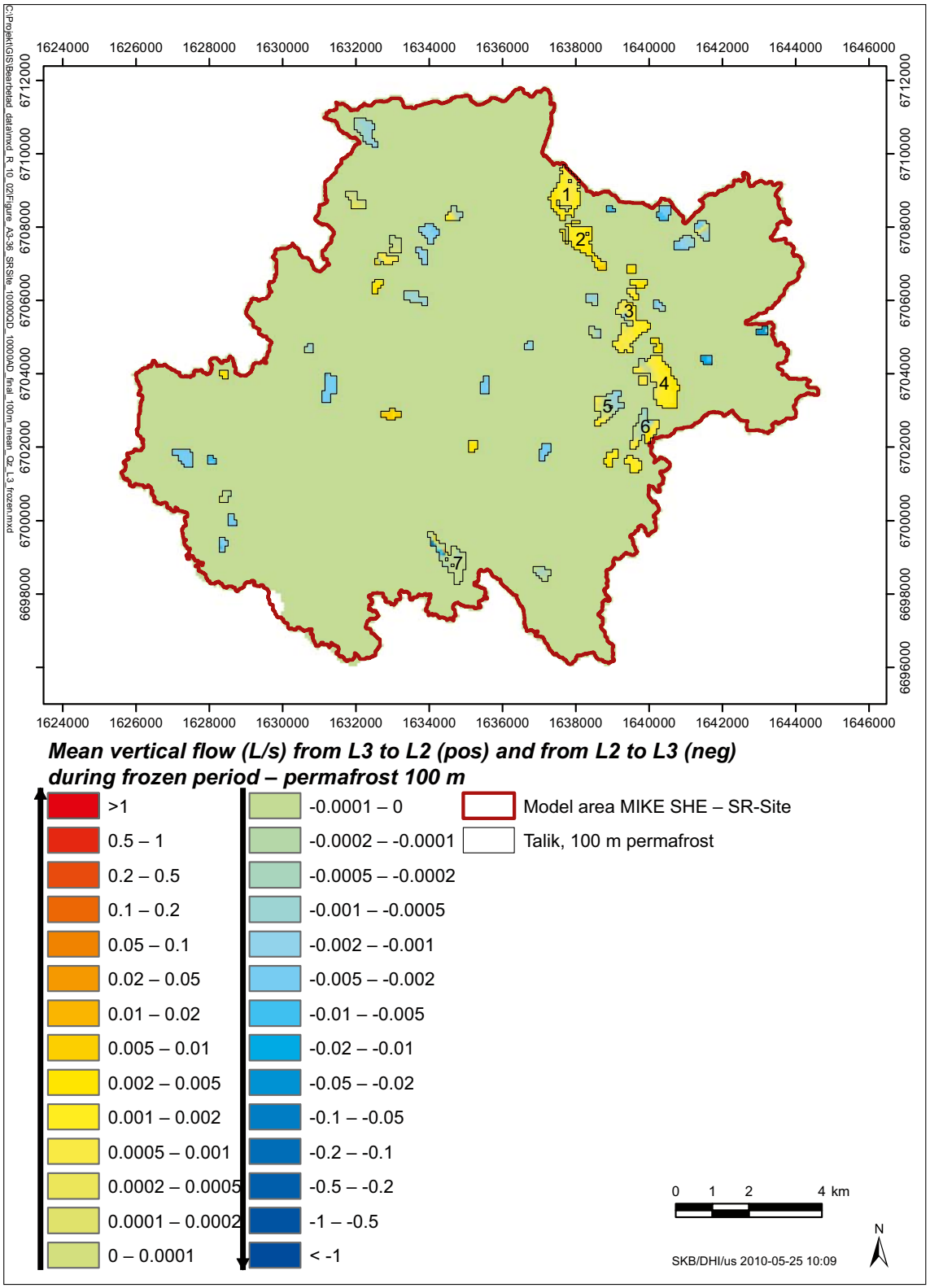

Figure A3-36. *Calculated mean vertical flow (units in l/s) between the two upper permafrost layers during the frozen period with a permafrost thickness of 100 m.*

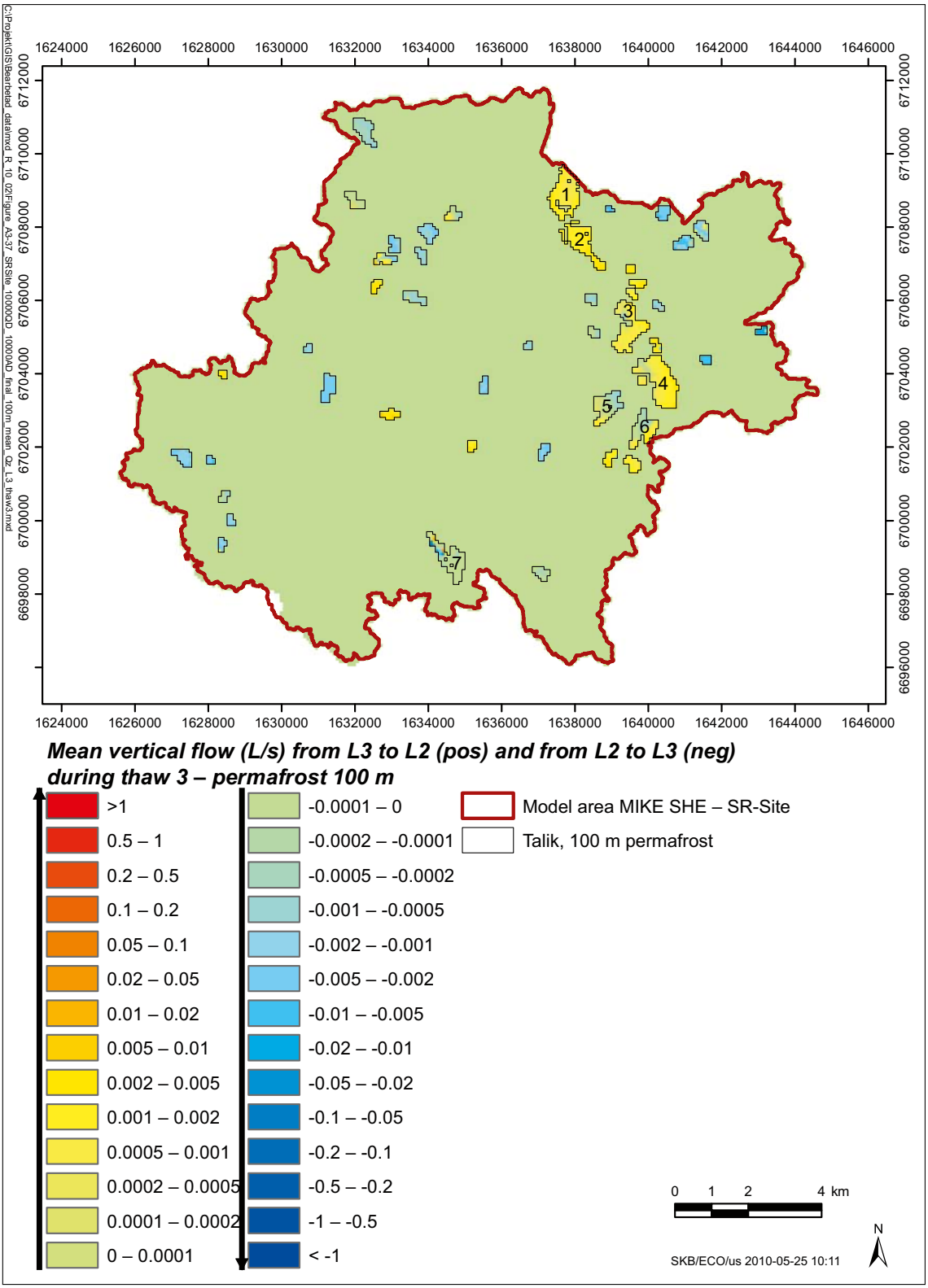

Figure A3-37. *Calculated mean vertical flow (units in l/s) between the two upper permafrost layers during the thaw3 period with a permafrost thickness of 100 m.*

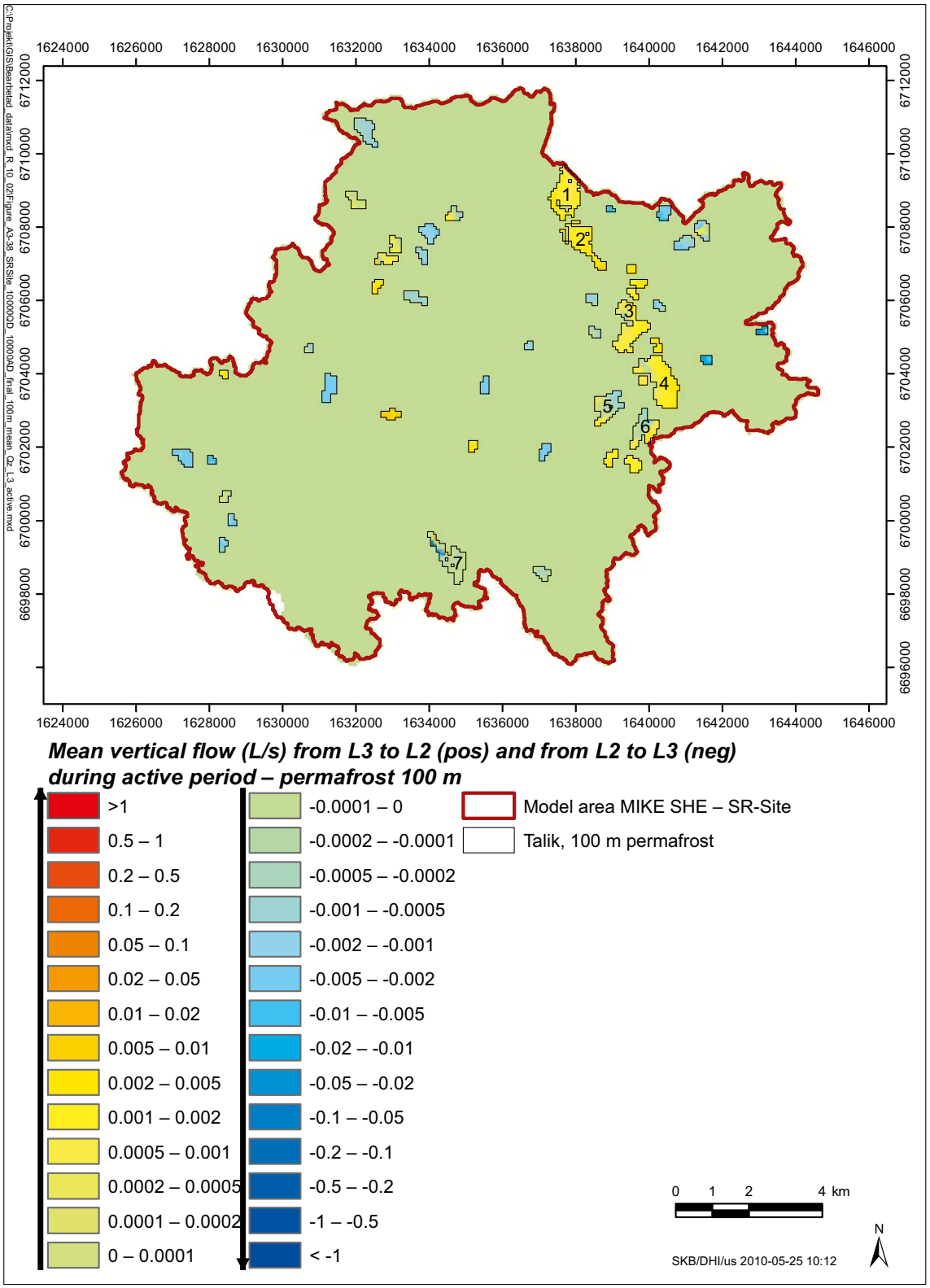

Figure A3-38. *Calculated mean vertical flow (units in l/s) between two upper permafrost layers during the active period with a permafrost thickness of 100 m.*

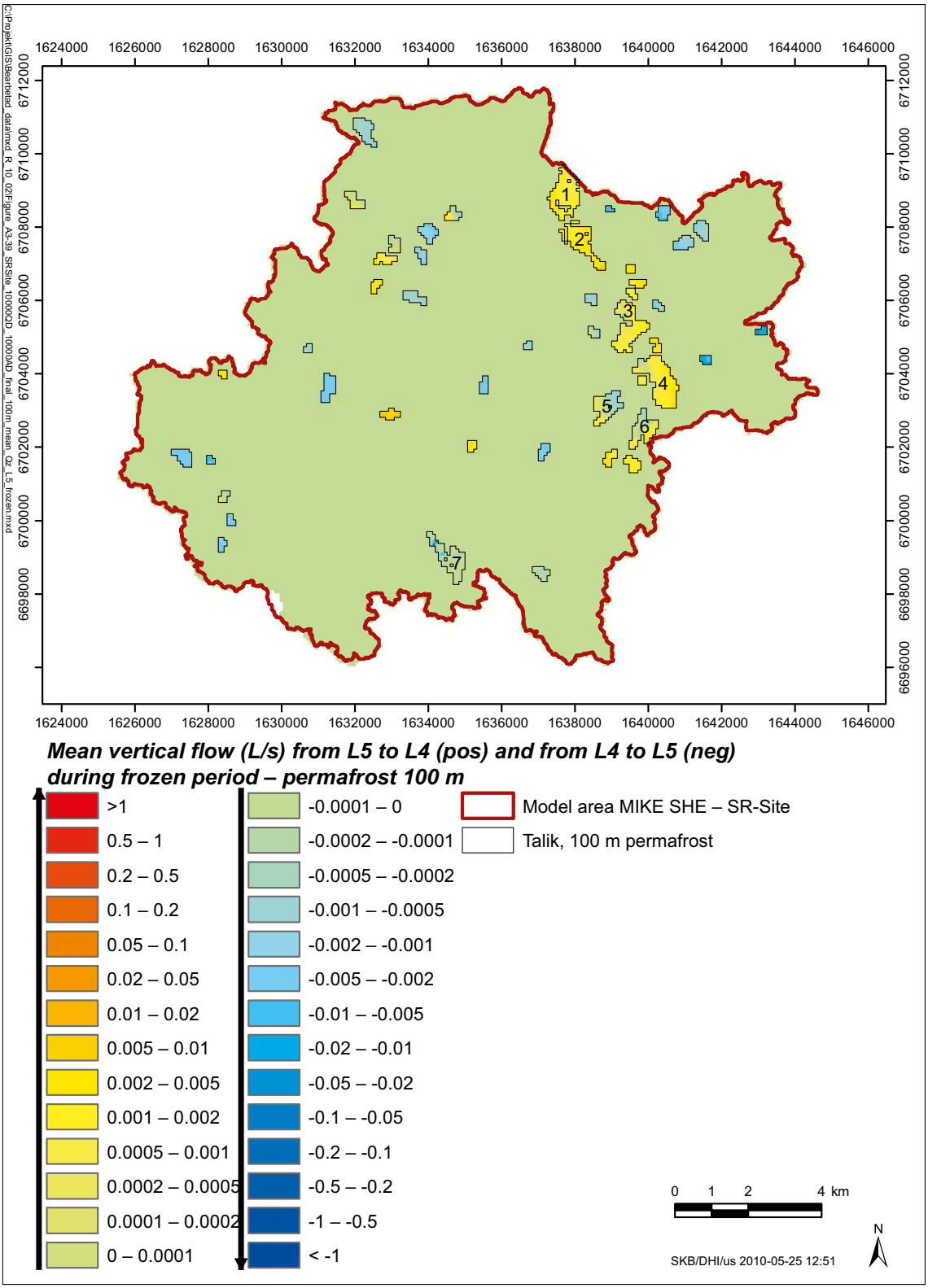

Figure A3-39. *Calculated mean vertical flow (units in l/s) between two middle permafrost layers during the frozen period with a permafrost thickness of 100 m.*

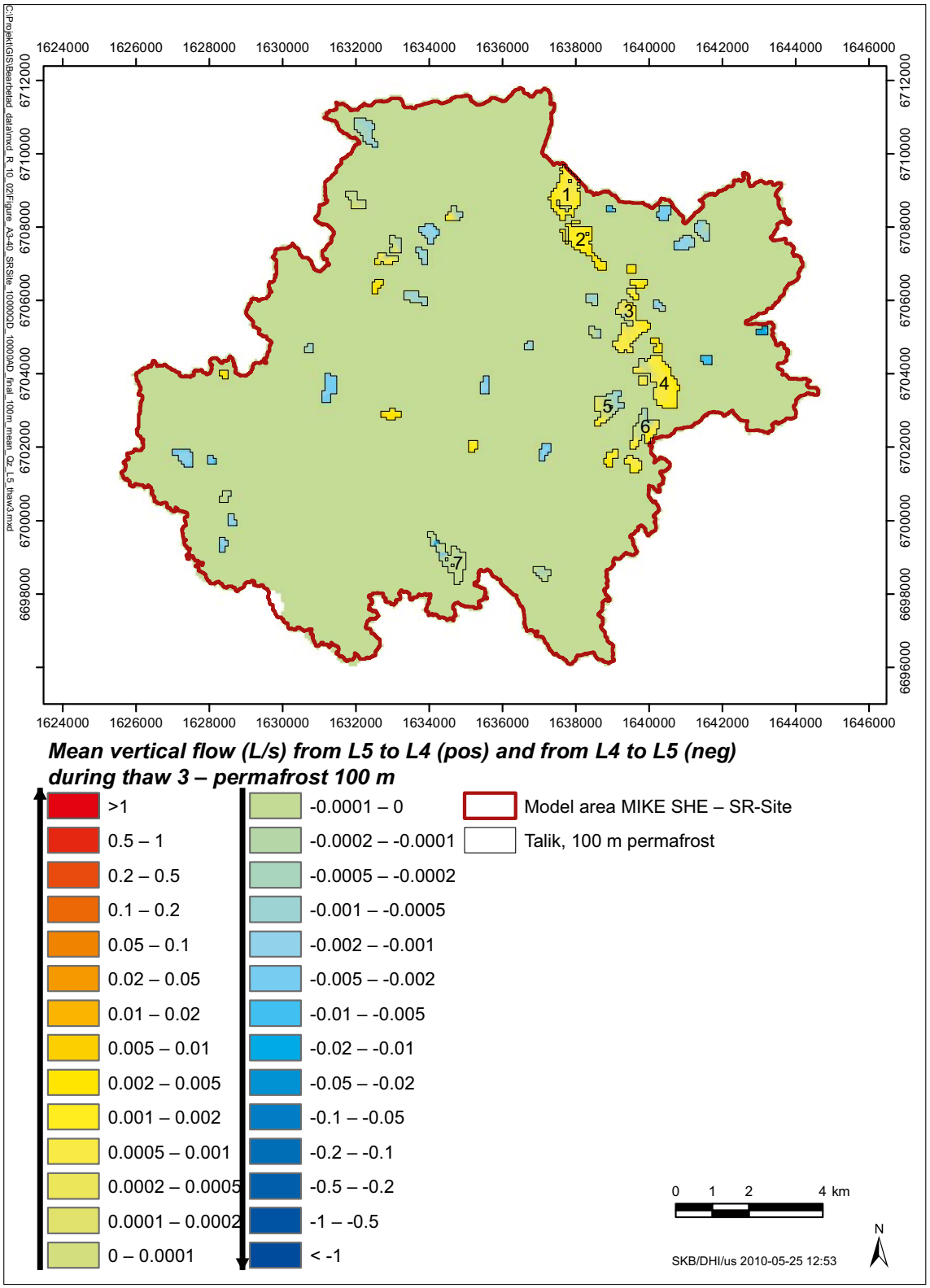

Figure A3-40. *Calculated mean vertical flow (units in l/s) between two middle permafrost layers during the thaw3 period with a permafrost thickness of 100 m.*

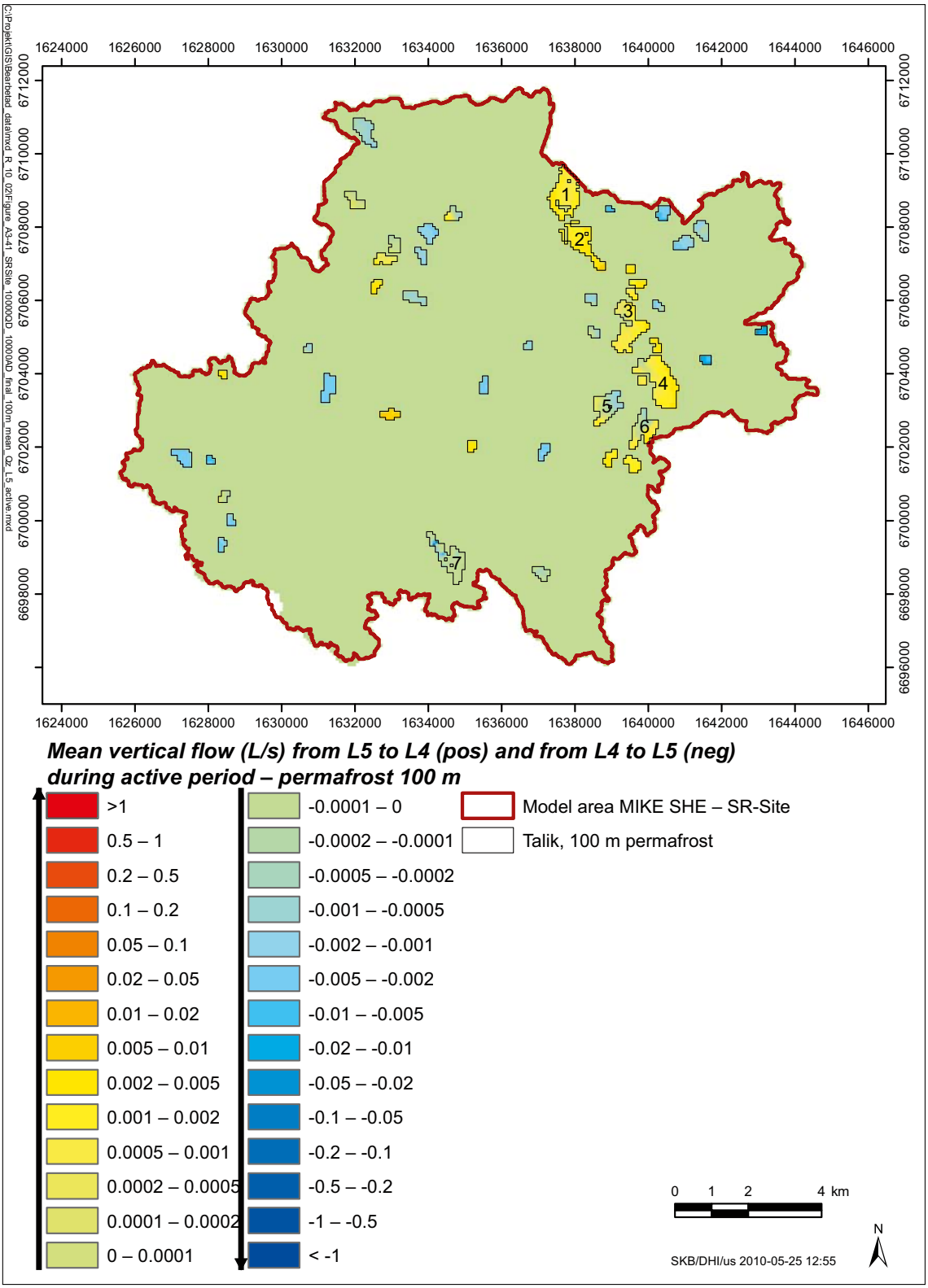

Figure A3-41. *Calculated mean vertical flow (units in l/s) between two middle permafrost layers during the active period with a permafrost thickness of 100 m.*

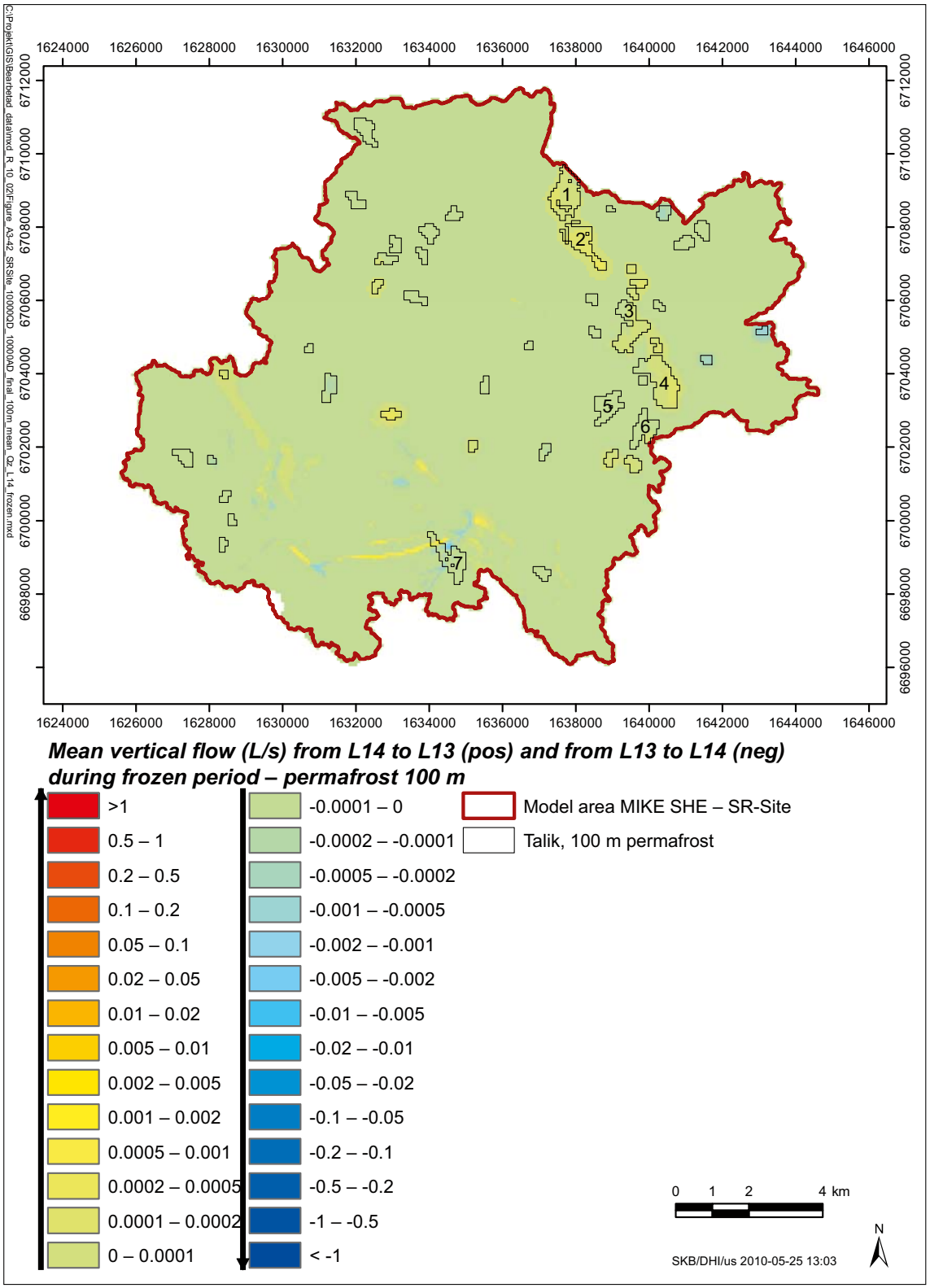

Figure A3-42. *Calculated mean vertical flow (units in l/s) between two deep unfrozen layers below the permafrost during the frozen period with a permafrost thickness of 100 m.*

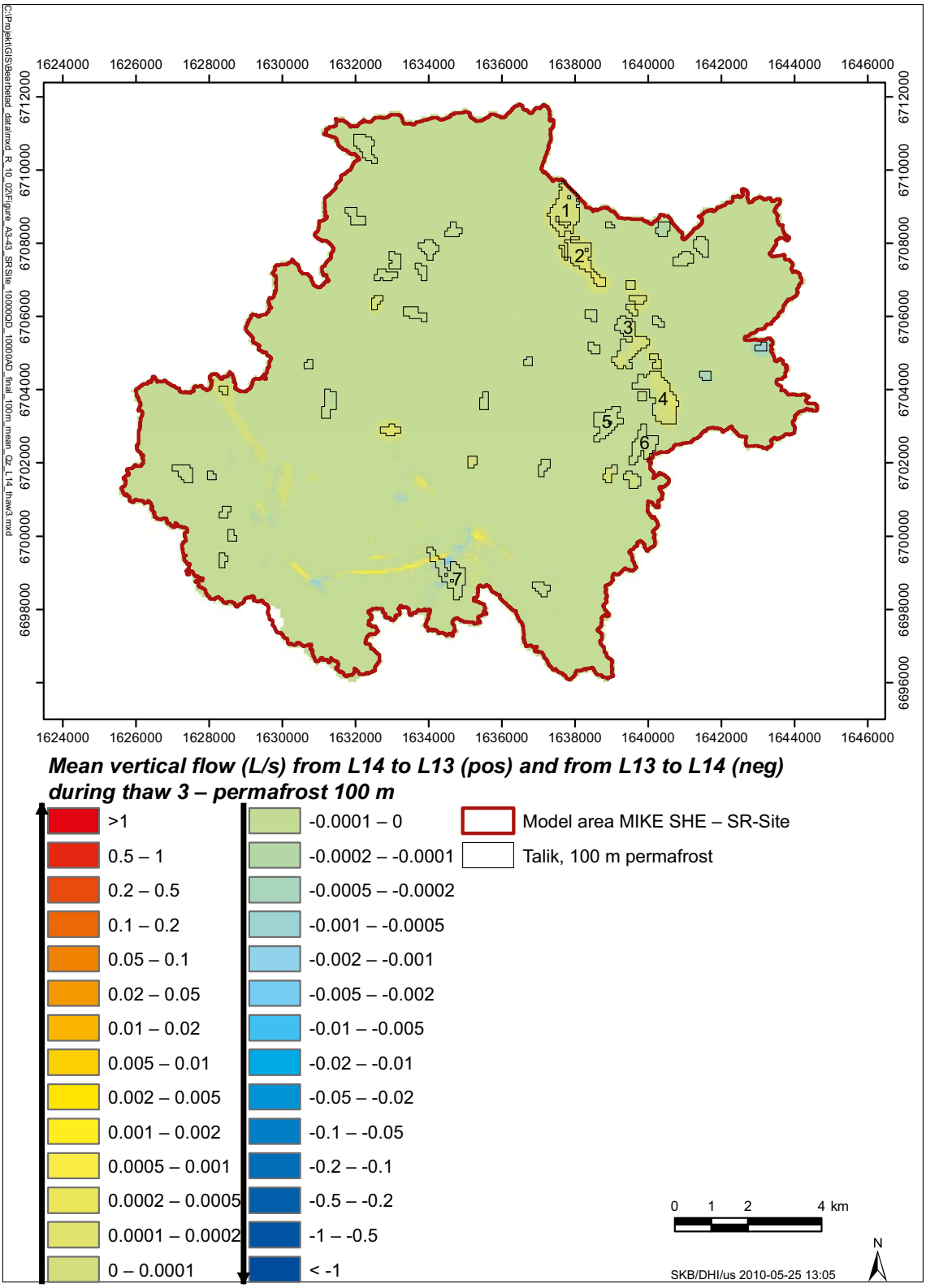

Figure A3-43. *Calculated mean vertical flow (units in l/s) between two deep unfrozen layers below the permafrost during the thaw3 period with a permafrost thickness of 100 m.*

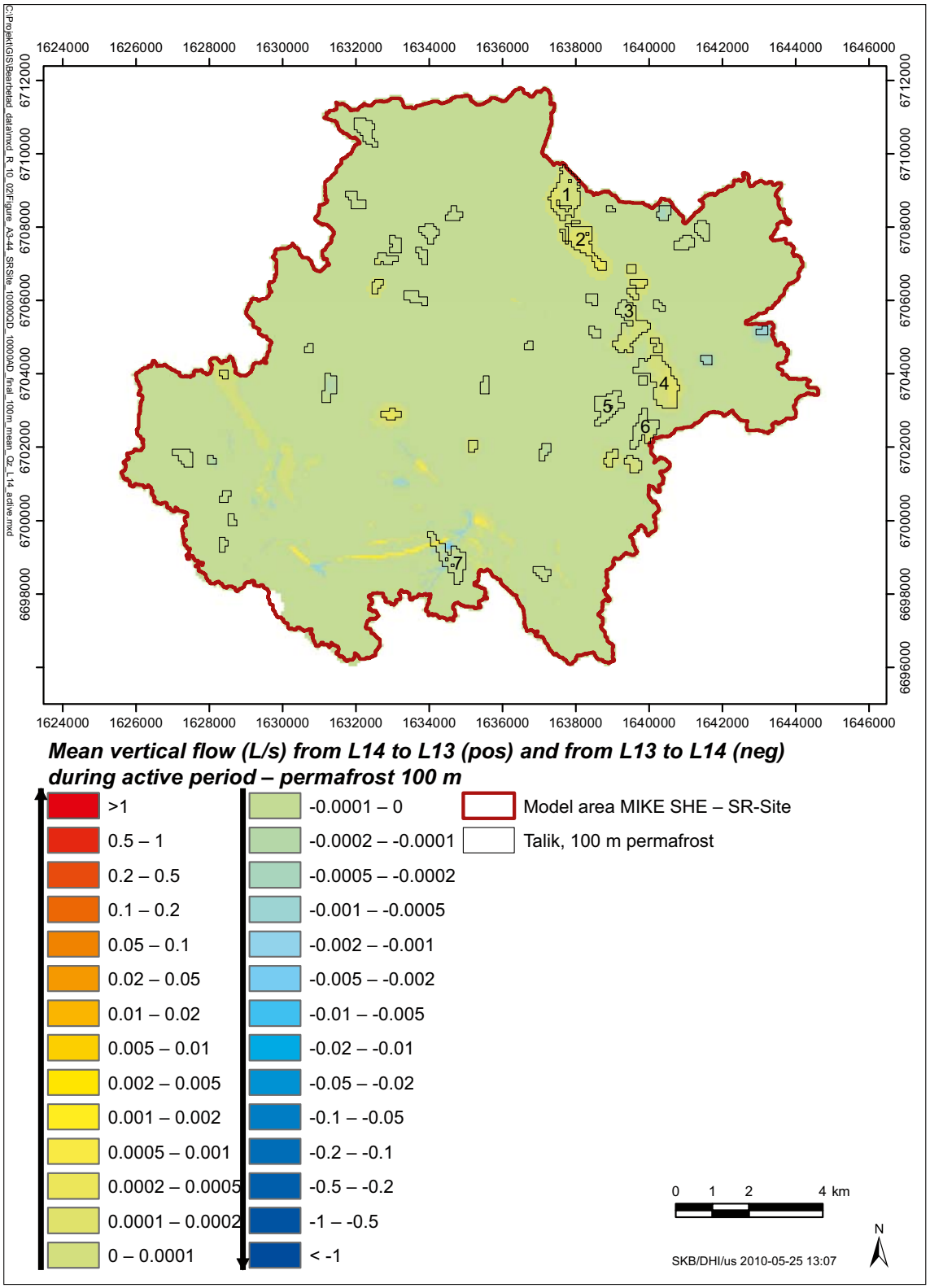

Figure A3-44. *Calculated mean vertical flow (units in l/s) between two deep unfrozen layers below the permafrost during the active period with a permafrost thickness of 100 m.*